UNIVERSITY OF ADELAIDE
11.09.02
LIBRARY

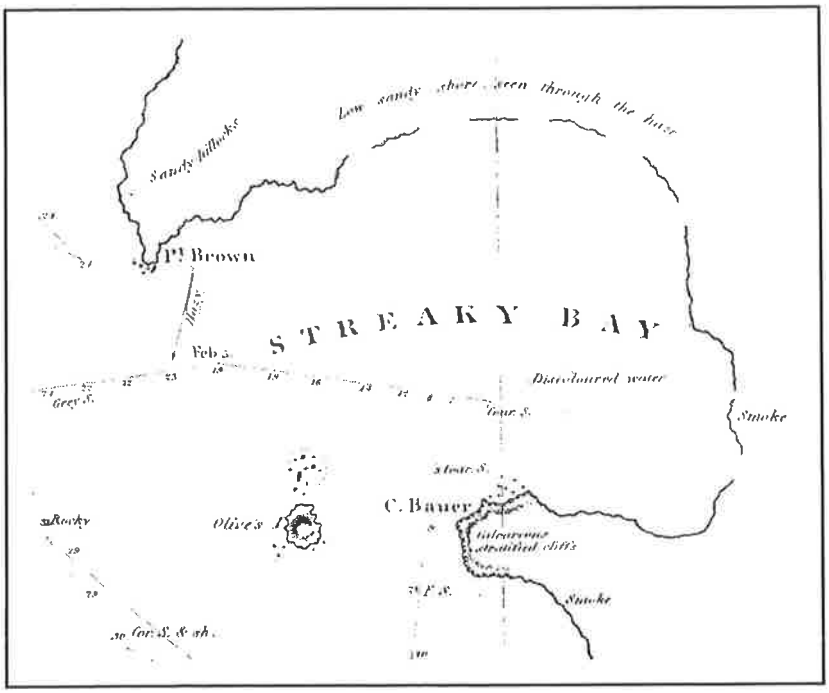
# Carbonate Sediments of a Cool-Water Embayment, Streaky Bay, South Australia

Richard F. Daniel B.Sc.




Department of Geology and Geophysics
ADELAIDE
UNIVERSITY
AUSTRALIA

Thesis submitted in fulfilment required for the degree of Doctor of Philosophy in the Faculty of Science, Adelaide University
March 2002




"....the water was much discoloured in streaks, at less than a mile from the ship with much refuse from the shore, as well as seaweed floating about. Smokes were rising in three different places; but as the wind was unfavourable, and there was no prospect of any opening, sufficiently large to admit the Investigator, I gave up the further examination of this place, and called it STREAKY BAY, (1802, February, Friday 5)."

Flinders, (1814, p 111)

# A Voyade to Terra Australis,
# The Unknown Coast;
# Nuyts' Archipelago,
# Being the Explorations of
# Captain Matthew Flinders RN
# along the shores of South Australia
# on board the Investigator.

# Table of Contents


Table of Contents i

List of Figures ix

Statement of Originality xiii

Abstract xiv

Acknowledgments xvi

**CHAPTER ONE** **1**

**INTRODUCTION: RECENT TEMPERATE CARBONATE INNER SHELF MARGINAL FACIES; EASTERN GREAT AUSTRALIAN BIGHT**

1.1 PREAMBLE 1

1.2 PURPOSE OF THIS STUDY 3

1.3 AIMS 4

**CHAPTER TWO** **5**

**GEOLOGICAL AND OCEANOGRAPHIC SETTING**

2.1 INTRODUCTION 5

2.1.1 MODERN COOL-WATER CARBONATE SEDIMENTS FROM THE SOUTH AUSTRALIAN MARGIN 6

2.2 REGIONAL GEOLOGY 8

2.3 GEOLOGY OF STREAKY BAY 9

2.3.1 PROTEROZOIC OUTCROP 9

2.3.2 PLEISTOCENE OUTCROP 9

2.3.2.1 Bridgewater Formation 9

2.3.2.2 Glanville Formation 9

2.3.3 LOCAL HOLOCENE GEOLOGY 10

2.3.3.1 St. Kilda Formation 10

2.4 LOCATION OF THE STUDY AREA 11

2.5 REGIONAL GEOMORPHOLOGY 11

2.5.1 GEOMORPHOLOGY OF STREAKY BAY 12

2.5.1.1 Streaky Bay Shoreline, Southern Margin 12

2.5.1.2 Streaky Bay Shoreline, Eastern Margin 13

2.5.1.3 Streaky Bay Shoreline, Northern Margin 13

2.6 REGIONAL OCEANOGRAPHY 14

2.6.1 OCEANOGRAPHY OF STREAKY BAY 16

2.7 REGIONAL CLIMATE 18

**CHAPTER THREE** **19**

**METHODS**

3.1 INTRODUCTION 19

3.1.1 TERMOLOGY 19

3.2 MARINE ACQUISITION 20

3.2.1. SEA-FLOOR SAMPLES 20

3.2.2. GRAVITY CORES 21

3.3. LAND OPERATIONS 21

3.3.1. DUMPY LEVEL SURVEYS 21

3.3.2. SLIP HAMMER CORES 22

3.4. LABORATORY ANALYSIS 22

3.4.1. GEOCHRONOLOGY 22

3.4.2. SEDIMENT GRAINSIZE 23

3.4.3. SAND COMPONENT 24

3.4.4. GRAVEL COMPONENT 25

3.4.5. IDENTIFICATION OF ORGANISMS 26

3.4.6. MUD 26

3.4.6.1. Acid Dissolution 27

3.4.6.2. X-ray Diffraction 27

3.4.6.3. Scanning Electron Microscopy 28

3.4.7. FACIES DETERMINATION BY WARD'S CLUSTER METHOD 29

3.5 DISCUSSION 30

3.5.1. MARINE ACQUISITION 30

3.5.2 LAND ACQUISITION 30

3.5.3 LABORATORY ANALYSIS 31

**CHAPTER FOUR** **33**

**LATE QUATERNARY GEOCHRONOLOGY AND RELATIVE SEA-LEVEL FLUCTUATIONS: STREAKY BAY**

4.1 INTRODUCTION 33

4.2 PREVIOUS WORK 34

4.2.1 AUSTRALIAN LATE PLEITOCENE 37

4.2.2 SOUTH AUSTRALIAN PLEISTOCENE 38

4.2.3 HOLOCENE SEA-LEVEL 39

4.2.4 AUSTRALIAN HOLOCENE 40

4.2.5 SOUTH AUSTRALIAN HOLOCENE 40
4.3 RESULTS 41
4.3.1 MID TO LATE PLEISTOCENE SEA-LEVEL DETERMINATION 41
4.3.2 FLAGSTAFF LANDING SECTION 42
4.3.3 POINT GIBSON SECTION 42
4.3.4 POINT COLLINSON PLEISTOCENE WAVE CUT PLATFORM 43
4.3.5 TIMING OF GLANVILLE FORMATION DEPOSITION 43
4.3.6 EVIDENCE FOR QUATERNARY INTERSTADIAL HIGH SEA-LEVEL 44
4.3.7 EVIDENCE FOR EARLY HOLOCENE SEA-LEVEL HIGH STAND 44
4.3.8 COMMENCEMENT OF EARLY HOLOCENE SHALLOW-WATER SEDIMENTATION 44
4.3.9 LATE HOLOCENE DEPOSITIONAL PHASE 46
4.4 DISCUSSION 48
4.4.1. MODERN DAY/ GLANVILLE FM COMPARISON (FLAGSTAFF LANDING) 48
4.4.2. MODERN DAY/ GLANVILLE FORMATION COMPARISON (POINT GIBSON) 48
4.4.3. PLEISTOCENE PLATFORM 49
4.4.4. TIMING OF GLANVILLE FORMATION 49
4.4.5. DEVELOPMENT OF NEAR SHORE LITTORAL TERRACE 50
4.4.6. EARLY HOLOCENE SEA-LEVEL HIGH STAND 50
4.4.7. COMMENCEMENT OF EARLY HOLOCENE SHALLOW-WATER SEDIMENTATION 51
4.4.8. HOLOCENE SEA-LEVEL HIGHSTAND 52
4.4.9. TIMING OF THE EMPLACEMENT OF SOUTH SAND AND NORTH BANK 53
4.5. CONCLUSIONS 53

**CHAPTER FIVE** **55**

**GRAINSIZE DISTRIBUTION OF RECENT SEDIMENTS**

5.1 INTRODUCTION 55
5.2 SUBSTRATE 56
5.2.2 SANDY SUBSTRATE 56
5.2.3 HARD ROCKY SUBSTRATE 56
5.3 GENERAL DISTRIBUTION OF LIVING BIOTA 57
5.3.1 MOLLUSCS 57
5.3.2 BRYOZOANS 57
5.3.3 FORAMINIFERS 57
5.3.4 CORALLINE ALGAE 58
5.3.5. MINOR BIOGENIC COMPONENTS 58
5.3.6 NON-BIOGENIC COMPONENTS 58

5.4 GRAINSIZE DISTRIBUTION 59
5.4.1 DESCRIPTION OF TRANSECTS 59
5.4.1.1 Transects 1, 2, 3. 59
5.5 RESULTS 60
5.5.1 BY TRANSECT 60
5.5.2 SPATIAL DISTRIBUTION 61
5.5.2.1 Gravel 61
5.5.2.2 Very Coarse to Coarse Sand 61
5.5.2.3 Medium to Very Fine Sand 62
5.5.2.4 Mud 62
5.6 SAND RATIO DISTRIBUTION 62
5.7 SKEWNESS 62
5.8 DISCUSSION 63
5.8.1 SAND RATIO 63
5.8.2 SKEWNESS 63
5.8.3 GRAINSIZE DISTRIBUTION OF RECENT SEA-FLOOR SEDIMENTS, EYRE PENINSULA 64
5.8.3.1 Comparison With Nearby Embayments 64
5.8.4 ORIGINS OF SAND-SIZED SEDIMENTS 65
5.9 CONCLUSIONS 67

**CHAPTER SIX** **68**
**COMPOSITIONAL DISTRIBUTION OF SAND-SIZED SEDIMENT**
6.1 INTRODUCTION 68
6.2. COMPONENT IDENTIFICATION 69
6.3. RESULTS 69
6.3.1. GENERAL DISTRIBUTION OF SEDIMENT COMPONENTS 69
6.4. SPATIAL DISTRIBUTION OF COMPONENTS 70
6.4.1. MOLLUSCAN GRAINS 70
6.4.2. FORAMINIFERS 71
6.4.3. BRYOZOAN GRAINS 71
6.4.4. ECHINODERM GRAINS 71
6.4.5. CORALLINE ALGAL GRAINS 71
6.4.6. ABRADED BIOCLASTIC GRAINS 72
6.4.7. CALCAREOUS AEOLIANITE GRAINS 72
6.4.8. QUARTZ/ LITHIC GRAINS 72
6.5 DISCUSSION 72
6.6 CONCLUSIONS 74

**CHAPTER SEVEN** 75
**DISTRIBUTION AND COMPOSITION OF MACROFOSSILS**
7.1 INTRODUCTION 75
7.2 RESULTS - TRANSECTS 77
7.2.1 STREAKY BAY TRANSECTS 77
7.2.2 SHELF TRANSECT 78
7.3 RESULTS - SPATIAL DISTRIBUTION 78
7.3.1 MOLLUSCS 78
7.3.2 BRYOZOANS 80
7.3.3 FORAMINIFERS 81
7.3.4 CORALLINE ALGAE 81
7.3.5 MINOR CARBONATE-PRODUCING ORGANISMS 82
7.3.5.1 Echinoderms 82
7.3.5.2 Brachiopods 83
7.3.5.3 Crustaceans 83
7.3.5.4 Serpulids 83
7.3.5.5 Sponges 83
7.3.5.6 Corals 83
7.3.6 QUARTZ AND LITHIC FRAGMENTS 84
7.4 DISCUSSION 84
7.4.1 MOLLUSCS 84
7.4.2 BRYOZOANS 85
7.4.3 FORAMINIFERS 86
7.4.4 CORALLINE ALGAE 86
7.4.6 QUARTZ/LITHIC 86
7.5 CONCLUSIONS 87

**CHAPTER EIGHT** 88
**ORIGIN AND COMPOSITION OF MUD-SIZED SEDIMENTS**
8.1 INTRODUCTION 88
8.2. CARBONATE CONTENT OF THE MUD FRACTION 89
8.2.1. RESULTS 89
8.3. CARBONATE COMPOSITION OF SEDIMENT BY XRD ANALYSIS 90
8.3.1. RESULTS 91

8.3.1.1. LMC 91
8.3.1.2. IMC 91
8.3.1.3. HMC 91
8.3.1.4. Aragonite 91
8.3.1.5. Dolomite 93
8.3.1.5. Minor and Trace Minerals 93
8.4. COMPOSITION OF SKELETAL ORGANISMS 94
8.4.1 RESULTS 97
8.5. MORPHOLOGY OF SKELETAL MICROSTRUCTURE 97
8.5.1. MOLLUSCS 98
8.5.2. FORAMINIFERS 99
8.5.3. BRYOZOA 99
8.5.4. CORALLINE ALGAE 101
8.5.5. ECHINODERMS 103
8.5.6. BRACHIOPODS 103
8.5.7. SPIRORBIDS AND SERPULIDS (ANNELIDA) 103
8.5.8. PORIFERA (SPONGES) 104
8.5.9 TUNICATES (ASCIDIANS) 104
8.5.10 CORALS 105
8.5.11 DIATOMS (CHRYSOPHYTA) 105
8.5.12 COCCOLITHS (CHRYSOPHYTA) 105
8.6 MORPHOLOGY AND COMPOSITION OF THE MUD FRACTION BY SEM 106
8.6.1 MORPHOLOGY OF MUD FRACTION 106
8.6.1.1 Prismatic Particles 106
8.6.1.2. Tabular To Blocky Particles 106
8.6.1.3. Porous Polygonally Sub-Equant Particles 106
8.6.1.4. Composite Particles 107
8.6.2. CARBONATE COMPOSITION OF MUD; EDAX PROBE RESULTS 107
8.7. DISCUSSION 109
8.7.1. CARBONATE CONTENT OF MUD 109
8.7.2. MINERALOGY (XRD) 110
8.7.2.1. Mud Mineralogy 110
8.7.2.2. Skeletal Mineralogy 111
8.7.2.3. Non Biogenic Mineralogy 112
8.7.3. COMPOSITION OF SKELETAL MATERIAL AND SEDIMENT (XRD) 113
8.7.4. PARTICLE MORPHOLOGY (SEM) 113
8.7.5. DISINTEGRATION PATHWAYS OF VARIOUS SKELETAL ORGANISMS 114

8.7.6. MORPHOLOGY OF TEMPERATE VERSUS TROPICAL MUDS 116
8.8. CONCLUSIONS 117

**CHAPTER NINE** **120**
**COOL-WATER CARBONATE LITHOFACIES**
9.1 INTRODUCTION 120
9.2 DISTRIBUTION OF FACIES COMPONENTS WITHIN STREAKY BAY 121
9.3 SEDIMENTARY LITHOFACIES 122
9.3.1 INTERPRETIVE LITHOFACIES 122
9.3.2 STATISTICAL DETERMINATION OF LITHOFACIES 123
9.3.2.1 Three Lithofacies 123
9.3.2.2 Four Lithofacies 124
9.3.2.3 Five Lithofacies 124
9.3.2.4 Six Lithofacies 124
9.3.2.5 Seven and Eight Lithofacies 125
9.4 FIVE LITHOFACIES MODEL 125
9.4.1 LITHOFACIES ONE: MOLLUSC/ CALCAREOUS AEOLIANITE/ QUARTZ/ BRYOZOAN, MEDIUM TO FINE SAND 126
9.4.2 LITHOFACIES TWO:- CALCAREOUS AEOLIANITE/ MOLLUSC/ QUARTZ, 127
VERY COARSE TO FINE SAND 127
9.4.3 LITHOFACIES THREE:- MOLLUSC/ FORAMINIFERA/ BRYOZOAN/ CORALLINE ALGAE, GRAVELLY FINE TO VERY COARSE SAND 127
9.4.4 LITHOFACIES FOUR:- BRYOZOAN/ MOLLUSC/ CALCAREOUS AEOLIANITE/ CORALLINE ALGAE, GRAVELLY MEDIUM TO VERY COARSE SAND 127
9.4.5 LITHOFACIES FIVE:- MOLLUSC/ ECHINOID/ QUARTZ/ FORAMINIFERA, FINE SANDY MUD 128
9.5. DISCUSSION 129
9.5.1. REGIONAL DISTRIBUTION OF LITHOFACIES, COASTAL EMBAYMENTS, WESTERN EYRE PENINSULA 129
9.5.1.1. Baird Bay 130
9.5.1.2. Tourville Bay 130
9.5.1.3. Coffin Bay 131
9.5.1.4. Fowlers Bay 131
9.5.2. STREAKY BAY TO GAB SHELF EDGE: TRANSECT FROM FR 03/98 132
9.6 LITHOFACIES OF THE SOUTHERN MARGIN, COMPARISON 134
9.6.1 BROAD-BASED SOUTHERN MARGIN FACIES 134
9.6.2 GREAT AUSTRALIAN BIGHT 134

9.6.3 LINCOLN SHELF 135
9.6.4 SOUTHERN SPENCER GULF, INVESTIGATOR STRAIT 136
9.6.5 LACEPEDE AND BONNEY SHELVES 136
9.7 CONCLUSIONS 137

**CHAPTER TEN**
**CONCLUSIONS** **140**

**REFERENCES** **145**

**APPENDIX** **162**
APPENDIX I Sample Stations - Latitude and Longitude 163
APPENDIX 2 Sediment Descriptions 171
APPENDIX 3 Grainsize Fractions 187
APPENDIX 4 Organism Distribution Gravel Fraction 191
APPENDIX 5 Discussion on Carbonate Muds 196

# List of Figures

**FRONTISPIECE.** Map drawn by Captain Matthew Flinders with an excerpt from the ship's log on naming Streaky Bay.

**CHAPTER ONE**

1.1 World-Wide Distribution of Cool-Water Carbonates 3
1.2 Australia Locality Map 3
1.3 Great Australian Bight - Lithofacies 4

**CHAPTER TWO**

2.1 Southern Margin Localities 6
2.2 Eyre Peninsula , South Australia Regional Geology 9
2.3 Streaky Bay Geology 9
2,4 Streaky Localities 12
2.5 Oblique view of Streaky Bay to the South West 12
2.6 Oblique view of Streaky Bay to the West 12
2.7 Oblique view of Acraman Creek Estuary 12
2.8 Bathymetry 12
2.9 Water Movement within Streaky Bay 18
2.10 Transport Directions within Streaky Bay 18
2.11 Surface and Sea-floor Salinity 18
2.12 Currents and Eddies 18

**CHAPTER THREE**

3.1 RV *Hero* and Supply Truck 21
3.2 Streaky Bay and Shelf Sample Stations 21
3.3 Dredge, Gravity Corer and Coring Tools 21

**CHAPTER FOUR**

4.1 Late Quaternary Oxygen Isotope and Sea-Level Curve 35
4.2 Holocene Sample Elevations for Sea Level Rise of Past 17ka 41
4.3 Holocene Sea Level Rise for Northern Queensland 41
4.4 Isotope Stage 5e Sea-Level, Flagstaff Landing 43
4.5 Isotope Stage 5e Sea-Level, Point Gibson 43
4.6 Isotope Stage 5e Sea-Level, Wave-cut, Point Collinson 43

4.7 Isotope Stage 5 a-c Near-shore Littoral Terrace/ Ultimate platform 45
4.8 Depth and Timing of Holocene Highstand 46
4.9 Sedimentation Rates Mid to Late Holocene 46
4.10 Mean Average Sea Surface Temperatures for Australian Waters 50

**CHAPTER FIVE**

5.1 Morphology of Streaky Bay 57
5.2 Substrate, Streaky Bay 57
5.3 Rocky Substrate, Outer Bay 57
5.4 Sand Waves And Crevice Fill, Outer Bay 57
5.5 Transect Locations 57
5.6 Relative Sediment Abundance 57
5.7 Transect 1 Sea-floor Profile, Grain-size distribution, Components -sand fraction, Components -gravel fraction 61
5.8 Transect 2 Sea-floor Profile, Grain-size distribution, Components -sand fraction, Components -gravel fraction 61
5.9 Transect 3 Sea-floor Profile, Grain-size distribution, Components -sand fraction, Components -gravel fraction 61
5.10 Transect 4 Sea-floor Profile, Grain-size distribution, Components -sand fraction, Components -gravel fraction 61
5.11 Transect 5 Sea-floor Profile, Grain-size distribution, Components -sand fraction, Components -gravel fraction 61
5.12 Transect 6 Sea-floor Profile, Grain-size distribution, Components -sand fraction, Components -gravel fraction 61
5.13 Transect 7 Sea-floor Profile, Grain-size distribution, Components -sand fraction, Components -gravel fraction 61
5.14 Transect 8 Sea-floor Profile, Grain-size distribution, Components -sand fraction, Components -gravel fraction 61
5.15 Shelf Transect Sea-floor Profile, Grain-size distribution, Components -sand fraction, Components -gravel fraction. 61
5.16 Distribution, Gravel 62
5.17 Distribution, Very coarse to coarse Sand 62
5.18 Distribution, Medium to Very Fine Sand 62
5.19 Distribution, Mud 62
5.20 Sand Ratio Isopleth 63
5.21 Ternary Textural Distribution of Sediments 63
5.22 Skewness 63

**CHAPTER SIX**

6.1 Distribution of Molluscan Grains (sand fraction) 72
6.2 Distribution of Foraminifera (sand fraction) 72
6.3 Distribution of Bryozoan grains (sand fraction) 72
6.4 Distribution of Echinoderm grains (sand fraction) 72
6.5 Distribution of Coralline Algal grains (sand fraction) 72
6.6 Distribution of Abraded Bioclastic grains (sand fraction) 72
6.7 Distribution of Calcareous Aeolianitic grains (sand fraction) 72
6.8 Distribution of Quartz/ Lithic grains (sand fraction) 72

**CHAPTER SEVEN**

7.1 Distribution of Gravel Fraction 77
7.2 Distribution of Molluscan fragments, (gravel fraction) 77
7.3 Distribution of Bryozoan fragments (gravel fraction) 82
7.4 Distribution of Coralline Algal fragments (gravel fraction) 82
7.5 Distribution of Echinoderm fragments (gravel fraction) 82
7.6 Distribution of Quartz/ Lithic fragments (gravel fraction) 82
7.7 Distribution of Bivalves and Gastropods, Transects 1, 2, 3, 4 82
7.8 Distribution of Bivalves and Gastropods, Transects 5, 6, 7, 8 82
7.9 Distribution of Bryozoan Structural Types, Transects 1, 2, 3, 4 82
7.10 Distribution of Bryozoan Structural Types, Transects 5, 6, 7, 8 82
7.11 Distribution of Coralline Algae Structural Types, Transects 1, 2, 3, 4 82
7.12 Distribution of Coralline Algae Structural Types, Transects 5, 6, 7, 8 82
7.13 Distribution of Bivalves and Gastropods, Bryozoan Structural Types and Coralline Algae Structural Types, Shelf Transect 82

**CHAPTER EIGHT**

8.1 SEM Disintegration Patterns of Molluscs 100
8.2 SEM Disintegration Patterns of Molluscs 100
8.3 SEM Disintegration Patterns of Molluscs 100
8.4 SEM Disintegration Patterns of Molluscs and Foraminifers 100
8.5 SEM Disintegration Patterns of Foraminifers 100
8.6 SEM Disintegration Patterns of Foraminifers and Bryozoans 100
8.7 SEM Disintegration Patterns of Bryozoans 100
8.8 SEM Disintegration Patterns of Bryozoans 100
8.9 SEM Disintegration Patterns of Bryozoans 100
8.10 SEM Disintegration Patterns of Bryozoans 100
8.11 SEM Disintegration Patterns of Bryozoans 100

8.12 SEM Disintegration Patterns of Bryozoans and Coralline Algae 100
8.13 SEM Disintegration Patterns of Coralline Algae 100
8.14 SEM Disintegration Patterns of Coralline Algae and Echinoderms 100
8.15 SEM Disintegration Patterns of Echinoderms and Brachiopods 100
8.16 SEM Disintegration Patterns of Brachiopods and Serpulids 100
8.17 SEM Disintegration Patterns of Serpulids 100
8.18 SEM Disintegration Patterns of Serpulids, Sponges and Ascidian spicules 100
8.19 SEM Disintegration Patterns of Ascidian spicules and Corals 100
8.20 SEM of Common Diatoms and Coccoliths 100
8.21 SEM Morphology of Mud Fraction 100
8.22 SEM Morphology of Mud Fraction, Prismatic and Blocky Particles 107
8.23 SEM Morphology of Mud Fraction, Prismatic Particles 107
8.24 SEM Morphology of Mud Fraction, Prismatic and Tabular Particles 107
8.25 SEM Morphology of Mud Fraction, Composite and Porous Polygonal Particles 107
8.26 SEM Morphology of Mud Fraction, Porous Polygonal Particles 107
8.27 SEM Morphology of Mud Fraction, Bladed and Cleavage Particles 107

**CHAPTER NINE**

9.1 Cluster Dendogram 124
9.2 Three Facies Model, Streaky Bay 124
9.3 Four Facies Model, Streaky By 124
9.4 Five Facies Model, Streaky Bay 124
9.5 Six Facies Model, Streaky Bay 124
9.6 Average Component Bar Graph, Five Facies 127
9.7 Mollusc/Foraminifer/Bryozoan Ternary Plot 127
9.8 Sediments of Facies 1, 2, 3 127
9.9 Sediments of Facies 4, 5 127
9.10 West Eyre Peninsula Facies Model (Energy, Substrate, Salinity) 131
9.11 Baird Bay Sea Chart 132
9.12 Coffin Bay Sea Chart 132
9.13 Fowlers Bay to Baird Bay Sea Chart 132

# Statement of Originality

This work contains no material which has been accepted for the award of any other degree or diploma in any university and that, to the best of my knowledge and belief, contains no material previously published or written by another person, except where due reference has been made in the text.

I hereby consent to this copy of my thesis, when deposited the University library, being available for loan and photocopying.

..... .....

Richard F. Daniel

# COOL-WATER CARBONATE SEDIMENT DISTRIBUTION PATTERNS, STREAKY BAY, SOUTH AUSTRALIA

**Abstract**

The interface between shallow cool-water marine shelf and terrestrial facies is rarely observed in Cainozoic limestones. An analogue for shallow marine carbonate sedimentation and deposition on a broad passive margin is described from the eastern Great Australian Bight.

Streaky Bay is a large embayment on the West Coast of Eyre Peninsula, South Australia. The climate is temperate, with cool waters offshore. It is partially protected from high wave attack and swells from the Southern Ocean by substantial headlands at the mouth. Islands and extensive shallow near-shore tidal deltas attenuate wave energy within the bay. Proterozoic felsic intrusives occur north and south of the bay as basement whereas the headlands are composed of Pleistocene Bridgewater Formation aeolianites. The marine bioclastic Pleistocene Glanville Formation outcrops in isolated areas around the perimeter of the bay. Two localities with stratigraphic and palaeontological control, of far field tectonic stability, were surveyed in conjunction with proximal modern beach profiles. Survey comparisons indicate sea-level was 1.8 m higher during the highstand of Isotope Stage 5e. than present day. These sediments have an estimated age of 125 ka and a depositional environment significantly warmer than present day.

Holocene sediments are predominantly biogenic in origin. Sampling and analysis of seafloor sediments collected on transects across the bay show distinct patterns in component and grainsize distribution. The sediments are mixtures of: 1) ubiquitous Holocene biogenic particles (~80%); 2) unidentifiable abraded bioclastic grains, localised to sand shoals, banks and spits (~20%); 3) calcareous aeolianite or relict carbonate grains, restricted to areas where the Bridgewater Formation is exposed (~10%) and 4) Proterozoic rock fragments, especially in the region of Olive Island (~10%). Significant Holocene biogenic sand-size components are fragments of, in decreasing order of abundance, molluscs, bryozoans, foraminifers and coralline algae. Minor contributors are echinoderms, brachiopods, various crustaceans, serpulids, corals, and sponge spicules. Molluscs, whilst present in significant quantities throughout the bay, are most abundant in the basinal and deeper tidal-delta areas (up to 75%). Foraminifers are concentrated in the central sea-grass meadows flanking the banks and tidal deltas and in the central area of the bay, where brown algae are also prolific. The highest percentage and diversity of bryozoans, including rare vagrants, occur centrally at the bay entrance, where there are suitable diverse substrates. Coralline algae are ubiquitous in all sediments collected. Diatoms are common in the very fine sand- to mud-sized sediment.

Allochthonous sediment sources are supplied from around the headlands and the bay entrance i.e. probably from deeper offshore shelf areas. These sediments have formed extensive spits abutting the north and south margins of the bay. Sediment has also accumulated across the inner half of the floor of the bay, forming two elongate sandbanks approximately 9 km in length. Large tidal deltas occur between and adjacent to these sandbanks. The sea-floor of the deeper outer areas is a rocky or loose pavement of eroded Bridgewater Formation, with isolated mobile sand waves. Sediment here is composed of significant biogenic fragments with terrigenous sediment derived from the nearby islands and isolated sea-floor highs.

The grainsize of the sediments ranges from gravel to mud size. Gravel-size sediments (up to 40%) occur at the mouth of the bay whereas only minor amounts of gravel (<5%) occur within the bay. Localised concentrations

of gravel are the result of current hydrodynamics, biogenic activity and erosion of the bay floor. Coarse to very coarse sands are abundant (up to 80%) at the mouth, centre and central tidal delta regions of the bay. The grain size of the sediments from the sandbanks and the tidal deltas is predominantly medium to fine sand, with minor areas extending to gravel size (<10%). Mud is present (up to 60%), along with medium to very fine sand, in the comparatively deep-water of the inner marginal basins. These are protected from the effects of the open sea by the sandbanks and tidal deltas. The fine sandy muds are characterised by silt-size grains. The calcium carbonate content of the mud is >95% and consists of aragonite and low, intermediate and high magnesium calcite. Scanning electron microscope examination of the muds reveal they are generally derived from the disintegration of molluscs (silt), bryozoa (silt to clay-size) and coralline algae (clay-size).

Five distinct lithofacies and distribution in the bay are;

- Mollusc/ calcareous aeolianite/ quartz/ bryozoan, medium to fine sand lithofacies; beaches, northern and outer sand shoals, banks and central inner terrace.
- Calcareous aeolianite/ mollusc/ quartz, very coarse to fine sand lithofacies; sand shoals, northern and southern terrace.
- Mollusc/ foraminifera/ bryozoan/ coralline algae, gravelly fine to very coarse sand lithofacies; central and southern terrace.
- Bryozoan/ mollusc/ calcareous aeolianite/ coralline algae, gravelly medium to very coarse sand lithofacies; entrance and central and outer northern terrace.
- Mollusc/ echinoderm/ quartz/ foraminifera, fine sandy mud lithofacies; inner marginal basins

Lithofacies of most marginal embayments on the West Coast of the Eyre Peninsula are characterised by similar variations of energy, salinity and seagrass meadows and contain several of the lithofacies described from Streaky Bay. The dominant skeletal component in lithofacies from these embayments is molluscan, in contrast to the inner shelf where molluscs equal bryozoa and the outer shelf where bryozoans dominate.

# Acknowledgments

To my supervisors Dr Yvonne Bone, Professor Chris von der Borch and Professor Noel James deep thanks for your enthusiastic contributions to all aspects from initiation to reviewing the thesis: Chris for suggesting the West Coast and help with collecting sediments and cores; Noel for suggesting Streaky Bay as a great place to study recent carbonate sediments, your expertise in the carbonate realm and your delightful habit of picking every lapse in my logic; Yvonne for your enthusiasm and encouragement for the long haul in taking the thesis from ideas to hard copy – your support has been immeasurable.

I would like to thank the late Dr Gunther Bischoff and Professor John Talent of Macquarie University for your enthusiasm in soft-rock geology and micropalaeontology that initially set me on the inquisitive road to research.

Thanks Dr John Bye for your help in collecting sediments, outlining your ideas on southern margin oceanography and, with Paul Clarke, your ideas on the oceanography of Streaky Bay. Dr George Matsumoto for your insights into invertebrate biology and your help in collecting samples at Streaky Bay. Thank you Dr Herb Veeh for your U/Th dating of corals and valuable background into Isotope Stage 5e problems. Thanks to Dr Adriana Dutkievicz, you have always been good for reassuring chats about the many ups and downs in the life of a postgrad.

Thanks are due to the School of Earth Science for a Grant to hire and transport the *RV Hero* from Adelaide to Streaky Bay. Thanks also to the Australian Institute of Nuclear Science and Engineering for their grant (95/084, AINSE-AMS Award) to date sediments at Streaky Bay.

Thank you to the technical crew at Flinders University in particular to Gail Jackson for your drafting capabilities, to Trevor McGrath, Bob Walker and Gert Johanssen for towing from Adelaide and navigating the *RV Hero* over the length and breadth of Streaky Bay in quite variable conditions (how crook was I?). Thanks to Joe Lorenzin for quite difficult thin sectioning of loose sediments. Thank you Peter Russ for suppling, organising materials and laboratory space and your friendship at Flinders University during research and teaching.

Thank you Professor Stewart Greenhalgh, Associate Professor Alex Grady, Dr Malcolm Abbott and Dr Vic Gostin for chewing the fat on subjects near and far in the geological realm and being a sounding board for maintaining the right track at Flinders and Adelaide Universities.

Thank you also to the technical crew at Adelaide University and in particular Dr Keith Turnbull for isotope analyses, Wayne Mussared for thin and polished sections and John Stanley for help with loads of XRDs. To Gerald Buttfield, Mary Odlum, Yvonne Philp and Sondra Gould for your organisational ability to keep plans running smoothly and make things work, thank you very much. Thank you

Sherrie Proferes and Ian Florence for an introduction into the mysteries and byways of the computer realm and the whimsical functioning of some programmes.

Thanks to the staff at CEMMSA, John, Craig, Linda, Angie and especially Lyn for teaching me how to drive the XL-20 and XL-30.

Identification of the numerous organisms encountered in Streaky Bay would not have been possible without the help of Karen Gowlett-Holmes (molluscs), Dr Yvonne Bone and Rolf Schmidt (bryozoans), Dr Peter Gell (diatoms) and Dr Charlie Veron (corals), Kirsty Brown with the machinations of crustose coralline algae.

I would like to thank the Carbonate Group at AU particularly Dr Yvonne Bone, Dr Liz Campbell, Kirsty Brown, Miles Davies, Rolf Schmidt and Paul Polito for your good company, support and on going tutorials on various computer programmes.

The Captains, Crews and Scientists of the CSIRO, Division of Oceanography, *RV Franklin* cruise 03/98 for access to sediments collected on the shelf off Streaky Bay.

Thank you to the Streaky Bay community and the local diving group for your friendliness and the information on the weather habits of Streaky Bay.

Thankyou Graham Williams for your guidance.

I wish to thank my parents, Dennis and Beryl Daniel, for your timeless support especially throughout my university career.

My deepest gratitude goes my partner, Ann Calvert and my daughter Lyrian Daniel, for all your understanding and support throughout these last few years.

# CHAPTER 1

# INTRODUCTION

# Recent Cool-Water Carbonate Inner Shelf Marginal Facies; Eastern Great Australian Bight

## 1.1 PREAMBLE

The importance of cool-water carbonates in the geological column was recognised by the early work of Teichert (1958); Chave (1967); Conolly and Von der Borch (1967); Davies (1970); Wass et al. (1970); Lees and Buller (1972), amongst others. Chave (1967) noted that the production of calcareous sediments was not restricted to the lower latitudes of the tropics. It was indisputable that thousands of square kilometres of temperate continental shelves in higher latitudes were dominated by biogenic carbonate sedimentation. Indeed, as more sediments from what were previously assumed to be "non-carbonate" areas were studied (Figure 1.1), it was realised that our ideas on temperate shelves needed a complete revision.

Major areas of wide cool-water carbonate dominated shelves are found off southern Australia and north-west Europe (Conolly and Von der Borch, (1967); Boillet, (1965); Wass et al., (1970)). It was also recognised that these sediments were appropriate analogues for limestones preserved throughout the Phanerozoic rock record (Nelson, 1978, 1988; Jones and Desrochers, 1992). Since this important

recognition, limestones with cool-water carbonate affinities have been reported throughout the Phanerozoic from most continents eg. Canada/ United States - Ordovician and Carboniferous (Brookfield, 1988; Pope and Reid, 1997; Brandley and Krause, 1997; Martindale and Boreen, 1997); Australia - Permian - Cainozoic (Draper, 1988; James and Bone, 1991, 1992, 2000, James et al., 1993); New Zealand - Cainozoic (Kamp et al., 1988; Nelson et al., 1978, 1988); Europe - Cretaceous, Tertiary (Carannante et al., 1997; Surlyk, 1997; Spjeldnaes and Moissette, 1997; Franseen et al., 1997) amongst others.

The southern continental margin of Australia is the largest open temperate shelf and site of active cool-water carbonate sediment deposition on Earth (James et al., 1992, 1994, 1997, 2001) (Figure 1.1). The deposition of cool-water carbonate sediments is continuous along this margin from south of the Ningaloo Reef in Western Australia (Collins et al., 1997) to off-shore shelf areas of sparse deposition in southern New South Wales (Ferland and Roy, 1997; Davies, 1979) (Figure 1.2). The southern margin has been established as an analogue for ramp and open shelf cool-water carbonate deposition for Cainozoic carbonates (Boreen and James, 1995; James and Bone, 1989, 1991; James et al., 1993; Nelson, 1978; Nelson et al., 1988) The latitude parallel section of the shelf has little terrigenous input as a result of the arid climate along southern Australia. The central section of this southern margin, encompassing the Great Australian Bight (GAB), is the most arid with minimal terrestrial input to the shelf through fluvial activity (Figure 1.2). The identification and distribution of GAB shelf facies for >40m water depth is delineated by James et al, 2001, which encompasses shelf sediments from Cape Pasley in the West to the southern tip of Eyre Peninsula in the East (Figure 1.3).

The shoreline of the Eastern Great Australian Bight is backed by laterally extensive thick calcarenite , Bridgewater Formation. Aeolian processes were responsible for the transport of much of the sediment in these Quaternary calcareous aeolianites on the eastern coast of the Great Australian Bight (Eyre Peninsula). The sediments, from which these dune deposits originate, are derived from lithoskels of biogenic calcium carbonate on the adjacent shelf and embayments. These high Quaternary coastal dune systems act as barriers to the incursion of sea during high stand inter-glacial periods. Active coastal erosion has breached some of these barriers to form numerous embayments (open to restricted circulation) along the western coast of the Eyre Peninsula (Figure 1.3). The sediments in these embayments were generally thought to consist of mostly sand sized grains (Reeckmann, 1988; Nelson et al, 1988) but this study found that significant concentrations of mud-sized sediments are deposited in the more sheltered embayments of this high energy coastline.

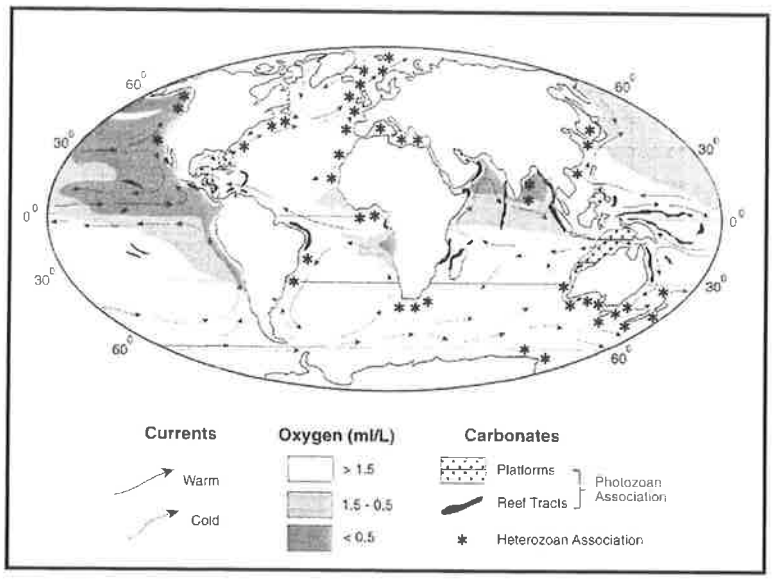



Figure 1.1. Distribution of Tropical (Photozoan) and documented Cool-water (Heterozoan) carbonates, low-oxygen marine waters and major ocean currents. (James, 1997)

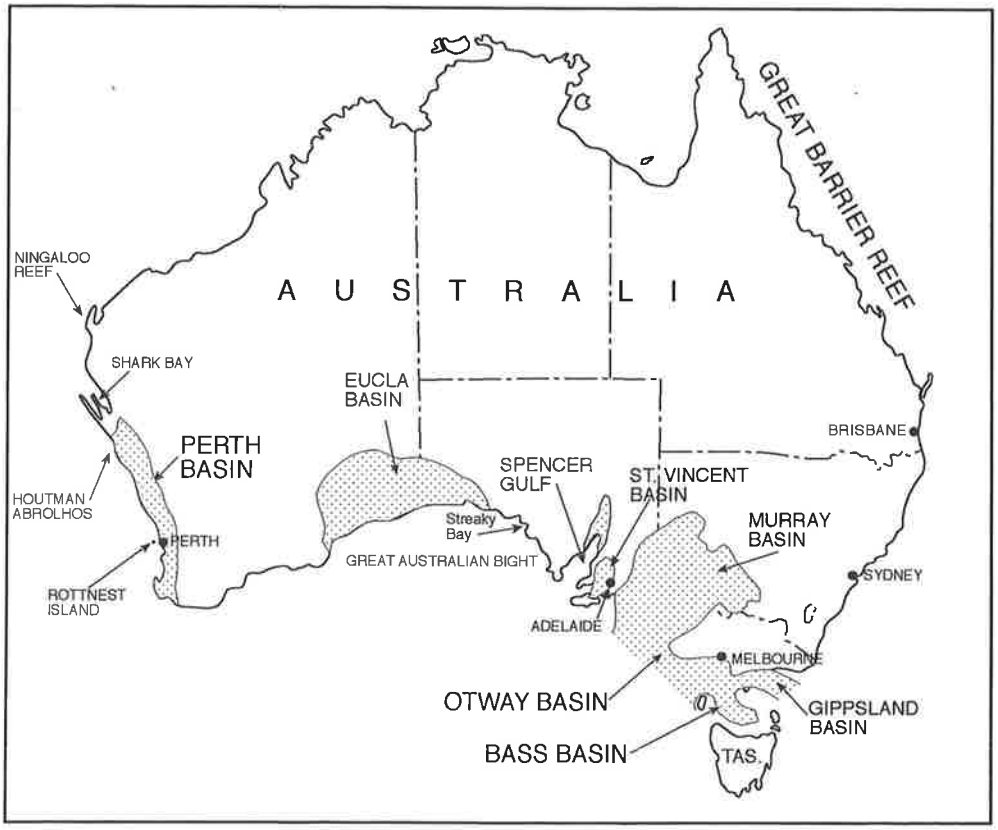



Figure 1.2. Distribution of southern Australian sedimentary basins that contain cool-water (temperate) shelf carbonate deposits. (after Reekmann, 1988)

## 1.2 PURPOSE OF THIS STUDY

Most studies of modern cool-water carbonates are based on the off-shore shelf environment in water depths > 30 m. This is because the researchers active in the field of marine geology are controlled by the capabilities of the larger research vessels. Consequently, one area of cool-water carbonate sedimentation that has received little attention is the near-shore depositional environment, especially in relatively low energy conditions. The eastern Great Australian Bight (GAB) offers the opportunity to examine these settings because, unlike other sectors, it consists of a series of large semi-protected embayments (Figure 1.3). The focus of this study is one such embayment, Streaky Bay.

There have been sparse reports on the sedimentology of Streaky Bay in the literature ie. Flinders (1814) briefly described two sediment samples from the bay, Short et al. (1986) included the bay in a geomorphological study of the coastal western Eyre Peninsula, and Clarke (1994) reported on a reconnaissance oceanographic study of the bay. Other embayments along this section of coastline have been the focus of brief reconnaissance sedimentological studies ie. Tourville Bay (Lablack, 1985); Coffin Bay (Freeman, 1985); Fowlers Bay (Belperio, 1988) and Baird Bay (Hill, 1994). Streaky Bay has a diverse range of lithofacies, including a relatively deep-water carbonate mud facies, which can be used as an analogue for typifying marginal marine lithofacies occurring in embayments along this ~1500km of indented coastline (Point Fowler to Cape Catastrophe; Figure 2.1).

Proximal cool-water carbonate sediments originating in temperate, marginal, marine environments limit the of thin but laterally extensive shelf carbonate deposits. The location of these sediments is important for delineating the marginal facies of a shelf sequence. The unique morphology and composition of these sediments can be a valuable tool in limiting the lateral extent of temperate shelf carbonates, especially the Cainozoic limestones of southern Australia and New Zealand. Backstepping carbonate mud deposition within the embayments occurring along these margins can indicate the full onset of HST (highstand systems tract) conditions and give an indication of sea-level height at the time of maximum flooding surface (MFS). Further evidence of MFS can be verified when the marine muds are related to beach deposits, ie. from the tidal and supra tidal environments. The morphology and composition of these marginal marine sediments are only sparsely represented in the literature Those reported are usually associated with significant terrestrial deposition (Alexandersson, 1979; Farrow et al, 1984; Nelson et al, 1988; Reeckmann, 1988).

The Tertiary cool-water limestones, described from sedimentary basins occurring along the southern of Australia primarily have been assigned lithologies of mid to outer shelf facies (James and Bone, 1991; James and Bone, 1992; James et al 1993). James and Bone (2000) assign a high energy, shallow water regime to mixed siliceous carbonates in the St Vincent Basin, although these sediments

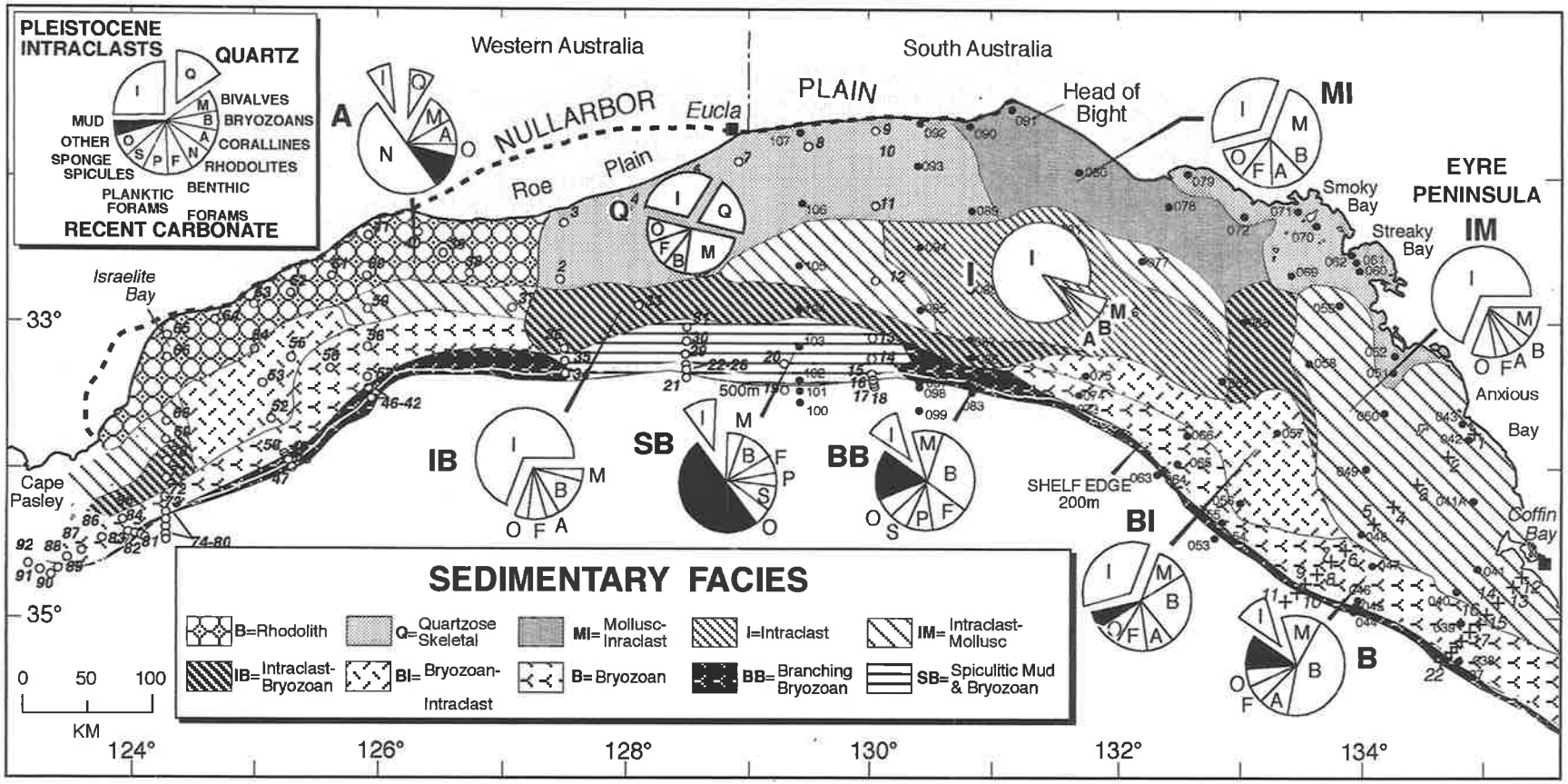



Figure 1.3 Distribution of cool-water carbonate lithofacies on the shelf of the Great Australian Bight. Numbers locate sediment sampling points collected on three separate cruises to the GAB region. 200m and 500m isobaths highlighted in grey. James (2001)

contain significant terrigenous material. Overlying marls and spiculites in this sequence have been deposited in a warm water setting. Shallow water or near-shore spongolite limestone facies are described from near Norseman in southern Western Australia (Clarke et al 1996

The lithofacies described from Streaky Bay represent the modern marginal facies of a shelf sequence, which may be analogous to a significant portion of the southern cool-water carbonate margin of southern Australia.

## 1.3 AIMS OF THIS STUDY

**1.3.1** To determine the geochronology of the late Quaternary to the present day embayment and thereby establish the sedimentological framework.

**1.3.2** To ascertain and describe the sediments from Streaky Bay and thereby also provide a sedimentary facies analogue for the western Eyre Peninsula embayments.

**1.3.3** To determine and describe how biota with calcareous skeletons become carbonate sediments with the emphasis on the production of carbonate mud in the shallow cool-water carbonate setting.

# CHAPTER TWO

# GEOLOGICAL AND OCEANOGRAPHIC SETTING

## 2.1 INTRODUCTION

The characteristics of cool-water carbonates were developed by Lees and Buller (1972), when they synthesised information from 92 publications on grain types and environmental factors from continental shelves between 60°N and 60°S. Approximately one third of the areas covered in the publications were between latitudes 30°-60° North and South - the temperate regions. Nelson (1988) used modern shelf carbonates of New Zealand, to further refine the characteristics of cool-water carbonates by direct comparison with warm-water varieties (Figure 1.1)

Tropical carbonate shelf systems are characterised primarily by latitude ie. between 30° North and 30° South. They are usually situated on rimmed shelves and stable platforms with a mean bottom sea temperature above 23°C and saturated with respect to carbonate. Flora and fauna typical of these areas are calcareous green and red coralline algae, hermatypic corals, benthic foraminifera and molluscs. Skeletons are usually thick and the rate of shell production is high. Aragonite is the dominant carbonate mineralogy with micrite commonly derived from floral breakdown and inorganic precipitation leading to seabed lithification.

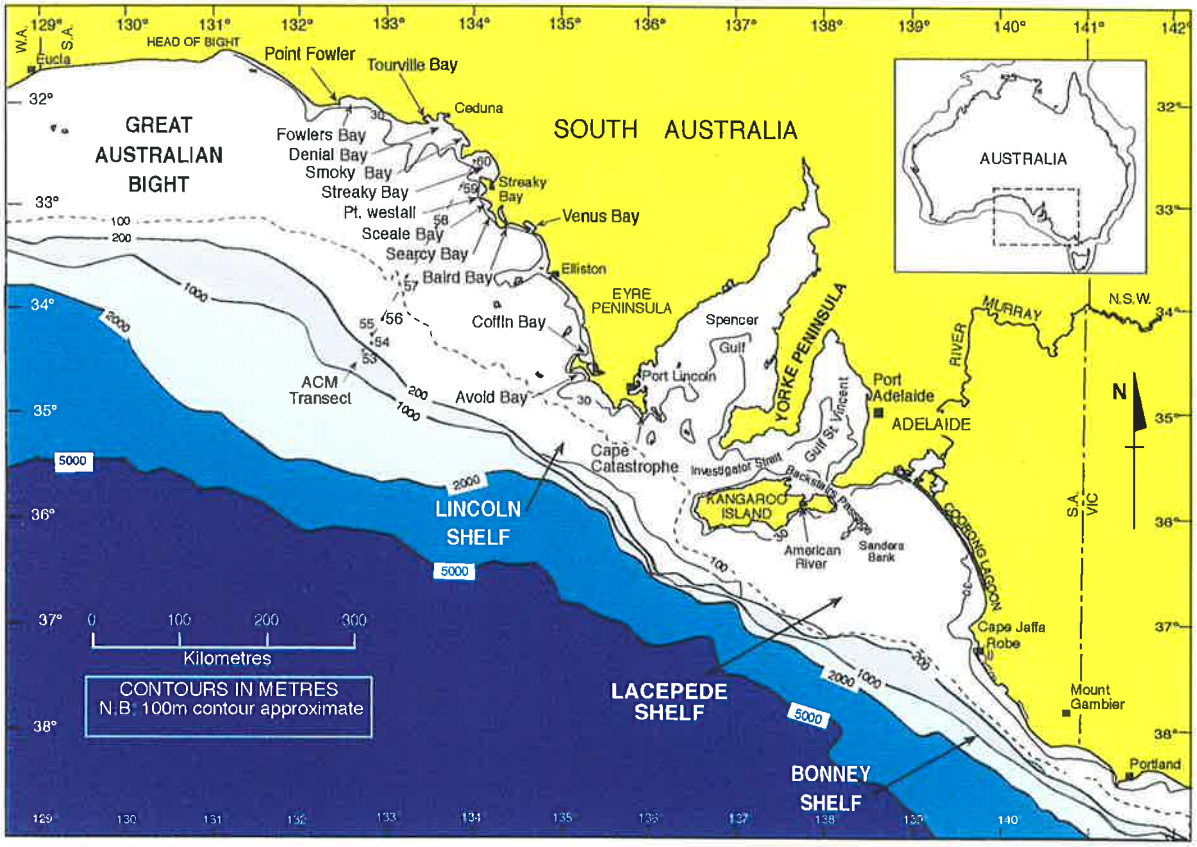



Figure 2.1 Principal localities on the southern margin and shelf of South Australia.

On the other hand non-tropical or cool-water carbonate systems are found polar-wards of the above latitudes on stable to unstable shelves and ramps with a mean bottom sea temperature below 23°C. The flora and fauna associated with these systems are coralline algae, coccolithophorids, bryozoans, molluscs (mainly as bivalves), benthic foraminifera, barnacles, echinoderms, serpulids and brachiopods. These groups typically have thinner shells and low to moderate rates of production compared to their tropical counterparts.

It was clear from these results that there were systematic differences in the organisms associated with tropical carbonates and carbonates formed in temperate waters. Terminology based on dominant biota in the two main carbonate types was created from this study. The term "chlorozoan" was proposed for tropical carbonates which was derived from the names of the principal organism groups present in the sediments ie. Chlorophyta and Zoantharia. For sediments derived from the temperate areas "foramol" was used because of the nearly ubiquitous presence of the foraminifers and molluscs. The inadequacy of the term foramol was also noted because of the large proportion of bryozoans, coralline algae, echinoids and barnacles which were present in the sediments. A series of terms were coined to accommodate the differing proportions of biota such as molechfor, bryomol, rhodalgal, choralgal etc. (Lees, 1975, Nelson, 1978, 1988; Carannante et al. 1988).

James (1997, p. 4) has since proposed a rationalisation of these terms under two major sediment associations and are summarised here: *"Heterozoan..... to represent associations of benthic carbonate particles whose producing organisms are* (not) *dependent on light but can incorporate red calcareous algae and Photozoan..... to represent benthic particle associations of skeletons of light dependent organisms, non skeletal particles ie ooids and peloids and can contain allochthonous particles from the Heterozoan association".*

### 2.1.1 Modern Cool-water Carbonate Sediments from the South Australian Margin

Sediments from the southern margin of Australia were first analysed by Matthew Flinders on his initial voyages of discovery along the "Unknown Coast" (Great Australian Bight) (Flinders, 1814). He reported that the inner shelf sea-floor sediment (Western Eyre Peninsula) was composed of fine to coarse shelly sands and isolated coralline sediments with scattered rocky substrate (see Frontispiece).

In recent times Conolly and von der Borch (1967) lead research cruises which sampled and described the carbonate sediments from the southern continental shelf in a series of cruises between 1960 and 1964. The results showed that surficial sediments of the shelf mainly consisted of coarse calcareous bioclastic sands. These sands were composed of "fragments of bryozoans, molluscs, foraminifera, echinoids, worm tubes, calcareous algae, sponges, pteropods, corals, crustaceans, asteroids, ostracodes and worn or unidentifiable calcareous lumps and reworked beachrock" (Conolly and von der Borch,

1967, p 198). Bryozoans, molluscs and foraminifers were found to be abundant in most samples although the molluscan fraction was significantly reduced in samples from the outer shelf. They also describe a range of grains ie. 'pale brown, polished and unidentifiable calcareous sands' being present across the shelf which correlates with relict and intraclastic sediments described on the Lacepede and 'Lincoln' (sensu, James et al., 1997) Shelves (James et al., 1992, 1997, 2001) and lower Spencer Gulf (Fuller et al., 1994) (Figure 2.1). Mud is rare, although it can be common locally with low to high magnesium calcite being common on the shelf.

Broad scale biolithofacies based on the distribution of bryozoan zooarial habit were interpreted for the shelf-break area from south-west Western Australia to south-eastern Victoria and eastern Tasmania (Wass et al., 1970). The refinement of the broad lithofacies of the southern continental shelf has continued since this time (Blom, 1988; Bone and James, 1993; Boreen et al., 1993; Cann and Clarke, 1993; Collins, 1988, 1997; Fuller et al., 1994; Ferland, 1997; Gostin et al., 1984; Harris, 1994; James and von der Borch, 1991; James et al., 1992, 1994, 1997; von der Borch and Hughes-Clarke, 1993; Rao, 1996 amongst others). The delineation of sedimentary facies of the Great Australian Bight (GAB) is presented by James et al. (2001), which is the culmination of three sampling cruises to the region (Figure 1.3)

The modern carbonates of this shelf have been closely correlated with Cainozoic shelf carbonates of the Bass, Otway, St Vincent, Murray, Eucla and Perth Basins, which occur along southern Australia (Conolly and von der Borch, 1967; Reeckmann, 1988; Boreen and James, 1995; Clarke et al., 1996; James and Bone, 1989, 1991; James et al., 1993; Shubber et al., 1996; Nicolaides,1995; Nicolaides and Wallace, 1997; Nelson and James, 2000) (Figure 1.2).

The sediments of shallow-water tidally influenced embayments represent sediment types that sensitively reflect a range of Holocene environments of deposition and in some areas they also record evidence of sea-level changes which have occurred, particularly from the late Pleistocene to the present (Figure 2.1). Particular focus has been on the upper reaches of Gulf St. Vincent and Spencer Gulf in South Australia (Figure southern margin) (Belperio et al., 1984; Belperio et al., 1988; Burne, 1982; Cann and Gostin, 1985; Cann et al., 1993; Gostin et al., 1988; Hails et al., 1984, 1983). Other smaller low energy embayments which have been briefly examined along the coast of South Australia include Tourville Bay (Lablack, 1985); Coffin Bay (Freeman, 1985); Pelican Lagoon (Millikan, 1994); American River (Wirtz, 1994); and Baird Bay (Hill, 1994).

## 2.2 REGIONAL GEOLOGY

The Streaky Bay region is composed of two distinct geological regimes. A Proterozoic basement that consists of felsic and minor basic intrusives and a relatively thin cover of Pleistocene aeolianites and shallow marine bioclastics.

The Streaky Bay region is centrally located marginal to the Gawler Craton (Figure 2.2), which is an extensive area of crystalline basement consisting of rocks from three major tectonic Precambrian cycles in the late Archaean, Palaeoproterozoic and Mesoproterozoic (Fanning et al., 1983, Rankin and Flint, 1991). The Lincoln Intrusive Complex was emplaced during the Palaeoproterozoic Kimban Orogeny. The emplacement of the Hiltaba Suite (acid intrusives) postdates the Kimban Orogeny (Figure 2.2). Extensive volcanics and fluvial sedimentation occurred during the Mesoproterozoic after which a change of tectonism led to the cratonisation of the Eyre Peninsula region. The tectonic events that lead to the Cambrian Delamerian Orogeny and the folding of the Adelaide Geosyncline did not affect the Eyre Peninsula apart from the easterly area around Port Augusta (Parker et al., 1983).

Polda Basin is a narrow east-west graben situated midway up the west coast of Eyre Peninsula. It contains Cambrian red beds, evaporites and subsurface Permian glacial beds. Jurassic coal-bearing formations (Polda Formation) are found in the upper sequences of the basin. Palaeozoic or Mesozoic sediments do not occur elsewhere on the Eyre Peninsula (Rankin and Flint, 1991).

A variably thin layer of diverse alluvial sediments was deposited over the Eyre Peninsula during the Cainozoic, with marine sands and limestones deposited in small embayments at the margins. Over the last one million years, extensive aeolian dune sands with regular pedogenic calcrete layers (Bridgewater Formation) and isolated marine sediments (Glanville Formation) have been deposited in a wide marginal belt along the South Australian coast. The aeolianite layers range from a few metres thick inland to 90 metres in the coastal areas (Parker et al., 1985, Wilson, 1991).

The Holocene St. Kilda Formation is present as a range of diverse sediments from skeletal sands of prograding spits, cheniers and marginal dune systems (Figure 2.3); organic subtidal to intertidal sandflats; shelly muds of mangrove woodlands and samphire flats to the calcareous and gypsiferous muds of the supra-extratidal flats in the distal areas of restricted embayments (Rankin and Flint, 1988).

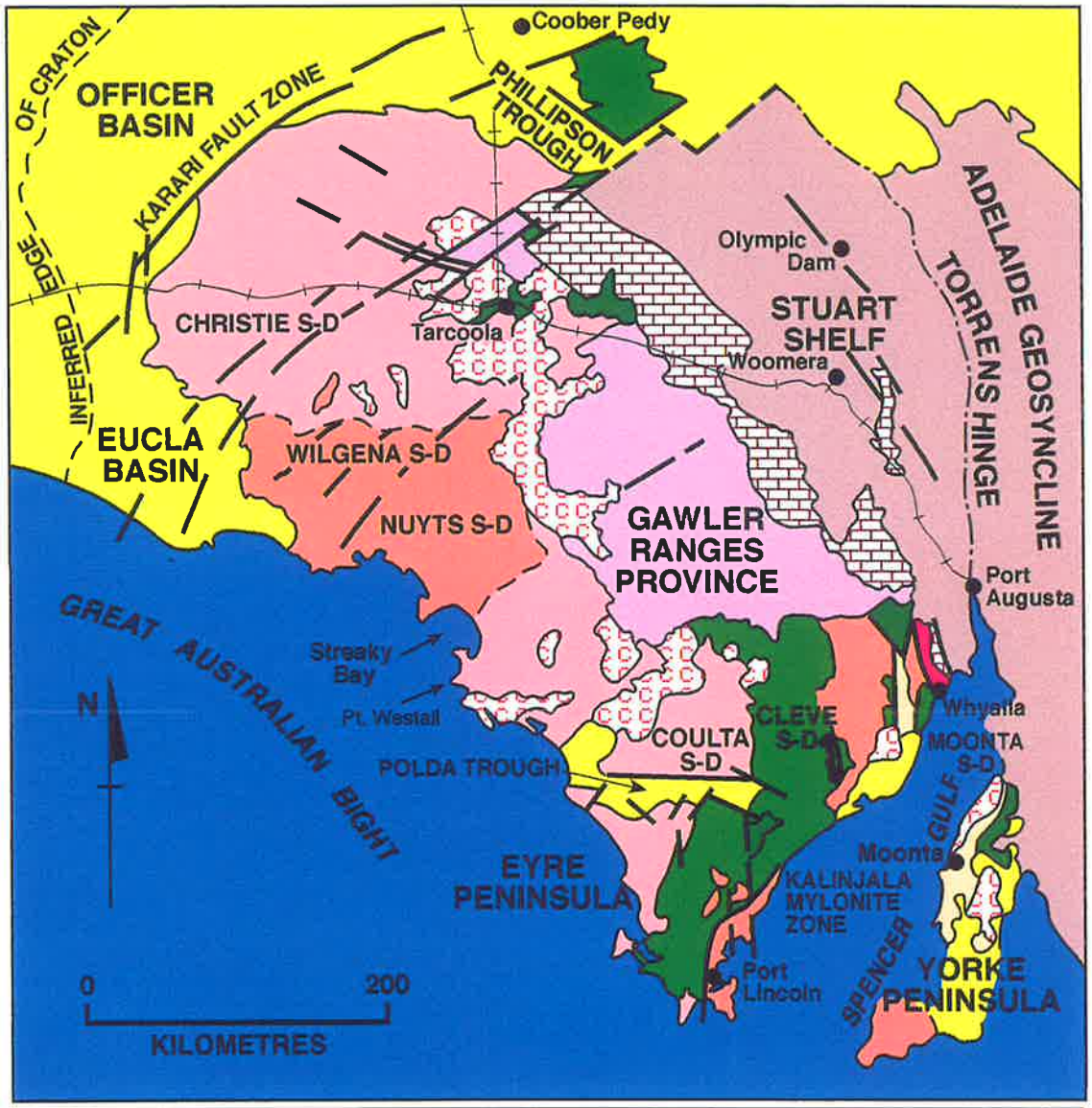



Figure 2.2 Geology and Tectonic framework of the Eyre and York Peninsulas, South Australia

Modified after Parker et al. 1985, 1993

**Legend**

PHANEROZOIC
- Basin sediments
- Adelaidean sediments
- Pandurra Fm
- Hiltaba Suite
- Lincoln Complex

**YORKE PENINSULA**

PROTEROZOIC
- Windearah Metasiltstone/ Willamulka Volcanics
- Moonta Porphyry/ Doora Schist

**EYRE PENINSULA/ NORTHWEST CRATON**

- Gawler Range Volcanics
- Tarcoola Fm/ Corunna Conglomerates
- Moonabie Fm/ McGregor Volcanics
- Myola Volcanics/ Broadview Schist
- Hutchison Group

ARCHAEAN
- Miltalie Gneiss
- Mulgathing Complex/ Sleaford Complex

- Fault

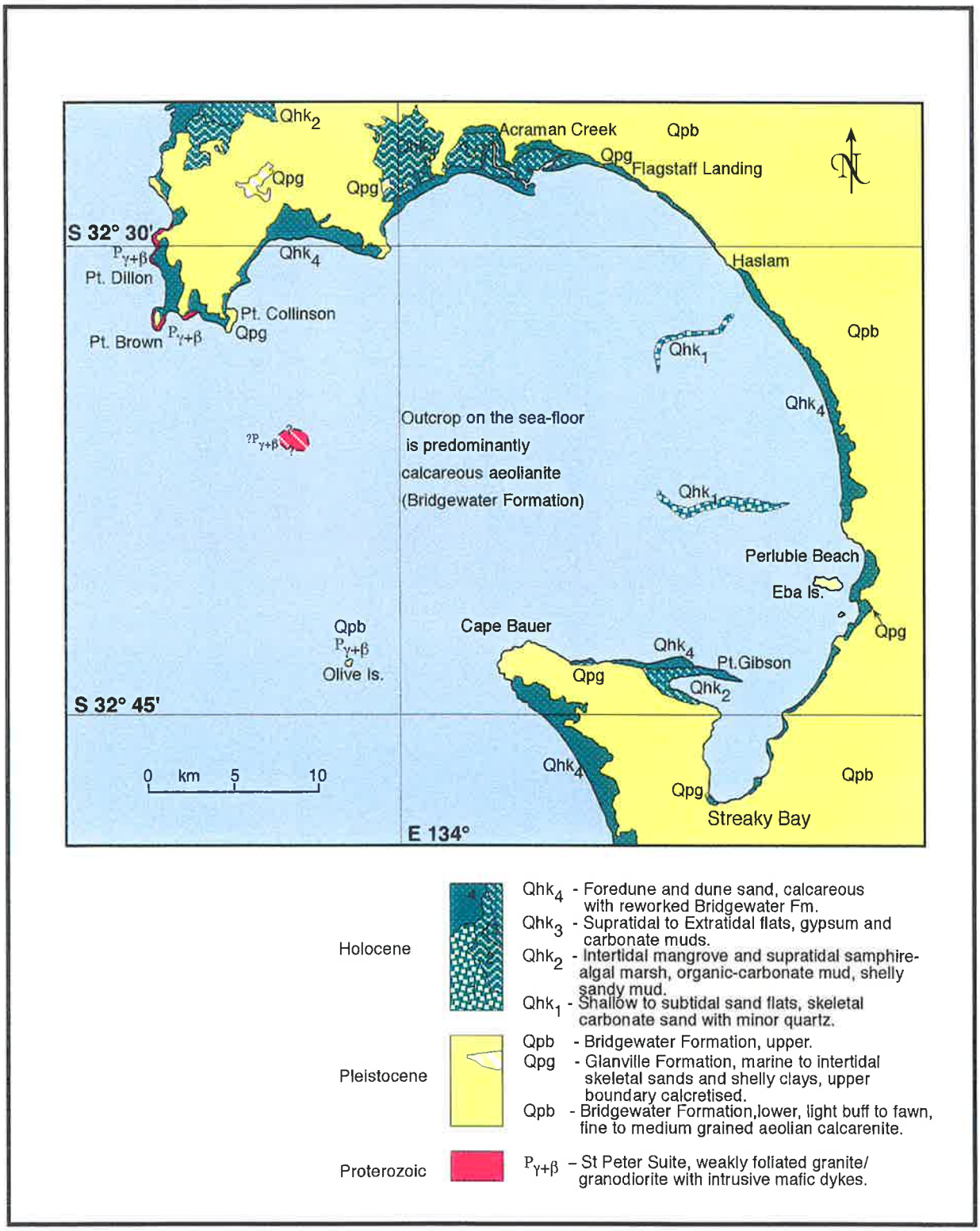



Figure 2.3 Geology of the Streaky Bay area. (After Rankin and Flint, 1991)
The rocks are calceous aeolianite and calcrete where outcrop occurs on the sea-floor.
A sea-floor high, South of Pt. Collinson, is most probably an outcrop of Proterozoic intrusive.

## 2.3 GEOLOGY OF STREAKY BAY

### 2.3.1 PROTEROZOIC OUTCROP

Rocks of the early Palaeoproterozoic St. Peter Suite (Lincoln Complex) and Mesoproterozoic Hitilba Suite outcrop around the margins of Streaky Bay. Fine to medium grained moderately foliated granite to adamellite with basic intrusions (Lincoln Complex) occurs on the northern shores of the bay at Points Brown and Dillon (Figure 2.3). Rocks of the Hitilba Suite are represented by medium to coarse-grained porphyritic orthoclase granite at the mouth of Streaky Bay on Olive Island (Rankin and Flint, 1991). Rocks of the St. Peter Suite occur to the south at Smooth Pool and Granite Rock at Point Westall and are weakly foliated granodiorite to porphyritic granite and medium to coarse grained granite gneiss (Figure 2.2) (Dove, 1997).

### 2.3.2 PLEISTOCENE OUTCROP

Pleistocene sediments outcrop over a wide area of the Eyre Peninsula. Specifically they comprise the extensive cliff-lines of coastal western Eyre Peninsula to the North and South of the entrance to Streaky Bay and the low cliff-lines flanking the bay itself (Bridgewater Formation). There are also isolated coeval deposits of low-lying marine bioclastic sands (Glanville Formation) flanking various parts of the bay (Figure 2.3).

#### 2.3.2.1 Bridgewater Formation

Calcareous aeolianites of the Bridgewater Formation outcrop extensively over a wide area of the Streaky Bay region and along much of the South coast of South Australia. Locally they form high (to 60 m) cliffs to the North and South of the entrance to the bay and are also present around the margins of the bay, with thicknesses from several to a few tens of metres. Carbonate soil and calcrete horizons are intercalated throughout the Bridgewater Formation indicating periods of arrested sedimentation resulting in pedogenesis and erosion (Rankin and Flint, 1985). These intercalations correlate closely with Pleistocene glacial sea-level lowstand periods. Most sedimentation occurred during interglacial periods, probably at the highest sea-level incursion - MFS (maximum flooding surface-; approximately the present sea-level) eroding the foredune areas and supplying sediment to the shallow embayments and remobilising existing dune fields (Wilson, 1991).

#### 2.3.2.2 Glanville Formation

The Glanville Formation was first described by Howchin (1888) in an excavation at the Glanville dock, Port Adelaide. A second section of marine sediment from this late Pleistocene transgression was exposed in an excavation at Dry Creek (near Port Adelaide). The section included *Ostrea angasi, Arca (Anadara) trapezia* and abundant foraminifera all of which have shallow marine habitats (Howchin, 1912). More recently, a new exposed reference section of the Glanville Formation has

resulted from quarrying operations near Dry Creek (Figure 2.1). This section also contains skeletal remains of tropical to semi-tropical fauna, which no longer inhabit the sea off South Australia (Cann, 1978).

The Glanville Formation was deposited during the late Pleistocene. It interfingers with the upper part of the Bridgewater formation. It outcrops at Point Collinson, the Acraman Creek/Flagstaff Landing area, Perlubie Beach, adjacent Streaky Bay township and West of Point Gibson (ref. Qpg in Figure 2.3). The formation is the marine equivalent of the upper section of the Bridgewater Formation and contains richly fossiliferous shelly sands that were deposited in subtidal to intertidal lagoonal and restricted environments (Cann, 1978, Wilson, 1991).

The Glanville formation is characterised by the fauna *Anadara trapezia, Pinctada carhariarium, Matra eximia, Euplica bidentata* and the foraminifer *Marginopera vertebralis* (Ludbrook, 1978). Locally, the coral *Goniopora somaliensis*, has been found with some of the above fauna in the Acraman Creek area. The age of the Glanville Formation has been variously dated from 90 ka. to 125 ka. using amino acid racemisation and U/Th discontinuous series dating, (Belperio et al., 1984;

Murray-Wallace et al., 1988; Wilson, 1991; Daniel et al., 1998) and was deposited during an interglacial period (Isotope Stage 5) when the relative sea-level was approximately 2m above the present level (Belperio, 1988, Daniel et al., 1998).

### 2.3.3 Local Holocene Geology

#### 2.3.3.1 St. Kilda Formation.

The Holocene St. Kilda Formation at Streaky Bay occurs in a range of depositional environments and the range of the occurrence is briefly described. Fine to coarse bioclastic sands are found in the areas of the North Bank, South Sand and the marginal dune systems flanking the bay. Accumulations of gravelly very coarse sands to fine sandy muds are variably distributed across the sea-floor . Organic shelly muds are found in the subtidal/ intertidal sandflats, mangrove woodlands and samphire flats which occur at Acraman Creek and the mangrove woodlands and restricted samphire flats occurring in the Point Gibson embayment. The supratidal salina to the immediate West of the Acraman Creek estuary is composed of gypsiferous and minor calcareous muds (Figure 2.3).

Sediments of the St. Kilda formation yield $^{14}C$ ages of 6800 years B.P. (Belperio et al., 1988). The measurements were carried out on fossil subtidal *Posidonia* sea-grass in sediments from Tourville Bay, near Ceduna. It appears from this determination that sediment accumulation and progradation was relatively rapid and mostly occurring within the first 2000 years of the Holocene highstand (Belperio et al., 1988).

## 2.4 LOCATION OF THE STUDY AREA.

Streaky Bay is located 720 km from Adelaide, approximately midway along the western coast of the Eyre Peninsula, South Australia. The embayment is approximately 37 km wide by 26 km long (Figure 2.4) with water depths ranging from 40 m in the entrance to low tide exposure on the elongate sand banks.

The embayment faces the Southern Ocean and is constantly subject to major wave action from the South and Southwest. The slope of the sea-floor is 0.03° seaward of the entrance area, where the water depth increases from ~36 m to ~42 m over a distance of 11 km. The water depth varies from 35 to 40 m at the mouth of the bay with patchy gravel sands on a rocky substrate with a 0.19° slope. There is a low angle (0.05°) terrace shorewards of the entrance, where the water depth ranges from 12 to 16 m. The sea-floor in this area is mostly rocky with patches of coarse to fine sand. The inner central section of the bay contains a channelled tidal delta complex including the Warburton, Dashwood and South Channels (Figure 2.4). The channels are separated by two large sigmoidal linear sand banks, the North Bank and South Sand (~7 km and ~9 km long respectively) (Figures 2.5, 2.6). The banks, which are exposed at low tide, are perpendicular to the beach. Shoreward of the tidal deltas are deeper water shallow basinal areas termed inner marginal basins, which are between and to either side of the linear banks. The basins are elongate and subparallel to the eastern shore. They occur in three discrete areas and have water depths up to 15 m. There is a comparatively sharp rise of 0.31° landwards from the basins to the beach, which in turn has a steeply rising beach. The relatively narrow beaches are flanked by stabilised to blown-out dune systems with isolated low cliff lines of Pleistocene age (Figure 2.7).

## 2.5 REGIONAL GEOMORPHOLOGY

Streaky Bay is the largest semi-protected bay on the West coast of the Eyre Peninsula. The bay is partially sheltered from energetic waves by substantial headlands to the North and South of the mouth of the bay. Olive Island and associated islands, together with the shallow nearshore tidal deltas lead to considerable attenuation and diminishment of wave energy at the shore-face (Short et al. '86)

The bay was formed by rising sea level and wave action breaching the high Pleistocene dune fields of the lower Bridgewater Formation (aeolianites from the lower to mid Pleistocene) creating a large embayment in the back dune corridor. This corridor is present, particularly along the upper west coast of the Eyre Peninsula, behind the high lithified coastal dune systems (Twidale and Campbell, 1985; Wilson, 1991). The aeolianitic sediments were concentrated in the region of the present coastline by

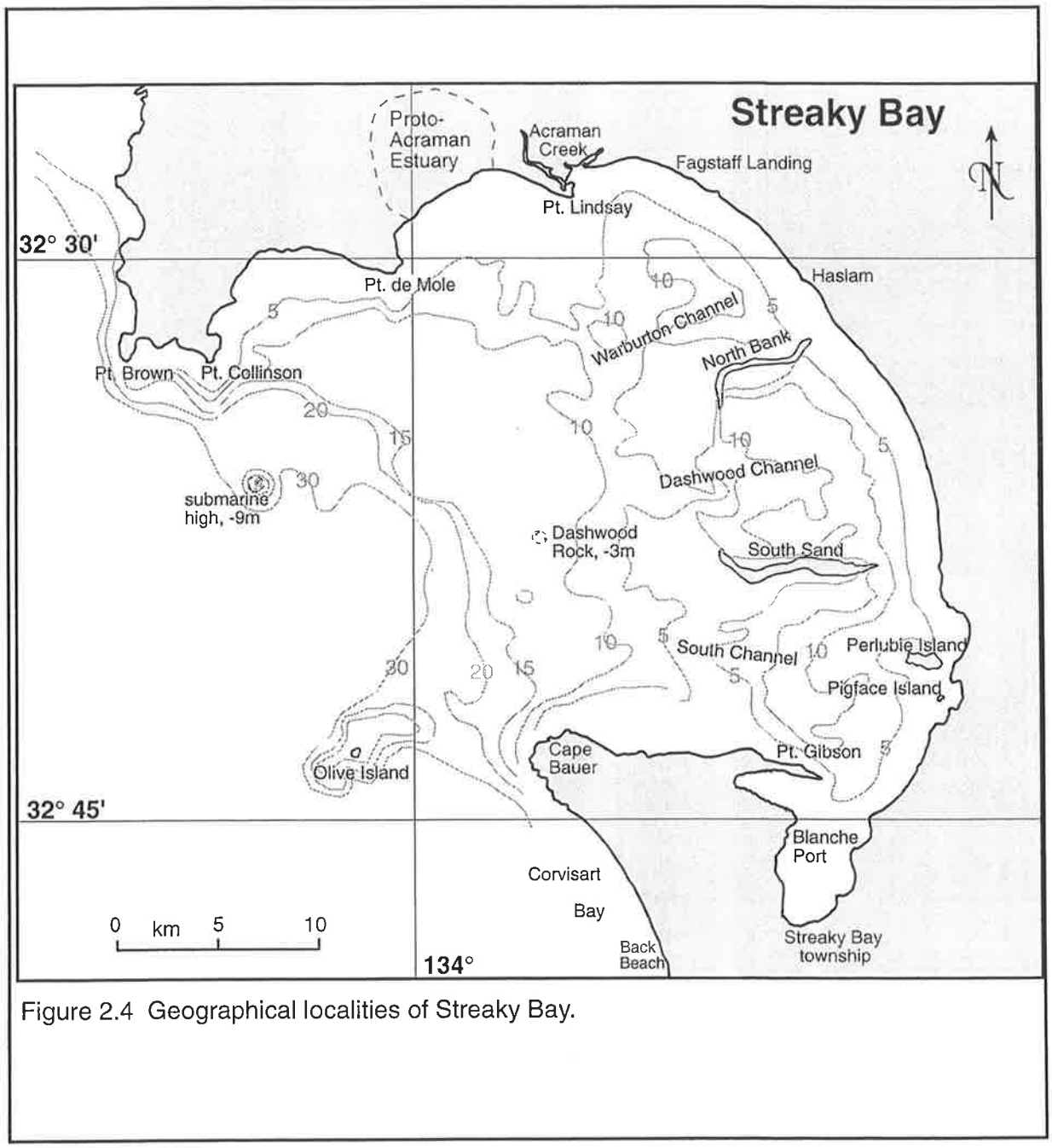



Figure 2.4 Geographical localities of Streaky Bay.




Figure 2.5 Oblique aerial view of Streaky Bay looking southwest across the blowout dunes of the eastern shoreline past the South Sand to Point Gibson (left) and Cape Bauer (far right). Blanche Port is the sheltered embayment to south of Point Gibson. Distance from South Sand to the southern shore approximately 11 km.

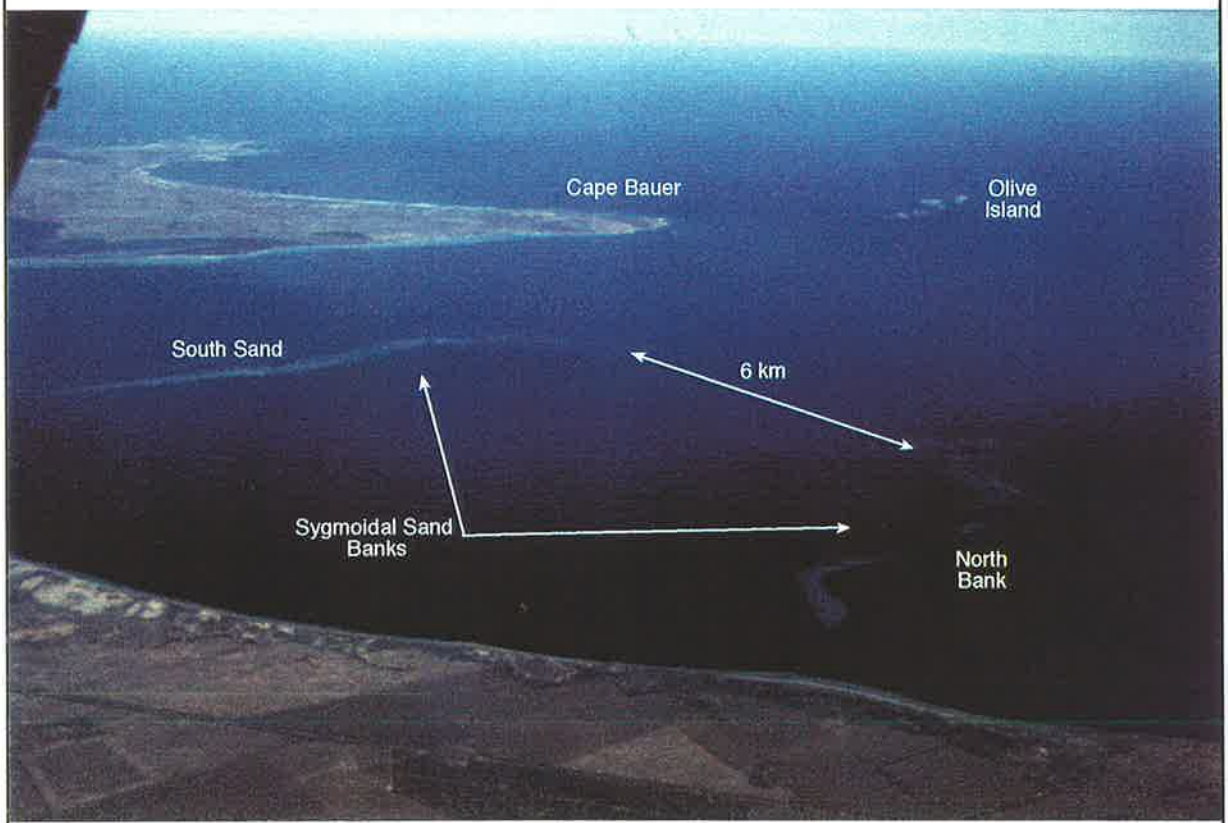



Figure 2.6 Oblique aerial view of central Streaky Bay showing the sygmoidal shape of the two sand bodies (South Sand and North Bank). Olive Island about 4.5 km off Cape Bauerand Corvisart Bay to the south of Cape Bauer. The seaward extremities of the sand bodies are approx. 6 km apart and the South Sand is approx. 9 km long.




Figure 2.7 Aerial view of the Acraman Creek estuary and Pt. Lindsay with the Acraman salina inland from Pt. De Mole. Pt. Collinson and Pt. Brown in the distance (Pt. De Mole to Pt. Brown, 14 km). Flagstaff Landing is approximately 1.5 km along the coast off the lower left of the photo.

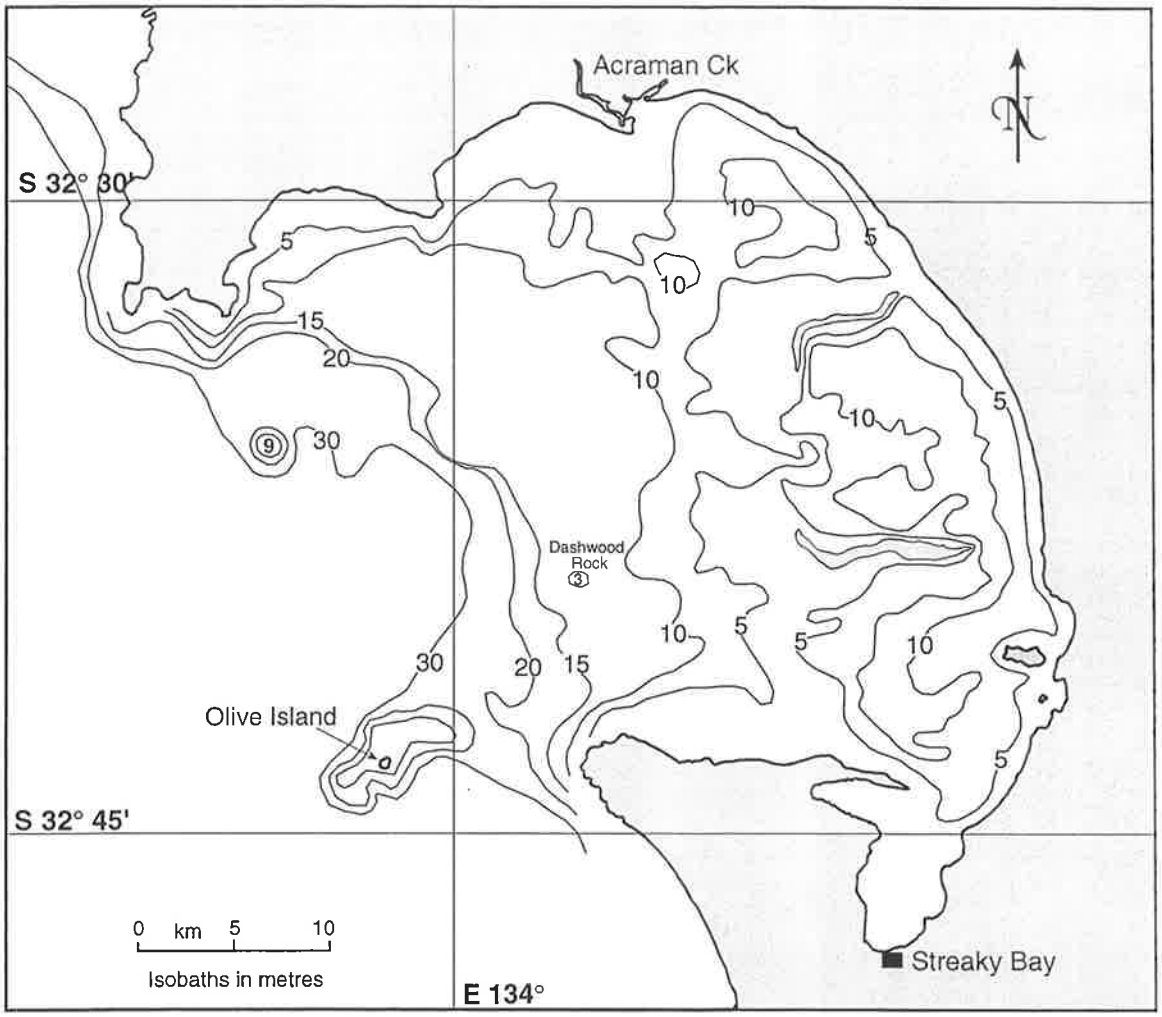



Figure 2.8 Bathymetry of Streaky Bay, depths from Admiralty sheet Aus 121 and verified with Raytheon depth sounder during sampling operations.

Pleistocene sea-level rises which rose to within -40m to+2 m of the present sea-level (Wilson, 1991). Pleistocene sediments in the bay were then supplied by migrating bottom sediments and low sea-level barrier/ dune systems (Short et al. 1986).

Substantial sediment has interpreted to have been supplied from the deeper shelf waters (Wilson, 1991) and from around the headlands to create three main sediment spits: two at Acraman Creek to the north (Point Lindsay and the adjacent unnamed spit) and Point Gibson on the southern side of the bay (Figure 2.4). Extensive transverse tidal delta deposits have also accumulated across the floor of Streaky Bay resulting in large scale shoaling across the inner face of the bay with two major sand banks up to nine kilometres in length orientated perpendicular to the shoreline. The sea-floor is dominated by seagrass within these inner areas of low wave energy where the sedimentation is relatively low (Short et al. 1986).

Flood tide deposits have filled much of the bay since the present sea-level highstand limiting Holocene dune transgression to present sites around the bay. Reactivation of the dune fields has occurred with land clearing and grazing taking place in areas since the 1920's eg. Flagstaff Landing and Perlubie Beach areas. Further supply of sediment during the Holocene is derived from erosion of the headland cliffs of calcareous aeolianite (Bridgewater Formation). Erosion at the base of the cliffs at the high water mark causes undercutting and eventual collapse of the overlying cliff . Chemical activity from salt spray and aerosols also etches the cliffs, producing jagged, scalloped surfaces and producing new mobile sediment (Short et al. 1986).

### 2.5.1 GEOMORPHOLOGY OF STREAKY BAY

The coastline of the bay is divided into three main geomorphological provinces based on the wave energy expended at beach and the presence of aeolianite outcropping as low cliffs or as a low tide wave-cut platform. Descriptions of the coastline are a result of research by Short et al. (1986) and this study.

#### 2.5.1.1 Streaky Bay Shoreline, Southern Margin

Aeolianite cliffs ranging from 35m (outer) to 6m (inner) are present along approximately one third of the length of the southern margin of Streaky Bay (Cape Bauer to Point Gibson) (Figure 2.4). The remainder consists of narrow beaches that extend to the end of the recurved spit, Point Gibson. The sediment is slowly moving eastward via shallow water sand waves as a series of minor spits. There are at least five episodes of spit development along Point Gibson, during the Holocene, with significant areas of accretion and erosion being measured from 1945 to 1979 (Short et al., 1986).

These periods of accretion and erosion were observed in a series of early aerial photographs taken of the coastline. Blanche Port, at the southern end of Streaky Bay, is a low energy bay protected by the Point Gibson spit. Blanche Port is mostly flanked by low relief cliffs of aeolianite of the Bridgewater Formation and encompasses an extensive mangrove woodland in the lee of Point Gibson (Figure 2.4).

#### 2.5.1.2 Streaky Bay Shoreline, Eastern Margin

The eastern margin of Streaky Bay runs from adjacent Point Gibson to Flagstaff Landing (Figure 2.4). It is subject to attenuated low energy southwest swells, and wind waves generated from the dominant west to south west winds (Short et al '86). The shoreline is isolated from sediment supply via the entrance of the bay by the deep marginal basins (Figure 2.8). These factors have led to only minor Holocene sedimentation along the margin, mostly restricted to the development of beach ridges and samphire flats in the Pigface to Eba Island area. Minor dune accretion has occurred along the southern part of the section. The areas where the dunes are mobile have been destabilised by grazing up to the beach dune margin. East of Pigface Island, the inner most foredune ridge has been dated at 3260 ±90 years showing Holocene progradation of approximately half of a kilometre since that time (Short et al 1986).

The beaches of the southern section of the shoreline are of a reflective type indicating a low energy environment with medium to coarse sand. The northerly beaches are of a low intermediate type indicating low to moderate energy with medium to fine sand. Occasional low relief Pleistocene aeolianite cliffs outcrop around the eastern margin of the bay.

#### 2.5.1.3 Streaky Bay Shoreline, Northern Margin

The northern section of Streaky Bay (Flagstaff Landing to Point Brown (Figure 2.4) is more exposed to higher energy southerly waves, either derived from the attenuated ocean swells or the wind generated south to south westerly waves. As with the southern margin, this section is the site of major sediment deposition in the form of multiple recurved spits and beach ridges (Fig 2.3). Two extensive recurved spit systems, ~4.5 km and ~5 km in length, to the east of Point de Mole have resulted in occluding an early Holocene bay (Proto Acraman Estuary) and creating an area (Acraman Creek) of extensive mangrove flats. Acraman Creek, behind Point Lindsay, is an active barrier/ spit enclosed estuary dominated by tidal flows with little or no fluvial input. Dating carried out by Short et al., (1986) on the innermost barrier ridge to the north of the tip of Point Lindsay.(Figure 2.4) show that intertidal deposits began accumulating in this area around 5850±90 yr BP.

The relatively steep beaches to the west of Point de Mole are more reflective to intermediate than the beaches on the other sections. Separating these beaches are the low aeolianite headlands of Point de Mole, Point Collinson and Point Brown. Proterozoic basement rocks are exposed at the base of the

cliffs at Point Brown and the adjacent minor headland to the east (Figure 2.7). The relatively steeper beaches between Point Collinson and Point Brown are result of significant quartz in the beach sands which are derived from these rocks.

## 2.6 REGIONAL OCEANOGRAPHY

Streaky Bay is situated on the eastern coast of the GAB, where the shelf is approximately 250 km wide. The area is dominated by a high energy, west-coast swell environment (Davies, 1980). Swells are predominantly from the southwest, being generated by the easterly movement of low-pressure systems, including gale force winds in the winter months.

Ocean currents in the GAB vary throughout the year depending on the weather systems and the rate of warming of the GAB waters. The inner GAB currents generally flow in an easterly direction due to forcing from the westerly anticyclonic/ cyclonic weather systems (Herzfeld, 1996, 1997, Herzfeld and Tomczak, 1997).

The 'Great Australian Bight Current' (informal name, James at al., 1997) moves eastwards across the shelf edge in an anticyclonic gyre during summer and autumn as the water mass warms up in the western GAB region. The anticyclonic gyre is formed by wind stress forcing from northerly and north-westerly winds. The gyre is advected easterly, by the eastward flowing arm of the gyre, to form a warm current across the shelf. The current is intensified in the eastern GAB by the upwelling Flinders Current (Bye, 1972, Herzfeld, 1996).

The Leeuwin Current flows into the western Bight during the winter months in the vicinity of the shelf break, where it connects with the GAB shelf water to form a band of warm water across the central and western shelf region of Australia. During this period it attains high velocities and high energy and has been recorded as a homogeneous water column. At other times of the year the Leeuwin Current weakens along the shelf break to the centre of the Bight (130°E ; Figure 2.1). The weakening of the current is a result of intermixing with cooler oceanic waters and the dispersal of energy into large gyres (up to 150 km in diameter) along the west and south of Australia (Cresswell, 1991, 1993; Herzfeld, 1996).

The Leeuwin Current has its origin in the area around Indonesia and the North West Shelf of Australia and is driven down the coast of Western Australia to Cape Leeuwin by a high steric (thermohaline) gradient. Sea level changes of up to 40 cm have been recorded on the North West Shelf in March and during May and June, off south-west Australia. The current appears to be initiated by the flow of

Pacific Ocean waters through the Indonesian Archipelago to the Indian Ocean -the Indonesian Gateway (Cresswell, 1993) and the heating of the shallow waters on the Northwest shelf (Cresswell, 1991). Seasonal variations in strength are a result of wind stress rather than differences in the steric gradient (Smith et al. 1991).

The Flinders Current, which appears as an upwelling in the eastern GAB during late summer and autumn months, has its origin south of Tasmania where it is possibly the result of an anticyclonic gyre of the East Australian Current flowing westwards (Bye, 1972). The current occurs at between 500 and 1800 m water depth with a maximum velocity at 900 m water depth. It is characterised by a lower salinity and temperature (<34.4‰, <8.5°C) from that of the surrounding water (Bye, 1972). The warm Bight current is found to respond to the momentum of the Flinders Current, which in turn is controlled by sea temperature stratification and sea floor topography where the upwelling occurs on the eastern Bight shelf (Herzfeld, 1996). The Flinders Current is strongest where it flows onto shelf areas, which have significantly higher topographical gradients and stratified water layers that maintains a steep north-south temperature gradient (Bye 1972). This in turn gives rise to a more extensive current (GAB Current), in terms of depth and area, flowing out of the eastern GAB (Herzfeld, 1996).

Wave movement along the Eyre coast, as observed by satellite and recorded by Chelton et al. (1981), shows significant deepwater wave heights of > 5.5 m with periods of 15 sec. Wave heights of < 2 m occurred only 2% of the time with 40% over 5 m. The observations of Chelton et al. (1981) were recorded over a three month period (July- Sept 1978). As this was winter, the peaks recorded are assumed to be greater than they would be in the summer period, once the cyclonic activity had migrated south of the continent (Chelton et al., 1981).

Wave maximum peaks of > 10 m (June) with occasional waves of > 5 m were recorded by Provis and Steedman (1985) at seven wave rider stations placed off-shore at Streaky Bay in water depths from 26 m (Stn 7) to 1150 m (Stn 1) over a 240 km transect. A 50% decrease in wave height and a 75% decrease in wave energy were observed between the station at 1150 m and the station just inside Streaky Bay at 26 m. The frequency of the waves remained the same between stations 1 and 7, with an average period of 15 sec. The wave velocity was observed to be approximately 24 $ms^{-1}$ with a wavelength of 360 m. This high energy-long wavelength swell can interact with sediment to a depth of 180 m.

As the western GAB water warms up and begins to move south easterly towards the shelf edge, gyres are formed in the central and eastern Bight area which are mixed with the cooler distal extents of the Flinders current moving to replace this warmer Bight water (Herzfeld 1996, 1997). The currents that

are important in the vicinity of Streaky Bay are the westward coastal flowing anticyclonic gyre of the Bight current and the eastward surface current due to the prevailing weather patterns.

### 2.6.1 OCEANOGRAPHY OF STREAKY BAY

The weather pattern of the GAB consists of easterly moving cyclonic/anticyclonic activity and hence generates a swell environment that is predominantly southwest to westerly. The Streaky Bay region, along with most of the West Coast can experience significantly high storm surges formed by barometric pressure differentials and weather changes caused by local wind conditions (Provis and Radok, 1979). The surface currents generated by the prevailing weather conditions tend to nullify its effects of the weak westerly moving Flinders current (< 0.13 $ms^{-1}$) in the region. The current is more significant in deeper offshore waters than the immediate coastal regions as a result of these conditions (Bye, 1972; Herzfeld, 1996).

Current velocities have been measured using current meters in the central tidal delta area of Streaky Bay, over a five day interval. One of the current meters was placed in the mouth of the channel, another was situated shorewards, at the edge of the cental basin (Figure 2.11) and both were located in ~10 m of water (Figure 2.9a and b) (Clarke, 1994). Maximum velocities were observed on alternate flood tides with the other flood tide rates similar to average ebb tide currents. Current velocities at the mouth of the central tidal delta were measured at rates up to 0.46 $ms^{-1}$ and averaging 0.30 $ms^{-1}$. Shorewards, at the second site, rates averaged 0.07 $ms^{-1}$ and peaked at 0.16 $ms^{-1}$. This disparity in current velocities is reflected in the distance between the sand banks at each site, ie. 6.3 km and 9.3 km. The net water movement (Figure 2.9a and 2.9b) was plotted from the results obtained from the current meters. Transport stream lines (Figure 2.10b) and residual velocities (Figure 2.10a), due to tidal forcing in the bay, were plotted and compared with the current data recorded at the two stations. These components were plotted using the FLOWC computer programme (Bye and Ng 1994). The computed results were less than (~0.118 $cm^{-1}$ sec) the observed residual velocities recorded at the current meter (~2.5 $cm^{-1}$ sec). The primary sites of sediment deposition can be correlated with the major patterns of water movement ie. the spits, sand shoals and sand banks.

Salinities were recorded by Clarke (1994) on alternate stations along the transects on which the present author collected the sediment samples for this study. Readings were recorded every half second so that surface (Figure 2.11a) and bottom (Figure 2.11b) salinities and any salinity stratification would be recognised when the information was plotted (April 1994). Minor differences of up to +0.5 ‰ (+ is higher bottom salinity) were observed in the main bay (southern two inner basins) with surface salinities ranging from 36 ‰ in the outer bay to 38.75 ‰ in the southern area of Blanche Port (Clarke, 1994) (Figure 2.11a and b). The 1998 CSIRO RV Franklin cruise (03/98

Australian Coastal Margin) recorded surface salinities at three stations from 35.52 to 35.49‰ at the entrance to Streaky Bay. A CTD deployed at station SB 119 (ACM 62, CTD 31, 03/98) showed a salinity value near the sea-floor of 35.68‰ (James et al., Records of RV Franklin cruise, 03/98). Both sets of observations were taken in April, four years apart and show comparatively minor variation over this time.

Water temperature was monitored continuously over a five day period (April,1994) at a site on the sea-floor near the jetty at Streaky Bay township and was found to vary between 17.3°C and 13.9°C. Bottom temperatures in the main bay were found to be similar to Blanche Port with an average temperature of 16.2°C being recorded in the vicinity of the mouth of the tidal delta (the temperatures taken from the CTDs were not recorded in the thesis). Further temperatures have been recorded at the mouth of the bay, during the R V *Franklin* (03/98, ACM) cruise in April 1998, from 16.2 - 17.2° C on the surface to 15.8°C on the sea-floor (SB 119, ACM 062, CTD 31) (James et al., Records of RV Franklin cruise, 03/98).

Clarke (1994) concluded that by comparing surface and sae-floor salinity the overall current movement is counter-clockwise ie. it moves in from the southern approaches of the bay, is deflected northwards by the shallow sand sheets and flows westerly out past the northwest headlands (Figure 2.11a and b). Smaller scale transport stream lines (tidal influence) can be seen in Figure 2.10b, which is the result of the FLOWC computer modelling programme (the highs represent cyclonic eddies and the lows are anticyclonic eddies).

Clarke (1994) noted that the significant turbulence in the vicinity of the headlands could be generated by friction effects as the seawater moves in and out of the bay with the tidal cycles. A computer plot of residual velocities for a 2 m tide are plotted in Figure 2.10a. Transports showing turbulent activity (ie. sediment transport) in the vicinities of the headlands and the flanks of the sand banks. It can be seen from the authors interpretation of the residuals and transport currents in Figure 2.10b that the linear banks occupy areas between cyclonic and anticyclonic eddies even though the general flow is parallel to the banks. As with the North Sea banks (a size order of > 10) there appear to be three types of current moving about the sandbanks; the general flow from the outer to inner bay chiefly through the central channel, the cyclonic anticyclonic eddies which in specific areas around the banks (Figure 2.12) and surface currents that move across the sand banks during high tide (Collins et al., 1995, Pattriartchi and Collins, 1987, Huthnance, 1982). The banks are asymmetrical with the steeper sides in the proximity of the eddies ie. the asymmetry varies from side to side with eddy occurrence. This points to a transference of the prograding edge of the banks from central distal ("x") to the outer proximal ("o") along their length ie. the two banks are an approximate mirror image of depositional dynamics (Figure 2.12) . This is not seen in the North Sea Banks as they are situated in open seas

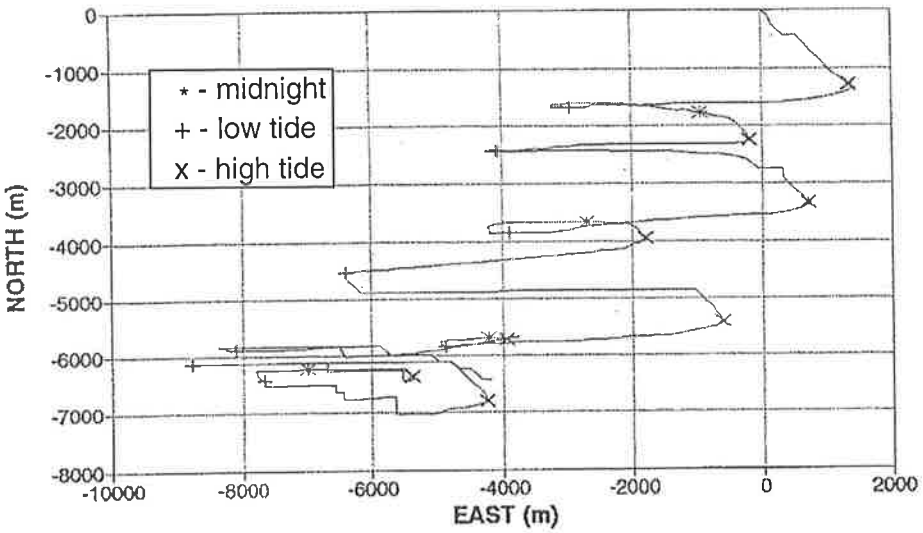



Figure 2.9a Water movement recorded by AANDERAA current meter (serial no.1802), started at (0, 0) on 11/5/94 and finished 15/5/94. Located at Station SB100 (Clarke, 1994).

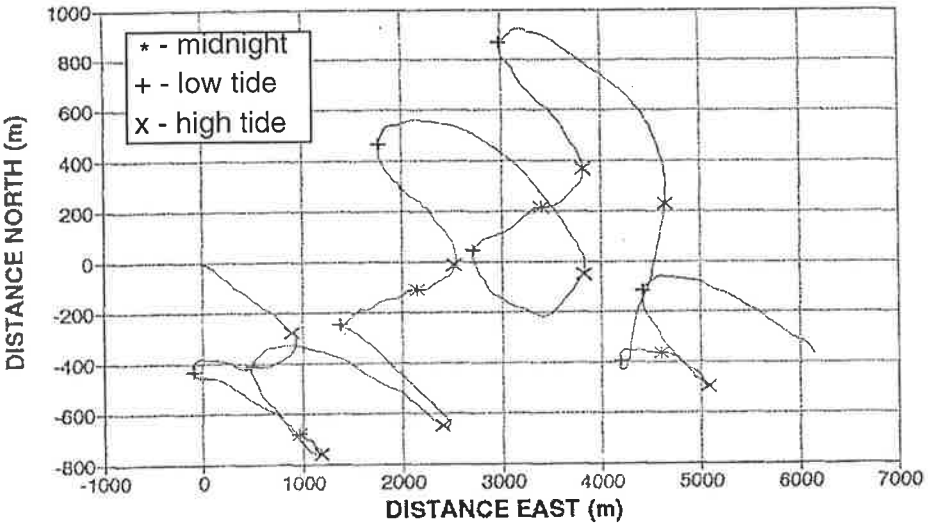



Figure 2.9b Water movement recorded by S4 current meter, started at (0, 0) on 11/5/94 and finished on 15/5/94. Located at Station SB103 (Clarke, 1994).

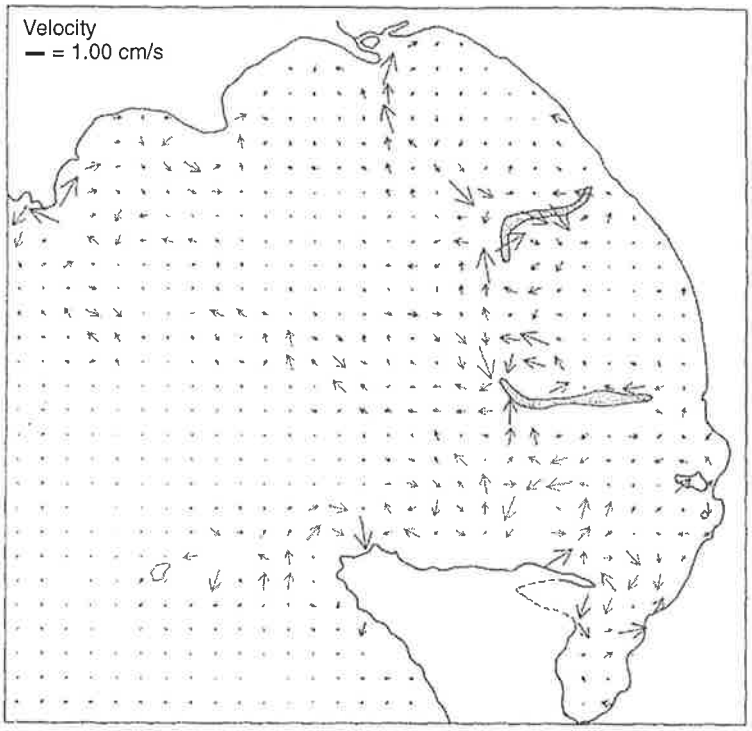



Figure 2.10a Residual velocities for a 2m tide with a sandy bottom (cm/s) showing direction and strength of residuals, FLOW-C modelling. (Clarke, 1994). Only fine muds ~<20 µm are transported by these currents (Hamblin and Christiansen 1995).

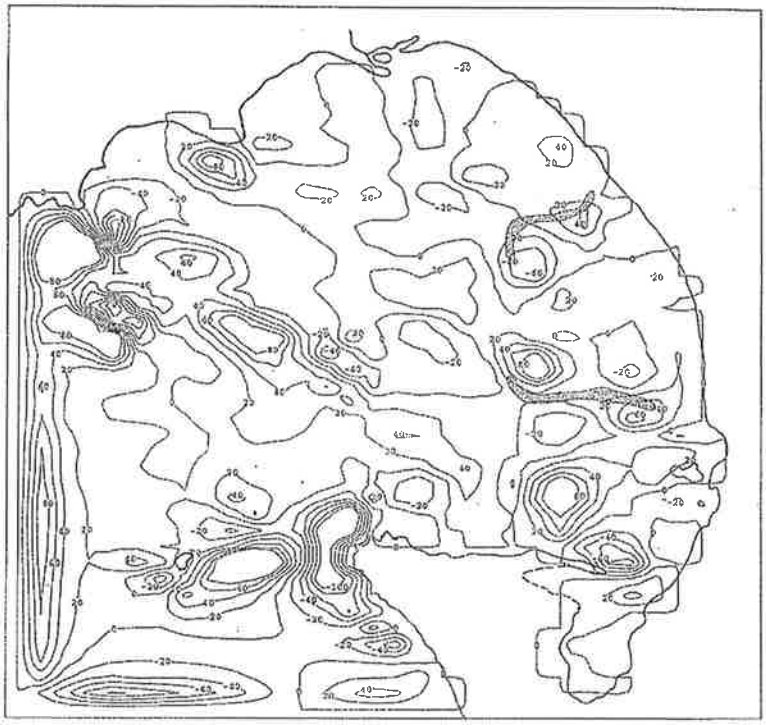


Figure 2.10b Transport lines for a 2m tide with a sandy bottom, FLOW-C modelling (water movement is parallel to transport lines; + values flow counter-clockwise; - values flow clockwise ) (Clarke, 1994). High values equate to elevated carrying capacity.

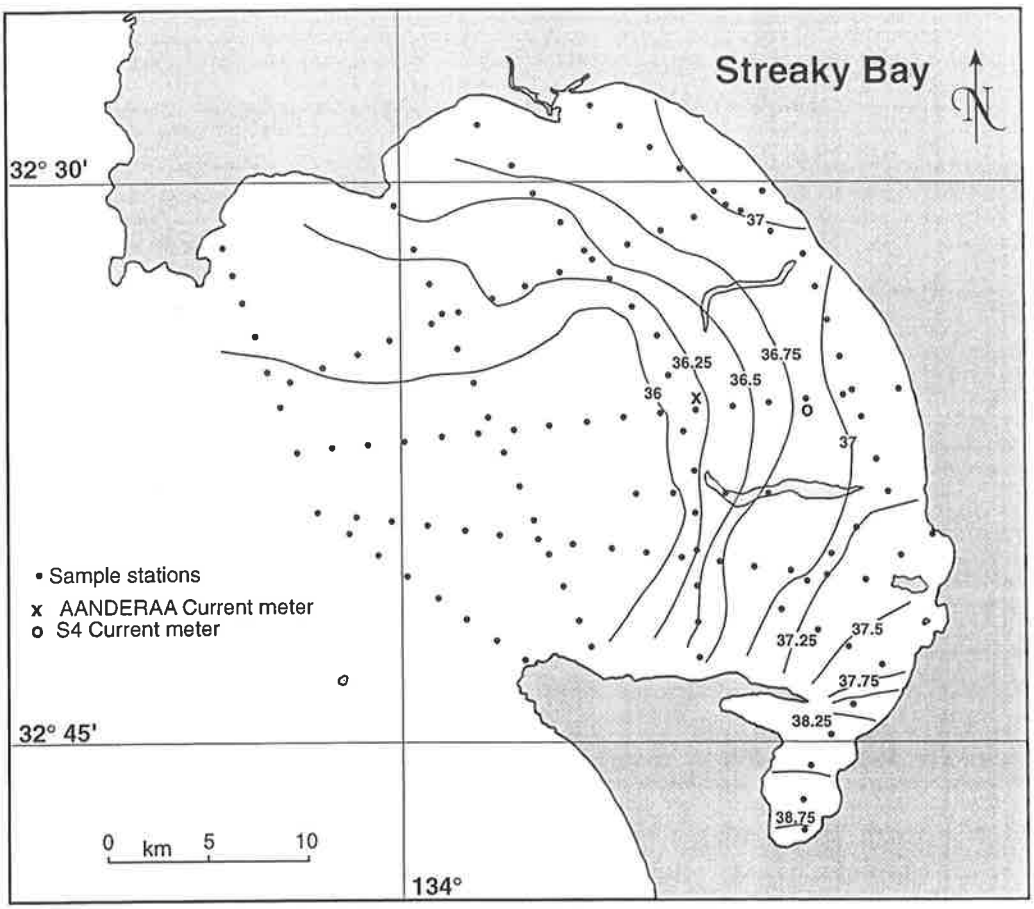



Figure 2.11a Surface Salinity, May 1994,(Clarke, 1994)

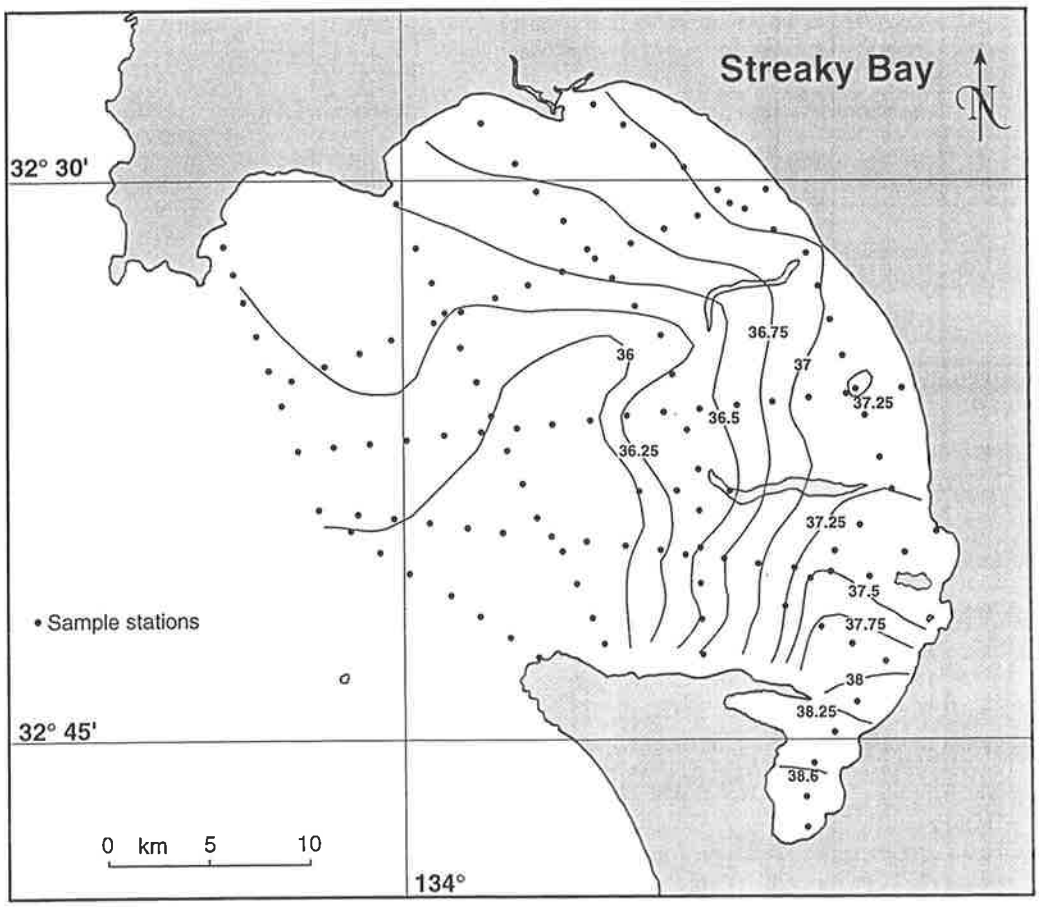



Figure 2.11b Bottom Salinty, May 1994, (Clarke, 1994)

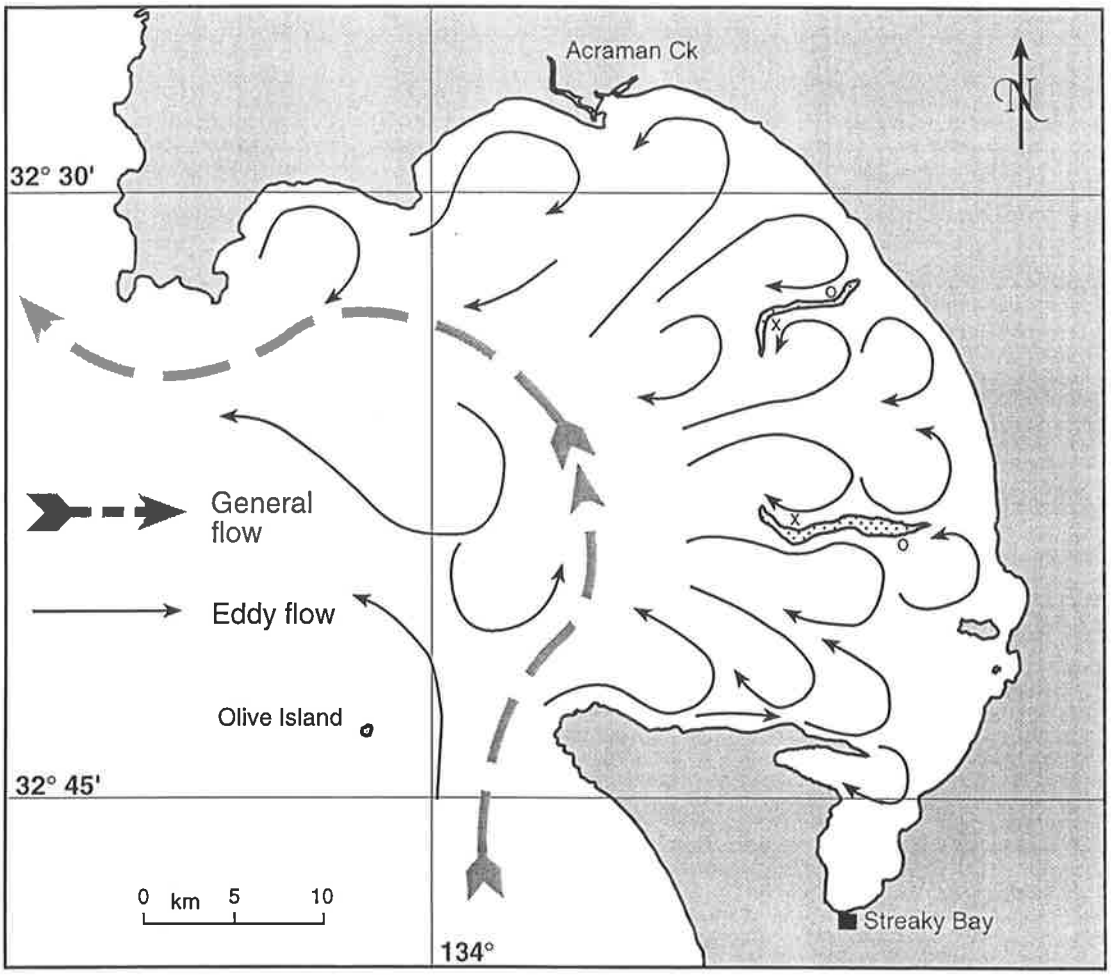



Figure 2.12 General sea movement and eddy circulation, Streaky Bay.
(modified after Clarke (1994) - Figures 2.14a, 2.15a and 2.15b)

where general sediment transport is perpendicular to the banks trending away from the coast. Minor transport is observed moving in a clockwise direction around the banks and also across the tops of the banks (Collins et al., 1995, Huthnance, 1982). The banks at Streaky Bay, therefore, represent areas of low transport capability (sparse to medium occurrence of *Amphibolis* sp across the top) and hence are the sites for a steady state of minor sediment deposition and transport (Daniel et al. 1998).

## 2.7 REGIONAL CLIMATE

The climate of the western Eyre Peninsula ranges from mild along the coast to hot and dry inland. Overall resembling a Mediterranean setting, with dry and warm, long summers and cool and wet short winters (Schwerdtfeger, 1985). Only 10% (~35 mm.) of the mean annual rainfall at Streaky Bay falls during the summer months. This period is dominated by mid-latitude high pressure systems moving slowly easterly across the continent. In the winter months Southern Ocean low pressure systems bring frontal activity and rain to the region. The mean annual rainfall for the Streaky Bay area is 350 mm. with mean summer temperatures around 28°C maximum/ 15°C minimum and mean winter temperatures of 17°C maximum/ 9°C minimum (Bureau of Meteorology data in Schwerdtfeger, 1985).

The winds are influenced by the latitudinal migration of the subtropical high-pressure belt that varies from 37°S in summer to 29°S in winter. This variation gives rise to a dominant northwesterly airstream in the winter, as the anti-cyclones are located over central and eastern Australia. In summer the high pressure cells move South over the Great Australian Bight and the Eyre Peninsula and give rise to a predominantly southeasterly airstream over the peninsula (Schwerdtfeger, 1985). The dominant wind direction at Streaky Bay is westerly in winter and southeasterly in summer (Bureau of Meteorology data in Short et al., 1986.

# CHAPTER THREE

# METHODS

## 3.1 INTRODUCTION

Scientific techniques utilised in this study are similar to those employed in studying surficial marine sediments, especially in the temperate to semi-tropical carbonate regimes of the continental shelves and embayments of southern to mid Australia and New Zealand (Nelson 1988; Fuller et al, 1994; Hill, 1994; James et al, 1992, 1997, 2001). Methods of research on the geochronology of Streaky Bay follow those as described, for example, by Belperio (1988), Barnett (1993), A summary of these methods and debatable terminology used in the study of sediments at Streaky Bay follows.

### 3.1.1 TERMINOLOGY

A majority of terms used in this thesis have been in common usage for some time but the reader may benefit at the outset from further clarification of the following terms and classification systems that are used in this thesis.

• Calcareous aeolianite grains, as sand or gravel, (McKee, 1983) are derived from the erosion of Bridgewater Formation and is variably equivalent to the shelf terminology ie. intraclasts (James et al., 2001) or relict grains (James et al., 1992, 1997 and Fuller et al., 1994).

• Maceration (sensu, Alexandersson, 1978, 1979) of skeletal carbonate refers to the disintegration of skeletons into their micrometre-sized structural components ie. flakes, needles, prisms and blocks by the primary degradation of fine organic sheaths that occur between the components. Dissolution is considered a factor in this breakdown process but appears to be minor in the overall skeletal

disintegration. Precise methods of quantifying rates and fabrics of dissolution in open sea-water are still questionable when the role of nanobacteria and nanophytes in bioerosion is not clearly known (Folk, 1993).

• The bryozoan architectural classification of the nine basic morphotypes (Bone and James, 1993) is used for general bryozoan descriptions within the sand and gravel fractions of the sediments in Streaky Bay.

## 3.2 MARINE ACQUISITION

The sediments, depth profiles and gravity cores from the sea-floor of Streaky Bay were acquired from on board the R.V. *Hero*, which is owned by the School of Earth Sciences, Flinders University and was towed 800 km from Adelaide to Streaky Bay. All oceanographic and sediment (marine and land) sampling equipment was carried to Streaky Bay by truck (Figure 3.1).

### 3.2.1 SEA-FLOOR SAMPLES

A multiple transect pattern was established over Streaky Bay using the Streaky Bay Admiralty Sheet (Aus 121) as a base map. Seven major transects were sited to characterise and maximise coverage across the bay and to sample sediments in the proximity to pronounced geographical features (inner marginal basins, elongate sand bars, sub-aqueous highs and an off-shore island) (Figure 3.2). Three transects (T1, southern; T2, central; T3, northern) were orientated in an East-West direction from the inner bay to the entrance. The other four transects were oriented North-South through inferred principal depositional environments of the bay (ie. inner marginal basins, sand shoals and seagrass meadows, central to outer terrace area and the deepwater entrance region entrance, which incorporates the region from Point Bauer to Point Collinson). A minor transect (T8) was sited along the South Sand and partially sampled but the water was too shallow and the tide moving too quickly for the research boat.

The sampling stations were plotted along the transects at intervals of approximately one nautical mile (1.853 km) (Figure 3.2). These were reduced to latitudes and longitudes (Appendix 1) for entry into a Garmon 75, Global Positioning System (G.P.S.) instrument (School of Earth Sciences, Flinders University). A Raytheon Depth Chart recorder was used to verify the profile of the seafloor of the bay, as recorded on the Admiralty sheet No. 121 (Streaky Bay).

The *RV Hero* was used for sampling during April 1994 and May 1995. Samples were collected using a toothed pipe dredge with a capacity of up to 3 kg of sediment (Figure 3.3). The sample was assumed to have been collected from the uppermost 5 to 10 cm of the sediment, due to the relatively light



Figure 3.1 The *RV Hero* en route to the Streaky Bay launching site and the start of the sampling programme. Professor Chris Von der Borch as scale.

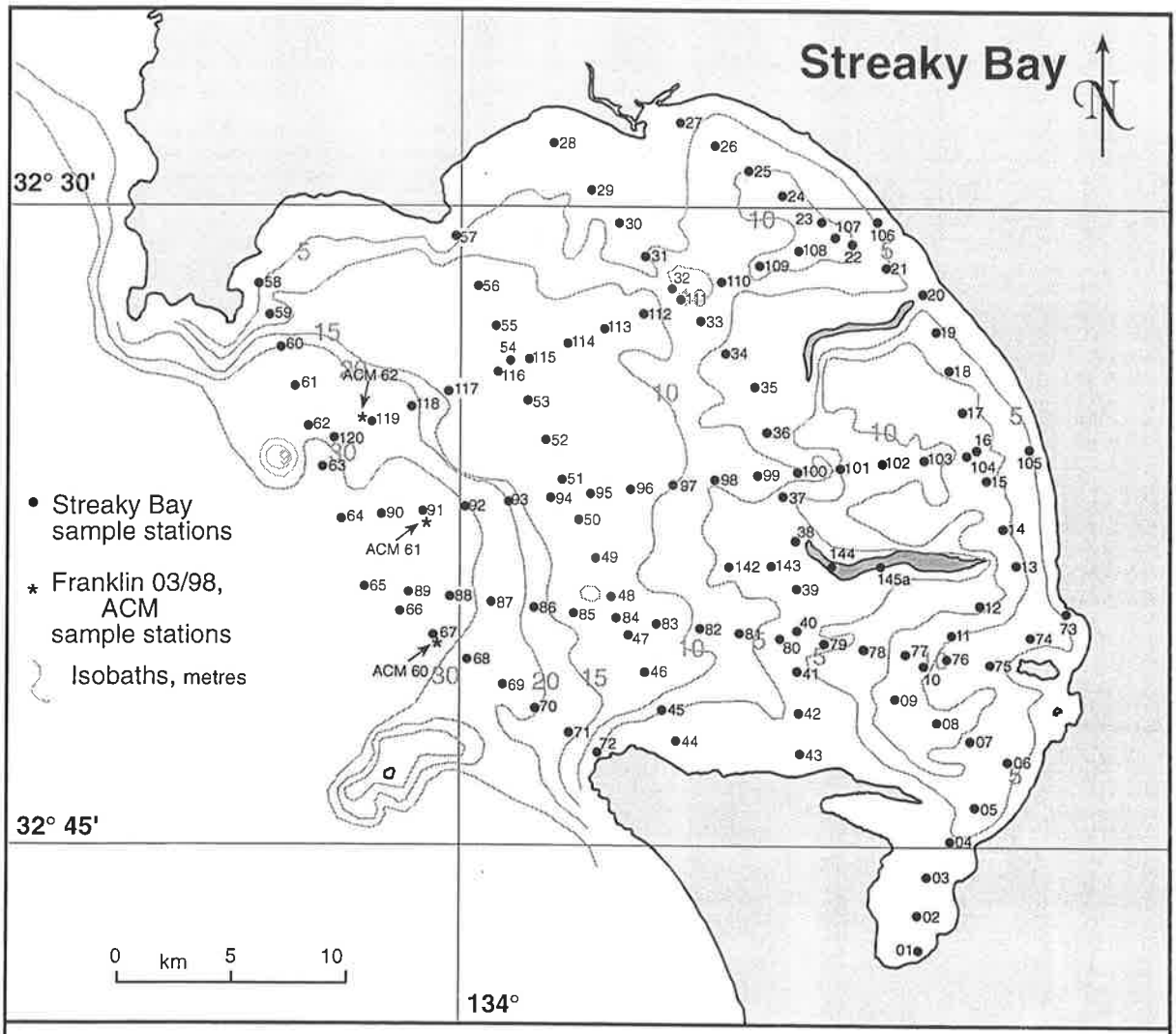



Figure 3.2 Location and number of sample points, Streaky Bay.
Dot points represent sediments collected in1994 and asterisk points represent samples collected on the CSIRO Franklin 13/98 cruise.

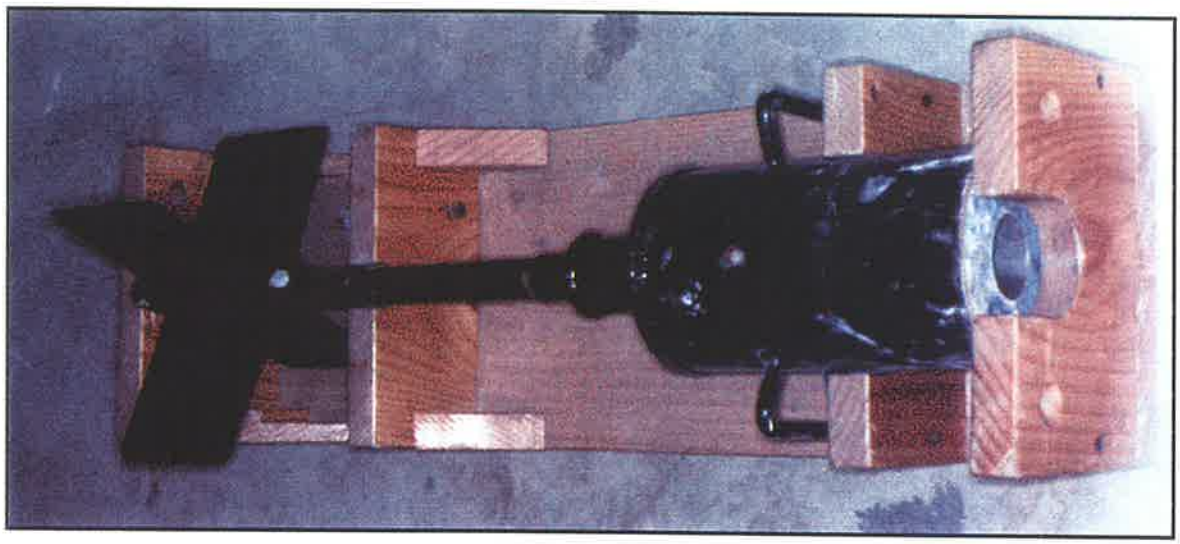


Figure 3.3a Gravity coring device. A one metre length of high grade plastic tubing, fixed with a core catcher is inserted and bolted in the opening (right). A retrieving rope (2-3 times water depth in length) is shackled to the eye at the left- hand end. An internal ball valve ensures the sediment moves easily up the tube and protects the resultant core from being washed out on retrieval.

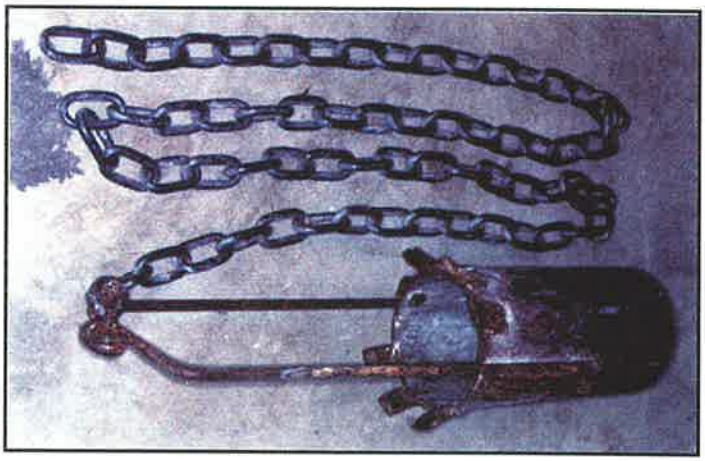
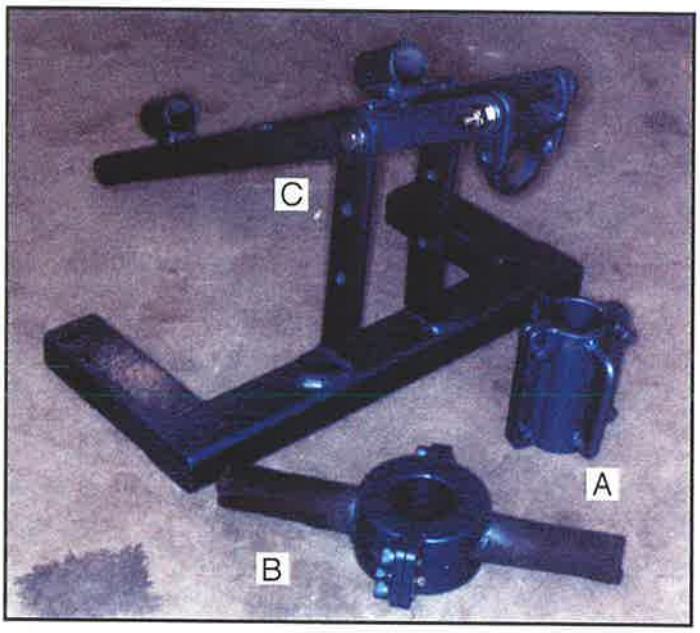


Figure 3.3b. Toothed pip dredge with lead chain attached. The fixed bridle and chain ensures that only the top 5-10 cm of sediment is sampled. The toothed rim aids in collecting sediment in areas of high density seagrass

Figure 3.3c Slip-hammer coring device. High grade plastic tubing (up to 6 m), fitted with a core catcher is hammered into sediment. The adjustable collar (A), which is clamped to the tube, is moved up as the tube penetrates the sediment. A slip-hammer (B) is hammered onto the collar which forces the tube into the sediment. The core jack (C) is used to lift the tube containing the core once coring has been completed.



weight nature of the dredge coupled with the 6 m of heavy gauge chain lead. Approximately two to three times the water depth in rope length was payed out at each sampling station which resulted in the dredge being deployed in a fairly horizontal fashion while being slowly towed behind the boat (<3 km/hr). This depth of sampling has been verified through direct underwater observations of the deployment of a similar dredge (James et al., 1992). The samples were refrigerated, on return to the laboratory, to preserve sediment and biota.

### 3.2.2 GRAVITY CORES

Five gravity cores were taken across the inner marginal basins of Streaky Bay. The sites were chosen initially from inferred low energy areas of the bay in order to gain stratigraphic information from the sediments. The best results were achieved when coring in muddy to fine sandy sediments. Other sites chosen consisted of gravels to coarse sand, which caused the plastic core tubes to shatter on impact.

The gravity corer has a shape similar to a classic bomb (Figure 3.3). It has guiding fins at the top and a driving weight (~45 kg) at the bottom. A core tube one metre long (50 mm, class 9 plastic pipe), with a core catcher, is bolted in a hole at the bottom of the gravity corer. This hole, which receives the core tube, continues through the device to allow for the displacement of water as sediment fills the tube. A moving rubber ball covers the top of the hole, as a valve, to prevent seawater washing the sediment out of the core tube during recovery. The gravity device was tethered to *RV Hero* with a line at least twice the water depth in length. This enabled its recovery via a winch attached to the side of the boat. Cores of up to 54 cm were obtained in 9 - 12 m deep seawater.

## 3.3 LAND OPERATIONS

Land based operations included verification and mapping of all Pleistocene Glanville Formation outcrops around Streaky Bay (Figure 2.3) and locating and coring the abundant Holocene sediment in the northern and southern depositional sites (Acraman Creek and Point Gibson).

### 3.3.1 DUMPY LEVEL SURVEYS

Dumpy level surveys were carried out to measure the heights above Mean Sea Level (MSL), and the Australian Height Datum (AHD), of elevated palaeontological and palaeomorphological features in the Glanville Formation (Isotope Stage 5e) and similar adjacent modern morphologies. These differences in height of similar beach morphologies were used to predict the height of palaeosea-levels above a local datum. These were correlated with tidal results produced by the National Tidal Facility (NTF, Flinders University) so that the heights of palaeo-sea-levels and present day sea-level could be reduced to MSL and AHD. Time adjustments (supplied by the NTF) for Streaky Bay tides were made

to Port Thevenard (Ceduna) tidal information so that the exact height above sea-level was calculated for each survey. Surveys were completed at Flagstaff Landing, Point Gibson and Point Collinson.

### 3.3.2 SLIP HAMMER CORES

A slip hammer-coring device (Figure 3.3) was used to obtain 14 cores to develop a profile of sediments from the spit/ mangrove areas flanking the north and south of Streaky Bay, ie. Acraman Creek area and the bay protected by Point Gibson (Figure 2.4). The core tube (50 mm diameter, class 9, 3 - 6 m long), with a core catcher attached, is fitted with a moveable steel collar clamp and a doughnut shaped slip hammer (~8 kg) with handles. This is used to drive the tube into the sediment. Cores of up to 3.2 m were collected, with the limiting factor being compact medium to very coarse sands, which cannot be penetrated easily by this method. Once the core had been retrieved, with the aid of a specially constructed pipe lifter, it was labelled, sealed and the depth of pipe penetration measured. This pipe measurement was used to determine the compaction factor of the recovered sediment. The cores were slabbed and refrigerated on return to the laboratory with half being archived, whilst the other was used for sub-sampling (photography, sedimentology and geochronology). A Garmon 75 G.P.S. instrument was used to determine an accurate position of the core sites. Unfortunately a number of coring attempts encountered shallow subcropping calcrete (< 30 cm), which caused the core tube to shatter around the leading edge.

## 3.4 LABORATORY ANALYSIS

Early laboratory analyses were carried out in the School of Earth Sciences, Flinders University and latterly in the Department of Geology and Geophysics, Adelaide University.

### 3.4.1 GEOCHRONOLOGY

The age determination of a Pleistocene coral (Glanville Formation) was carried out by Dr. H.H. Veeh (Flinders University, 1996) using the $^{234}U/^{230}Th$ discontinuous series radiometric dating (ß ray collection) technique as described by Veeh and Burnett (1982). The sample used was selected on freshness, lack of boring and lack of material caught within the septa. It was cleaned in 10% bleach solution for 48hrs to dissolve any organic matter within the corallites. A thin surface layer of the coral and the septa were ground off with a dental drill to clean off and out any contaminant material that was caught up in these areas before the analysis was performed. The coral was sub-sampled and analysed by X-ray diffraction to check the aragonite content

Holocene dates (for sediments at Acraman Creek and Point Gibson) were determined by AMS $^{14}C$ dating (Accelerated Mass Spectrometer) by the Australian Institute of Nuclear Science and

Engineering (AINSE) at the Lucas Heights Research Facilities in New South Wales, Australia. AINSE awarded a grant (95/084) to the author for dating 10 sediment samples in the Streaky Bay area. The samples were taken from the slip-hammer cores located at Point Gibson, Acraman Creek and the Proto-Acraman embayment (Figure 2.4). Two further samples were taken from gravity cores in the central Inner Marginal Basins (IMB). Their locations in the cores were carefully measured and noted during sampling. The shells were articulated and in living position and the seagrass samples were present as thin fibrous matts intercalated with the sediment. The dating was carried out using the technique described by Hedges and Gowlett (1986) and Williams et al. (1998). The samples (approximately 0.5 gm) were prepared for AINSE by immersion in a sonic cleaner for 15 minutes to clean extraneous particles from the shell and seagrass material. Further examination of the samples by binocular microscope to check on possible lodged or adhering grains, which were scraped off when found. The samples were packaged and sent to ANSTO for analysis.

Holocene Carbon 14 dating of shell from a core (ACC No. 9) in the Proto-Acraman Creek area (Figure 2.4) was determined by the direct $CO_2$ absorption method for radiocarbon analysis by the CSIRO Division of Water Resources, Adelaide, South Australia, following the method described by Leaney et al. (1994). This method is not as accurate as the AMS method, however availability and cost were important factors in method selection. The sample, which was sent to CSIRO, was pretreated similarly to the ANSTO samples.

Verification of some anomalous carbon 13 isotope data, through ANSTO, were determined by mass spectrometry (Fisons, model Optima, mass spectrometer) at the Department of Geology and Geophysics, Adelaide University using techniques outlined by from Kyser (1995). Carbon 13 isotope analysis was not available at ANSTO when the samples were dated and were sent to ANU laboratories for determination. The anomalous data was compared with stable isotope mass spectrometer results on the shell samples at the Department of Geology and Geophysics (see results Chapter Four).

### 3.4.2 Sediment Grainsize

Bulk samples were wet sieved into the principal fractions of gravel (coarse fraction, < 2 mm), sand (2 mm - 63 μm) and mud (<63 μm). Each fraction was dried, weighed and recorded as a percentage of the total weight. The sand fractions were dry sieved into three fractions (2.0 mm-0.5 mm, 0.5 mm-0.25 mm and 0.25 mm-0.0625 mm), weighed and tabulated as a percentage of the sample weight. These sediment and sand fraction divisions are the same as used by researchers on surficial sediments on the southern margin of Australia (James et al., 1992; Boreen et al.1993; Fuller et al., 1994; James et al., 1994, 1997, 2001). Further detailed size fractions are not considered practical for studying carbonate sediments as suites of new grains across the size spectrum are being added continually as calcareous skeletal organisms die.

Percentage isopleth (contour) maps were drawn up of the principal sediment fractions, (ie gravel, very coarse to coarse sand, medium to very fine sand, and mud). These maps were utilised by Fleming (1977) to emphasise the concentrations of the different grain-size fractions.

A sand ratio isopleth (contour) map was also drawn to demonstrate the grainsize distribution across the bay. The ratio (vc sand+c sand/m sand+f-vf sand) indicates the trends in fining grainsizes ie. ratio < 0.5 indicates finer sediments; ratio > 1 indicates coarser sediments. This style of map was also used to effect by Fleming (1977) to highlight the overall distribution of sediments in Saldanha Bay and Langebaan Lagoon, South Africa.

Skewness was also calculated on the grain-size distribution of the sediments. The skewness of sediment measures the degree of asymmetry in grainsize distribution and also indicates, by a positive or negative sign, the direction of skew. Sediments with excessive coarse fraction show negative values and sediments with excessive fine fraction show positive results, while sediments with a normal distribution have a skewness of zero (Folk, 1968; Fleming, 1977; Tucker, 1988). The skewness of the sediments at Streaky Bay is a useful tool for mapping sediment migration, as the general grain-size frequency curves are unimodal and approximate normal distribution apart from where the sediments are highly skewed to either the gravel or mud fractions (Figures 5.3 - 5.11).

### 3.4.3 Sand Component

The sand component is described first in the text as a result of this fraction's dominance in the sediments on the bay-floor. The composition of sand grains is established through a series of important diagnostic properties, which have been used to identify the grains through a reflecting binocular microscope. Supportive data on the attributes of biota and resultant grain morphology was obtained from Bathurst (1983); Scoffin (1987) and Milliman,1974). The component percentages of the sand fractions were calculated on the results of 300 grain counts (Harwood, 1988).

The grains are grouped under the following components; molluscan, bryozoan, foraminifera, echinoderm (principally echinoid), coralline algae, abraded bioclastic, calcareous aeolianite and quartz/ lithic grains. The quartz/ lithic grains are subdivided into quartz, potassium feldspar, lithic igneous and lithic aeolianite. The quartz, potassium feldspar and lithic subdivisions are grouped together (as terrigenous sediment) in the point counting analyses.

Distribution graphs of grainsize, sand components and gravel components from each transect are correlated with water depth and presented in one figure (Chapter Five). The graphs are generated using Microsoft Excel package combined with Macromedia's Freehand package.

It was decided to utilise a point counting technique and compare with the shelf data, as most of the component percentages for the shelf studies are based on visual estimates (James et al., 1992, 1997, 2001). Estimation is considered reliable for temperate carbonate sediments as groups of organisms have different disintegration pathways, eg. a bryozoan will breakdown to large or small fragments depending on the energy regime, whereas an ophiuroid will disarticulate completely within a relatively short time after dying, creating a significant number of fragments even though it may be smaller than the bryozoan structure. This comparison can be repeated with many calcareous skeletal organisms within the temperate real

### 3.4.4 GRAVEL COMPONENT

A numerical system of describing component density or occurrence has been used to facilitate graphing procedures (Table 3.1). Gravel from each sediment was evenly spread over a picking tray to determine the component density of each group.

| Population Frequency | Numerical Value | Population of Fragments |
|---|---|---|
| Absent | 0 | 0 |
| Rare | 1 | 1 - 4 |
| Common | 2 | 5 – 10 |
| Abundant | 3 | more than 10 |

Table 3.1 Population frequency of gravel components versus numerical value (for graphing purposes) in relation to fragment population. Frequency is based on the occurrence of fragments evenly spread on a picking tray (5x9 cm).

The results were plotted on a distribution graph for each transects. They show the occurrence of the components at each sample station on a frequency scale from 0 to 3 (absent to abundant). Sediment was not collected from a number of sample stations ie: SB 55, SB 58, SB 59, SB 61, SB 71, SB 72, SB93, SB98 and SB 118. This is a result of the rocky substrate having a thin veneer of overlying sediment or the conditions being too dangerous for sampling at the station point. As a consequence there was an aberration in the graphs where the results of the above sediments are shown as zero in the distribution graphs, which would imply that the sparse sediment at these locations has no grainsize or components. These stations were deleted to facilitate a clear understanding of the trends in the gravel components. Sediments without gravel fractions are graphed as zero.

### 3.4.5 IDENTIFICATION OF ORGANISMS

The organisms of significance within Streaky Bay have been identified using the following sources:

• Mollusc identification ; Ludbrook (1984, 1988); Gowlett-Holmes, K., pers com. (1996).

• Foraminifera identification; Brasier (1980); Cann and Gostin (1985); Lablack (1985); Hill (1994); Q. Li, pers. com. (1999).

• Bryozoa identification; Bock (1982); Bryozoa, Past and Present.; Winzar (1998), Y Bone and R Schmidt, pers com. (2000)

• Coralline Algae identification; Wommersley, (1996); Wray, (1977); K Brown, pers. com (2000).

• Echinoderm identification; Baker, (1982a, 1982b).

• Brachiopod identification; Richardson, (1997), James et al., (1997) and Y. Bone, pers com. (1999).

• Serpulid identification; Knight-Jones et al., (1973).

• Coral identification; (Shepherd and Veron, 1982); Veron pers com. (1997).

• Diatom identification; Foged, (1978, 1979); Barnett, (1993); Round et al., (1996); Edwards, (1998); P. Gell pers com., (2000).

• Coccolith identification; Honjo, (1976)

### 3.4.6 MUD

Muds from the inner marginal basins were analysed and compared by acid dissolution, X-ray diffraction analysis and scanning electron microscopy. The sediments selected for the XRD analysis were the same used in the acid dissolution tests.

The samples were analysed;

- as a bulk sample,
- as the mud fraction
- as the residue fraction from the 10 % hydrochloric acid dissolution.

A suite of ten sediments was selected from stations along Transect No. 4 that was indicative of the four locations of high percent mud, ie. northern, central and southern inner marginal basins and

Blanche Port. The sediments from the basins were chosen on the basis of high mud content, deep-water occurrence, and maximum distance from the shore.

A selection of calcareous skeletal organisms was also analysed. These organisms were collected at stations mostly in the outer portion of the bay. They were selected from this area because of their significant contribution to the gravel and sand fractions. However specimens of calcareous algae, bryozoans and molluscs were collected from the central seagrass meadow area because of their contribution to the mud fractions in the IMB. Samples of calcareous skeletal organisms were also were taken from the basins where they were not subject to significant transportation and were available as fresh specimens. The organisms found in the basins (pristine to highly eroded) are important as they may indicate the amount of mud-sized sediment being added to the basins from in situ biodegradation and maceration.

#### 3.4.6.1 Acid Dissolution

The selection of samples, used for determining the carbonate content of the mud fraction, was based on mud content and distance from the shore and sand shoals surrounding the basins. They were selected so that any transport variations of significance could be minimised. These variations could be due to the proximity of the shore and contamination by wind born sediments or transportation of sediment across the sand shoals and through the tidal deltas to the basins during storms and king tides. The carbonate percentages were recorded from samples collected in water depths from 10 – 14 m in the open bay and ~7 m in Blanche Port, adjacent to Streaky Bay township. The amount of $CaCO_3$ present in the mud fraction was determined by digesting a known dry weight of the sediment fraction to completion (usually ~ 24 hours) in 10 % hydrochloric acid. The resultant residue was dried, weighed and the carbonate percentage calculated and tabulated.

#### 3.4.6.2 X-ray Diffraction

The carbonate composition of the bulk sample and mud fraction, and the composition of the residue was determined by X-ray diffraction (XRD). A Phillips P W 1050 Diffractometer with a Cobalt Kα radiation source was used to carry out the analyses. The samples to be analysed were ground to a powder of < 125 μm for no more than two minutes. This was to lessen the effects of structural damage and mineralogical change to the carbonate minerals that can be caused by heat and pressure build up during an extended grinding process (Milliman, 1974, Tucker, 1988). Energetic grinding times over two minutes and up to 32 minutes results in a nearly geometric reduction in peak intensity on the diffractogram. At 32 minutes the diffractogram curve is only undulating at the absorption sites of the minerals. The distortion due to grinding time is more noticeable in calcite than in aragonite. Calcite also shows a more than proportionate reduction in peak intensity than aragonite with increasing grinding time when compared to analyses from a < 2 minute grinding (Milliman, 1974).

### 3.4.6.3 Scanning Electron Microscopy

A Philips XL-30 Field Emission Scanning Electron Microscope, with an integrated EDAX Energy Dispersive X-ray Analyser package, was used to characterise the morphology and the elemental components of particles within the mud fraction and representative dominant calcareous organisms from Streaky Bay. A representative sample of the mud for stub mounting was obtained by thoroughly mixing the fraction, then taking a small sub-sample with a small spatula (< 0.1 g) and allowing it to cascade over the adhesive area of the stub. Sediment that remained unstuck on the stub was gently blown off or the stub was gently tapped on the table to release loose sediment which overcomes unnecessary charging of grains while operating the microscope. These stubs were then prepared by vacuum coating with gold and carbon or gold depending on the potential of the grains to charge up during the SEM operation. A suite of representative organisms from the bay was also prepared for the SEM. Some of the stubs containing samples and specimens appear to have been coated with too much gold as artefacts are seen in images of high magnification (resolutions of < 5 μm) not unlike those described by Folk (1993) and Folk and Lynch (1997). These artefacts can appear as a result of vacuum gold coating times in excess of 30 seconds (Folk and Lynch, 1997). If high resolution SEM microscopy is required it is desirable to coat the stubs in a special cryogenic vacuum chamber which can minimise the high magnification artefacts (Waterhouse, L., CEMMSA, pers. com. 2000).

The state of preservation of the skeletal material of the specimens was imaged so that a spectrum of maceration or shell breakdown (*sensu*, Alexandersson, 1979) (either biogenic, physical or chemical) could be observed and correlated with images of the mud particles. This was to determine whether morphological and elemental comparisons could be made with the calcareous skeletal organisms present in the bay. The skeletons of the organisms that were used for the comparisons were either recently dead or starting to disintegrate at the time of sampling.

A significant portion of the SEM research on the muddy sediment was carried out on the mud fraction. This fraction was obtained by wet sieving, with the resultant sediment and water standing for at least two to hours before decanting. The standing time allowed grainsizes of > 4 μm to settle or approach settlement near the bottom of the beaker (Folk, 1968). A majority of this water was decanted and the rest allowed to evaporate over several days in an oven heated to 40° C until the sample was nearly dry. The sample was then air-dried and bagged, this was to curtail the unnecessary formation of loosely compacted secondary 'clasts' of sediment during the drying operation.

Trial SEM experiments with bulk unwashed sediment proved to be unsatisfactory as many micrometre-sized particles adhered to and subsequently masked the larger particle morphology. This masking was readily observed when comparing the difference between SEM micrographs of washed

and unwashed samples. The smaller sub-micrometre particles were also responsible for excessive particle charging during SEM operations to the point where successful clear imaging was very difficult. Larger and smaller particle morphology was studied from sub-samples of the washed samples. The morphologies of the smaller particles (micrometre-sized) were compared with those obtained from unwashed samples to ensure the morphologies of particles (although not necessarily populations) were comparable.

Percentages of calcium and magnesium were calculated by the EDAX-ZAF element quantification subroutine and converted to mol % $MgCO_3$ via the method used by Smith and Nelson (1998).

### 3.4.7 Facies Determination by Ward's Cluster Method

The results of point-counting the sand fraction were entered into a spread sheet in the JMP statistical programme and the samples were clustered as a dendogram (Figure 9.1) based on the variants or components of the samples. Three to six clusters were calculated and saved from the clustering dendogram that could probably represent the lithofacies in the bay. Several anomalous single station clusters were recognised when running the data through the programme several times. These stations were deleted from the data base so that a clearer picture of the dominant clusters or lithofacies could be established. The data set of the Abraded Bioclastic component was also excluded as these data represent a proportionate sum of recognised bioclastic constituents within each sediment sample and is not a separate bio- or litho-component.

A range of three to six clusters were plotted against the sample station sites on separate maps and highlighted to delineate possible lithofacies (Figures 9.2 to 9.5). The samples were also calculated for two, seven and eight clusters. The first was lacking in detail and the second and third contained an abundance of detail but the general delineation of lithofacies was considered too complex to be of practical use. The range of possible lithofacies distribution according to the various clustering is described and illustrated in the models.

Definition of Ward's Method: *"In Ward's minimum variance method, the distance between clusters is the ANOVA sum of squares between the two clusters added up over all the variables. At each generation, the within-cluster sum of squares is minimised over all partitions obtainable, by merging two clusters from the previous generation. The sums of squares are easier to interpret when they are divided by the total sum of squares to give the proportions of variance (squared semipartial correlations)."* (Milligan, 1980).

## 3.5 DISCUSSION

The methods utilised to acquire samples and data in this study are similar to those which have generally been utilised by researchers in the fields of shallow marine sedimentology and Quaternary chronostratigraphy in relatively remote areas.

### 3.5.1 MARINE ACQUISITION

This was the most difficult section of the field work to organise as all the equipment for marine sampling together with the research vessel (~3 tonnes) and extra oceanographic equipment for a concurrent project, had to be carried on the truck or towed the ~800 km from Adelaide.

Seven primary transects were sited to maximise sediment sampling from the diverse depositional environments present. This was coupled with the need to sample continuously from inner to outer and from South to North over the width of the bay to highlight any sedimentological trends which may be present. The sediments were collected with a toothed pipe dredge which was set up with a heavy chain lead so as to sample only the top 5 to 10 cm. This sampling depth has been verified by direct observation (James et al 1992; Bone pers.com. 1995). Samples were refrigerated on return to the laboratory to stabilise the biota and carbonate minerals contained within the sediments. This slows down the disintegration of live biota and the subsequent production of an acidic environment, which could produce artificial dissolution textures on the carbonate material within the samples.

The gravity coring method was selected for studying accumulations of sediment in deep-water areas of the bay. This was to build a framework of sediment accumulation across the sea-floor and correlate with the land based cores. Gravity cores were initially selected at sites within the IMB (15 m water depth) and entrance (35 m water depth) areas. The selection of sites assumed adequate fine grained sea-floor sediment cover and water depth for the coring device to operate efficiently. However, the sediments of the entrance proved too coarse and patchy in distribution resulting in the core barrels being shattered on the medium to coarse sands and resistant rocky substrate. The limiting factors of further gravity coring sites were relatively shallow waters (< 10 m) and sandy or rocky substrate. The cores recovered from the IMB are < 54 cm in length, which is probably due to washed core and the limitations of the device. Possible significant unknowns are whether the top of the cores is the sea/sediment interface or a washed surface, and that the amount of compaction. The latter means that the actual sedimentation rates are higher than calculated as no compaction has been assumed.

### 3.5.2 LAND ACQUISITION

The aims of the dumpy level surveys were to survey prominent palaeo- (of the Glanville Formation and early Holocene sediments) and similar modern day beach morphologies. As a result of the low energy and relatively stable nature of the modern beach profile (visually checked over a period of 3

years), it was determined that a measured comparison could present a clear picture of sea-level height for Isotope Stage 5e and possibly for the early Holocene. The Flagstaff Landing section was based on height differences of similar morphologies. Several readings of each point were noted and the mean of these used in the calculations. Point Gibson was measured on modern day Low Mean Tide height compared with the maximum heights of in situ articulated *Anadara trapezia* and *Katelysia rhytipora* bivalves. The infaunal bivalve *A. trapezia* is observed inhabiting muddy substrates to the Low Mean Tide level on the east coast of Australia at the present day, which also agrees with Ludbrook (1984). Comparing the mean of the maximum heights of these bivalves outcropping in the Glanville Formation with the present day Low Mean Tide indicates the height difference in sea-level.

The slip-hammer coring device was used to obtain cores up to 3.2m. This core length would appear to be near the limit for the sediments being cored as the core catchers and the leading edges of the core barrel were tearing away and being shattered, respectively. Significant compression of the sediment was observed in recovery. It is not known whether the sediment compresses through the elimination of water or that some of the sediment is forced outside of core barrel during coring. The latter has been observed to be the case when coring muddy sediments in Lake Alexandrina, South Australia (Barnett, 1993).

### 3.5.3 Laboratory Analysis

The methods used in the grainsize analysis of carbonate sediments has been found to be reliable on a local ie. Coffin Bay, Baird Bay, American River and Pelican Lagoon (Kangaroo Island) and lower Spencer Gulf to a regional scale ie. the Otway, Bonny, Lacepede, Lincoln, Great Australian Bight, Eucla, Rottnest and Abrolhos Shelves (Freeman, 1985; Hill, 1994;Wirtz, 1994; Millikan;1994; Fuller et al., 1994; Boreen et al., 1993; James et al., 1992, 1997, 2001, Collins, 1988; Collins et al., 1997)

Analysis of the mud fraction of surficial cool-water carbonate sediments (60 m-83 m water depth) has been described from the Bass Basin, Australia, and although these muds contain a significant proportion of terrestrial clays and quartzose silt(up to 50%) the biogenic carbonate content and components were identifiable using similar techniques as this study ie. XRD, acid dissolution and scanning electron microscopy.

Statistical clustering has been utilised extensively by Li (1996, 1999) to delineate foraminiferal biofacies on the Southern margin, ie. Bonny/ Lacepede Shelves, Lincoln Shelf and the Southern shelf of Western Australia. The multivariate nature of the sediments in Streaky Bay offered a unique opportunity to utilise this technique and broadly compare it with the preliminary lithofacies interpretation. The technique appears to be robust as the overall facies boundaries remain intact as

subfacies or new facies are developed. A drawback to this technique is the generation of data through point counting and component identification in the carbonate sands especially the very fine sands.

# CHAPTER FOUR

# LATE QUATERNARY GEOCHRONOLOGY AND RELATIVE SEA-LEVEL FLUCTUATIONS: STREAKY BAY

## 4.1 INTRODUCTION

The timing and variation in the relative sea-level high-stands along the South Australian coast during the Pleistocene have been constrained by a series of late Pleistocene dates obtained from rocks of the Glanville and Bridgewater Formations found proximal to the coastal areas of South Australia (principally the southeast and west coasts). The West Coast of the Eyre Peninsula, in particular, is also isostatically constrained by the far-field stability of the Precambrian Gawler Craton and therefore represents a coastline, which more significantly reflects the eustatic movements of sea-level during the late Quaternary

Significant marine sedimentation occurred on the west coast of the Eyre Peninsula when relative sea-level was in the vicinity of the present height (MSL) during the late Pleistocene and early Holocene (from approximately 7300 years BP). The foci of deposition are principally found within the embayments along this coastline. The sediments have been transported to these sites from three main sources ie. biogenic production of sediment both from within and proximal to the embayments, erosion of Pleistocene aeolianitic cliffs that are common along the west coast and erosion of similar

aeolianitic cliffs within the embayments, and erosion of the sea-floor within and proximal to the embayments.

The purpose of this chapter is to establish the timing of high-stand marine conditions and determine the late Pleistocene and early to mid Holocene sediment transport patterns, deposition rates and relative sea-level heights.

## 4.2 PREVIOUS WORK

The fluctuations and timing of relative sea-level during the Quaternary is primarily delineated on a world wide basis using data from uplifted coral terraces (Veeh and Chappell, 1970; Bloom et al., 1974; Chappell, 1974, Chappell and Veeh, 1978; Chappell and Shackleton, 1986, amongst others). This was subsequently verified and refined using the oxygen isotope ratio curves ($\delta^{18}O/\ \delta^{16}O$) obtained from deep-sea sediment cores (Shackleton and Opdyke, 1973, 1976; van Donk, 1976, Chappell and Shackleton, 1986) (Figure 3.2. sea-level). Research on direct dating ($^{234}U/^{230}Th$) and oxygen isotope ratios ($\delta^{18}O/\ \delta^{16}O$) of marine sediment cores from the Bahamas has also added to the refinement in timing of the late Pleistocene sea-level high (Slowey et al. 1996).

Uplifted coral terraces can represent the occurrences of sea-level highs (periods of high stand at maximum transgression) in tectonically active areas where the rate of uplift is overtaken by rising sea-level (Chappell and Shackleton, 1986). Coral terraces (reefs) form just below the high-stand sea-level, during these sustained periods, as long as climatic conditions are favourable. The rate of uplift elevates the last coral terrace to above the current sea-level at maximum transgression within the intervening cycle of relative sea-level fall and rise. Eleven major succeeding coral terraces have been accurately surveyed and dated on the Huon Peninsula in New Guinea cycles (Chappell and Shackleton, 1986). The four earliest dates and sea-level height inference are estimations because of the lack of an earlier sea-level datum. This is due to an increasing probability of errors in the dating technique (see below) and unverified morphostratigraphy in the upper section. The dates of diagenetically unaltered corals from these areas were determined using $^{14}C$ dating (ß ray collection (radiometric) and Accelerated Mass Spectrometry (AMS) techniques), for the Holocene and $^{234}U/^{230}Th$ dating methods (ß ray collection (radiometric) and Thermal Ionisation Mass Spectrometry (TIMS), for pre-Holocene dates. This provided a time frame for the formation of the coral terraces and hence for the sea-level highstands over the past 240 ka (Figure 3.3).

The oxygen isotope record ($\delta^{18}O/\ \delta^{16}O$) from the deep water Pacific Ocean core V19-30 was used to correlate with the high resolution Huon Peninsula sea-level record for the last 130 ka (Figure 4.1). There was a significant correlation between the two records up to coal reef VIIa (Isotope Stage 5e),

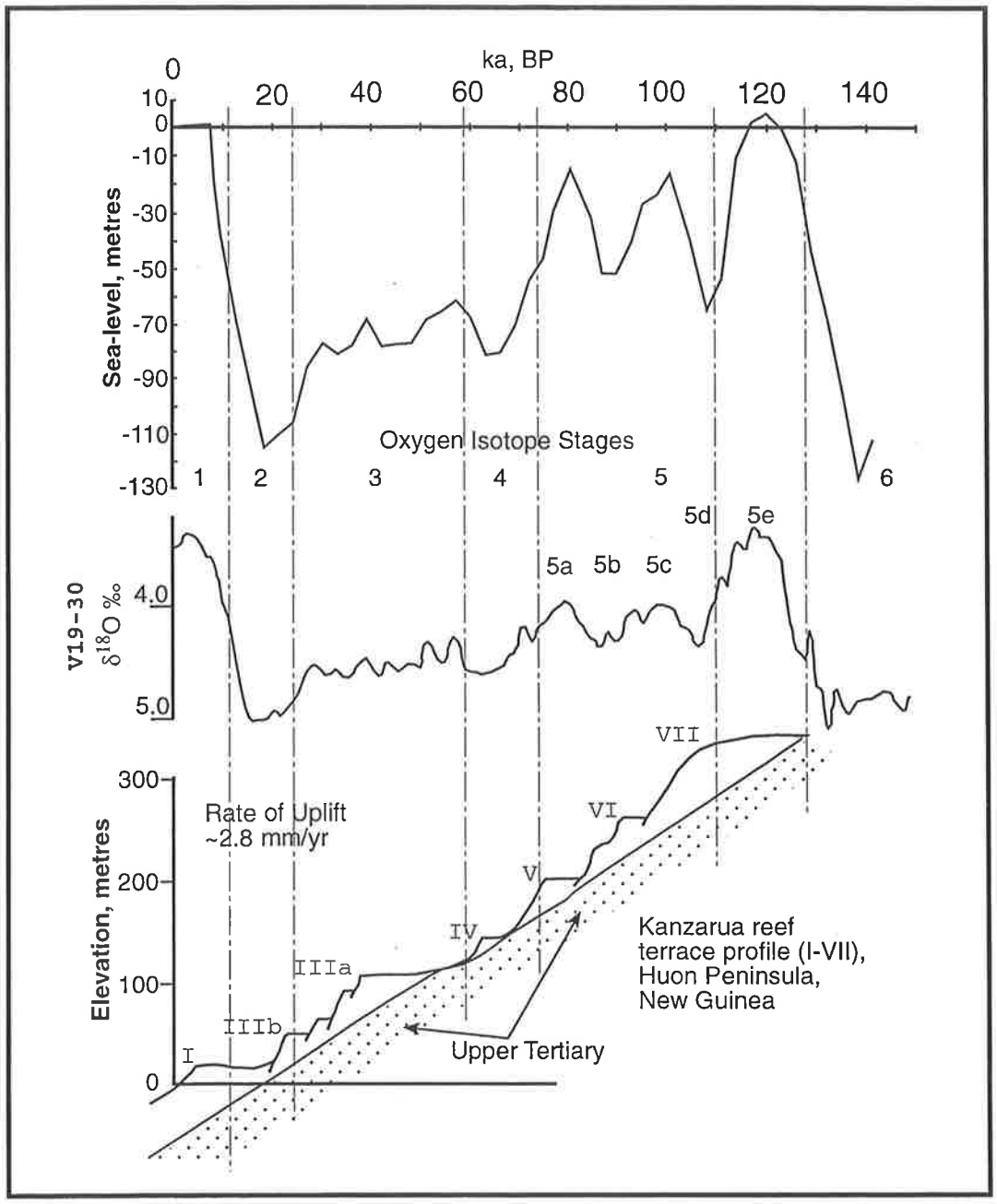



Figure 4.1 Sea-level, Oxygen Isotope and Uplft relationships, Huon Peninsula. Modified after Chappell and Shackleton, 1986 and Chappell, 1994.

after which the timing of the sea-level record is attenuated. This is possibly derived from experimental error and also due to averaging the timing of sea-level highs at each high stand event from the seven sections measured on the Huon Peninsula (Chappell and Shackleton, 1986). The recalibration of the timing of the sea-level high stands meant that the sea-level height variation was also modified because the rate of uplift had to be recalculated from the revised timing data. A new discrepancy resulted between the two curves (sea-level and isotope) from the recalibrations and it was surmised that the deep Pacific Ocean must have cooled more rapidly than predicted, to 0° C during Isotope Stage 4 (<110 ka), then to -1° C at 40 ka, with slow warming to 0° C by 18 ka and warming to the 1.5° C at the present day. Rapid expansion of the continental ice packs was also proposed as an alternate hypotheses, but further work is needed in this area to determine its veracity (Chappell and Shackleton, 1986).

Resurveying, resampling and redating the Huon Peninsula transects to higher standards of precision has resulted in the sea-level data correlating more closely with the deep sea benthic/ planktonic foraminifera oxygen isotope record ($\delta^{18}O/\delta^{16}O$) ie. the sea-level during the last glacial period (Oxygen Isotope Stage 2 to 5d) was lower than predicted in previous studies (Chappell, 1994).

Oxygen isotope ratios ($\delta^{18}O/\delta^{16}O$) can be determined from marine biogenic carbonate material found in sediments ie. molluscs, brachiopods, tests of foraminifera and other calcareous biota (Matthews, 1986). This gives the variation in the oceanic oxygen isotope ratios for a known environment. Benthic foraminifera, which are obtained from the cores of deep ocean sediments, provide the most accurate figures because of the slow and stable sedimentation rates. These values plotted against time reflect a history of eustatic sea-level change (Matthews, 1986). The ratios vary with the volume of isotopically light ice locked in the ice caps and ice sheets, ie. during the growth of ice sheets seawater becomes enriched in the heavier $\delta^{18}O$ and the ice sheet becomes enriched in the lighter $\delta^{16}O$ through evaporative fractionation of the isotopes. The vapour from this fractionation process becomes further depleted with respect to $\delta^{18}O$ as it condenses into rain or snow (Matthews, 1986). Planktonic foraminifera have not been used since the early 1980's because it has been found that they will be affected by variations in sea-surface salinity, seasonal growth structure and variable depth habitat (Chappell and Shackleton, 1986).

The Quaternary dates, sea-level and oxygen isotope data from the coral terraces and deep sea cores were presented as a series of graphs which were then correlated with each other. A close approximation of relative ocean volume and relative sea-level fluctuation for the Quaternary was established on a global basis (Figure 4.1). The values of the ratios presented range from 0.011‰ $\delta^{18}O/\delta^{16}O$ / metre of sea-level (Matthews, 1986) to 0.0097 ‰ $\delta^{18}O/\delta^{16}O$ / metre of sea-level (Chappell and Shackleton, 1986) and recently this figure has been refined by Chappell et al. (1996) to

0.009‰ / metre of sea-level. Although these values are reproduced as ratios on a m scale, in reality the ratios are beyond the precision level of mass spectrometers which typically produce significant values to two decimal places. Also these figures contain uncertain inaccuracies due to possible variations in $^{18}O$ depleted ice sheet, changing ocean water temperatures with the effect on the isotopic composition of benthic foraminifera and possible diagenetic alteration of foraminiferal tests (Plint et al. 1992). The above variations mask any significant difference between the $\delta^{18}O/\delta^{16}O$ ratio for seawater in the late Pleistocene and the present day.

Sea-level variation on a global scale has been summarised by various authors and perhaps the most complete overview is presented by Plint et al. (1992) where the mechanisms of sea-level change are discussed. These mechanisms relate to the changing volume of the Earth's oceans through:

- steric (thermohaline) changes;
- glacial build-up and melting;
- the amount of water retained on land in aquifers and lakes;
- crustal deformation including isostatic rebound and sedimentation which changes the shape and size of the containing sea-floor.

The question of Quaternary sea-level variation on a global scale is highlighted by the undulation in the Earth's geodetic sea-level. This can vary up to several metres in amplitude (Christie-Blick, 1990; Morner,1987a,b; Bowen, 1978). Variations in the geoid, which is a function of Earth's gravity, may be partially responsible for anomalous global sea-levels during the Holocene transgression. It was also suggested that "sea-level curves of global significance" were of limited value because of this variation, especially when coupled with variable global tectonism (Devoy 1987).

Pirazzoli (1991) also discussed the problem of erecting a global Holocene sea-level curve when tectonic movement, isostatic uplift/ subsidence from glaciation and changing patterns of the exchange of oceanic waters around the continents account for significant global sea-level variation. Tooley *Ed.*(1987) and authors therein, discussed late Pleistocene and Holocene sea-level variation at various localities in countries throughout the world. These discussions are not uniform, on a global level, in their treatment of Pleistocene and Holocene sea-level, although the latest details of research from nine major areas are presented. To highlight these variations, benthic marine molluscan assemblages in north-eastern Argentina have been used to correlate present day with mid-Holocene assemblages which indicated that the sea-level was 4-5 m above present MSL from 2500 to 6000 years BP (Aguirre, 1993). This is in contrast to coastal areas in Australia where sea-levels were below MSL during the same period (Hopley (ed), 1983; Chappell, 1987, amongst others)

Sea-levels for Australia during the Pleistocene and Holocene are discussed by Chappell (1987), where field examples for the Holocene sea-level rise are used from northern Queensland fringing coral reefs and prograding coast-lines in the Gulf of Carpentaria, and the coastal carbonate banks of the upper Spencer Gulf, South Australia. Late Pleistocene sites from Western Australia, South Australia, northern New South Wales and far northern Queensland are discussed. Most of the sea-level maxima from these sites range between 2 to 8 m for Isotope Stage 5e. The timing of Isotope Stage 5e and late Stage 7 has also been determined directly on cored marine sediments from the Bahamas by $^{234}U/^{230}Th$ dating and found to be 127-120 ka BP and 190-189 ka BP respectively (Slowey et al. 1996).

The 'global' relative sea-level window-curve has been modified to regional sea-level curves throughout the world, where the isostatic stability of the lithosphere in any given area is taken into account. Variations in coastlines from narrow to wide continental shelves gives rise to different rates of sea-level response when loaded with melt water ie during the Late Pleistocene and over the last 7000 years (Nakiboglu et al., 1983; Lambeck and Nakada, 1985 1992; Cloetingh et al 1986; Nakada and Lambeck, 1985). The isostatic rebound of the crust in response to glacial, seawater and erosional (sediment) unloading on a global and regional setting/environment is also confusing the sea-level variation derived directly from the melt water curve. This variation in subsidence and uplift (as rebound) has been shown to be dependent on the rheology and the flexural stresses of the Earth's mantle (Stephenson and Lambeck 1985; Nakada and Lambeck, 1988, 1989; Lambeck and Nakada, 1985). Western Australia and South Australia were chosen by Nakada and Lambeck (1989) as far field observation areas (areas at a considerable distance from possible sediment loading by glacial outwash during the disintegration of ice sheets) for determining the rheological response of the mantle to loading during the Holocene transgression. This enabled the possibility of separating the effective mantle response and the different rheological response between the upper and the lower mantle from the variable melting histories of the ice caps without the interference of tectonism.

### 4.2.1 AUSTRALIAN LATE PLEISTOCENE

Australian evidence for, and discussion on, Late Quaternary sea-level variation has been summarised extensively from field evidence of palaeo-shorelines and coral reefs which occur at many localities around the Australian coastline: Schofield (1971); Thom and Chappell (1975); Hopley (1983); Hopley and Thom (1983); Hails et al.(1984); Thom and Roy (1985); Thom and Hopley (1985); Chappell (1987); Buckley et al. (1987); Blom (1988); Murray-Wallace et al. (1988); Murray-Wallace and Belperio (1991); Belperio et al. (1995), amongst others. The variation in sea-levels from these localities range from -7 to +22 m above present sea-level. The age estimate for these sea-level highs, obtained from coral reefs in Queensland and Western Australia averages 125 ka, ie. Isotope Stage 5e (Chappell, 1987, Murray-Wallace and Belperio, 1991).

Veeh and France (1988) constrained the deposition of terrestrial phosphate derived from guano, and hence the timing of the present and last sea-level high to 4700 years and 120 ka (derived from coral reefs in the Pelsaert Reef Complex). Stirling et al. (1995) conducted precision dating on four late Pleistocene coral reefs in Western Australia and found the timing for the last interglacial sea-level high was between 127-122 ka, with a sea-level of approximately 2 m above present MSL. This interval indicates the timing of the major reef building event, but not necessarily the interglacial period itself ie. 130- 117 ka. Late Pleistocene sea-level evidence (Woodroffe et al., 1995) from Lord Howe Island indicates the timing of Isotope Stage 5e to be a mean of 136 ka using $^{234}U/^{230}Th$ discontinuous series dating and between 138 ka and 116 ka using thermoluminescence dating. The sea-level at this time was approximately 1.5 m above present day MSL (Woodroffe et al., 1995). Field evidence of the late Pleistocene sea-level is found in the Warrnambool-Port Fairy district of western Victoria (Gill and Amin, 1975). Flat lying Miocene marine strata has been eroded and a low cliff line, with a shelly conglomerate at the base, has been preserved. The shells, found within the conglomerate, which is 7.5 m above present MSL, yielded $^{234}U/^{230}Th$ dates of around 125 ka. A date from a marine gastropod (*Subninella undulata* sp.) found on a secondary terrace at +3.6 m MSL indicated that this terrace was possibly formed during Isotope stage 5d or 5c (Gill and Amin, 1975).

### 4.2.2 South Australian Pleistocene

The evidence for late Quaternary relative sea-level rise in South Australia has been discussed and summarised by Howchin (1888); Schwebel (1978); Burne (1982); Belperio et al. (1983); Belperio et al. (1984); Hails et al. (1984); Buckley et al. (1987); Belperio (1988); Belperio et al. (1988); Murray-Wallace et al. (1988); Short (1988); Cann et al. (1993); Belperio (1995); Daniel et al. (1998); Harvey et al. (1999).

The timing and variation in the sea-level high stand along the South Australian coast during the Pleistocene has been constrained by a series of late Pleistocene dates taken from samples of the Glanville Formation found in the southeast to the west coast of South Australia. The dating techniques used were primarily amino acid racemisation (AAR) (Belperio et al., 1984; Murray-Wallace et al., 1988, 1991, 1993; Murray-Wallace and Belperio, 1991; Wilson, 1991) and $^{234}U/^{230}Th$ discontinuous series (Schwebel, 1978; this study) with sporadic thermoluminescent dating (Belperio et al. 1984; Wilson, 1991).

A lateral equivalent ("upper member of the Bridgewater Formation") of the Glanville Formation in the southeast of South Australia was dated by Schwebel (1984), who suggested an $^{234}U/^{230}Th$ age of 125 ka ±20 ka BP, based on $^{234}U/^{230}Th$ dating of mollusc shells and 100 ka ±30 ka BP dating of aragonitic mud from the lagoonal facies of the "member". This timing has been the primary datum for AAR

research and has subsequently enabled the results of this research from the late Pleistocene to be correlated to an absolute time scale, and to create an AAR time scale. The AAR research has been mainly carried out by Murray-Wallace (1988, 1991, 1993) and to a lesser extent Belperio (1984) and Wilson (1991). The timing, as then applied to various sites in South Australia, has revealed a common age for the deposition of the Glanville Formation at approximately 125 ka BP. These localities are: Dry Creek; Port Wakefield (near Adelaide) and Denial Bay with interstadial marine deposition sites in Gulf St Vincent (Figure 2.1).

Late Pleistocene sea-level heights have been reported as having an average elevation of +2 m MSL, but clearly presented evidence for this height in South Australia is not generally common. The evidence of Stage 5e sea-level elevation ranges between -0.25 m and 1.25 m when corrected for an uplift rate of 0.07 mm/year for the Pleistocene section in the southeast (Robe to Naracoorte) of South Australia (Murray-Wallace and Belperio, 1991; Belperio, 1995) A sea-level of +3 m MSL is indicated by the shoreline facies of the Glanville Formation that is present in the Port Wakefield area of Gulf St Vincent (Belperio, 1995). An approximate sea-level of +2 m MSL, is indicated by flat lying intertidal facies of the Glanville Formation at Fowlers Bay on the western Eyre Peninsula (Murray-Wallace and Belperio, 1991). A direct comparison of Late Pleistocene with present day sea-level is possible, using coastal outcrops of the Glanville Formation and adjacent beach morphology, at Streaky Bay (Section 4.3).

The interstadial maximum sea-levels in Gulf St. Vincent has varied from -8 m during Isotope Stage 5c (Hails et al., 1984) to a low of -28 m during Isotope Stage 3 (Cann et al., 1993; Murray-Wallace et al., 1993). The sea-levels and timing, during Oxygen Isotope Stage 3 from the Gulf St Vincent, were used to refine the Huon Peninsula data for the same period. The high sea-level was determined to be approximately -40 m for the Huon Peninsula transgressive stage IIIb (Chappell and Shackleton, 1986) and has subsequently been refined to -24 m (Cann et al. 1988) and -27 m (Cann et al. 1993). The timing of the sea-level high (Stage 3)in the Gulf St. Vincent was refined by AAR and found to be 46.5 ka BP (Murray-Wallace et al., 1993). A sea-level high for either Stage 5a or 5c is indicated by an extensive submerged coastal terrace (ultimate terrace) at Streaky Bay. The terrace, which is interpreted as a near-shore littoral terrace, has an elevation between 12 m and 14 m below MSL. This depth correlates with shallow marine conditions at either the interstadial of 100 ka or 80 ka.

### 4.2.3 Holocene Sea-Level

A graphic plot compiled of radiocarbon dates (<17 ka) versus elevations acquired from many sources (Newman, 1986) on a world-wide basis demonstrated the difficulty in constructing a meaningful global Holocene sea-level curve (Stanley, 1995). The elevations in this plot varied, with a maximum

variation at approximately 10 ka, from –120 m to +200 m (Figure 4.2). Also highlighted was the sea-level rise curve from the Netherlands against the sea-level fall curve from the St. Lawrence river and gulf area. These curves are practically mirror images of each other and thus lead to the author's qualification in the title; ".....: the impossible dream?" (Stanley, 1995) (Figure 4.2). However when only dates and sea-levels are graphed from inferred tectonically stable areas, the scatter curve shows a relatively fast rise of sea-level from -90 m to -10 m (17 ka to 8 ka BP) with a gradual rise from -10 m to present MSL ie. 8 ka BP to the present ( Stanley, 1995) (Figure 4.2). The above two figures demonstrate the differences between relative and absolute sea-level and the difficulties in establishing an absolute sea-level curve for any region.

### 4.2.4 AUSTRALIAN HOLOCENE

Sea-levels and timing for Australia during the Holocene are discussed by Chappell and Polach (1991), Pirazzoli (1991), Chappell (1987), Hopley and Thom (1983), Thom and Roy (1983) amongst others. It must be stressed that sea-levels are being discussed in local context and as such are relative sea-levels rather than absolute. The significant of hydro-isostatic flexure has not been fully ascertained over many areas incorporating the data sets. Field examples for the mid-Holocene sea-level highstand are used from northern Queensland fringing coral reefs (~6 ka BP, maximum +1 m) and prograding coast-lines in the Gulf of Carpentaria (~6 ka BP at least +2 m ), and the coastal carbonate banks of the upper Spencer Gulf, South Australia (early Holocene max +3 m).

Examples from Western Australia indicates early Holocene sea-levels of up to +2.5 m occurred about 6400 years BP, after which the relative sea-level fell to approximate present day MSL then rose ~1.5 m between 3100 and 2200 years BP. A 'window curve' for south eastern Australia has been presented by Thom and Chappell (1975) which is a compilation of over 20 points from the coast of northern New South Wales to western Victoria. The sea reached the present MSL at approximately 6500 years BP and rising to ~+1.5 m by 6000 years BP (Thom and Chappell 1975). A high resolution sea-level curve that is the result of a compilation of 364 radiocarbon dates is presented for the central Great Barrier Reef shelf by Larcombe et al. (1995) (Figure 4.3) . This curve also incorporates sample elevation data of Thom and Roy (1983) and Chappell and Polach (1991) and shows an episodic sea-level rises from 10 ka to 5.5 ka with a double sea-level paracycle between 8.5 -8.2 ka BP.

### 4.2.5 SOUTH AUSTRALIAN HOLOCENE

The onset of Holocene marine sedimentation, as represented by the St Kilda Formation, has been dated by Belperio (1995) at 6460 ±170 years BP at elevations close to present MSL. Research at Tourville Bay, Eyre Peninsula (Belperio et al. 1988) indicated that seagrass meadows actively commenced growing approximately 6800 years BP at a depth of 4 to 5 m below present MSL. The timing of the onset of seagrass development was determined by the radiocarbon dating of seagrass

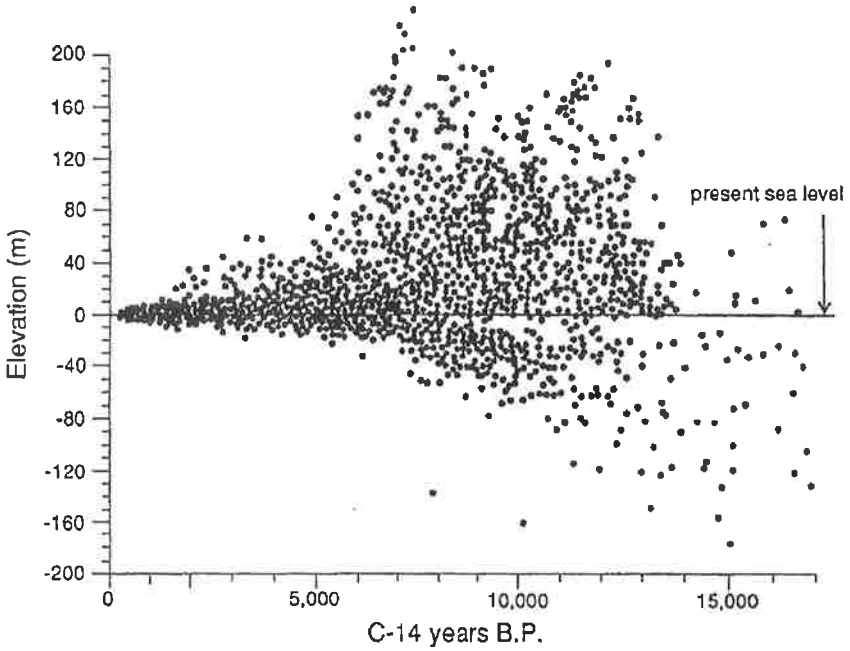



Figure 4.2a. "Graphic plot, compiled from many soursces on world basis, depicting samples dated for the past ~17,000 years and their elevations plotted above and below present sea level." (from Stanley 1995)

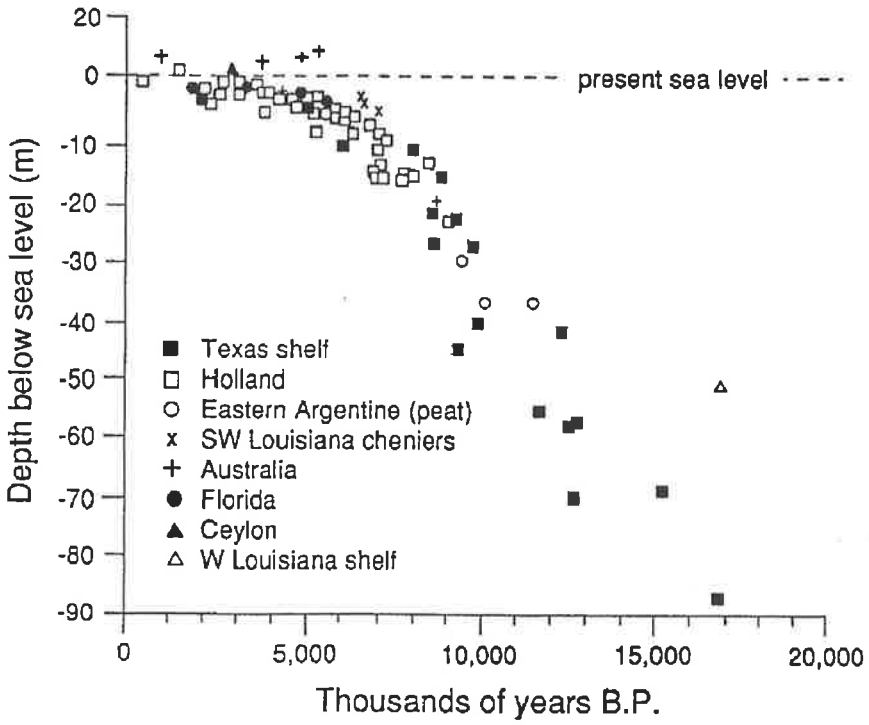



Figure 4.2b. "Example of a global sea-level curve compiled to depict eustatic rise, using radiocarbon -dated samples collected from inferred stable areas that are presently submerged." (from Stanley, 1995)

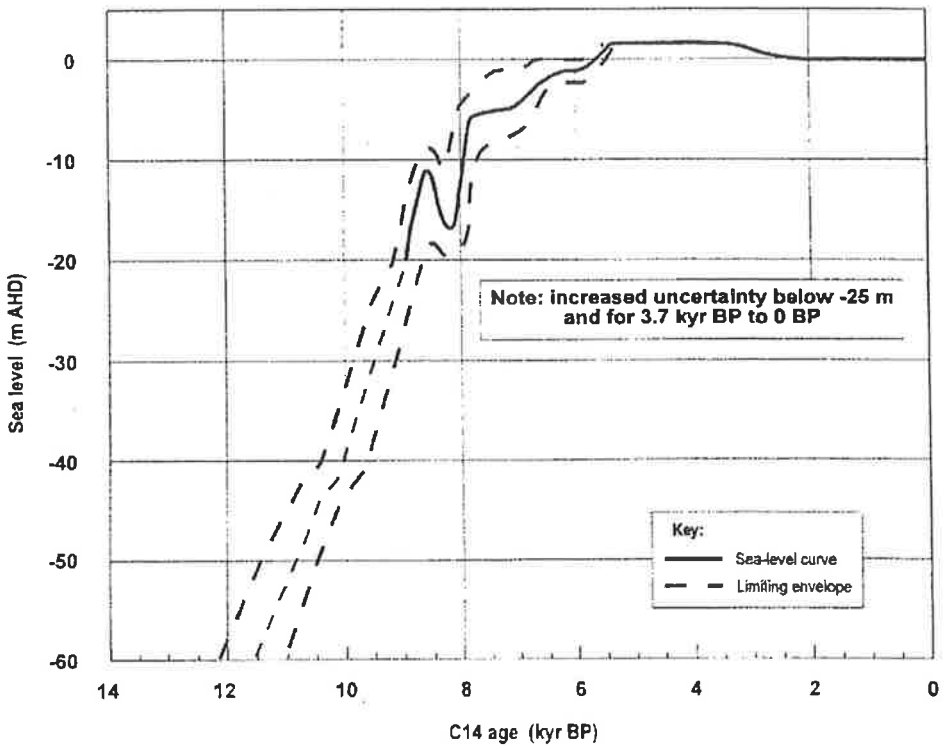



Figure 4.3. High resolution mean sea-level curve for the Holocene of the central Great Barrier Reef, Queensland. The sea level curve is represented by the solid line with limiting values (dashed lines). (Larcombe et al., 1995, p. 27.)

fibres found near the base of several vibrocores, which were drilled in a transect across Tourville Bay. Sea-grass fibres in basal Holocene marine sediments have been dated from the upper Spencer Gulf at Redcliff and at Port Pirie and are found to have an average age of 6300 years BP and 6700 BP respectively (Belperio, 1995; Harvey et al., 1999). This indicates that the marine facies of the St Kilda Formation was well developed by this time. The approximate elevation of the sampled intervals, range from 0 m to 3 m below the Low Water Datum (LWD) or approximately 1-4 m below MSL, see general Holocene sea-level curve for South Australia (Figure 4.8).

A relative fall in sea-level, in the southeast of South Australia, of approximately ~1 m since the early Holocene, is the result of coastal uplift (Belperio, 1995). A resultant fall in sea-level of approximately 0.5 m is indicated from the early Holocene to the present when this fall has been corrected for the general rate of uplift in the area (0.07 mm/yr). The west coast of the Eyre Peninsula is considered to be tectonically stable (Nakada and Lambeck,1989) so that any variation in relative sea-level can be viewed as a variation in ocean volume due to climatic change (Belperio et al., 1983, 1988). A summary of uncorrected heights of early Holocene sea-level maxima in South Australia is shown in Table 4.1. The curve of sea-level rise in South Australia is drawn as a series of straight lines from known points of time and elevation due to the paucity of Holocene sea-level data. For this reason Short (1988) proposed a series of evolutionary morphostratigraphic shoreface types to typify the Holocene transgression.

They are categorised under a seven shoreface types (scheme) (prograding to eroding) with up to four primary steps in their evolution from 10 ka to the present (Short, 1988). These models are based on the Holocene sea-level highstand beginning approximately 6.5 ka BP. Before this time, abundant sediment had been transported from the continental shelf to provide material for the high energy dune systems, infilling of interdunal depressions and forming prograding barriers. During the mid to late Holocene the supply of sediment from the shelf was exhausted and sediment from the erosion of sea-cliffs and dunal ramps supplied material at a reduced rate to the now stabilising dune systems. The interdunal and back barrier depressions were the loci for beach ridges, tidal flats and cheniers, behind which limited mangrove forests colonised suitable intertidal environments (Short, 1988).

## 4.3 RESULTS

### 4.3.1 MID TO LATE PLEISTOCENE SEA-LEVEL DETERMINATION

Significant outcrops of Glanville Fm occur at Acraman Creek, Point Gibson, Perlubie Beach, and a disturbed outcrop at the southern end of Blanche Port in the Streaky Bay township.(Figure 2.3).

### 4.3.2 FLAGSTAFF LANDING SECTION

The Flagstaff Landing section just to the east of Acraman Creek on the northern margin of Streaky Bay (S32° 43' 26.4", E134° 06' 57.6") (Figure 2.3). A low cliff, up to 8 m high immediately west of Flagstaff Landing shows a marginal marine facies section of the Glanville Formation. Figure 4.4 depicts the Glanville Formation lying unconformably on a calcrete of the Bridgewater Formation and is now limited by the calcretised upper section of the Glanville Formation.

The thickness of the formation varies from 4 cm, higher in the cliff section, to ~80 cm at the base of the cliff. It grades up slope from cobble sand with whole to coarse bioclasts and cobbles of reworked calcrete to a bioclastic fine sand where the formation thins to 4 cm. The formation has a micritic matrix, which is possibly contiguous with the overlying calcrete bed or the result of the breakdown of coralline algae and bryozoans. Also present in this fauna are the species *Goniopora somaliensis*, *Anadara trapezia* and *Marginopora vertebralis*.

A transition from fine-medium sand to coarse sand grainsize is seen in the more elevated part of the formation (Point a, Figure 4.4). This grades to a very coarse-coarse sand into a gravelly sand transition zone (point b). The grainsize further coarsens along the section where the gravel in the sandy sediment has increased to cobble size (Point c).

**• Modern Day Beach Profile**

The nearby present day beach profile is shown in the inset of Figure 4.4. The beach is of an intermediate to reflective type (Short et al. 1986), which indicates a low to moderate energy environment. A change in grainsize occurs point d (Inset, Figure 4.4). This marks the transition from the upper beach slope to the proximal dune environment and marks the transition from a wave dominated to a wind dominated transport mechanism.

The present limit to the high tide swash zone (point e) is delineated by the lower limit of a thick ribbon of seagrass debris present on the beach and also by a change in grainsize from gravelly coarse sand to coarse sand.

The elevation difference between these two points, ie. the modern day and Glanville Formation profiles, is 1.77 m.

### 4.3.3 POINT GIBSON SECTION

This Glanville Formation outcrop is situated approximately halfway between Point Gibson and Cape Bauer on a low slope leading down to the shore (S32° 27' 27.7"; E134° 07' 51.6") (Figure 2.3). The Glanville Formation, at this site, appears to be an onlap deposit overlying the calcrete and aeolianite of the Bridgewater Formation (Figure 4.5). The Glanville Formation is represented by a medium to fine bioclastic sand with a marine molluscan fauna, particularly the bivalves *Anadara trapezia* and

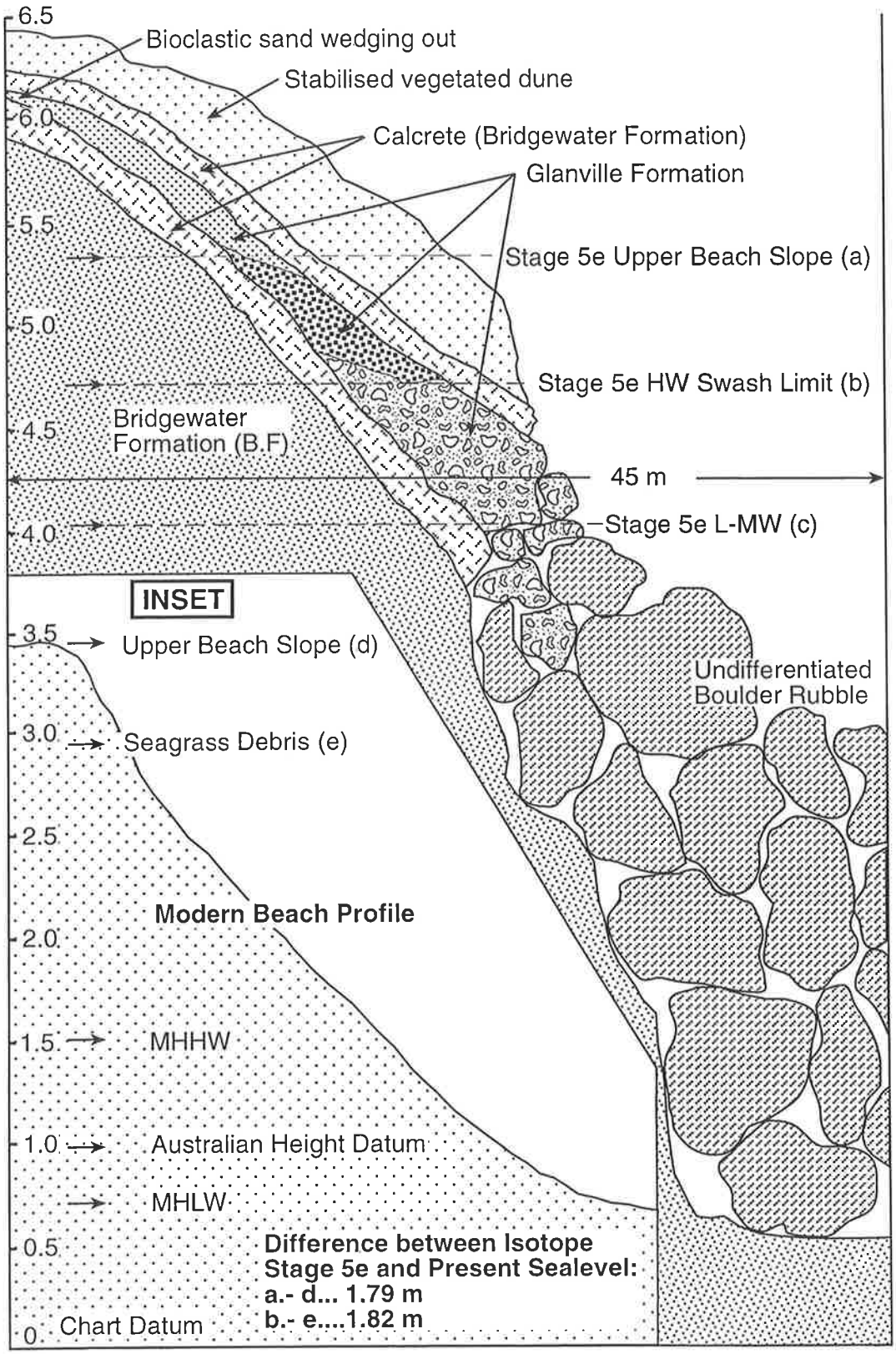



Figure 4.4 Height comparisons of similar morphologies between the Glanville Formation (Isotope Stage 5e) and an adjacent modern beach , results in a height difference of ~ 1.8 m. This indicates the sea-level was ~1.8 m higher during Isotope Stage 5e. Flagstaff Landing, Streaky Bay

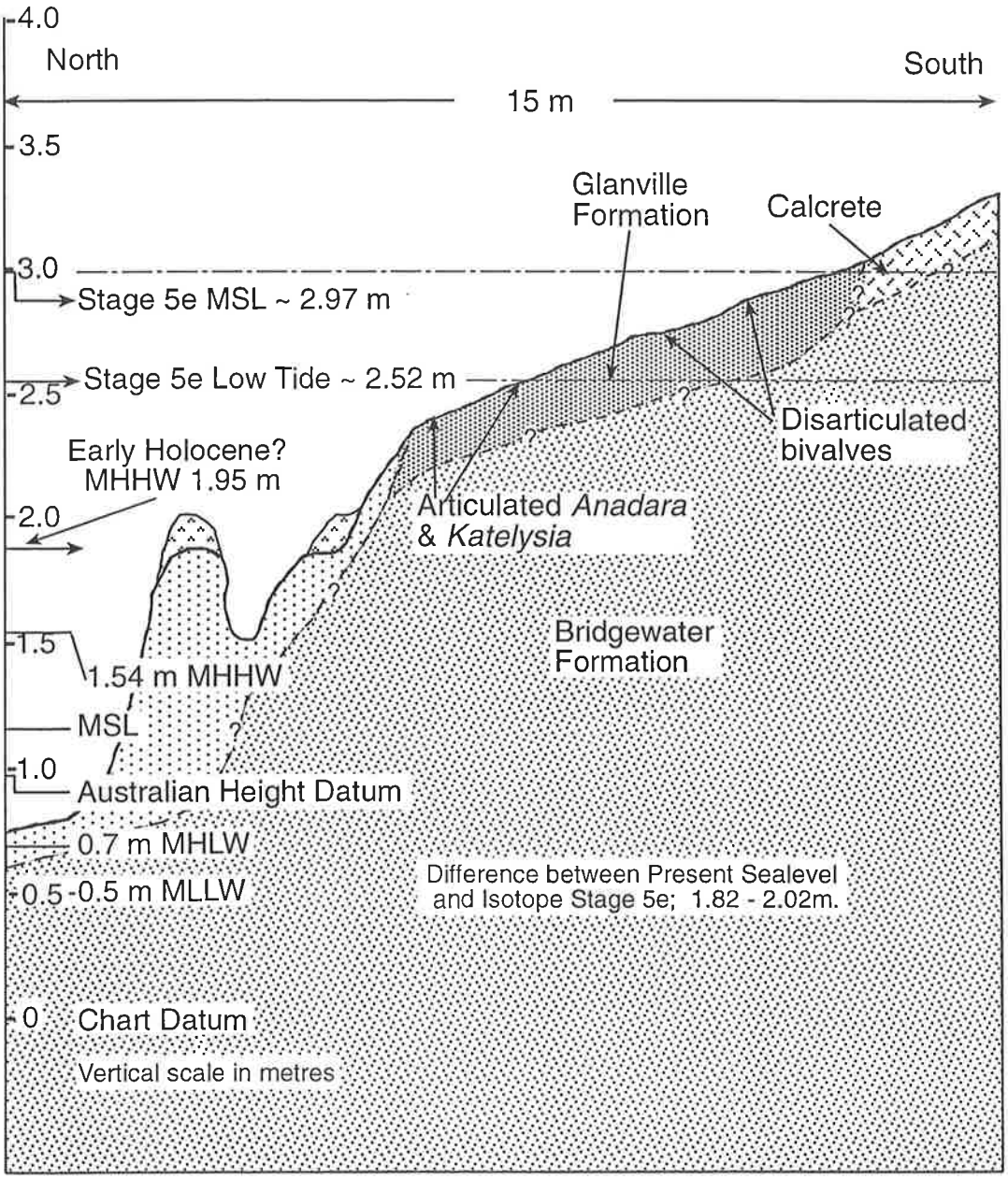



Figure 4.5 An estimate of low tide in a section of the Glanville Formation is based on the habitat of *Anadara trapezia* and *Katelysia scalarina* (minimum low tide). This is compared with the Mean Low Low Water mark of present day. The difference ranges from 1.82 m to 2.02 m, indicating that sea-level during Isotope Stage 5e averaged 1.9 m above that of present day. Point Gibson, Streaky Bay.

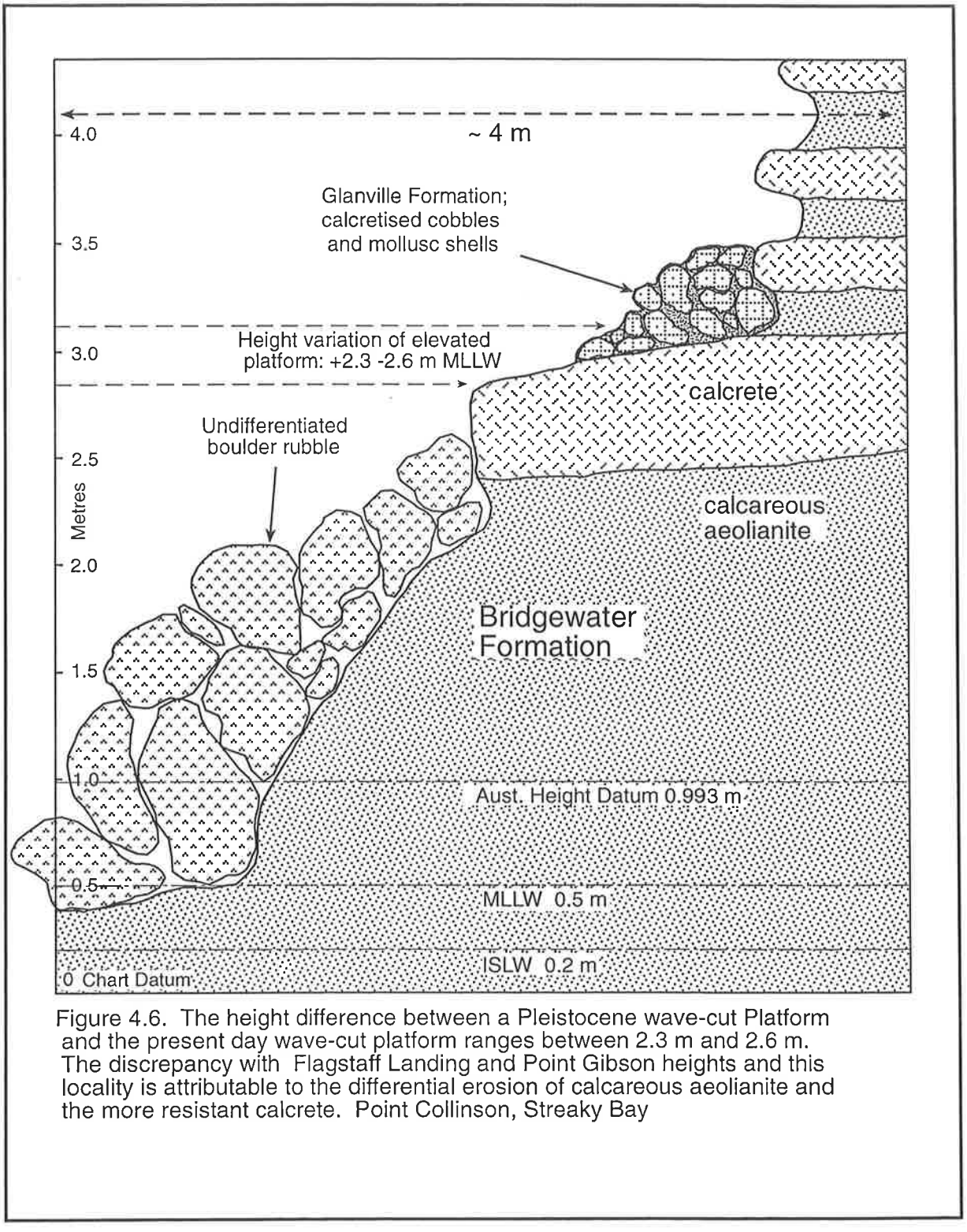



Figure 4.6. The height difference between a Pleistocene wave-cut Platform and the present day wave-cut platform ranges between 2.3 m and 2.6 m. The discrepancy with Flagstaff Landing and Point Gibson heights and this locality is attributable to the differential erosion of calcareous aeolianite and the more resistant calcrete. Point Collinson, Streaky Bay

*Katelysia rhytipora*. These are present, in some instances, as articulated forms in the lower part of the outcrop. These articulated forms can be used to delineate the approximate height of the High Low Water mark during the time of the deposition of the sediments in the Glanville Formation. This is based primarily on the observation of the habitat of present day *A. trapezia*, which is found living in estuarine and muddy substrates on the east coast of Australia just below the High Low Water mark (Ludbrook 1984).

The average difference in height between the Pleistocene and modern day High Low Water marks is 1.82 m.

### 4.3.4 Point Collinson Pleistocene Wave cut Platform

Point Collinson is located on the north western coast of Streaky Bay, (Figure 2.3) (Location; S32° 32' 26", E133° 53' 34"). The cliffs at this site are up to 10 m and consist of interbedded aeolianite and calcrete beds of the Bridgewater Formation. The height of the stepped cliff, at the site chosen for the survey, is approximately 5 m (Figure 4.6). The presence of a Pleistocene wave-cut platform was determined by the occurrence of an overlying 30-50 cm thick , cobble sediment which has been cemented by calcrete. The cobble-sized grains are composed of rounded calcareous aeolianite and calcrete. Whole, pristine to abraded valves of *A. trapezia* and other bivalves (*Katelysia sp.* and *Pinna sp.?*) are found in the finer grained sediment between the cobbles (Short et al., 1986; Buckley et al., 1987; pers. obs., 1995). It most probably represents a platform cut during either Isotope Stage 5e or Stage 7 (Short et al., 1986; Buckley et al., 1987). The age of the sediment cemented on the platform was further determined to be Pleistocene by $^{14}C$ dates obtained from shells present in the sediment. The shells had an age of > 40 ka and were interpreted to be approximately 120 ka (Isotope Stage 5e), based on established data of sea-level highstands for the late Pleistocene (Buckley et al., 1987).

- **Modern-day Wave-cut Platform**

It was possible to delineate the present day wave-cut platform during the survey as the tide was near low tide (NTF Tidal Data). The tide was approximately 20 cm above the platform at the time of the survey and the sea was dead calm. This also allowed limited access to the platform to measure the differences between the two platforms (Figure 4.6).

The range of differences between the two platforms was between 2.6 m - 2.3 m and averaged 2.46 m.

### 4.3.5 Timing Of Glanville Formation Deposition

The timing of the Glanville Formation sediments was determined using $^{234}U/^{230}Th$ discontinuous series radiometric dating on a colonial coral, which is found in the Glanville Formation that outcrops at Flagstaff Landing and in a costean at Acraman Creek. Large fragments (< 6 cm) of the coral are

found as allochthonous, fresh fragments to abraded pebbles throughout the Glanville Formation at these two localities. XRD analysis on fresh coral showed that the coral was composed entirely of aragonite. The lack of calcite in the coral indicates that it had not undergone any post depositional diagenesis and that the data from the analysis are based on original carbonate. The coral was identified as *Goniopora somaliensis,* which is restricted in distribution today to the areas north of Moreton Bay in southern Queensland and Ningaloo Reef in Western Australia (J. Veron; pers. com. 1996, Veron, 1986).

The result of the radiometric dating on the coral in the Glanville Formation was 124±9 Ka BP.

### 4.3.6 Evidence For Quaternary Interstadial High Sea-Level

There is little evidence in the Streaky Bay area of the high sea-levels of Isotope Stages 5a, 5c, 4 or 3. Although the author has speculated that the broad terracing in the mid- to outer portion of the bay may be a result of near-shore littoral abrasion during Isotope Stages 5a and 5c which would coincide with shallow waters over the terrace at these times (Figure 4.7). This terrace is up to 7 km wide and varies marginally from 12 m. to 14 m (±1 m) water depth. It may also be the result of littoral abrasion during a "double sea-level paracycle" in the sea-level curve in the mid Holocene. Abundant evidence of this paracycle is found in mangrove muds, intertidal shells and palaeosols of the mid-northern Queensland coast and micro-atolls of the Great Barrier Reef. This paracycle occurred from 8.5 to 8.2 ka and between 16 and 12 m AHD (Larcombe et al. 1995)

### 4.3.7 Evidence for Early Holocene Sea-Level High Stand

Evidence of the early Holocene high stand may be present in the Point Gibson area where the present high tide levels are 50 to 60 cm below the present day supra-tidal flat (Figure 4.5). Holocene, medium to coarse bioclastic sands, which are capped with 10-20 cm of organic soil, are found at this location (S32° 27' 27.7", E134° 07 ' 51.6"). This soil contains very coarse sand to fine gravelly shells and calcrete clasts. The underlying medium to coarse bioclastic sands are similar to those found in the present-day tidal zone and it is speculated that the top of these coarse bioclastic sediments (~40 cm above MSL) represents similar proximal shoreline deposits of the early Holocene. This shoreline, based on the Carbon 14 dated shell from the central IMB would be been present from ~7.2 ka BP.

### 4.3.8 Commencement of Early Holocene Shallow-Water Sedimentation

The beginning of the Holocene deposition of shallow water environment infilling-sediments has been determined by $^{14}C$ dating as beginning 6800 years BP. at Tourville Bay, near Ceduna (Belperio et al., 1988). Carbon 14 dating at Streaky Bay (Table 4.2) indicates that slightly deeper water (~12 m below present MSL) sedimentation commenced in the central inner marginal basin at least 7300 years BP

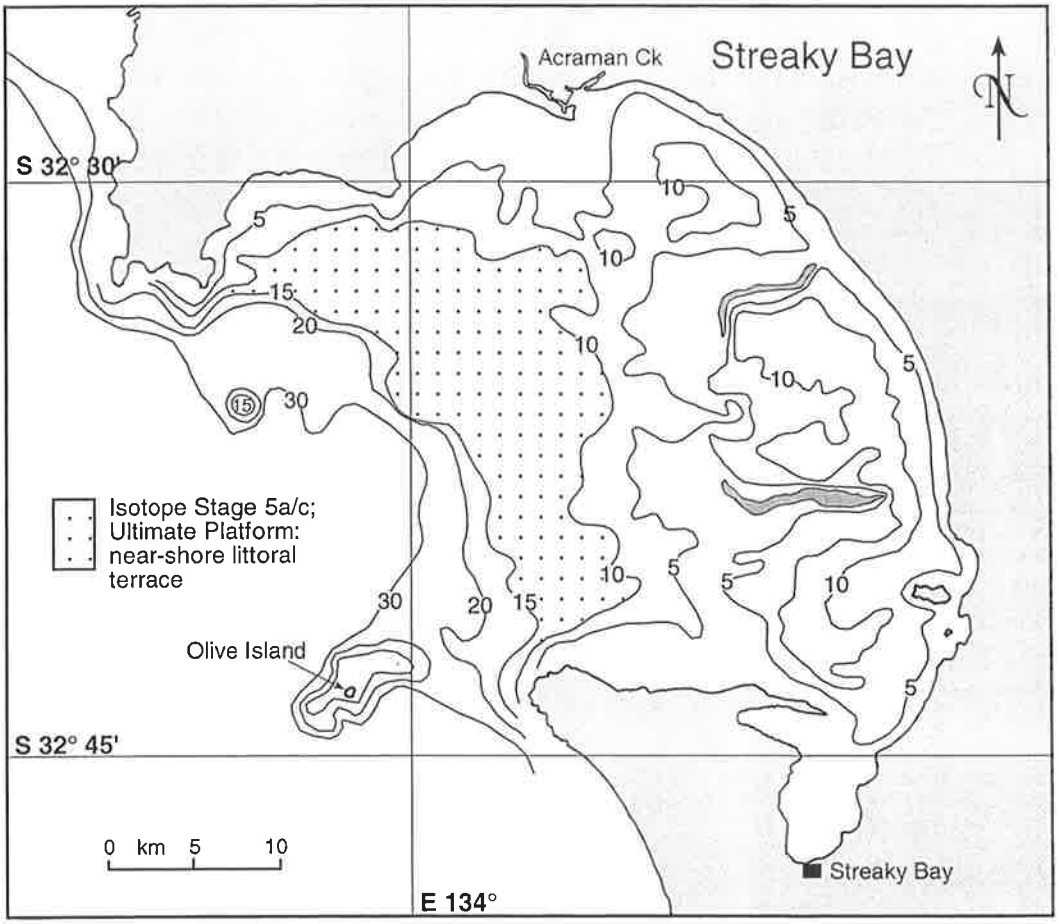



Figure 4.7 The sea-floor terrace in the outer bay is covered with 10 m - 15 m of sea-water. This depth represents an shallow littoral abrasion zone during Isotope Stage 5a-c when the sea-level was approximately 12 m below present MSL.

(Figure 4.10). However, marine access for the sedimentation in the inner basins was through either of the three existing channels. These vary in depth from 3 m to 8 m at the present. The date was determined by AMS $^{14}C$ dating technique (Sample No. OZB909U, ANSTO, Table 4.2) on an articulated valve of *Tellina victoriae* from a gravity core (SBGC No. 1, depth - 54 cm ) taken in the central inner marginal basin (Figure 4.9).

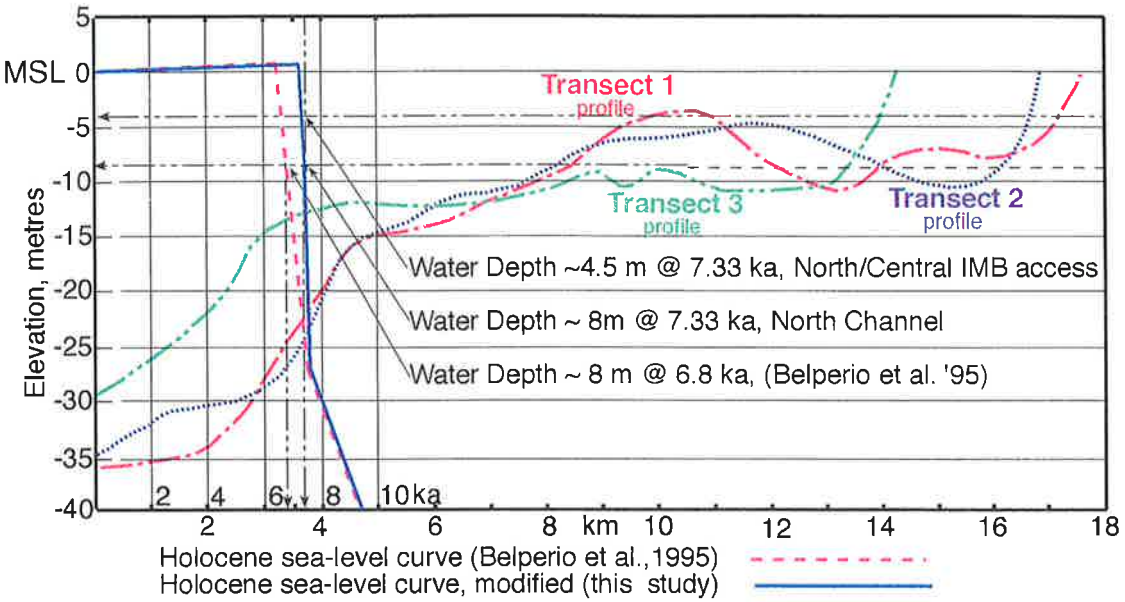



Figure 4.8 Sea-floor profiles of Streaky Bay compared with the timing of the South Australian Holocene sea-level rise. Lowest sea-water entry point to the inner marginal basins is via the northern channel at -8 m MSL. This represents a minimum level as the Bridgewater Formation is being actively eroded in this channel. The central and southern channels have a soft sediment base so the channel floors maybe higher at present than in the early Holocene. The access channel around North Bank from the northern to the central IMB is 4.5 m deep which represents the maximum sea-level for marine conditions to establish in the central IMB . Carbon 14 dating of an articulated shell (from a gravity core 54 cm below the sediment/water interface) in the central IMB suggests that marine conditions were established by 7.33 ka. When this figure is included in the esta blished sea-level curve of (Belperio et al.,1988) at either -8m or -4.5m, the timing for the Holocene high stand is approximately 7.2 ka. The 40 cm rise above present MSL depicted in the early Holocene is derived from Belperio et al. (1988) and speculative observations of coarse bioclastic sediments (top ~40cm above MSL) covered by soil creep on Point Gibson, Streaky Bay.

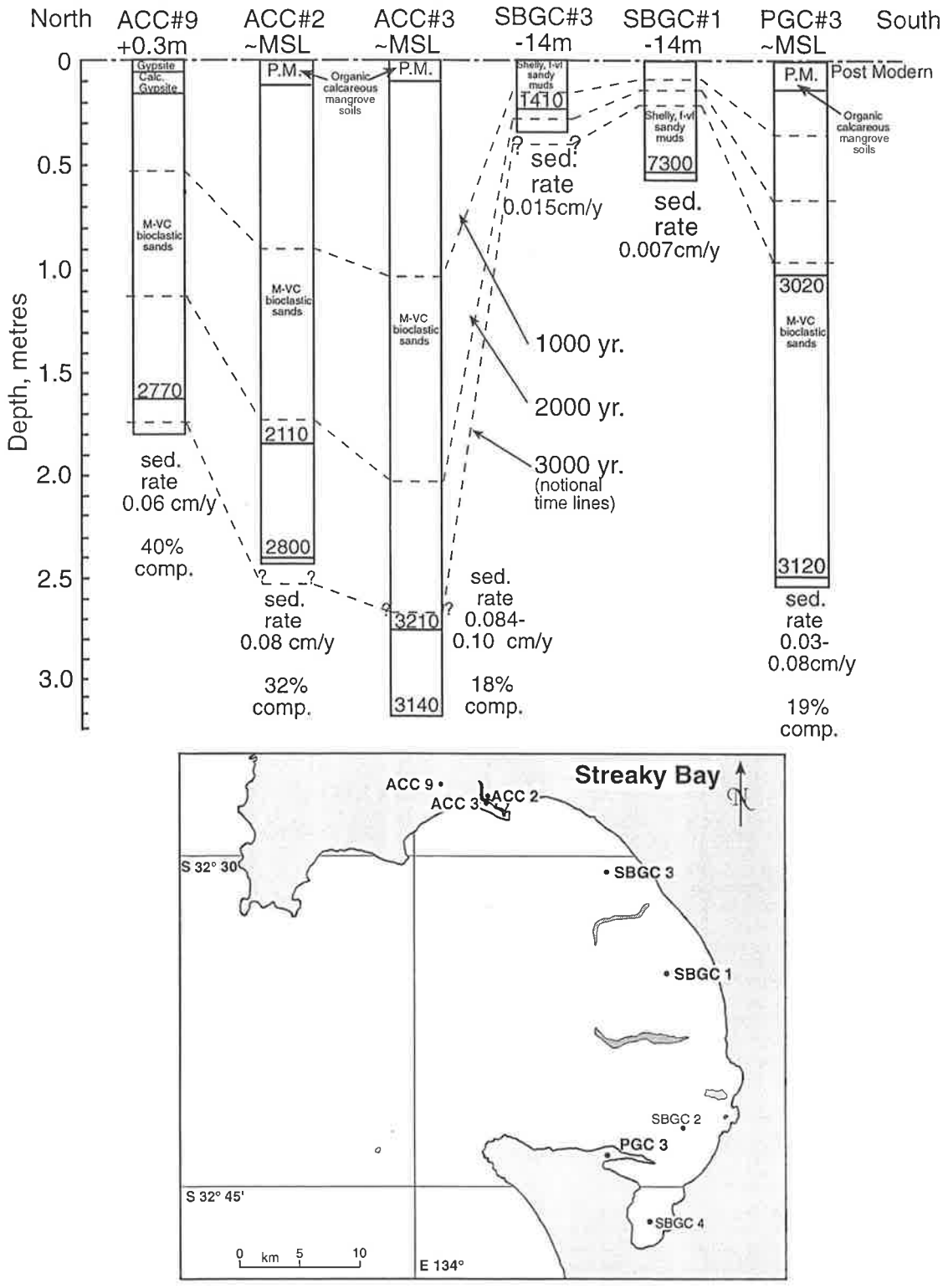



Figure 4.9 Holocene sedimentation rates and core locations. Sedimentation rates ranges from 0.26 cm/yr to 0.39 cm/yr at the spits (Point Gibson and Point Lindsay) and 0.007 to 0.13 cm/yr in the inner marginal basins. Depth and age of sediment cored at the spits was 325 cm (3190 yr BP) at ACC No. 3 (North) and 255 cm (3490 yr BP) at Point Gibson (South). Maximum age of sediment sampled in the IMB was 7550 yr BP , central basin. 1000 yr notional time lines highlight the variability of sedimentation rates.

| Streaky Bay ID & Description | Elevation ~MSL m | ANSTO CODE | $\delta C^{13}$/ ml ANU lab. | % Modern Carbon | | Conventional $C^{14}$ Age* | |
|---|---|---|---|---|---|---|---|
| | WD; water depth | AMS Dating, 1995 | | % PMC | 1 σ error | Age (BP) yrs | 1 σ error yrs |
| **1** Seagrass fibre, ACC#2 | -1.65 | OZB905U | -12 est. | 67.8 | ± 0.66 | 2800 | ±130 |
| **2** Seagrass fibre, ACC#2 | -1.25 | OZB906U | -12 est | 73.5 | ± 0.52 | 2110 | ±120 |
| **3** Seagrass fibre, PGC#3 | -2.03 | OZB907U | -8.4 | 64.5 | ± 0.47 | 3120 | ±130 |
| **4** Seagrass fibre, PGC#3 | -0.82 | OZB908U | -12 est. | 66.6 | ± 0.77 | 3020 | ±110 |
| **6** Seagrass fibre, PGC#3 | -0.16 | OZB910U | -12 est. | 117.5 | ± 0.30 | post-modern | |
| **8** Seagrass fibre, ACC#3 | -2.35 | OZB912U | -12 est. | no data | | 3210 | ±120 |
| **9** Seagrass fibre, ACC#3 | -2.51 | OZB913U | -12 est. | no data | | 3140 | ±130 |
| **10** Seagrass fibre | -0.16 | OZB914U | -12 est. | 105.0 | ± 0.75 | post-modern | |
| | | | | | | | |
| **5** Shell , SBGC#1 | -14.54 ~14m WD | OZB909U | +0.2 | 38.4 | ± 0.20 | 7300 | ±110 |
| **7** Shell , SBGC#3 | -14.22 ~14m WD | OZB911U | - 0.3 | 79.5 | ± 0.33 | 1410 | ±110 |
| *Corrected for marine reservoir effect, South Australian open waters (average 400±110 yrs) (Bowman and Harvey, 1983; Belperio, 1988, Harvey et al,. 1999) | | | | | | | |

**Table 4.2.** Results of 14 C analyses performed at ANSTO 1995. The ANSTO laboratories were not able supply 13 C data and results that were returned from the ANU proved to be anomalous. The 13 C results for the shells were obtained from the stable isotope mass spectrometer at the Dept of Geology and Geophysics, Adelaide University. Unfortunately all the seagrass samples were used for the AMS dating procedures so a marine plant average for $\delta C^{13}$/ ml of -12 was applied.

| Streaky Bay ID & Description | Elevation ~MSL m | CSIRO CODE | $\delta C^{13}$/ ml | % Modern Carbon | | Conventional $C^{14}$ Age* | |
|---|---|---|---|---|---|---|---|
| $CO_2$ Absorption Conventional Dating, 1998 | | | | % PMC | 1 σ error | Age (BP) yrs | 1 σ error yrs |
| SBC 9 Shell ACC#9 | -0.67 | CS1458 | -0.3 | 67.4 | ± 1.8 | 2770 | ± 230 |
| *Corrected for marine reservoir effect, South Australian open waters (average 400±110 yrs) (Bowman and Harvey, 1983; Belperio, 1988, Harvey et al,. 1999) | | | | | | | |

**Table 4.3.** Results of 14 C analysis performed at CSIRO Land and Water, Adelaide

### 4.3.9 Late Holocene Depositional Phase (Commencement of Rapid Deposition)

The $^{14}C$ AMS dates from marine and estuarine sediments at Streaky Bay show that up to 3.1 m (+18% compaction) of sediment has accumulated in the last 3200 years BP (Figure 4.9). The compaction (as a %) of cores, as a result of slip hammer coring, is recorded to highlight the difference between the depth the core tube penetrated and the length of cored sediment recovered. The difference in the two measurements is due to the following causes:-

- compaction of the sediment during coring by forcing a tighter grainsize packing arrangement;
- dewatering of the sediment during the coring operation;
- forcing sediment around the outside of the core-tube through higher friction loads inside the tube (especially when alternating sand and mud sediments are involved).

Relatively rapid deposition rates, up to 0.10 cm/yr (Acraman Creek Core No. 3), are shown in sediments beneath the mangroves in the Point Gibson embayment and the Acraman Creek estuary.
The sediments that make up the majority of the sediments in the cores are similar to those currently accumulating on the nearby spits (ie. medium to coarse bioclastic sands with a significant number of whole bivalve shells (some articulated) in lags and throughout the sediment). The relative rates of deposition for the Point Gibson and Acraman Creek areas are shown in Figure 4.8. The timing for the main development of the spits at Point Gibson, (southern Streaky Bay), and at Point Lindsay at Acraman Creek, has been determined by $^{14}C$ AMS dating, to have occurred during the last 3000 years. Both spit areas were at least 2 m below MSL before this time. The early Holocene embayment in the 'Proto' Acraman Creek area (Figure 2.3) has also changed from an estuarine shallow-water environment (Acraman Creek Core 5) to a gypsum-based salina in the late Holocene. Spits and chenier ridges migrating across the entrance of the embayment have been responsible for occluding marine access within the last ~1000 years using notional time lines as in Figure 4.8.

Deposition rates for the muddy sediments in the inner marginal basins during the mid to late Holocene were between 0.015 cm/yr (northern basin) and 0.007 cm/yr (central basin) (Figure 4.9). Carbon 14 dates on seagrass from just below (down to 35 cm) the rich organic upper muds of the mangrove forest have given Post Modern dates (Samples OZB910 (Point Gibson) and OZB914 (Acraman creek), ANSTO ,Table 4.2). This indicates that the mangrove woodlands may have become established recently or that the sediments overlying the seagrass layer have been subject to intense bioturbation and contaminated the layer of seagrass.

## 4.4 DISCUSSION

### 4.4.1 MODERN DAY/ GLANVILLE FM COMPARISON (FLAGSTAFF LANDING)

The points highlighted in the two profiles can be correlated as similarities in the depositional environments, represented as morphological and sedimentological changes. Minimal changes were observed in the beach profile over a period of three years. This particular section of the shoreline is a low energy environment (protected by the sand shoals), where the shoreline and near beach profile has been stabilised by a mat of seagrass. It was observed on a recent visit to the area that the seagrass mat was still present and stabilising the shoreline (Brown pers com., 1999).

The transition from fine-medium to coarse grainsize seen in the more elevated part of the Glanville Formation represents an upper beach slope (Figure 4.4, point a) to a proximal dune environment whereas the very coarse-coarse sand to gravelly sand transition can be inferred as a high tide swash-limit environment (Figure 4.4, point b). Mid- to low-tide is located where the gravel in the sandy sediment increases to cobble size (Figure 4.4, point c). Points "a" and "d" represent an upper beach slope where the significant grainsize changes from coarse sand to medium-fine sand. The difference in elevation between these two points, ie. the modern day profile and in the Glanville Fm., is 1.8 m (1.82 m).

Points "b" and "e" represent the limit of the high tide swash zone as characterised by the lower boundary of the seagrass debris, associated with very coarse-coarse sand on the modern beach and the significant fining of the gravelly very coarse bioclastic sand to a very coarse-coarse bioclastic sand in the Glanville formation section. The elevation difference between these two points ie., the modern day profile and the Glanville Fm., is 1.8 m (1.77 m).

### 4.4.2 MODERN DAY/ GLANVILLE FORMATION COMPARISON (POINT GIBSON)

The sea-level difference between the Pleistocene (IS 5e) and present day was a straight forward oceanographic problem once the equivalent tidal mark in the Glanville Formation was determined. The area of formation exposure encompassed the upper zone of articulated bivalves and sufficient outcrop above this point to check for higher placed articulates (Figure 4.5). The present day height of the Mean High Low Water is +0.7 m for Streaky Bay (National Tidal Facility, Flinders University, NTF). The average height above the chart datum of the articulated bivalves in the Glanville Fm. section is +2.52 m. The difference between the present day High Low Water mark and the inferred High Low Water mark in the Glanville Fm. is 1.8 m (1.82 m) using NTF Tidal information for Ceduna and adjusted for Streaky Bay.

### 4.4.3 PLEISTOCENE PLATFORM

The height differential between the Pleistocene (IS 5e) and present day platform is 2.46 m The results agree with those of Buckley et al. (1987), although they questioned whether the upper platform was of high tide or low tide origin. The latter is considered the more likely because; a) the upper surface of the sediment is level, indicating the absence of sub-aerial erosion (Buckley et al., 1987) and, b) the deposit is similar in morphology to present day low-tide boulder deposits around the shores of Streaky Bay, ie. Flagstaff Landing, Perlubie Beach.

This height difference may not be truly indicative of a Pleistocene sea-level, as there are numerous alternating aeolianite and calcrete beds which, through preferential weathering by seawater and aerosols, can cause a platform to be formed out of 'geomorphological context' Buckley et al. (1987). Thus, the top of a calcrete horizon in the general region of low tide (either higher or lower) could become the locus for a wave-cut platform if the adjacent lithology is more susceptible to abrasion and saturation. The bed immediately below the Pleistocene platform consists of calcrete, which is more resistant to weathering and could represent a preferential weathering surface. However, the present low tide platform appears to be cut midway into a fairly massive bed of Bridgewater Formation calcareous aeolianite. This resistance to weathering could explain the higher estimate of late Pleistocene sea-level (IS 5e) at this site, when compared with those estimates from Flagstaff Landing and Point Gibson. It is generally agreed, however, that shore platforms are not highly reliable indicators of sea-level but are only related to sea-level in a general way (Twidale and Bourne, 1990; Short et al. 1990).

### 4.4.4 TIMING OF GLANVILLE FORMATION

The depositional timing of the Glanville Formation at Flagstaff Landing, Streaky Bay of 124±9 ka is within the accepted constraints of Isotope Stage 5e, which ranges from 128 ka to 114 ka (Williams et al., 1998). It is interpreted that the occurrence of *Goniopora somaliensis* in the waters of Streaky Bay during this Stage points to the water temperature and climatic regime being significantly warmer than present . The interpretation of warmer water for IS 5e is a direct present-day habitat correlation of *Goniopora somaliensis*, whose most southerly occurrences are to the north of both Ningaloo Reef, WA and Moreton Bay, Qld (Veron, 1986). The seawater in these regions is significantly warmer than the waters of the central southern margin of Australia, ie. average mean annual SST for Ningaloo Reef, WA - 25°C, Moreton Bay, QLD - 23°C and inner GAB waters - 16°C (CSIRO Marine Research, 2001)(Figure 4.10). It is speculated that the higher sea-levels that have been determined for IS 5e are most probably a result of these warmer climatic conditions.

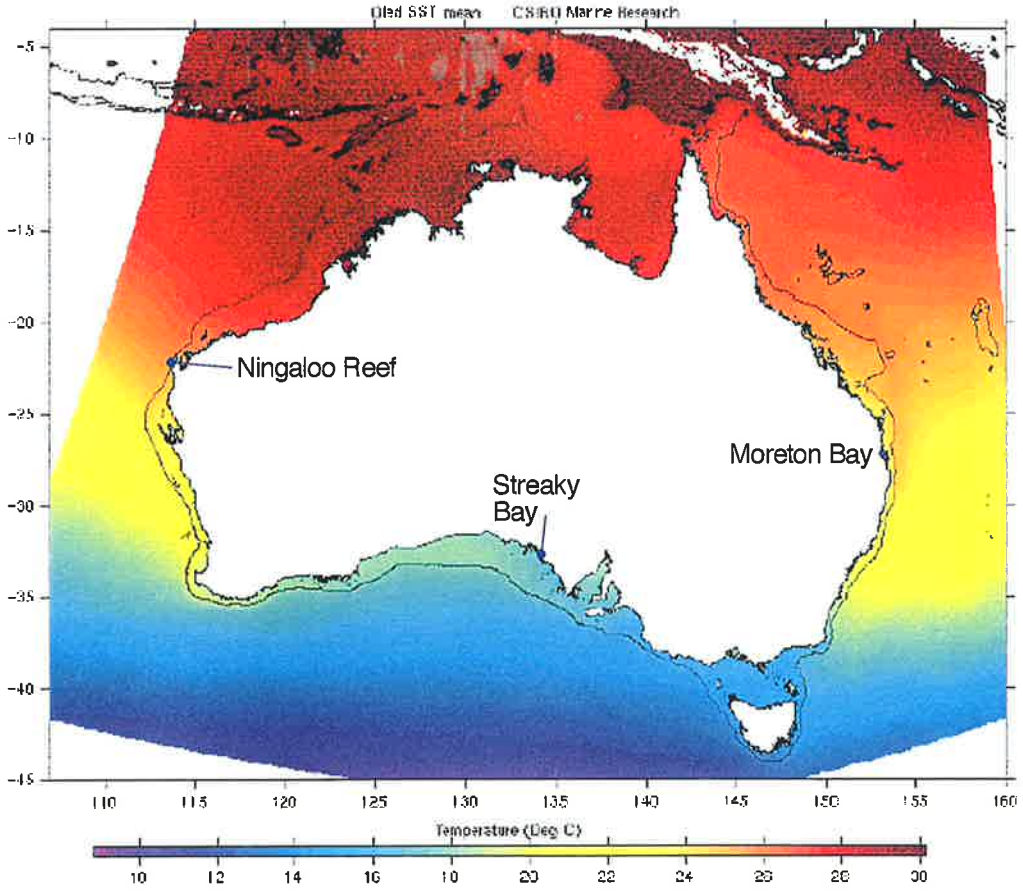



Figure 4.10 Average Annual Sea Surface Temperatures for Australian waters (CSIRO, Marine Research, 2001). The temperature differential is highlighted between South Australian Bight waters and those of Ningaloo Reef, W.A. and Moreton Bay, Qld. The latter two localities represent the present day southern limits of the coral *Goniopora somaliensis*, in contrast to the coral being present in GAB waters during Isotope Stage 5e.

### 4.4.5 Development of Near Shore Littoral Terrace

The sea floor terrace in the outer region of Streaky Bay is interpreted as a near-shore littoral terrace, which is similar to an ultimate terrace (sensu Jutson, 1939, 1940, 1948, 1949) and a submarine terrace (sensu Sherbon Hills, 1972). The terrace was actively eroded to a nearly horizontal aspect on the sea floor in a high energy surf-zone as described by; for example Dietz (1963), Bathurst (1975), Friedman and Sanders (1978) Walker and Plint (1992), and Lewis and McConchie (1994). It is speculated that the periods of high sea-levels during Isotope Stage 5a and 5c (100 ka and 80 ka) or the "double sea-level paracycle" of the mid-Holocene (8.5-8.2 ka) (Larcombe et al., 1995), may have provided the time, shallow seas and the high wave energy that was required for this terracing abrasion process to occur (Figure 4.7). In contrast to this, there may not have been sufficient time for the formation of such a wide terrace to occur during the Holocene event as observations of present day wave cut platforms and shallow marine terracing on the Eyre Peninsula margin indicate widths of < 100 m for wave cut platforms and < 1 km for shallow marine terracing.

The inner areas of Streaky Bay have been sites of minimal deposition of the upper Bridgewater Formation. This can be seen by the presence of thin calcrete and aeolianite layers above the Glanville Formation in the Flagstaff Landing Glanville Formation sequence. Wilson (1991) also notes that only minor aeolianite and calcrete was deposited after Glanville Formation time, until the onset of the deposition of the St. Kilda Formation during the Holocene.

### 4.4.6 Early Holocene Sea-level High Stand

Early Holocene beach sediments are interpreted to have been deposited in an equivalent depositional environment as present day. Based on this, the resultant height difference of 40-50 cm depicts the difference between the present sea-level and the early Holocene sea-level high stand. Unfortunately suitable material for carbon dating this event was not available in this area.

| Locality | Height above MSL (metres) | Timing, years BP |
|---|---|---|
| Ceduna, Eyre Peninsula, SA[1] | 0.4 | ~6100 |
| Coffin Bay, Eyre Peninsula, SA[1] | 0.8 | ~6200 |
| Port Gawler, Gulf St. Vincent, SA[1] | 2.1 | ~6300 |
| Port Pirie, Spencer Gulf, SA[2] | 2.2 | ~6700 |
| Port Wakefield, Gulf St. Vincent, SA[1] | 3.0 | ~6500 |
| Northern Spencer Gulf, SA[1] | 4.5 | ~6800 |
| Streaky Bay, Eyre Peninsula, SA[3] | ~0.4 | ~7300 |

[1]Belperio, 1995; [2]Harvey et al., 1999, [3]This study.

**Table 4.1** Relative heights of the Holocene sea-level maxima from the South Australian coast.

### 4.4.7 Commencement of Early Holocene Shallow-water Sedimentation

Timing of the onset of marine deposition in the IMB is constrained by the water depth at the tidal deltas located near the distal ends of the sand banks (Figure 2.13). The floors of the central and southern channels are sites of prograding tidal deltas and as such it is difficult to determine their water depth during the early Holocene. Aeolianite and calcrete of the Bridgewater Formation are exposed and being eroded on the floor of the northern channel, the height of which represents the maximum depth below present sea-level of sea-level incursion during the Holocene (Figure 4.8).

The present depth of 4 m in the central channel would constrain the early Holocene sea-level only if a relatively constant rate of progradation of the flood and ebb tidal deltas is assumed (Figure 4.8). This depth of 4 m can be assumed to have been stable because the presence of deeper water on either side of the tidal channel allows abundant accommodation space for transported sediment deposition, on either direction across the delta, with no loss of accommodation space on the channel or tidal delta. The tidal currents (reflecting transport capability) are also assumed to have remained relatively constant since the time of the sea-level highstand because the morphology of the bay does not appear to have altered significantly since the mid Holocene (refer to FLOWC modelling Figure 2.15).

If this constant rate of sediment transport in the central tidal channel were not so and the water depth was significantly shallower, the northern channel could have provided marine access. The water depth in this channel is now 8 m and is actively eroding into the sediments of the Bridgewater Formation. This, therefore represents a maximum channel depth or lowest sea-level height for the mid-Holocene (7300 years BP). However, a further impediment to marine access via the northern channel to the

central basin is the North Sand which only has a 4 m deep connecting channel between the eastern end of the bank and the beach (Figure 2.13), which has constrained the upper limit of sea-level as described.

The radiocarbon dates of Belperio et al (1988) were derived from subtidal sea-grass deposits (*Posidonia australis* sp.) in sediments from vibro-cores taken at Tourville Bay, Eyre Peninsula (Figure 2.1). These dates suggest that sediment accumulation and progradation were relatively rapid and that it mostly occurred within the first 2000 years of the Holocene highstand (Belperio et al.,1988). This indicates that either the central tidal deltas in Streaky Bay must have been significantly lower (ie. ~25 m) than the present sea-level or the Holocene sea-level must have been at least at -8 m MSL by 7300 years BP. This would have been the minimum depth of the northern channel at this time because the Bridgewater Formation is presently being eroded in the floor of the channel at a depth of 8 m. (Figure 4.8, Transect 3 sea-floor profile). It is possible that the sea-level was higher at this time because the minimum depth of the central channel at present is ~4 m. However there may have been an interconnection between the three inner basins, the more important access being between the central and the northern basin (Figure 2.13). A connecting channel to the East of the North Sand provides marine access via the northern basin to the central basin that is 4 m deep (Figure 2.13). It is interpreted that due to the restrictions to the central inner basins provided by the tidal channels and the sand bank-beach channels the mid- Holocene sea-level was approximately -4 m MSL at 7300 years BP (Figure 4.8). There is considerable reliance on the dating of a single articulated shell on which to base sea-level rise and onset of the Holocene highstand at Streaky but it does compare with the two dates, which have been utilised at Tourville Bay for the west coast region by Belperio et al. (1988).

### 4.4.8 Holocene Sea-level Highstand

The sea-level can be interpreted to have been between -8 and -4 m below present sea-level at approximately 7300 years BP from the above evidence (Figure 4.8). This level depends on the marine access channel used for the determination. It demonstrates that the relative sea-level, at this time, was rising significantly faster (between 40 mm/yr and 47 mm/yr) than that proposed by Belperio et al. (1995) (24 mm/yr from 8 ka- 6.7 ka). If these figures are used and the relative sea-level rise was uniform, the early Holocene sea-level can be projected to have reached the present day level between 7210 and 7100 years BP (Figure 4.10) rather than 6800 years BP as predicted by Belperio et al., (1988). This modified curve is similar to that proposed by Hails et al. (1984) for the northern Spencer Gulf and the generalised curve from the east coast of Australia (Thom and Roy. 1983; Gindrod and Rhodes, 1984 and Hopley, 1984).

### 4.4.9 TIMING OF THE EMPLACEMENT OF SOUTH SAND AND NORTH BANK

The precise timing of the emplacement of the two elongate sygmoidal sand banks in the bay (South Sand and North Bank) is problematic. Clarke (1994) showed that the sand bodies occupy areas of significantly low residual water velocity between the clockwise and counter clockwise circulation gyres in the bay.(Figure 2.17) This was demonstrated using a tidal residual current computer model, developed by Bye and Ng (1994). The elongate sand banks were not included in the model because of the difficulties in modelling the bodies mathematically, so the results of the current residual velocities were derived by using the broad physical parameters of the bay with the sand bodies excluded. When these results were superimposed on a map of Streaky Bay the elongate bodies were found to lie in the areas of very low residual velocity. It is interpreted, that by taking the above data into account, the banks formed principally up to and around the Holocene highstand when sediment from the near shelf was moving into the shallow proximal shore areas. These sand bodies also may have been formed wholly or partially during the late Pleistocene sea-level high (Isotope Stage 5e), given that the shape of the bay has not changed significantly since Isotope Stage 5e times and that consequently the sea circulation patterns would also be similar (according to the FLOW C model, Clarke, 1994). The formation and maintenance of these sand banks is similar to the linear sand banks that have formed in the North Sea (Collins et al., 1995, Pattriartchi and Collins, 1987, Huthnance, 1982) see Chapter Two, Oceanography of Streaky Bay.

## 4.5 CONCLUSIONS

The present-day sea-level on the west coast of Eyre Peninsula has been established as high stand conditions, which is approximately 1.8 m below the high stand sea-level of Isotope Stage 5e. This sea-level agrees with heights established across the globe in areas of tectonic stability. The Eyre Peninsula has also been established as a tectonically stable far field region and therefore the sea-levels determined at Streaky Bay, and other areas on the Eyre Peninsula, can be regarded as mainly representing eustatic sea-level movements during the late Quaternary.

The height and timing of the sea-level during Isotope Stage 5e is established as being approximately 1.8 m above present day sea-level and occurring at 124 ±9 ka BP. This date establishes this maximum sea-level height on the Eyre Peninsula as approximately mid- Isotope Stage 5e. The geochronology of the Glanville Formation outcropping at Streaky Bay is also verified as being deposited during the late Pleistocene (Isotope Stage 5e). This can be correlated with similar outcrops of the Glanville Formation flanking Gulf St Vincent and the South East coast of South Australia.

The discovery of the present-day tropical coral *Goniopora somaliensis*, along with *Anadara trapezia* and *Marginopora vertebralis* within the Glanville Formation, has inferred that the seawaters, at least on the inner GAB shelf, were significantly warmer (7 - 9 °C) during Isotope Stage 5e than present day conditions.

An extensive near-shore littoral terrace (or the development of an ultimate platform/ submarine ramp) was formed in Streaky Bay during Isotope Stage 5a and 5c or the early Holocene approximately 12m below the present sea-level. It is most probable that the terrace was developed during the late Pleistocene as there is no record on the development of significant terracing, on the scale found at Streaky Bay, during the early Holocene.

Marine conditions became re-established in the Streaky Bay region during the early Holocene prior to 7300 years BP. This has moved the onset of early Holocene sedimentation on the West Coast of the Eyre Peninsula back approximately 500 years when compared to 6800 years BP established in Tourville Bay near Ceduna.

Early Holocene sea-level reached present day mean sea-level between 7200 and 7100 years BP and attained a maximum height of between 7180 and 7080 years BP. This height was approximately 40 - 50 cm above present-day sea-level in the Streaky Bay area and agrees with established data on the Eyre Peninsula.

Extensive sedimentation occurred along the coastal margins of the inner bay during the past 3500 years, with maximum sedimentation rates occurring around 3000 years BP when the occlusion of the Proto Acraman Creek estuary occurred. This has been established from the results of coring over the extensive northern and southern spits at Streaky Bay. Significant sedimentation has led to the continued expansion of the shallow sand shoals in the central portion across Streaky Bay.

# CHAPTER FIVE

# GRAINSIZE

# DISTRIBUTION OF RECENT SEDIMENTS

## 5.1 INTRODUCTION

Research on sediments from the inner shelf of the western Eyre Peninsula has been fairly sparse to date. Studies have been carried out on recent sediments at Baird Bay (Hill 1994), Tourville Bay (Lablack 1985) and Coffin Bay (Freeman 1985), but little quantitative data is available. A report from the Department of Mines and Energy (SA) has also described the Quaternary coastal sediments and the results of rotary drilling from around Fowlers Bay (Belperio 1988). The distribution of sediments from the outer to the inner shelf, incorporating the regional shelf area near Streaky Bay, have been described by Conolly and von der Borch, (1967), Wass et al., (1970), Fuller et al., (1994), James et al., (1994, 1997, 2001).

The aim of this chapter is to highlight the grain-size distribution in relation to the variation of wave energy, water depth and substrate across the bay. The spatial distribution of grain-size across the bay are related to those in a range of embayments on the Eyre Peninsula, which represent the marginal

facies of the shelf high stand depositional environment. The distribution of grainsizes are compared the with the adjacent shelf sediments as a continuum from the shore face to the shelf edge.

## 5.2 SUBSTRATE

Substrate composition of the sea-floor is linked closely with the morphology of the bay (Figure 5.1). These compositions are divided into three broad predominant regimes from the inner to the outer bay (Figure 5.2). The distribution of rocky substrates is summarised in Figure 5.6 where the presence of rocky substrate or limited sediment sample is highlighted.

### 5.2.1 SOFT MUDDY SUBSTRATE

Confined to the inner marginal basins in water depth that varies from ~ 7 m to 15 m. The fine sandy calcareous mud is present in the three open basins of greater Streaky Bay and Blanche Port in depths of > 4.5 m. The predominant organisms present on this substrate are molluscs with epibionts such as serpulids, barnacles, minor bryozoans and coralline algae with abundant diatoms and rare echinoids (Figure 5.2).

### 5.2.2 SANDY SUBSTRATE

Occurs centrally in the bay and ranges from exposed sand at high tide on the elongate banks and spits to sand in the shallow waters of the tidal deltas and sand shoals. This includes sparse to densely populated seagrass meadows of *Posidonia* sp. and *Amphibolis* sp. which flank these more exposed areas. Sediments are predominantly calcareous fine to coarse sand with common organisms including molluscs, foraminifers and coralline algae (Figure 5.2).

### 5.2.3 HARD ROCKY SUBSTRATE

Typical of the outer half of the bay in conjunction with mobile sand waves and crevice fill (Figure 5.3). This rocky substrate consists predominantly of calcareous aeolianites and calcretes of the Bridgewater Formation (Figure 5.3). The loose sediments consist of calcareous medium to very coarse sand with quartzo-feldspathic coarse sand to fine pebble gravel (Figure 5.4). Figures 5.3a-f highlight the rocky substrate in the entrance and outer terrace areas. Low thickets of algae, sponges and bryozoans are abundant in these areas. Figures 5.4a-f show the depositional framework of loose sediment in the same general area. Figures 5.4a-c are migrating sand waves with a gravelly lag present in Figure 5.4b. Figure 5.4d-f depict areas of crevice fill with sediment fill ranging from medium to gravelly very coarse sands, which are flanked by prolific growth on the adjacent rocky substrate. A wide diversity of biota (epiphytic, epizoal, epibenthic to infaunal) such as molluscs, bryozoans, foraminifers, coralline algae and representatives of minor groups are common. Abundant

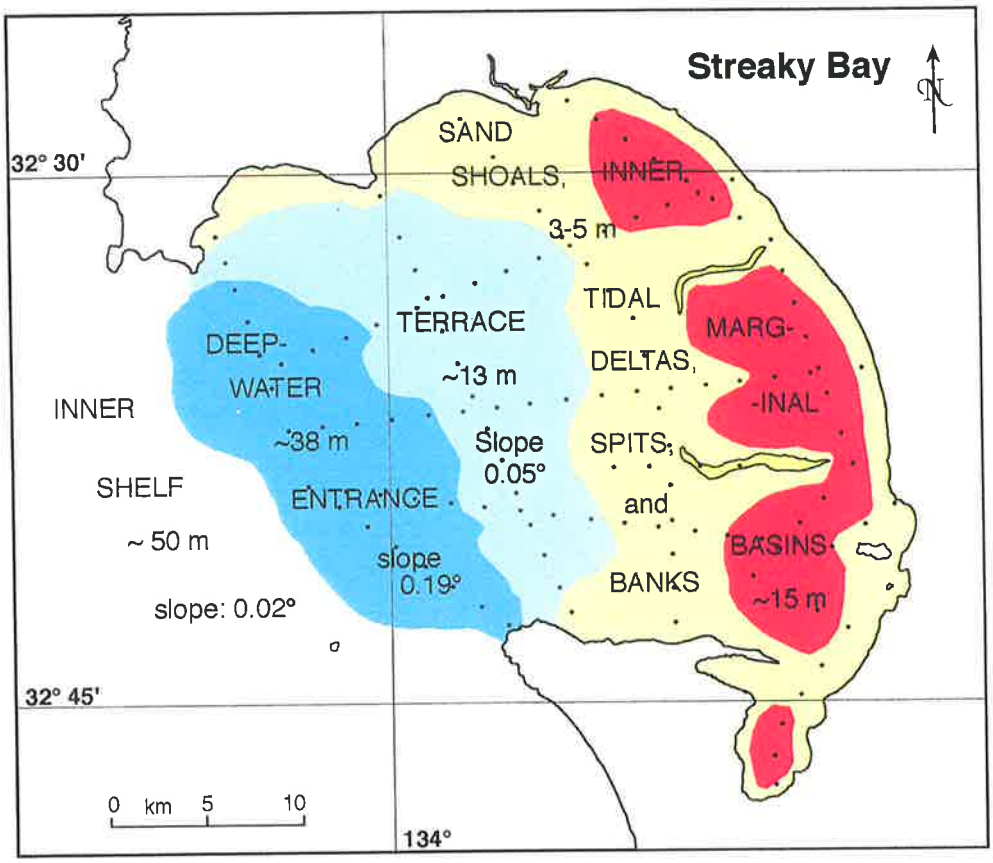



Figure 5.1 General sea-floor morpholgy of Streaky Bay.

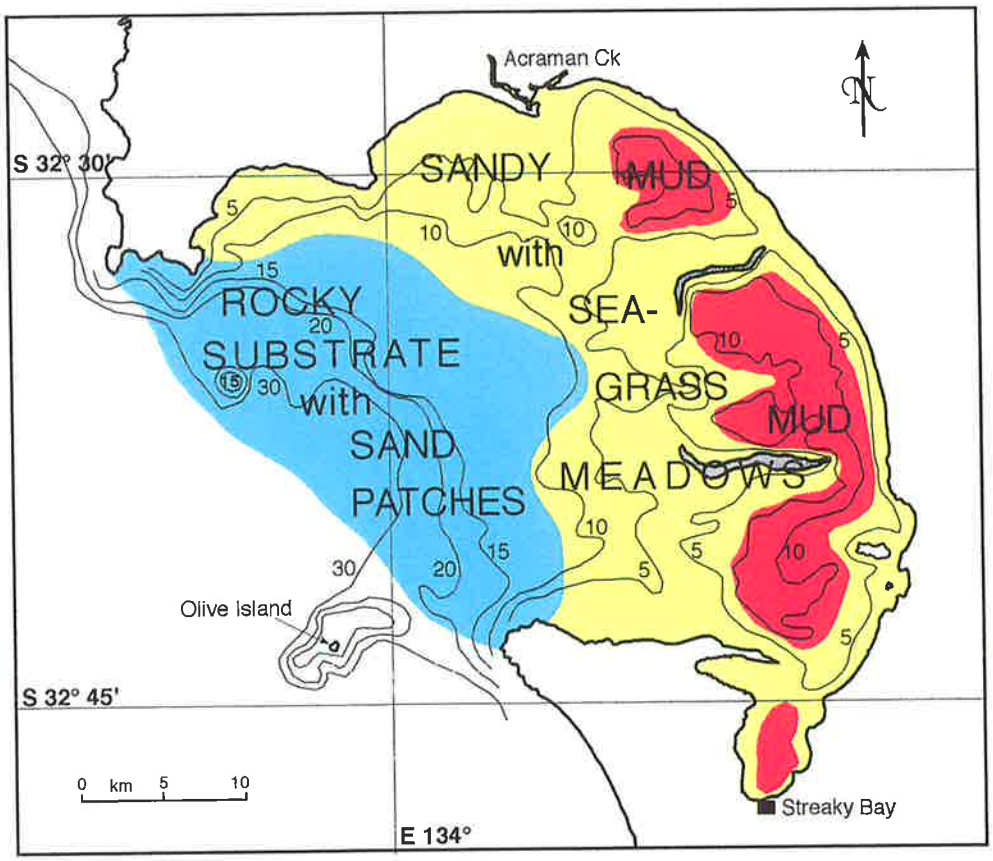



Figure 5.2 Substrate distribution, Streaky Bay

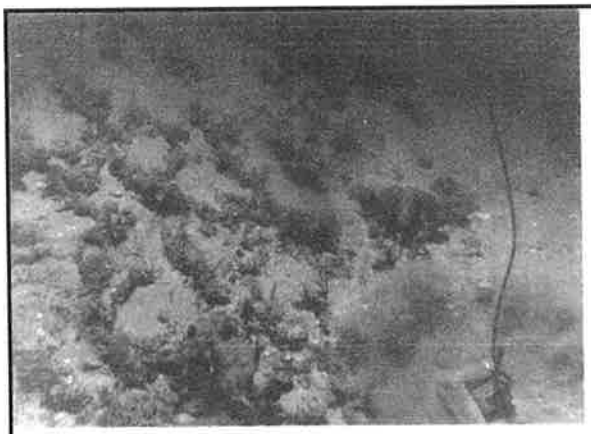


Figure 5.3a Rocky substrate in the vicinity of the entrance and outer terrace. A thin veneer of sediment is draped over the rocky sea-floor with robust benthic organisms growing through the loose sediment.
Scale bar 15 cm square.



Figure 5.3b Rocky substrate of the outer terrace highlighting low shrubby growth in response to high energy conditions. Soft and coralline algae, sponges and bryozoans predominate.
Scale 15 cm square

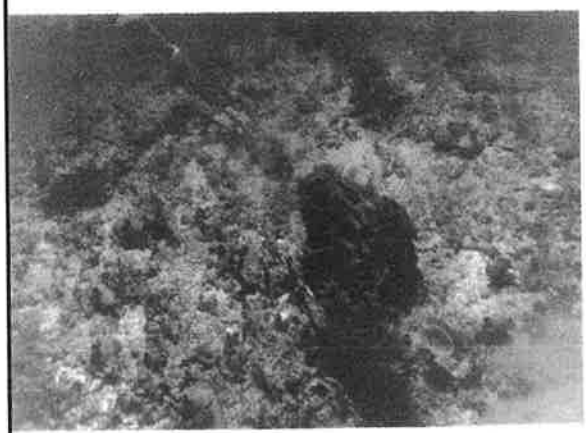


Figure 5.3c Detail of rocky substrate indicating prolific sponges and mollusc shells with a thin veneer of sediment.
Scale bar similar to 5.3a, b.

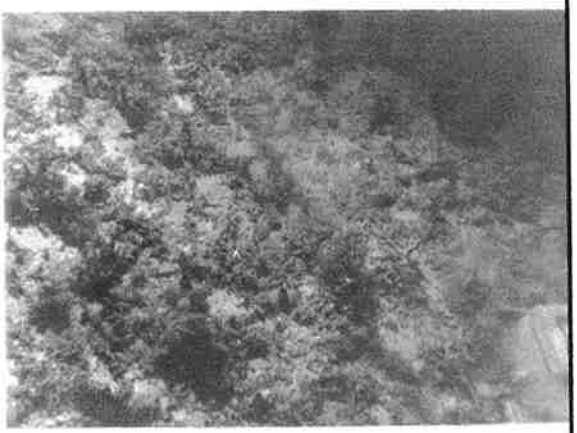


Figure 5.3d Low thickets of sponges, soft and coralline algae and bryozoans on an undulose slope.
Scale bar 15 cm square.

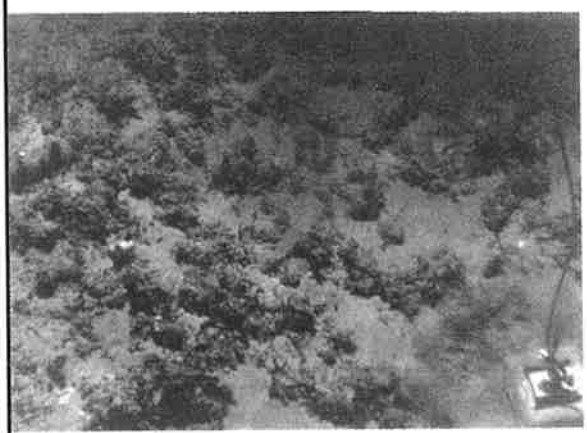


Figure 5.3e Thicker veneer of sediment decreases the density of benthic growth.
Scale bar 15 cm square.

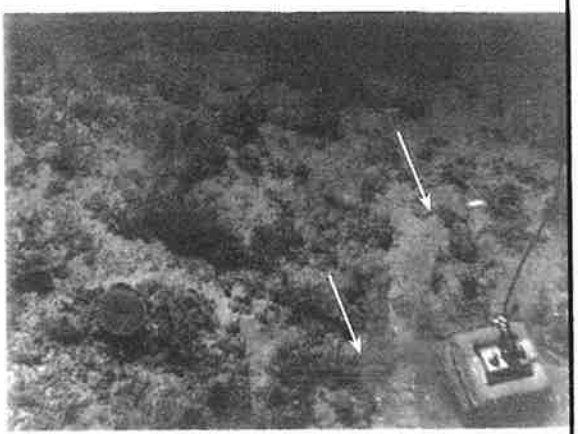


Figure 5.3f Calcrete substrate (arrowed) expoed on the sea-floor.
Scale bar 15 cm square.



Figure 5.4a Sea-floor in the vicinity of station SB 90 (outer terrace). Active sand waves of medium-coarse sand migrating across the sea-floor, biogenic gravel remaining as a lag (upper right).
Scale bar 15 cm square.



Figure 5.4b Detail of migrating sand wave leaving behind a gravelly lag of predominantly molluscan shells.
Scale bar 15 cm square.

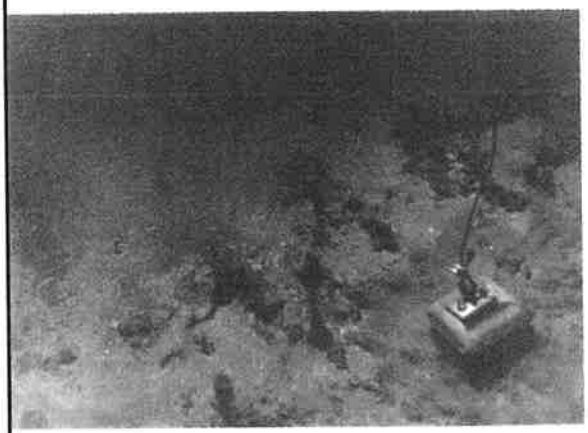


Figure 5.4c Coarsely rippled sand with large shell fragments and sparse sponge and algae growth.
Scale bar 15 cm square.



Figure 5.4d Rippled coarse sand deposited in an open crevice in the rocky substrate. Entrance and outer terrace areas.
Scale bar 15 cm square.



Figure 5.4e Rippled sand as crevice fill between outcrops of bridgewater Formation.
NB steeply inclined position of scale marker.
Scale bar 15 cm square.

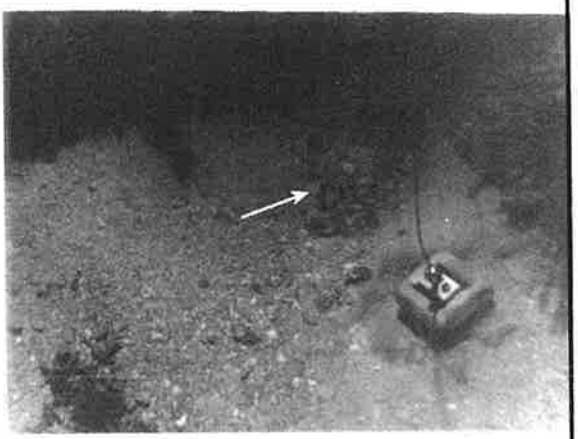


Figure 5.4f Detail of gravelly crevice fill (arrowed) in the lower part of the crevice with finer sands in the lower lee of the rocky walls (indicative of high energy conditions).
Scale bar 15 square

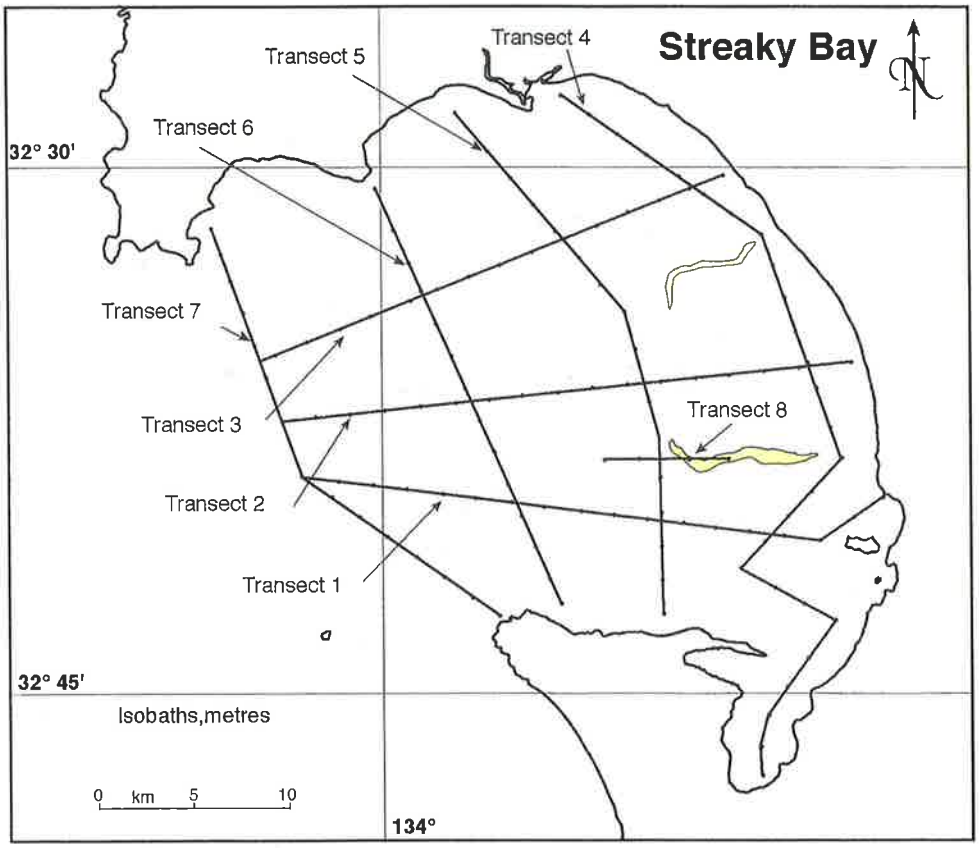



Figure 5.5 Transect locations.

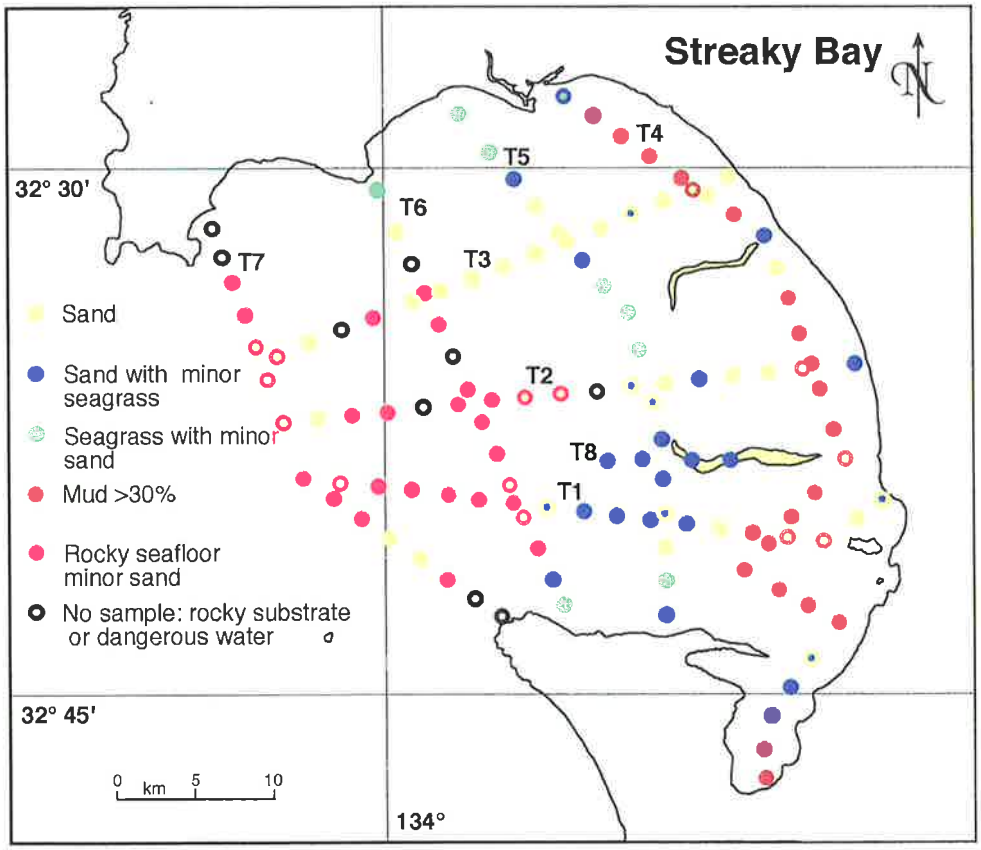



Figure 5.6 Areas of relative sediment abundance (yellow), abundant with minor seagrass (blue), abundant with major seagrass (green), paucity (red) and absence (black). The two stations at either end of Transect 7 were not sampled as a result dangerous conditions.

brown algae (*Petalonia* sp. and *Ecklonia* sp.) are common on these substrates. Note that the photographs in Figures 5.3 and 5.4 were taken in >30 m water depth with the flash inoperable.

## 5.3 GENERAL DISTRIBUTION OF LIVING BIOTA

### 5.3.1 MOLLUSCS

Molluscs show the highest abundance in the inner marginal basins and central tidal delta whilst common in sediments throughout the bay. Bivalves are the commonest form in these areas, with representatives from infaunal (*Dosinia* sp., *Fulvia* sp., *Pecten* sp.) and swimming (*Chlamys* sp.) forms in the basin. Gastropods are a common constituent in the outer rocky areas being up to 40% of the molluscs in the coarse fraction with ~25% in the sand shoals. regions

The sand shoal/ seagrass areas include bivalve forms from infaunal (*Venerupsis* sp., *Katelysia* ssp., *Mactra* sp., *Macomona* sp., *Chioneryx* sp.), semi infaunal (*Pecten* sp.) to epifaunal (*Modialus* sp., *Thalotia* sp., *Clanculus* sp.). Common gastropods are *Batilleria* sp., *Fusinus* sp., *Bulla* sp. and *Calytraea* sp. - representatives of grazing and predatory types

The outer shelf is typified by the infaunal *Glycymeris* sp. and the epifaunal *Modialus* sp.

Gastropods are represented by *Batilleria* sp., *Phasianella* sp., *Calytraea* sp., *Turbo* sp.

### 5.3.2 BRYOZOANS

Confined to the outer portion of the bay where there is significant variation in substrate from rocky to loose sediment. A large variety of structural forms are present; commonly encrusting and foliose; with less common delicate branching, foliose fenestrate and articulated branching. Rare abraded vagrants are present in the sediments from the deeper central area at the mouth of the bay.

Few bryozoans are recognised from the inner half of the bay, although encrusting bryozoans are common on the seagrass leaves. These are not obvious in the sediment but scanning electron microscopy on the muds from the basins show < 50 μm sized fragments attributable to bryozoans.

### 5.3.3 FORAMINIFERS

Common in the central area sea grass meadows (*Posidonia* sp. and *Amphibolis* sp.), and in the outer terrace region where abundant brown and red algae are present. *Rotaliids* and *Miliolinids* are common in the shallow seagrass areas with rare *Textulariids*. The numbers of *Rotaliids* remains fairly constant in the deeper waters with *Miliolinids* and *Textulariids* increasing. The tests become larger and more robust as the wave energy increases.

### 5.3.4 CORALLINE ALGAE

Found in significant numbers throughout the sediments of the bay, higher concentrations are found in the central terrace area and the gravelly/ rocky substrates of the mouth. The inner marginal basins are areas of low concentration, however it is noted that the seagrass flanking the basins support a significant population of encrusting coralline algae, which is not discernible within the sands. The main architectural types represented in the areas of abundance are fragments of articulated branching, encrusting and rhodolith forms.

### 5.3.5 MINOR BIOGENIC COMPONENTS

- **Echinoderms** are distributed across the bay as ophiuroids and epifaunal echinoids in the mouth of the bay - to epifaunal and infaunal echinoids in the central area with small epifaunal forms in the muddy substrate.
- **Brachiopods** are present as a trace only in areas of rocky substrate and mobile sand waves.
- **Crustacea -**
    - **Ostracodes** are found in most sediments in low numbers, the robustness of their valves reflecting the energy of the environment.
    - **Barnacles** are found as epifauna on larger biota and occasional substrate fragments at the mouth.
- **Serpulids** also occur as epifauna on larger biota and larger grains at the mouth.
- **Sponge** spicules are only seen in the finer sediments of the shoals and in the muds of the basins, although sponges were dredged in the central and outer areas.

### 5.3.6 NON-BIOGENIC COMPONENTS

- Abraded bioclastic ie unrecognisable modern biogenic fragments which are mostly confined to the lower energy areas of the bay, probably transported from the carbonate factory in the region of the terrace and mouth
- High of Calcareous Aeolianite have been recognised in areas where the bay floor is being actively eroded or material is being transported into the bay from the headlands or sea-floor highs.
- Concentrations of quartz/ lithic (granitic) material are found in the lees of Olive Island and sea-floor highs.

## 5.4 GRAINSIZE DISTRIBUTION

The distribution of sediment grainsize has been determined and plotted on transect graphs and distribution map of significant grainsize fractions using the methods described in Chapter 3. The components of sediments and their distribution is treated in Chapters 6, sand fraction; Chapter 7, gravel fraction and Chapter 8, mud fraction.

### 5.4.1 DESCRIPTION OF TRANSECTS

Three East-West transects and four North-South transects with a minor transect onto the South Sand were established on the Streaky Bay Admiralty Sheet (Aus 121). An auxiliary transect extends from Streaky Bay to the shelf edge (Figure 2.1) This transect was part of the CSIRO Franklin 03/98 Southern Margin Cruise and is incorporated in James et al.(2001) as part of the overall GAB lithofacies. Figure 5.6 highlights sample stations where rocky substrate was encountered and sediment recovery was limited. Localities mentioned in these descriptions are found in Figure 2.4.

#### 5.4.1.1 Transects 1, 2, 3.

The three, east west transects start at the entrance of the bay with T 1 being the southern most, T 2 central and T 3 the northern most transect. The water depths at the western ends of the transects, are 36, 35 and 30 m respectively. Each of the transects was extended from the mouth through the centres of the three tidal deltas, across the inner marginal basins and finishing at the near shore areas, Perlubie Beach (south), Haslam (north) and midway between these two localities.

**Transect 1** commences in the southern entrance area of the bay, in the lee of Olive Island, and finishes near Perlubie Beach on the eastern shore. The water depths (ISLW- Indian Spring Low Water) along the transect ranges from 36 m at the entrance to 2.8 m in the South Channel tidal delta, down to 11.5 m in the inner marginal basin and then shallowing up to the shore (Figure 5.7).

**Transect 2** was sited from the entrance of the bay in 35m water depth, through the central tidal delta (Dashwood Channel, 4.5 m), across the central IMB (11 m) to the eastern shore (Figure 5.8).

**Transect 3** commences in 30 m of water at the entrance to the bay and extends through Warburton Channel (8.5 m), into the northern IMB (11 m) and finishes close to the Haslam jetty (Figure 5.9).

**5.4.1.2. Transects 4, 5, 6 and 7** are generally north-south transects each encompassing the detail of the four major water depth zones (Figure 2.8).

**Transect 4** is the major transect extending along the eastern face of the bay, including the inner marginal basins, from Blanche Port (Streaky Bay township) in the south to near the Acraman Creek estuary in the north. Water depths range from 3 to 5 m in the Blanche Port and Acraman Creek areas to a maximum of 12 m in the inner marginal basins (Figure 5.10).

**Transect 5** extends from Point Gibson to the area west of Point Lindsay. It passes immediately to the west of the South Sand and North Bank and includes the three major tidal channels. Water depths along the transect vary from a maximum of 9 m in the channels to 2 m in the vicinity of the sand banks (Figure 5.11).

**Transect 6** is sited across the terrace area, in the outer portion of the bay, from the northerly Point de Mole to approximately 4 km east of Cape Bauer. The water depth on this terrace area (up to 13 km wide) does not vary significantly from 12 m.(Figure 5.12).

**Transect 7** covers the entrance area, extending from inside Point Collinson to the head of Cape Bauer. A dogleg in the transect enabled samples to be collected from the proximity of Olive Island and the sub-aqueous high west of stations SB 62 and SB 63. The profile of the entrance floor along the transect is roughly curved with a maximum water depth at the centre of 37 m (Figure 5.13).

**Transect 8** is a short transect over the western end of the South Sand which extends from station SB 49 to SB 145a where the water was too shallow for *RV Hero* to proceed. The water depth varies from 11 m at SB 49, to 5 m at SB 143, to 0.6 m (high tide depth) at SB 145a (Figure 5.14).

## 5.5 RESULTS

A majority of the sediments in Streaky Bay are located in the S (sand) and gS (slightly gravelly sand) when plotted on Folk's textural ternary graph. Approximately 60 % of the sediments plot in the S and gS fields, ~ 20 % in the mS and sM fields and the remainder in the gmS and Sg fields. The sediments are coloured by lithofacies type for location within the bay (Lithofacies distribution - Figure 9.4)

### 5.5.1 BY TRANSECT

The grain-size generally trends (West to East) from gravelly very coarse sands at the entrance reducing rapidly to a medium to fine sand on the terrace area. Grainsize continues to fine towards the tidal delta regions where the grainsize again reduces rapidly to fine-very fine sandy muds in the inner

Figure 5.7a Sea-floor Profile

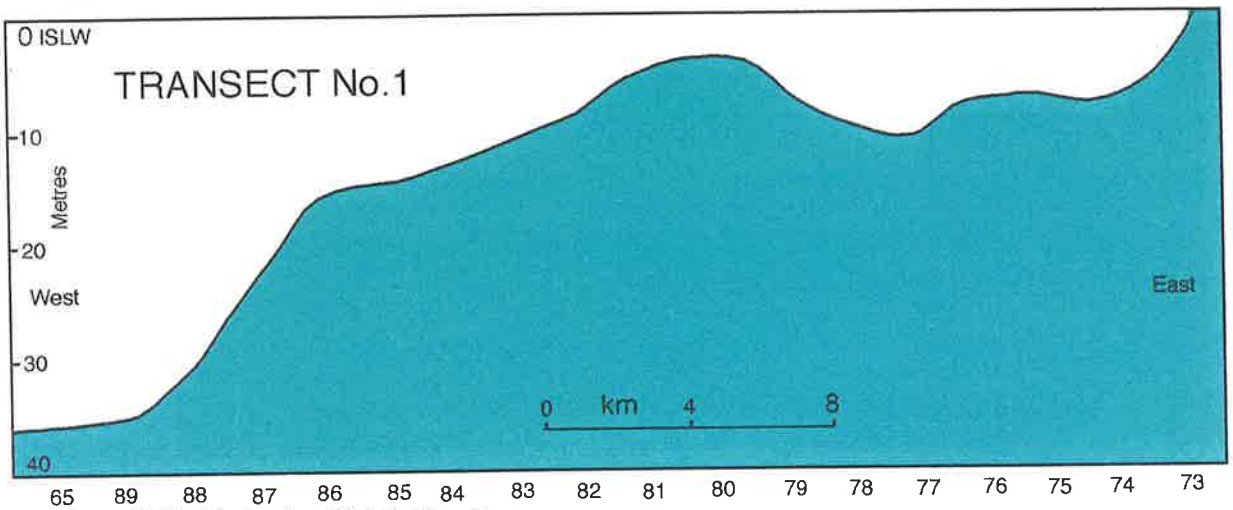



Figure 5.7b Grainsize Distribution %

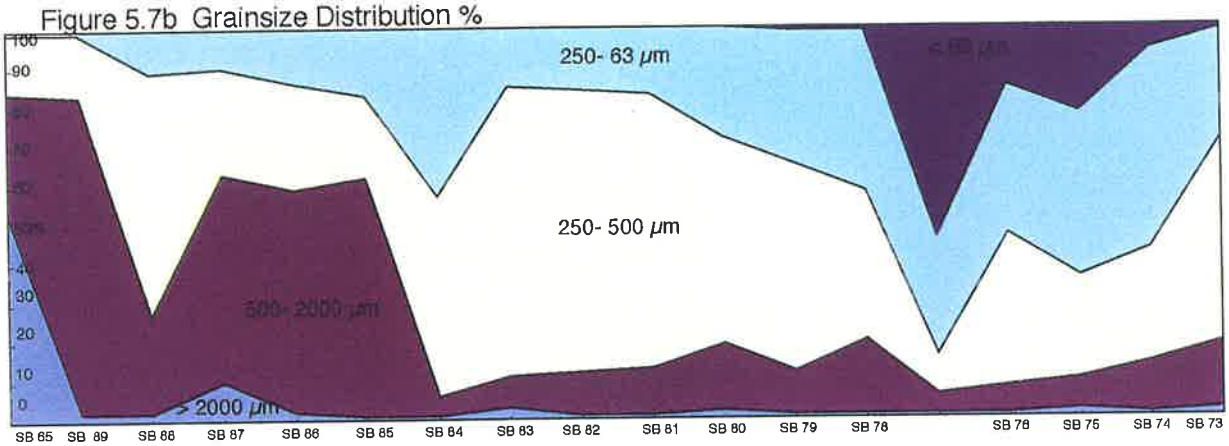



Figure 5.7c Component Distribution %, Sand Fraction

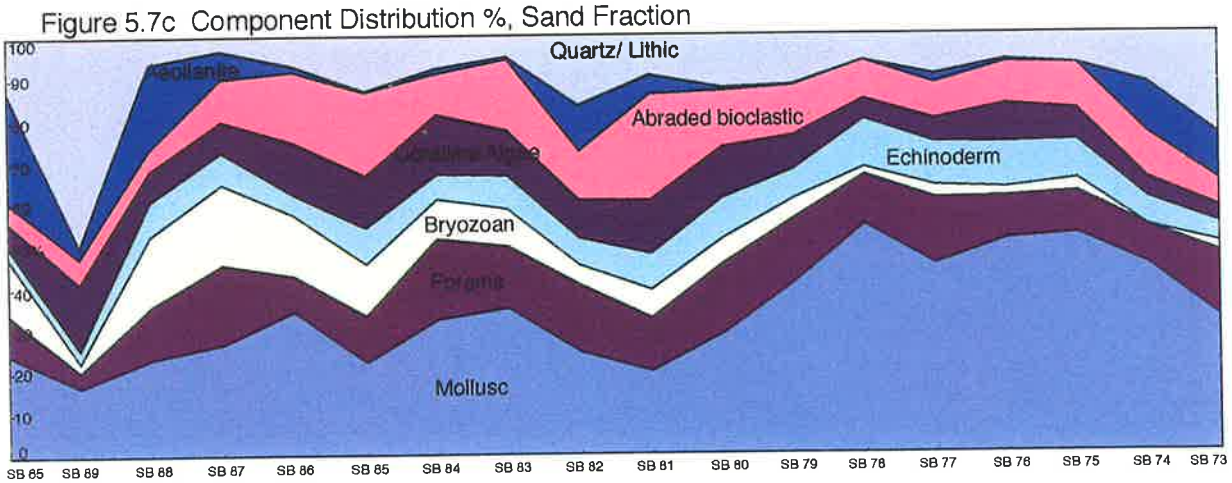



Figure 5.7d Component Distribution and Density, Gravel Fraction

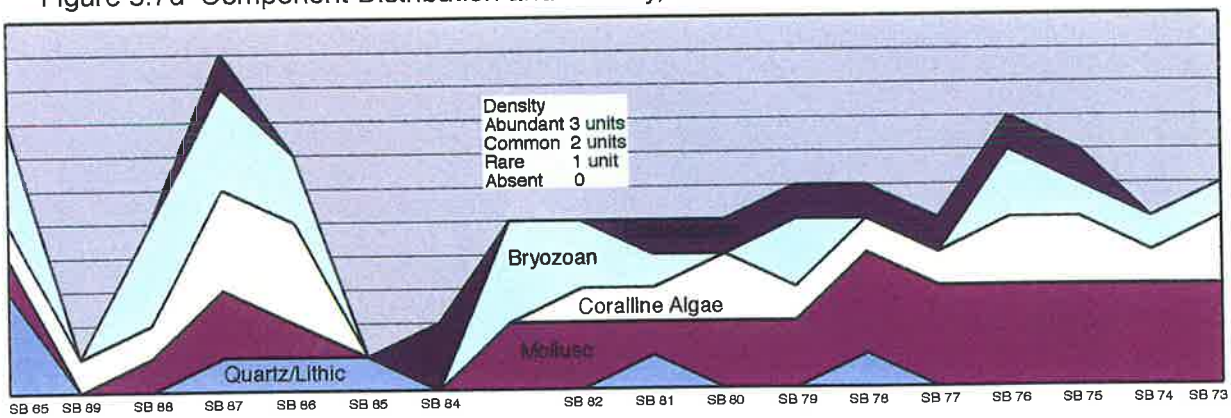


Figure 5.8a Sea-floor Profile

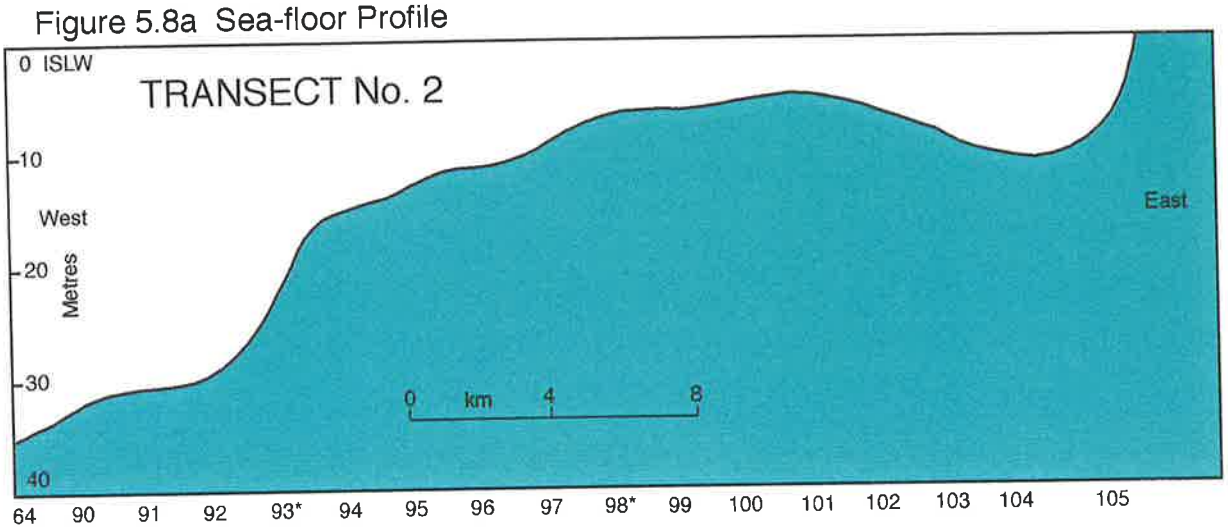



Figure 5.8b Grainsize Distribution %

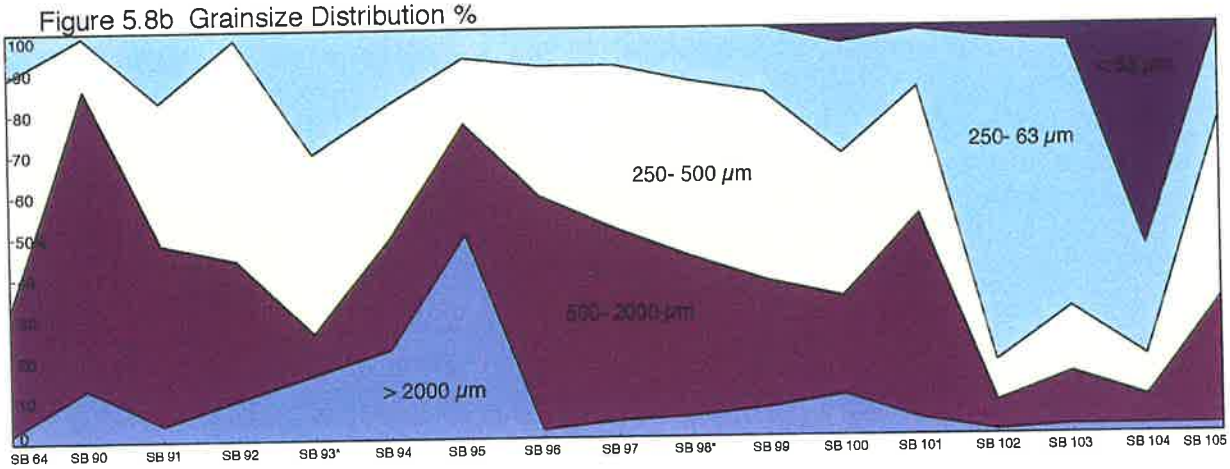
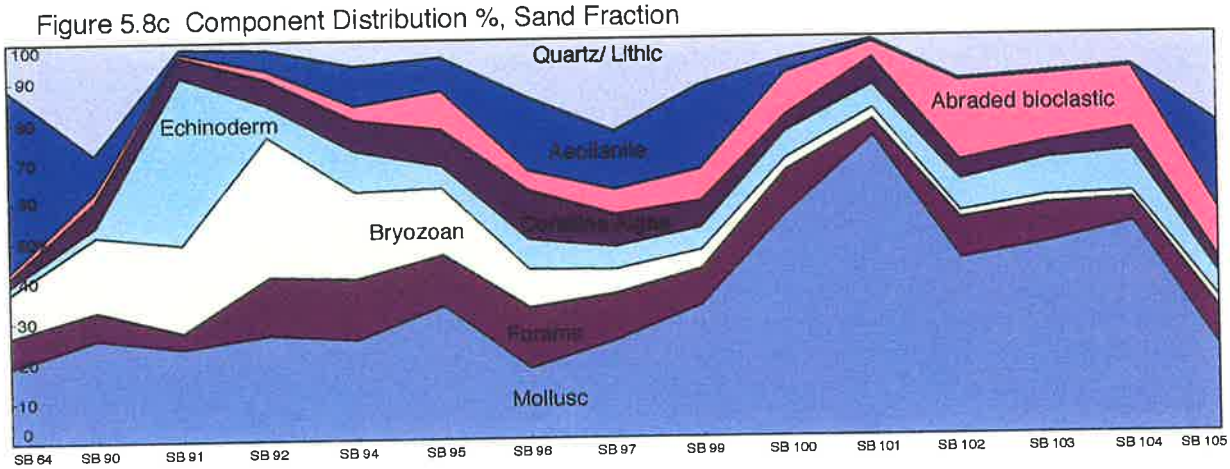



Figure 5.8c Component Distribution %, Sand Fraction




Figrue 5.8d Component Distribution and Density, Gravel Fraction

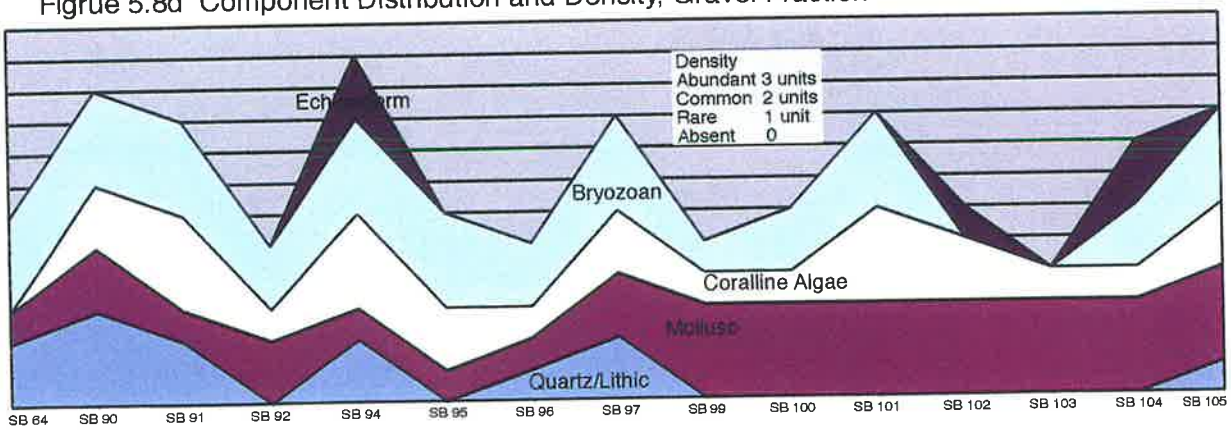
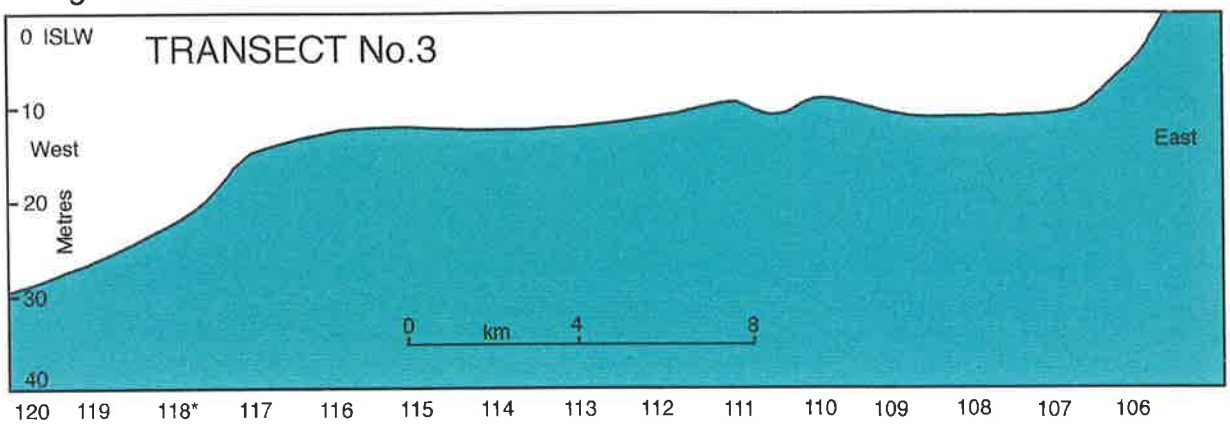


Figure 5.9a Sea-floor Profile




Figrue 5.9b Grainsize Distribution %

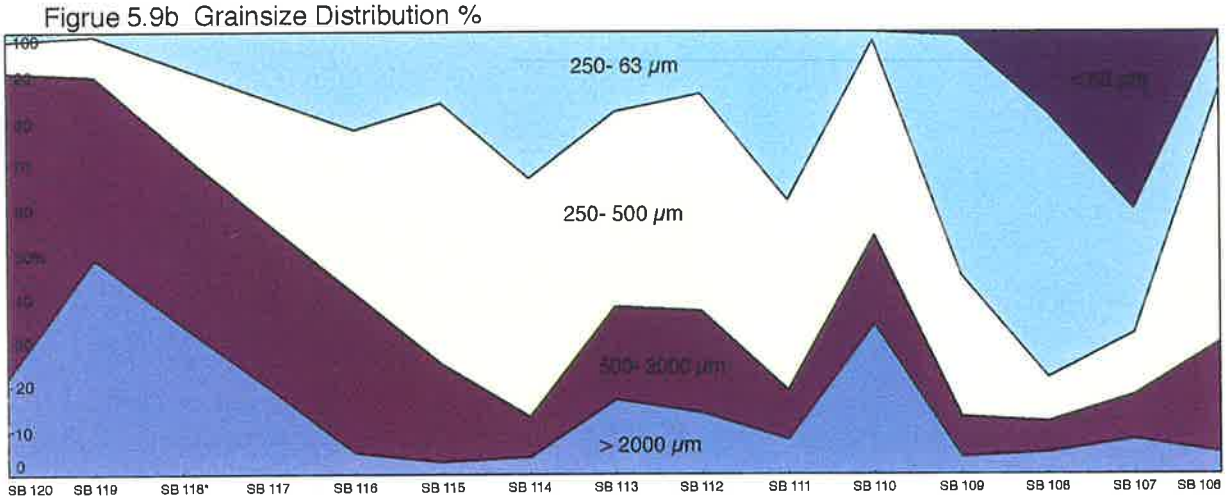



Figure 5.9c Component Distribution %, Sand Fraction

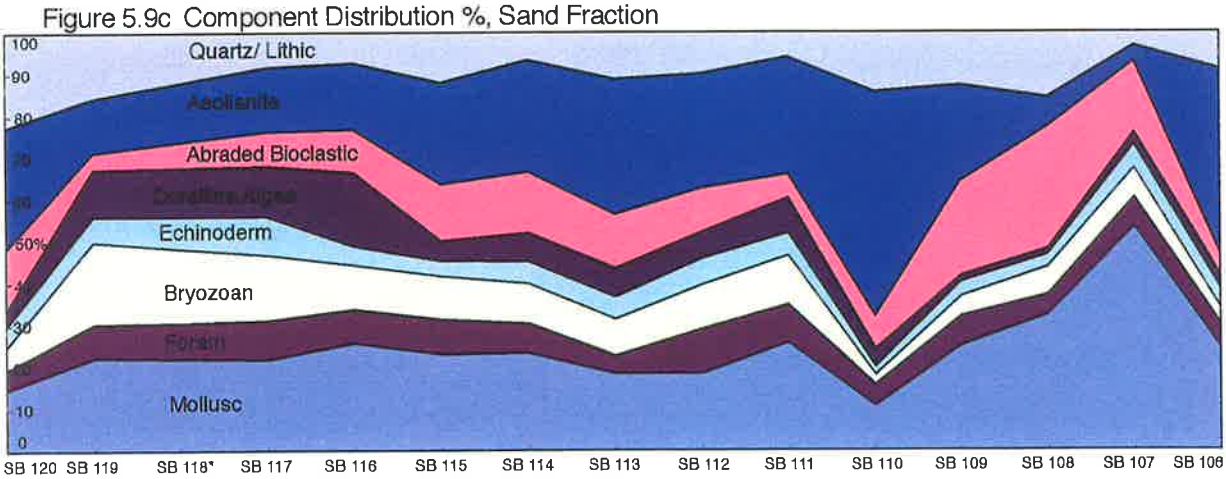



Figure 5.9d Component Distribution and Density,

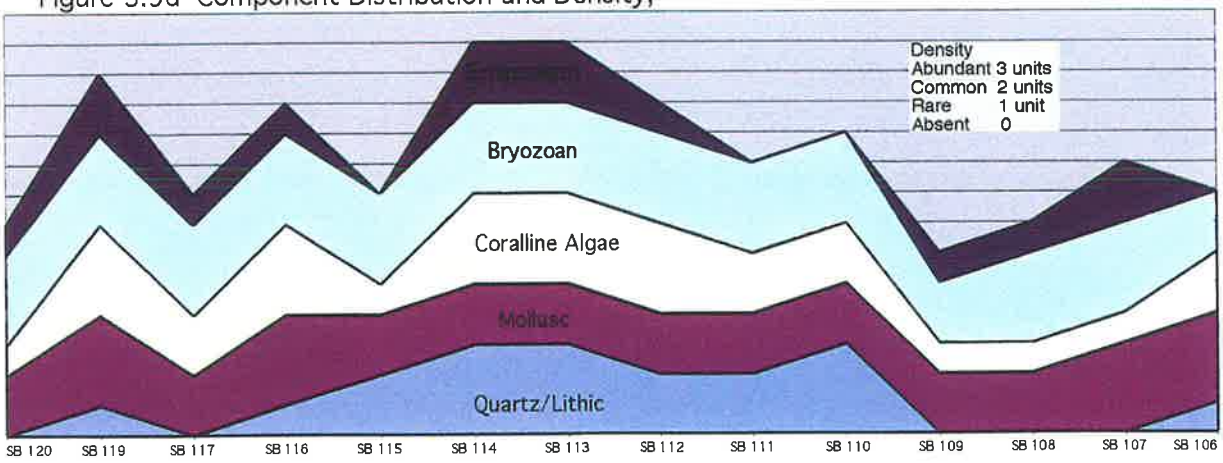


Figure 5.10a Sea-floor profile

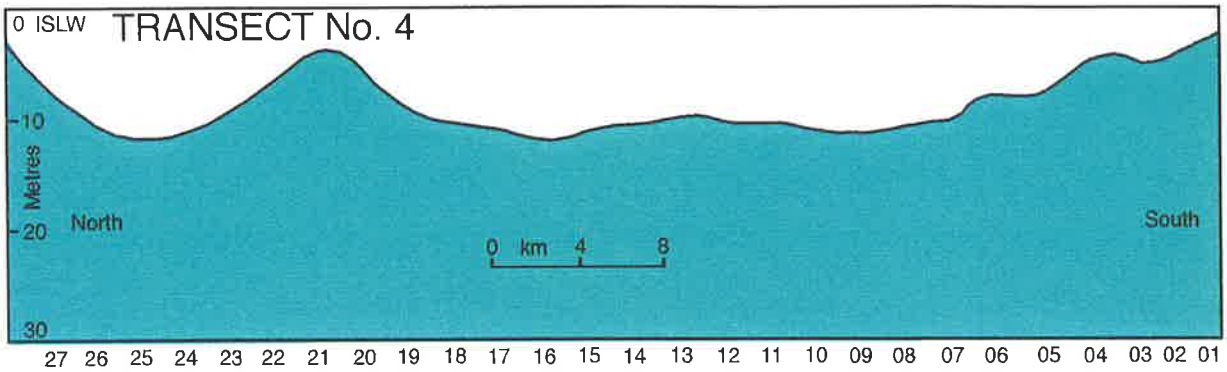



Figure 5.10b Grainsize Distribution %

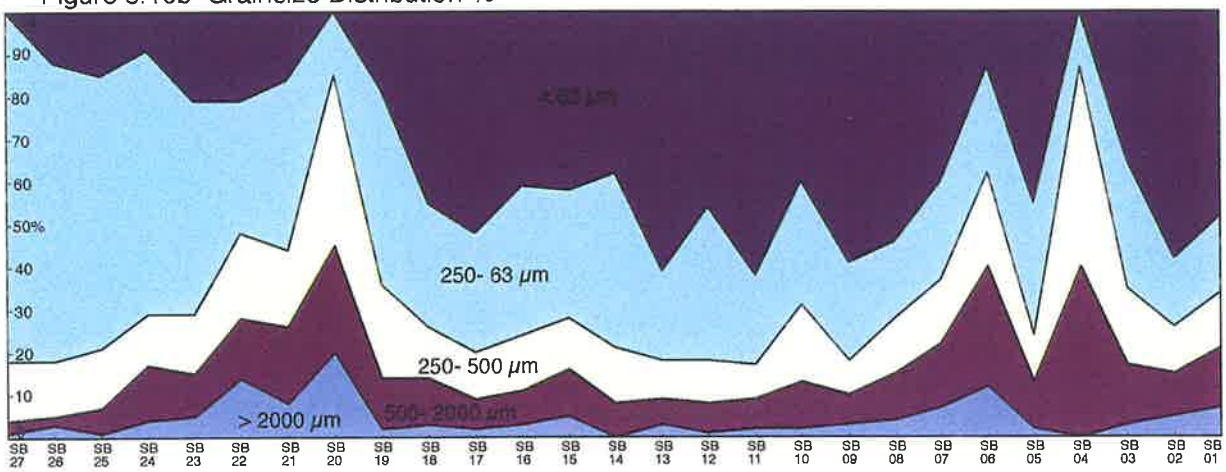



Figure 5.10c Component Distribution %, Sand Fraction

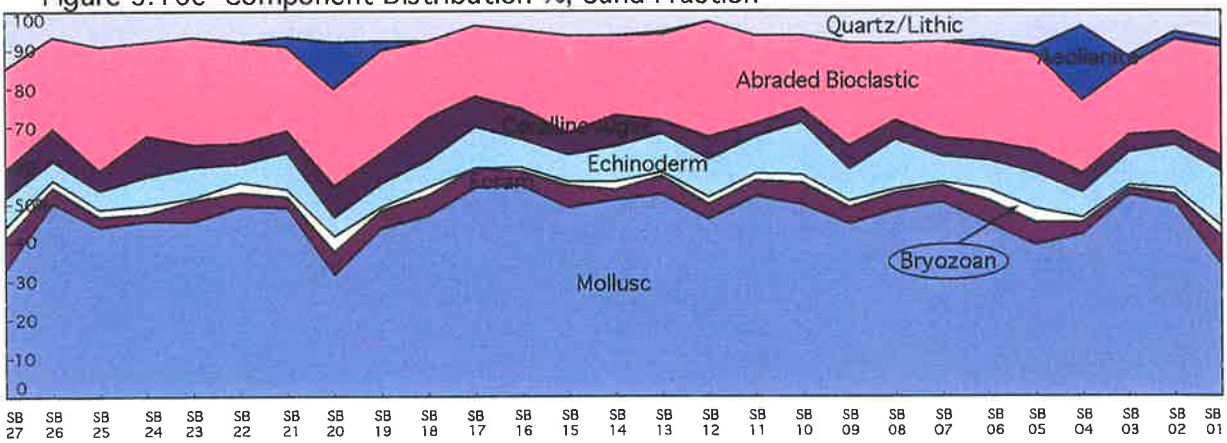



Figure 5.10d Component Distribution and Density, Gravel Fraction

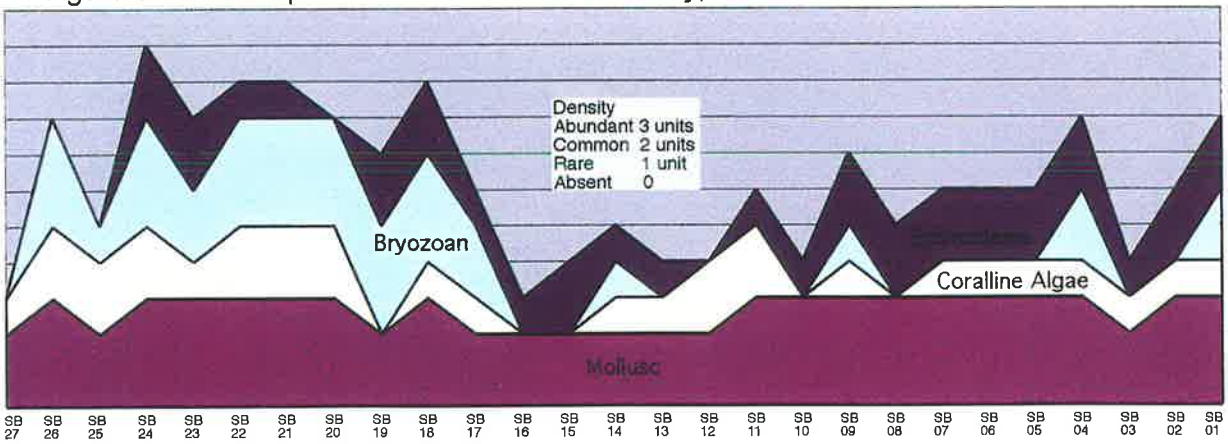


Figure 5.11a Sea-floor Profile

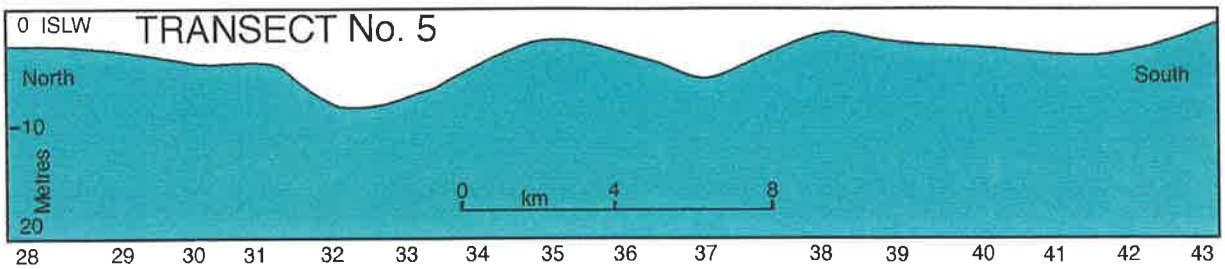



Figure 5.11b Grainsize Distribution %

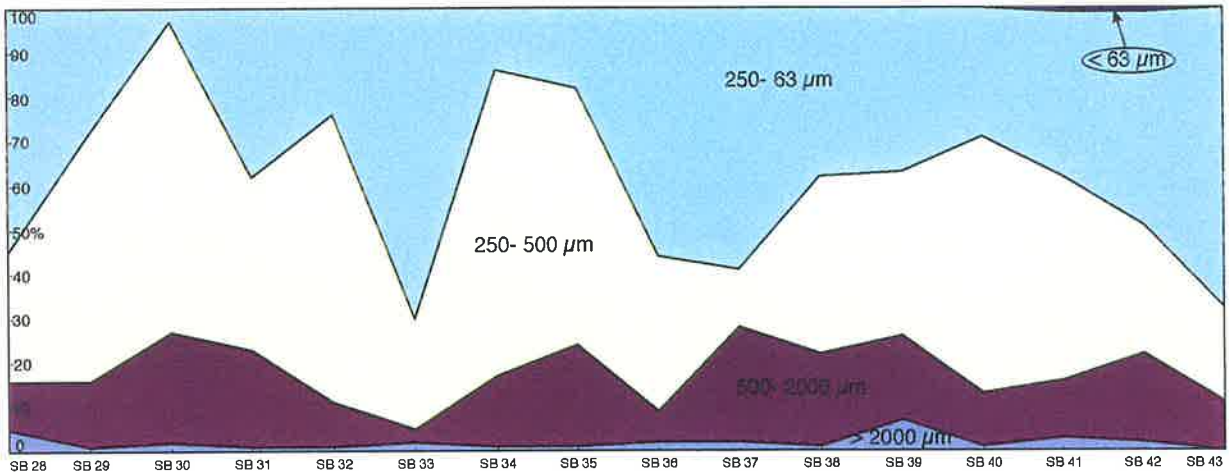



Figure 5.11c Component Distribution %, Sand Fraction

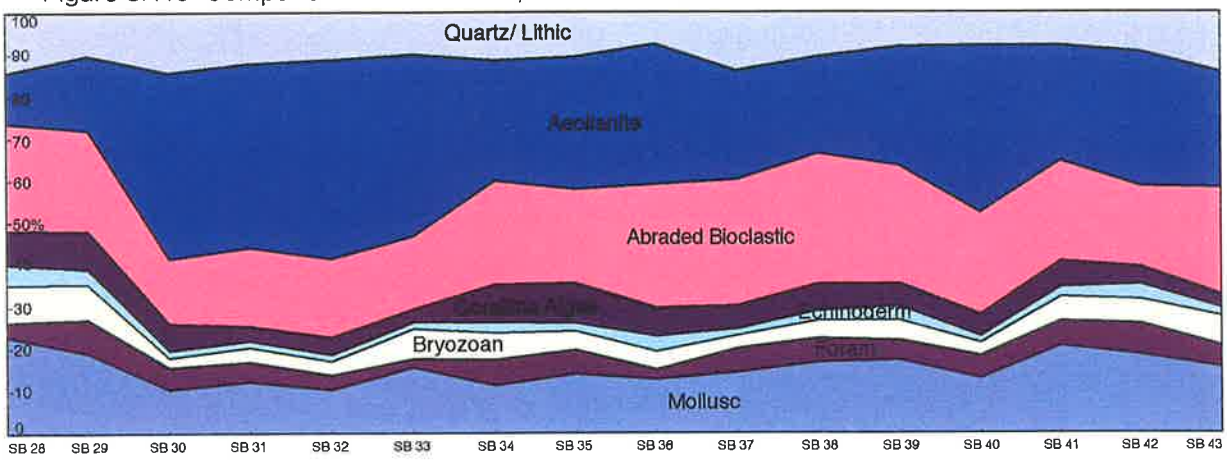



Figure 5.11d Component Distribution and Density, Gravel

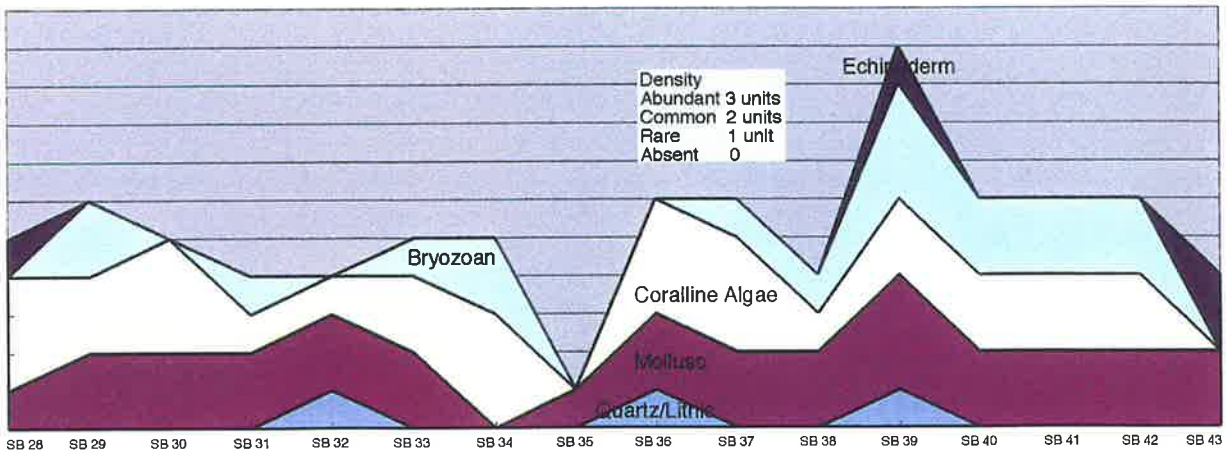


Figure 5.12a Sea-floor Profile

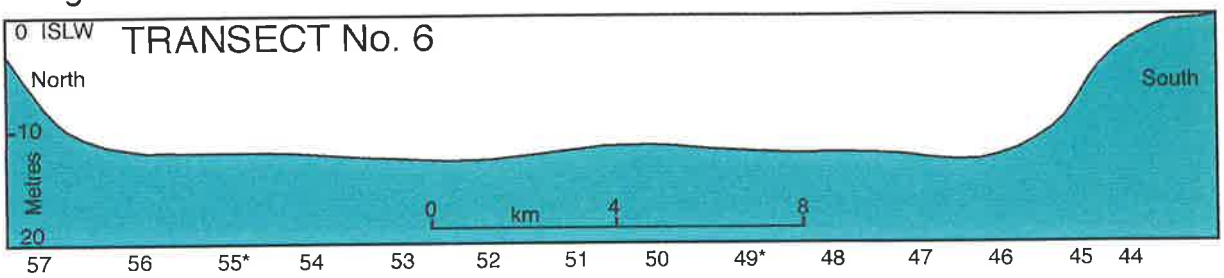



Figure 5.12b Grainsize Distribution %

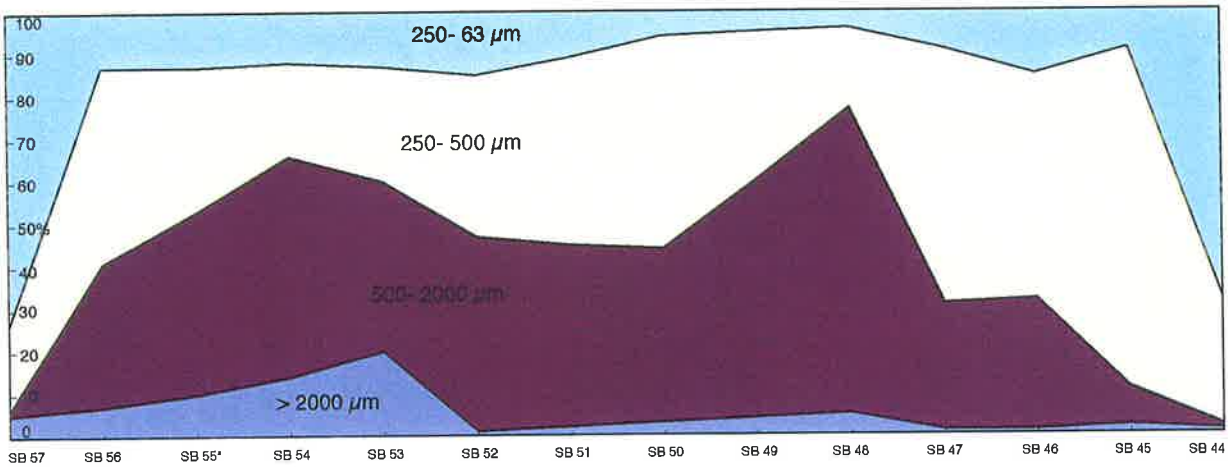



Figure 5.12c Component Distribution %, Sand Fraction

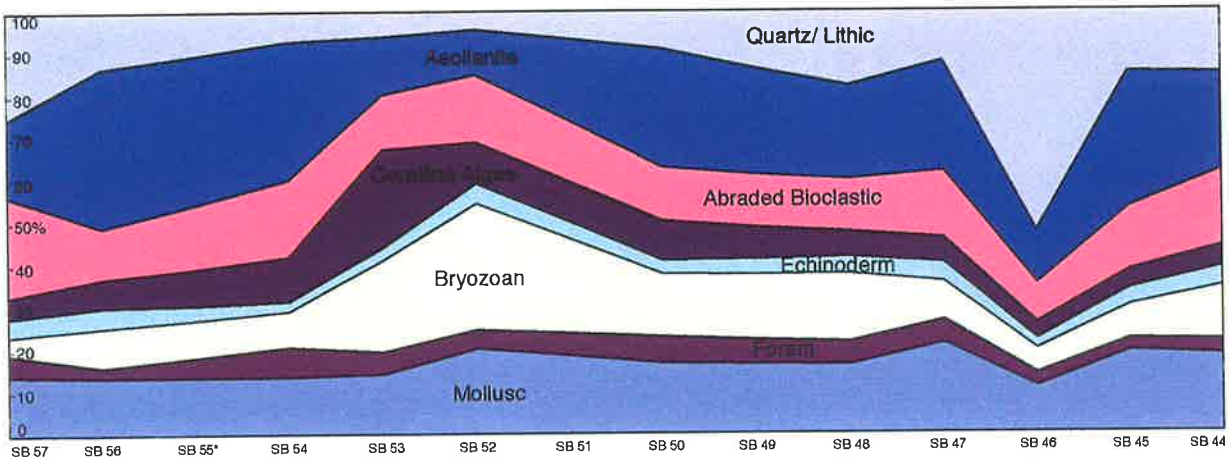



Figure 5.12d Component Distribution and Density, Gravel Fraction

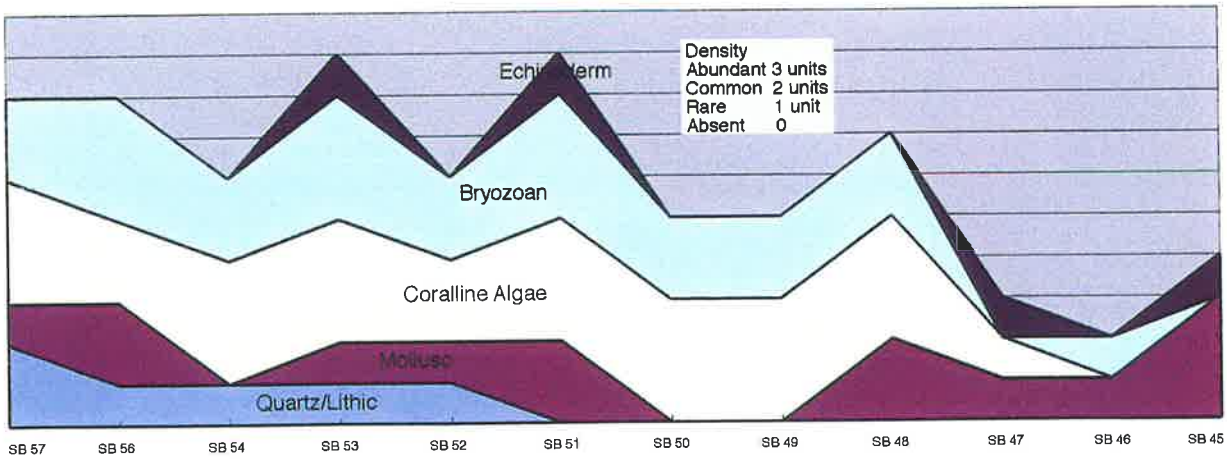


Figure 5.13a Sea-floor Profile

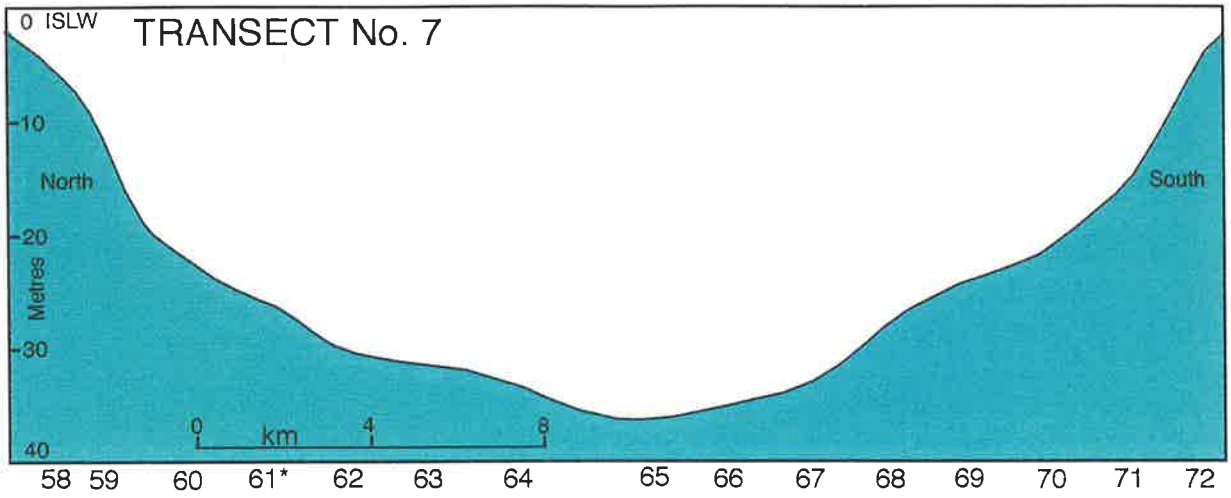



Figure 5.13b Grainsize Distribution %

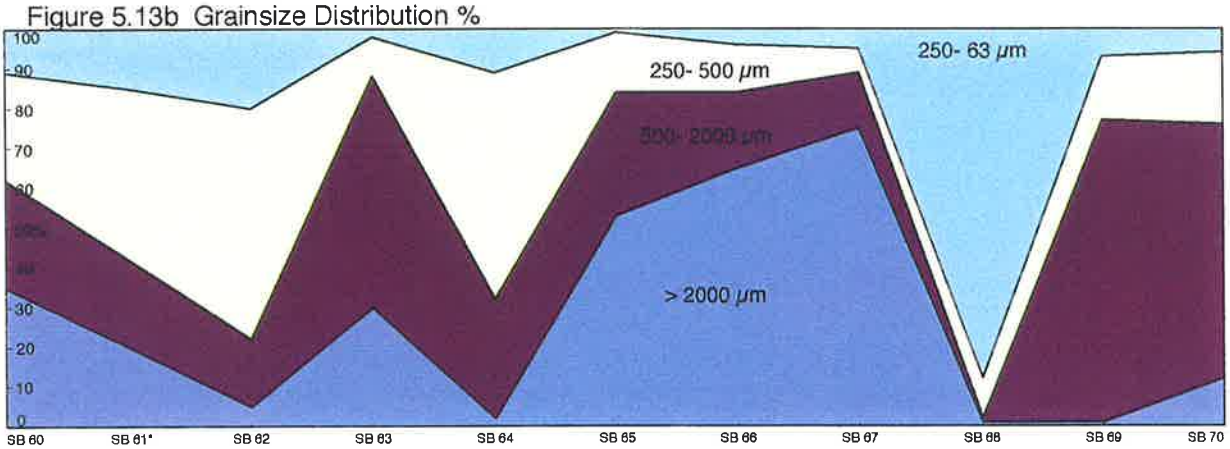



Figure 5.13c Component Distribution %, Sand Fraction

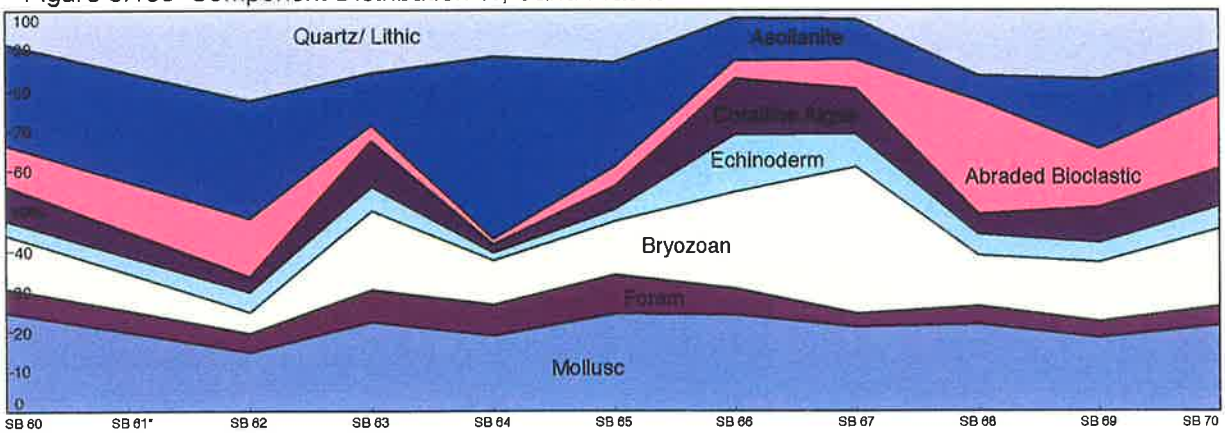



Figure 5.13d Component Distribution and Density, Gravel Fraction

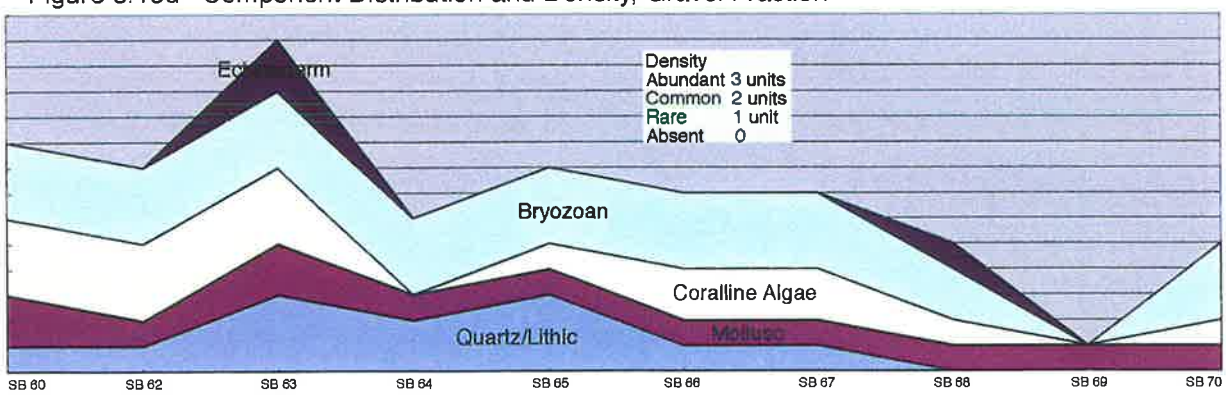


Figure 5.14a Sea-floor profile

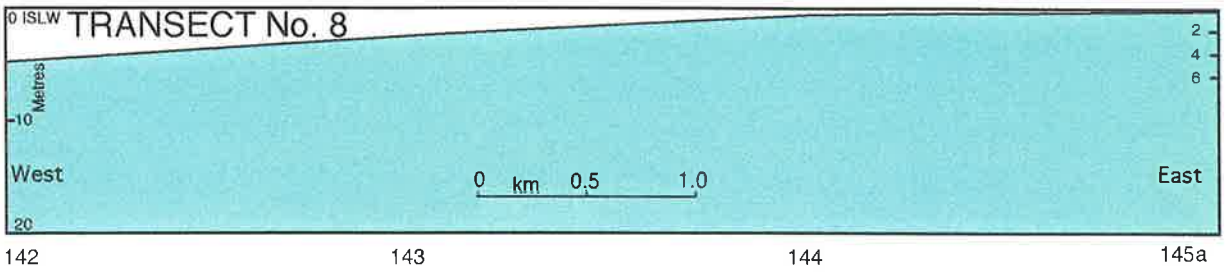



Figure 5.14b Grainsize Distribution %

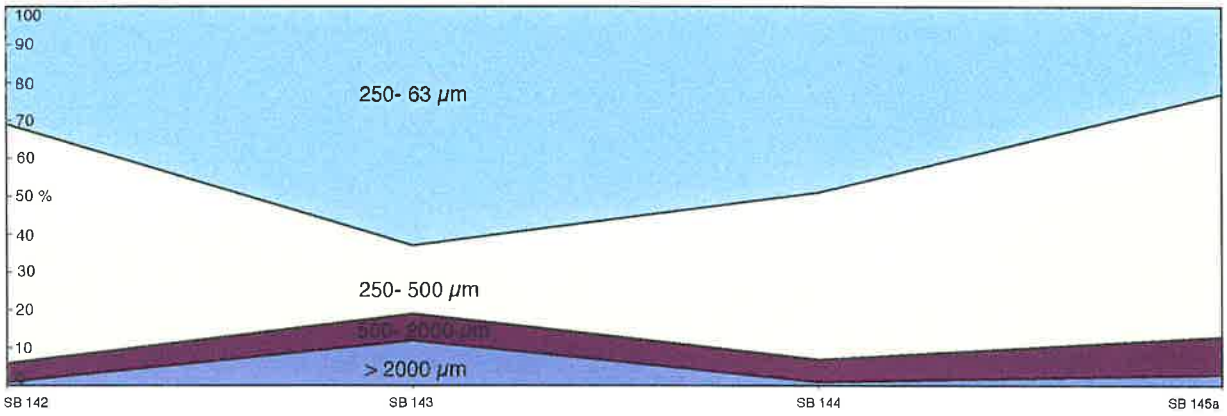



Figure 5.14c Component Distribution %, Sand Fraction

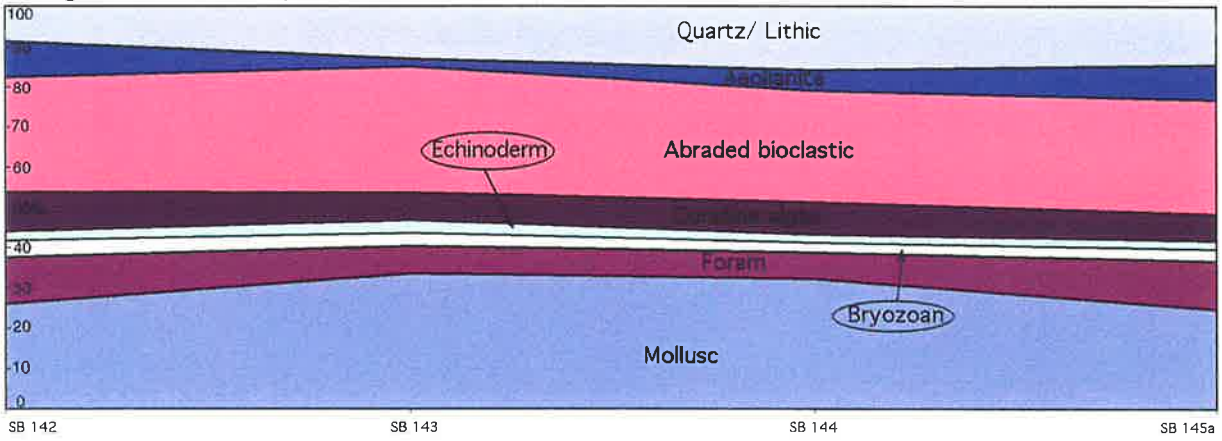
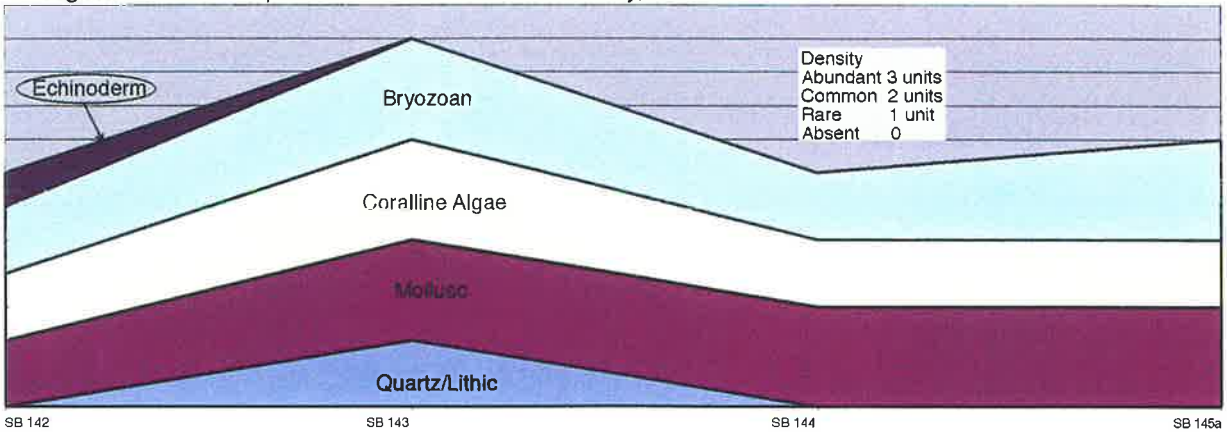
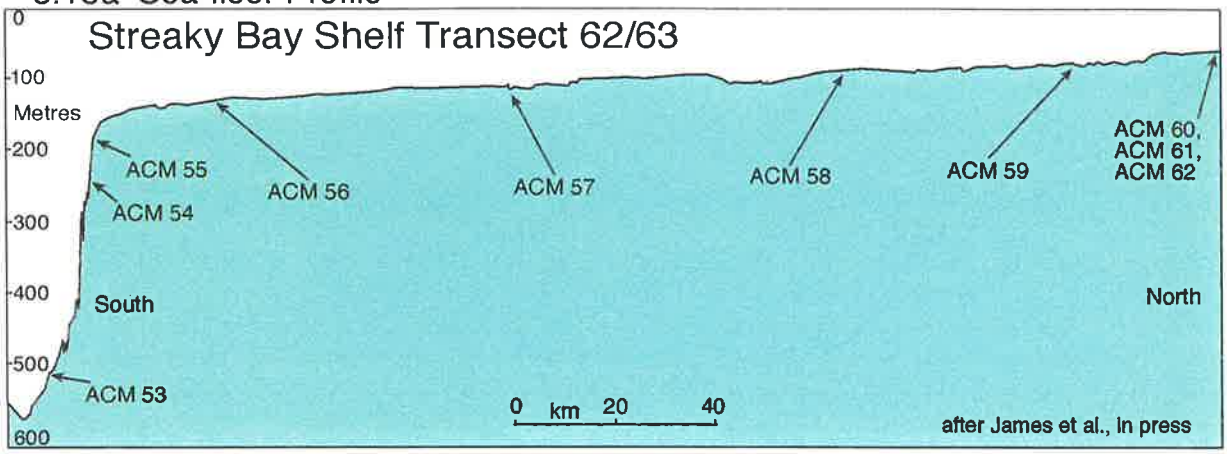


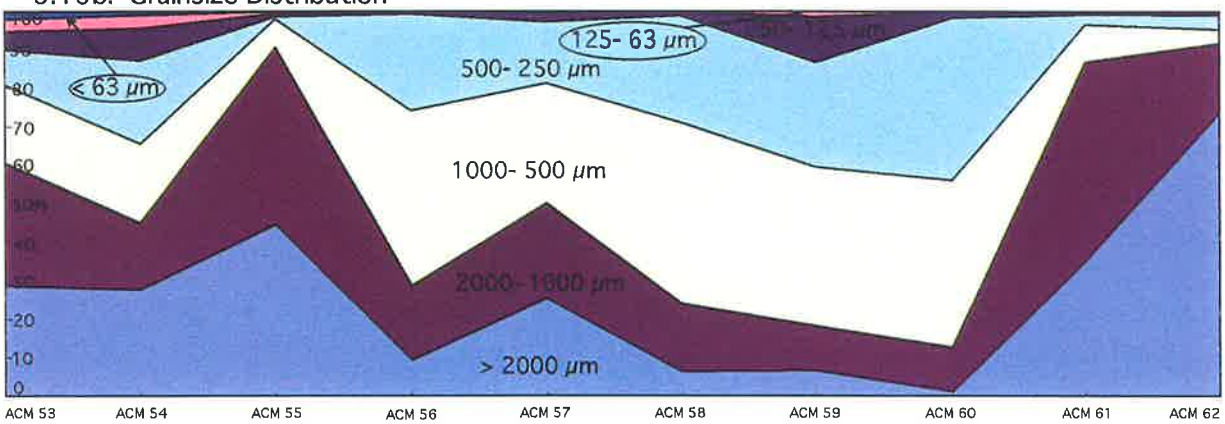

Figure 5.14d Component Distribution and Density, Gravel Fraction



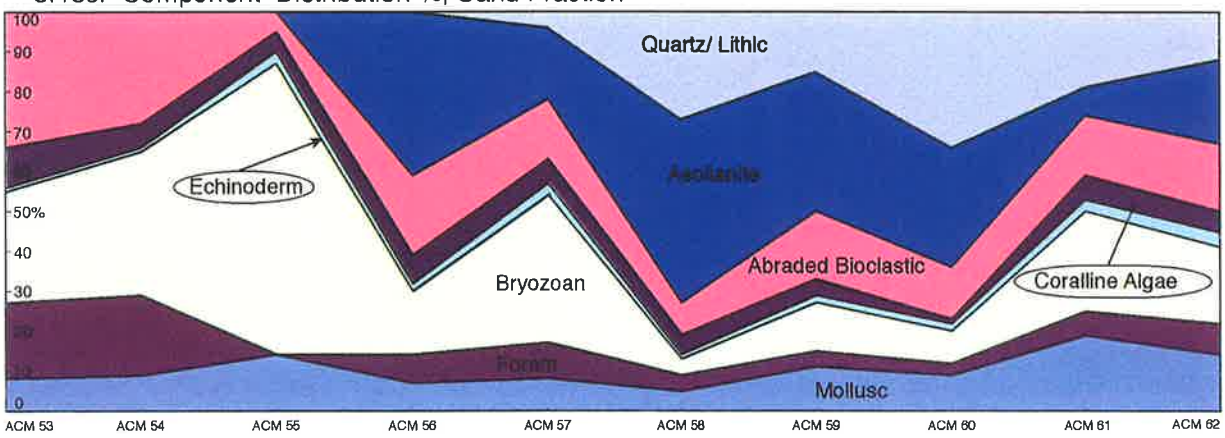
5.15a Sea-floor Profile



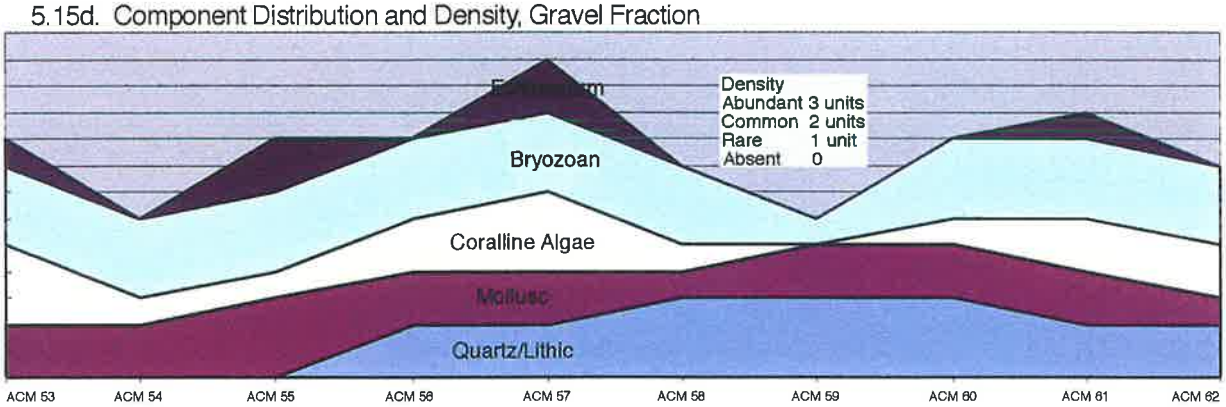

5.15b. Grainsize Distribution




5.15c. Component Distribution %, Sand Fraction




5.15d. Component Distribution and Density, Gravel Fraction



marginal basins. An increase in grainsize occurs towards the beaches on the inner bay (Figures 5.7 – 5.9).

The sediments from each of the north-south transects (T 4, T 5, T 6, T 7) reflect the above general trend. They also indicate a coarsening of sediment grainsize in the northern areas of the bay. The sediments on the western South Sand area (Transect 8) are predominantly medium to very fine sand (~90 %) (Figures 5.10 – 5.14).

Grainsize distribution on the ACM transect is not truly indicative as significant amounts of the fine fractions were lost during sample recovery and washing on deck. Generally the sediment becomes finer off-shoe, however, the gravel fraction becomes significant on the mid- to outer shelf in areas of active bryozoan thickets (Figure 5.15).

### 5.5.2 Spatial Distribution

The percentage of each principal grain size fraction was plotted and contoured onto a base map of Streaky Bay. A separate distribution map for each principal sediment fraction is presented and described.

#### 5.5.2.1 Gravel

Abundant gravel is located in the entrance of the bay (Figure 5.16). Local high concentrations are found on the central terrace and in the northern Warburton Channel, with a small area of lower concentration between the North Bank and the shore. The overall composition of the gravels across the bay is predominantly biogenic, consisting of whole or fragmented biota, some of which was alive at sampling. However, the composition of the gravels in the outer bay does have a significant quartzo-feldspathic component. The inner bay gravel concentrations are also predominantly biogenic, with the addition of eroded fragments of the Bridgewater Formation. Local areas, such as the eastern end of the North Bank and the western end of the South Sand, have abundant biogenic gravels.

#### 5.5.2.2 Very Coarse to Coarse Sand

The significant portion of the very coarse to coarse sand is located as two large lobes extending from the central areas of the entrance to the mid-terrace region (Figure 5.17). These lobes extend towards the central and northern tidal deltas, but in lesser concentrations, apart from the local high in the central tidal delta. Highs of up to 20 % occur in the northern and southern deltas. These lobes are separated by a low percentage area where abundant medium to very fine sand and gravel occur.

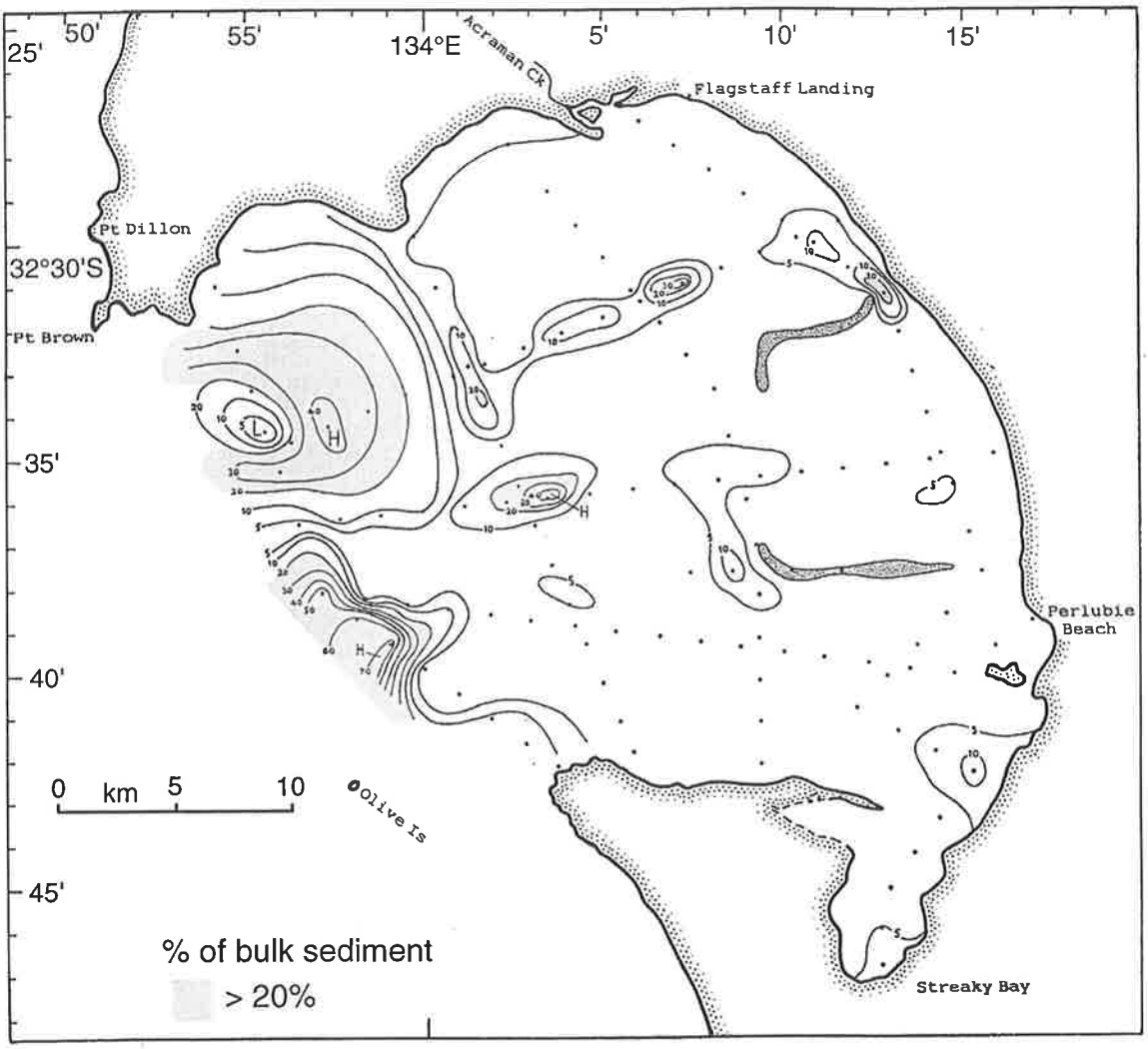



Figure 5.16 Distribution of the gravel fraction, surficial sediments, Streaky Bay

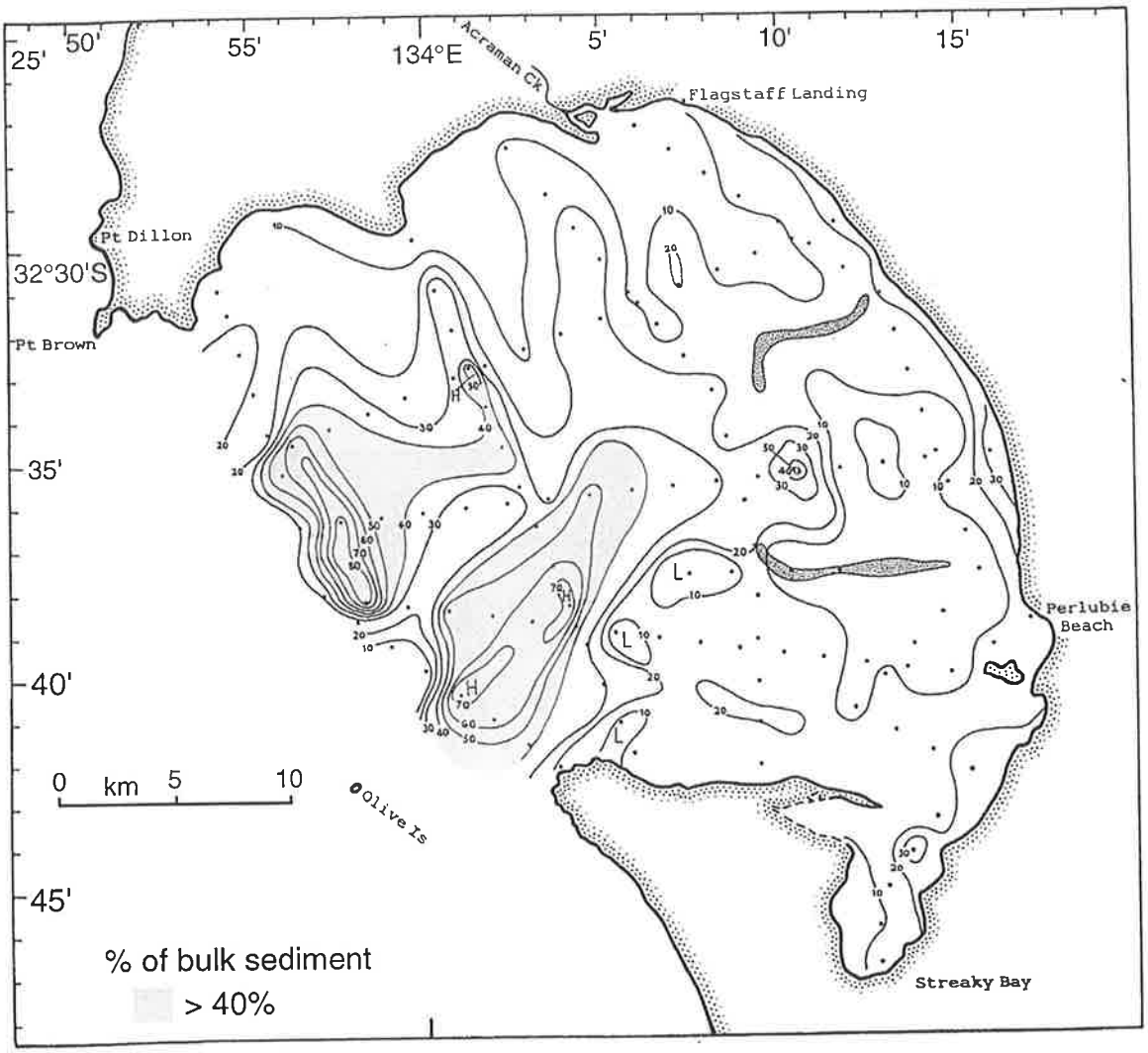



Figure 5.17 Distribution of very coarse to coarse sand, surficial sediments, Streaky Bay.

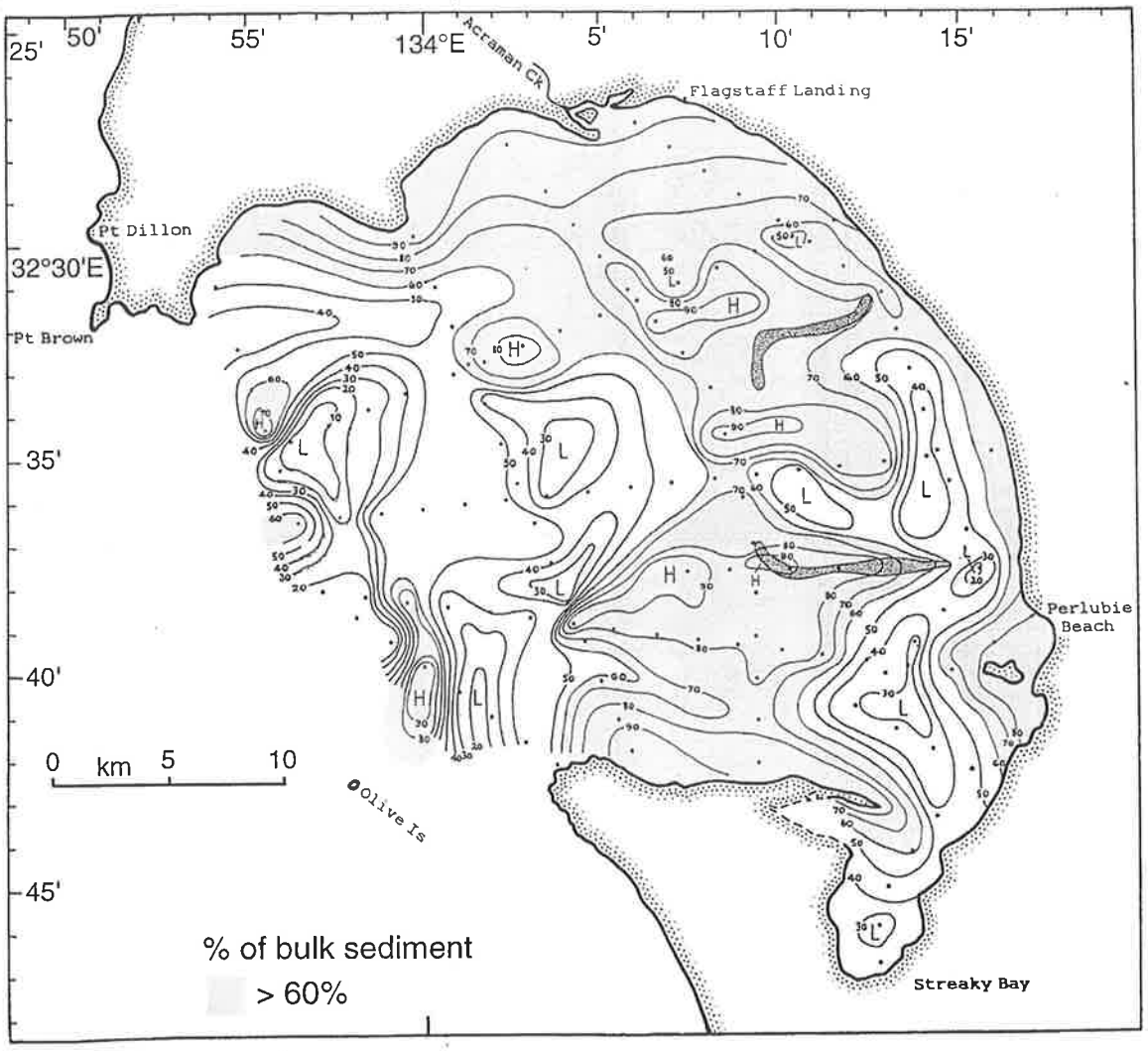



Figure 5.18 Distribution of medium to very fine sand, surficial sediments, Streaky Bay

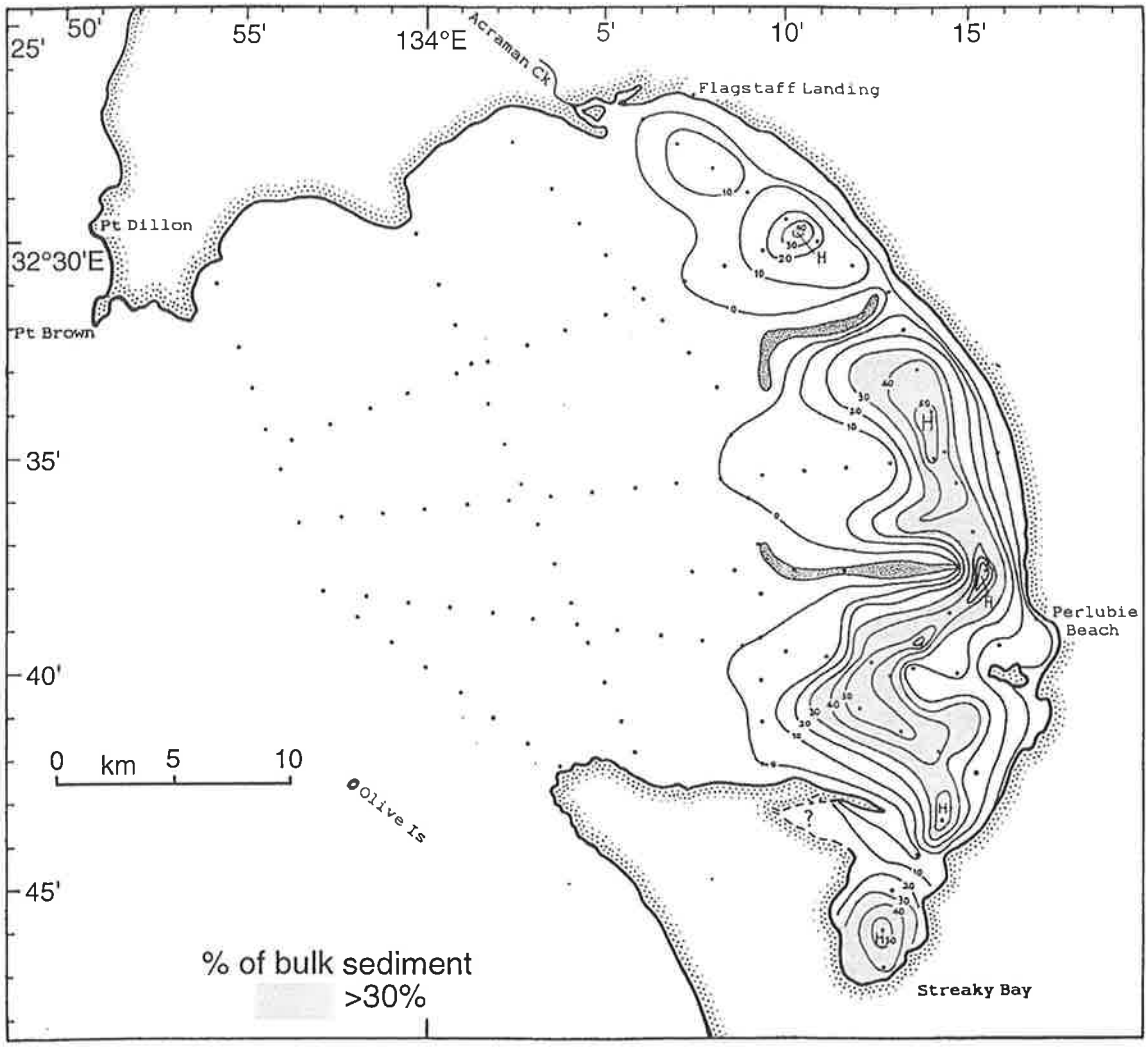



Figure 5.19 Distribution of mud (<62.5 μm), surficial sediments, Streaky Bay.

#### 5.5.2.3 Medium to Very Fine Sand

Most of the floor of the inner bay is covered by at least 60 % of medium to very fine sand (Figure 5.18). This includes the sand shoal/seagrass areas, sand banks and the margins of almost the entire shoreline to a depth of 3 m, abundant medium to very fine sand occurs in the areas of the tidal deltas, the sand banks, the northern and southern central terrace and locally across the entrance. Sparse medium to very fine sand is located in the central, southern and Blanche Port (Figure 2.3) marginal basins in the inner bay with the central terrace and entrance areas having concentrations down to 10 %. Overall the medium to very fine sand component is the dominant sediment fraction for Streaky Bay, with only minor areas in the bay containing less than 20 % of the total sample.

#### 5.5.2.4 Mud

Most mud sized sediment is confined to the inner marginal basins (Figure 5.19). The mud content in the basins increases from the north to the south, both in percentage and spatial distribution. Minor high concentrations and a more restricted occurrence of mud occurs in the northern basin. High abundance of mud occurs in the central and southern basins with an extensive presence of low percent distribution on the basin flanks. This high mud content is also present in the southern area of Blanche Port where up to two thirds of the deposit is mud.

## 5.6 SAND RATIO DISTRIBUTION

Grainsize distribution can be summarised by way of a sand ratio contour map (Figure 5.20). The ratio formula used to determine this distribution is vcS+cS/m-vfS. High ratios (very coarse to coarse sand) are shown at the entrance with low ratios predominantly in the basins. The central lows represent an abundance of medium to very fine sand. There is a significant correlation between the sand ratio map when it is compared with the gravel and the mud isopleths. The low ratios (0.1) shown on the sand ratio map in the central and northern areas, do not contain mud as do the low ratios in the inner marginal basins.

## 5.7 SKEWNESS

The skewness of a sediment measures the degree of asymmetry in grainsize distribution and also indicates, by a positive or negative sign, the direction of skew (Chapt 3, Methods). Sediments with excessive coarse fraction shows negative values and sediments with excessive fine fraction shows positive results, while sediments with a normal distribution have a skewness of zero (Folk, 1968). Skewness can indicate the hydraulic energy regime and transportation influence on a depositional

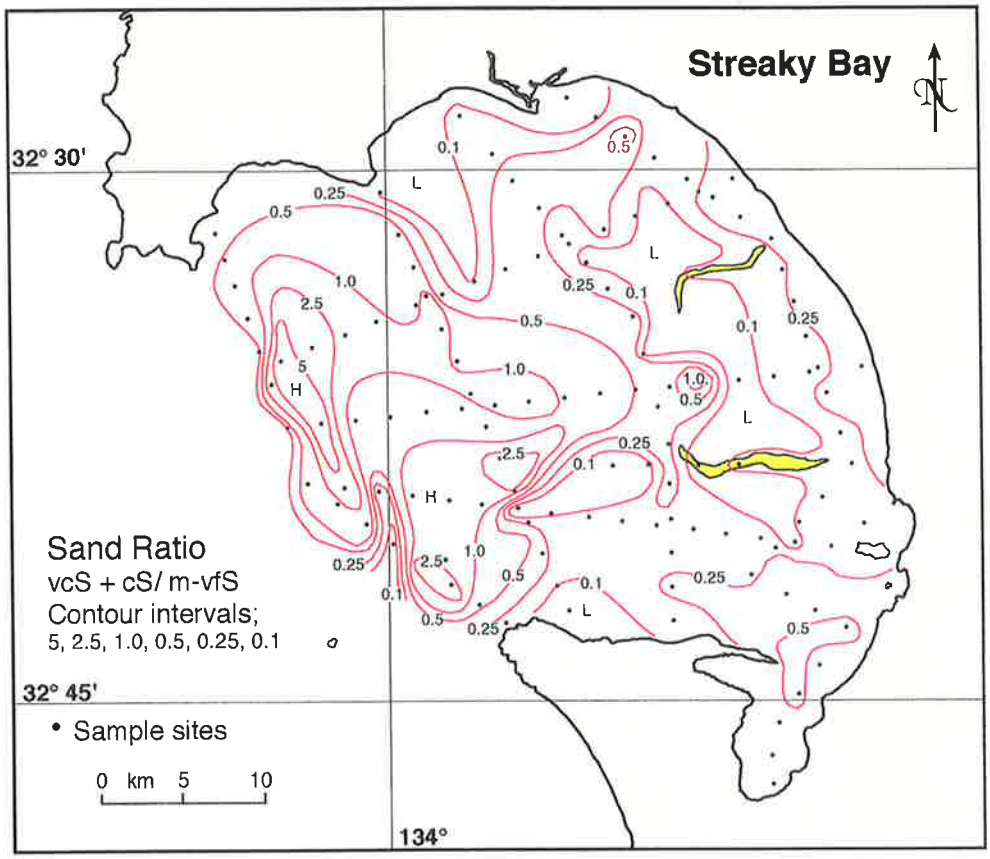



Figure 5.20 Sand Ratio Map, showing the devellopment of finer grain sedimentsed towardthe inner bay also highlighting the zones ofhigh and low energy in terms of depostional environment. higher units represent coarser sediments and lower units, finer sediments.

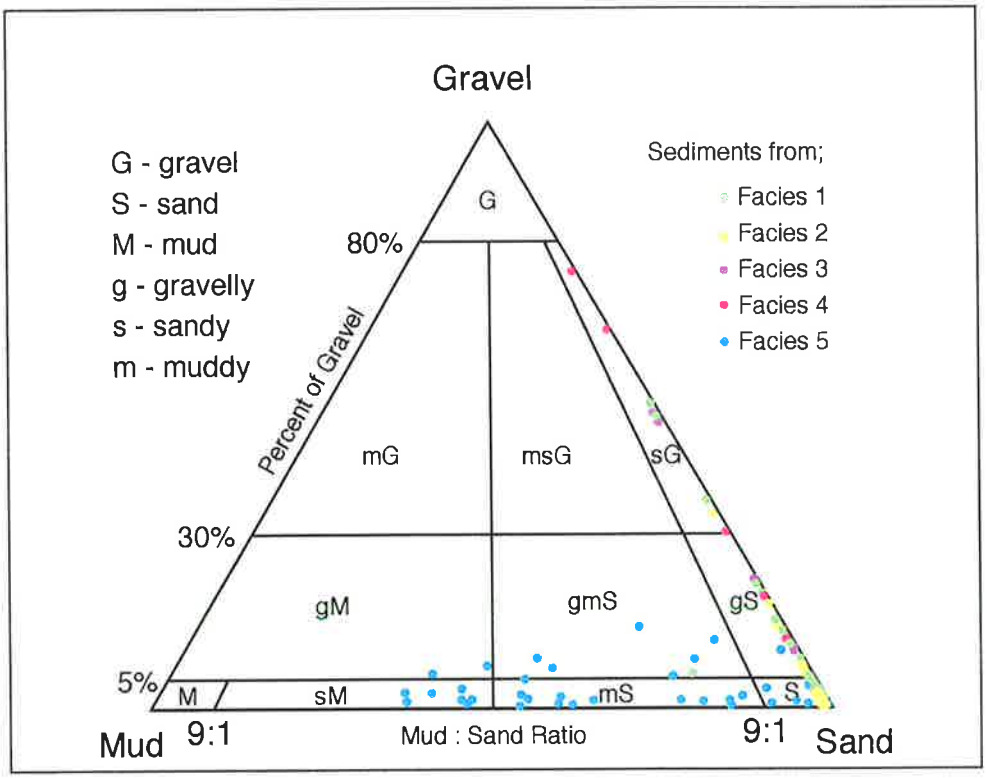



Figure 5.21 Textural distribution of sediments in Streaky Bay.
(~65% of sediments are located in the S and gS fields)

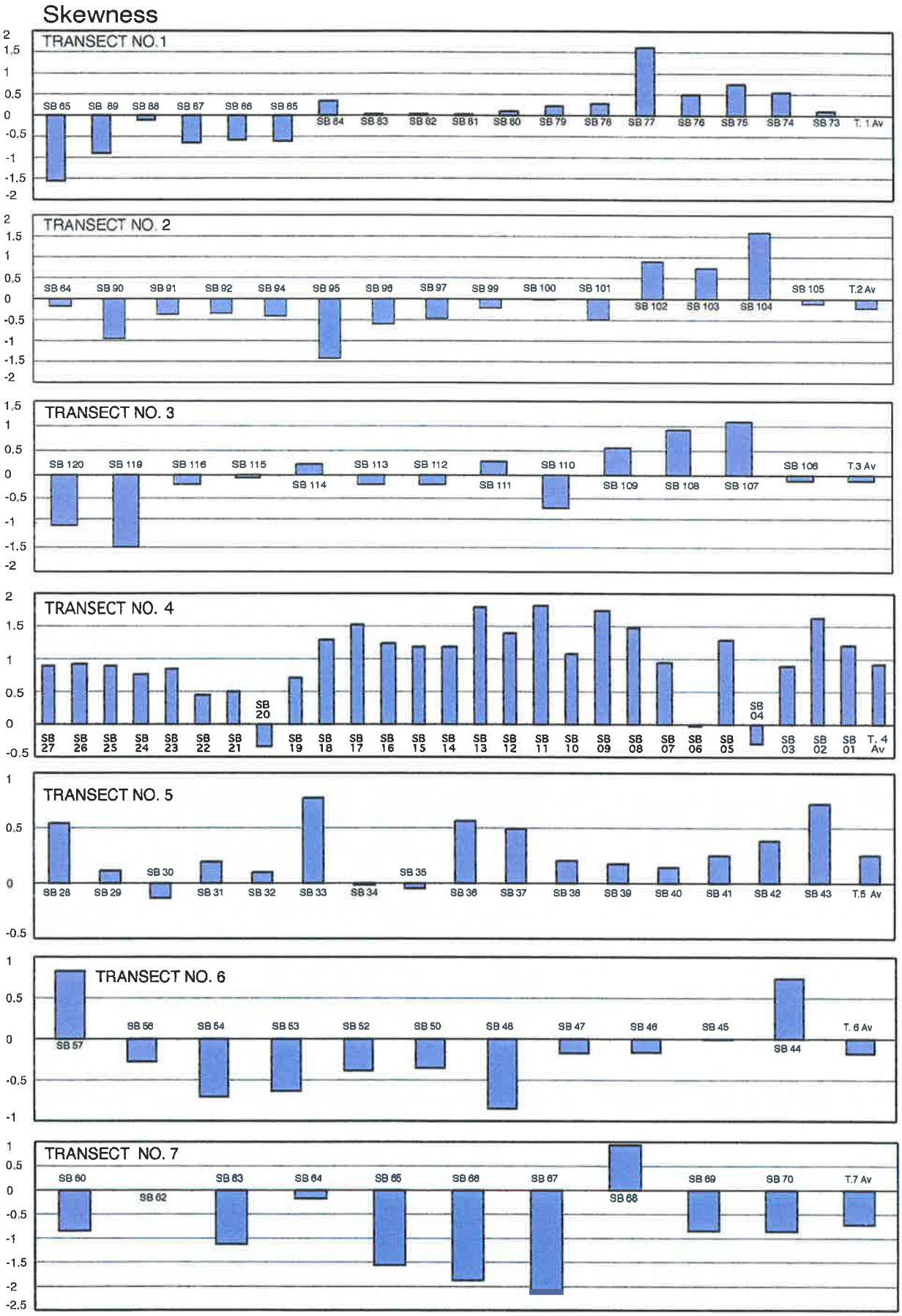



Figure 5.22 Transects 1 to 3 show a negative skewness in sediments in the outer bay representing excessive coarse fraction in the grainsize distribution and a positive skewness in the inner bay where sediments have an excess of fine fraction. Transects 4 to 7 verify this at each morphological change across the bay.

environment (Fleming, 1977) in terrigenous sediments and to a degree in bioclastic carbonate sediments.

The sediments in Streaky Bay show a general trend of negative skewness at the entrance to positive in the inner marginal basins (Figure 5.22). Sediments with negative skewness occur in the entrance and terrace area with negativity highest in the central entrance. Sediments from the sand shoals (Transect No.5) have low positive and occasional low negative values, whilst the sediments from the inner marginal basins have high positive values.

## 5.8 DISCUSSION

### 5.8.1 SAND RATIO

The sand ratio highlights the grainsize distribution, showing the development of finer grain sediments toward the inner bay and also highlighting the zones of high and low energy in terms of depositional environment. The ratio map implies that areas that have ratios < 0.1 contain mud by correlation with the inner marginal basins but the central and northern areas contains abundant fine to very sands and no mud, this is the only significant distortion of overall grainsize distribution using this ratio. The value of this ratio map lies a the clear overall view of grainsize distribution.

### 5.8.2 SKEWNESS

Skewness measures excessive departures in grainsize to a normal distribution. Skewness is only truly indicative of sediment grainsize departure when there is no *in situ* sediment production, as there is in Streaky Bay. However, skewness will give an indication of departure from normal grainsize distribution.

The graphs of skewness highlights the excessive gravels in the outer bay and the muds and fine sands of the inner bay. The sediments in the region of the sand shoals and parts of the terrace are near to normal distribution. These graphs also clearly represent the grainsize distribution of sediment across the sea-floor. It is interpreted that the grainsize skewness can indicate the distribution of energy and the general robustness of architecture of organisms across the bay. In the high energy outer bay organisms are either of a robust nature or of an encrusting style, that is stable against high levels of agitation from the prevailing swells. It also can be interpreted that skewness can also highlight the hydrodynamic regime and transportation influence on the sediments. The average of skewness for sediments from the three East-West transects approaches zero which implies that the sediments as a whole are normally distributed. It is the hydraulic regime that sorts the sediments into a continuum of grainsize from the entrance to the basins. Continuing biogenic production (local carbonate factory) in the entrance and outer terrace maintains supply for the dispersion of carbonate sediment into the inner

bay. It is also recognised that biogenic activity and maceration (degradation) are occurring throughout the bay as a whole.

### 5.8.3 GRAINSIZE DISTRIBUTION OF RECENT SEA-FLOOR SEDIMENTS, EYRE PENINSULA

#### 5.8.3.1 Comparison With Nearby Embayments

Broad grainsize distribution patterns of the nearby embayments have been determined from the texts, as quantitative grainsize data is not available.

• **Baird Bay** is a long, shallow inverse estuary situated about 50 km south of Streaky Bay (Hill, 1994) (Figure 2.1). Biogenic very coarse to fine carbonate sands are common throughout the bay with the exception of areas of carbonate very fine sandy peloidal bioclastic mud, which is restricted to low energy environments in water depths of >2 m in the upper reaches of the bay. Reworked medium to coarse carbonate sands (aeolianite) are most common in the northern region beach areas, whereas in the southern areas medium to very coarse quartz/feldspar sands are found in high concentrations especially at the eastern mouth of the bay in the tidal channel (Hill, 1994).
The range and locations of sediment grain-sizes encountered in Baird Bay are similar to Streaky Bay although the very coarse predominantly quartz/potassium feldspar sands of Baird Bay are not common and the peloidal mud is not present in Streaky Bay. The common sediments that are found in the southern third of Baird Bay are indicative of normal salinity and medium to low energy from tidal influences similar to the sand shoals and seagrass meadows in Streaky Bay

• **Tourville Bay** is a shallow embayment situated 15 km to the west of Ceduna, on the western side of Denial Bay (Figure 2.1). Sedimentary textures are described by Lablack (1985). The sandy subtidal environments are similar to those of the shallower seagrass meadows in the North and South of Streaky Bay. Fine bioclastic sands and very fine sandy carbonate muds occur in the tidal channels, usually <2 m deep, which meander into the mangrove mangles. Similar sediments occur in the mangrove mangles at Acraman Creek and the lee of Point Gibson and minor occurrences on the flanks of the inner marginal basins. Medium to very fine sandy carbonate muds that are bound by blue-green algal mats are typical of low energy subtidal to intertidal zones of tidal flats. These algal bound sediment are not found at Streaky Bay, however, similar medium bioclastic muddy sands are present on the inner lower energy beaches (Blanche Port)

• **Coffin Bay** is located at the south-western tip of the Eyre Peninsula (Figure 2.1) with the mouth of the bay facing to the north northwest, along the west coast of the peninsula (Freeman, 1985).
The sea floor of most of the inner regions of the bay in depths of over 8 m, or shallow low energy bays are characterised by bioclastic gravelly fine to very fine sandy muds containing up to 20 % shell hash,

which is similar to the fine sandy muds of the inner margins basins in Streaky Bay. Fine to medium bioclastic sands occur from these deeper water sediments to the inner bay beaches. Coarse to medium bioclastic sand constitutes a majority of the sediments in the outer regions of Coffin Bay. The components of the sands are predominantly reworked sediment (aeolianite) from the Bridgewater Formation and modern biogenic material, which is similar to the outer bay sediments in Streaky Bay.

• **Fowlers Bay** is an open bay, situated approximately 140 km west of Ceduna, with a southerly aspect facing the high energy swells of the Southern Ocean (Figure 2.1). Recent sediments found in this area are high wave energy very coarse to medium bioclastic beach and dune sands and low energy lagoonal and intertidal shelly and gypsiferous muds (Belperio, 1988). Gravelly very coarse to coarse bioclastic sands containing predominantly foraminifer, mollusc and calcareous algae fragments (CSIRO Franklin 03/98 log, and James et al., 2001) are found immediately off-shore Fowlers Bay. These are similar to some of the outer terrace and entrance sediments found at Streaky Bay, although the component percentages differ slightly. Shelly muds and overlying gypsiferous muds found inland, are typical of sediments retrieved from the upper sections of the Proto Acraman Creek cores (Figure 1.3 and 4.11-Acraman Creek Core No.9)

• **Shelf Sediments adjacent West Coast, Eyre Peninsula** are predominantly very coarse sandy gravels near headlands and islands with gravelly medium to coarse sands between. The near shelf sediments in the vicinity of Streaky Bay are mostly a veneer of slightly gravelly medium to fine sands with sediments becoming coarser off-shore (Figure 5.15). The increasing gravel fraction is composed predominantly of biogenic fragments.

### 5.8.4 Origins Of Sand-Sized Sediments

Transport and maceration is occurring continually from the high energy entrance of the bay to the principal lower energy deposition sites ie. the sand shoals (spits and banks) with mud sized sediment being transported to the inner basins. These basins are slowly being filled with sediment transported via the extensive tidal flood deltas located on the seaward side of the basins. There is a marked attenuation of wave energy and hence grain transport capacity from the entrance to the Inner Marginal Basins. In noting the general decrease in grainsize ratio landwards it can be interpreted that this is also due a continuum of maceration of the skeletal material which originates from where biota dies and begins the process of maceration and transport. This is shown through the development of skewness values (negative to positive) from the outer to the inner bay.

The prolific robust organisms present in the outer bay are influencing the skewness of the sediments in this area. The subsequent transportation of macerated small biogenic grains from the entrance and

terrace to the inner marginal basins are highlight by the positive skewness of grainsize distribution in that area. It is interpreted that the excess coarser grains present in the outer bay are due to diverse substrate environments which are ideal habitats for a wide range of organisms and the excess fine grains in the inner bay are due to the transportation of fines from the outer bay while also maintaining a coarse fraction by virtue of the biota present in all areas.

The energy being expended by the high energy storm swells, approaching from the south west, at the relatively steep-sloped entrance and terrace to Streaky Bay ensures high rates of transport from the site of high diversity and abundance of calcareous biota. It can be interpreted that the terrace and entrance are sites of high diversity and abundance from the results of the identification and relative occurrence of gravel components. It appears that once any biota has been dislodged from its habitat through breakage or death, it can be transported into the bay via migrating sand waves or becomes fill for the many crevices observed on the entrance floor of the bay and undergo further maceration (Figure 5.3 and 5.4).

The relative ages of grains within the sediments do not appear to show marked finer populations towards the inner bay apart from the abraded bioclastic grains, which are highly concentrated in the IMB. The relative ages of the sediments has been divided into three categories:

A) Yellowed well rounded bioclastic grains are attributed to sediments of the Bridgewater Formation and occur on the sea-floor, where this formation is being actively eroded in situ or they have been transported into the bay from adjacent sites of erosion ie. the cliffs to the north and south. These sediments, even as a result of their age, do not appear biased to finer grain-sizes towards the inner areas of the bay.

B)White sub-angular to well rounded abraded bioclastic grains, possibly mid- to late Holocene, show high concentrations towards the inner areas of the bay. These abraded grains of indistinguishable biogenic origin are either the results of elevated rates of bioerosion, maceration and dissolution or extended periods of time in the abrasion zone of the sand shoals and inner terrace before being transported to the IMB.

C) Fresh white angular fragments of discernible biota are of recent origin and do have not been subjected to extended periods of degradation.

Substrates vary across the west-coast embayments from low energy sandy muds to sand banks and seagrass meadows to gravelly coarse sands to rocky outcrop. The rocky seafloor is the most prolific of these substrates in terms of biological growth and activity (James et al., 1992; 1997, 2001, Nelson et al., 1992). These rocky substrates occur from the mid- to inner shelf (<60m) and the entrance to inner terrace off and in Streaky Bay. Rocky substrates are not common in the other embayments along the west coast and hence a commensurate lack of faunal diversity.

This accumulation of sediment is showing a reverse style of progradation, typical of the west coast embayments, from gravelly coarse sediments at the entrance to the very fine sands of the tidal deltas which are prograding onto the muds of the inner embayments. This is also highlighted by the general decrease in sand ratio values towards the inner shores, which indicate that transport coupled with energy attenuation, maceration, and occasional abrasion from high energy storms, is occurring in a continuum from the high energy entrance of the embayments to the low energy principal deposition sites i.e sand shoals and inner mud dominated basins.

## 5.9 CONCLUSIONS

The spatial distribution of sediment grainsize in Streaky Bay generally becomes finer towards the inner areas of the bay. This gradation of grainsize ranges from gravelly very coarse sands occur at the entrance and outer terrace to coarse and medium sands on the inner terrace area becoming finer sand in the region of the tidal deltas and muddy in the inner marginal basins. Further broad gradational coarsening of grainsize occurs from South to North due to an increasing energy regime from the swells of the Southern Ocean.

Local relatively high energy conditions modify the overall gradation of grainsize distribution in areas such as the elongate sand banks, spits and beaches, which are also submerged diurnally. Significant accumulations of gravels are found at the entrance to the bay where the amplitude of the long swells of the Southern Ocean is rapidly attenuated with the shallowing water depth and resultant high energy conditions on the sea-floor to concentrate these sediments. These high energy conditions, albeit attenuated, are found in the Warburton Channel (northern) with the resultant accumulations of gravels eroded proximally from the seabed.

The significant attenuation of wave energy in the central shallow sand shoal region has allowed favourable conditions for the deposition of very fine sandy mud over a considerable area of the deeper inner bay. These accumulations of mud, which is deposited in the deeper inner basins, is unusual in a normal shallowing marine setting and as such has provided an opportunity to study the development of marine carbonate mud.

# CHAPTER SIX

# COMPOSITIONAL DISTRIBUTION OF SAND-SIZED SEDIMENT

## 6.1 INTRODUCTION

The aim of this chapter is to determine and delineate the distribution of the significant calcareous and significant accessory components in the sand fraction of the sediments. The composition of the sands and the distribution of these components is an important indicator in determining the sedimentary facies in the bay. The dominance of the sand fraction in sediments of Streaky and other bays of the West-coast, Eyre Peninsula, attest to the importance of delineating these compositions especially in relation and correlation to the overall composition of shelf sediments. It is necessary to determine the composition and variations of these marginal cool-water carbonate sediments so that an analogue for marginal marine limestones can be presented.

The dominant components of the sands are; Holocene identifiable biogenic fragments (molluscs, bryozoans, foraminifers, echinoderm (principally echinoid), and coralline algae), abraded bioclastic grains, calcareous aeolianite or relict carbonate grains and Proterozoic granitic grains (predominantly quartz and potassium feldspar). Percentage composition of these components is calculated through point counting, transferred to distribution graphs and plotted and contoured on a Streaky Bay base map to determine the spatial distribution of each component (Chapter 3 - Methods).

## 6.2 COMPONENT IDENTIFICATION

The grains in the sand are recognised by the properties as outlined in Table 6.1. This table summarises the more important diagnostic properties, which have been used to identify the grains by reflecting microscope while point counting. The grains are grouped under the following components; molluscan, bryozoan, foraminifer, echinoderm (principally echinoid), coralline algae, abraded bioclastic, calcareous aeolianite and quartz and lithic grains, which are subdivided into quartz, potassium feldspar, lithic igneous, lithic aeolianite. The quartz, feldspar and lithic subdivisions are grouped together for the point counting analyses.

## 6.3 RESULTS

### 6.3.1 General distribution of Sediment Components

The grain components of the sediments have similar distribution patterns on each of the East-West transects (Figures 5.3c, 5.4c, 5.5c, 5.6c, 5.7c, 5.8c, 5.9c). Molluscan grains increase from the entrance (West) to a maximum in the inner marginal basins, decreasing towards the beach. Foraminifera have a maximum in the sand shoals and inner terrace and decrease to the beach and the entrance. Bryozoan grains increase from the beach to a maximum at the entrance and outer terrace. Echinoderm grains are uniformly distributed in the sediments with a maximum in the inner marginal basins and the outer terrace on Transect 2. Coralline algae grains increase centrally from lows at the beach and the entrance to a maximum on the terrace. Abraded bioclastic grains increase from the entrance and the beach to a maximum on the terrace and inner marginal basins. Calcareous aeolianite grains are concentrated in the entrance, on the sand shoals and the near beach areas. Quartz-lithic grains increase from the inner marginal basins to a maximum in the entrance. Abraded bioclastic aeolianite and quartz/lithic grains are concentrated to the North and South areas of the bay. Generally the grains derived from recent organisms occur in higher concentrations in the central areas of the bay.

| Component | Grain morphology | Grain/Skeletal Structure, Growth patterns | Colour, Reflectivity | Ornamentation |
|---|---|---|---|---|
| **Molluscan** | tabular to prismatic | lamellar, perpendicular, chevron, oblique | bright white to off-white opaque, 'dense' /dull reflective | rare costal grooves |
| **Bryozoan** | irregular tabular, planar/curved | fine lamellar | white to translucent, dull to medium reflective | with or without frontal wall ornamentation |
| **Foraminifer** | usually complete test, or major fragment | very fine lamellar, fine perpendicular, agglutinate | white to buff, highly reflective | typical foram ornamentation, with or without pores, agglutinate chambers |
| **Echinoderm** | plates, spines, ossicles, irregular polygonal grains | open porous network, crystal continuity | white to semi translucent, medium to highly reflective | rare spine boss and porous ambulacral plates |
| **Coralline Algae** | irregular nodular to polygonal grains, disarticulated segments | very fine porous | off-white, chalky, low flat reflectivity | surface pores in cross and long section |
| **Abraded Bioclastic** | rounded, amorphic, fresh in appearance | indistinct growth layers, biogenic in origin | relatively white, medium reflective | No ornamentation, smooth |
| **Calcareous Aeolianite** | well rounded, sub spherical | biogenic in origin, polished, occasional cemented grains | buff to yellowish, medium to dull reflective | no ornamentation, smooth |
| **Quartz** | well rounded to sub angular, sub spherical | abundant micro-fractures, dull to polished | transparent to white translucent, high to medium reflective | some pitting to smooth |
| **Potassium Feldspar** | well rounded to subangular, sub spherical | grains fractured | dark yellow to orange, highly to dull reflective | isolated pitting to smooth |
| **Lithic, igneous** | prismatic to sub-spherical | fragments of felsic rock, qtz-fsp-hbe | white-yellow-dark green to black, medium to dull reflective | isolated pitting to smooth |
| **Lithic, Bridgewater Formation** | gravelly to coarse grain, sub angular | cemented grains of calcareous aeolianite, biogenic origin | buff to yellow, medium to dull reflective | no ornamentation, smooth to uneven |

Table 6.1 Identification table of principal sediment components, for reflecting binocular microscope.

## 6.4 SPATIAL DISTRIBUTION OF COMPONENTS

### 6.4.1 MOLLUSCAN GRAINS

Molluscan grains are concentrated on the eastern side of Streaky Bay in the inner marginal basins, with an increasing concentration in the central to southern portion of the bay (Figure 6.1). Lowest concentrations occur on the seaward side of the northern tidal channel to the northwestern beach. Molluscan grains are the most abundant sediment component with a major proportion of the inner bay containing > 30% and areas of the inner marginal basins > 45%. Minor central and outer areas contain < 20% with a small northern pocket of sediment containing < 10% molluscan grains.

### 6.4.2 FORAMINIFERS

Significant concentrations of foraminifers (> 15%) are located on the outer to central terrace area where abundant brown and soft red algae are present, the southern and central seagrass meadows/ sand shoal/ tidal delta region and further east in the area of Perlubie Beach/ Eba Island (Figure 6.2). Lowest concentrations (< 5%) occur in the central and northern inner marginal basins, northern and southern portions of the bay and Blanche Port.

The Rotaliid*s* *(Discorbis* ssp., *Cibicides sp., Elphidium ssp.)* and Miliolinid*s* (*Triloculina* ssp., *Quinqueloculina* ssp., *Peneroplis* ssp. *Spiroloculina* ssp.) are common with rare *Textulariids* (*Textularia* ssp., *Cibrobulimina* ssp.) in shallow seagrass areas. There is a general increase in foraminifers numbers in the central deeper waters where the ratio of Rotaliid*s* to Miliolinids and Textulariid*s* falls and the population of Miliolinids remains approximately the same as the sea grass areas.

The foraminifers that are common in the outer region are:
Miliolinids- *Triloculina* ssp., *Quinqueloculina* ssp., *Peneroplis* ssp. and *Trochammina* sp.;
Rotaliids- *Elphidium* ssp., *Discorbis* ssp., *Cibicides sp.* and rare *Sorites* sp.;
Textulariids- *Textularia* sp., *Cribrobulimina* sp.
The tests of a significant proportion of the foraminifers become larger and more robust in the outer terrace to entrance areas.

### 6.4.3 BRYOZOAN GRAINS

Bryozoan grains occur in high concentrations in the sediments associated with the rocky substrates in the central entrance to outer terrace area (up to 35 %) (Figure 6.3). The bryozoan sand content of the sediment diminishes towards the seagrass/ sand shoals and shallowing entrance areas with lowest bryozoan grains occurring in the tidal deltas and inner marginal basins (< 5%).

### 6.4.4 ECHINODERM GRAINS

Echinoderm grains do not occur in significant numbers in Streaky Bay sediments although they are present in restricted concentrations of ~ 12 % in the inner marginal basins, the southern tidal channel and the outer central terrace area (Figure 6.4). Echinoid grains are of mostly epifaunal varieties (where identifiable) with only trace amounts of infaunal types; ophiuroid fragments are confined to the terrace and entrance areas.

### 6.4.5 CORALLINE ALGAL GRAINS

Significant concentrations of coralline algal grains are confined to the northern terrace with lesser amounts in the central entrance area and the north portion of the central inner marginal basin (Figure

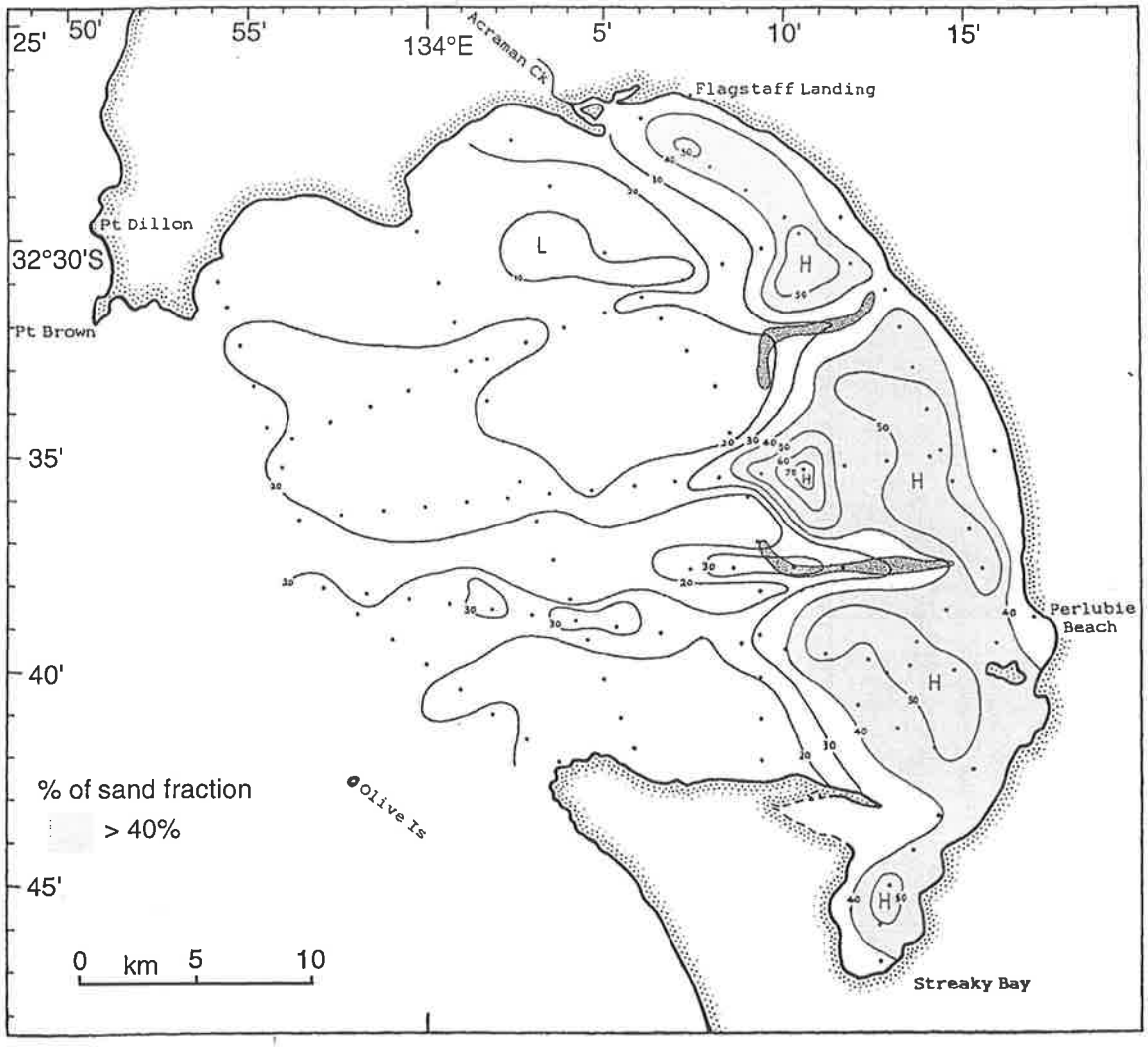



Figure 6.1 Distribution of molluscan grains, (sand fraction).

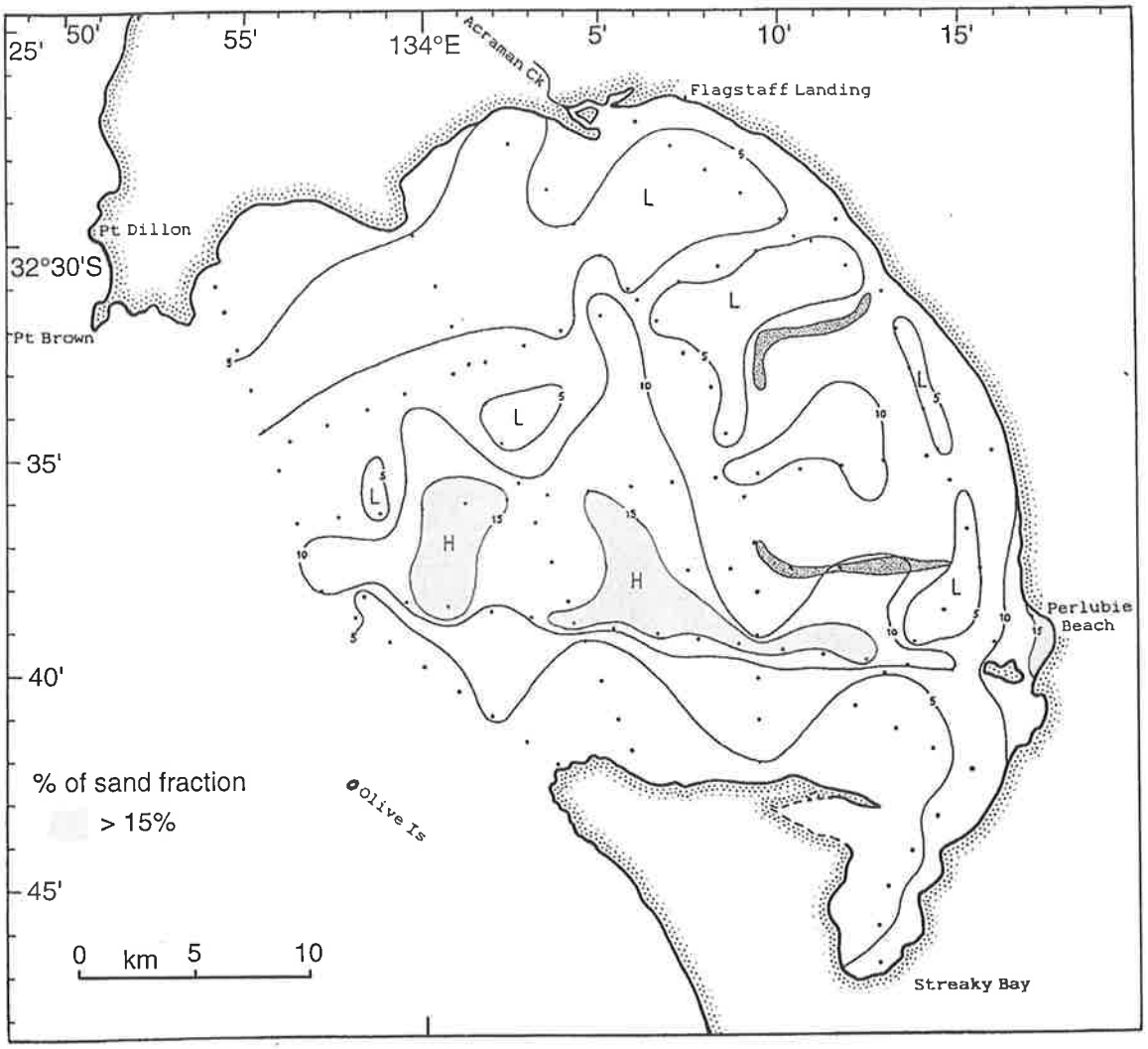



Figure 6.2 Distribution of foraminifer grains (sand fraction).

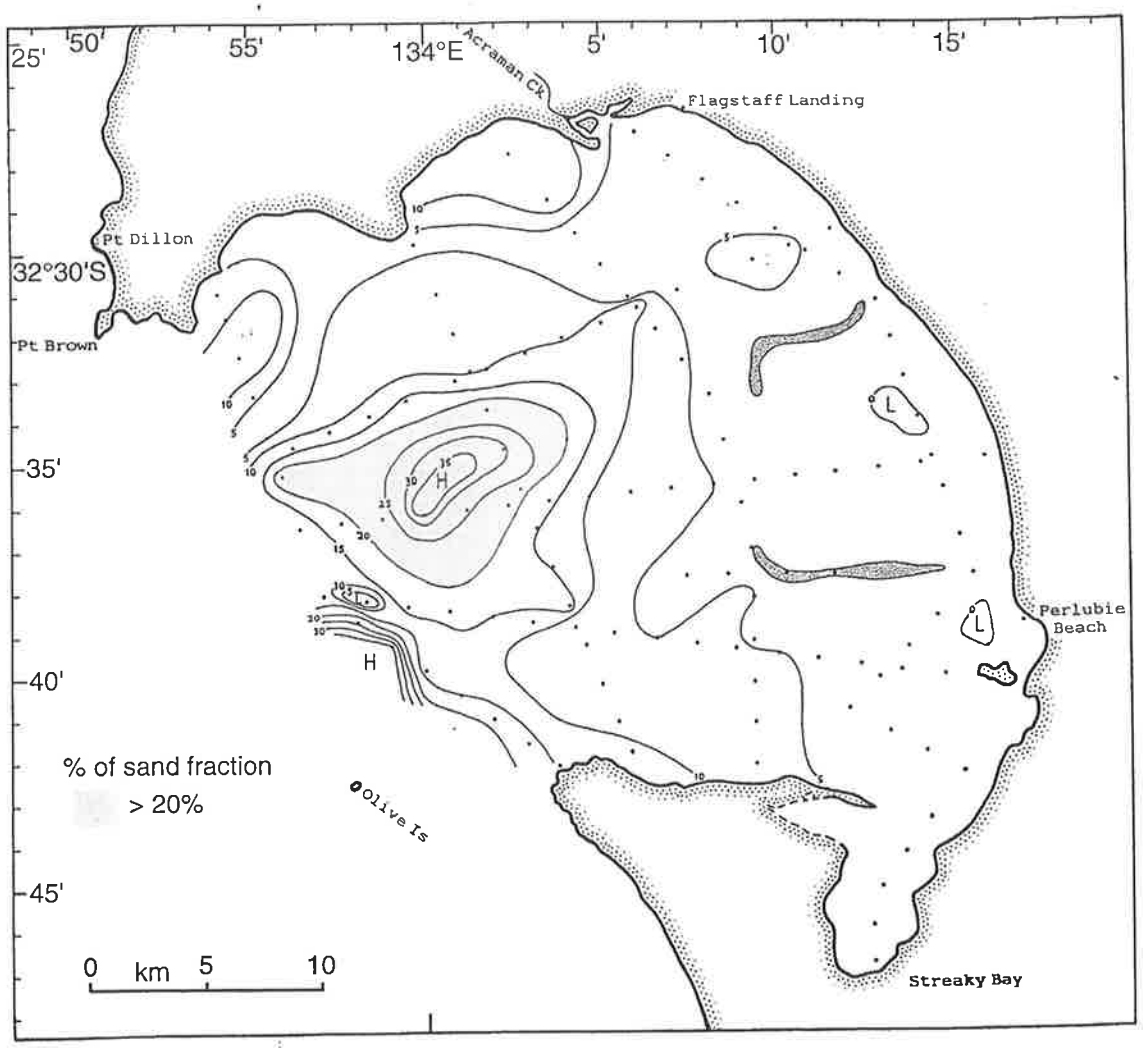



Figure 6.3 Distribution of bryozoan grains (Sand Fraction)

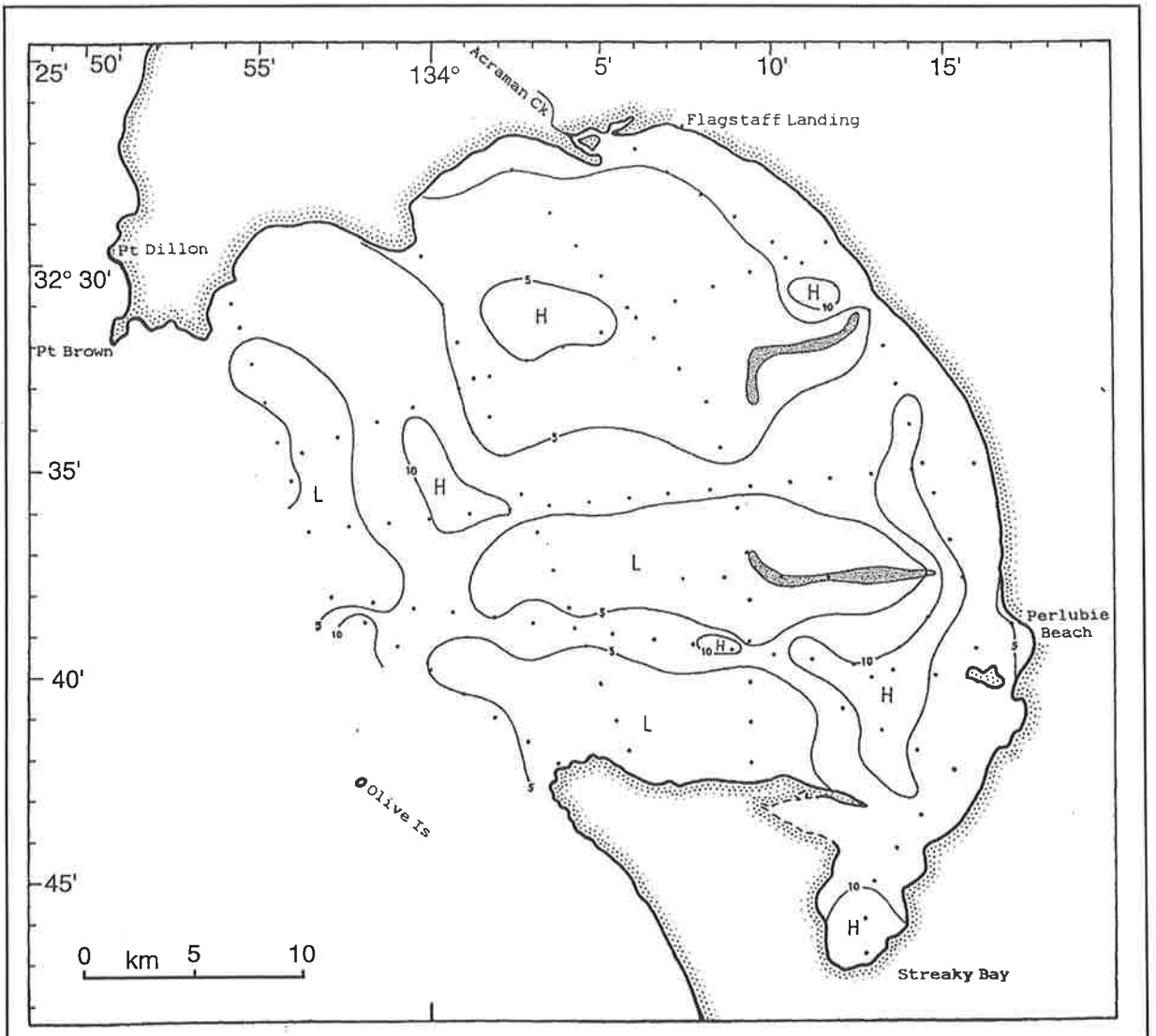



Figure 6.4 Distribution of Echinoderm grains (Sand Fraction).

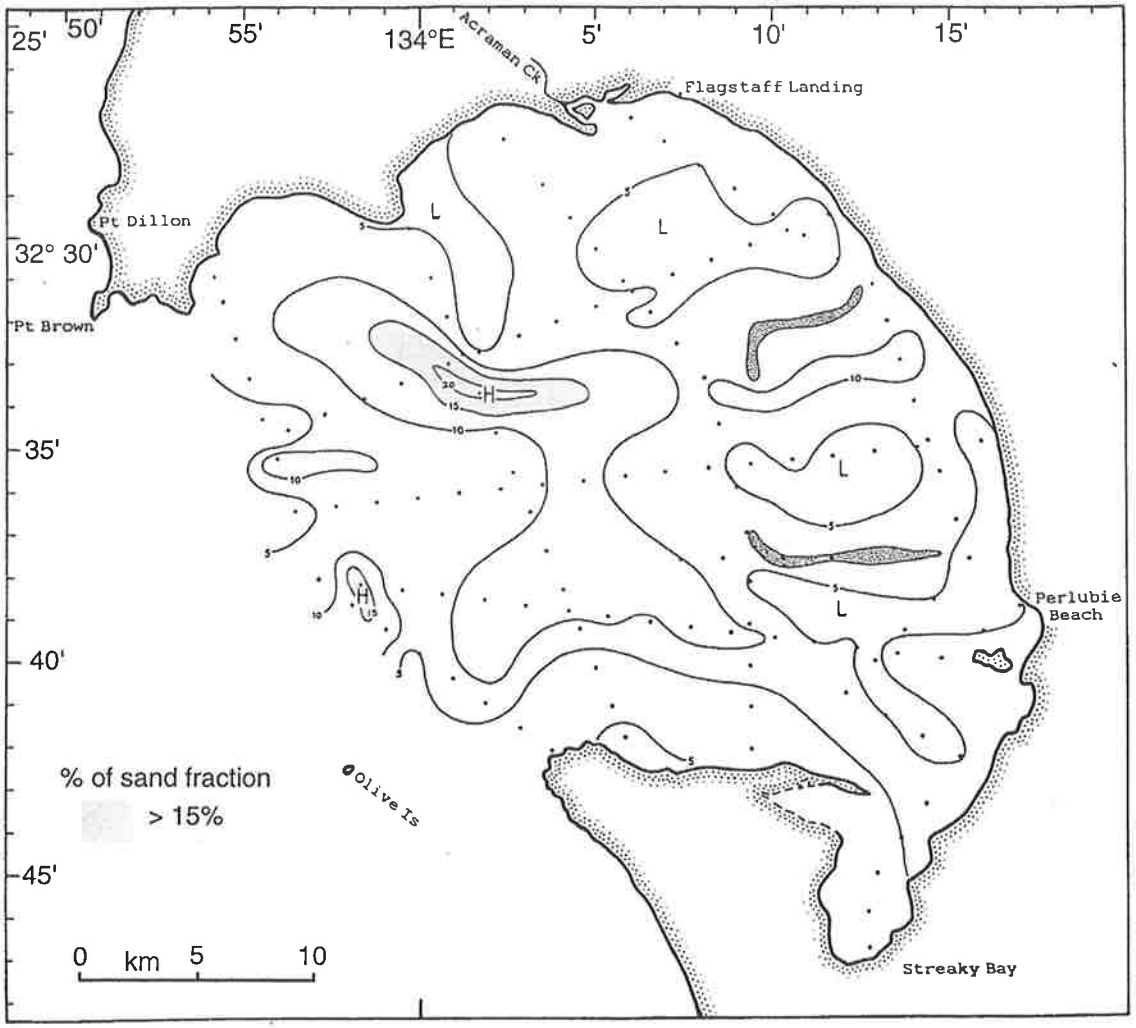



Figure 6.5 Distribution of coralline algae grains (Sand Fraction).

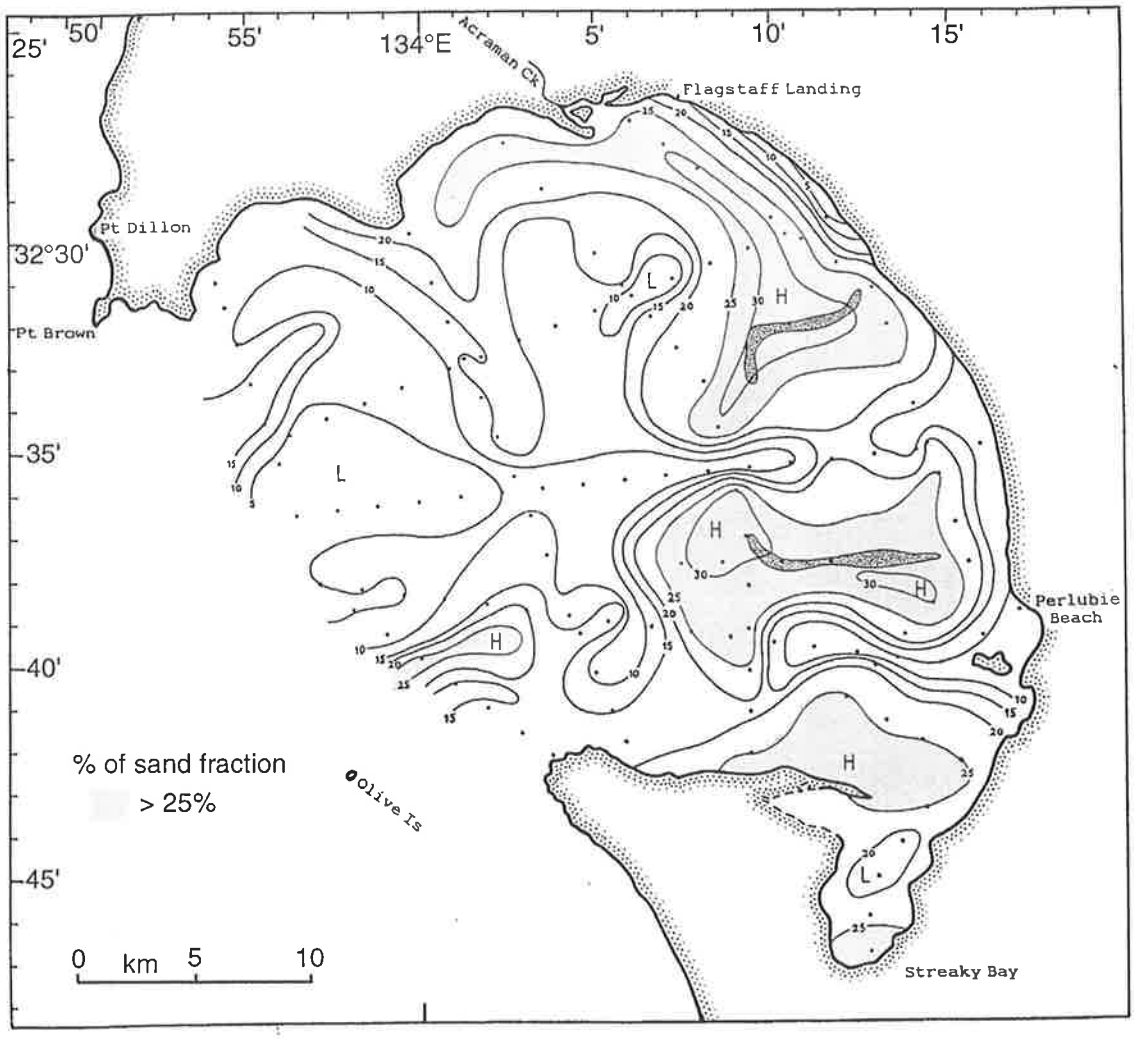



Figure 6.6 Distribution of abraded bioclastic grains, (Sand Fraction).

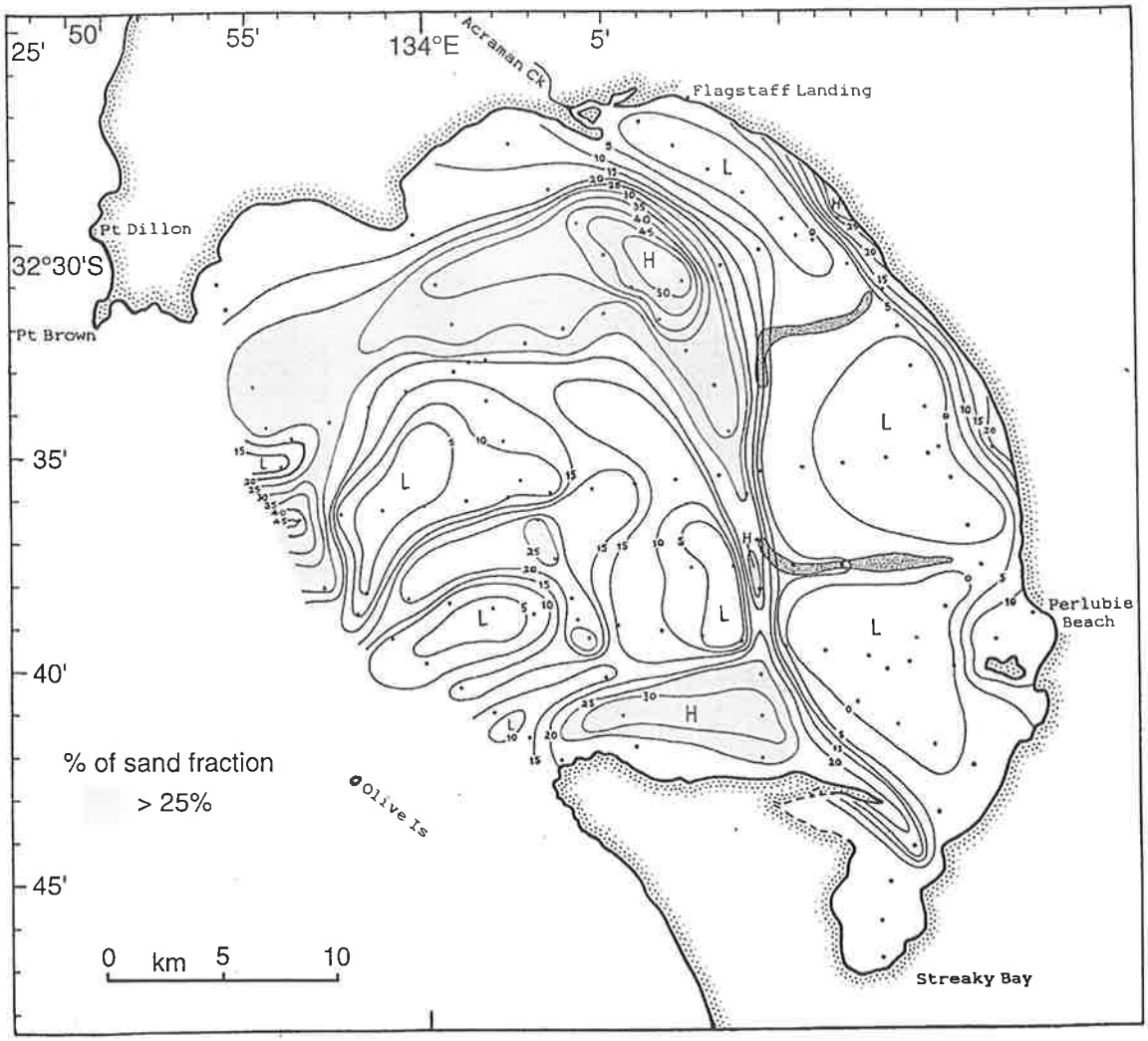



Figure 6.7 Distribution of calcareous aeolianite grains, (Sand Faction)

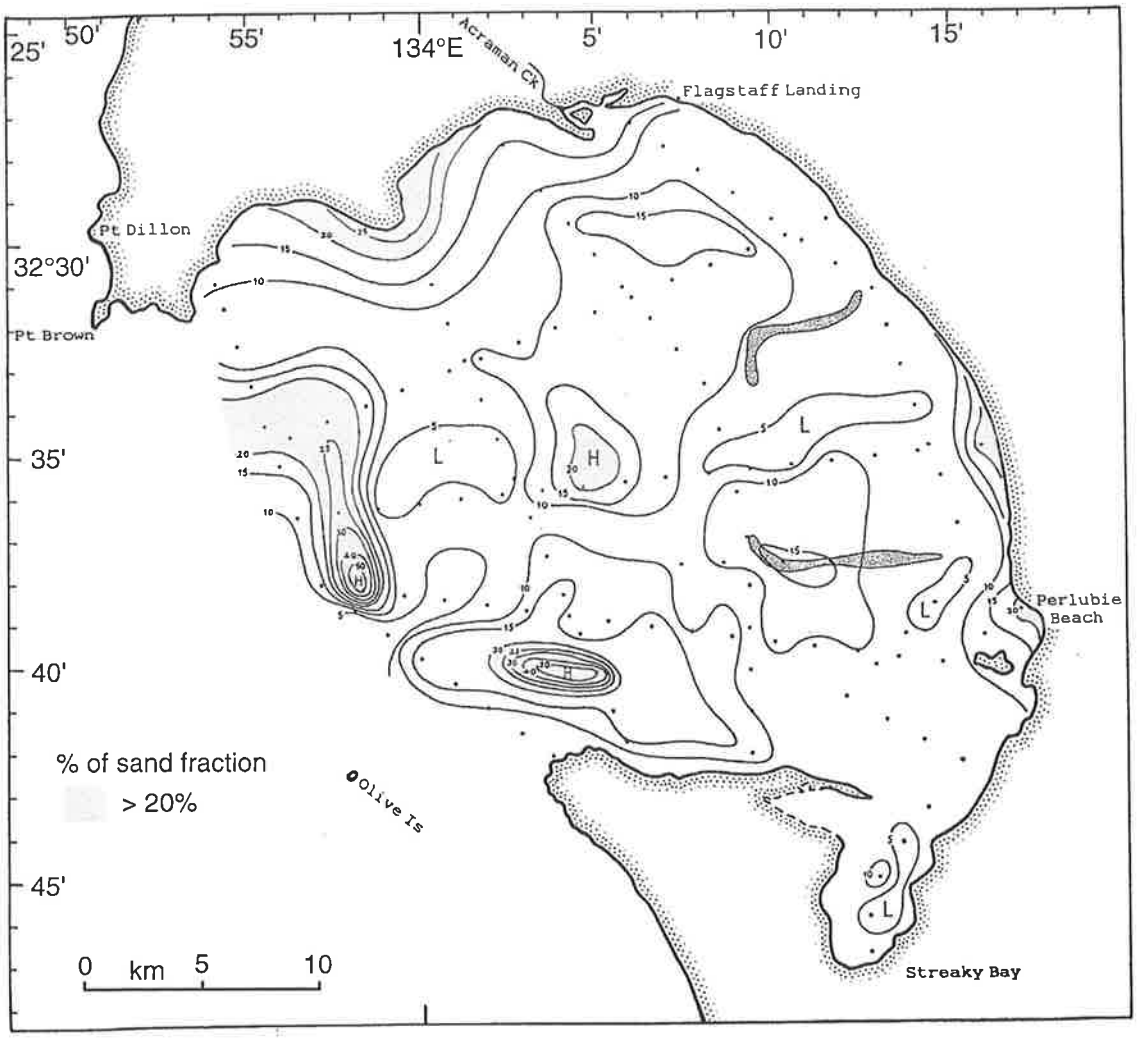



Figure 6.8 Distribution of quartz/lithic grains, (Sand Fraction).

6.5). Generally the fragments are confined to the terrace area with low concentrations in the inner marginal basins and the areas of the northern and southern margins.

### 6.4.6 Abraded Bioclastic Grains

The elongate sand banks, the north and south spit regions and southern Blanche Port are where most abraded bioclastic grains occur with another high concentration at the entrance in the lee of Olive Island (Figure 6.6). Low percentages occur in the tidal channels and across the central terrace to the deep-water entrance area. The deep-water tracts of the inner marginal basins contain variable amounts of abraded bioclastic grains from 10% to 30%.

### 6.4.7 Calcareous Aeolianite Grains

Locations with more than 25 % calcareous aeolianite are situated in the northern part of the bay from the entrance to the Warburton Channel and across to the North Bank, with a smaller area just off-shore of the southern margin from Cape Bauer to half way along Point Gibson (Figure 6.7). The highest concentrations occur in Warburton Channel and central entrance area with low concentrations in the inner marginal basins, central sand shoals and the northwest lee of Olive Island.

### 6.4.8 Quartz/ Lithic Grains

High concentrations of quartz/lithic grains occur in the central and southern entrance areas with a significant plume extending northwards from the central high concentration area (Figure 6.8). Lesser concentrations occur in the vicinities of the central terrace, the northern and central eastern shore margins. Low concentrations of quartz/lithic grains are present in the inner marginal basins, outer terrace and central entrance areas

## 6.5 DISCUSSION

• **Molluscan** grains are concentrated in the inner marginal basins. This higher population is a result of abundant infaunal habitats that exist in the softer muddy sediments. The lower energy environment is also favourable for epifaunal bivalves whose grains are common in this area. Lower concentrations occur in the outer bay where the rocky substrate is not so conducive for abundant bivalves although small whole gastropods are significant within the sand fractions of some sediments (Figure 6.1).

• **Foraminifers** are concentrated where abundant brown and soft red algae are present. It is interpreted that foraminifers found on fresh leaves from the seagrass meadows are transported to the inner beach areas along with the significant amount of discarded seagrass leaves rather than accumulating in situ. Lowest concentrations occur in the muddy inner marginal basins and Blanche Port also the areas of higher energy proximal to the northern and southern coastal margin (Figure 6.2).

• **Bryozoan** grains are associated with the occurrence of abundant bryozoans on the rocky substrates in the central entrance to outer terrace area (see Chapter 7). It is interpreted that the bryozoan content of the sediment diminishes from this area towards the inner bay as a result of the fragile skeletons disintegrating to fine sands and muds. These are subsequently transported to the inner marginal basins where they are recognised in the mud fraction (Figure 6.3)(see Chapter 8).

• **Echinoderm grains** are distinguished by isolated small juvenile forms occurring in the sand fraction and have generally been found in areas of low energy soft substrate. Some ophiuroid grains are distinguished by the typical morphology of the ossicles from rare small juveniles that are found in the sand fraction of sediments mostly associated with rocky substrates (Figure 6.4).

• **Coralline Algal** grains occur in significant numbers to the northern terrace and represent concentrations of disintegrated articulated coralline algae. It is interpreted that the live coralline algae is situated on the terrace growing on the substrate and the root areas of the common soft brown algae and are transported on dying and disintegration, into the bay to the outer sand shoals. The minor concentrations, which are found in the entrance, are dense crustose forms growing mostly on the quartzose and felspathic very coarse to coarse sand grains. Grains attributed to rhodolithic algae are also recognised in the entrance ie. dull irregular prismatic grains (Figure 6.5).

• **Abraded Bioclastic** grains are concentrated the elongate sand banks, the north and south spit regions and southern Blanche Port occur as a result of transportation and abrasion in the shallow higher energy areas of the bay. This occurs with the transportation of macerated carbonate skeletons from areas of higher productivity to shallower regimes where abrasive processes are significant. Hence lower concentrations occur in areas of low energy, deeper water or a combination of both (Figure 6.6).

• **Calcareous Aeolianite** grains are concentrated in the proximity of Bridgewater Formation exposure ie. the northern part of the bay from the entrance to the Warburton Channel and across to the North Bank, with a smaller area from Cape Bauer to half way along Point Gibson proximal to the beach. It is interpreted that the exposures of Bridgewater Formation are sites of active erosion either as the flanking cliffs or high energy areas of aeolianitic sea-floor (Figure 6.7).

• **Quartz/ Lithic** concentrations occur in the central and southern entrance areas proximal to Olive Island where quartzo-felspathic intrusives outcrop (Figure 2.2). It is interpreted that as the island flanks are eroded, the resulting gravelly to coarse sandy sediment is transported into the bay and deposited. The centrally located high concentration is most probably a result of an eroding sea-floor high, which is also composed of felsic minerals. Low concentration ubiquity results from further abrasion of these deposits that are subsequently transported throughout the bay (Figure 6.8).

The presence of these components in the sediments are variably similar to those in the other embayments on the west coast and adjacent shelf (Hill., 1994; Lablack, 1985; Freeman, 1985; Belperio, 1988; Fuller et al., 1994 James et al., 1997, and 2001). The sediments generally present in the West coast embayments are largely composed of molluscan, foraminifera and reworked aeolianite with minor echinoid grains. An exception is offshore Fowlers Bay where significant bryozoan grains occur with molluscan and foraminifera grains (Belperio, 1988; James et al., 2001). The adjacent shelf sediments are composed dominantly of molluscan and lesser bryozoan and rhodolithic grains with 10-30% terrigenous grains. This composition is similar to sediments of outer terrace and entrance to Streaky Bay. The degree of correlation of these sediments may be probably due to the deeper waters and partially exposed rocky substrates of both areas.

## 6.6 CONCLUSIONS

The biogenic composition of the sediments is that of a cool-water carbonate heterozoan assemblage or more specifically variations between a foramol and a bryomol with abundant dilution from the surrounding aeolianite cliffs and minor dilution from granitic intrusives at the entrance to the bay. This assemblage is similar to the shallow water GAB shelf sediments and is similar to assemblages found in the shallow cool-water shelf regions of the Northern and Southern Hemispheres.

Molluscs are the dominant fauna in the bay with bivalves habiting the softer substrate and gastropods the firm or rocky substrate and also are abundant on seagrass meadows. Sub-dominant fauna of foraminifers, bryozoans and coralline algae vary in concentrations across the bay depending on the substrate encountered. Foraminifers and coralline algae are concentrated on the seagrass sand shoals (ie. the coralline algae lives on the seagrass) with bryozoan concentrations occurring on the rocky substrates of the outer terrace and entrance areas. These four faunal groups are modified by echinoderms in the outer bay and the inner marginal basins.

Abraded bioclastic grains, which are composed of the above faunal groups, are concentrated on the elongate sand banks, the north and south spit regions and southern Blanche Port is due to the breakdown and transportation of skeletal carbonate from high energy deeper waters (outer bay) and maceration in the shallow lower energy areas near the sites of deposition proximal to the faunal habitat.

The heterozoan assemblages in Streaky Bay are differentiated from cool-water assemblages on a global scale by the dilution of calcareous aeolianite and quartz/lithic grains. This modification appears to be only within the embayments on the West Coast of the Eyre Peninsula.

# CHAPTER SEVEN

# DISTRIBUTION AND COMPOSITION OF MACROFOSSILS

## 7.1 INTRODUCTION

The aim of this chapter is to determine the distribution and identify the significant macrofossil component skeletons within the gravel fraction of the sea-floor sediments and further subdivide these groups into morphological types and correlate these with substrate type. The occurrence and density of the macrofossils together with transport directions are keys to the origins of the finer sediments and to the distribution of resultant sedimentary facies of a region. The distributions of these organisms in the sediment has been determined by reflecting macro and microscopic observation and numerically tabulated (Chapter 3). The significant carbonate-producing organisms include, as with the sand fraction, molluscs, bryozoans, coralline algae and echinoderms. The skeletons from these groups encompass living organisms at the time of collection, recently dead skeletal material and abraded skeletal material including large fragments, which can be identified as belonging in the above groups and their subgroups. Subdivisions based on the distribution of structural forms of molluscs, bryozoans and coralline algae are tabulated and graphed.

The ability to identify the organisms is dependant on the degree of maceration, mastication and abrasion to which an organism or fragment has been subjected. The degree of abrasion is dependent on the energy being expended at the sea-floor by the action of waves and sea currents. There may be rounding of the grains through the cyclic movement of the waves on the sea-floor, although it appears

that no significant breakage of biogenic carbonate material occurs outside of the surf zone although some may occur on rocky substrates from the movement of larger cobbles (Boreen et al., 1993; Scoffin, 1988 Dietz, 1963 amongst others). Therefore, apart from possible breakage during the sampling process, significant breakage of the marine organisms can be attributed to maceration by larger organisms ie. crustaceans, fish, molluscs, echinoderms, rays, and weakened by boring and scraping organisms ie. sponges, molluscs, echinoderms, algae, annelids and calcimicrobes, amongst others. Boring and scraping is evident in biogenic fragments from samples on the terrace and entrance areas of the bay, and is particularly noticeable in the gravel fraction of samples SB 62 and SB 112.

The distribution of the quartz/lithic component is included as it is a significant component especially in the outer bay. This component encompasses the following rock and mineral types; aeolianite, calcrete, felsic intrusive, quartz, feldspar and amphibole. The aeolianite and quartz/lithic components have been combined in the tabulation of the gravel fraction because of their limited abundance in restricted areas of the bay. Significant percentages of gravel sediment is concentrated at the entrance and in the northern areas while minor concentrations < 5% occur over the majority of the bay (Figure 7.1).

The details of biota and distribution in the gravel fraction of the sediments is tabulated in Appendix. Four. This table summarises information derived from the sediments collected on the sea-floor at Streaky Bay and sediments along a transect to the shelf edge (FR 03/98). The table also includes a full descriptive sediment name and water depth from which it was sampled. The distribution of forms from within the different biotic groups that were found is summarised.

Distribution graphs of the components of the gravel are presented in Figures 5.3d to 5.11d (Chapter 5). A numerical system of describing component density or occurrence has been used to facilitate graphing procedures (Table 7.1). Gravel from each sediment was evenly spread over a picking tray to determine the component density of each group (see Chapter 3, Methods).

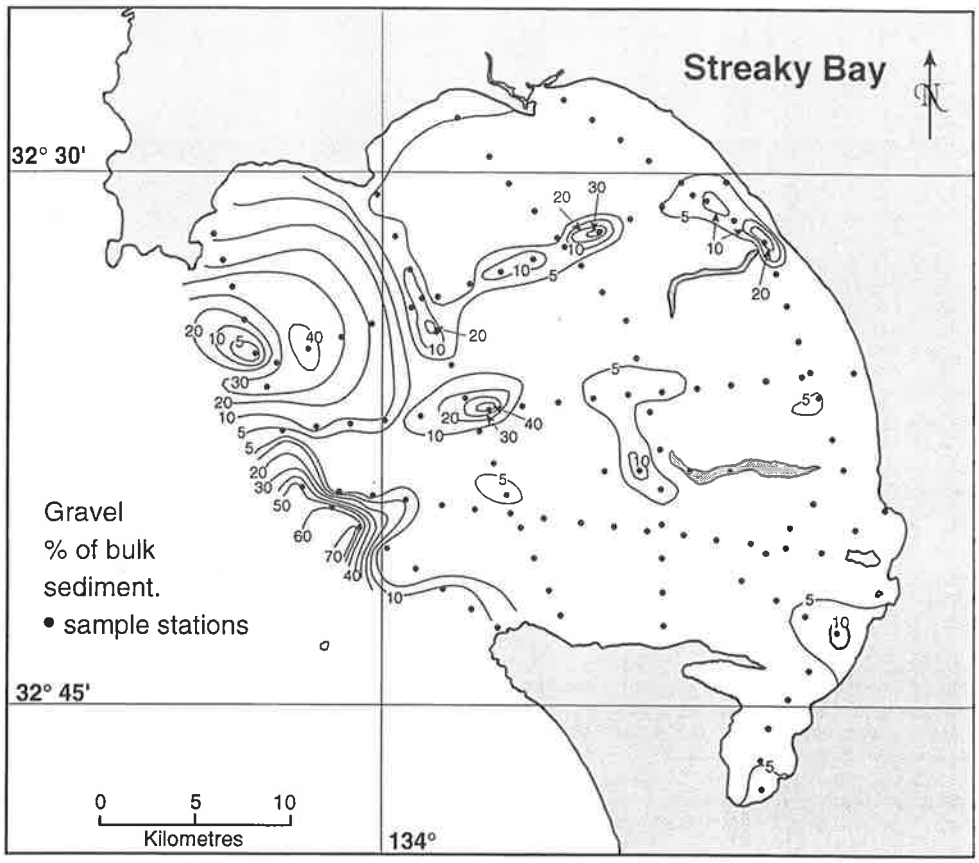



Figure 7.1 Distribution of the gravel fraction as a percentage of bulk sediment.

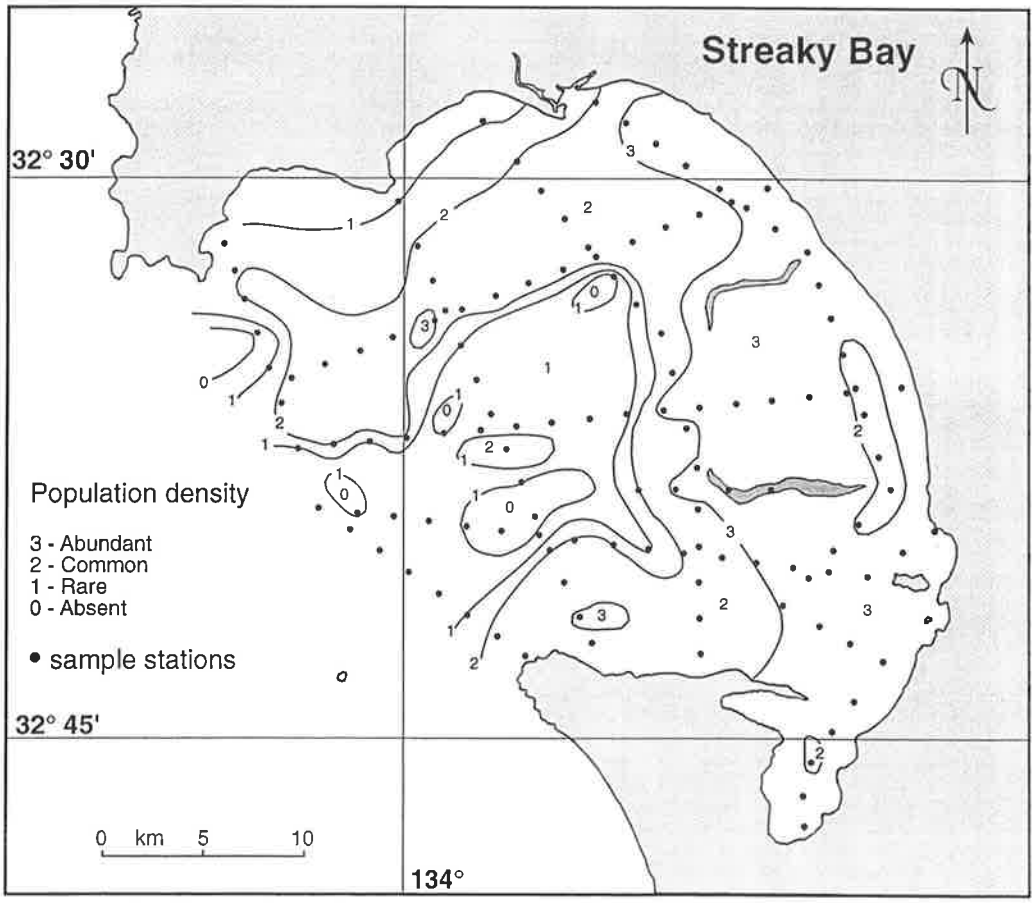



Figure 7.2 Distribution of molluscan gravel. Numerals indicate the density of fragments.

| Population Frequency (density) | Numerical Value | Number of Fragments |
|---|---|---|
| Absent | 0 | 0 |
| Rare | 1 | 1 - 4 |
| Common | 2 | 5 – 10 |
| Abundant | 3 | more than 10 |

Table 7.1 Population frequency of gravel components versus numerical value (for graphing purposes) in relation to fragment numbers.

The results were plotted on a distribution graph for each of the transects. Sediment was not collected from a number of sample stations (ie.; SB 55, SB 58, SB 59, SB 61, SB 71, SB 72, SB93, SB98 and SB 118). This is a result of the rocky substrate having no overlying sediment or conditions being too dangerous for sampling at or near the station point. As a consequence there would be an aberration in the graphs where the results at the above stations are shown as zero in the distribution graphs. This would imply that the sparse sediment at these locations has no grainsize or components. These stations were deleted to facilitate a clear understanding of the trends in the gravel components. Sediments are graphed as zero which recorded no gravel in the sieve analysis. The results of these observations are summarised by general transect trends and described in detail by spatial occurrence.

## 7.2 RESULTS - TRANSECTS

### 7.2.1 Streaky Bay Transects

The general trend of molluscs varies from abundant-common in the basins and inner beaches to common-absent at the entrance (Figures 5.3d, 5.4d, 5.5d). Coralline algae are abundant at the entrance with crustose, articulated branching and rhodolith forms present and common-rare in the inner bay where they occur predominantly as crustose forms on shells and seagrass. Bryozoans are common to absent in the inner bay becoming abundant on the outer terrace and entrance and showing a wide structural diversity. Echinoderms are common to rare in the central entrance, sand shoals and inner marginal basins as infaunal and epifaunal echinoids in the IMB with epifaunal echinoids and ophiuroids in the entrance, and absent-rare on the terrace. Quartz-lithic fragments are abundant in the entrance (granitic material) and northern terrace (fragments of Bridgewater Formation) but are absent to rare in the inner bay.

Trends in gravel components from South to North (Figures 5.6d, 5.7d, 5.8d, 5.9d) reflect the diversity and concentration of biota in sediments from Transects 1 to 3. Molluscs are generally abundant in the south decreasing to common-absent in the north. Bryozoans and coralline algae increase from

common-rare in the south to abundant in the northern areas. The patchy distribution of rare-common Echinoderms are reflected in the North-South transects with common occurrences mostly in sediments from Transect 4. The common-abundant distribution of quartz-lithic gravel in the northern area and absence in the south is also highlighted in sediments from these transects.

### 7.2.2 SHELF TRANSECT

Quartz and lithic fragments are common-abundant in outer Streaky Bay and the inner shelf, but they are absent on the mid- to outer shelf (Figure 5.11). Molluscs are rare-common in the gravels from the inner shelf samples and common-abundant in the mid- to outer shelf samples from this transect (Figure 2.1). Coralline algae are abundant to common on the mid- to outer shelf and common to rare on the inner shelf. Bryozoans are abundant in sediments from the inner shelf to the outer shelf apart from sediment ACM 59 on the inner shelf where their occurrence is rare. The diversity of bryozoan structural architecture increases proportionately with distance off-shore. Rare-common echinoderms were observed in isolated sediments from the transect, with most of these occurrences being on the mid- to outer shelf (CSIRO Franklin Cruise 03/98).

## 7.3 RESULTS - SPATIAL DISTRIBUTION

The spatial distribution of organisms from the gravel fraction is plotted in terms of occurrence of density, ie abundant, common, rare and absent (Chapter 3; Methods). Further results are derived from graphs differentiating the architecture within the major biogenic groups (Figures 7.7 to 7.13).

### 7.3.1 MOLLUSCS

Molluscan shells and fragments are most abundant in the inner marginal basins, Blanche Port, and central and southern tidal deltas, whilst also being a significant gravel component in most of the sediments throughout the bay (Figure 7.2). Molluscs are rare to absent in the central areas of the entrance and terrace, and the northern tidal delta. They usually range from juvenile to mature forms, although the latter may only be present as large fragments (Figures 7.7, 7.8 and 5.3 to 5.11 and Appendix Four).

Bivalves are the most common molluscs in the inner marginal basins and central tidal delta area, and include infaunal, semi-infaunal and mobile benthic (swimming) forms. The bivalves represented in the deeper rocky areas are generally epifaunal and robust semi-infaunal forms.

Bivalves show a distinct reduction in population from abundant-common in the inner marginal basins (Transect 4), to rare-absent in the outer terrace and entrance areas (Transects 6 and 7) apart from

isolated areas of abundance (Transect 3). They also show a general reduction from abundant-common to common-rare occurrence from the southern area of the bay to the north (Transect 5). The occurrence of bivalves on the shelf increases from rare-absent at the entrance of Streaky Bay to abundant-common at the outer shelf and shelf break (Figures 7.7 and 7.8).

Gastropods are the most common mollusc in the outer rocky sea-floor areas, comprising up to ~60% of the molluscs in the gravel fraction. They also comprise up to 25% of the molluscs present in the sand shoal regions. They are epibenthic to semi-infaunal and have representatives from diverse feeding styles ie. grazers (seagrass, red and brown algae), predators, suspension feeders and scavengers.

The occurrence of gastropods varies in population from abundant to absent in the gravel fraction. Generally they are common to absent in the inner portion of the bay and increase from common to abundant in the terrace and entrance areas (Transect 4 and 6, Mollusc). Gastropods also show a significant increase in population from the southern to the central and northern areas of the bay (Transect 4, 7, 1 and 3). This higher population of gastropods at the entrance is also reflected in the ACM Shelf Transect which shows a decrease on the inner shelf, an increase to abundant on the mid shelf, with rare to common occurrences towards and including the shelf break (Figures 7.7, 7.8 and 7.13).

The common bivalves from the samples from the inner marginal basins have representatives from infaunal (*Dosinia* sp., *Fulvia* sp., *Anomia* sp.), semi-infaunal (*Ostrea* sp. and *Pecten* sp. and fragments of *Pinna* sp.) and swimming (*Equichlamys* sp.) forms. The gastropods represented in the samples from the inner marginal basins are typically epibenthic grazers, ie *Batillaria* sp., *Bulla* sp. and semi infaunal molluscan predator types, ie. *Thais* sp. and *Penion* sp.
The sand shoal/ seagrass areas include the infaunal bivalves (*Venerupsis* sp., *Katelysia* spp., *Mactra* sp., *Macomona* sp., *Acrosterigma* sp., *Chioneryx* sp., and *Glycymeris* sp.), semi infaunal (*Ostrea* sp. and *Pecten* sp.) to epifaunal (*Modialus* sp. and *Chlamys* sp.). Common gastropods in this area which are representatives of both grazing, predatory, burrowers and suspension feeder types are *Batillaria* spp., *Fusinus* sp., *Bulla* sp., *Thalotia* sp., *Clanculus* sp., *Oliva* sp. with rare *Serpulorbis* sp., *Calyptraea* sp. and the slit patellid, *Emarginula* sp.

Bivalves of the outer terrace and entrance area are typified by the infaunal *Glycymeris* spp., *Neotrigonia* spp., *Dosinia* sp. with rare *Katelysia* sp. and *Circomphalus* sp. and common epifaunal bivalve *Modialus* spp. Gastropods are represented in these areas by grazers, burrowers, suspension feeders, and rare predators, ie. common *Batillaria* spp., *Phasianella* sp., *Calyptraea* sp., *Turbo* spp., *Fusinus* sp., *Cassis* sp., and rare *Siliquaria* sp. in areas of deeper water.

### 7.3.2 BRYOZOANS

A wide variety of structural forms of bryozoans (see Chapter 3; Methods) occur in sediments collected from Streaky Bay (Figure 7.9 and 7.10). They occur most prolifically in the central to outer portion of the bay where there is significant variation in substrate environments. These environments range from eroded rocky sea-floor to soft sandy sediments which appear to be present either as sand waves or as crevice fillings (Figure 2.11 and 2.12).

The frequency and range of bryozoan architectural types (Figures 7.9 and 7.10), which are present in the outer area are;

- common to abundant, encrusting and fenestrate forms,
- common to rare, foliose, delicate branching, and articulated branching forms,
- rare, articulated zooidal, flat robust, nodular and vagrant forms. The vagrants are pristine to abraded, and are only present in the sediments collected from the deeper central area at the entrance of the bay.

Encrusting bryozoans are the dominant form found in the inner half of the bay (Transects 4, 1, 2, and 3). Other structural forms present here are, rare fenestrate, articulated zooidal, delicate branching and articulated branching forms. The variety of structural forms increases from the inner bay to the outer terrace and entrance areas (Transects 4, 5, 6 and 7).

Cheilostome bryozoans are predominant in the inner areas of the bay with minor cyclostomes. The few cyclostomes present are predominantly encrusting with rare delicate and articulated branching forms. Both the encrusting cheilostomes and cyclostome occur on fragments of seagrass (*Posidonia* sp. and *Amphibolis* sp.) which are found in the gravel fraction.

Cheilostomes common in the inner bay are; *Celleporaria cristata*, *Membranipora membranacea*, *Orthoscutella* sp. and *Pyripora* sp.

Cheilostomes common in the outer bay are; *Adeona* sp., *Adeonellopsis* sp., *Arachnopusia* sp., *Cellarporaria* sp., *Gigantopora* sp., *Iodictyum* sp., *Membranipora perfragilis*, *Orthoscutella* sp., *Osthimosia amplexia*, *Petraliella* sp. *Porina gracilis*, *Smittina* sp., *Steginoporella truncata*,

The cyclostomes comprise <5% of the bryozoans present in the gravel fraction of samples from the inner bay (*Crisia* sp., *Diaperoecia* sp. and *Lichenopora* sp. however, their occurrence increases significantly to 30-40% in the outer areas of the bay. Cyclostomes present in the outer bay include common delicate branching (*Crisia* sp., *Diaperoecia* sp., *Hornera* sp., *Idmidronea* sp., *Mesonea* sp. and *Nevianopora* sp.) and encrusting (*Lichenopora* sp. and *Tubulipora* sp.) forms.

Bryozoans from Transect ACM show that maximum diversity of structural variety occurs towards the mid- to outer shelf with all structural varieties being represented in sediments from the outer shelf.

### 7.3.3 FORAMINIFERS

Although foraminifers are present mainly in the sand fraction, there are larger forms present in the gravel fraction of sediments collected from the outer terrace and entrance. A significant proportion of these larger foraminifers has morphologically similar forms in the shallower, less energetic, sand shoal sea-grass regions.

The large Rotaliid (*Elphidium* sp.) is the most common foraminifer in the gravel fraction which occurs in the outer terrace and entrance areas. Other rare large foraminifers present are the agglutinate Textulariid forms (*Textularia* sp., *Cribrobulimina* sp.) and the Miliolinids; *Peneropolis* ssp., *Triloculina* sp. and *Quinqueloculina* sp. These rare specimens which are found within the gravel fraction in the outer areas of the bay are significantly larger and more robust than their inner bay counterparts.

### 7.3.4 CORALLINE ALGAE

Abundant coralline algae are found in the sand shoal and central terrace area and also the gravelly/rocky substrates of the entrance to the bay (Figure 7.4). The inner marginal basins are areas of rare to common concentrations. It was observed that seagrass fragments (*Posidonia* sp and minor *Amphibolis* sp.) found in the gravel fraction supported a significant population of crustose coralline algae.

The main structural forms of coralline algae, represented in areas of abundance are crustose and articulated branching (Figures 7.11 and 7.12). Fragments of crustose coralline algae are generally common to abundant in the gravel fraction from all the samples collected (Figures 5.3 to 5.11). Rare to abundant rhodoliths occur predominantly on the terrace and in the entrance areas of the bay (Transects 1, 2, 3, 5 and 6). Higher concentrations are found in the mid- to outer northern areas of the bay (Figures 7.11 and 7.12).

Crustose and rhodolith forms are usually present as whole plants (thalli) whereas articulated branching, and some crustose forms, are found as parts of the whole plant. Whole crustose forms are found growing on lithic gravel grains and fragments of larger biota ie seagrass blades, molluscs, barnacles, echinoids or as partial plants when the encrusting substrate has been fragmented through natural process or broken during sampling. Articulated and delicate rhodolith forms are usually found as disarticulated or broken fragments, apart from rare occurrences where whole live plants were collected and not broken or disarticulated during the sampling and preparation process. All these forms, in general, are mostly present as fragments rather than whole plants.

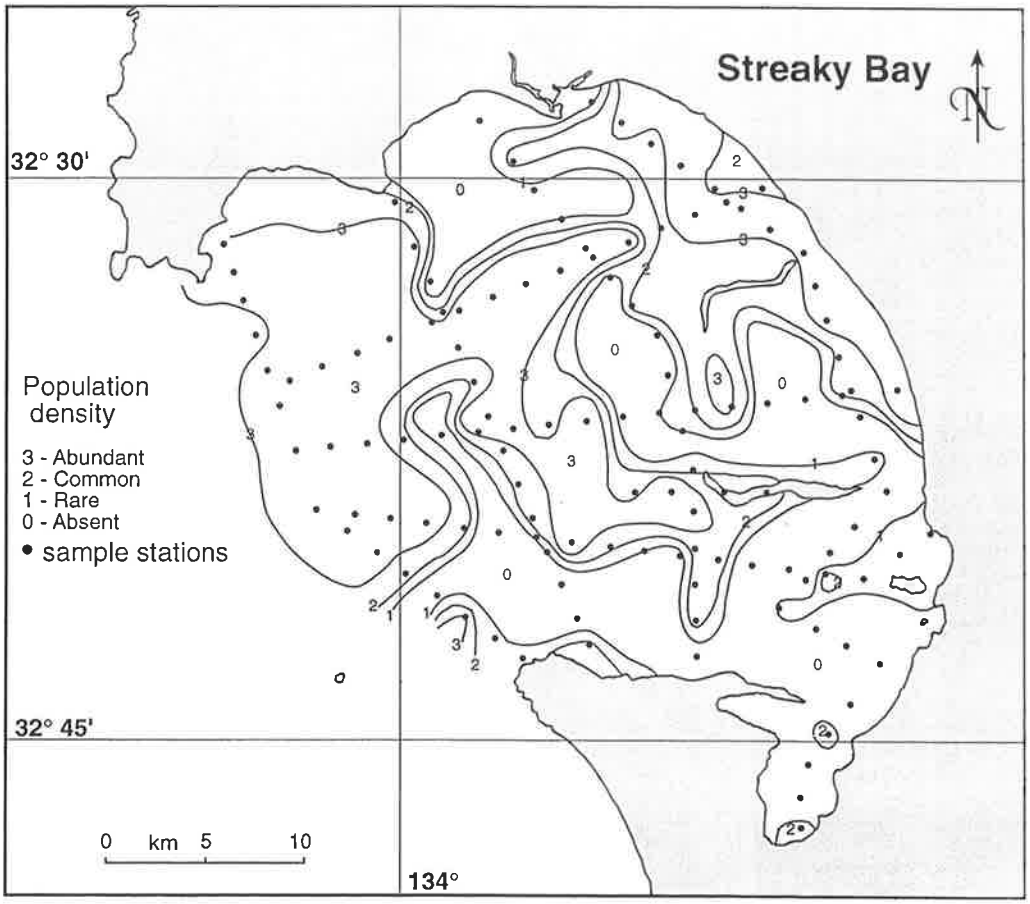



Figure 7.3 Distribution of bryozoan fragments in the gravel fraction.

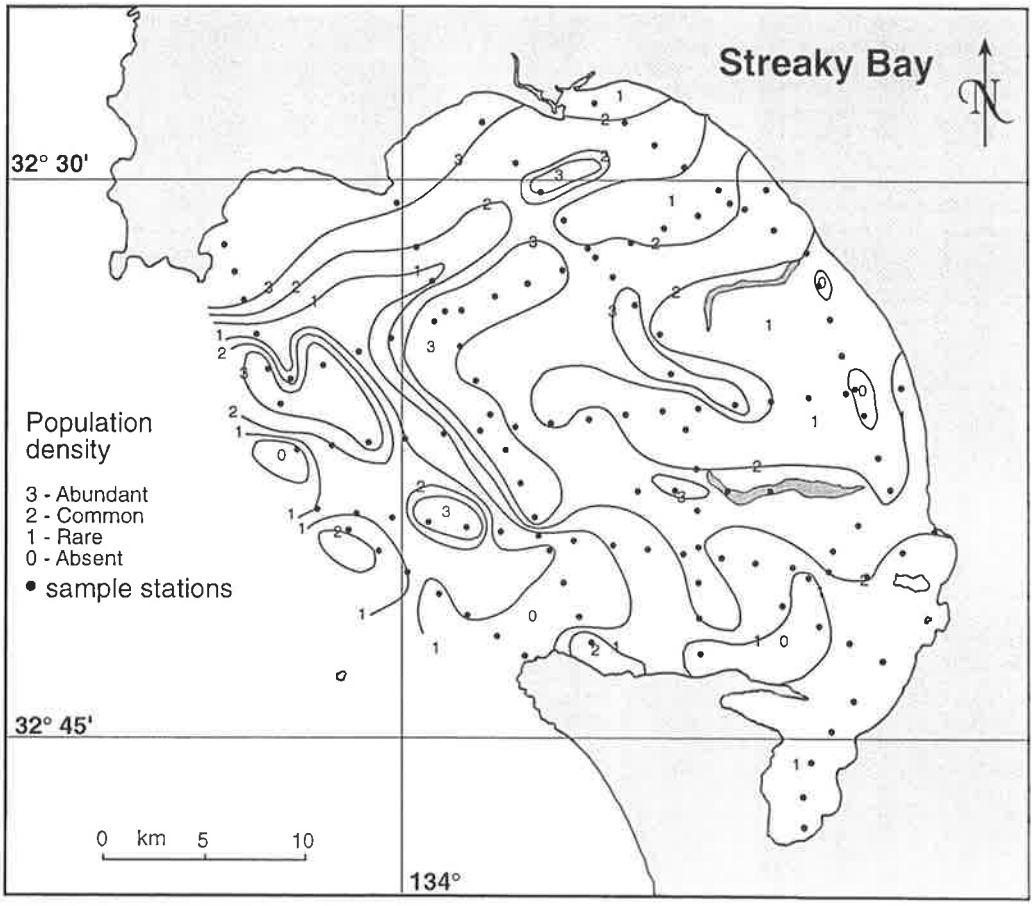



Figure 7.4 Distribution of coralline algal fragments in the gravel fraction Numerals indicate the density of fragments.

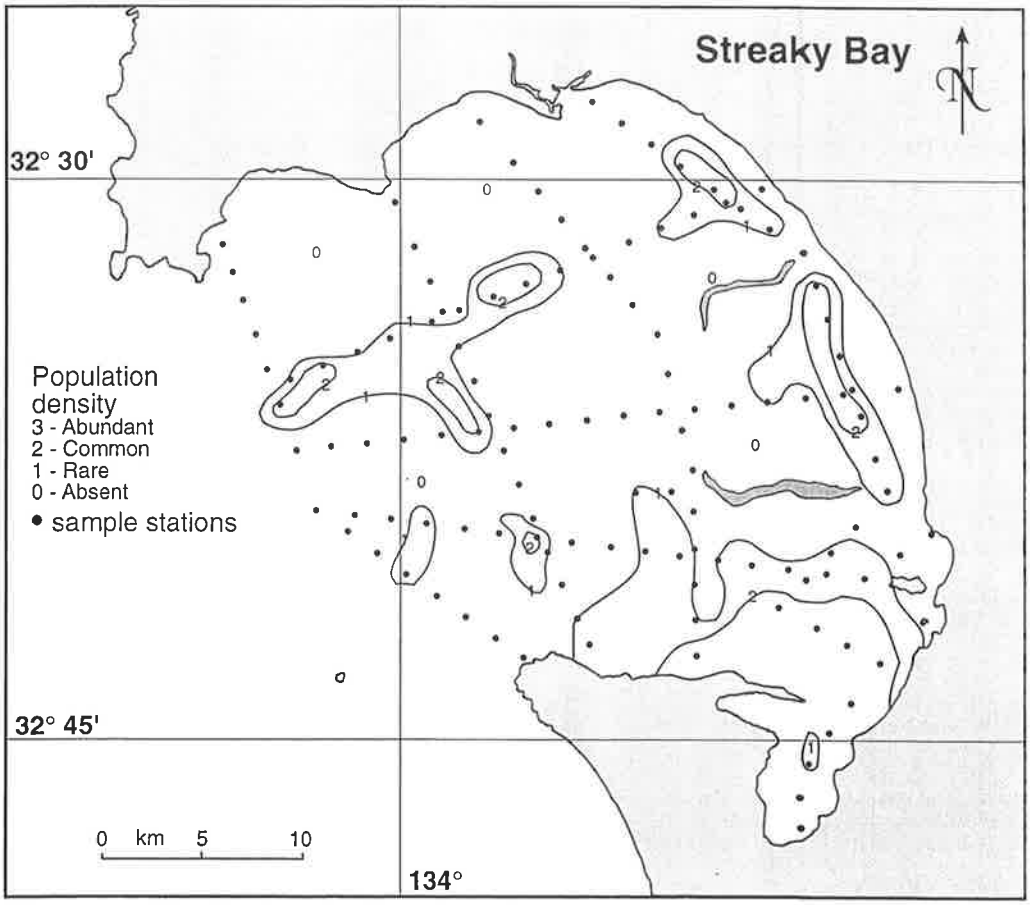



Figure 7.5 Distribution of echinoderm fragments in the gravel fraction.

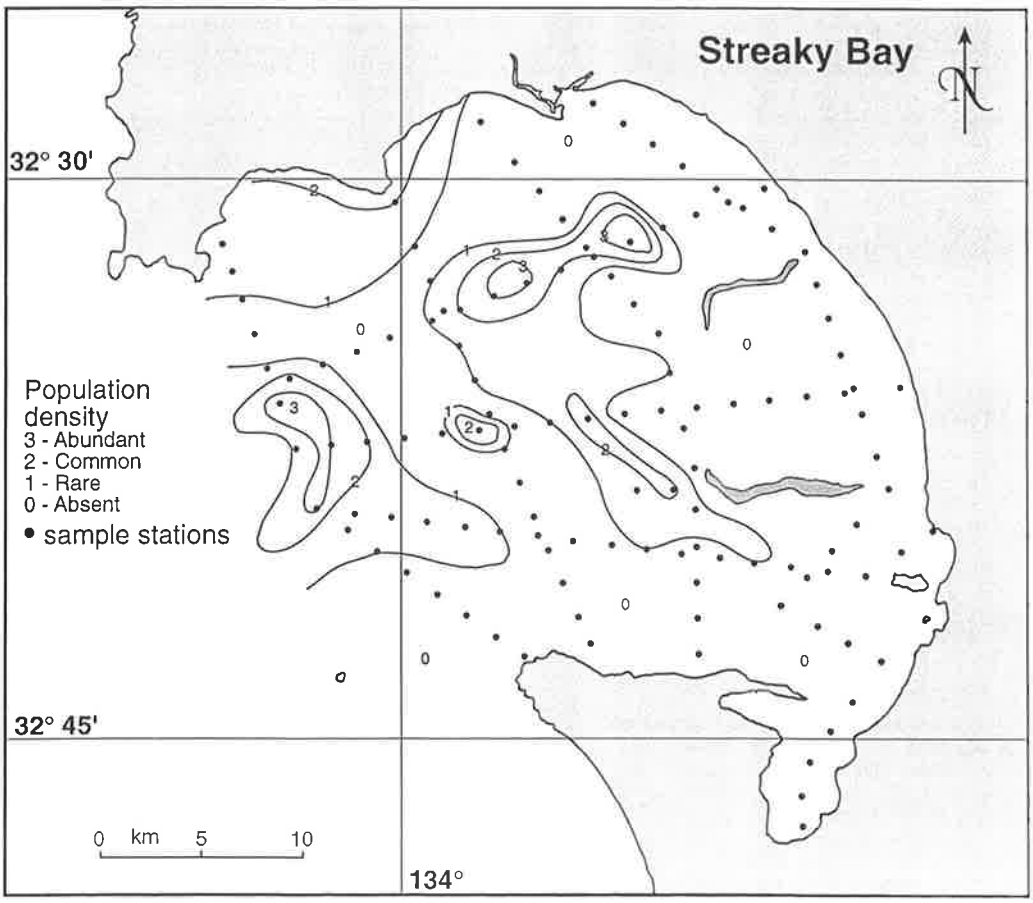
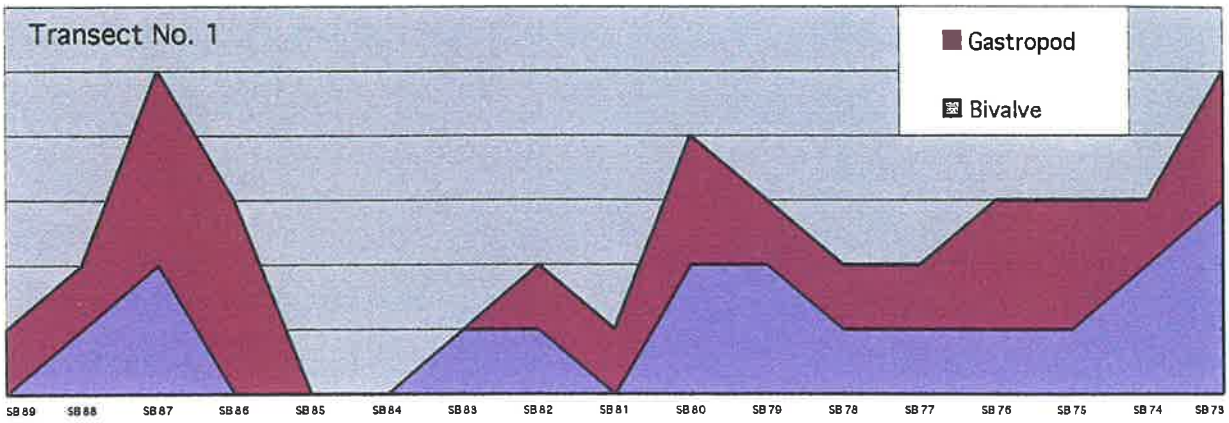
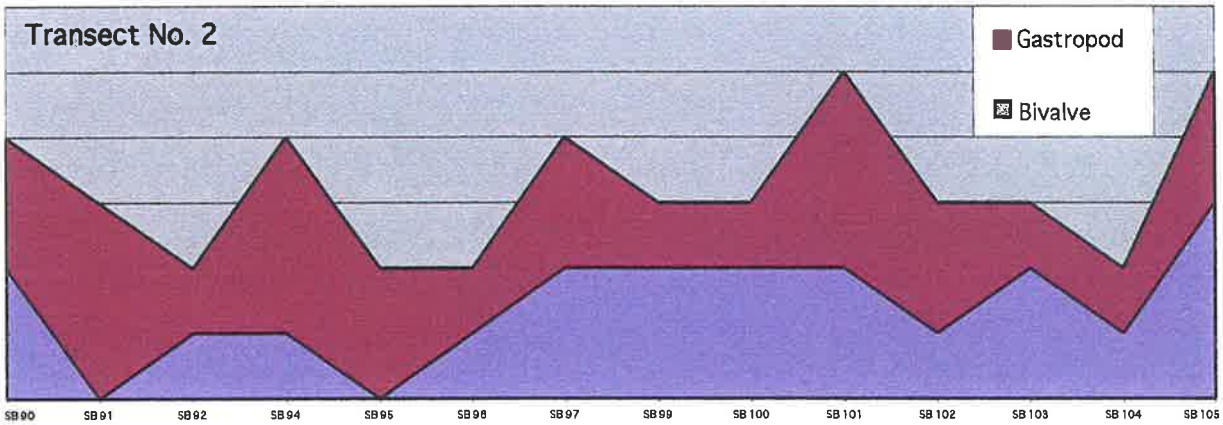
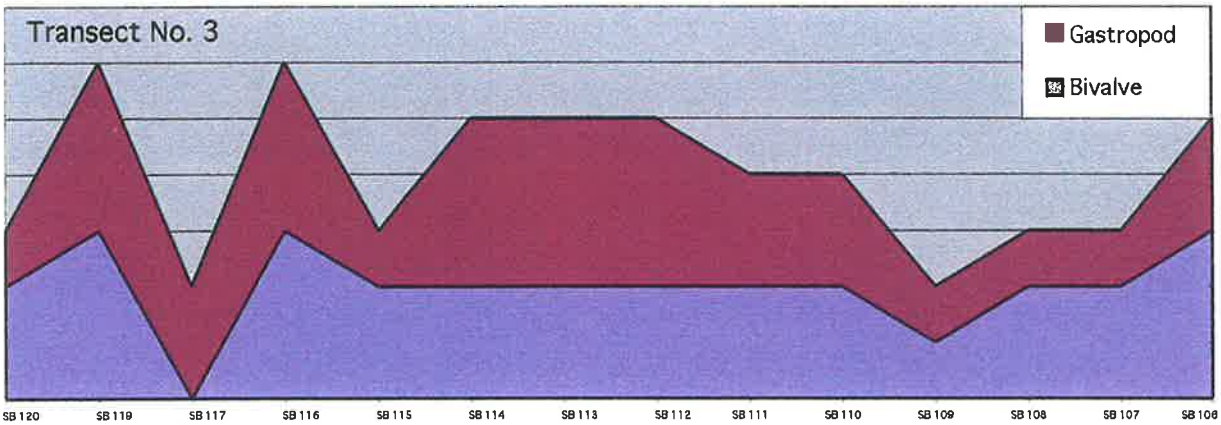


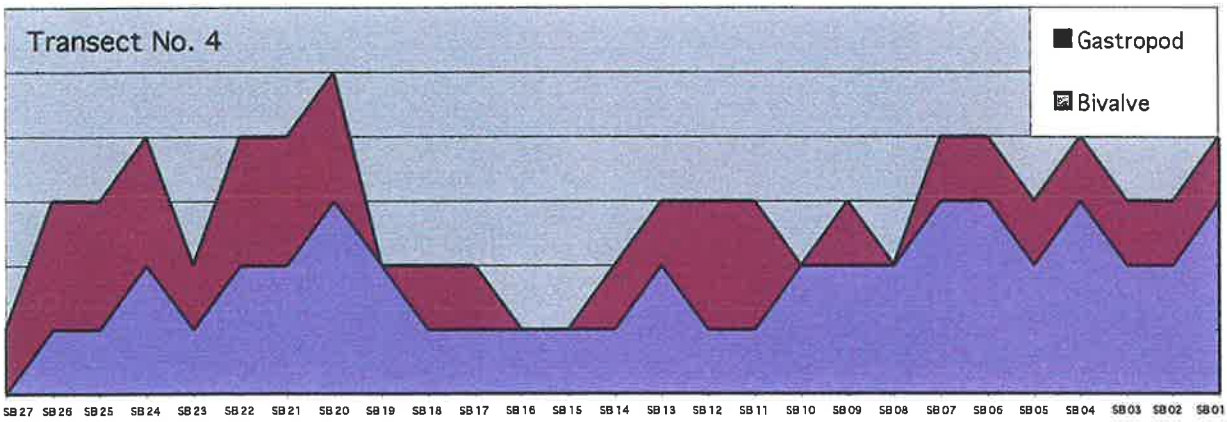

Figure 7.6 Distribution of quartz/lithic fragments in the gravel fraction. Numerals indicate the density of fragments.

## 7.7 Mollusc Distribution, Gravel

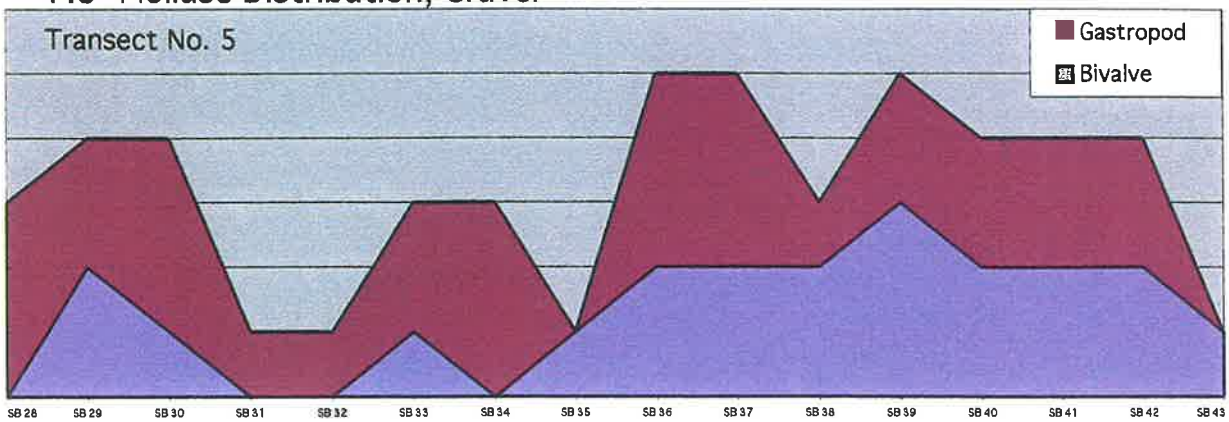


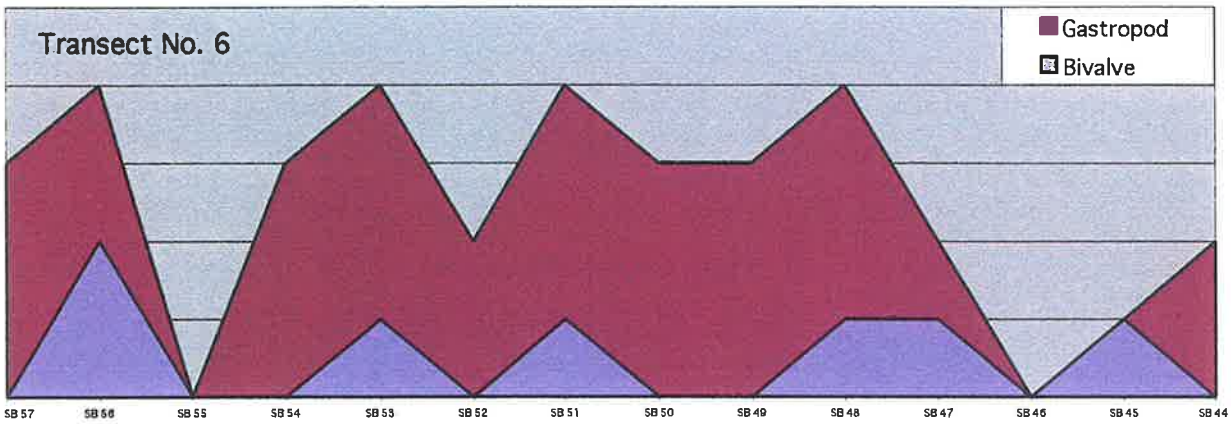



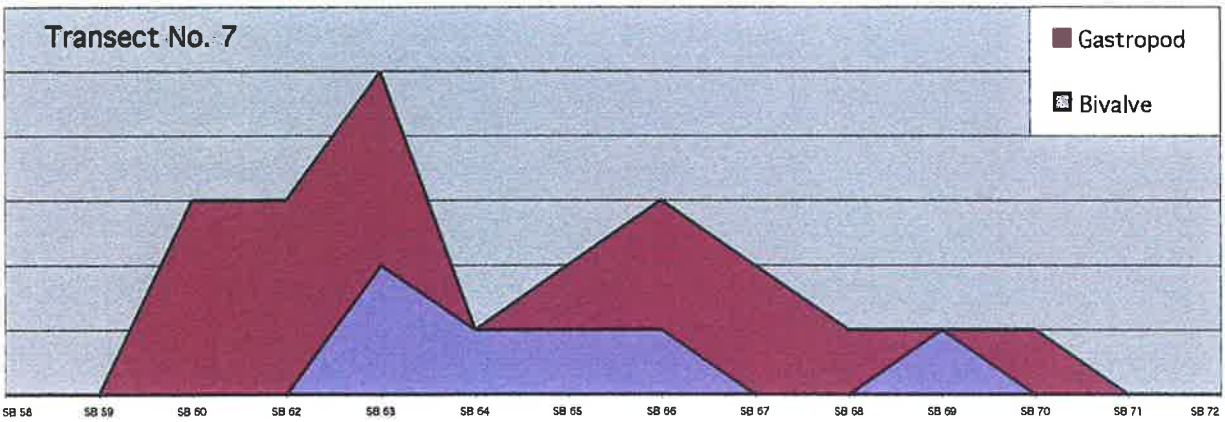



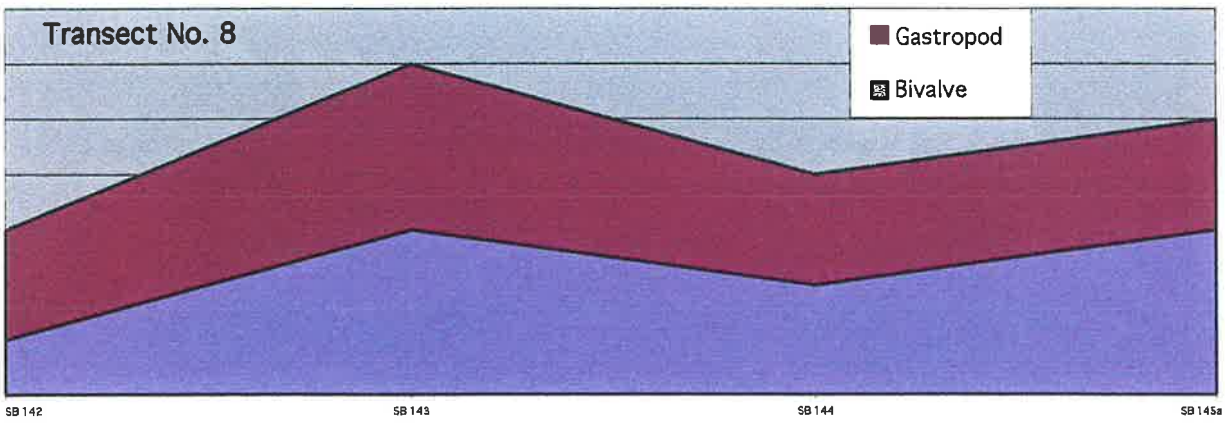



## 7.8 Mollusc Distribution, Gravel

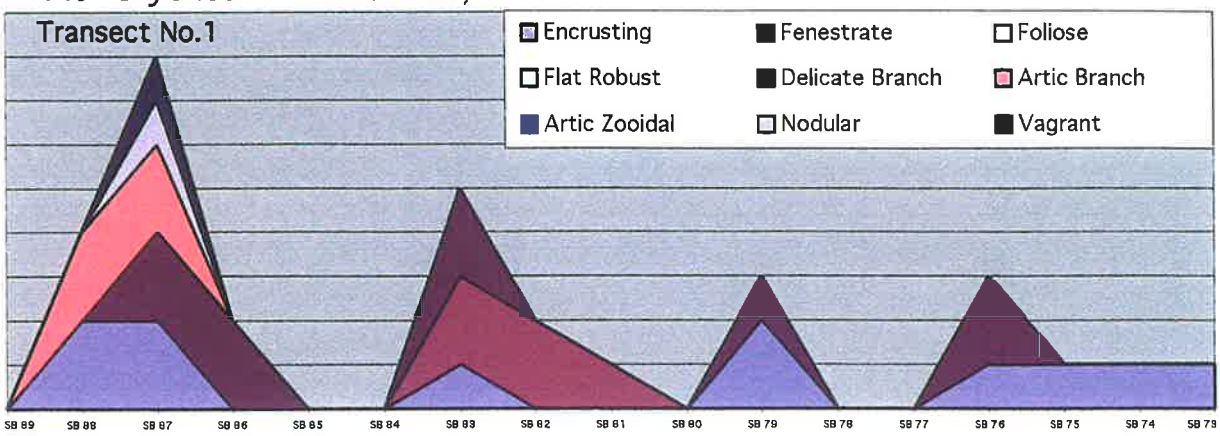


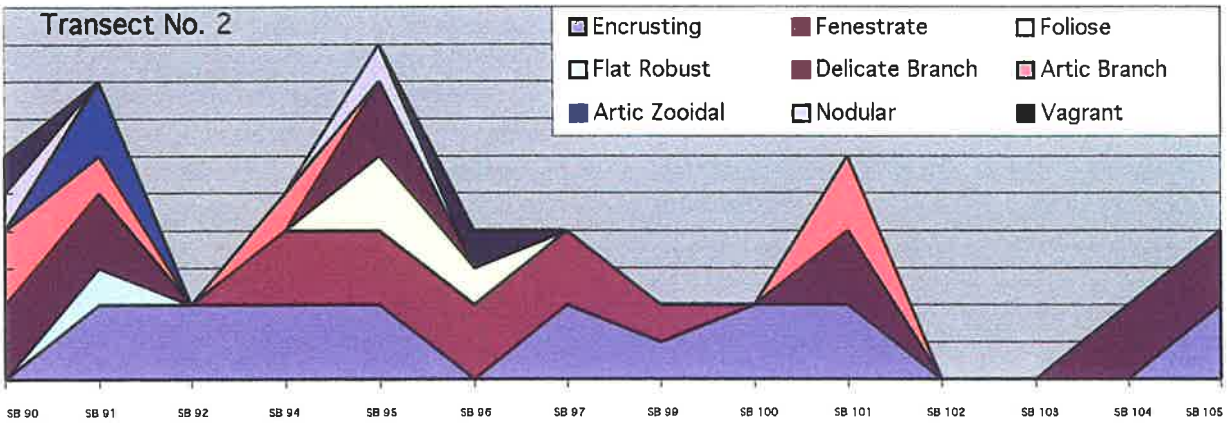



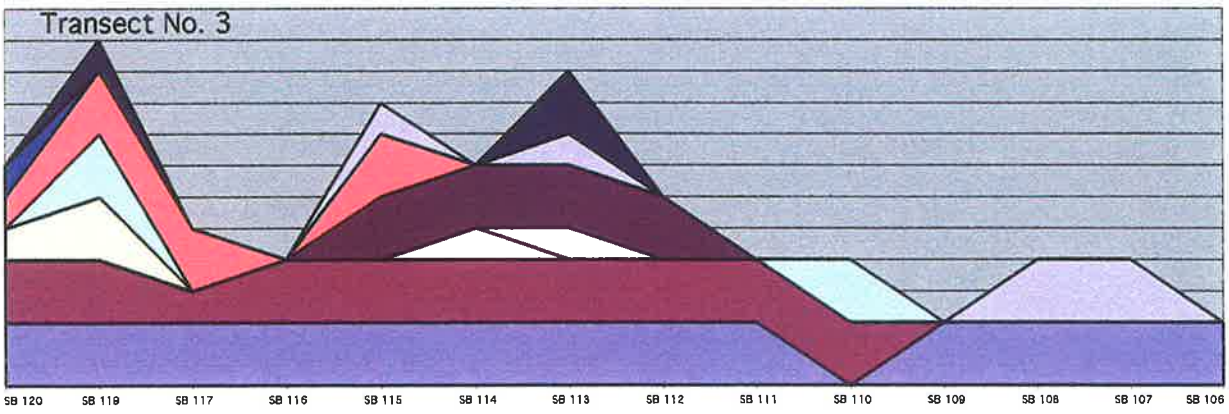



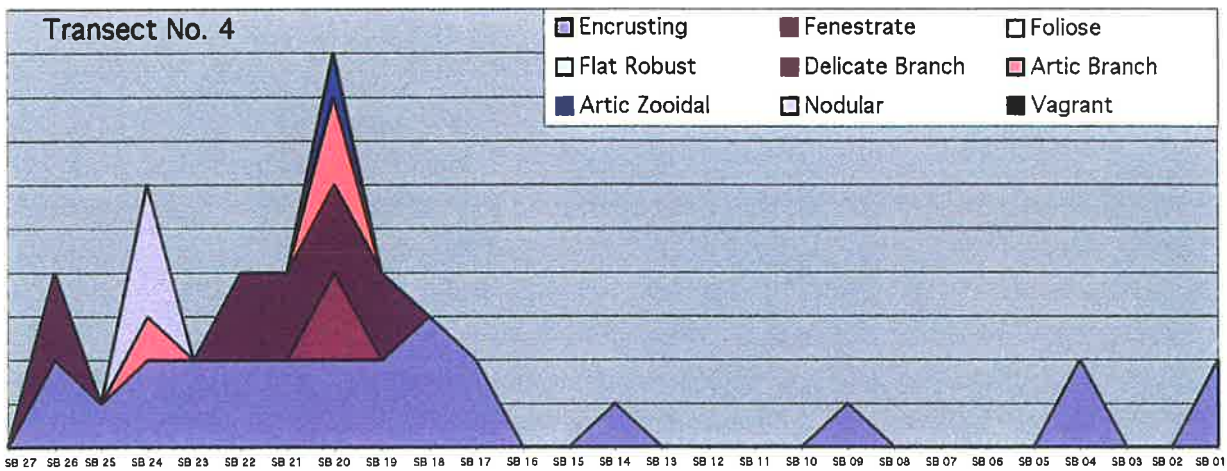



## 7.9 Bryozoan Distribution, Gravel

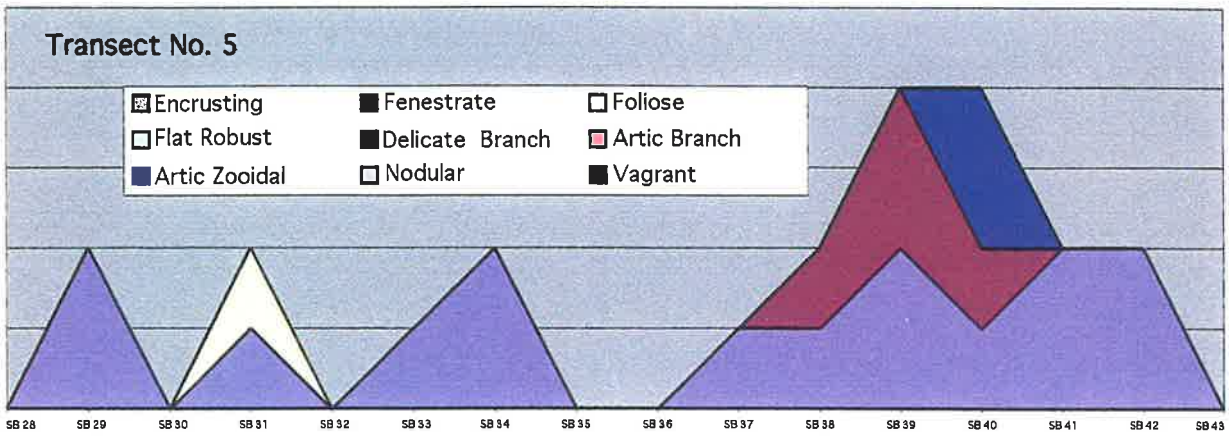


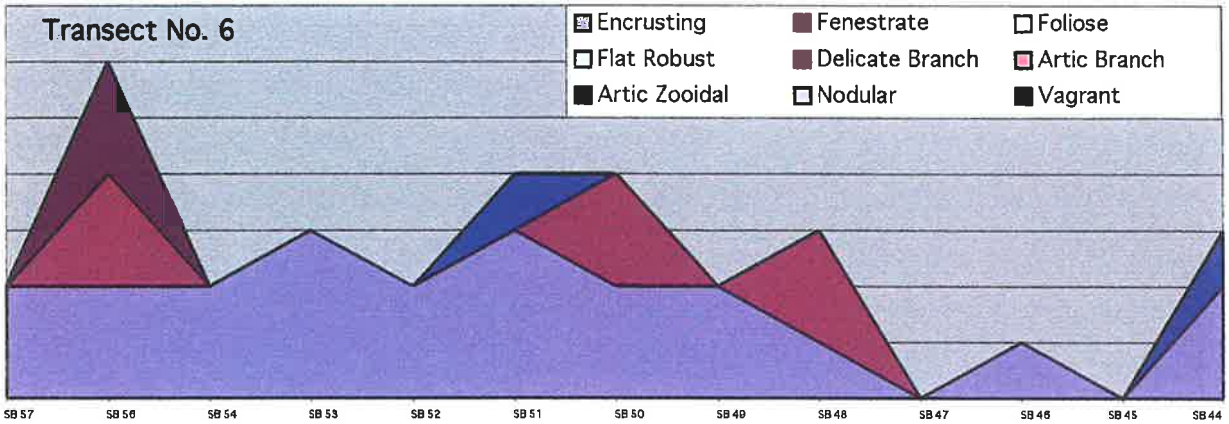



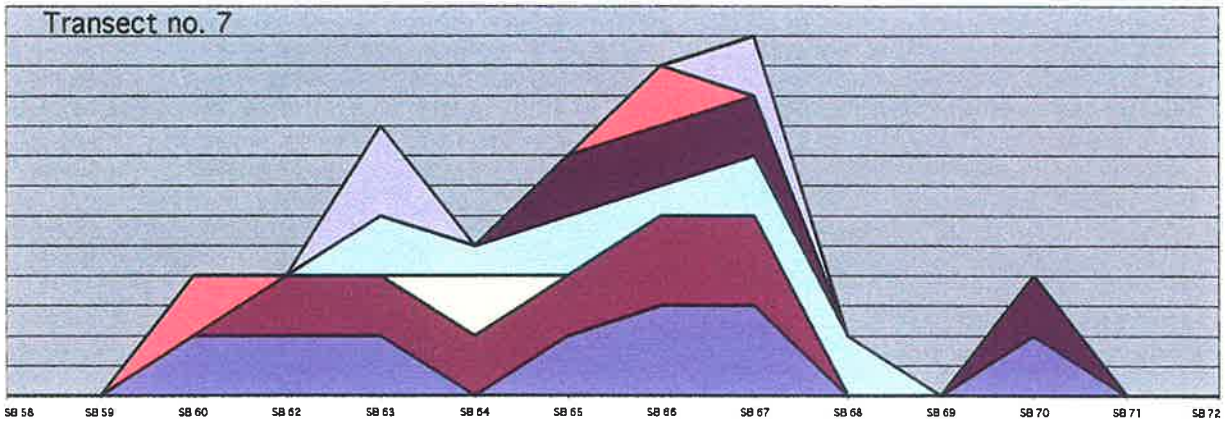



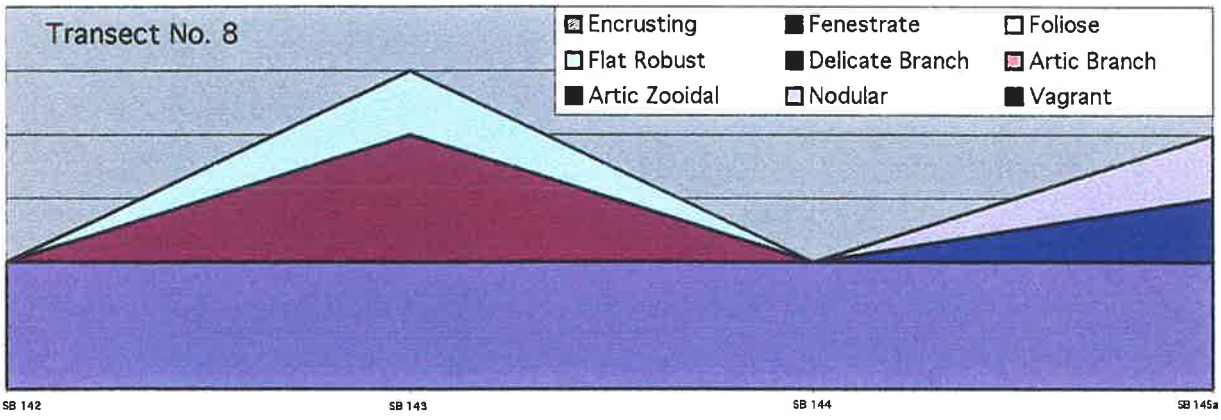



## 7.10 Bryozoan Distribution, Gravel

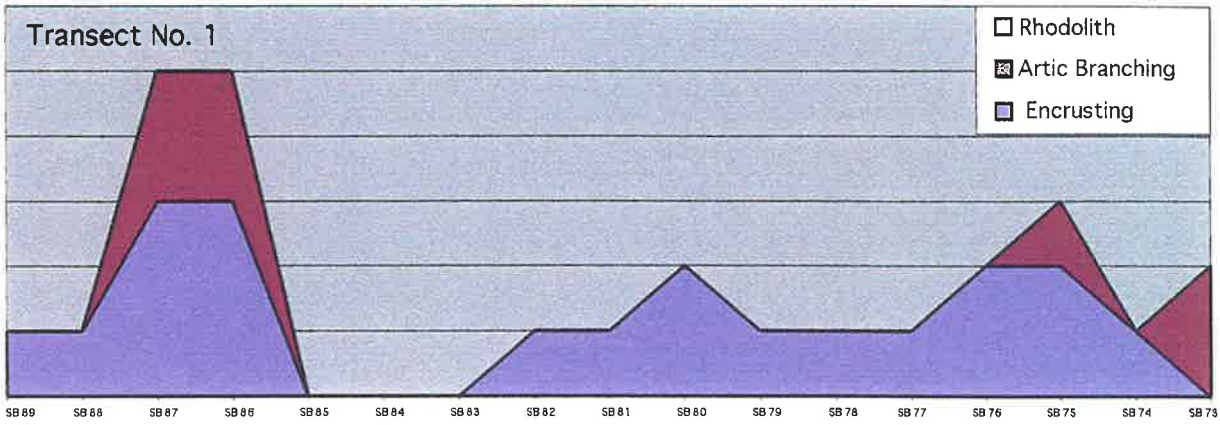


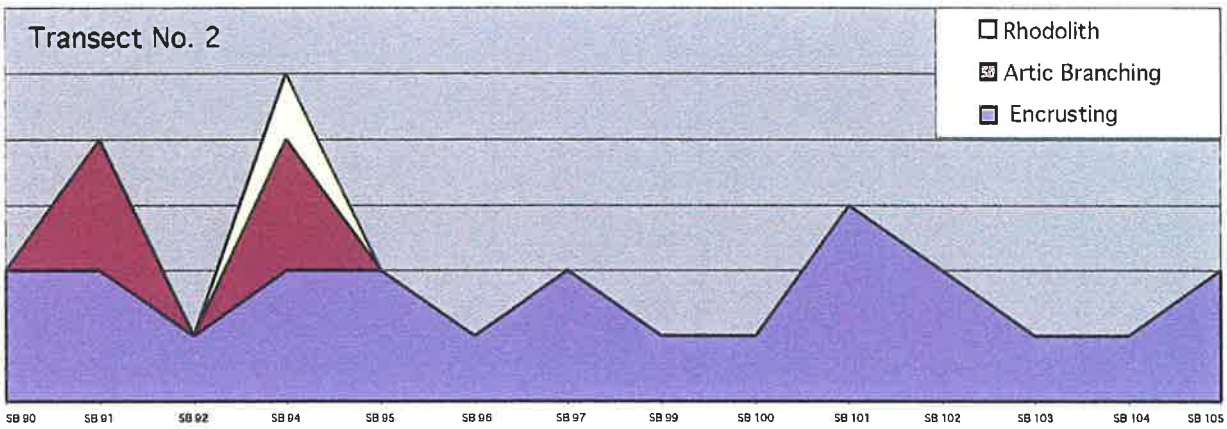



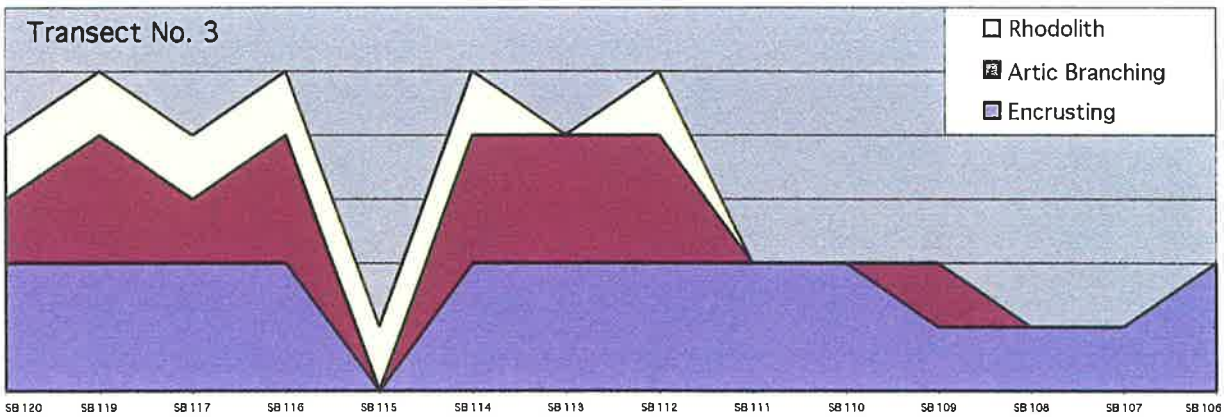



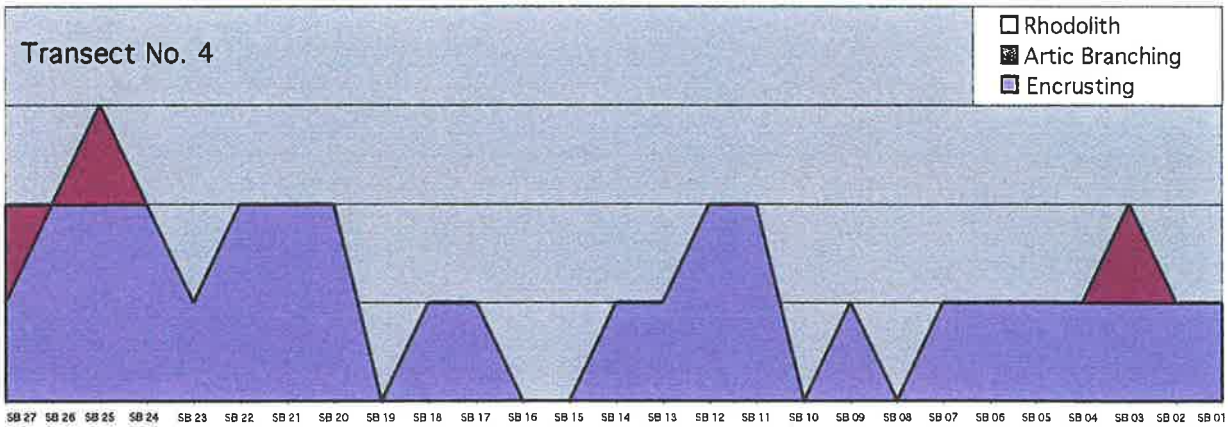



## 7.11 Coralline Algae Distribution, Gravel

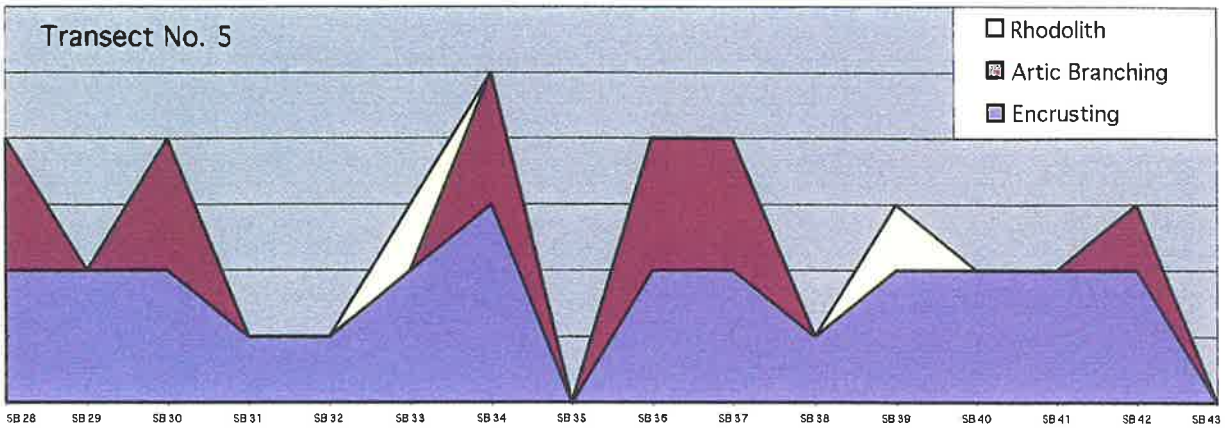


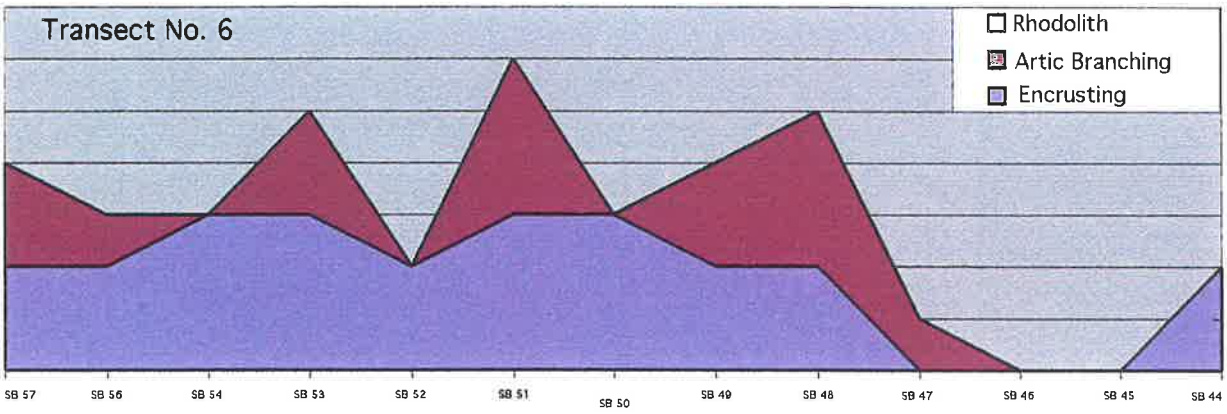



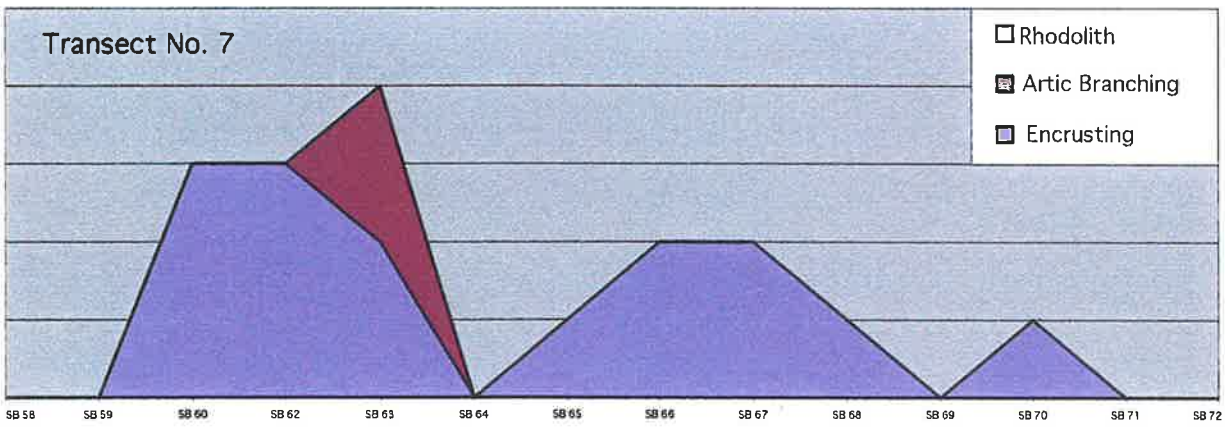



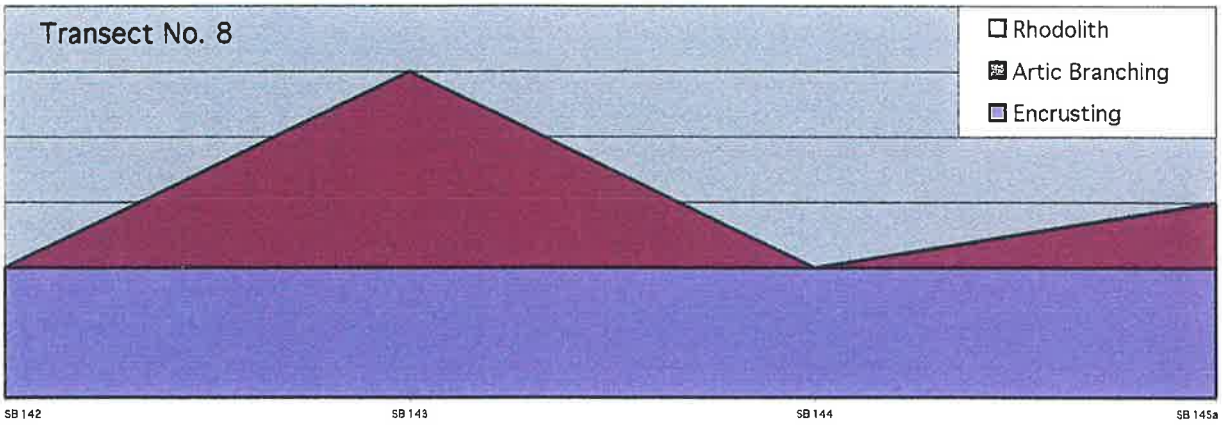



## 7.12 Coralline Algae Distribution, Gravel

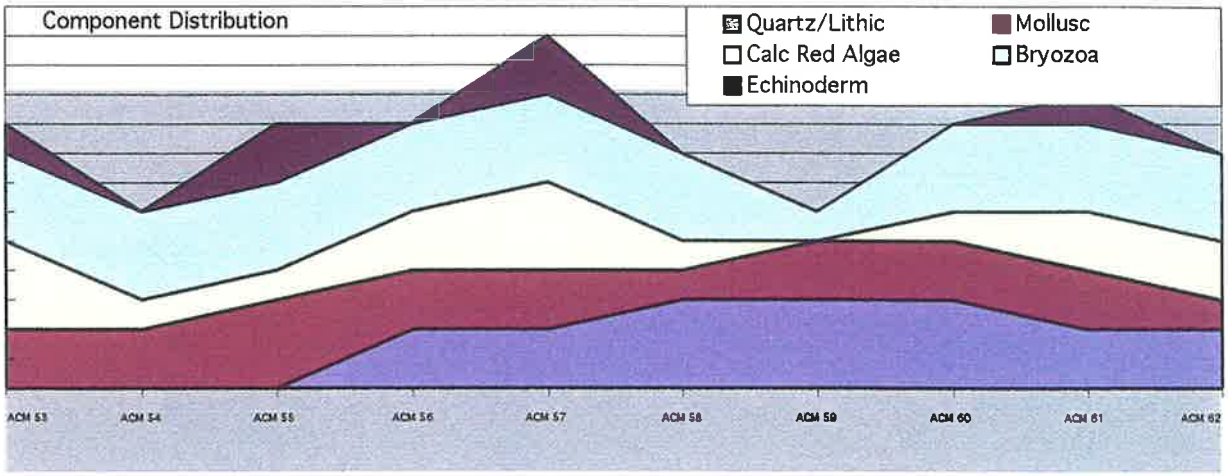


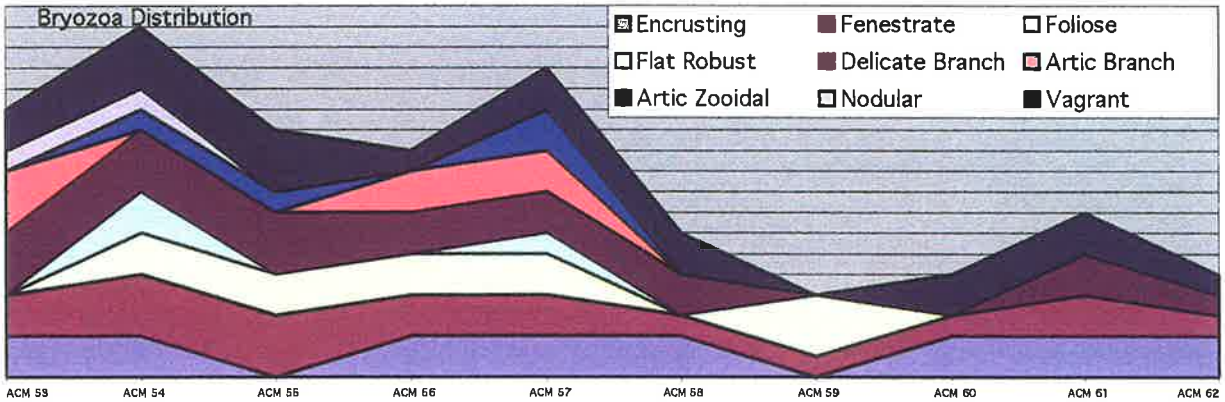



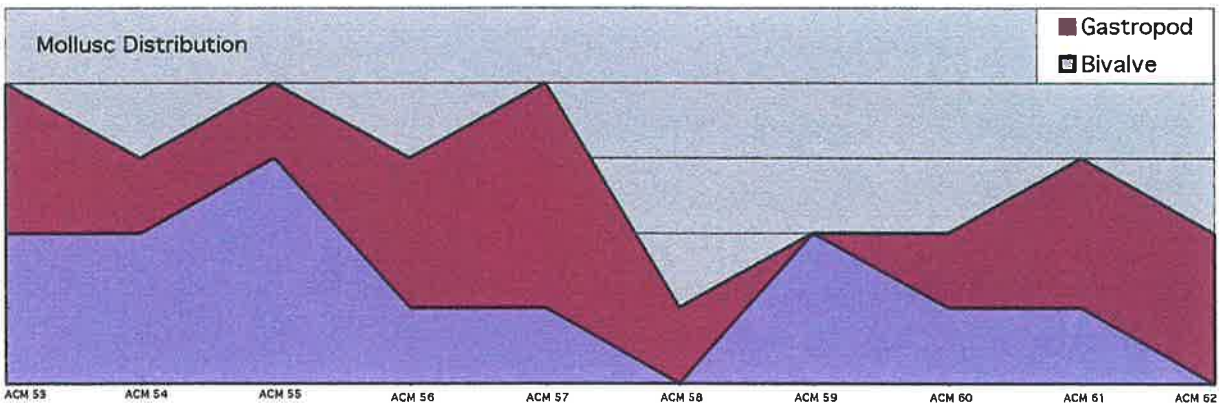



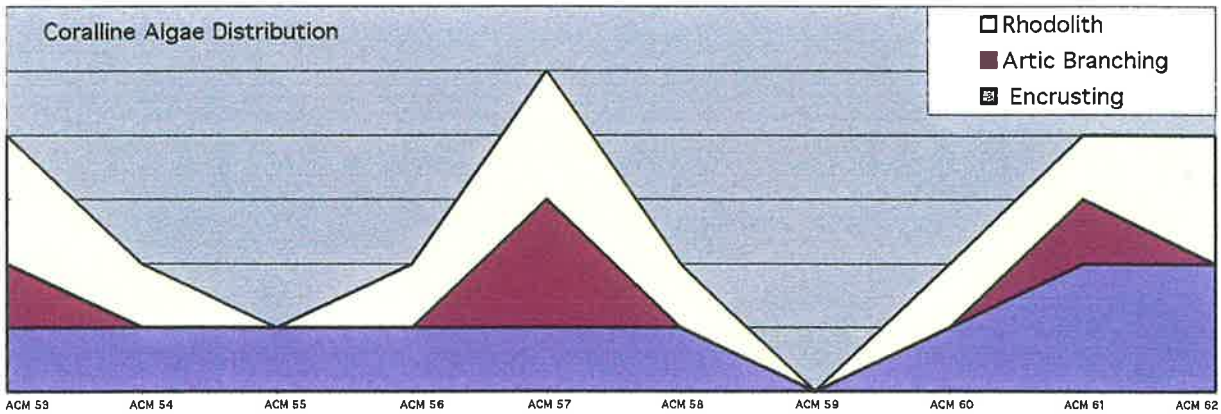



## 7.13 ACM Streaky Bay Transect, Gravel



Genera found in the outer areas, are *Lithothamnion* sp., *Goniolithon* sp. (rhodoliths), *Phymatolithon* sp., *Lithophyllum* sp. (crustose) and *Corallina* ssp., *Arthrocardia* sp., *Jania* ssp. and *Metagoniolithon* sp. (articulated branching).

The crustose coralline algae that is commonly found on the stems and leaves of the sea grasses *Posidonia* sp. and *Amphibolis* sp. are; *Lithothamnion* sp. (common on the leaves of *Posidonia* sp.) and *Hydrolithon* sp., *Pneophyllum* sp. (stems and leaves of *Amphibolis* sp.).

### 7.3.5 Minor Carbonate-producing Organisms

The minor carbonate producing organisms represented in the gravel fraction of the sediments are as follows:

#### 7.3.5.1 Echinoderms

Rare to common occurrences of echinoderms are found in the gravel fraction from sediments throughout the bay (Figure 7.5). They are present as rare whole tests of echinoids and fragments of echinoids and ophiuroids. Ophiuroids (*Ophionereis* sp.) and epifaunal echinoids are found in the mouth of the bay while epifaunal and infaunal echinoids are present in the central sand shoal area with small (< 10 mm) epifaunal echinoids found on the muddy substrate. The plates and spines vary from fine delicate spines and thin plates in the inner areas of the bay to thick ornamented spines and robust plates on the outer terrace and entrance area of the bay.

The echinoderms and their locations are described;

- Plates and smooth striated spines of the epifaunal *Heliocidaris* sp. are found in isolated samples from most areas in the bay. The nature of the plates and spines indicate that the test and spines change from a delicate in the inner regions (sand shoals and inner marginal basins) to a robust structure in the outer regions (outer terrace and entrance) reflecting the energy of the waves in each environment.
- The plates and robust thorny spines of the epifaunal *Goniocidaris* sp. are found in isolated samples in high energy areas of the terrace and in the entrance.
- Fine spines and small broken tests of the infaunal *Holopneustes* sp. occur in samples from the low energy areas of the inner sand shoals and inner marginal basins.
- A single small test of the delicate infaunal echinoid, *Echinocardium* sp. was found in the medium to coarse sands on the generally rocky substrate at Sample Station, SB 116.
- Living Ophiuroids were observed from the outer rocky and the inner muddy environments within Streaky Bay. These ophiuroids subsequently disarticulated and degraded during the sampling and storage process so it was difficult to ascribe a genus to these brittle stars, but is thought to be *Ophionereis* sp. which is a common shallow water species in southern Australia.

#### 7.3.5.2 Brachiopods

Brachiopods are present as whole valves or large fragments only in trace numbers. These are present in the areas of the terrace and entrance where the substrate consists of eroded aeolianitic rock with scattered sand patches (Figure 2.11 and 2.12). Two species are represented in these occurrences, namely *Anakinetica cumingi* and *Magellania flavescens*. *A. cumingi* is a small free-living and sand dwelling, whereas *M. flavescens* is larger and common in coarse sandy seagrass meadows. Both brachiopods belong to the family Terebratulidae and are common in waters on the southern margin of Australia.

#### 7.3.5.3 Crustaceans

This group is represented in the gravel fraction of the samples, by two groups ie barnacles (Cirrapedia) and crabs (Malacostraca), in order of abundance.

- Barnacles are found as epifauna on larger biota and occasional large substrate fragments at the mouth and outer terrace.
- Rare crab claw fragments are found in samples from the seagrass meadows in the central area of the bay.

#### 7.3.5.4 Serpulids

The calcareous exoskeleltons of Annelids occur as epifauna on larger biota (commonly mollusc valves) and larger lithic grains at the mouth and are common on blades of *Posidonia* sp. in the seagrass meadows of the central area of the bay. The genera which are common in the bay are the spirorbids *Protolaeospira* sp., *Janua* sp. and *Romanchella* sp. in the seagrass meadows and entrance and the serpulid *Galeolaria* sp. in the entrance area.

#### 7.3.5.5 Sponges

Living sponges are found in samples from the central to the outer areas. Large triaxon (calcareous and siliceous) and broken tetraxon (siliceous) spicules were found in the gravel fraction of the sediments in the outer terrace to entrance areas of the bay.

#### 7.3.5.6 Corals

Rare corals (Scleractinia) are represented as a single azooxanthellate species in reptoid colonial form. They are present on the outer shelf and entrance area where there are suitable rocky substrates for the colony to attach. Recruitment for these corals appears to be difficult because of competition with encrusting bryozoans. The corals collected at Streaky Bay vary from small distinct colonies to colonies surrounded by encrusting bryozoans to such an extent that only the calyx was visible. The corals were found in the samples SB 67, SB90, SB91, SB116 and ACM 57.

### 7.3.6 QUARTZ AND LITHIC FRAGMENTS

Quartz and lithic components in the gravel fraction range from highly polished/well-rounded to dull/angular fragments . These components are abundant to common in the northern tidal channel, central to northern entrance area (Figure 7.6). They are common to rare on the central and northern shoals, northern shoreface and central entrance area. The fragments observed in this fraction are similar to the quartz/lithic types observed in the sand fraction ie.

- Quartz grains, which are transparent to white translucent due to micro fractures, occur in the central sand shoals and northern entrance.
- Potassium feldspar grains, which are predominantly dark yellow to orange, have significant occurrences on the northern outer terrace and entrance areas,
- Lithic fragments are comprised of fragments from both igneous and sedimentary-derived sources. The igneous felsic material consists of feldspar and quartz with traces of dark green amphibole (hornblende). The feldspar in these fragments is composed of K feldspar and a trace of pale buff coloured plagioclase. These fragments are derived from felsic intrusives which occur to the north and at the entrance of Streaky Bay (Dove, 1997). Rare gravel-sized grains of amphibole (hornblende) possibly originate from the altered mafic rocks of the Hiltaba suite which has intruded the felsic St. Peter Suite.

The sedimentary lithic gravel fragments attributable to the Bridgewater Formation are present as either fragments of cemented aeolianite or large fragments of rounded calcrete (Figure 9.8c and 9.9 d). These rare fragments are limited to the northern tidal channel and northern outer terrace.

## 7.4 DISCUSSION

The distribution of the gravel-sized sediment in the bay has to be taken into account when discussing the composition and the distribution of the components. A significant portion of the sediments in the bay contain less than 5 % gravel while local areas have > 30% and an isolated area at the entrance comprises > 70 % gravel (Figure 7.1). These concentrations of gravel are localised to the northern tidal delta, the central and northern terrace and the central and northern entrance areas (see Chapter 5). In general, component composition of gravel tends to be > 50 % quartz /lithic fragments where concentrations of gravel are > ~15 %. The composition of the gravel is mostly biogenic where the fraction is < 10 %.

### 7.4.1 MOLLUSCS

The areas of maximum abundance of molluscs are restricted to the inner marginal basins, other isolated abundant occurrences of are found on the northern and southern areas of the terrace. It is

interpreted that these low energy environments allow the deposition of a finer and thicker sea-floor sediments, which are the preferred habitat for a significant range of swimming and infaunal molluscs. The central areas of the entrance and terrace support sparse populations due to high-energy swells sweeping into the bay maintaining a mobile substrate. This effect is magnified to an extent by the morphology of the outer bay funnelling and concentrating the energy of these swells with the steep rise of the sea-floor from the entrance to the outer terrace (Figure 2.8). As a consequence of this winnowing, the finer sediment is moved shorewards to the sand shoals and the inner marginal basins leaving only a patchy thin layer of coarser sand and gravel sediment generally occurs in the outer portion of the bay. This outer area is only marginally habitable for infaunal species but is a suitable environment for epibenthic (mobile and sessile) species. The environment is typical, on a smaller scale, of the continental shelf on southern margin of Australia, where the sediments are palimpsest and the finer fractions occur as migrating sand waves and fill within the ravined rocky substrate of the shelf (James et al., 1992; 1994; 1997; 2001; James and von der Borch, 1991; Boreen and James, 1993).

The distribution of molluscs in Streaky Bay reflects this variation in energy and resultant sediment veneer. Infaunal, mobile and sessile benthic bivalves are abundant in the inner marginal basins and the central and southern flood deltas, which are areas of low energy as reflected in the grainsize distribution (Figure 5.16). As the environmental energy increases the composition of the significant mollusc population commonly changes from infaunal and mobile bivalves to gastropods and byssally attached bivalves. The mature forms of these molluscs in the high energy environment are generally robust, heavy weight and well ornamented (Sediment Descriptions, Appendix Two). The seagrass meadows are host to grazing and predatory gastropods as well as smaller light to medium weight infaunal bivalves.

### 7.4.2 BRYOZOANS

The structural diversity of the bryozoans increases proportionately with the firmness of the substrate which is available for bryozoans to inhabit (Bone and James, 1993, James et al, 1992, 1997). This variation is particularly noticeable from the inner marginal basins and sand shoals where diversity is low, to the highly variable rocky and patchy sediment substrates of the terrace and entrance areas where the structural diversity is high (Figures 7.9, 7.10 and Sample Descriptions- Appendix Two). The low structural diversity of bryozoans in the inner bay can be correlated with the delicate nature of the encrusting bryozoans which attach to the leaves of the seagrasses *Posidonia* sp. and *Amphibolis* sp. and the further lack of suitable hard substrate on which many of the structural forms depend The outer bay environments are host to a majority of the structural forms which are utilised by the cheilostome and cyclostome bryozoans. This can be compared directly with the bryozoan structural diversification on the adjacent mid- to outer shelf where all the described structural forms (James et al,

1992) are represented in the sediments (Figure 7.13). This wide variation of structural diversity on the mid- to outer shelf is also seen on the Central GAB (James et al., 2001), Lincoln (James et al, 1997) and Lacepede (James et al, 1992) shelves, whist the inner shelf structural diversity, similar to that of Streaky Bay, is seen in sediments from the southern Spencer Gulf (Fuller et al, 1994)

### 7.4.3 FORAMINIFERS

The relatively large *Elphidium* sp. is the most common foraminifer in the gravel fraction and occurs in the outer terrace and entrance areas. Other rare large foraminifers present are *Textularia* sp., *Cribrobulimina* sp., *Peneropolis* ssp., *Triloculina* sp. and *Quinqueloculina* sp. These specimens are mostly found in the outer areas of the bay are significantly larger and more robust than their inner bay counterparts. Large-sized foraminifers are not recorded from other coastal embayments on the western Eyre Peninsula although the large foraminifers *Heterostigina* sp. and *Miniacina* sp. occur sparsely at the entrance to Streaky Bay (James et al., 2001).

### 7.4.4 CORALLINE ALGAE

The coralline algae, present in the gravel fraction depicts the observed occurrence in the sand shoal/seagrass meadows as being common to occasionally abundant. It is interpreted that this frequency of occurrence is understated as a result of the habitat substrate of prolific crustose coralline algae in this area. The leaves extensive seagrass is the site for prolific coralline growth and while thalli grow larger than 2 mm, they disintegrate quickly into smaller grain sizes (Chapter 9 Mud). Articulated coralline algae is common on the rocky substrates of the outer bay and also on the rocks which outcrop in the littoral zone around the headlands and discontinuously outcrops along the inner shore lines. It has also been observed attached to the root bosses of the seaweed *Ecklonia* sp. and to a lesser extent, around the roots of seagrasses. Significant coralline algal fragments, which are confined to the northern terrace, are concentrations of disintegrated articulated coralline algae. It is interpreted that live articulated coralline algae growing on the terrace substrate and the root areas of soft brown algae are transported to the sand shoals on dying and disintegration.

### 7.4.6 QUARTZ/LITHIC

The areas of quartz/lithic gravel abundance, especially at the entrance, can be directly correlated with the presence of felsic intrusives and aeolianite on Olive Island, which is being actively eroded by the continual action of the southwesterly oceanic swells. It is interpreted that the felsic (quartz and feldspar) and to a lesser extent aeolianitic sediment produced by this action is being transported into Streaky Bay. A lobe of quartz/ lithic gravel, which extends from the entrance into bay with NNE orientation. This orientation of this lobe correlates with swell direction and the position of Olive Island. The area of low quartz/lithic gravel immediately to the northeast (leeside) of Olive Island is the deposition site of more sandy sediments with a higher biogenic content (Figure 5.9). The

abundant occurrence of quartz /lithic fragments on the central terrace is the result of the erosion of the subaqueous pinnacle (Dashwood Rocks) which is probably an outcrop of felsic intrusive. Erosion on the northern tidal channel floor (Warburton Channel) has produced the highly abundant aeolianite gravel on both the ebb and flood tidal deltas. This occurrence is localised due to the current action of the tides and the friable nature of the aeolianite. This friable nature is a result of poor cementation within the aeolianite, the cement of which is predominantly contact (Wilson, 1991). The layers of calcretised aeolianite, which are found within the Bridgewater Formation, have produced rounded coarse pebble to coarse sand grains in the same proximity as the aeolianite. The plumes of sediment derived from this erosion in the channel are significant when the distribution and quantity of aeolianitic grains in the sand fraction are also taken into account (up to 50 %) (Figure 6.6).

## 7.5 CONCLUSIONS

The abundance of gravel at the entrance and outer terrace reflects the prolific biogenic diversity and population densities of calcareous fauna in this area As in the sand fraction, the molluscs are the dominant group which represents a range of infaunal and epifaunal bivalves and grazing and predatory gastropods. The inner bay is characterised by infaunal, mobile and sessile epibenthic bivalves and grazing gastropods, while in the outer bay byssally attached bivalves and predatory gastropods predominate. These zonations are principally a result of substrate distribution and characterise sediment production from mollusc disintegration from both substrates along the west coast of the Eyre Peninsula.

The structural diversity of bryozoans increases proportionately with the proportion of rocky substrate habitable for bryozoans. More robust forms also with significant populations characterise the outer rocky substrates of the bay. This compares with a low diversity and population of bryozoans in the inner bay with encrusting, delicate branching and articulated delicate branching forms common.

Abundant articulated and robust crustose coralline algae and rare patches of rhodoliths occur on the high energy outer bay rocky substrates, while delicate crustose and articulated coralline algae occurs in the lower energy sand shoals and near beach areas associated predominantly with the seagrass meadows

The gravels on the rocky outer bay substrate are composed of significant quartz/lithic gravel components that can be directly correlated with the presence and erosion of Proterozoic felsic intrusives and Bridgewater Formation aeolianite. These areas of quartzo-feldspathic gravel are concentrated proximally to Olive Island, Point Brown and a sea-floor high in the outer bay.

# CHAPTER EIGHT

# ORIGIN AND COMPOSITION OF MUD-SIZED SEDIMENTS

## 8.1 INTRODUCTION

Reports and research on the production, accumulation and occurrence of temperate (cool-water) shallow-water open marine carbonate muds from around the world are not abundant. Temperate carbonate muds have been sampled from intertidal, estuarine and supratidal zones in protected marine temperate localities (Cann and Gostin, 1985; Gostin et al., 1984; Andrews et al., 1997, Larsonneur, 1975, Lablack, 1985; Hill, 1994 and Wirtz, 1994 amongst others. Deeper water (>40 m) carbonate muds from temperate regions is reported from the outer continental shelf of the southern half of Australia (James et al., 1992, 1994, 1997, 1999; Collins et al., 1997; Boreen, 1993; Ferland, 1997; Collins, 1988; Jones and Davies, 1983; Conolly and Von Der Borch, 1967, amongst others); Bass Basin, (Blom and Alsop, 1988); from the continental shelf of New Zealand (Gillespie and Nelson, 1997; Nelson et al., 1988; Nelson, 1978); from the temperate continental shelf of western Europe; (Alexandersson, 1979; Farrow and Fyfe, 1988); and the temperate continental shelf of North America (Young and Nelson, 1985).

The deposition of semi-protected marine carbonate muds in semi-protected areas in water depths from 8 m to 15 m, in a cool-water environment has not been recorded in the literature. The inner marginal basins of Streaky Bay typify such an environment.

The aims of this chapter are:

- To determine the composition and origins of the muds in the bay.
- To compare the bulk sediment with the mud fraction.
- To ascertain whether there is a neomorphic change (i.e. leaching of magnesium and replacement by calcium) occurring during the process of larger grains and fragments disintegrating to mud.
- To characterise particles found within the mud fraction and correlate them with particles produced by the disintegration of calcareous organisms found in the bay and the mud fraction.
- To determine whether there is a mineralogical correlation with the dominant skeletal organisms in the bay.

## 8.2 CARBONATE CONTENT OF THE MUD FRACTION

The carbonate content of the bulk sediment and mud fraction was determined using the methods outlined in Chapter 3, Methods.

### 8.2.1 RESULTS

The $CaCO_3$ content (aragonite, LMC, IMC and HMC) of the mud fraction of the sediment varies, in selected samples, along the length of the inner marginal basins from 87.6% to 99.3%. The selection of these samples was determined by high mud content of these sediments along the inner marginal basins.

| Sample | Bulk sample % [1] | Mud fraction % [1] | Sand fraction % [2] |
|---|---|---|---|
| SB 02 | 86.5 | 87.6 | 94.7 |
| SB 08 | 93.1 | 89.5 | 91.7 |
| SB 09 | 90.3 | 95.6 | 91.7 |
| SB 10 | 95.8 | 96.2 | 93.7 |
| SB 15 | 93.3 | 91.9 | 93.7 |
| SB 16 | 93.3 | 93.4 | 95.0 |
| SB 17 | 96.7 | 97.0 | 96.3 |
| SB 23 | 92.3 | 93.6 | 92.2 |
| SB 24 | 92.3 | 98.2 | 93.3 |
| SB 25 | 90.1 | 99.3 | 92.0 |
| Average | 92.4 | 94.2 | 93.4 |
| [1]Results from acid dissolution [2]Results from point-counting | | | |

Table 8.1 Carbonate content of bulk sample, mud fraction and sand fraction of selected sediments from the Inner Marginal Basins and Blanche Port. (Figure 3.2 for sample locations).

The carbonate content of the 10 bulk samples from the inner marginal basins has a modal average of 92.4%. The content is higher than average in the central basin (94.4%), average in the southern(93.1%) and northern (91.6%) basins and significantly lower than average in Blanche Port.

The carbonate content of the mud fraction of the sediments from the inner marginal basins ranges from 85.6% to 99.3% with a modal average of 94.2%. The content of the mud in the southern and central basins averages 93.4% and 94.1% respectively, the northern basin is higher than average with 97% and Blanche Port is lower than average with 87.6% carbonate in the mud fraction. It is also higher in the northern area of each basin and is lower in the southern areas of the basins and lowest in the central area of Blanche Port.

## 8.3 CARBONATE COMPOSITION OF SEDIMENT BY XRD ANALYSIS.

The principal minerals targeted for the XRD analysis were Low, Intermediate and High Magnesium Calcite (LMC, IMC, and HMC respectively), Aragonite, Dolomite and Quartz. Intermediate magnesium calcite is an arbitrarily designated mineral in the Australia - New Zealand cool-water setting (Bone and James, 1993, 1997). The skeletal mineralogical composition of > 50 % of bryozoans fall approximately midway between the normal LMC (≤ 4.0 mol % $MgCO_3$), HMC (> 12.0 mol % $MgCO_3$) and IMC values, ie between 5.0 and 11.0 mol % $MgCO_3$ (Bone and James, 1993, 1997, Smith et al., 1998). The IMC mineral becomes important as a result of the high occurrence of bryozoans and their contribution to the carbonate sediments found in these temperate shelf settings (Bone and James, 1993, 1997, Smith et al., 1998).

The mole % $MgCO_3$ contained in the different magnesium calcite species is shown in Table 8.2.

| Magnesium Calcite species | Mole % Mg $CO_3$ |
|---|---|
| Low Magnesium Calcite (LMC) | < 3.99 |
| Intermediate Magnesium Calcite (IMC) | 4.0 – 11.99 |
| High Magnesium Calcite (HMC) | > 12.0 |

Table 8.2 Mole % $MgCO_3$ defining the Magnesium Calcite species; LMC, IMC, HMC (Bone and James, 1993, 1997).

### 8.3.1 RESULTS

The results of XRD analysis are shown in Table 8.3. Carbonate constituents are shown as a percentage, and terrigenous shown as dominant (>50%), minor (<~2%) or trace (< ~0.5%). The carbonate composition of the bulk samples and mud fractions show a subequal dominance of aragonite and magnesium calcite of varied mol % $MgCO_3$ (Table 6.3). Low magnesium calcite (LMC) is significant throughout the sediments and is usually co-dominant with IMC. High magnesium calcite (HMC) is significant in a number of analyses, but where present, is not represented in both the bulk and mud fraction of the sample.

**8.3.1.1 LMC** is present in the bulk and mud fractions of all the sediments (1% – 52%) and varies from 0.0 to 3.5 mol % $MgCO_3$. The difference in composition of LMC in the mud fraction to the bulk sediment ranges from zero to 3.5 mol % $MgCO_3$. The mol % $MgCO_3$ is lower in the bulk fraction than in the mud in a majority of the sediments, although the opposite is found in samples SB 02 and SB 08.

**8.3.1.2 IMC** is significant in the bulk and mud fractions of the sediments (9% - 48%) except for the mud fraction of sediments SB 17 and SB23 where IMC was not detected. Two different compositions of IMC are found in the bulk samples of SB 16 and SB 25 and their compositions are 8.5 and 11.0 mol % $MgCO_3$ and 6.0 and 9.0 mol % $MgCO_3$ respectively. The IMC present in the mud fraction is generally 0.5 – 1.0 mol % $MgCO_3$ higher than the corresponding bulk sample. Sample SB 16 is the exception to this where the IMC is 1.0 mol % $MgCO_3$ less than that of the bulk sediment.

**8.3.1.3 HMC** is present in only four analyses (11% - 29%), all of which have a composition of 13.0 mol % $MgCO_3$. Three of these analyses are from mud fractions (SB 10, SB 17 and SB 23) and the remaining one from the bulk sediment of SB 09.

**8.3.1.4 Aragonite** is present in all fractions, ranging from 29% to 58% of the carbonate present. There is a general trend in aragonite content from the abundance (58%) occurring in the Blanche Port sediment to the northern basin where the content falls to 29%. In general, the percentage content is less in the mud fraction than in the bulk sediment.

| Sample Bulk, Mud, Residue | Low Magnesium Calcite Mol % $MgCO_3$ Abundance | Intermediate Magnesium Calcite Mol %$MgCO_3$ Abundance | High Magnesium Calcite Mol % $MgCO_3$ Abundance | Aragonite, Abundance % | Accessory Component Relative Abundance |
|---|---|---|---|---|---|
| SB 02 Bulk | 3.0 - 29% | 9.0 - 9% | - | 58% | Qtz - m<br>Dol - tr |
| SB 02 Mud | 1.5 - 1% | 10.0 - 38% | - | 58% | Qtz - m<br>Dol -tr<br>Fld - tr |
| SB 02 Res. | - | - | - | - | Qtz - d<br>Fld - tr<br>Kaol - tr |
| | | | | | |
| SB 08 Bulk | 3.5 - 34% | 8.5 - 11% | - | 53% | Qtz - tr<br>Fld - tr |
| SB 08 Mud | 0.0 - 29% | 9.0 - 21% | - | 48% | Qtz - tr |
| SB 08 Res. | - | - | - | - | Qtz –d<br>Fld –tr<br>Kaol - m |
| | | | | | |
| SB 09 Bulk | 1.0 - 23% | 9.0 - 12% | 13.0 - 11% | 52% | Qtz - tr |
| SB 09 Mud | 3.0 - 32% | 10.0 - 19% | - | 48% | Qtz - m |
| SB 09 Res | - | - | - | - | Qtz d<br>Fld - m |
| | | | | | |
| SB 10 Bulk | 1.0 - 52% | 8.0 - 15% | - | 31% | Qtz - tr<br>Dol - tr<br>Fld - tr |
| SB 10 Mud | 1.0 - 27% | 8.5 - 18% | 13.0 - 13% | 41% | Qtz - tr<br>Dol - tr<br>Fld - tr |
| SB 10 Res | - | - | - | - | Qtz - d<br>Fld -tr<br>Kaol - m |
| | | | | | |
| SB 15 Bulk | 2.0 - 21% | 9.5 - 20% | - | 57% | Qtz - tr<br>Dol - tr |
| SB 15 Mud | 2.5 - 47% | 10.0 - 13% | - | 39% | Qtz - tr |
| SB 15 Res | - | - | - | - | Qtz - d |
| | | | | | |
| SB 16 Bulk | 1.0 - 22% | 8.5 + 11.0 - 28% | | 48% | Qtz - m<br>Dol - tr |
| SB 16 Mud | 3.5 - 22% | 7.5 - 32% | | 45% | Qtz - tr |
| SB 16 Res | - | - | - | - | Qtz - d<br>Fld - m<br>Kaol - tr |
| | | | | | |

| Sample Bulk, Mud, Residue | Low Magnesium Calcite Mol % $MgCO_3$ - Abundance % | Intermediate Magnesium Calcite Mol %$MgCO_3$ - Abundance % | High Magnesium Calcite Mol % $MgCO_3$ - Abundance % | Aragonite, Abundance % | Accessory Components & Relative Abundance |
|---|---|---|---|---|---|
| SB 17 Bulk | 3.0 - 38% | 7.5 - 8% | | 54% | Qtz - tr |
| SB 17 Mud | 3.0 - 45 % | - | 13.0 - 19% | 35% | - |
| SB 17 Res | - | - | | - | Qtz - d |
| | | | | | |
| SB 23 Bulk | 2.5 - 19 % | 9.0 - 35% | | 45 % | Qtz - m<br>Dol - tr |
| SB 23 Mud | 3.5 - 36% | - | 13.0 - 29% | 32% | Qtz tr<br>Dol - tr |
| SB 23 Res | - | - | - | - | Qtz - d |
| | | | | | |
| SB 24 Bulk | 2.0 - 20% | 9.0 - 41% | | 7% | Qtz - m<br>Dol - 1 |
| SB 24 Mud | 3.5 - 25 | 10.0 - 39% | | 33 % | Qtz - tr<br>Dol -tr |
| SB 24 Res | - | - | - | - | Qtz - d |
| | | | | | |
| SB 25 Bulk | 1.0 - 20% | 6.0 + 9.0 48% | - | 30% | Qtz - tr<br>Fld - tr<br>Dol - tr |
| SB 25 Mud | 3.5 - 29% | 7.0 - 40% | - | 29% | Qtz - tr<br>Dol - tr |
| SB 25 Res | - | - | - | - | Qtz - d<br>Fld - tr |
| Qtz - quartz; Fld - feldspar; Dol - dolomite, Kaol - kaolinite; | | | | | |
| d – dominant; cd – codominant; sd – subdominant; m – minor; tr - trace | | | | | |

Table 8.3 Details of the XRD composition of samples with respect to the calculated mol % $MgCO_3$ in Calcite, with the percentages of LMC, IMC, HMC, Aragonite. Accessory components ie Quartz, Dolomite and Feldspar and their relative abundance are shown in the right hand column. The analyses of acid residues indicate the presence of clay (kaolinite) with the other minor-trace minerals found in the mud fraction. (Figure 3.2 for sample locations).

**8.3.1.5 Dolomite** is present in a majority of the bulk samples and one mud fraction. It is predominantly found in the sediments from the northern and central IMB and Blanche Port. Dolomite is present in one sediment from the southern IMB. The presence of dolomite in the mud fraction is restricted to the northern IMB, SB10 and SB 02. Dolomite is absent in the analysis of the residue fractions, which is not unusual given the time over which the acid dissolution process was conducted (~24 hours).

### 8.3.1.5 Minor and Trace Minerals

**Quartz** is ubiquitous throughout the analyses ranging from minor to trace in the bulk sediment and mud fraction, to dominant in the acid residue . Trace to minor amounts of quartz are found in the bulk samples with traces being common in the southern section of the bay apart from a minor presence in

Blanche Port (SB 02). Minor amounts of quartz are also indicated in the northern section apart from a trace in SB 17.

**Feldspar** occurs in the sediments throughout the IMB, but rarely occurring in the three analyses from the one sediment. The presence of feldspar occurs in the sediments from the southern section of the bay, including Blanche Port. Sample SB10 contains trace feldspar in the bulk sample, mud fraction and acid dissolution residue. It occurs in the bulk sediments of SB 08, SB 10, and SB 25, the mud fraction of sediments SB 02 and SB 10 and the acid dissolution residues of SB 02, SB 08, SB 09, SB 10, SB 16 and SB 25.

**Kaolinite** is present in analyses of the residue fractions from SB 02, SB 08, SB 10 and SB 16. The analyses show that a minor to trace amount occurs in the two sediments from the southern IMB and traces are found in the acid dissolution residues from Blanche Port and the northern IMB.

## 8.4 COMPOSITION OF SKELETAL ORGANISMS

The sediment-producing biota refers to the organisms from which the sediment originates and not necessarily the organisms that created the sediment either by mastication or ingestion. Examples of the latter processes would be echinoids (skeletal material; HMC) or sponges (skeletal material; silica) boring into bivalves or gastropods, thus producing LMC and aragonitic particles whilst their own skeletal material will produce HMC or silica fragments after dying.

The composition of significant calcareous skeletal organisms in Streaky Bay is determined by X-Ray analysis as described in Chapter 2 (Methods). A review of the skeletal carbonate compositions of major and minor biogenic groups encountered in Streaky Bay is detailed in Table 8.4

| Taxon | Calcite, Mol % $MgCO_3$ | Aragonite | Aragonite and Mg Calcite |
|---|---|---|---|
| Coralline Algae | 8 – 32 | | |
| Coccoliths | < 1 | | |
| Foraminifera -Benthic<br>ie, Miliolinids<br>Peneroplids<br>Rotaliids<br>Discorbids<br>Elphidiids | 0 – 16, rare up to 26<br>6 – 18 (10 –13)*<br>15 - 18<br>1 - 20<br>4 -15<br>2 – 4 (1.5 - 3)* | O | |
| Sponges - Calcareous | 7 – 15 (*11.5) | O | |
| Brachiopoda -<br>Terabratulid | 0 – 7 (*0.5) | | |
| Coral - Scleratinian | | X | |
| Bryozoa<br>Cyclostomata<br>Cheilostomata | 1.5 – 11.5<br>3<br>av 7.9 | X | O |
| Mollusc – Bivalves | 0 – 4 | X | X |
| Mollusc - Gastropods | 0 – 4 | X | X |
| Annelid - Serpulids | 2 – 10<br>values for cool-water (6 – 13.5) | X | X |
| Arthropod – Barnacles | 0 – 5<br>values for cool-water (0.7 – 2.5) | | |
| Arthropod – Ostracodes | 2 - 9 | | |
| Echinoderm – Echinoids | 3 – 16<br>values for cool-water (9 – 11) | | |
| X – Common; O – Rare | | *values for cool-water (17°C) | |

Modified after Scholle (1978), Milliman (1974) and Scoffin (1987) and Table 8.5 (this chapter).

Table 8.4 The general skeletal carbonate composition is tabulated for a majority of organisms from the cool-water realm. It reflects the importance of the IMC category that indicates a significant amount of skeletal material falling within the % mol $MgCO_3$ limits of IMC. Aragonite is also shown to be present in the skeletons of a significant number of common organisms

| Sample | Low Magnesium Calcite Mol % $MgCO_3$ – Abundance % | Intermediate Magnesium Calcite Mol % $MgCO_3$ – Abundance % | High Magnesium Calcite Mol % $MgCO_3$– Abundance % | Aragonite Abundance% |
|---|---|---|---|---|
| SB 26, bivalve *Chlamys bifrons* | 0.5 – 90 | - | - | 10 |
| SB 112, bivalve *Modialus areolatus* | 0.5 - 5 | - | - | 95 |
| SB 110a, bivalve *Dosinia victoriae* | - | - | - | 100 |
| SB 110b, bivalve *Ostrea angasi* | 1.5 – 100 | - | - | - |
| SB 107, bivalve *Fulvia tenuicostata* | - | - | - | 100 |
| SB 15, gastropod *Bulla quoyii* | - | - | - | 100 |
| SB 21, gastropod *Fusinus australis* | 1.5 - 0.5 | 9.5 - 2 | - | 97 |
| SB 33, gastropod *Thalotia chlorostoma* | - | 10.5 -1.5 | | 98 |
| SB 143, gastropod, *Phasianella* sp. | - | - | - | 100 |
| SB 01, echinoid, *Holopneustes* sp. | - | 11.0 - 100 | - | - |
| SB 201, artic. coralline algae, *Corallina* sp. | - | - | 12.5 - 100 | - |
| SB 36, crustose coralline algae, *Lithothamnion* sp. | - | - | 12.0 -100 | - |
| SB 87c, rhodolith coralline algae, *Lithothamnion* sp. | 0.5 - 1 | - | 13.5 - 98 | tr |
| SB 206, rhodolith coralline algae, *Lithothamnion* sp. | - | - | 14.5 - 100% | - |
| SB 210, rhodolith coralline algae, *Lithothamnion* sp. | - | - | 15.0 - 100 Lower Spencer Gulf | - |
| SB 67, coral, *Culicia* sp. | 3.0 - tr | - | - | 100 |
| SB 87b, barnacle, Balanus sp. | 1.5 - 98 | - | - | 1.5 |
| SB 200, calcareous sponge, *Sycon gelatinosum* | - | 11.5 - 100 | - | - |
| SB 87a spirorbid | - | - | 13.5* - 35 | 65 |
| SB 202, serpulid, *Galeolaria* sp. | - | 7.0 - 2 | 13.5* - 98 | |
| SB 203, brachiopod, *Anakinetica cumingi* | 0.5 - 100 | - | | - |
| SB 24, arborescent bryo, *Celleporaria* sp. | - | 7.5 - 100 | - | - |

| Sample | Low Magnesium Calcite Mol % $MgCO_3$ – Abundance % | Intermediate Magnesium Calcite Mol % $MgCO_3$ – Abundance % | High Magnesium Calcite Mol % $MgCO_3$– Abundance % | Aragonite Abundance% |
|---|---|---|---|---|
| SB 67a, foliose bryo, *Adeonellopsis folacea* | - | - | - | 100 |
| SB 67b, fenestrate bryo, *Iodictyum phoeniceum* | - | 9.0 - 100 | - | - |
| SB 67c, cyclo, del. bran. bryo, *Nevianopora* sp | 3.9 - 100 | - | - | - |
| SB 91-1, encrusting bryo, *Membranipora membrancea* | - | 4.5 - 100 | - | - |
| SB 91, unilam. bryo, *Membranipora perfragilis* | 3.0 ~ 4 | 8.5 - 96 | - | - |
| SB 205, unilam. bryo, *Petralia undata* | - | 7.5 - 54 | - | 46 |
| SB 207, unilam, foliose bryo, *Bugula dissimilis* | - | 9.5 - 100 | - | - |
| SB 208, encrusting bryo, *Cellarporaria cristata* | - | 8.0 - 100 | - | - |
| SB 209, foraminifera, *Elphidium* sp. | 1.5 - 100 | - | - | - |

Table 8.5 Results of XRD analysis of common calcareous skeletal remains dredged from sample stations in Streaky Bay.

### 8.4.1 Results

The compositions of the skeletal material from organisms found in Streaky Bay are shown in Table 8.5

The mineralogical composition of the skeletons of organisms analysed from Streaky Bay fall broadly into the combinations of carbonate mineralogy as presented in the table based on the results of Scholle (1978), Milliman (1974, and Scoffin (1987), (Table 8.4).

The organisms which are found to have dominant LMC include molluscs, bryozoans, foraminifers, brachiopods and barnacles. IMC is dominant in bryozoans, echinoderms and calcareous sponges and co-dominant with aragonite in some unilaminate bryozoans. HMC is dominant in coralline algae (crustose, articulated branching and rhodolith forms) and serpulid annelids and subdominant in spirorbid annelids. Aragonite is dominant in corals, bryozoans, some gastropods and spirorbid annelids and co-dominant in some unilaminate bryozoans.

## 8.5 MORPHOLOGY OF SKELETAL MICROSTRUCTURE OF MAJOR ORGANISMS.

The intrinsic micro- and nanostructure of the significant organisms found in the bay are examined in this section for their potential pathways of disintegration. The associated particles that are produced from this disintegration are highlighted in Section 8.6.

The skeletons of calcareous and minor siliceous organisms that contribute significantly to the composition and volume of the sand and gravel fractions of the sediment in Streaky Bay are analysed by scanning electron microscope using techniques described in Chapter 3 (Methods).
These organisms are studied for their potential to disintegrate and contribute to the mud fraction and are discussed in the same order as in Chapter 6 and Chapter 7.

### 8.5.1 MOLLUSCS

Molluscs, classes Bivalvia and Gastropoda, are the dominant carbonate producers within the sediments examined from Streaky Bay. This is evident from the component analysis of the sand fraction and the faunal density analysis of the gravel fraction. Molluscan shells are prone to breakdown from their laminate, prismatic or cross-lamellar structures into carbonate platelets or prisms through the presence of alternating organic proteinaceous (conchiolin) layers (Bathurst, 1983). These organic layers are secreted during the growth periods or between each carbonate layer. When the mollusc dies, the breakdown of this conchiolin accentuates the disarticulation and disintegration of the platelets and prisms, which can also be attributed to shell boring, maceration and abrasion (Bathurst, 1983). This is seen in the gastropod *Thais orbita*, where the layered and prismatic structures of the gastropod, are disintegrating into < 5 μm particles (Figures 8.1c, 8.1d). Bivalves also exhibit this style of disintegration into platelet and prismatic particles, particularly in the Superfamilies – Mytilacea, Pinnacea, and Pteriacea, all of which are common in Streaky Bay. The breakdown of crossed-lamellar structure and thin parallel layering in bivalves is shown in the transverse section in Figure 8.1e. Relatively large scale (~0.5 mm) laminar exfoliation leading to small scale (sub-μm) laminar breakdown can be clearly traced in the detailed SEM series, Figures 8.2a, 8.2b, 8.2c, 8.2d. Microboring is a common facilitator of shell disintegration where the crossed-lamellar and parallel layering is exposed through algal and annelid microboring (Figure 8.1f). This exposure through boring accentuates the rate of breakdown at the leading edge of the shell and leads to the formation of elongate platelets where crossed-lamination and prismatic layering is encountered (Figures 8.3a, 8.3b, 8.3c).

Homogenous bivalve and gastropod crystalline shell structure, which is composed of irregularly rounded particles, appears more likely to undergo intense boring at micro- (< 5 μm) and meso- (> 5 – 20 μm) scale (Figures 8.3d, 8.3e, 8.3e). These mollusc fragments, when reduced to mud size, appear as prismatic to blocky particles that usually contain abundant evidence of boring (Figures 8.2e, 8.2f). Further disintegration of bivalve shells is observed on large fragments from both the inner and outer areas of the bay. The series of micrographs (Figures 8.4a, 8.4b, 8.4c) show a fragment of *Katelysia* sp. valve with basin-shaped pitting located mostly between the growth-line ridges on the exterior surface. This pitting averages a width of 10 μm, with a depth of ~ 5 μm. These pittings have subsequently become a receptacle for smaller sub-μm particles. Further biogenic degradation of

bivalve shells is observed in Figure 8.4d where a significant area of the valve interior is marked with groups of short scratches. These scratches appear to radiate out from the muscle scars and thicker nacreous areas of the valve. The sub-μm particles resulting from these scratchings adds to the finer mud fractions (see discussion).

### 8.5.2 FORAMINIFERS

Whole foraminifera rarely occurred in this fraction. Rare benthic foraminifers (mostly Rotaliids) and an isolated planktonic foraminifer were found. It was difficult to definitively distinguish smaller mud-sized particles that belonged to this group due to the robust nature of the tests and the sub-μm prismatic crystallites, which are similar to other biogenic breakdown material produced by maceration i.e. coralline algae. Recognisable fragments of foraminifera were only occasionally observed in the mud fraction, apart from fragments and rare complete Rotaliids (Figure 8.19b, 8.22d). Rare fragments of what are possibly *Marginopora vertebralis* were observed but the particles were too charged for SEM imaging. These may have originated from the erosion of the marine sediments of the Glanville Formation. The principle method of breakdown of foraminifera tests appears to be through maceration and gradual disintegration with limited microboring (Figures 8.4e, 8.4f, 8.5a - *Elphidium* sp.) rather than the biogenic pathway of microboring. The organic coating on the cell walls of the foraminifera has been recognised as being particularly resistant to disintegration (Corliss and Honjo, 1981). It can be seen in Figure 8.5b (detail of Figure 8.4f), Figure 8.5e (*Discorbis* sp.) and Figure 8.5c, 8.5d (*Discorbis* sp.) that μm scale particles are continually exfoliating from the foraminifer surface. These exfoliations are further degraded into sub-μm crystallites as indicated in Figure 8.5f. Possible minor dissolution is indicated in the tests of agglutinated foraminifers (Figures 8.6a, 8.6b - *Cribrobulimina* sp.) and on the disintegrating edge of layer exfoliation (Figure 8.6c - *Discorbis* sp.). The dissolution fabric is recognised when comparing nearby unmarked surfaces to the porous or etched surface. The larger foliated particles can be identified when proximal to the foraminifera by a tight laminar structure that has no indication of an organic layer between the laminae, but recognition of the released particles in the mud fraction is circumspect.

### 8.5.3 BRYOZOA

Bryozoan fragments are a significant component of the sediment from the outer terrace on the sea-floor of Streaky Bay. Here they comprise < 35 % of the sand fraction, but generally, over a large area of the bay, the fragments are < 10 %. These areas include the inner marginal basins, the sea-grass meadows and the southern and northern terrace (Chapter Six). The distribution of bryozoan fragments within the gravel fraction ranges from abundant on the outer terrace, the seagrass meadows of the sand shoals and northeast shore area to absent in the far northern and southern areas of the bay which includes the central and southern inner marginal basins, Blanche Port and southern terrace. Mud-sized particles of bryozoan are present in all of the selected mud samples, occurring as porous foliose to

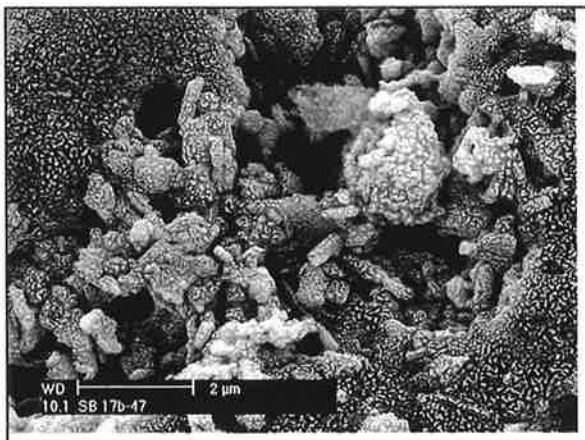



Figure 8.1a SEM Artifacts. Coarse gold artifacts,caused by coating on an unwashed carbonate sediment showing a pervasive distribution of gold globules. Scale bar 2 µm.

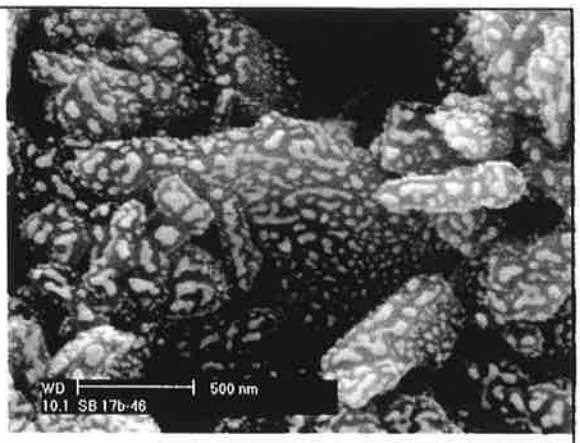



Figure 8.1b SEM Artifacts. Detail of gold artifacts (light coloured) coating the unwashed sediment. This can occur when coating sediments with grainsizes < 5 µm or when coating times have exceeded 30 secs.
Scale bar 500 nm.

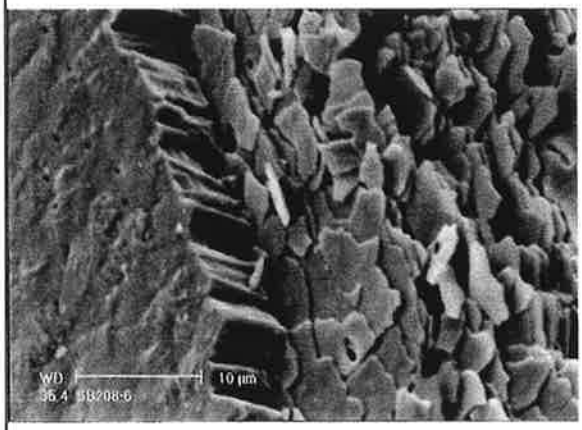



Figure 8.1c Layered and prismatic structure of *Thais orbita* (gastropod) illustrating the disintegration of the shell wall into platelets and prismatic particles.
Scale bar 10 µm.

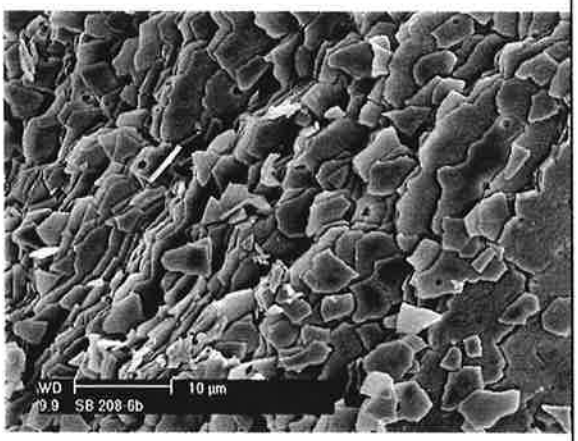



Figure 8.1d Detail of the layered shell structure of *Thais orbita*, illustrating the progressive formation of < 5 µm platelets.
Scale bar 10 µm.

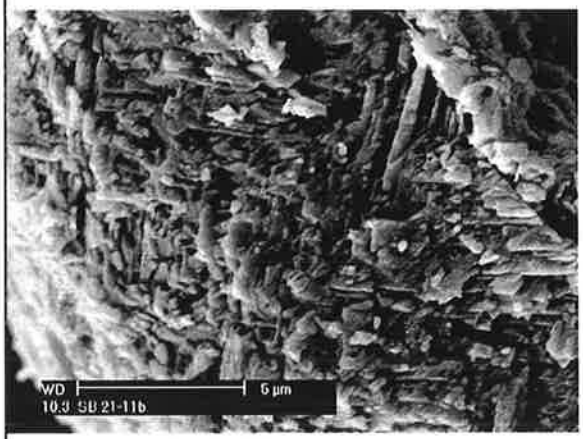



Figure 8.1e Shell disintegration patterns of crossed-lamellar structure in bivalves, showing the production of elongate prisms and irregular platelets.
Scale bar 10 µm.

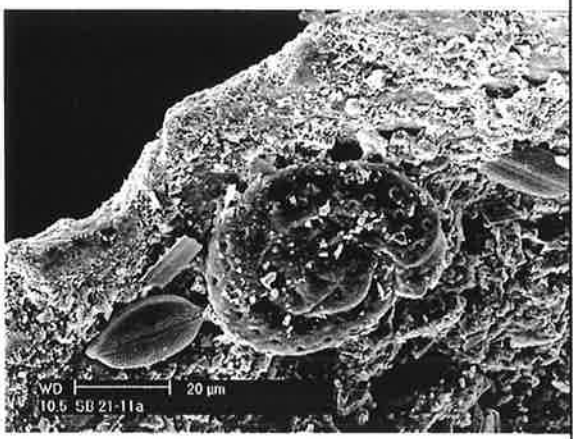



Figure 8.1f Maceration of bivalves is facilitated by algal microboring and epibionts. The maceration at the shell edge also accentuates the rate of shell breakdown.
Scale bar 20 µm.

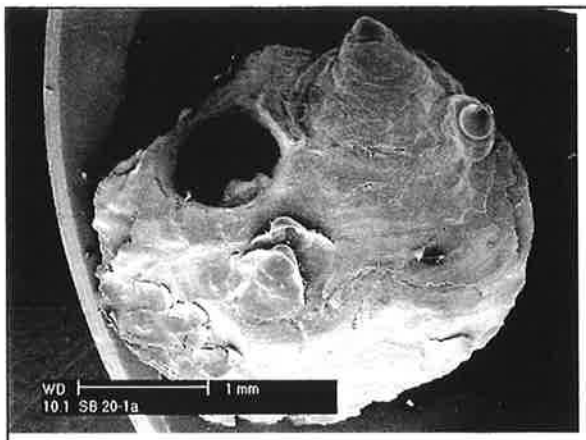



Figure 8.2a Large scale laminar exfoliation in juvenile forms of the bivalve *Ostrea* sp., also inferred μm sized particle production from gastropod boring. Scale bar 1 mm.

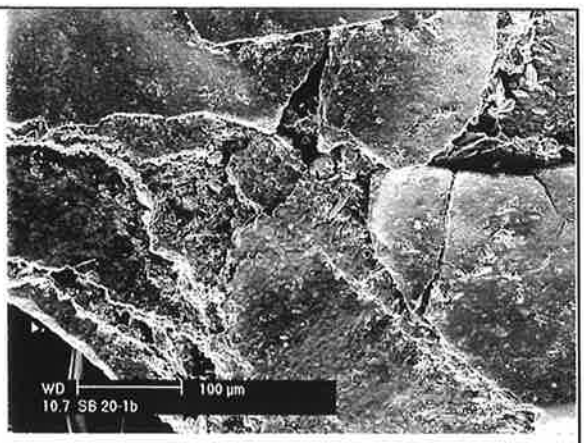



Figure 8.2b Detail of Ostrea sp. shell disintegration and macro-platelet formation. Scale bar 100 μm.

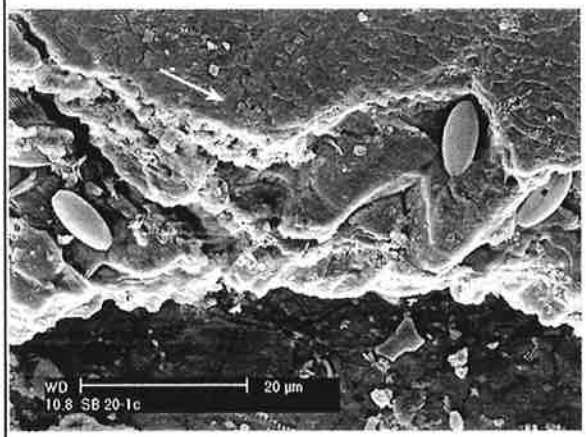



Figure 8.2c Detail of the macro-platelets (8.2b) indicating a sub-structure of microplatelets (arrowed).
Scale bar 20 μm.

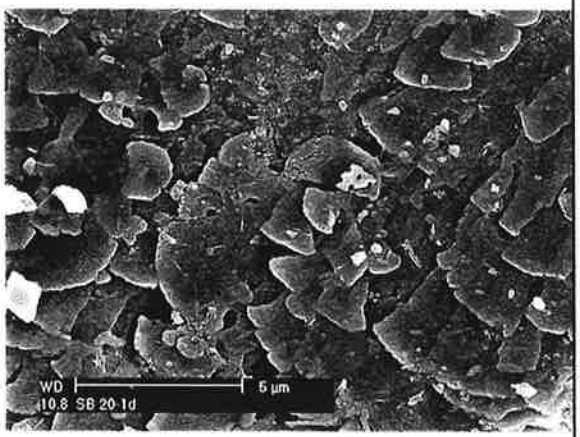



Figure 8.2d Detail showing the morphology of microplatelets resulting from the disintegration of *Ostrea* sp.
Scale bar 5 μm.

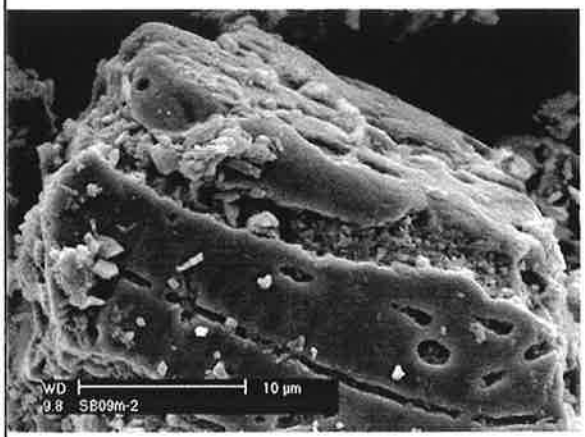



Figure 8.2e Blocky molluscan particle disintegrating through boring. Boreholes tend to be oriented with growth lines, which can be seen on the upper face .
Scale bar 10 μm.

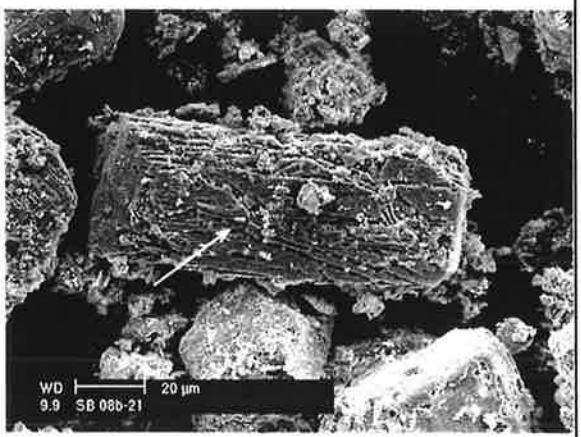



Figure 8.2f Abundant boring (arrowed) and laminar exfoliation of a prismatic molluscan particle.
Scale bar 20 μm.

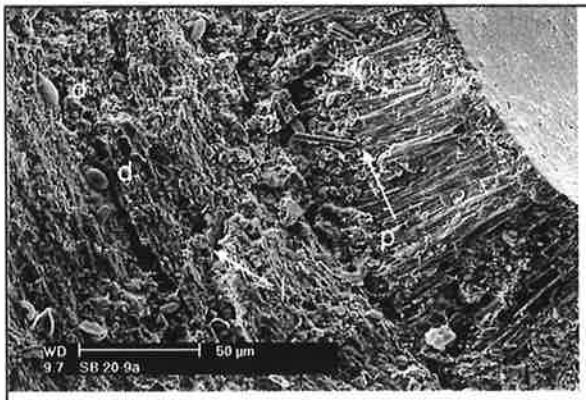



Figure 8.3a Production of layered(l) and elongate prismatic(p) particles in a disintegrating gastropod. Note proliferation of diatoms.
Scale bar 50 µm

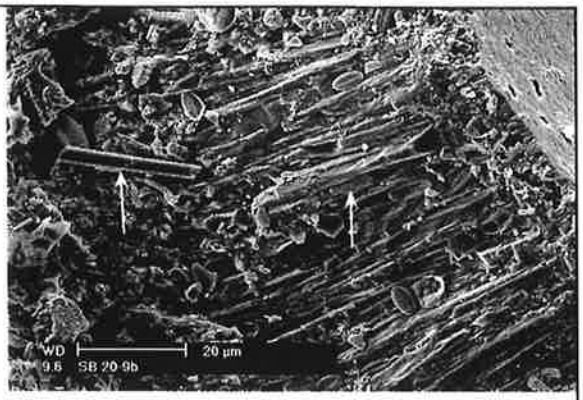



Figure 8.3b Detail of disintegration of the prismatic layer in some gastropods into elongate irregular needles (arrowed).
Scale bar 20 µm

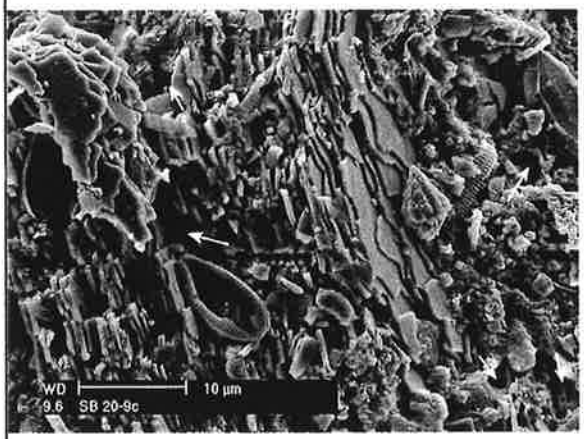



Figure 8.3c Detail of platelet production during gastropod disintegration. Microboring into the laminar layer (arrowed) accelerates degradation of interlamellar organic tissue.
Scale bar 10 µm.

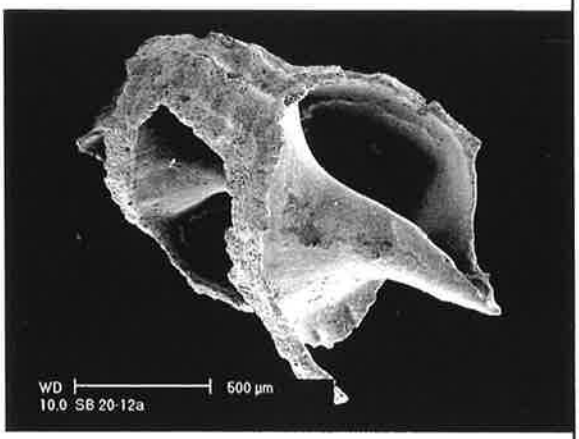



Figure 8.3d Disintegrating gastropod with a homogeneous shell microstructure.
Scale bar 500 µm.

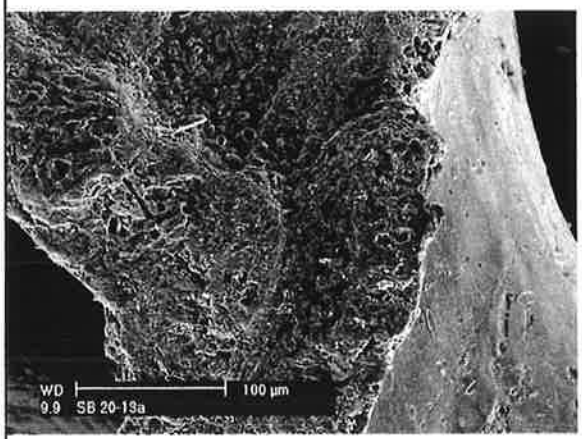



Figure 8.3e Detail of gastropod structure showing abundant microboring in a relatively homogeneous shell.
Scale bar 100 µm.

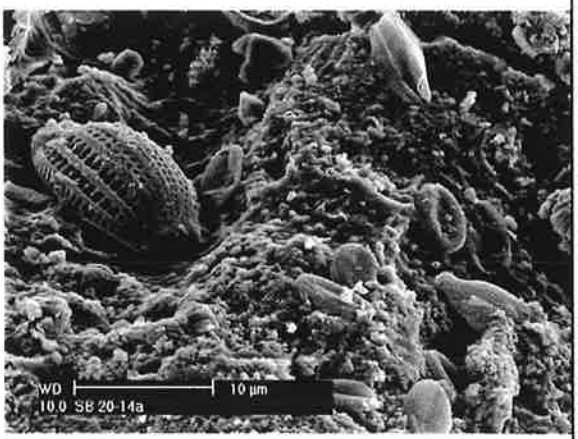



Figure 8.3f Detail of homogeneous gastropod shell structure, which breaks down to blocky particles. Note abundant diatoms.
Scale bar 10 µm.

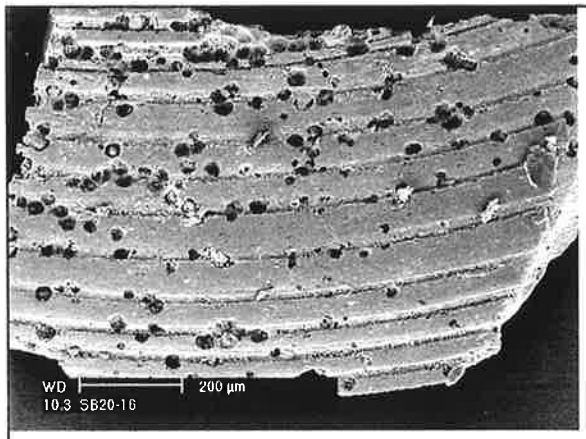



Figure 8.4a Fragment of the bivalve *Katelysia* sp. with basin shaped pitting between the growth ridges.
Scale bar 200 µm.

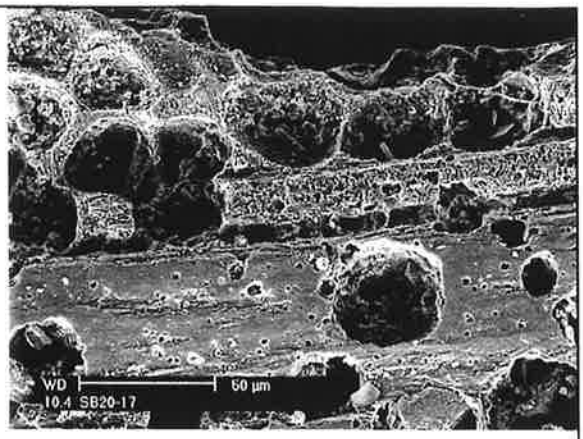



Figure 8.4b Detail of pitting and microboring in 8.4a, also active shell disintegration in the heavily pitted areas (upper portion of micrograph). Pits approximately 10 µm by 5 µm deep.
Scale bar 50 µm

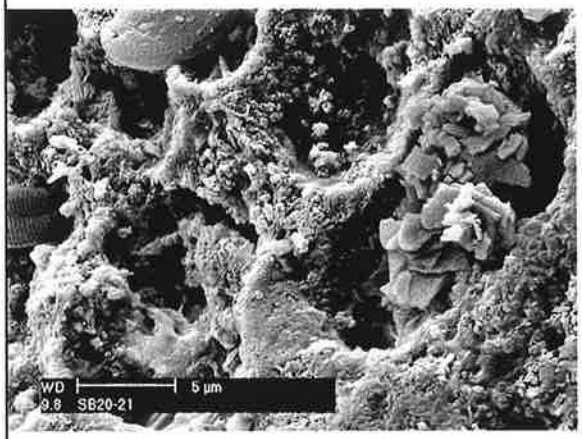



Figure 8.4c Detail of pitting, which becomes a receptacle for micron-sized particles and refuge for diatoms. Clionid sponges are probably responsible for this type of pitting.
Scale bar 5 µm

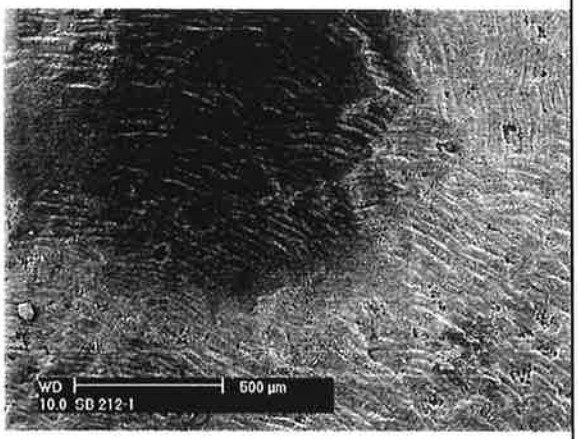



Figure 8.4d Example of grouped short scratches on the interior of bivalves, usually radiating away from the muscle scars. Scratches are attributable to gastropods rasping at the proteinaceous surface.
Scale bar 500 µm.




Figure 8.4e Disintegrating foraminifer, *Elphidium* sp., showing breakdown progression at the test margins and along the porous radial elements.
Scale bar 1 mm.

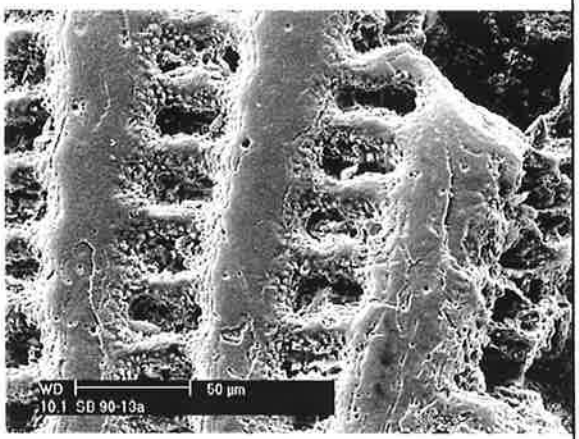



Figure 8.4f Detail of *Elphidium* sp. lamellar disintegration on the radial ridges.
Scale bar 50 µm.

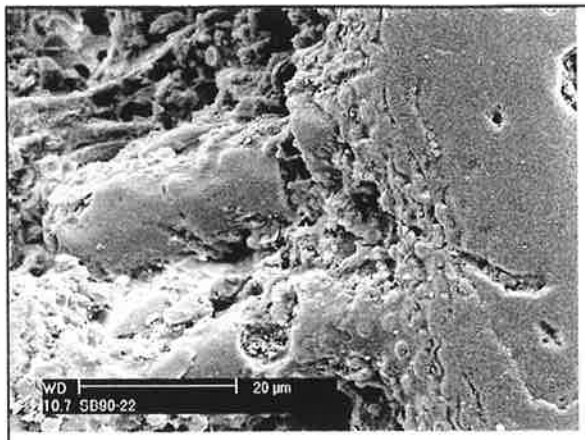
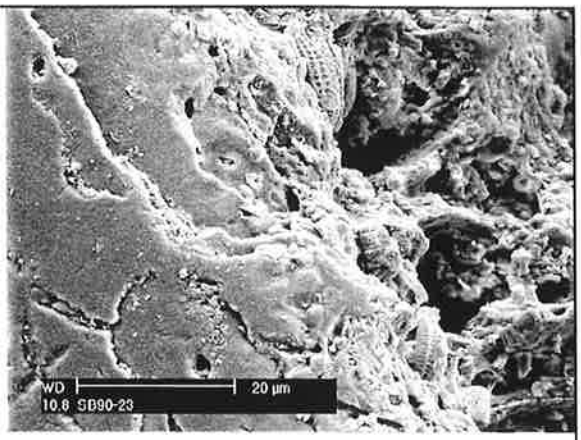



Figure 8.5a Detail of foraminifer, *Elphidium* sp., degrading by gradual exfoliation and limited microboring into µm-sized elongate particles. Scale bar 20 µm.




Figrue 8.5b Detail of *Elphidium* sp. degrading into subparallel layered particles 10- 20 µm. Scale bar 20 µm.

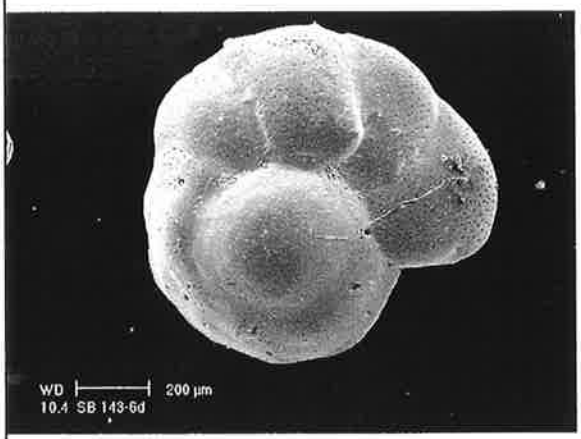



Figure 8.5c The foraminifer, *Discorbis* sp., showing limited signs of microboring around the periphery.
Scale bar 200 µm.

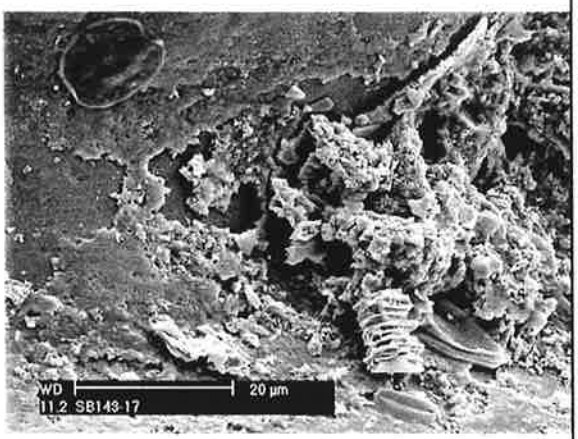



Figure 8.5d Detail of exfoliation on the test of *Discorbis* sp. resulting in µm size-particles. Scale bar 20 µm.

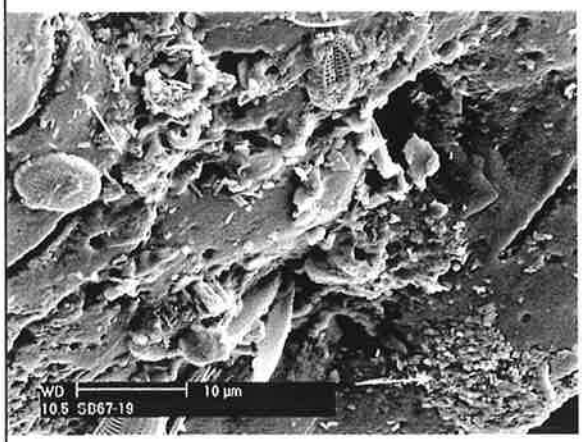



Figure 8.5e Detail of exfoliation on *Discorbis* sp. indicating further disintegration into sub-µm crystallites (arrowed).
Scale bar 10 µm.

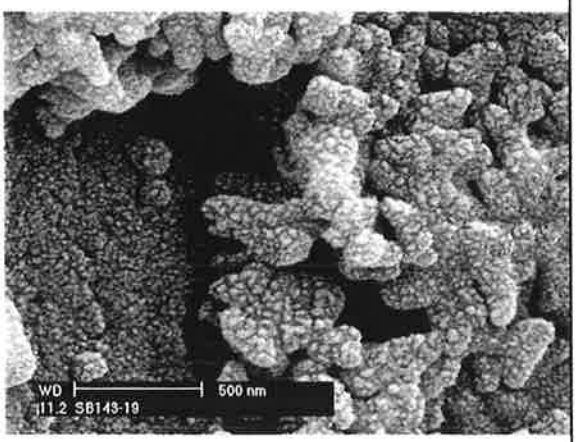



Figure 8.5f Detail of the exfoliation platelets of *Discorbis* sp. showing details of the sub-µm crystallites. (surface texture is attributed to coating artifacts).
Scale 500 nm.

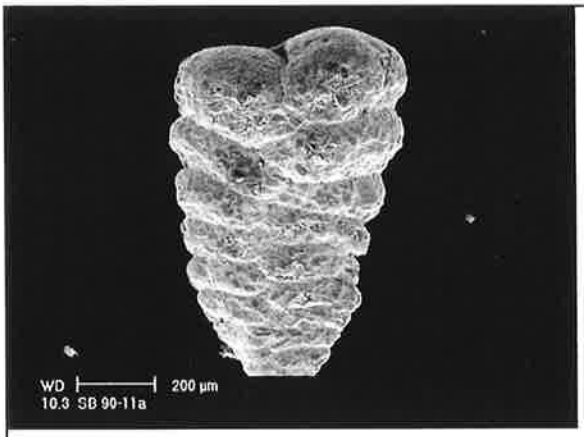



Figure 8.6a Agglutinated grains within the test of the foraminifer, *Cribrobulimina* sp., indicating minor microboring and possible dissolution.
Scale bar 200 µm.

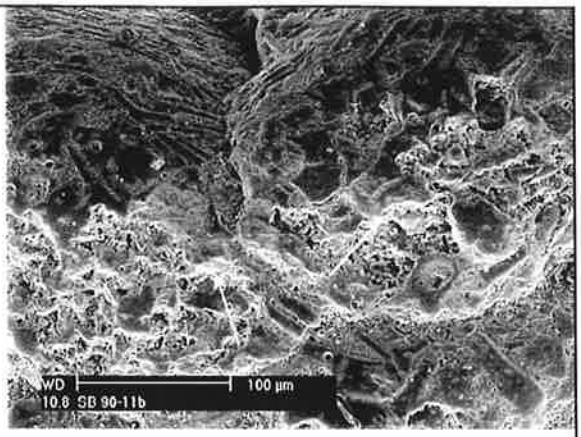



Figure 8.6 b Detail of *Cribrobulimina* sp. with possible dissolution of some agglutinated grains within the test. Possible dissolution of the cement (arrowed) is also indicated by the smooth surface texture.
Scale bar 100 µm.

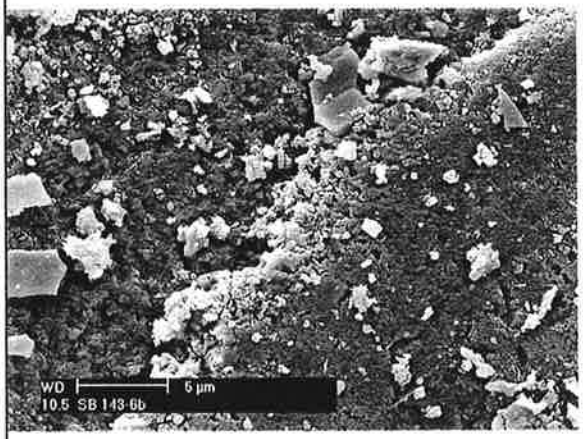



Figure 8.6c Leading edge of exfoliation on the foraminifer, *Discorbis* sp., test indicating a possible hackly dissolution surface texture as the layer is disintegrating into sub-µm crystallites.
Scale 5 µm.

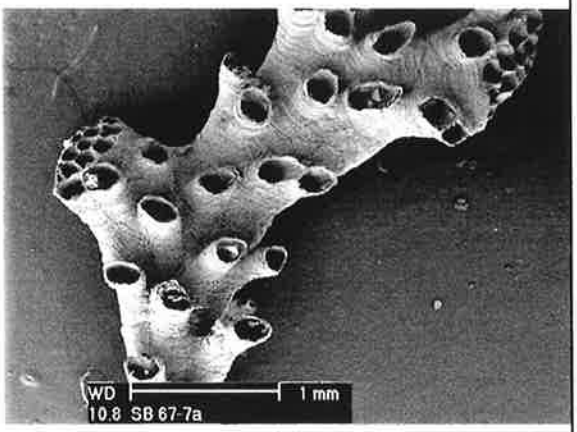



Figure 8.6d Nevianopora sp. highlighting general bryozoan cyclostome morphology.
Scale bar 1 mm.

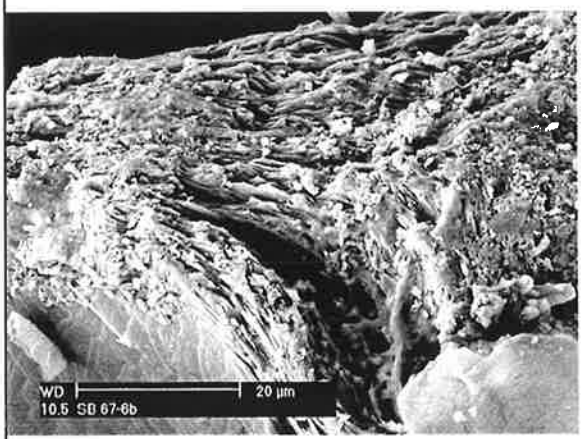



Figure 8.6e Layered morphology of platelets of the zooid aperture of *Nevianopora* sp., also showing imbricate structure of the platelets in the zooid wall (arrowed).
Scale bar 20 µm.

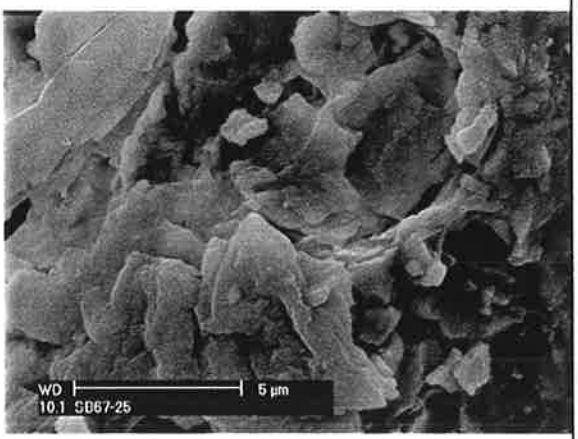



Figure 8.6f Detail of platelets in the zooid walls of *Nevianopora* sp., highlighting thin sub-µm curved to tabular platelets.
Scale bar 5 µm.

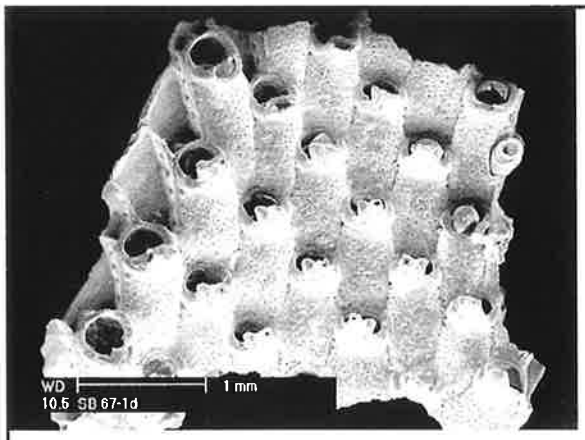



Figure 8.7a Encrusting cheilostome bryozoan, general structure, *Serripetraliella* sp.
Scale bar 1 mm.

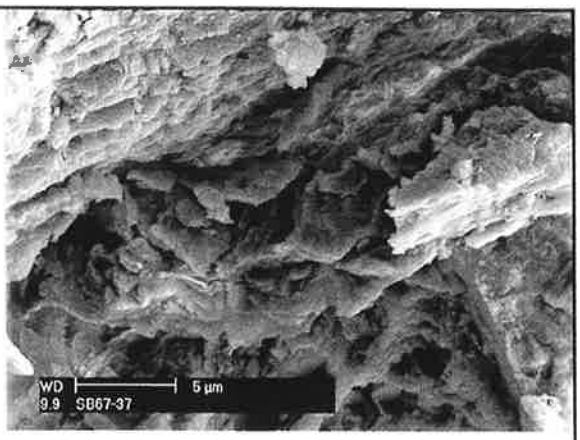



Figure 8.7b Detail of general cheilostome microstructure showing the production of µm to sub-µm irregular platelets during disintegration.
Scale bar 5 µm.

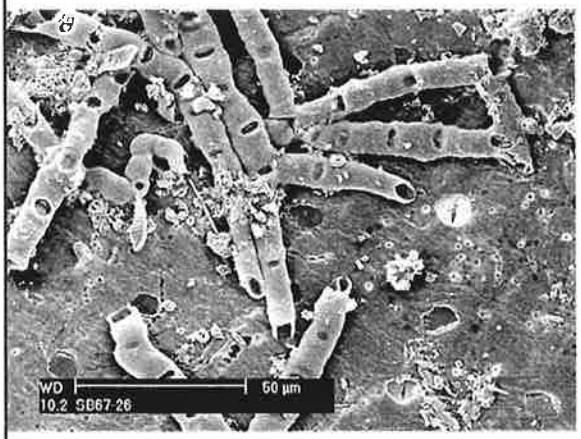



Figure 8.7c Encrusting cheilostome with delicate branching morphology on cyclostome (*Nevianopora* sp.)
Scale bar 50 µm.

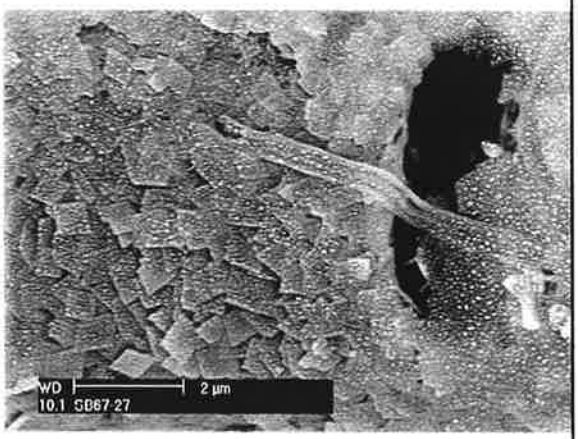



Figure 8.7d Detail of "runner" cheilostome showing the imbricate structure of the sub-µm platelets (coating artifacts present).
Scale bar 2 µm.

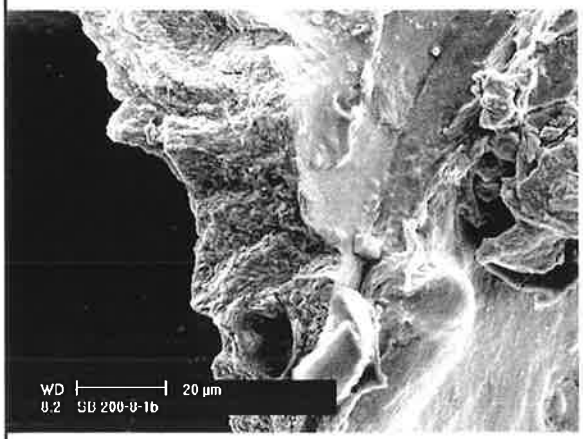



Figure 8.7e Basal and wall thickening lead ot a more robust microstructure i.e. Adeoniform, robust branching and encrusting bryozoans.
Scale bar 20 µm.

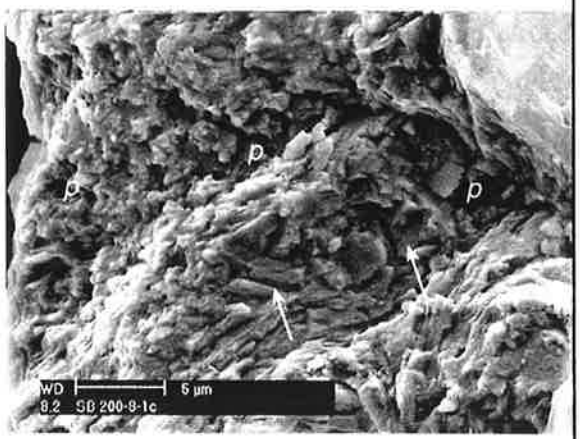



Figure 8.7f Detail of encrusting bryozoan *Ostimosia* sp. highlighting the production of elongate rhombic particles in the zooecial walls and the development of porosity with continued maceration (p).
Scale bar 5 µm.

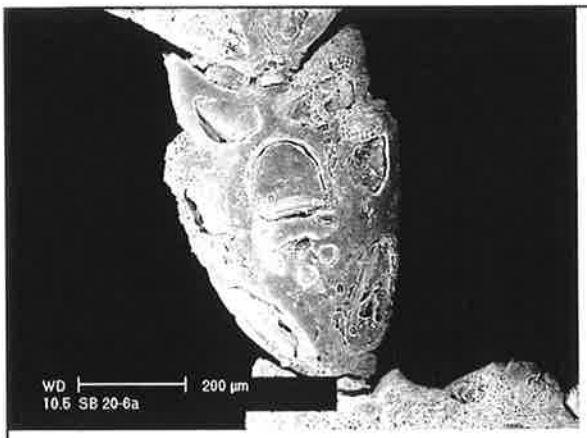



Figure 8.8a Microboring and probable dissolution are the significant disintegration pathways for this articulated bryozoan (*Othoscuticella* sp.).
Scale bar 200 µm.




Figure 8.8b Detail of microboring (arrowed) in *Othoscuticella* sp. Possible dissolution textures are highlighted by rounding of the pathways of microboring 'd'.
Scale bar 50 µm.




Figure 8.8c Detail of micoboring and possible dissolution at the thin exposed edges (arrowed) (*Othoscuticella* sp.).
Scale bar 20 µm.

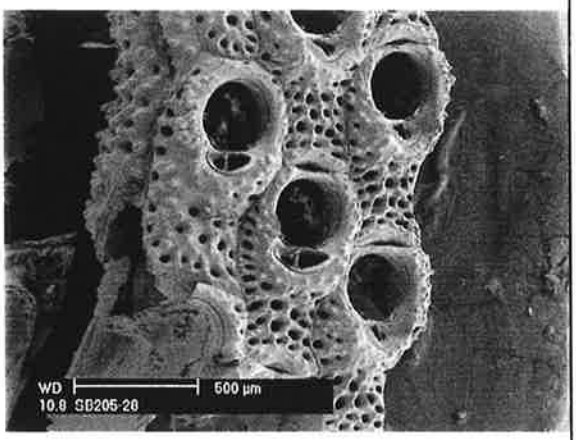



Figure 8.8d The bryozoan *Petralia* sp. is composed of a dense equi-granular skeletal structure.
Scale bar 50 µm.

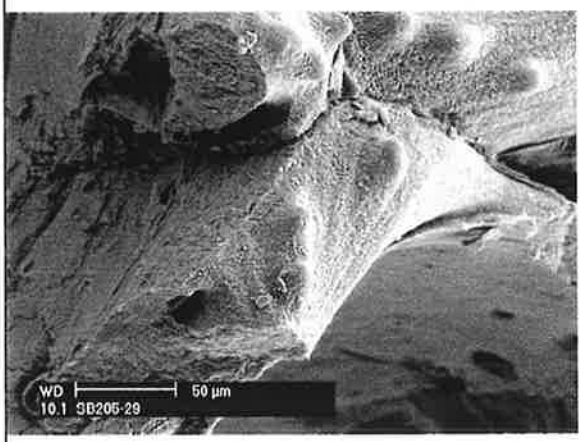



Figure 8.8e Detail of the dense equi-granular structure of *Petralia* sp.
Scale bar 50 µm.

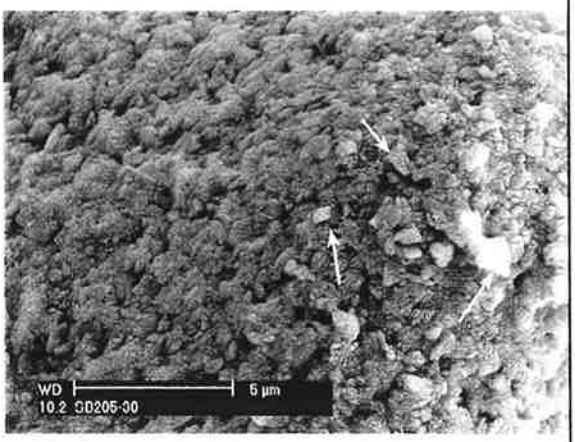



Figure 8.8f Detail of 8.8e highlighting the dense structure of the zooid wall showing randomly oriented blocky particles with occasional rhombic particles exposed at the surface.
Scale bar 5 µm.

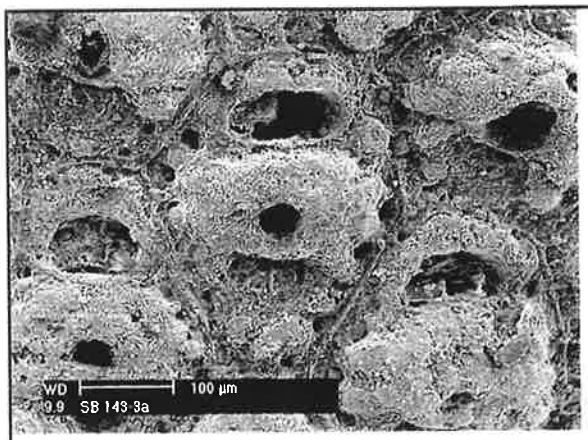



Figure 8.9a Encrusting bryozoan showing disintegration through microboring and possible dissolution.
Scale bar 100 µm.

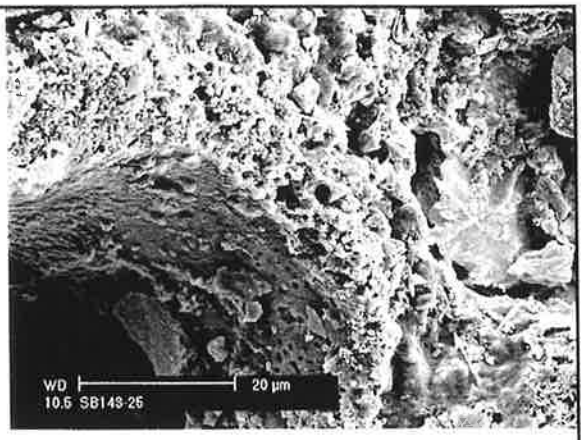



Figure 8.9b Detail of abundant microboring and possible granular dissolution texture at the mouth of the zooecium of the bryozoan in 8.9a
Scale bar 20 µm.

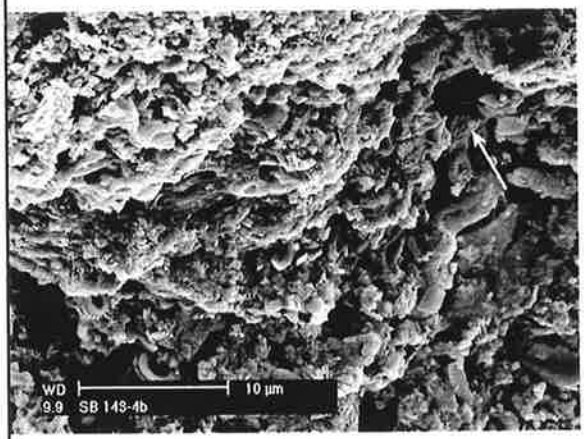



Figure 8.9c Detail of possible granular textured dissolution (maceration) surface with microboring present. The disintegration of this bryozoan produces sub-rhombic and sub-µm particles.
Scale bar 10 µm.

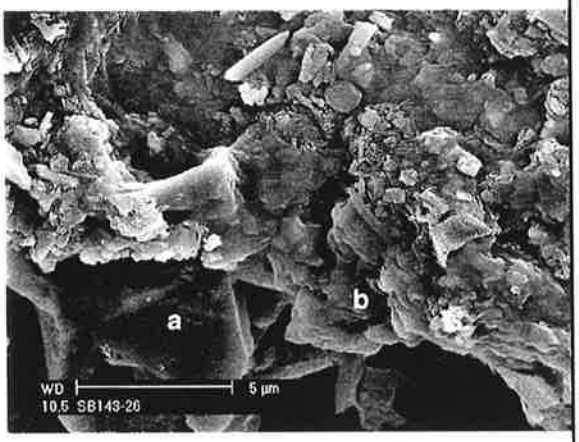



Figure 8.9d Detail of sub-rhombic particles (a) and irregular thin platelets (b) produced by encrusting bryozoans.
Scale bar 5 µm.

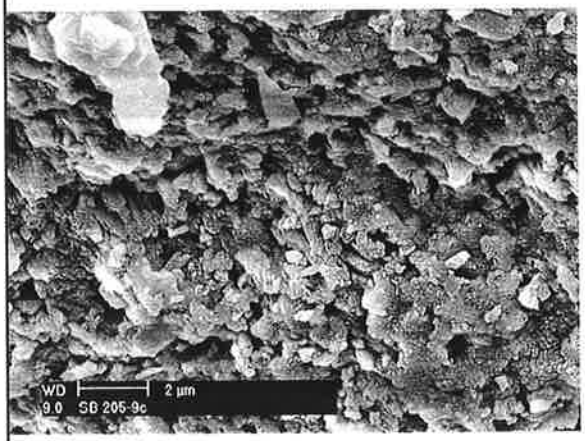



Figure 8.9e Detail of the zooecial wall of the bryozoan *Petralia* sp. showing microboring, possible dissolution and limited exfoliation as active agents of disintegration.
Scale bar 2 µm.

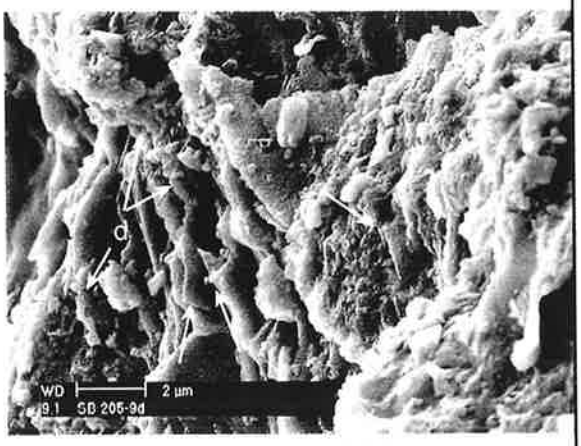



Figure 8.9f Detail of 8.9e highlighting stacked layer platelets showing etched embayments similar to dissolution patterns (d), sub-rhombic morphology of some particles are indicated (arrowed).
Scale bar 2 µm.

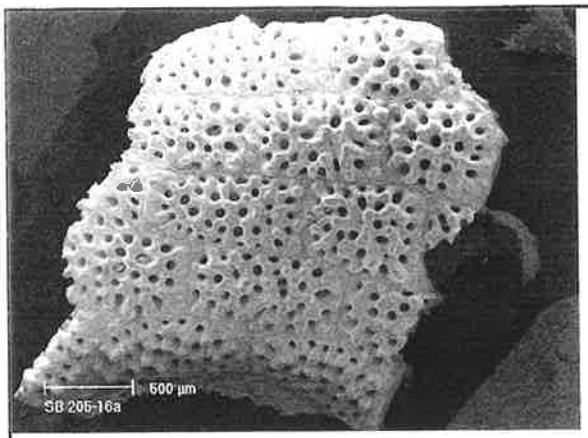



Figure 8.10a Basal plate of a foliose bryozoan indicating degradation at the zooecial boundaries.
Scale bar 500 µm.

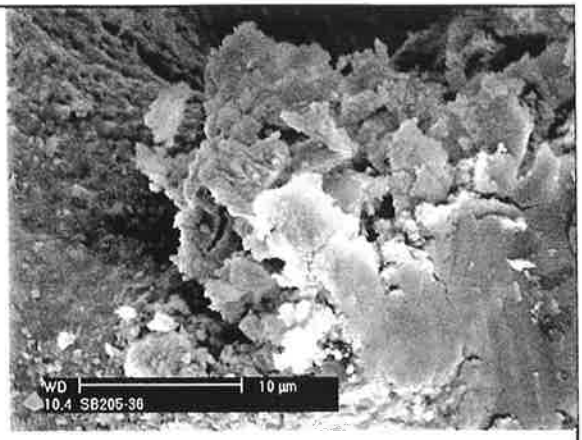



Figure 8.10b Detail of artificial maceration produced by a sharp probe on the bryozoan 8.10a. This highlights the probable effects of rasping and boring organisms in producing sub-µm bryozoan particles.
Scale bar 10 µm.

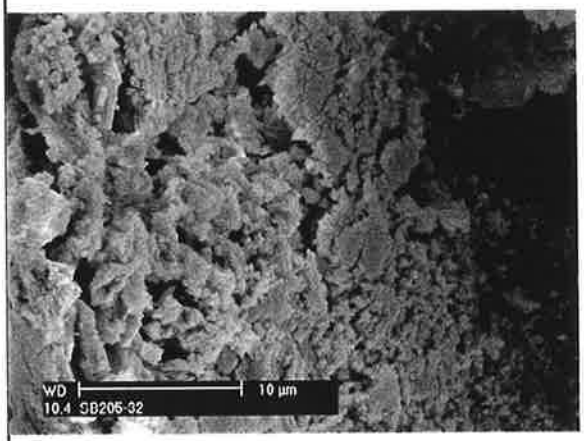



Figure 8.10c Detail of bryozoan, 8.10a, highlighting possible dissolution fabric producing µm to sub-µm particles and porous textures.
Scale bar 10 µm.

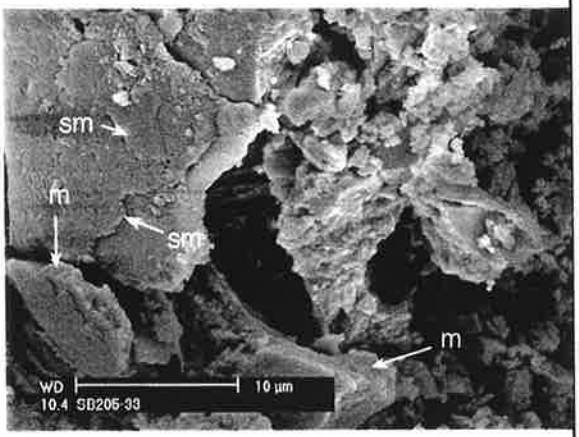



Figure 8.10d Flaking of layered particles is common at the zooecial boundary, both µm (m) and µm (sm) size on the bryozoan 8.10a.
Scale bar 10 µm.

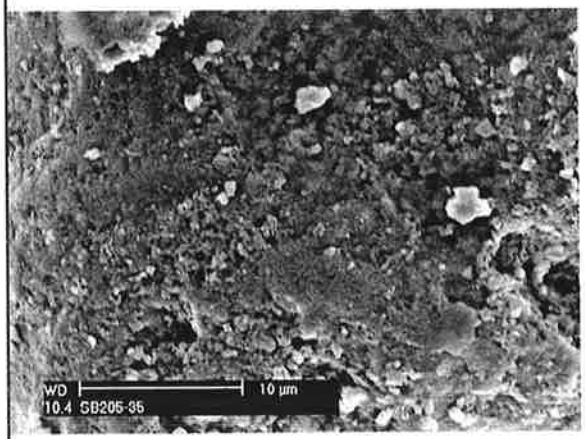



Figure 8.10e Detail of flaking on skeletal ridge of the base plates where exfoliation is occurring and producing sub-µm to µm particles on the bryozoan of 8.10a.
Scale bar 10 µm.

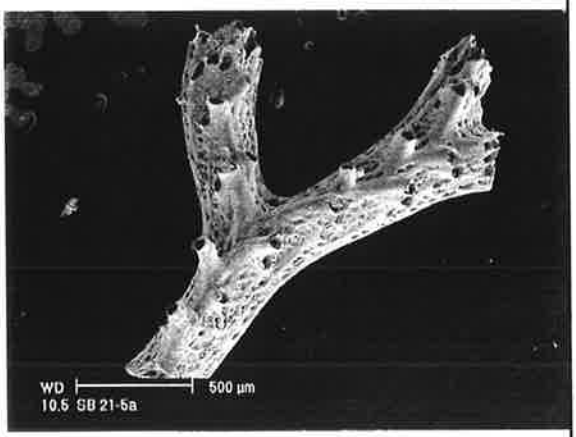



Figure 8.10f Delicate branching cyclostome bryozoan, *Mesonea* sp., is composed of sub-rhombic imbricate platelets.
Scale bar 500 µm.

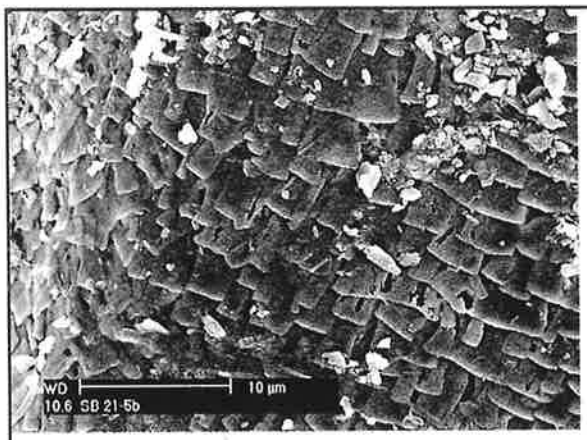



Figure 8.11a Detail of sub-rhombic imbricate platelets of the bryozoan (*Mesonea* sp.), indicating possible production of ~ 5 µm platelets on disintegration.
Scale bar 10 µm.

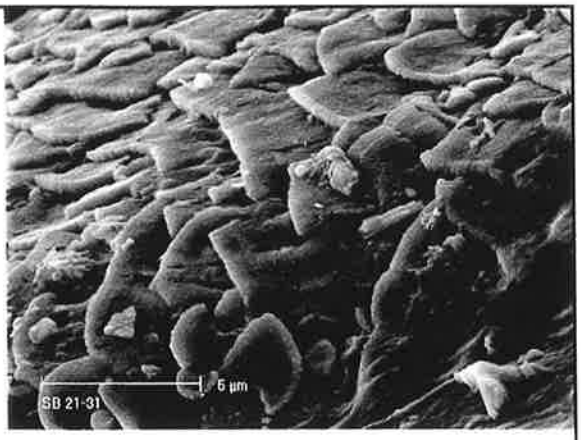



Figure 8.11b Detail (8.11a) of imbricate structure, highlighting an undulose sub-rhombic laminar morphology (*Mesonea* sp.).
Scale bar 5 µm

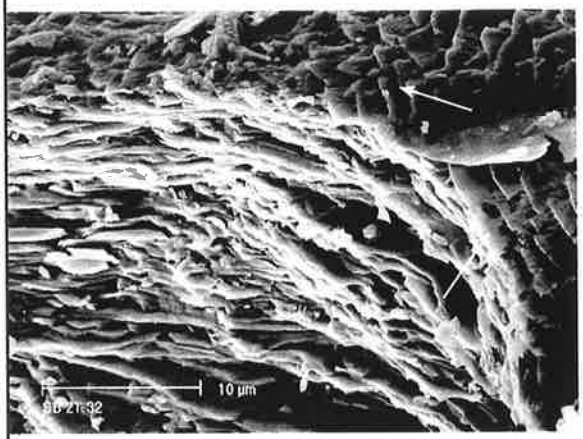



Figure 8.11c Detail of cyclostome structure showing more pronounced rhombic platelet morphology (arrowed) than cheilostomes.
Scale bar 10 µm.

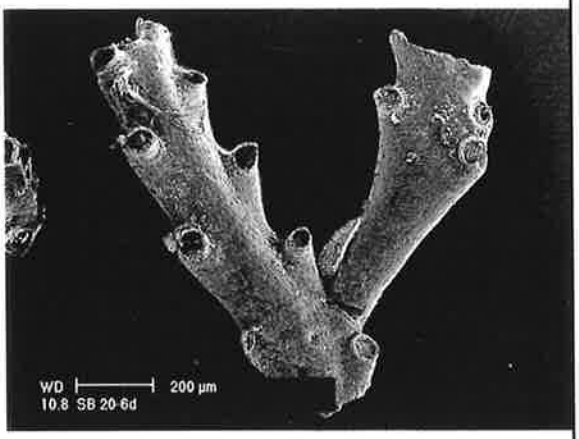



Figure 8.11d Pronounced platelet layering at the orifice is evident in the cyclosstome bryozoan, *Crisia* sp.
Scale bar 200 µm.

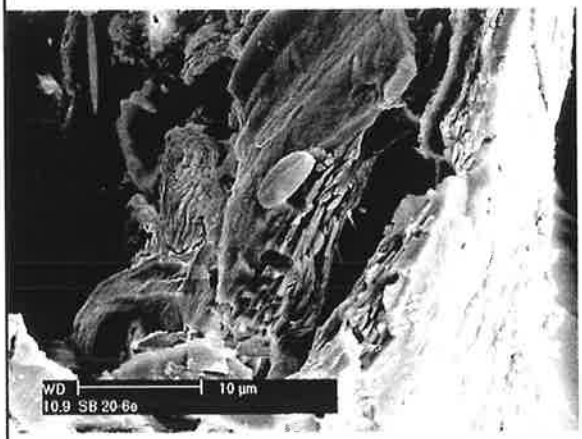



Figure 8.11e Detail of *Crisia* sp. structure highlighting layering at the orifice, that on disintegration will produce < 5 µm particles.
Scale bar 10 µm.

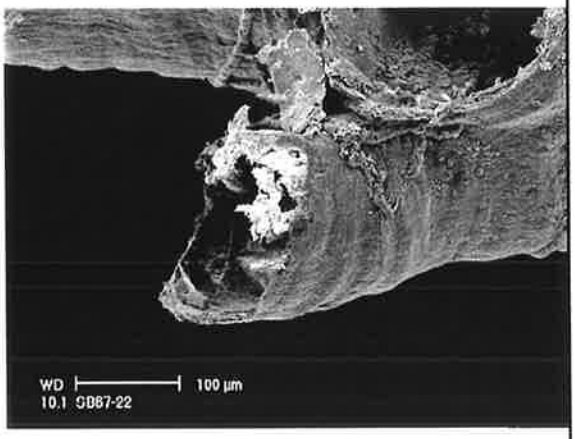



Figure 8.11f Orifice of *Nevianopora* sp. showing commencement of disintegration and particle production.
Scale bar 100 µm.

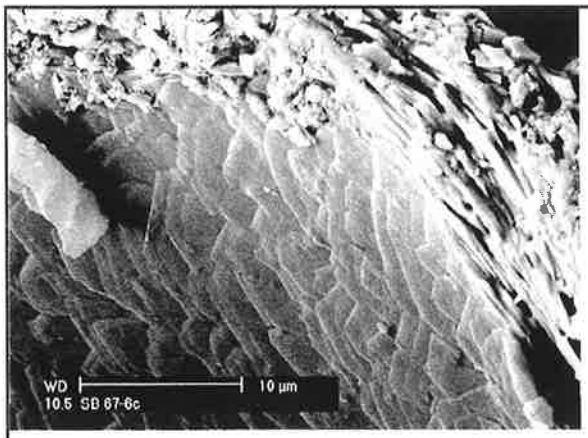



Figure 8.12a Detail of *Nevianopora* sp. orifice highlighting layered and sub-rhombic structure of the platelets. Disintegration produces particles < 5 µm.
Scale bar 10 µm.

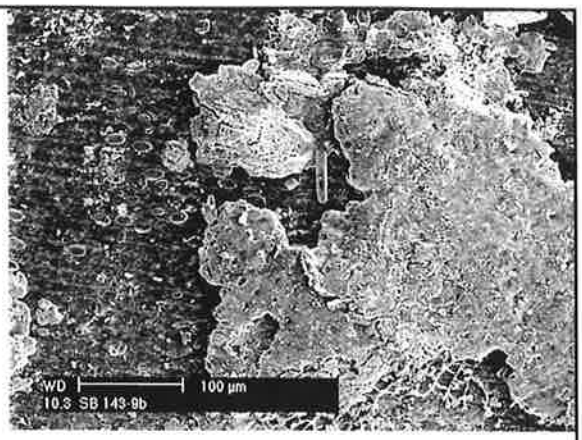



Figure 8.12b Overlapping crustose coralline algae on seagrass highlighting > 50 µm scale flaky nature.
Scale bar 100 µm.

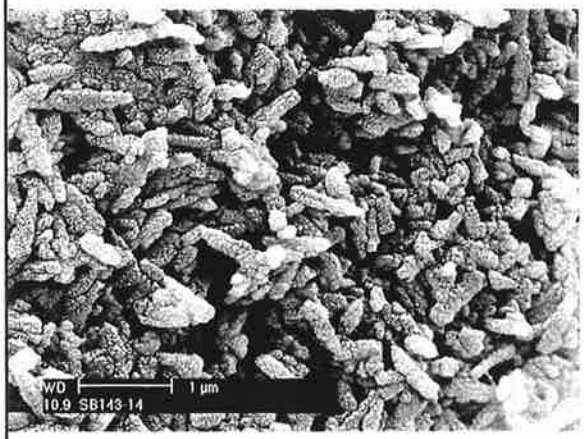



Figure 8.12c Detail of crustose coralline algae showing disintegration of cell wall and release of tapered sub-µm crystallites.
Scale bar 1 µm.

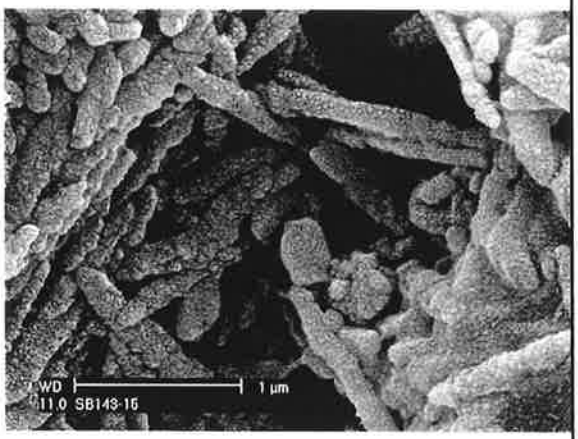



Figure 8.12d Detail of crystallites produced by crustose coralline algae.
Scale bar 1 µm.

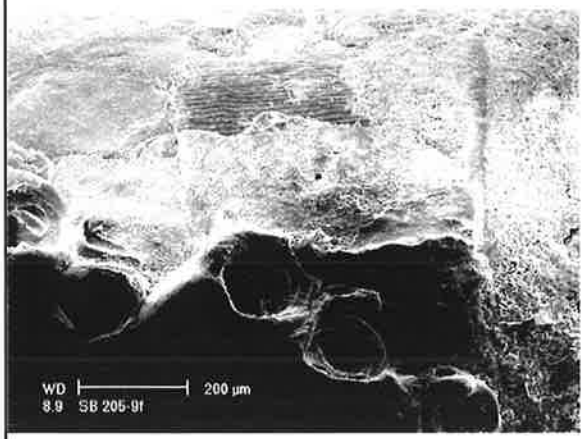



Figure 8.12e Thick crustose coralline algae solid substrate incorporates a rigid multi-layered cell structure.
Scale bar 10 µm.

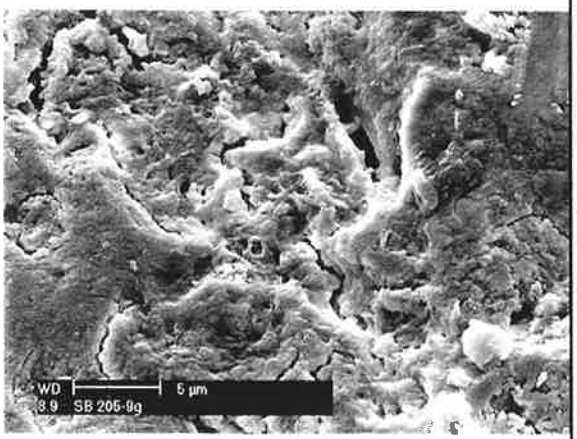



Figure 8.12f Detail of thick crustose coralline algae showing little intrinsic morphology, mostly irregular platey particles.
Scale bar 5 µm.




Figure 8.13a Thick crustose coralline algae similar to Figure 8.12e, on an echinoid spine. Scale bar 100 μm.

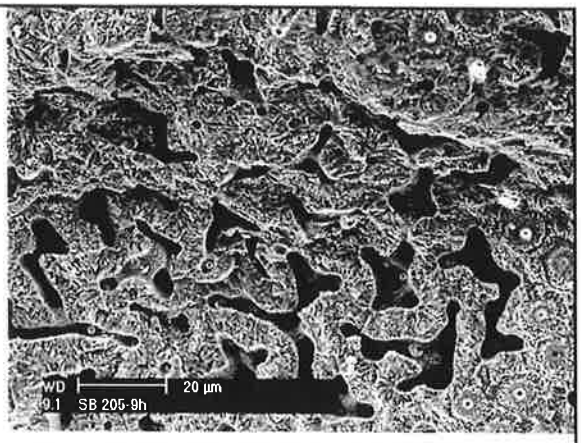



Figure 8.13b The thickened cell walls of rhodoliths provide structural rigidity in for high energy conditions.
Scale bar 20 μm.

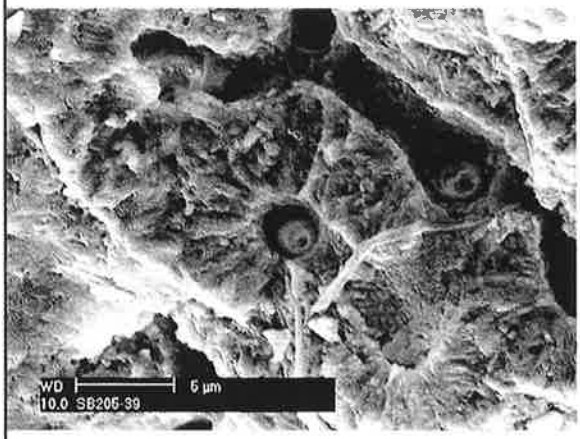



Figure 8.13c Detail of thickened rhodolith cell wall, showing dense structure and perpendicular orientation of crystallites.
Scale bar 5 μm.

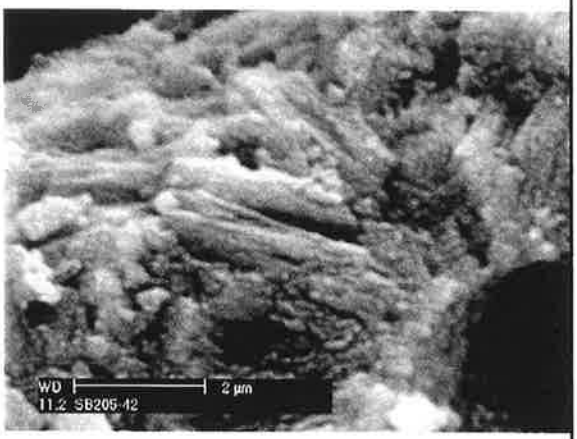



Figure 8.13d Detail of perpendicularly oriented crystallites in the cell walls of rhodoliths. There is a potential for a disintegrating rhodolith to produce micron sized elongate particles.
Scale bar 2 μm.

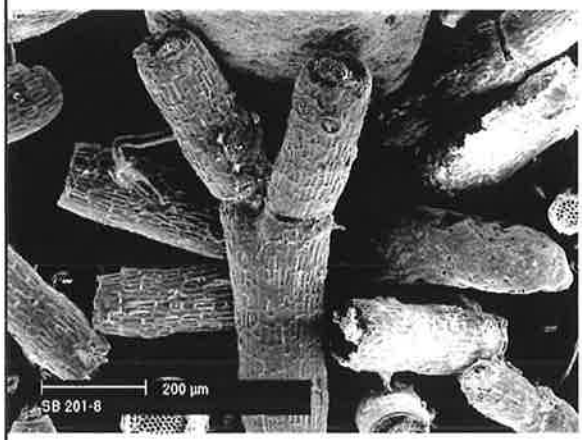



Figure 8.13e Articulated coralline algae showing primary breakdown into 200- 500 μm segments
Scale bar 200 μm.

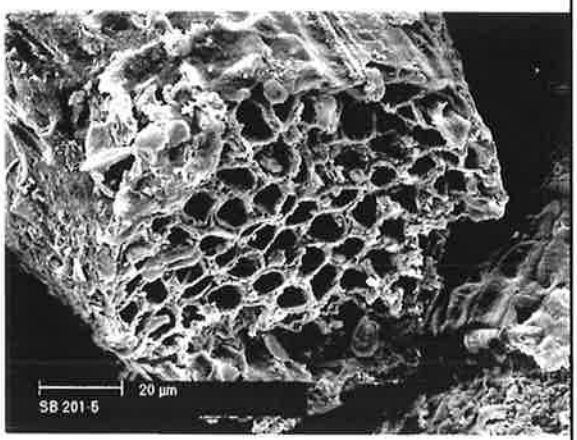



Figure 8.13f Detail of an end section of articulated coralline algae, showing honeycomb structure.
Scale bar 20 μm.

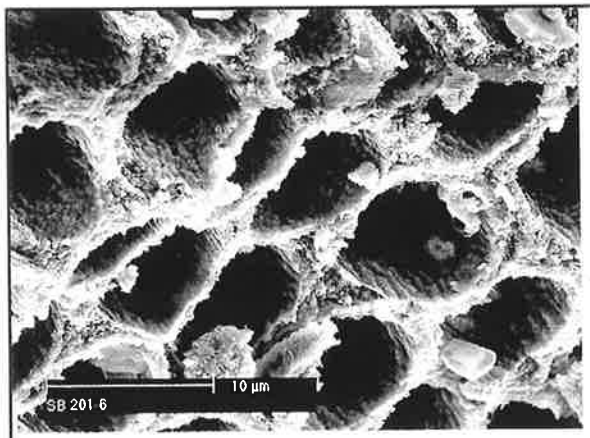



Figure 8.14a Detail, cross section of articulated coralline algae. Light areas are loci of disintegration and particle production.
Scale bar 10 µm.

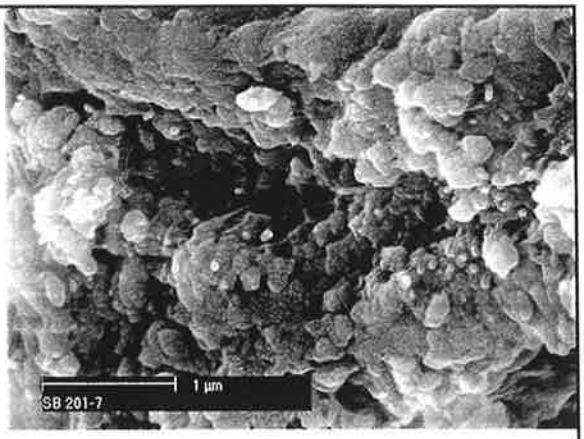



Figure 8.14b Detail of cell wall structure of articulated coralline algae indicating a structure of short ellipsoidal and granular particles (articulated coralline algae).
Scale bar 1 µm.

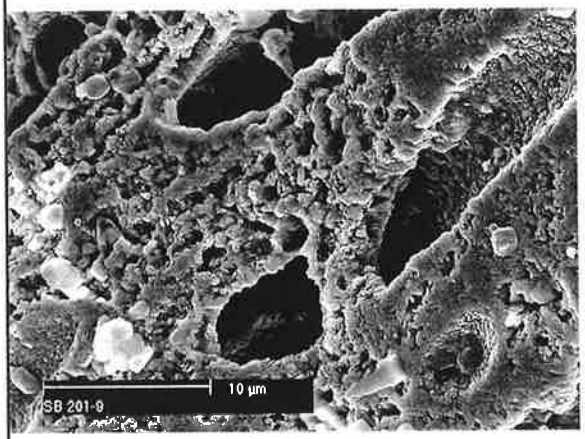



Figure 8.14c Oblique section of articulatedcoralline algae showing pore structure within the cell walls and potential particle production.
Scale bar 10 µm.

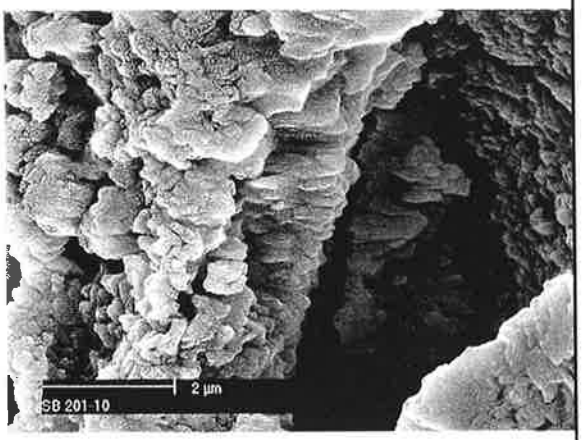



Figure 8.14d Detail of articulated coralline algae highlighting cell wall with outer perpendicularly oriented crystallites and internal granular particles.
Scale bar 2 µm.

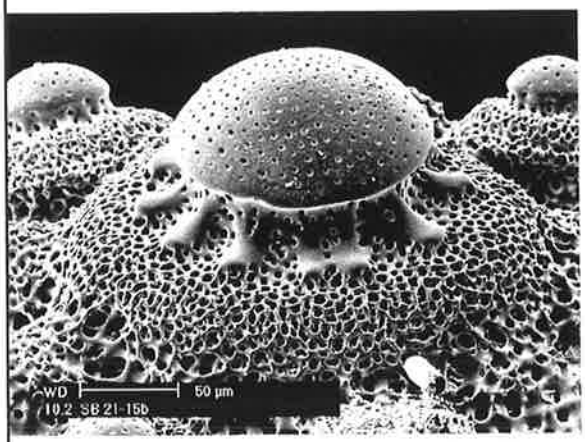



Figure 8.14e Detail of a regular echinoid stereom highlighting the open structural framework.
Scale bar 50 µm.

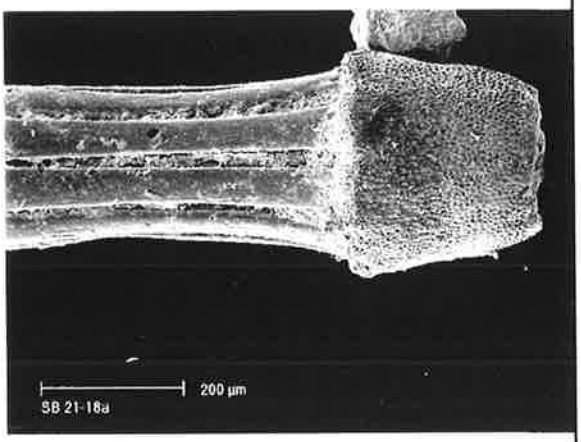



Figure 8.14f Echinoid spine showing the porous attachment area and the relativly dense portion of the spine away from the articulating area.
Scale bar 200 µm.

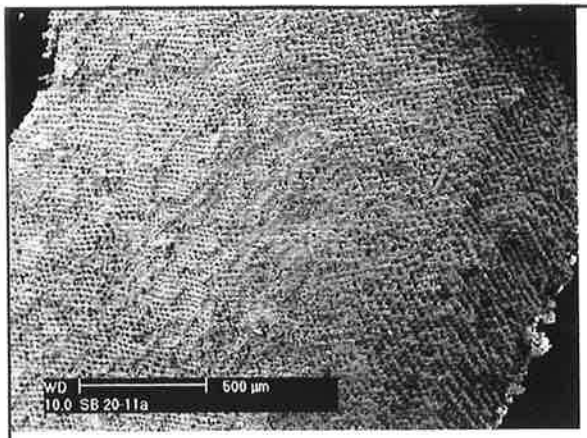



Figure 8.15a Fragment of disintegrating echinoid plate highlighting the regular nature of the open porosity.
Scale bar 500 µm.

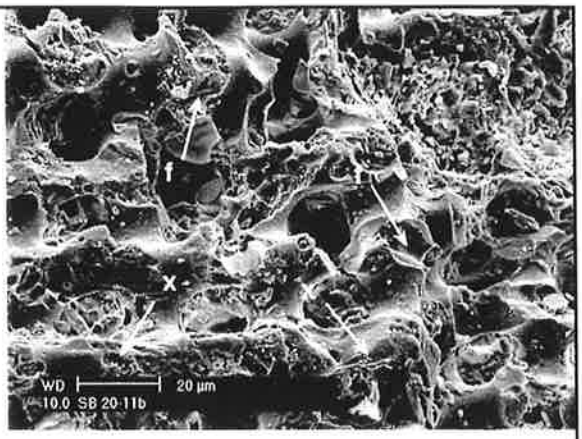



Figure 8.15b Detail of echinoid fragment showing brittle fracturing at the suface (x), which produces irregular dense particles. Some exfoliation is evident (x).
Scale bar 20 µm.

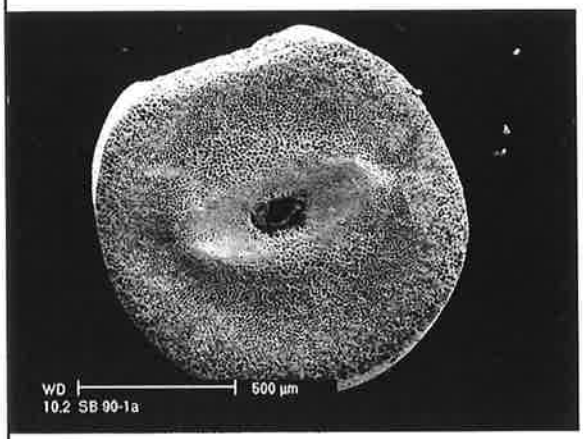



Figure 8.15c Open porous nature of ophiuroid ossicles. Distintegration is occurring on the rim and outer disc region.
Scale bar 500 µm.

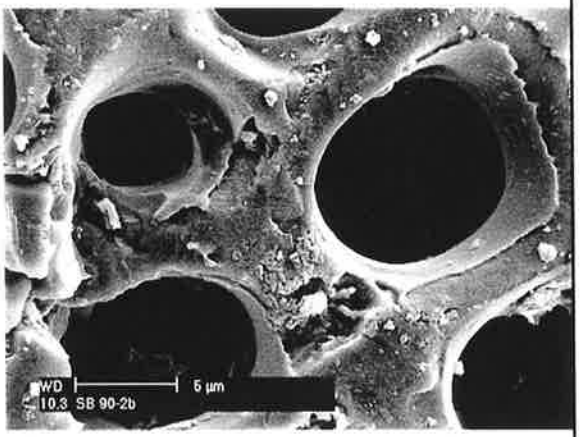



Figure 8.15d Detail of ophiuroid ossicle disintegration highlighting exfoliation of the outer protective layer and exposing the inner skeleton which is producing rhombic particles.
Scale bar 5 µm.

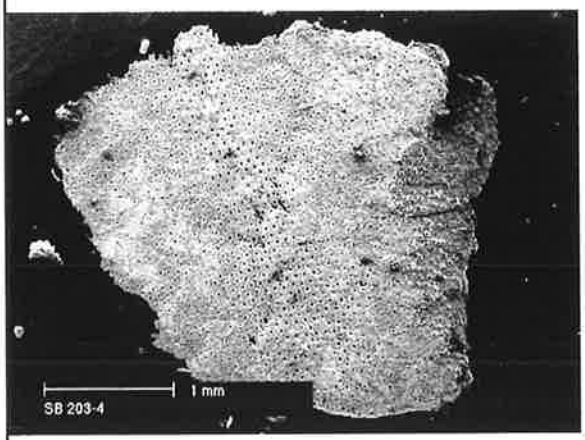



Figure 8.15e Punctate brachiopod fragment, highlighlighting the regular array of punctae and the irregular disintegration edge.
Scale bar 1 mm.

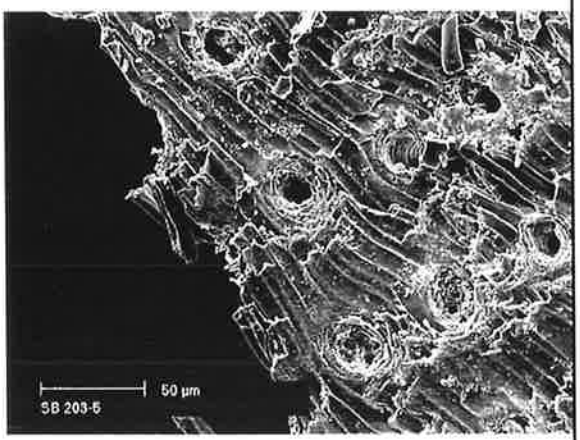



Figure 8.15f Detail of brachiopod fragment showing punctae and breakdown fracture patterns of the valve, producing elongate tabular particles

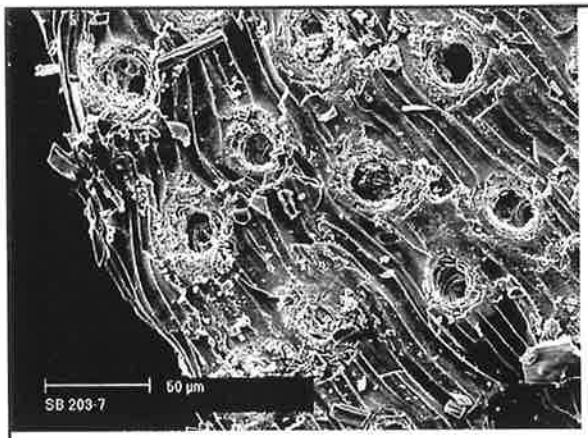



Figure 8.16a Detail of brachiopod fragment showing distribution of punctae and the curved elongate particles, which are produced during disintegration.
Scale bar 50 µm.

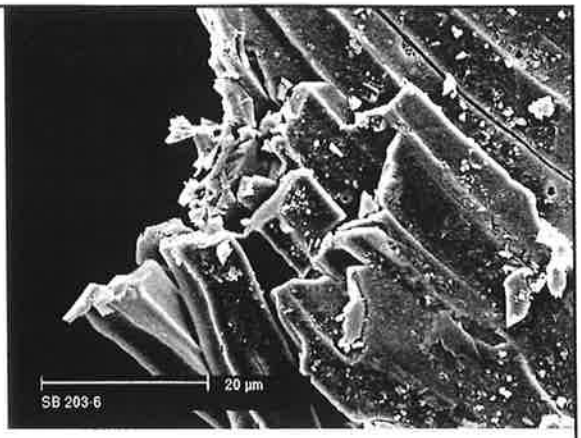



Figure 8.16b Detail of brachiopod fragment showing oblique cross sections of the elongate particles
Scale bar 20 µm.

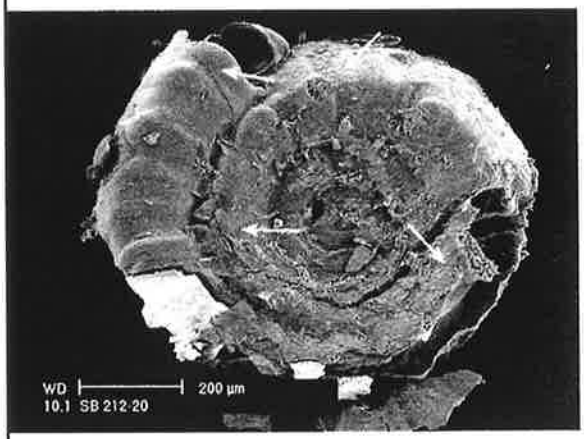



Figure 8.16c Disintegrating spirorbid with crustose coralline (arrowed) covering part of the shell.
Scale bar 200 µm.

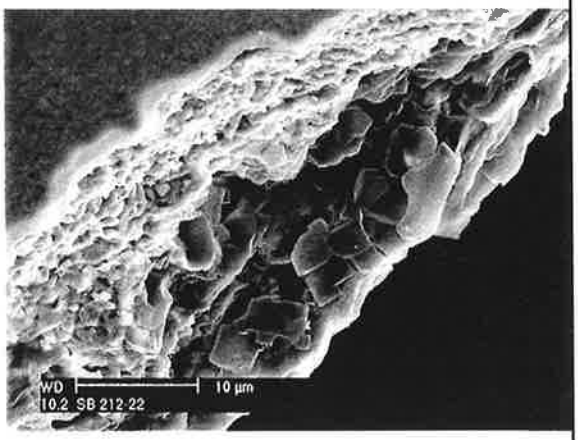



Figure 8.16d Detail of spirorbid breakdown producing sub-µm plates from the inner layer and ~4 µm rhombic plates from the outer layer.
Scale bar 10 µm.

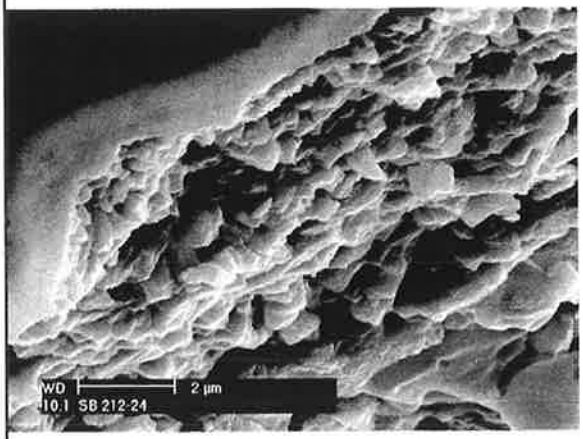



Figure 8.16e Detail of spirorbid inner layer and potential irregular platey particles.
Scale bar 2 µm.

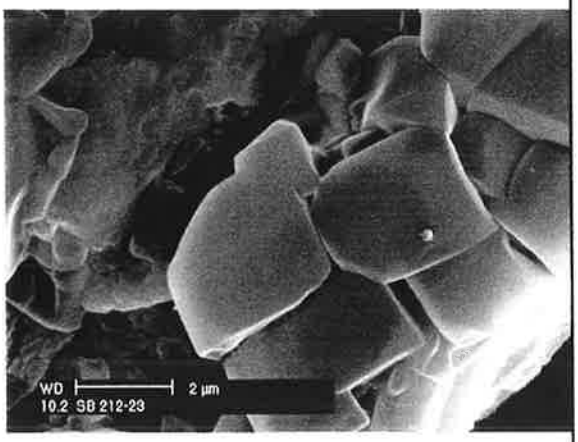



Figure 8.16f Detail of spirorbid outer layer and potential rhombic platelets.
Scale 2 µm.

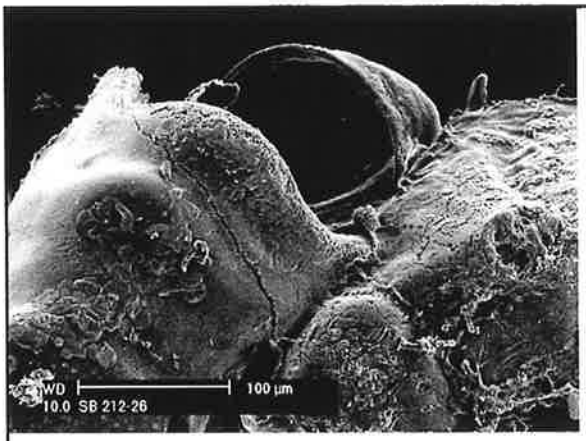



Figure 8.17a Detail of spirorbid with surficial crustose coralline algae. from a *Posidonia* sp. leaf on the sand shoals.
Scale bar 100 µm.

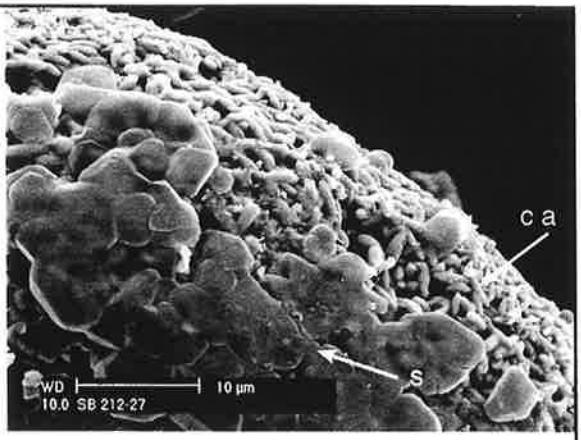



Figure 8.17b Detail of an intercalated crustose coralline algae (ca) in the outer ornamental layer of a spirorbid (s).
Scale bar 10 µm.

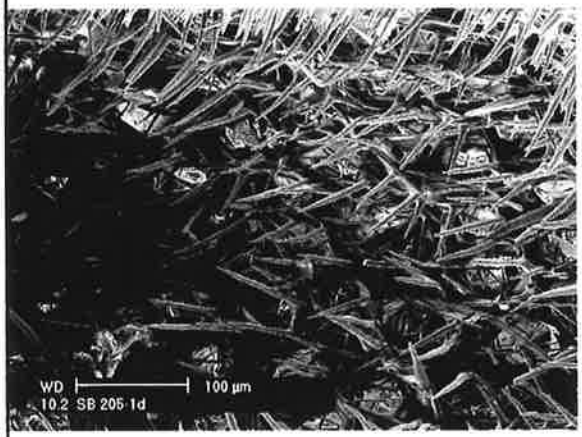



Figure 8.17c Calcareous triaxon spicules in the sponge, *Sycon gelatinosum*, internal array.
Scale bar 100 µm.

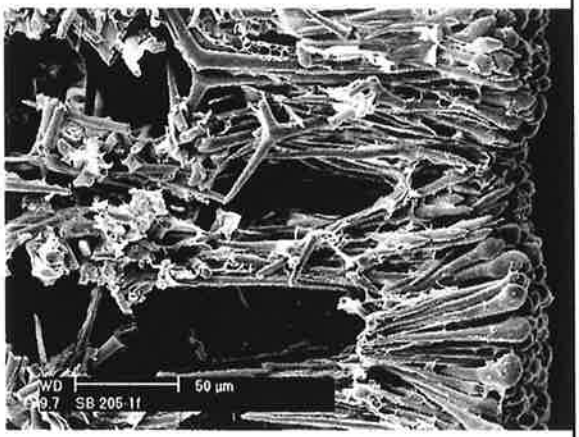



Figure 8.17d Detail of monaxon and triaxon spicules, and radial canals in a cross section of the epidermal area of the sponge in 8.17c
Scale bar 50 µm.

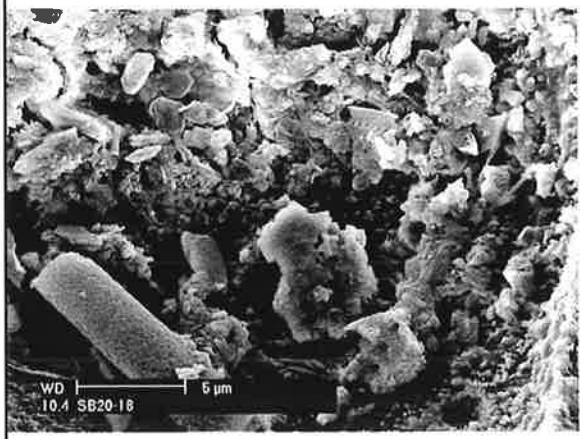



Figure 8.17e Detail of scalloped pit attributed to a boring *Clionid* sponge. The pit becomes a repository for degraded sub-µm particles of molluscs, bryozoans, coralline algae, and diatoms.
Scale bar 5 µm.




Figure 8.17f Detail of tunicate spicule showing signs of degradation and particle production.
Scale bar 10 µm.

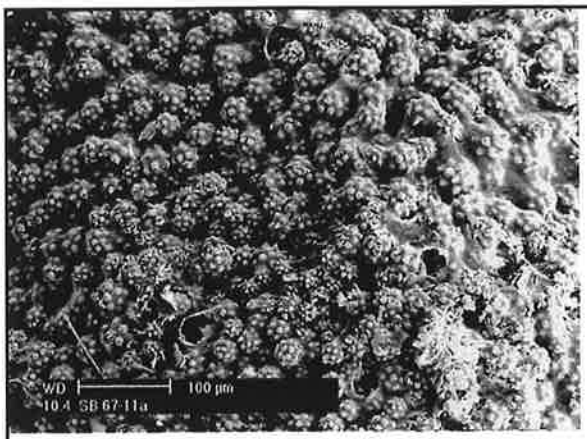



Figure 8.18a Preserved section of a tunicate body (*Tridemnum* sp.) showing spicule density.
Scale bar 100 µm.

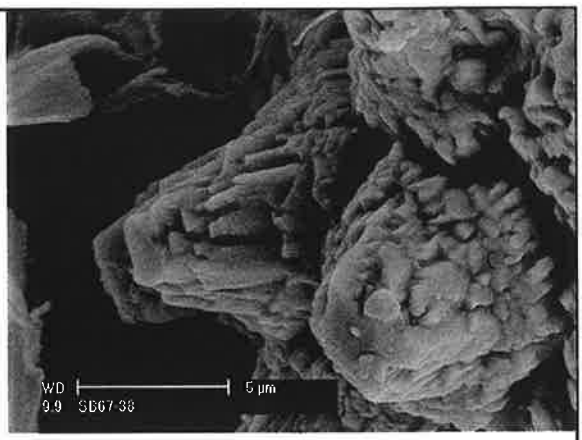



Figure 8.18b Detail of a tunicate spicule showing the production of µm-sized aragonite prisms as the spicule degrades.
Scale bar 5 µm.

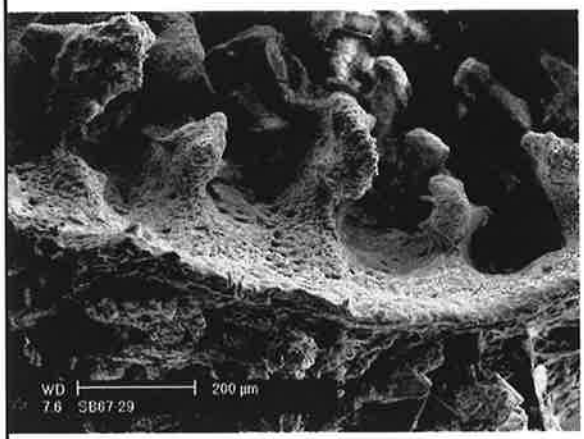



Figure 8.18c Corallite wall detail (*Culicia* sp.) highlighting sub-parallel layering in the corallite wall and densely structured septal ridges. (Coral, *Culicia* sp.)
Scale bar 200 µm.

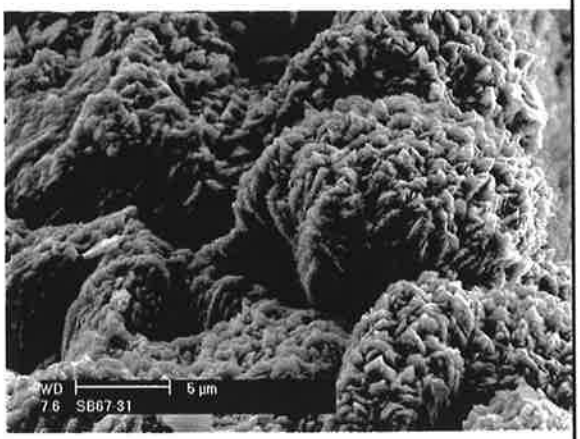



Figure 8.18d Potential sub-rhombic tabular µm-sized particles on a macerating corallite septal ridge.(Coral, *Culicia* sp.)
Scale bar 5 µm.

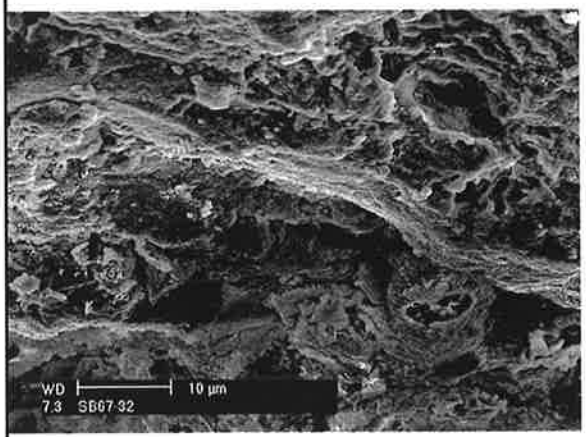



Figure 8.18e Detail of corallite wall with sub-parallel layering and resultant irrregular platelet production with disintegration. (Coral, *Culicia* sp.)
Scale bar 10 µm.

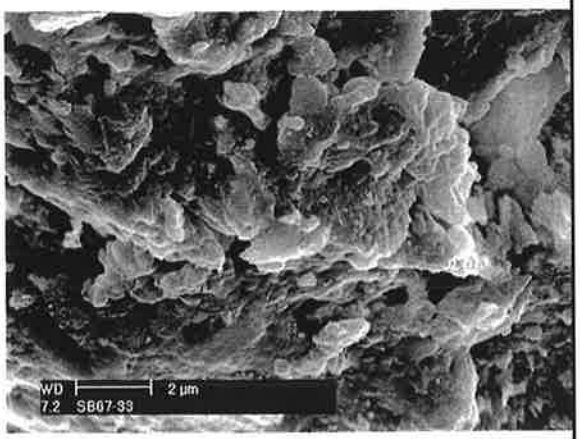



Figure 8.18f Detail of corallite wall highlighting teh production of irregular platelets and polygons. (Coral, *Culicia* sp.)
Scale bar 2 µm.

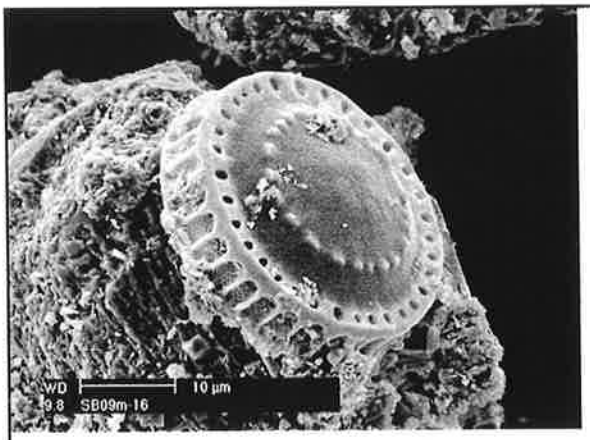



Figure 8.19a Centric diatom, *Thalassosira* sp. adhering to laminate blocky particle as a separate entity.
Scale bar 10 µm.

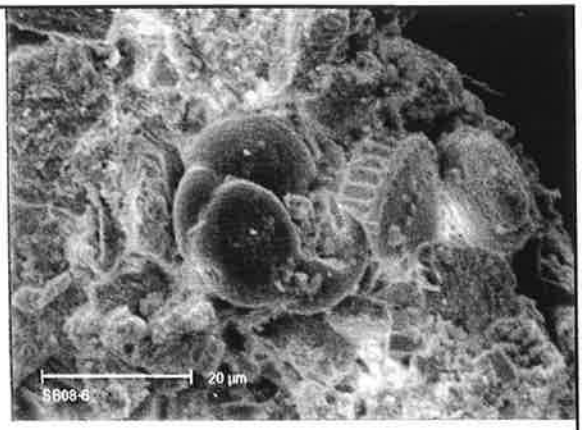



Figure 8.19b Centric diatoms (and foraminifer) within a composite particle (possibly of faecal origin) *Thalassosira* sp.
Scale bar 20 µm.

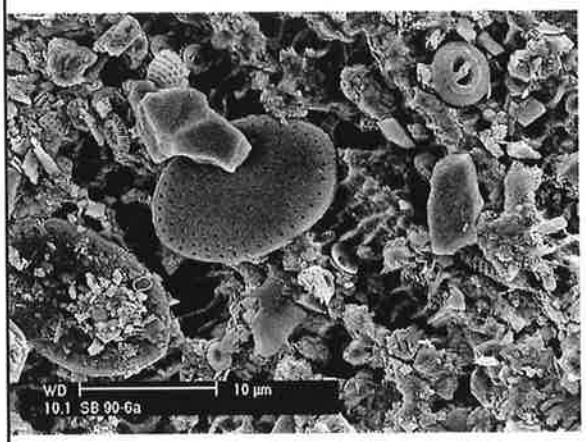



Figure 8.19c Pennate diatoms adhering to ornamental microstructure of molluscs. NB coccoliths and µm-sized diatom hash.
Scale bar 10 µm.

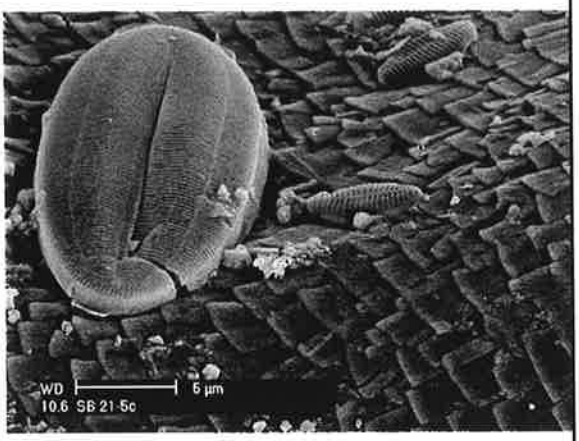



Figure 8.19d Pennate diatoms adhering to a cyclostome bryozoan colony (large diatom-*Cocconeis* sp.)
Scale bar 5 µm.




Figure 8.19e Pennate diatoms adhering to a foraminifer possibly resulting in dissolution of the foraminifer test.
Scale bar 50 µm.

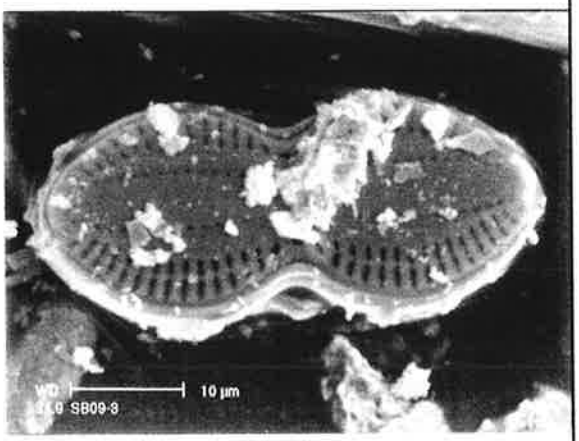



Figure 8.19f Pennate diatoms also are commonly found as separate particles in the mud fraction (*Psammodictyon* sp).
Scale bar 10 µm.



Figure 8.20a *Actinotypus* sp. centric diatom as a disceet particle from the inner marginal basins.
Scale bar 20 μm.

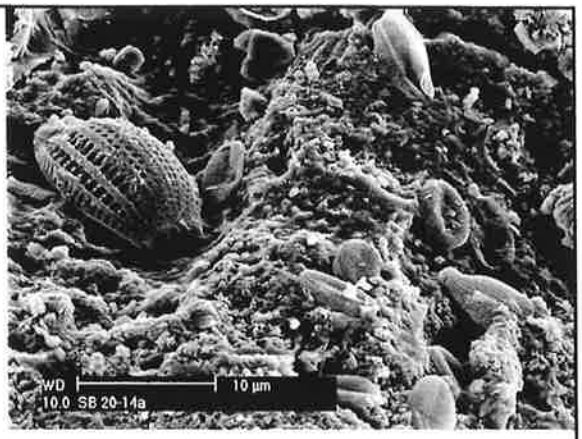



Figure 8.20b *Cocconeis* sp. (large diatom) and *Psammodictyon* sp. (small diatom).
Scale bar 10 μm.

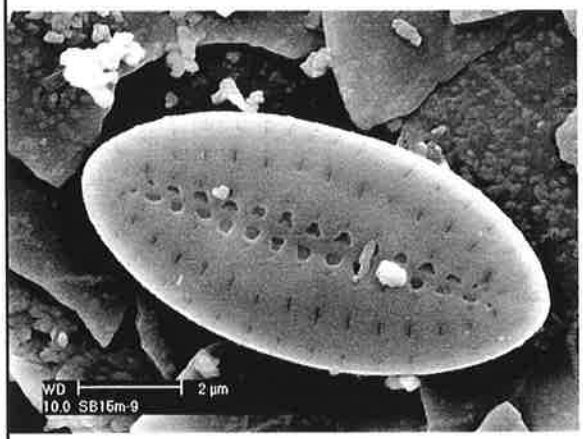



Figure 8.20c *Cocconeis* sp. (diatom) in a composite particle of μm-sized platelets.
Scale bar 2 μm.

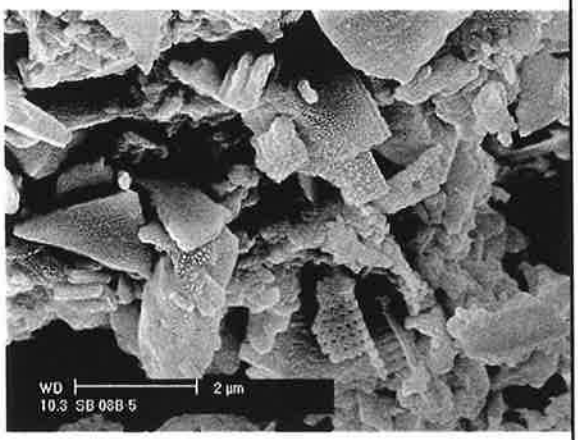



Figure 8.20d Diatom, bryozoan and molluscan hash with no visible cementing and abundant porosity.
Scale bar 2 μm.

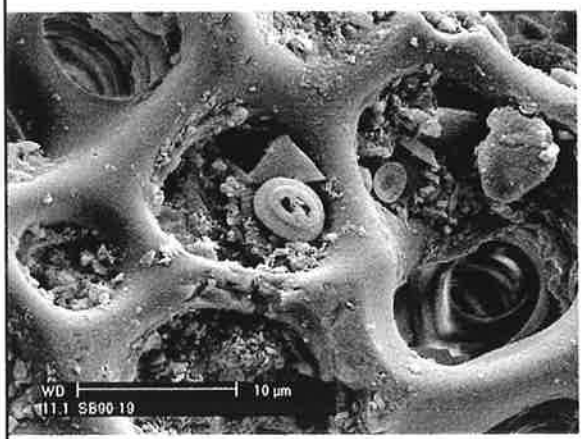



Figure 8.20e Coccoliths (*Geophyrocapea ?oceanica*) adhering to an echinoderm spine
Scale bar 10 μm.

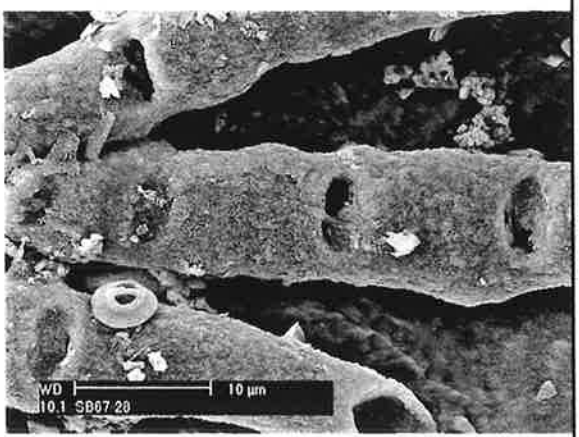



Figure 8.20f Coccolith (*Geophyrocapea ?oceanica*) as a particulate adhering to an encrusting bryozoa .
Scale bar 10 μm.

elongate crystalline particles. The dimensions of these particles commonly range from the mud cut-off at 62.5 μm to 10 μm. Particles below this size tend to disaggregate into < 2 μm platelets as indicated by general cheilostome structure. Examples of this can be seen in *Serripetraliella* sp. (Figures 8.7a, 8.7b), encrusting cheilostome structure (Figures 8.7c, 8.7d) and general cyclostome structures, e.g. *Nevianipora* sp. (Figures 8.6d, 8.6e, 8.6f).

The thickness of the cheilostome bryozoan wall varies significantly within the zooecia, from the finely sculptured frontal wall to the more robust basal area and lateral walls where thickening provides structural rigidity, protection form predators and dendritic thickening (structural support, i.e. adeoniform) for the zooaria as a whole (Figures 8.7e, 8.7f). The zooecial wall is generally composed of IMC and rare aragonite interspersed with proteinaceous material. This proteinaceous material ranges from < 10% to ~50 % in cheilostomes and < 10% in cyclostomes, depending on the amount of calcification of the zooid skeleton (Milliman, 1983).

The structure of particles which can originate from bryozoans are identifiable once the colony has died and the protecting proteinaceous material has commenced to breakdown. The breakdown causes the skeleton to be in contact with sea-water and biogenic activity which results in the observable structure of the variable open porous nature of the macerating calcite skeleton (Figures 8.7e, 8.7f – arrowed central area). These scanning electron micrographs of the encrusting bryozoan (*Osthimosia* sp.) show increasing magnification up to the point where the layered rhombic nature of the calcitic zooecial walls are readily seen. The IMC in this structure is disarticulating into ~1 μm platelets as the degradation of the interleaved organic layers occur. Dissolution and microboring appears to be the major destructive diagenetic pathway taking place in the articulated bryozoan *Orthoscuticella* sp. (Figures 8.8a, 8.8b, 8.8c). This is indicated by the rounding of the exfoliating fragments and the roughly cylindrical and channelled porous nature of the zooid microstructure. Similar disintegration is indicated in the micrograph series Figures 8.9a, 8.9b, 8.9c. Figures 8.9b and 8.9c in particular show abundant porosity from microboring and possible dissolution. Even the apparent 'dense' equigranular structure of *Petralia* sp. at low magnifications (Figures 8.8d, 8.8e, 8.8f) show that when subject to higher magnifications, dissolution, exfoliation, and microboring still are active agents in the disintegration of the skeleton (Figures 8.9e, 8.9f).

Possible dissolution patterns are discernible at the boundaries of the zooid basal plates of a foliose bryozoan (Figure 8.10a, 8.10c). The flaking of uneven layers of skeletal material is common at the plate boundary and on the skeletal ridges between the pores in the base plate (Figures 8.10d, 8.10e). Micrometre-scale particles are produced as these layers breakdown and are released into the environment (Figures 8.10d, 8.10e).

A significant number of cyclostome species found in Streaky Bay have an imbricated skeletal micro structure consisting of sub-rhombic platelets with dimensions ranging from 1.5 to 4 μm (Figures 8.10f, 8.11a, 8.11b - *Mesonea* sp.). These platelets are slightly larger, thicker and more rhombic in morphology than that of the cheilostomes (Figure 8.11c) and are usually composed of LMC (Table 8.5). Pronounced layering is also evident at the zooid aperture of the cyclostomes *Crisia* sp. (Figures 8.11d, 8.11f), and *Nevianopora* sp. (Figures 8.11f, 8.12a).. However, cyclostomes can occasionally display a breakdown fabric in the peristomal covering similar to that of the cheilostome fabric (Figure 8.7b).

Hence, it may be possible to distinguish between cyclostome and cheilostome platelets due to thicker platelets and interleaved organic layers in cyclostomes and slightly curved, thinner and more polygonal platelets in the cyclostomes (Figure 8.11e - cyclostome and Figure 8.7b – cheilostome).

### 8.5.4 Coralline Algae

Coralline algae are the dominant epiphytes in the *Posidonia* sea-grass meadows and inner terrace. The presence of coralline algal fragments in the sediments is also significant in Streaky Bay. However, they commonly only comprise < 10 %, and rarely up to 20 %, of the sand fraction in the seagrass meadows and inner terrace (Chapter Six). They are also common to abundant in the gravel fraction over a significant portion of the bay (Chapter Seven). Particles of coralline algae are identifiable as squat to elongate crystallites but do not appear as a highly significant component in the mud fraction.

The microstructure of coralline algae consists of interlocking crystallites (tenths of μm in length) of HMC, which support the algal morphology (Scoffin, 1987). These crystallites are arranged in layers at right angles to each other within and between the double layered cell walls. The cells are roughly rectangular and approximately 5 μm in size. The thallus is prone to early destructive diagenesis on dying as a result of losing its cellular structure and transforming to a micritic mass (Scoffin, 1987).

This is especially valid for the thin crustose thalli which form as epiphytes on the flexible leaves of the seagrasses, *Posidonia* sp. and *Amphibolis* sp. Scanning electron micrographs of crustose coralline algae from seagrass leaves, display thalli that have a flaky porous structure with indications that several generations of thalli have occupied overlapping spaces at a macro-scale (Figure 8.12b). This open flaky nature is susceptible to rapid breakdown as the organic material of the plant degrades. A view of the crustose algae on a nano-scale shows disintegration occurring in the carbonate cell structure with the release of tapered sub-μm carbonate crystallites (Figures 8.12c, 8.12d).

Thicker crustose coralline algae eg *Goniolithon* or *Lithothamnion* that form on solid substrates, display thicker and more rigid cell walls, which take a progressively longer time to degrade depending

on the robustness of the skeleton. These cell walls incorporate a multi-layered interlocking structure (Figures 8.12e, 8.12f). The layering consists of nano-scale platelets with little intrinsic morphology at the μm scale as indicated in Figure 8.12f. Also evident in this figure is the comparatively wide size range of the flaking particles. This style of crustose coralline algae is also evident on different substrates as indicated in the detailed image of an echinoid spine (Figure 8.13a).

Rhodoliths and thicker encrustations on solid sea-floor material take longer to degrade either because of interstitial cementation (predominantly tropical marine diagenesis) or as a result of slower pathways of biodegradation (i.e. boring activity from sponges, algae and fungi) and dissolution/abrasion (Scoffin, 1987; Alexandersson, 1978). Cell wall disintegration rather than cementation is likely to occur, in cool-water environments, although at a reduced rate because of the more compact nature of these forms (Alexandersson, 1978). Rhodoliths also have a denser, more rigid structure than the crustose forms as a result being separate (ie non encrusting) from the substrate. This requires the plant to provide structural rigidity to the thallus with thickened cell walls, which results in a comparatively higher mass than the thalli of crustose coralline algae (Figure 8.13b). The thickened cell wall impedes a rapid rate of disintegration or dissolution as a result of the rigid and compact crystallite structure (Figures 8.13c, 8.13d). When a rhodolith dies as a result of being smothered by sediment it becomes part of autochthonous gravel fraction and may, depending on the conditions of carbonate saturation, start to dissolve as in Figure 8.13c or precipitate small crystallites of calcite in the internal pore canals (e.g. Ryan, 1998 - Plate 4e). Unless rhodoliths are buried on dying, the thalli become new loci on which coralline algae can grow as a regenerated rhodolith (Ryan, 1998).

Rhodoliths provide only a small amount of mud-sized particles to the sedimentary system as a result of slow growing and their limited occurrences. They only appear to die when they are smothered or buried by other rhodoliths or sediment and are usually preserved as pavements in the stratigraphic column (Ryan, 1998). Maceration occurs at or below the sediment/ water interface with the rhodolith becoming less dense through the loss of cellular organic matter and gradual dissolution of the crystalline structure. Rhodoliths do not add significantly to the mud fraction of the sediment, as they are sparse at Streaky Bay.

Articulated corallines tend to disarticulate following death. They are transformed rapidly into sand-sized grains either through maceration or destructive abrasion (Scoffin, 1987). The structure of the thalli segment consists of elongate cavities running the length of the segment bounded by calcareous multicellular walls similar to a honeycomb structure (Figures 8.13e, 8.13f, 8.14a, 8.14b). The cell walls are composed of short ellipsoidal to equigranular crystallites. The ellipsoidal crystallites are arranged perpendicular to the elongate cavities and the granular particles fill the area between the

adjacent crystallite layers. Hence disintegration of the inner and outer cell walls occurs at μm to sub-μm sizes (Figures 8.14c, 8.13d). This is aided by possible dissolution at the exposed surface of the segments which is clearly seen in Figure 8.14.

### 8.5.5 ECHINODERMS

A significant population of Echinoderms are present in Streaky Bay and is represented by Echinoid and Ophiuroid calcareous skeletal fragments. Their contribution to the sediment composition in the sand fraction ranges from 1 % to 14 % (average ~ 5 %), comprising 42 % of the grains in the sand fraction at one station (Chapter Six). The distribution of echinoderms in the gravel fraction is broadly restricted to the inner marginal basins and the northern terrace area (Chapter Seven).

Echinoderm fragments are conspicuous by the highly porous structure of the stereom (skeleton) (Figure 8.14e – echinoid, boss area, Figure 8.14f - echinoid spine, Figures 8.15a, 8.15b - echinoid plate and Figures 8.15c 8.15d - ophiuroid ossicle). These fragments represent the common genera of echinoderms (*Holopneustes*, *Heliocidaris*, *Gonoicidaris*, *Echinocardium, and Ophionereis*) which are found in Streaky Bay. Observations at a micro-scale show fragments with a structure that appears relatively open and robust. The disintegration and dissolution patterns become apparent when the fragments are examined at a μm -scale,

### 8.5.6 BRACHIOPODS

Rare Terabratulid brachiopods are found in the bay, typically in the gravel fraction of samples taken from the variable substrates of the outer terrace and entrance area. Grains derived from brachiopods are rare (ie < 2/300 grains) in the sand fraction. Their presence is noted in several samples from the outer area of the bay (SB48, SB66, SB67 and SB87). These grains are recognisable in the sand fraction by the punctate structure of their valves (Figure 8.15e). Brachiopod particles are difficult to recognise in the mud fraction through the lack of discernible microstructure. The punctae are not a useful diagnostic feature for macerated or masticated particles of < 30 μm (Figures 8.15f, 8.16a), as they are typically distributed relatively evenly at 40 – 50 μm apart in the valves. The particles produced from this disintegration are elongate, tabular and are usually slightly bent along the length of the particle (~ 20 μm x 10 μm). Further breakdown into indistinguishable μm -sized particles occur at the abrading edges of the shell fragment (Figure 8.16b).

### 8.5.7 SPIRORBIDS AND SERPULIDS (ANNELIDA)

The calcareous exoskeletons of Annelids commonly found in the bay are the planispiral Spirorbid*s* in the seagrass meadows and entrance areas and rare sinuous Serpulids on larger lithic and biofragments also in the entrance area. Their contribution to the sediment volume is not significant as a result of the low populations (< 0.3 %) observed in the sand and gravel fractions. Examination of grab samples of

seagrass from the sand shoals indicate an approximate Spirorbid population of 5 to 8 individuals per 20 cm of *Posidonia* leaf. The structure of serpulids and spirorbids consist of concentric laminate inner layers with a low angle laminate cone in cone outer layer (Figure 8.16d, Milliman, 1974). The disintegration of the calcareous tubes (e.g. Spirorbid, Figure 8.16c) results in the formation of sub-μm polygonal platelets from the inner layer (Figure 8.16e) and larger rhombic platelets from the outer layer (~2 μm, Figure 8.16f). Spirorbids incorporate thin layers of crustose calcareous red algae in the outer more ornamental layer, due to the close association with coralline algae, especially on the leaves of seagrass (Figures 8.17a, 8.17b).

### 8.5.8 PORIFERA (SPONGES)

Siliceous and calcareous sponge spicules are found in Streaky Bay. Traces to rare triaxon spicules are found in the gravel and sand fraction of samples from the outer terrace. The spicules in the sand fraction occur mostly as broken monaxons with rare triaxial bosses. The siliceous spicules belong to sponges from the Class *Demospongea*. These spicules are mostly monaxon or fragments of broken tetraxon spicules. The calcareous triaxon spicules shown in Figures 8.17c and 8.17d are from the calcareous sponge *Sycon gelatinosum* in the Class *Calcarea*. The spicules are tightly interlaced around the radial canals and maintain the principal structure of the sponge. Monaxons are found in the epidermal area and serve as protection. The calcareous sponges do not contain spongin or silica so when the animal dies a large a number of spicules are released into the sediment comparatively rapidly. Scanning electron micrographs and EDAX probes of the mud from the inner marginal basins show that both siliceous and calcareous spicules are present.

Boring sponges (*Cliona*) have also added to the sediment supply by releasing particles during the process of boring (Young and Nelson, 1985). The typically scalloped particles are seen in the samples studied, but the resultant scalloped pits are evident on bivalve shells (Figures 8.4a, 8.4b). These pits have subsequently become a repository for sub-μm sized particles from degraded molluscs, bryozoans, calcareous algae, sponges and diatoms (Figure 8.17e).

### 8.5.9 TUNICATES (ASCIDIANS)

The occurrence of the stellate spicules of ascidians (Chordata) is significant in the muds at Streaky Bay. They are more common in the central and northern basins than elsewhere. Since their dimensions range from 10 μm to 30 μm, they are not observed in the sand or gravel fractions. A preserved section of the ascidian soft body containing the spicules is shown in Figures 8.18a, 8.18b). These aragonitic spicules are typical of those in the family Diademnidae and belong to the genus *Tridemnum*. This genus predominantly lives as an epiphyte on seagrass and algae in water depths from 1 m to 6 m (Kott, 1980; Jones, 1990). Once the ascidian dies μm to sub μm –sized prisms of aragonite are produced as the spines on the spicules disintegrate (Figure 8.17f).

### 8.5.10 CORALS

Rare azooxanthellate corals (*Culicia* sp.) are found in the outer areas attached to solid substrates such as the rocky substrate, robust bivalves and thick encrustations of dead bryozoans and calcareous red algae. Grains attributable to coral disintegration were not recognised in the sand fraction. Their contribution to the sediment supply is minimal, based on the small number of corals present in the gravel fraction of the samples (Appendix Two, Sample Descriptions). The microstructure of recently dead coral indicate that the septa will produce sub μm crystallites and the corallite wall will produce μm -sized sub-rhombic tabular particles on disintegration (Figures 8.18c, 8.18d and 8.18e, 8.18f).

### 8.5.11 DIATOMS (CHRYSOPHYTA)

Diatoms are common in the mud-sized sediments from the inner marginal basins and as epiphytes on skeletal material within Streaky Bay. The size of the test or frustule normally ranges from 5 μm - 2000 μm (Brasier, 1980). However, in the bay they range from 5μm up to the sieve limit of 62.5 μm (NB. no diatoms were found in the sand fraction). The diatom frustules are composed of silica and hence are a source of silica in the resulting sediments. Diatoms occur in two distinct shapes according to their ecology: pennate diatoms thrive in epiphytic benthic marine habitats (amongst others) and centric diatoms occupy the marine planktonic niche, especially at temperate and sub-polar latitudes. They require light for photosynthesis so they are restricted to the photic zone (< 200 m). Centric diatoms (usually the larger frustules) are found as separate particles within the mud fraction of the sediments (Figure 8.19a) and within composite mud particles of possible faecal origin (Figure 8.19b). Pennate diatoms are commonly found adhering to larger organisms e.g. fragments of molluscs (Figure 8.19c), bryozoan colonies (Figure 8.19d) and foraminifera (Figure 8.19e) and also in the mud fraction as separate particles (Figure 8.19f).

Diatoms found in the muds from the inner bay are species from the genera of *Actinoptychus* (Figure 8.20a), *Cocconeis* (Figure 8.20b – large diatom, 819d, 8.20c), *Diploneis* (Figure 8.19e), *Navicula* (Figure 8.1f), *Psammodictyon* (*Nitzschia*) (Figure 8.20b – small diatom, Figure 8.19f), *Thalassosira* (Figure 8.19a) and Cyclotella.

### 8.5.12 COCCOLITHS (CHRYSOPHYTA)

Plates of Coccolithophores are found as a trace throughout the mud sediments. The dimensions of these encapsulating plates range from 2 to 5 μm in the sediments at Streaky Bay and as a result of this, they are difficult to identify or encounter by chance when examining the sediment with the scanning electron microscope, at a 20 μm – 50 μm scale. The plates are usually found embedded in the pores of larger calcareous skeletons (Figure 8.20e - coccoliths in the pores of an echinoid spine) or adhering to skeletal fragments (Figure 8.20f - coccolith adhering to the surface of an encrusting bryozoans).

The coccoliths encountered in the sediments of Streaky Bay belong to the genera *Geophyrocapea* and are similar to *G. oceanica* (Honjo, 1976).

## 8.6 MORPHOLOGY AND COMPOSITION OF THE MUD FRACTION BY SEM

### 8.6.1 MORPHOLOGY OF MUD FRACTION

Scanning electron microscope resolutions of 50 μm : 1 cm (x170) indicate that the mud fraction is primarily composed of long prismatic, tabular to blocky and porous polygonally sub-equant particles (Figures 8.21a, 8.21c, 8.21d, 8.21d, 8.21e, 8.21f, 8.22a). The grain-size of the particles range from 62.5 μm to < 0.5 μm. There is a skew in grainsize towards the larger end of the fraction, although many larger porous particles (~20 - 50 μm) consist of aggregated μm -sized particles (composite particles) (Figures 8.22b, 8.22c).

**8.6.1.1 Prismatic particles** are dominant and larger in most of the mud fraction samples. The morphology varies from sub-hexagonal to sub-rectangular prisms and the axis ('c') of the prism is usually significantly longer than the shorter axes (Figures 8.22a, 8.22e, 8.22f, 8.23a). Perpendicular ('c') growth lines are common in these particles ranging from indistinct on the fresher, more angular particles to pronounced on particles that have evidence of abrasion and maceration (Figures 8.23b, 8.23c). Details of sub-μm disintegration through maceration and abrasion is evident in the micrographs of a particle and detailed enlargement in Figures 8.23d and 8.23e. Significant microboring is evident on more sub-rounded prismatic particles (Figure 8.23f).

**8.6.1.2 Tabular to blocky particles** are common and show less distinct growth lines, although as abrasion and maceration occur they become more prominent. The growth lines, when they occur, are usually perpendicular to the shorter 'c' axis (Figures 8.24a, 8.8.24b, 8.24c). Exfoliation of laminar platelets < 5 μm are common where the growth lines are perpendicular to the 'c' axis (Figures 8.24d, 8.24e). A combination of micro-boring and disintegration by maceration are commonly associated with these particles (Figures 8.8.2f, 8.2e. 8.24e). A tabular particle in the advanced stages of disintegration through abrasion, maceration and limited microboring is highlighted in a the series of micrographs. These reveal that the end products of disintegration are sub-μm platelets and prisms (Figure 8.25a, 8.25b, 8.25c – chevron layer in molluscs). Another example shows the sub-μm crystallite production resulting from the inner layer disintegrating in a tabular foraminifer particle once maceration of the outer layer commences (Figure 8.22d).

**8.6.1.3 Porous polygonally sub-equant particles** are common throughout the samples and the range of their morphology is noticeably variable (Figures 8.24f, 8.21f, 8.25d, 8.24d). These particles are

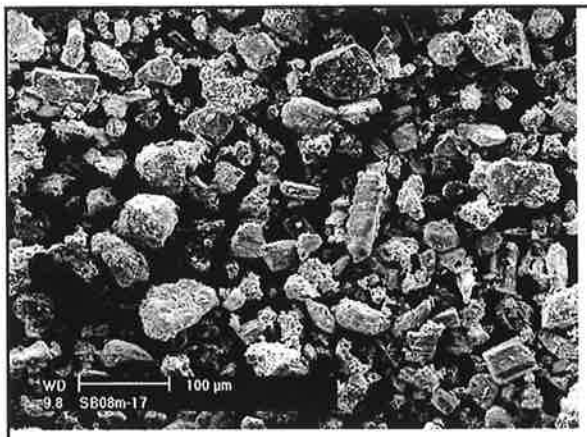



Figure 8.21a Particles from the mud fraction in the southern inner marginal basin (IMB), highlighting prismatic, tabular, blocky and composite particles.
Scale bar 100 µm.

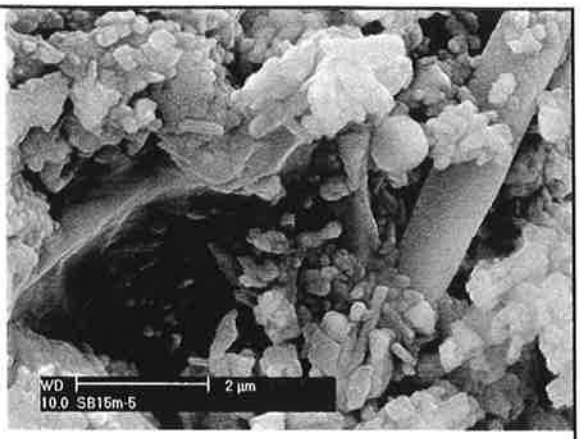



Figure 8.21b Detail of composite particle highlighting spherical, cylindrical, prismatic, and blocky to laminate sub-µm particles
Scale bar 2 µm.

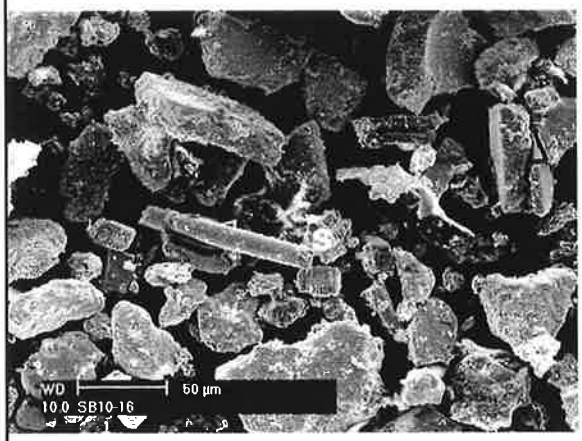



Figure 8.21c Mud fraction from southern IMB highlighting tabular prismatic and blocky particles. Carbonate spicule (s).
Scale bar 50 µm.

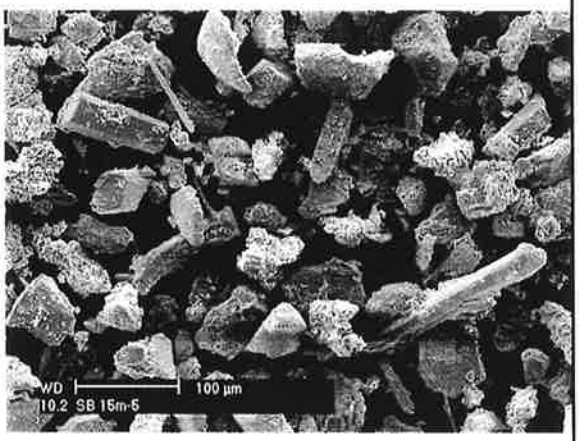



Figure 8.21d Mud fraction from central IMB, highlighting prismatic and composite particles.
Scale bar 100 µm.

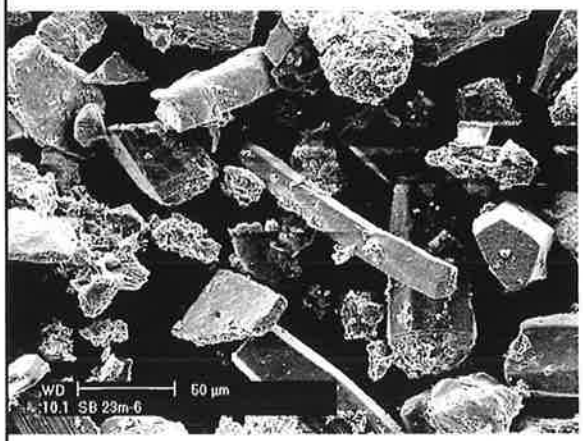



Figure 8.21e Detail of mud faction from the northern IMB, highlighting elongate tabular, prismatic and occasional composite particles.
Scale bar 50 µm.

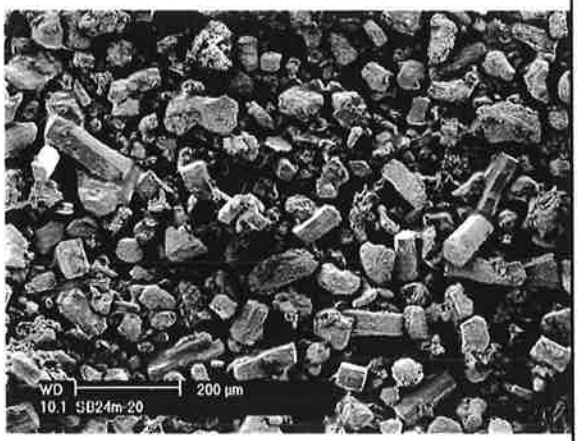



Figure 8.21f Mud fraction from the northern IMB, highlighting an area of predominantly prismatic, blocky and occasional composite particles.
Scale bar 200 µm.

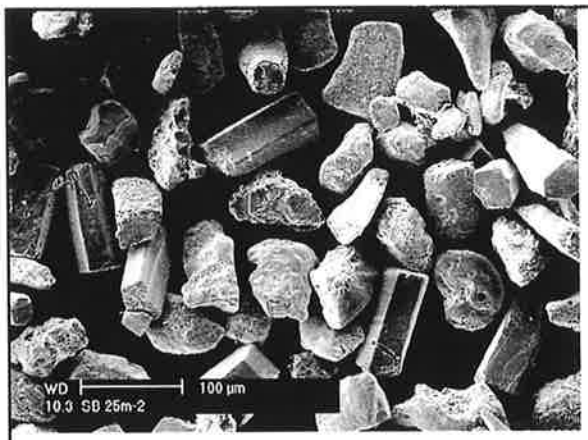



Figure 8.22a Mud fraction (washed) from the northern IMB, detailing prismatic, tabular, and porous polygonal particles.
Scale bar 100 µm.



Figure 8.22b Mud fraction (unwashed) from the central IMB, highlighting aggregates of µm-sized particles and the skew to larger particles within the fraction.
Scale bar 100 µm.

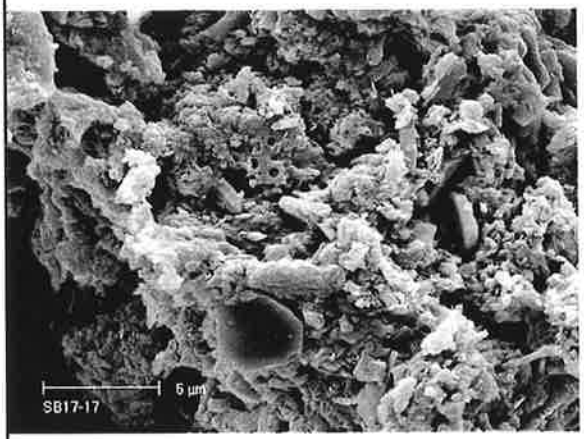



Figure 8.22c Aggregates of micron-sized particles forming larger composite particles (cementing not obvious).
Scale bar 5 µm.

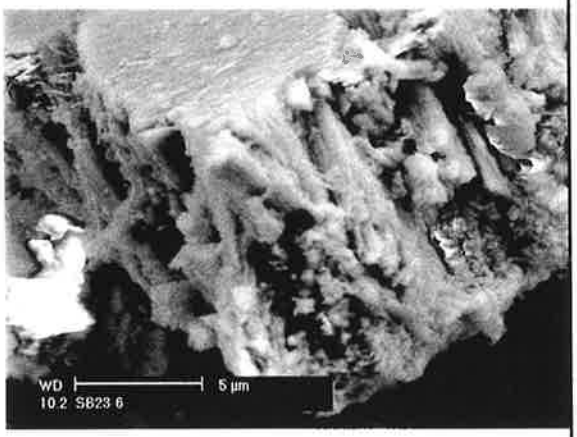



Figure 8.22d Tabular particle highlighting perpendicular crystallite structure and possible production of sub-µm crystallites on disintegration (foram).
Scale bar 5 µm.

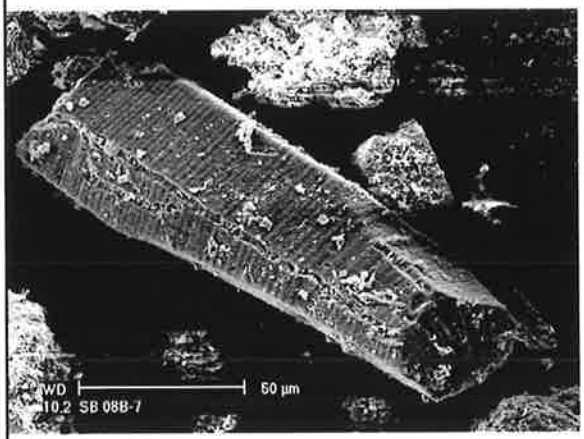



Figure 8.22e Pronounced growth lines perpendicular to the long axis are common in prismatic particles. NB micoboring on the long edge (minor) and perpendicular abundant) face.
Scale bar 50 µm.

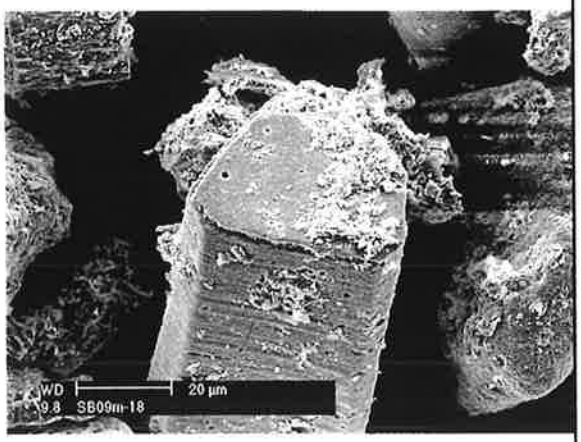



Figure 8.22f Detail of perpendicular face and growth lines of a prismatic particle with noticeable rounding of the edges from abrasion and maceration.
Scale 20 µm.

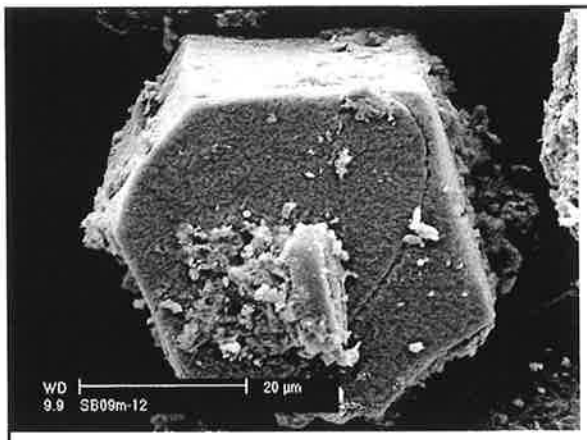



Figure 8.23a Detail of a fresh hexagonal prismatic particle indicating possible dissolution texture and limited microboring on the facing surface.
Scale bar 20 µm.

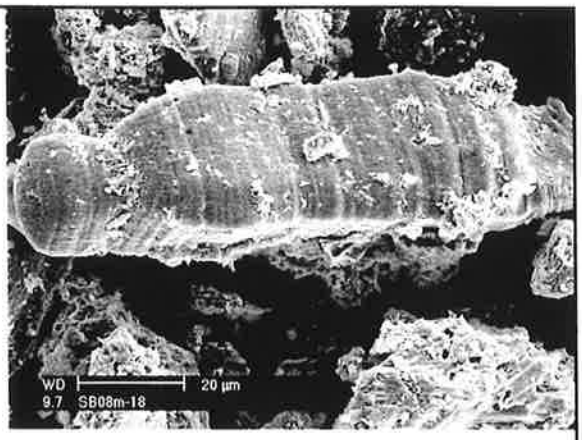



Figure 8.23b Rounded prismatic particle showing evidence of maceration and abrasion with preferential disintegration occurring on some growth layers.
Scale bar 20 µm.

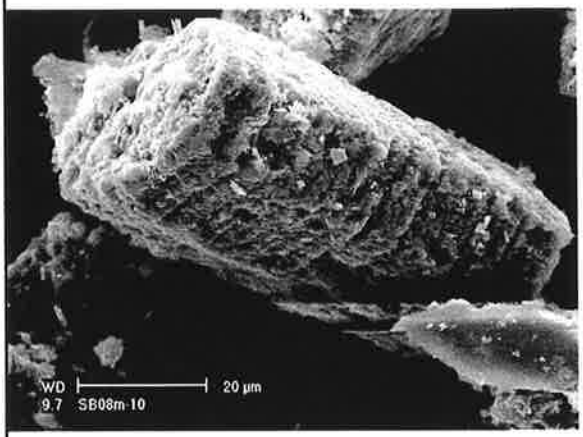



Figure 8.23c Evidence of maceration and possible dissolution creating a porous effect in on prismatic particle.
Scale bar 20 µm.

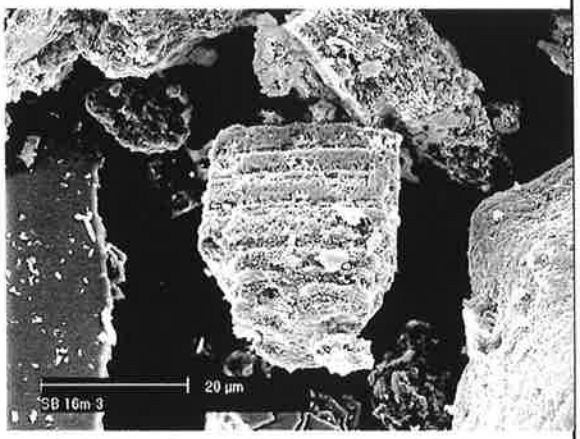



Figure 8.23d Detail of a blocky particle indicating the potential for sub-µm particle production through maceration and possible dissolution.
Scale bar 20 µm.

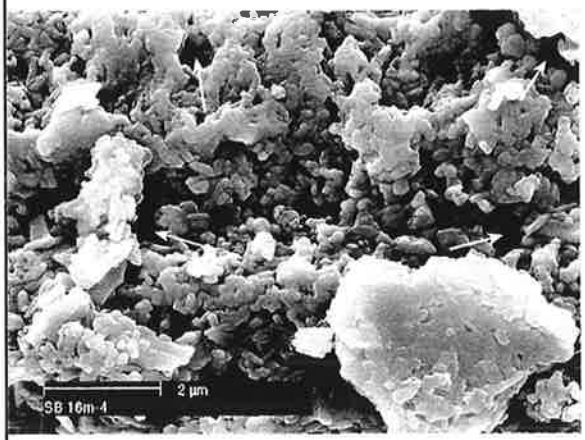



Figure 8.23e Detail of 8.23d showing advanced maceration and the liberation of sub-µm particles. NB porosity (arrowed)
Scale bar 2 µm.

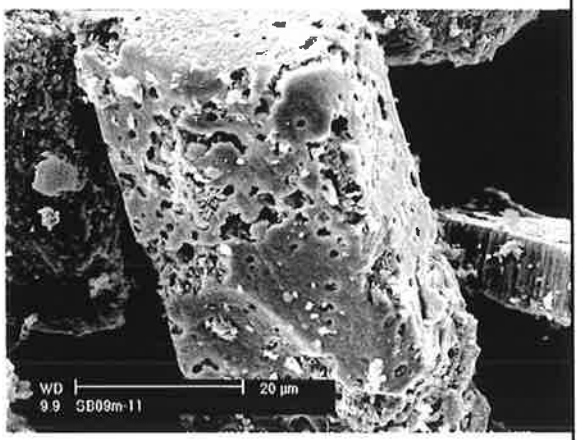



Figure 8.23f Significant microboring, which shows a preference for particular growth layers is more evident in sub-rounded prismatic particles.
Scale bar 20 µm.

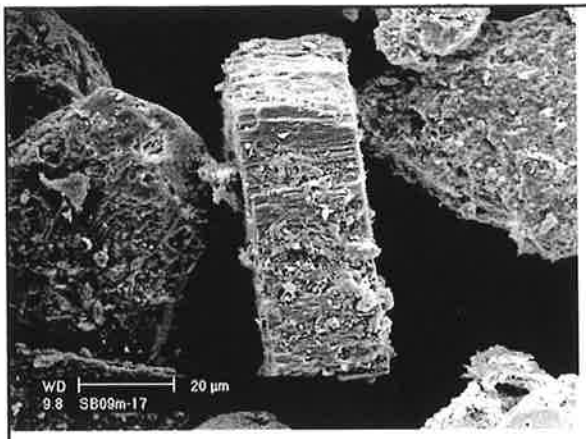



Figure 8.24a Tabular to blocky particles show less distinctive growth layers but when present are perpendicular to the shorter "c" axis.
Scale bar 20 µm.

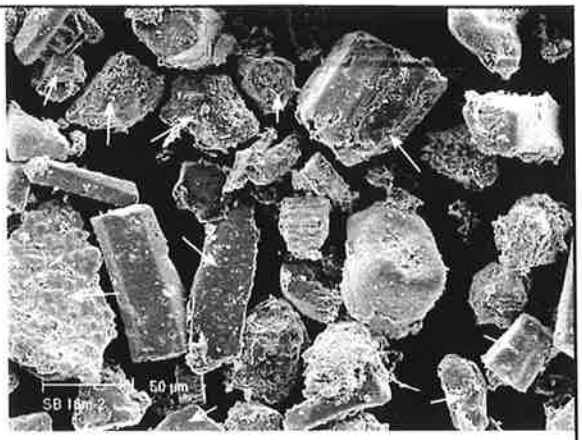



Figure 8.24b Tabular to blocky particles (arrowed) highlighting diverse morphology and states of maceration.
Scale bar 50 µm.

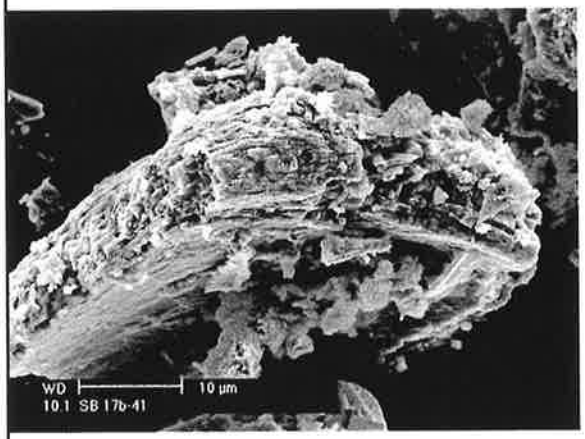



Figure 8.24c Detail of tabular particle with short 'c' axis and perpendicular growth layers. Particle is also disintegrating and producing sub-µm particles.
Scale bar 10 µm.

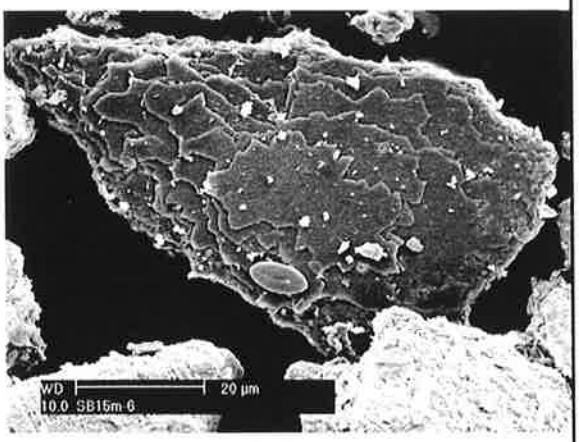



Figure 8.24d Detail of exfoliating tabular particle, highlighting patterns of disintegration to produce µm-sized platelets.
Scale bar 20 µm.

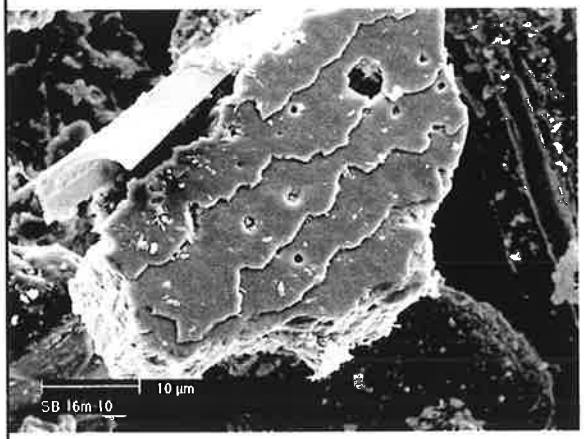



Figure 8.24e Detail of tabular particle, showing the exfoliation of lamellar platelets. NB, microboring perpendicular to growth layers.
Scale bar 10 µm.

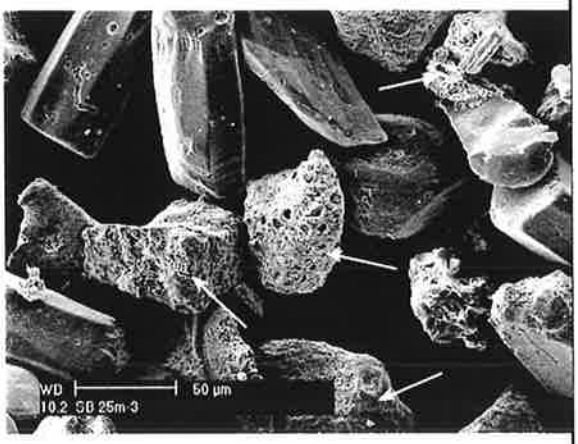



Figure 8.24f Porous polygonally sub-equant particles (arrowed) are common and their range of morphology is variable.
Scale bar 50 µm.

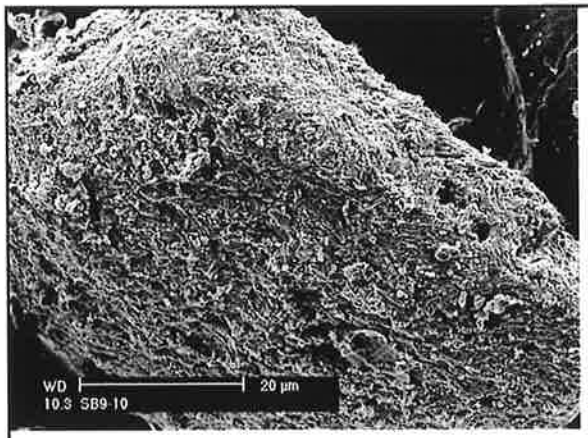



Figure 8.25a Tabular particle in advanced stages of disintegration through abrasion, maceration and microboring (chevron layer, molluscs).
Scale bar 20 µm.

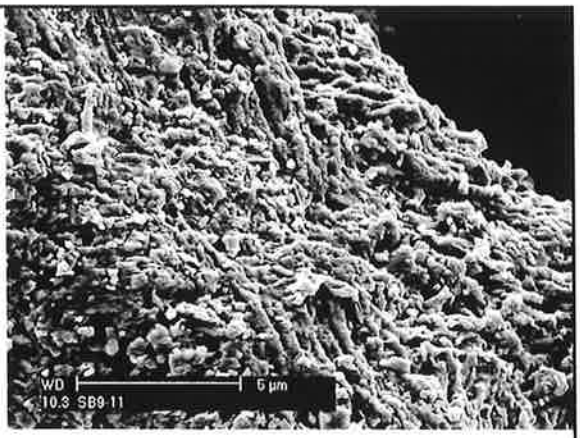



Figure 8.25b Detail of 8.25a (tabular particle) highlighting production of sub-µm prisms in the chevron layer of molluscs.
Scale bar 5 µm.

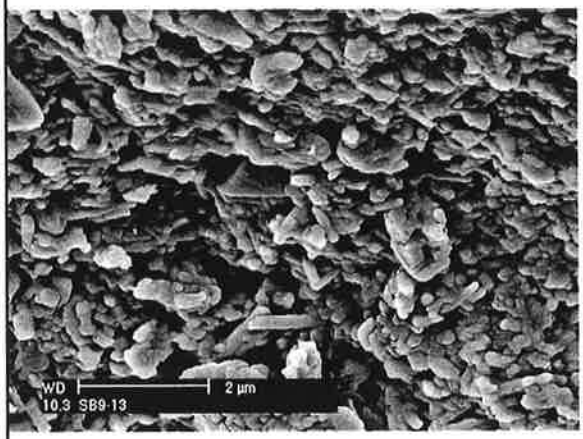



Figure 8.25c Detail of 8.25a (tabular particle) highlighting the production of sub-µm platelets and prisms (chevron layer, molluscs)
Scale bar 2 µm.

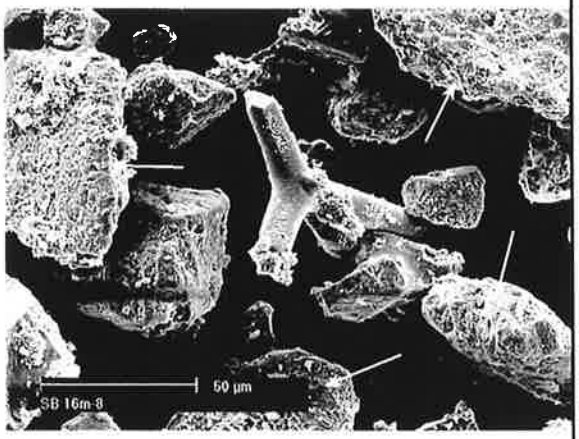



Figure 8.25d Porous polygonal particles (arrowed) are common throughout the sediments. The particles are usually in advanced stages of disintegration.
Scale bar 50 µm.

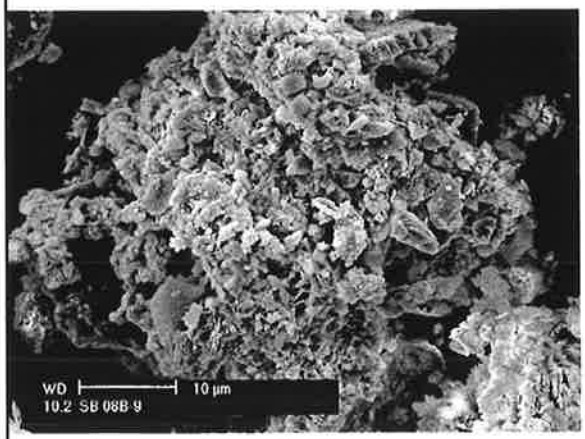



Figure 8.25e Loosely bound composite particle composed of platelets, prisms and elongate tabules with fragments of diatoms. NB, high apparent porosity.
Scale bar 10 µm.

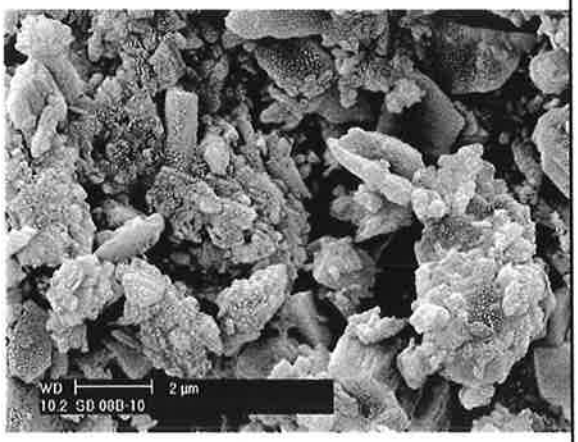



Figure 8.25f Detail of 8.25e (composite particle) showing prismatic, elongate tabular and platey sub-µm particles, with abundant porosity.
Scale bar 2 µm.

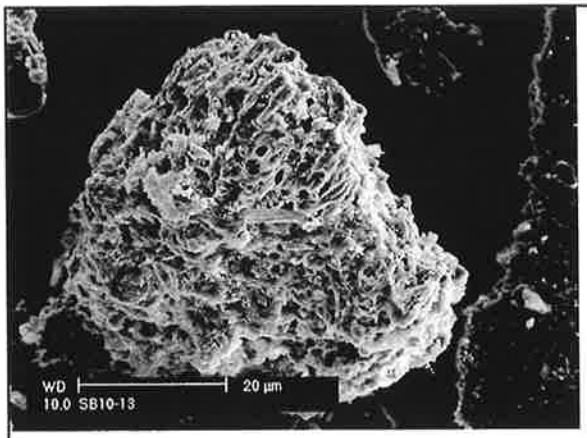
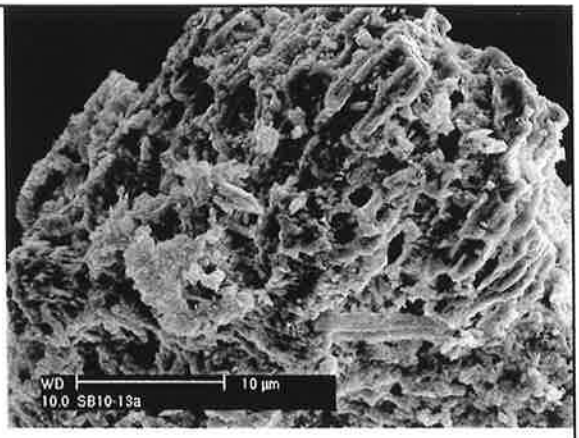



Figure 8.26a Porous polygonal particle showing advanced maceration and microboring.
Scale bar 20 µm.




8.26b Detail of 8.26a highlighting the progressive production of sub-µm particles with maceration and microboring.
Scale bar 10 µm.

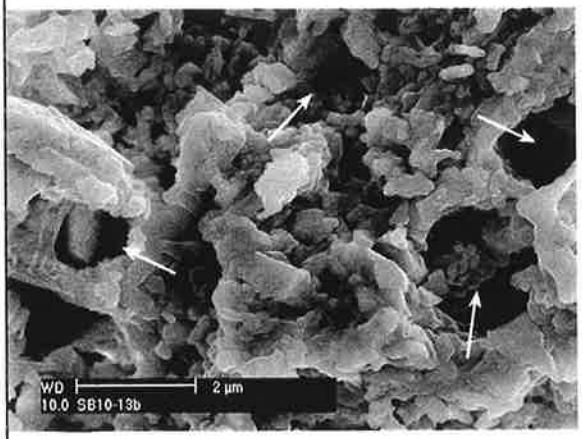



Figure 8.26c Detail of 8.25b highlighting small diameter microbores (arrowed) and sub-µm irregular platelets.
Scale bar 2 µm.

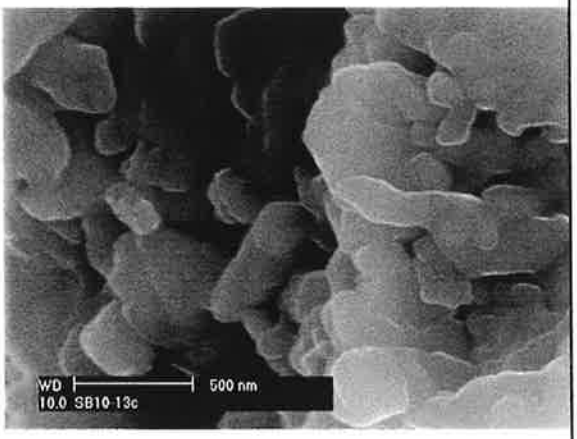



Figure 8.26d Detail of 8.26c showing the irregular nature of the microboring and also the rhombic morphology of some platelets. Platelet sizes ranging down to 200 nm.
Scale bar 500 nm.

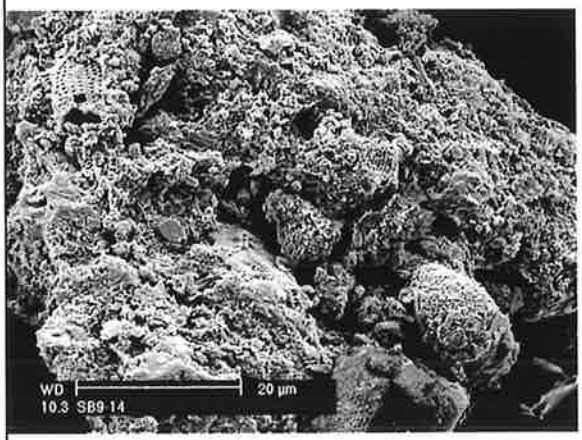



Figure 8.26e Composite particle highlighting loosely bound sub-particles. Component sub-particles can exhibit a wide variation in size.
Scale bar 20 µm.




Figure 8.26f Detail of 8.26e showing elongate tabular, platelet, crystallite, cylindrical and prismatic constituent particles.
Scale bar 5 µm.

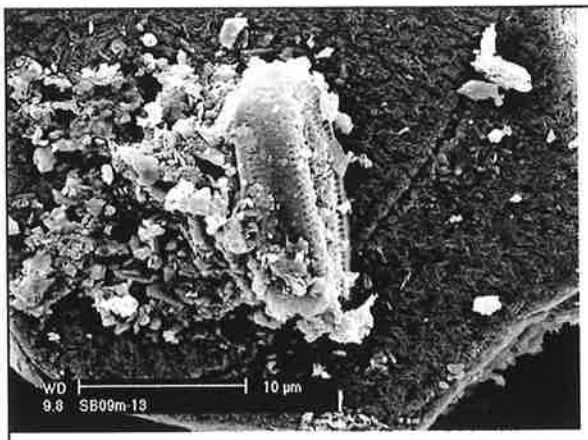



Figure 8.27a Individual sub-µm particles are also present in mud fraction adhering to larger particles.
Scale bar 10 µm.

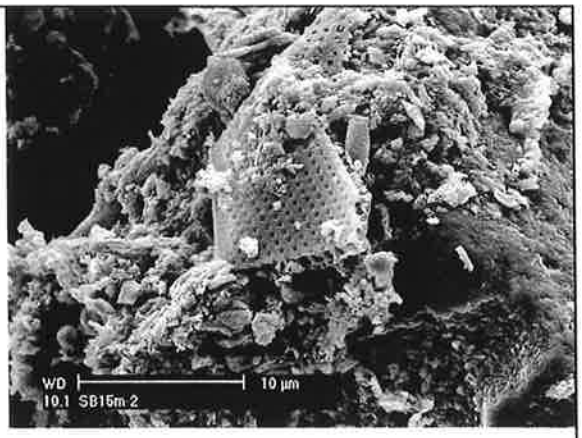



Figure 8.27b individual sub-µm particles adhering to larger particles (washed sediment). The size range remains similar to unwashed sediments with prismatic, tabular and platey morphologies.
Scale bar 10 µm.

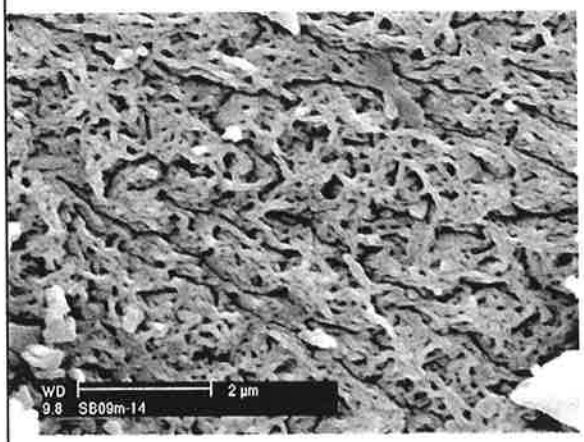



Figure 8.27c Detail of a high magnesium calcite macerated polygonal porous particle with sub-µm platelet and crystallite constituents.
Scale bar 2 µm.

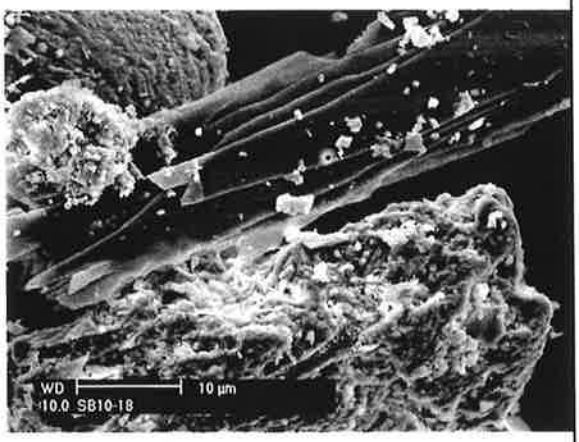



Figure 8.27d Larger bladed particles are attributed to brachiopod disintegration.
Scale bar 10 µm.

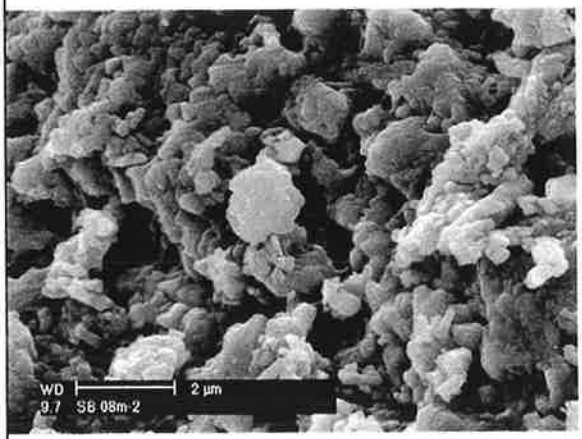



Figure 8.27e Sub-micron platelets, which are the result of the disintegration of denser structured bryozoans.
Scale bar 2 µm.

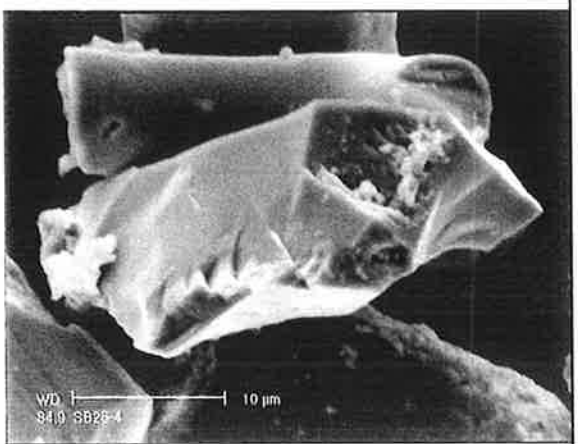



Figure 8.27f Fractured particle attributed to an echinoderm, highlighting the rhombic cleavage morphology typical of the echinoderm crystalline stereom.
Scale bar 10 µm.

either 'solid' or 'composite' in structure. The solid particles have structural continuity through the particle whereas the composite particles are heterogeneous in structural composition. A series of micrographs, of increasing detail, of a solid particle highlights abundant evidence of abrasion, microboring and maceration with the synchronous disintegration of the particle into sub-μm platelets (Figures 8.26a, 8.26b, 8.26c, 8.26d).

**8.6.1.4 Composite particles** are typified by a loosely bonded aggregate of μm to sub-μm -sized particle morphologies eg platelets, prisms, cylinders, blades and spheres. These composite particles with constituent sub-particles are illustrated in high-resolution micrographs (Figures 8.20d, 8.25e, 8.25f and 8.26e, 8.26f and 8.21b). The composite particle in Figures 8.25e and 8.25f incorporates elongate prismatic, irregular tabular and sub-rhomboidal laminate morphologies. Bladed, prismatic, and laminate morphologies are represented by μm to sub-μm particles in the larger composite particle of Figures 8.26e and 8.26f. The composite particle in Figure 8.21b is composed of sub-μm particles that range from spherical, cylindrical, prismatic, blocky to laminate in morphology.

The constituent sub-μm particles are also present as individual particles within the fraction, although they are commonly loosely adhering to larger particles, as observed in the detailed micrographs of the unwashed sediments (Figures 8.19b, 8.24c) and washed mud fraction (Figures 8.27a, 8.27b).

Minor readily identifiable particles observed in this fraction are diatoms, coccoliths, ascidian spicules, sponge spicules and rare benthic and planktonic foraminifera. These skeletal remains are figured and described under the corresponding sections in Section 8.5.1.

### 8.6.2 Carbonate Composition of Mud; EDAX Probe Results

Analyses from the EDAX probe on the FEG-30 SEM show that the modal average calcium carbonate composition of the mud samples is 3.6 mol % $MgCO_3$. The carbonate compositions are tabulated as an average as the EDAX programme only recognises the overall carbonate composition and not individual calcium magnesium carbonate species. These species include calcite, Mg calcite species, aragonite and dolomite. Diatoms and sponge spicules appear to be responsible for the silica that is found in most of the sediments as terrigenous quartz particles were not identified during the scanning electron microscope spectrogram analyses, either in the sediments and their constituent particles or the calcareous and siliceous biota (Table 8.6)

| Sample No. | Average Mol % $MgCO_3$ | Mg Wt % | Si wt % |
|---|---|---|---|
| SB08-17 | 0.0 | 0.0 | 0.0 |
| SB08b-20 | 1.7 | 0.49 | 0.0 |
| SB08m-13 | 2.8 | 0.81 | 30.85 |
| SB09-3 | 5.1 | 1.41 | 2.01 |
| SB09m-30 | 5.2 | 1.42 | 1.77 |
| SB09m-4 | 0.0 | 0.0 | 0.29 |
| SB10-10 | 6.0 | 1.68 | 1.86 |
| SB15-1 | 6.6 | 1.84 | 1.82 |
| SB15m-5/29 | 6.0 | 1.68 | 2.12 |
| SB16-1 | 0.5 | 0.16 | - |
| SB16-4 | 0.5 | 0.15 | 12.6 |
| SB16m-1 | 6.6 | 1.84 | 1.64 |
| SB17-15 | 3.3 | 0.92 | 1.26 |
| SB17b-40 | 5.8 | 1.66 | 2.25 |
| SB17b-45 | 3.8 | 1.08 | 0.0 |
| SB17b-50 | 5.4 | 1.55 | 1.56 |
| SB17b-7 | 4.9 | 1.38 | 1.38 |
| SB23m-4 | 2.0 | 0.57 | 0.0 |
| SB24-1 | 0.0 | 0.0 | 0.33 |
| SB24-4a | 1.1 | 0.52 | 0.54 |
| SB24m-30 | 5.4 | 1.45 | 1.90 |
| SB25m-1 | 6.6 | 1.84 | 1.64 |

**Table 8.6** Average Mol % $MgCO_3$ composition of mud samples from the inner marginal basins, Streaky Bay (EDAX field of view ~ 200 µm).
Conversion of Mg Wt. % to Mol % $MgCO_3$, after Smith and Nelson (1993)

The carbonate compositions of particles within the mud fraction vary from 0.0 mol % $MgCO_3$ to 6.6 mol % $MgCO_3$ when based on the EDAX-ZAF element quantification subroutine. The carbonate composition, with respect to mol % $MgCO_3$, of the particles can be correlated with the morphology of the particles (Table 8.7). The prismatic and to a lesser extent blocky particles tend to be composed of low average mol % $MgCO_3$ calcite minerals, whereas the tabular, composite and polygonal particles are generally composed of higher average mol % $MgCO_3$ calcite minerals. Ascidian spicules and foraminifer particles contain zero to low mol % $MgCO_3$. Calcite minerals and the sub-µm carbonate particles adhering to particles of siliceous sponge spicules are pure calcite.

| Sample | Particle description | Mg wt % | Mol % Mg $CO_3$ |
|---|---|---|---|
| SB10-14 | ascidian spicule | 0.0 | 0.0 |
| SB25-2 | ascidian spicule | 0.0 | 0.0 |
| SB08-3b | blocky | 0.13 | 0.4 |
| SB08-5 | blocky | 0.21 | 0.7 |
| SB08m-15 | blocky | 0.30 | 1.0 |
| SB09m-2 | blocky | 1.1 | 3.9 |
| SB10-4 | blocky/ composite | 0.28 | 1.0 |
| SB15m-13 | blocky/dissol/bored | 0.57 | 2.0 |
| SB08m-19 | composite | 0.80 | 2.8 |
| SB08b-22 | composite | 1.67 | 5.9 |
| SB17b-6 | composite | 0.38 | 1.4 |
| SB08m-12 | composite | 1.21 | 4.3 |
| SB09-6 | composite +diatom | 0.59 | 2.1 |
| SB15m-4 | composite particle | 1.2 | 4.3 |
| SB10-11 | composite/ foram | 0.17 | 0.5 |
| SB16-5 | diatom/ blocky | 0.12 | 0.4 |
| SB10-7 | foram particle | 0.0 | 0.0 |
| SB15m-16 | foram particle | 0.59 | 2.1 |
| SB09m-9 | polygonal porous | 1.00 | 3.8 |
| SB16-8a | polygonal porous | 0.36 | 1.3 |
| SB09m-14 | polygonal porous | 2.03 | 7.3 |
| SB10m-8 | polygonal porous | 2.48 | 8.8 |
| SB10-13b | polygonal/ porous | 0.18 | 0.6 |
| SB10m-4 | prismatic | 0.92 | 3.4 |
| SB08-4b | prismatic | 0.0 | 0.0 |
| SB16-10 | prismatic | 0.0 | 0.0 |
| SB16-3 | prismatic | 0.0 | 0.0 |
| SB08-7 | prismatic | 0.27 | 0.9 |
| SB09-1 | prismatic | 0.38 | 1.3 |
| SB16-6 | prismatic | 0.50 | 1.7 |
| SB23-4a | prismatic | 0.52 | 1.8 |
| SB10-17c | prismatic | 1.02 | 3.6 |
| SB25-4 | rhombic blocky | 1.88 | 6.7 |
| SB08a | sponge spic. $SiO_2$ | 0.0 | 0.0 |
| SB08m-9 | tabular | 0.85 | 3.0 |
| SB09-5 | tabular | 0.33 | 1.1 |
| SB08m-9 | tabular | 1.48 | 5.3 |
| SB16m-7 | tabular | 1.59 | 5.7 |
| SB08-1b | tabular /laminate | 0.37 | 1.3 |
| SB08m-8 | tabular, dissolution | 1.41 | 5.0 |
| SB08-5b | tabular/ elongate | 1.71 | 6.1 |
| SB08-3 | tabular/ laminate | 0.0 | 0.0 |
| SB08-2b | tabular/ laminate | 0.14 | 0.4 |
| SB09-7a | tabular/ laminate | 0.28 | 1.0 |
| SB16-11 | tabular/ laminate | 0.28 | 1.0 |
| SB10m-14 | tabular/ laminate | 1.23 | 4.4 |

Table 8.7. Ranked general morphology (1) and composition (2) (mol % $MgCO_3$) of selected mud-sized particles from the bulk and mud fraction samples, Inner Marginal Basins, Streaky Bay. The Mg weight % is taken from the SEM XL-30-EDAX element probe results. The mol % $MgCO_3$ is calculated from the Mg weight % using the conversion of Mg Wt. % to Mol % $MgCO_3$, after Smith and Nelson (1993).

## 8.7 DISCUSSION

### 8.7.1 Carbonate Content of Mud (Acid Digestion)

The carbonate content of the mud fraction can be generally correlated with that of the sand fraction. This varies from 91% to 96.3% and has a modal average of 93.4%. The sand fraction of the central basin and Blanche Port have a carbonate content higher than average (95% and 94.7%) and those of the northern and southern basin are slightly lower than average (92.4% and 92.5%). These percentages are taken from the results of grain counts on the sand fraction. (see Chapter 5). The higher carbonate content of these sediments is most probably due to the low energy conditions in the

central inner marginal basins (IMB) and Blanche Port, and the distance from the bulk of migrating sediments on the Northern and Southern shorelines, which have significantly more quartz.

### 8.7.2 MINERALOGY (XRD)

The XRD compositions of the bulk sample and its mud fraction are compared, to ascertain whether there are diagenetic changes occurring during the process of disintegration as the larger grains and fragments in the sediment are converted to mud-sized particles (Table 8.3). This is observed by comparison as grainsize diminishes, assuming increasing stability results as a consequence of neomorphism of the Mg-calcite minerals, ie. with the loss of Mg from HMC and IMC fragments. This comparison incorporates particles produced within and without the basins. Direct evidence for mud particle transport is not readily observable, however, as the sediment distribution is gradually skewed to finer grained to the inner areas of the bay. It is likely that fine particles have been transported from regions outside the IMB.

#### 8.7.2.1 Mud Mineralogy

The carbonate composition of the bulk samples and mud fractions consists of a mix of aragonite and magnesium calcite of varied mol % $MgCO_3$ (Table 8.3). The mol % $MgCO_3$ is generally less in the mud fraction than in the bulk sample. The difference represents a pattern of higher Mg calcite species being preferentially leached of magnesium ions from the grains during the early stages of diagenesis (Bathurst, 1975, Scoffin 1987, Nelson et al., 1988, James, 1997). This leaves the grains with a mineralogy trending towards the LMC end of the LMC - HMC continuum. The leaching (inversion) occurs during the degradation of a skeleton by physical (disarticulation, abrasion), biogenic (boring, mastication, ingestion and microbial disintegration) and chemical (maceration, dissolution) processes as the fragment or grain is being diminuted to mud-sized particles. The greater surface area created by the diminution of grainsize via these pathways accelerates the leaching process. This results in a higher proportion of the mud-sized sediment having the more stable lower Mg calcite species (Milliman, 1974).

Aragonite is ubiquitous throughout the bulk samples and mud fractions. Aragonite is generally dominant in both the bulk and mud fraction in two samples. The loss through dissolution of aragonite in the mud fraction of the samples is due to instability of aragonite grains as they degrade to silt-sized and more particularly sub-μm particles (Scoffin, 1987:Milliman, 1974, Bathurst, 1983). The dissolution (Henrich and Wefer 19860 or neomorphism (Reid and Macintyre, 1998) of aragonite, HMC, IMC and LMC particles occurs in a stability sequence where HMC is the unstable polymorph and LMC is most stable polymorph. The continuum of stability from least to most, depending on the ambient environment is:

HMC < ARAGONITE< IMC < LMC (Milliman, 1974, Bathurst,1975)

The occurrence of zero mol % $MgCO_3$ LMC is restricted to one sample (SB 08), and is co-dominant with IMC. This is because of the common occurrence of bivalves (especially Pectinids in the IMB), and bryozoans which are common epiphytes on the seagrass meadows on the seawards flank of southern IMB. LMC is sub-dominant throughout the samples and is usually sub-equal with IMC. This coupling correlates with the sequential loss of Mg from bryozoan fragments as they become diminuted within the mud fraction. HMC is sub-dominant in a significant number of sediments, but where present, it is not represented in both the bulk and mud fraction of the sediments analysed. The sources of HMC in the IMB is probably from coralline algae, serpulids (and foraminifera, possibly *Peneropolids* and *Miliolinids* mentioned by Milliman, 1974) all of which are found as epiphytes on the seagrasses of the sand shoals. HMC is not common in the mud fractions due to the ease with which crustose coralline algae (the most common contributor) disintegrates into μm -sized particles and is available to the magnesium leaching process.

**8.7.2.2 Skeletal Mineralogy**

The dominance of aragonite in all samples is probably due to a continual source of new biofragments, mostly originating from the abundant gastropods, bivalves and bryozoans in the immediate area. The skeletons of these fauna supply raw material for the ongoing disintegration of fragments through to mud-size, which on a large scale may be due to maceration, mastication or abrasion, which on the μm scale (mud) further maceration and possibly dissolution becomes dominant processes. The time that elapses during disintegration allows for aragonite to dissolve into the seawater either at the abrading edge or on a biodegrading surface or via mastication/ ingestion of grains.

The compositions of these samples can be compared with those of calcareous skeletons of organisms that inhabit the bay. Direct comparison of mud fraction to contributing organisms is difficult because the direct links from a given organism (to a generic level) to a particular skeletal fragment or particle cannot be confidently resolved. A broad comparison of calcareous skeletal animal and plant groups can give an indication of participating organisms contributing to the composition of the mud. These comparisons are based on frequency of skeletal grains within the sand and gravel fractions and their susceptibility to breakdown.

The common to abundant fauna and flora (described in section 8.5, i.e. bivalves, bryozoans, gastropods and coralline algae) appear to be the major contributors to the mud sized sediments. These contributors are highlighted by the variation of Mg carbonate composition within the sediment

analyses in Table 8.3 and are correlated with the skeletal compositions enumerated in Table 8.5 and the more general Table 8.4.

The dominant composition of the mud fraction is aragonite with significant skeletal material composed of LMC and IMC. The aragonite component volume appears to be relatively stable in the IMB when compared with IMC and HMC, although both aragonite and the IMC/HMC mol % $MgCO_3$ are both reduced in mud fraction when compared with the bulk sediment. It is interpreted that the Mg calcite/aragonite skeletal material in the mud fraction may have elevated rates of disintegration and dissolution (sensu Henrich and Wefer, 1986) and is in general outstripping the production of high Mg calcite/aragonite skeletal mud. The resultant particles either fully dissolve or are transported and deposited to the lower energy marine environment (inner marginal basins). The minimum size of particles observed being deposited in the inner marginal basins is approximately 0.2 μm (200nm).

#### 8.7.2.3 Non Biogenic Mineralogy

A minor source of allochthonous mud (see XRD results) in the inner marginal basins is of non-biogenic origin and is primarily siliciclastic. It occurs as quartz grains with fresh and altered accessory minerals (potassium feldspar, kaolinite). The quartz component probably originates from the erosion of quartz rich Precambrian felsic intrusive basement and the erosion of the Pleistocene Bridgewater and Glanville Formations. These Pleistocene formations contain between 5 % and 12 % 'terrigenous' material (Farrand and Belperio, 1987; Belperio, 1988; Wilson, 1991).

Feldspar is also a major constituent of the felsic intrusives that occur at the entrance to Streaky Bay. These are probably the main source of the feldspar in the mud fraction, as the sand and gravel fractions proximal to Olive Island (Figure 2.4) and the subaqueous outcrops contain significantly higher quantities than elsewhere in the bay. Trace feldspar is also recorded in sediments from the Bridgewater and Glanville Formations.

Dolomite is a significant component of the Bridgewater and Glanville Formations. It is present as rare rounded rhombs in the framework, as isopachous rinds, as a cryptocrystalline matrix, and as veins in the calcretised sediments of these formations (Farrand and Belperio, 1987; Belperio, 1988; Wilson, 1991). The dolomite that is recorded in the analyses occurs at locations inboard from sites where the sea-floor (Bridgewater Formation) is being actively eroded, ie the northern tidal channel and the central and northern inner terrace. It is also found in the Blanche Port sample where the shorelines are lined with eroding low cliffs of the Bridgewater Formation and remnant shore flanking outcrops of the Glanville Formation.

### 8.7.3 Composition of Skeletal Material and Sediment (XRD)

The compositions of bryozoans analysed at Streaky Bay fall within the compositional range of bryozoans found in Australia and New Zealand waters (Smith and Nelson, 1993; Bone and James 1993, 1998). The bryozoans range in composition from 7.5 to 9.5 % mol $MgCO_3$ with one analysis including aragonite and another including 3.0 % mol $MgCO_3$ LMC. The composition of the bulk of the species analysed (48) in New Zealand fall in the range from 3.5 to 10 % mol $MgCO_3$ with all species falling in the range from ~1 to 11 % mol $MgCO_3$. A significant proportion of the New Zealand bryozoans is bimineralic with both Mg calcite and aragonite being present in the structure (Smith and Nelson, 1993).

The serpulid and spirorbid analyses differ from the established % mol $MgCO_3$ in Table 6.4. The reported compositional range for cool-water serpulids and spirorbids is between 6 and 8 % mol $MgCO_3$. This IMC is a minor component in the serpulid analysis, whereas both analyses contain co-dominant 13.5 % mol $MgCO_3$. The serpulid (*Galeolaria* sp.) is composed of HMC with minor IMC and the spirorbid (*Romanchella* sp. or *Pileolaria* sp.) is composed of aragonite with sub-dominant HMC.

Spirorbid exoskeletons usually increase in aragonite content with increasing water temperature. Bornhold and Milliman (1972) showed that at 10° C they contain little or no aragonite and at 18° there is an increase to ~ 15% aragonite. The spirorbids at Streaky Bay are composed of approximately twice the aragonite to HMC, which could be a result of warmer water in the vicinity of the shallow sand shoals.

Aragonite recorded in barnacles and rhodoliths may have lodged as mud sized particles in the small pores and chambers of these skeletons as the presence of aragonite is not recorded from these groups in the literature.

### 8.7.4 Particle Morphology (SEM)

The significant particle morphologies that dominate the mud fraction are prismatic and tabular. These prolific morphologies are principally the result of the disintegration of the prismatic and nacreous layers in mollusc skeletons. The composition of the prismatic particles is usually LMC or aragonite (Table 8.7) with rare prismatic particles composed of IMC. The composition of the porous polygonal particle is high IMC, which is a combination of the particle and sub-μm particulate hash (platelets and crystallites) adhering to the particle. The tabular particles range in composition from calcite/ aragonite to high mol % $MgCO_3$ IMC. These particles are also varied in origin, as is the composition; ie from molluscan nacreous/foliate layers, larger bryozoan laminate particles and exfoliation laminae of foraminifera. The larger laminate particles of bryozoans are an intermediate breakdown component before further degradation to sub-μm platelets.

The average carbonate composition of the blocky particles is in the range of LMC-aragonite and the morphology is comparable with homogeneous structure of molluscan skeletons which are composed of sub-μm crystallites. The porous polygonal particles range in composition from LMC to high mol % $MgCO_3$ IMC. The porosity of these particles is due to extensive μm sized boring and significant disintegration, which gives the particle an open loosely bound structure of elongate platelets or crystallites. These particles are derived from the disintegration of bryozoans by ingestion, dissolution and boring, which exposes the laminate micro-structure, and the homogenous, significantly bored and dissolved structure of some molluscs. The highly porous composite particles are composed of the products of disintegration of numerous skeletal organisms that have a composition of IMC to HMC. The carbonate component of sub-μm particles are derived principally from bryozoans (platelets), coralline algae (crystallites), molluscan nacreous layers (platelets), foraminifera (crystallites and larger platelets) ascidians and coccoliths. Rare larger bladed particles are attributable to the disintegration of brachiopod valves (Figure 8.27d). Fragmented siliceous diatom lustreless and sponge spicules are a ubiquitous component of the composite particles (Figure 8.20.d).

### 8.7.5 DISINTEGRATION PATHWAYS OF VARIOUS SKELETAL ORGANISMS

Molluscs disintegrate into larger prismatic, tabular and blocky particles which have a grainsize from 10 μm to 62.5 μm. These particles in turn break down into μm to sub-μm platelets and crystallites depending on the mineralogy of the skeleton. The principal modes of disintegration of prismatic particles is through abrasion, boring and maceration. Maceration does not appear to be a major factor in mollusc disintegration because of the stability of the constituent minerals of the skeletons although the laminate particles appears to disintegrate relatively rapidly once separated from the prismatic layer.

Weaknesses in the bryozoan carbonate skeleton as a result of the degradation of fine organic layers between the laminae induce μm -scale layers to flake off the larger particle as indicated on the fragment edge (Figure 8.10d) and the fragment face between the pores (Figure 8.10e) (see also Alexandersson 1978). Micrometre–sized platelets were produced by gently using a fine needle probe as a scraper or artificial masticator (Figure 8.10b). These platelets can represent the effects and products of rasping graziers and borers (gastropods, chitons, sponges, algae and fungi) on the bryozoan skeleton. The μm to sub-μm platelets that are produced when bryozoan laminar particles disintegrate, become rounded and smaller through maceration during transport to the IMB and constitute part of the sub-μm 'matrix' of the mud fraction (Figure 8.27e). Micrometre-sized sub-crystallites and thick platelets are produced on the disintegration of bryozoans (some cheilostomes) with polygonal fracturing patterns and porous nature (Figures 8.7e, 8.7f), which are present in the scanning electron micrographs of the bulk sediment of SB17b and SB08b in particular.

The disintegration of foraminifera primarily produces tabular particles which on further maceration liberates sub-μm crystallites and irregular rhombs. Foraminifera provide comparatively little material to the sub-μm fraction. This may be a result of high diatom populations providing a biochemical protection against dissolution once the chambers have been breached and a conducive micro-habitat created (Echoless, 1993). The breaching of the foraminiferal chambers can occur by ingestion and selective corrosion by carnivorous gastropods and bacterially induced dissolution of the chamber wall (Freiwald, 1995).

Occurrence of coralline algae particles are not common in the larger sized mud fraction as result of the tendency to degrade rapidly through maceration, ingestion and the degradation of fine organic material in the thallus. The μm crystallites resulting from the disintegration of gravel fragments and sand-sized grains may either migrate downwards through the permeable pathways in the predominantly sandy substrate, or be transported and deposited in the inner marginal basins where currents are low enough to allow deposition. This deposition depends on the tides and wind forced currents, which can mobilise these particles for deposition within the bay or transport them from the bay out to the low energy shelf edge.

The primary substrate for the growth of the common crustose coralline algae in the bay are the leaves of the seagrass *Posidonia* sp. which are actively growing over a significant portion of the sea-floor in the shallower central sand shoal area. The crustose thalli present on the leaves have a size variation ranging in diameter from < 0.1 mm as newly established thalli, up to ~5 mm where they tend to coalesce and form a continuous layer over the surface of the leaf. The life span of an average blade of seagrass is approximately three months (McComb et al., 1981). After this time the blades become detached from the plant and are subjected to currents and wave action. The blades at this stage may have a coverage of 70% coralline algae and other epiphytes (bryozoans and serpulids). Often these blades, particularly after a storm, accumulate on beaches with thickness reaching up to 50 cm in places. These accumulations reach to 3 m deep on some beaches along the coast of South Australia (Brown et al., 1998). The organisms become separated and deposited into the sediment on the disintegration of the blade. It is interpreted that the crystallites of coralline algae resulting from the disintegration of these thalli from these blades are transported and probably deposited in the inner marginal basins or other low energy deposition sites. Between 10 g/m$^2$ and 400 g/m$^2$ of calcium carbonate maybe produced from seagrass crops and a significant proportion of this is crustose coralline algae (Brown et al., 1998). Articulated coralline algae present on the blades disintegrates into rods and may accumulate as sand in the seagrass meadows.

Dissolution and rhombic-fracture patterns are discernible on most of the echinoderm particles that have been scanned by SEM and are similar to the dissolution fabrics of Henrich and Wefer (1986). The particles produced by the biological breakdown from echinoids, fish and sponges have a typical rhombic morphology (Figure 8.27f). The echinoderm particles show abundant evidence of pitting (Figure 8.15b), which is interpreted to be point dissolution marks possibly resulting from bacteria infesting the surface, which then become the locus for further dissolution of the particle (Freiwald, 1995). Dissolution fabrics are also evident on fracture surfaces and the surfaces of micro-bores indicating that maceration is exacerbated by mastication, boring and chipping (Figure 8.15b).

Brachiopod valve disintegration is indicated in the mud fraction by bladed laminar particles, which are typical of late stage degradation (Figure 8.27d). The pattern is similar to that of the nacreous layer of molluscs except brachiopod particles are significantly elongate and the dissociating laminae appear thinner than molluscan platelets. These particles are rare in the mud fraction reflecting the low population of brachiopods.

### 8.7.6 Morphology of Cool-water versus Tropical Carbonate Muds

The disintegration of crustose coralline algae provides an analogue for the disintegration of temperate carbonate organisms and the production of cool-water carbonate muds. It is interpreted that crystallite production is achieved through disintegration of macerated coralline algae. This is similar to the disintegration of calcareous green algae in the tropical realm. Cool-water carbonate production is curtailed by nutrient supply (James, 1997), maceration and dissolution (Henrich and Wefer,1986) rather than enhanced by prolific growth and further inorganic precipitation as is the case of tropical marine carbonate production (Reid and Macintyre, 1998). There is difficulty in determining the difference, at the μm level, between some temperate and tropically produced carbonates when comparing the component biogenic particles with the SEM micrographs of Lasemi and Sandberg (1993 - figure 13.1b & c), Greenstein (1995) and Bathurst (1983). However, difference becomes significant when including the full suite of tropical components, ie. oolites, aragonitic microspar and peloids.

Research at the μm-level indicates that some tropical micritic 'inorganic' carbonate precipitation is being mediated by algal or microbial/bacterial activity even though the carbonate is not directly derived from the organism (Folk, 1993). This points to a more encompassing realm of organic carbonate production. However, Reid and Macintyre (1998) conclude that inorganic syndepositional recrystallisation with significant textural changes is occurring with overgrowth extensions of crystallites or in the formation of blocky micrite. The mineralogy in this process is either remaining the same, converting from aragonite to Mg calcite.

It is possible that at this scale both the temperate and tropical pathways of organic carbonate production rely on the same basic molecular structure to create the primary organic crystallites and platelets so it is not surprising that some of the particles have similar morphologies. The organic platelets and crystallites that are liberated during maceration processes in the temperate regime appear similar to the Mg calcite and aragonite particulates which are produced in the tropical or warm water realm (figure 13.1b & c, Lasemi and Sandberg 1993). The difference in mud accumulation lies with the significantly higher rates of dissolution (Henrich and Wefer, 1986), maceration and the low skeletal growth rate in the temperate regions, versus the relatively higher skeletal productivity, propensity for precipitating cements as skeletal overgrowths and micritic crystallites, oolites, micritic aggregates and the stability of carbonates in the tropical realm.

## 8.8 CONCLUSIONS

The unusual morphology of several embayments on the West Coast of the Eyre Peninsula i.e. relatively deep water inner regions, has provided sites for the deposition of mud derived from marine sources. This feature has presented an opportunity to analyse and characterise muds from environments that represent a significant shallow marine marginal lithofacies present in embayments along this 1500 km section (West Eyre Peninsula) of the largest cool-water carbonate province on Earth.

Broadly, the dominant mineral component of the muds from these inner marginal basins is calcium carbonate, which, when using Streaky Bay as model, averages 93% in the mud and the sand fractions. This carbonate content is dominantly aragonitic with subequal portions of low (LMC) and intermediate (IMC) magnesium calcite and minor high (HMC) magnesium calcite. The aragonite content of the bulk sediment is significantly higher than the mud fraction with LMC being of higher content than IMC. IMC is generally higher in the mud fraction and predominantly derived from disintegrating bryozoan particles.

The compositions of the sediments can be compared with the bulk composition of the calcareous skeletons of organisms that inhabit the bay. A broad correlation of calcareous skeletal animal and plant groups present and their susceptibility to disintegration can give an indication of participating organisms contributing to the composition of the mud. This comparison of bulk composition of skeletal material correlates closely with that of organisms found in other cool-water carbonate realms both in the southern and northern hemisphere. A notable exception has been the serpulids and spirorbids whose shells contain HMC and aragonite with minor LMC. The referenced composition is usually LMC (6 to 8 % mol $MgCO_3$). The origins of significant calcium carbonate particles in the

mud fraction, in order of abundance, are from molluscs, bryozoans, coralline algae, foraminifers, echinoderms, sponge spicules, serpulids and minor contributions from brachiopods, tunicates, corals and coccoliths.

Significant biogenic silica in the carbonate sediment is attributed to sponges and abundant diatoms. Contributions of minor non-biogenic origins to the mud fraction are siliciclastic particles i.e. quartz, potassium feldspar and kaolinite, which originate from the erosion of quartz-rich Precambrian felsic intrusive basement, and the Pleistocene Bridgewater and Glanville Formations. Minor dolomite, which occurs in some sediments, is derived from the eroding Bridgewater and Glanville Formations.

The disintegration of skeletal material, which composes the muds, appear to be produced through maceration coupled with medium to high energy sea movement. Possible dissolution of mud-sized skeletal material appears to be occurring in Streaky Bay. This is similar to studies of dissolution processes in waters of the Drake Passage, South America.

The dominant morphology of particles in the mud fraction are prismatic and tabular. The grainsize of these particles range from 20 to 63 μm, which is a significant fraction of the mud. The prismatic particles are composed of LMC or aragonite and the tabular particles are composed of LMC of aragonite and high mol % $MgCO_3$ IMC. Other significant particle morphologies are porous polygonal, blocky and composite particles. Polygonal particles are composed of LMC to high mol % $MgCO_3$ IMC and consist of sub-μm platelets and crystallites whereas blocky particles are usually composed of LMC or aragonite with an homogenous structure consisting of sub-μm crystallites. Composite particles are composed of a range of mineralogies from LM < IMC and HMC. They consist of disintegrated particles from numerous skeletal organisms i.e. bryozoans (platelets), coralline algae (crystallites), molluscan nacreous layers (platelets), foraminifera (crystallites and larger platelets) ascidians and coccoliths, and appear in some instances to be of faecal origin.

The skeletal disintegration of the faunal groups into mud-sized particles fall into distinct pathways in this cool-ware realm i.e:

- Molluscs disintegrate into larger prismatic, tabular and blocky particles which have a grainsize from 10 μm to 62.5 μm. These particles in turn break down into μm to sub-μm platelets and crystallites depending on the mineralogy of the skeleton.
- Bryozoans disintegrate to coarse laminate particles then on further maceration, μm -scale layers are induced to flake off the larger particles. Micrometre-sized sub-crystallites and thick platelets are also produced on the disintegration of some cheilostome bryozoans with polygonal fracturing patterns and porous nature.

• The disintegration of crustose coralline algae produces friable platey particles, which on further disintegration produces the significant μm -sized HMC crystallites observed in the composite particles. Articulated coralline algae disintegrates into rods and further into squat sub-μm crystallites, but this process appears to take much longer than with the crustose coralline algae

• The disintegration of echinoderms typically produces sub-rhomboidal particles, which show abundant evidence of pitting from bacterial infestation and subsequent dissolution.

• Foraminifera primarily produce tabular particles, which on further maceration liberate sub-μm crystallites and irregular rhombs.

• Brachiopod valves disintegrate into curved bladed laminar particles. Their sparsity reflects the low population of brachiopods.

Throughout the study no evidence of skeletal overgrowth was observed on the disintegrating particles in the mud fraction, which verifies the unsaturated condition (with respect to carbonate) of the marginal cool-water environment.

A similarity at the micrometre level (0.5 - 5 μm) is observed between cool-water composite particles and micrographs of tropical sediments of the same resolution, especially where calcareous algae (coralline red and green) disintegration is significant. The presence of inorganic aragonite needles in tropical muds signify the difference in settings. When cool-water carbonate muds are observed at lower magnifications in the silt range (10 - 50 μm) the differences become immediately obvious with dominant prismatic and tabular particle morphology. The difference in mud accumulation between these two environments lies with maceration and the low skeletal growth rate and significant rates of dissolution in the temperate regions, and the relatively higher skeletal productivity, propensity for precipitating cements as skeletal overgrowths and micritic crystallites and the stability of carbonate muds in the tropical realm.

# CHAPTER NINE

# COOL-WATER CARBONATE LITHOFACIES

## 9.1 INTRODUCTION

The lithofacies in Streaky Bay reflect the local:- abundance and variation of marine life; hydrodynamics; substrate; and surrounding lithology. The bay is ideal for studying the lithofacies continuum from a marginal high energy semi-protected setting to the inner shelf facies of the eastern GAB as it represents a variety of depositional environments that is common in embayments on the western Eyre Peninsula (Figure 2.1) . The comparison of this continuum with shelf facies was facilitated by examining sediments collected on a transect from Streaky Bay to shelf edge (CSIRO Franklin 03/98 cruise- James et al. 2001).

Shelf investigations on the southern margin have been confined to the open relatively deeper off-shore shelf waters (Conolly and von der Borch, 1967; Wass et al., 1970; Exon and Lee, 1987; Davies et al., 1989; Wilcox et al., 1988; Fuller et al., 1994; Bone and James, 1993; Boreen et al., 1993; James et al, 1992, 1994, 1997, and 2001) James and von der Borch, 1991; von der Borch and Hughes-Clarke, 1993). The studies of Lablack (1985), Freeman (1985) and Hill (1994), investigated the coastal embayments of Tourville, Coffin, and Baird Bays on the western Eyre Peninsula, but they are relatively well protected from the swells of the Southern Ocean. Fowlers Bay, on the far west of the peninsula (Figure 2.1), is an open embayment with a minimal protected shallow water area, whereas

Streaky Bay has a combination of deeper open and shallower protected areas within the embayment, which represent all these environments.

## 9.2 DISTRIBUTION OF FACIES COMPONENTS WITHIN STREAKY BAY

The distribution of major carbonate producing organisms and terrigenous sediment contributing to the sand-size fraction at Streaky Bay has been delineated in Chapter 6. The component content of the sand-sized fraction of the samples was determined by point count, with reference to the major biogenic groups and eroded terrigenous components. The major components (i.e. mollusc, foraminifera, bryozoa, echinoderm, coralline algae, aeolianite and quartz/ lithic fragments) in the sand fraction have been used for the basis of the lithofacies. These lithofacies have been modified and refined by sediment texture and the dominance of recognisable organisms (plant and animal) and terrigenous sediment in the gravel fraction.

The distribution of biota and minor terrigenous sediment from the sand and gravel fraction of sediments is shown in Appendix Two. This appendix summarises information derived from the samples collected from the sea-floor at Streaky Bay and the transect to the shelf edge (CSIRO RV *Franklin* 03/98), as well as the descriptive sediment name and water depth from which it was sampled. The distribution of organisms and terrigenous sediments found in the gravel fraction of the samples are also tabulated in Appendix Two. Significant concentrations and the locations of these principal components are briefly summarised.

**Molluscs** and fragments show greatest abundance in sediments from the inner marginal basins and central tidal delta and are common in the northern outer terrace whilst being the dominant component in sediments throughout the bay (Figure 6.1).

**Bryozoans** occur mostly in the central outer portion of the bay where there are significant variations in substrate environment from eroded rocky sea-floor to soft sandy sediments. They are also abundant in the north-eastern near-shore area of the bay (Figure 6.3). A significant amount of < 63 μm sediment can be attributed to bryozoans (Chapter 8)

**Foraminifers** are present in highest concentrations in the sea grass meadows of the central area (*Posidonia* sp. and *Amphibolis* sp.), and in the outer terrace region where abundant brown and calcareous red algae are present (Figure 6.2).

**Coralline algae** fragments are found in significant numbers throughout all the sediments in the bay. Highest concentrations are found in the central terrace area and the gravelly/ rocky substrates at the entrance (Figure 6.5). Seagrass meadows support a significant population of encrusting coralline algae. Fragments are not readily discernible within the sand and gravel but are recognised in the mud fraction (Chapter 8).

**Echinoderms** are most common in the central and northern terrace areas and the inner marginal basins, particularly the central and southern basins (Figure 6.4).

**Calcareous Aeolianite** fragments occur in high concentrations along the northern coastal margin, northern tidal channel, southern coastal margin, and northern entrance area in the vicinity of the central submarine topographic high (Figure 6.7). The calcareous aeolianite is derived from erosion of the Bridgewater Formation, which is present as the seafloor rocky substrate and low to high cliffs surrounding the bay.

**Quartz/ Lithic** components occur in highest abundance in the central and southern entrance area in the lee of Olive Island with a local high on the central inner terrace near a sea-floor high. Significant concentrations (> 5 %) are distributed over most of the bay (Figure 6.8). Quartz/lithic grains are derived from intrusive igneous and metamorphic rocks, which are present at the entrance of the bay on Olive Island and the northern area of the entrance

## 9.3 SEDIMENTARY LITHOFACIES

The determination of lithofacies can be based on visual estimations of dominant sediment components and grain-size distribution over a given area. This is, however, based on an educated subjective (qualitative) view of components and their spatial distribution. The lithofacies of Streaky Bay were developed in two ways, firstly in the preliminary interpretation of the data and secondly by statistical methods. The preliminary interpretive facies (based on data from Transect 1) were proposed before the statistical facies analyses. Significant correlation was found between the two methods.

### 9.3.1 INTERPRETIVE LITHOFACIES

Initial interpretive lithofacies were based on preliminary point count results before statistical clustering of sand components in sediments from all transects. This preliminary information included component sand grain counting and gravel component dominance in sediments from the East-West Transect No. 1. The distribution of these initial interpretative lithofacies was based on textural distribution, sand and gravel composition and related to bay morphology (Daniel and von der Borch, 1994). These preliminary lithofacies were as follows:

(i) Reworked calcareous aeolianite/ molluscan sand;

(ii) Fine sandy molluscan/ echinoid mud;

(iii) Molluscan sand

(iv) Fine to medium molluscan/ foraminiferal sand;

(v) Coarse quartzose mixed bioclastic sand.

The distribution of the lithofacies is controlled mainly by water depth and substrate type:

(i) <2m:- near-shore and linear sandbanks- predominantly molluscan;

(ii) 2-7m:- seagrass, medium sand- molluscs, encrusting bryozoans, foraminifera;

(iii) 7-12m:- fine sandy mud- molluscs, echinoids;

(iv) 12-20m:- coarse sand to rocky bottom- molluscs, bryozoans, red algae, brachiopods, ophiuroids, ahermatypic corals and brown algae;

(v) >20m:- outer deep water (to 40m - limit of study) very coarse sand to gravel with rocky substrate- predominantly molluscan with pockets of abundant quartz.

The distribution of the lithofacies became complex as more data was incorporated into the study, with similar isolated pockets of lithofacies being found in disparate areas of the bay. It was clear that a statistical clustering method for determining lithofacies would be the most appropriate as these preliminary lithofacies were based on only one transect. Nevertheless, the principal result of this interpretive method suggested that the lithofacies and their delineation were controlled by bay morphology.

### 9.3.2 Statistical Determination of Lithofacies

Quantitative methods of determining lithofacies by statistical analysis presents a more accurate result than the interpretative method, by using sample correlation by clustering. The component percentages of the sand fraction (the dominant grain-size across the sea-floor of Streaky Bay) were entered into a data base and clustered according to Wards Method (Chapter 3, Methods).

The JMP statistical programme package (SAS Institute Inc., USA, 1994) was used to cluster the samples from three to six clusters, excluding single samples as clusters after comparing their component details with the encompassing facies. The results were overall well defined images of lithofacies distribution. The components of each facies are listed in order of abundance when described in the models below. A range from three to six clusters are plotted against sample station sites on separate maps and highlighted to delineate possible lithofacies (Figures 9.2 to 9.5). Lithofacies numbers used are those based on the numbers used in the five cluster model, so that numbers in the different models represent the same facies.

#### 9.3.2.1 Three Lithofacies

Lithofacies 1, an aeolianite/ mollusc/ quartz lithofacies where the dominant components are aeolianite and molluscs. Lithofacies 3, a molluscan/ bryozoan/ coralline algae/ foraminifera/ aeolianite lithofacies with dominant components of molluscs and bryozoans. Lithofacies 5, a molluscan/ echinoid/ quartz/ foraminifera lithofacies in which the mollusc component is dominant.

The lithofacies are delineated by three clusters show a distribution similar to the substrate type i.e.;

Lithofacies 1; sand shoals, northern and southern terrace and isolated areas at the entrance,

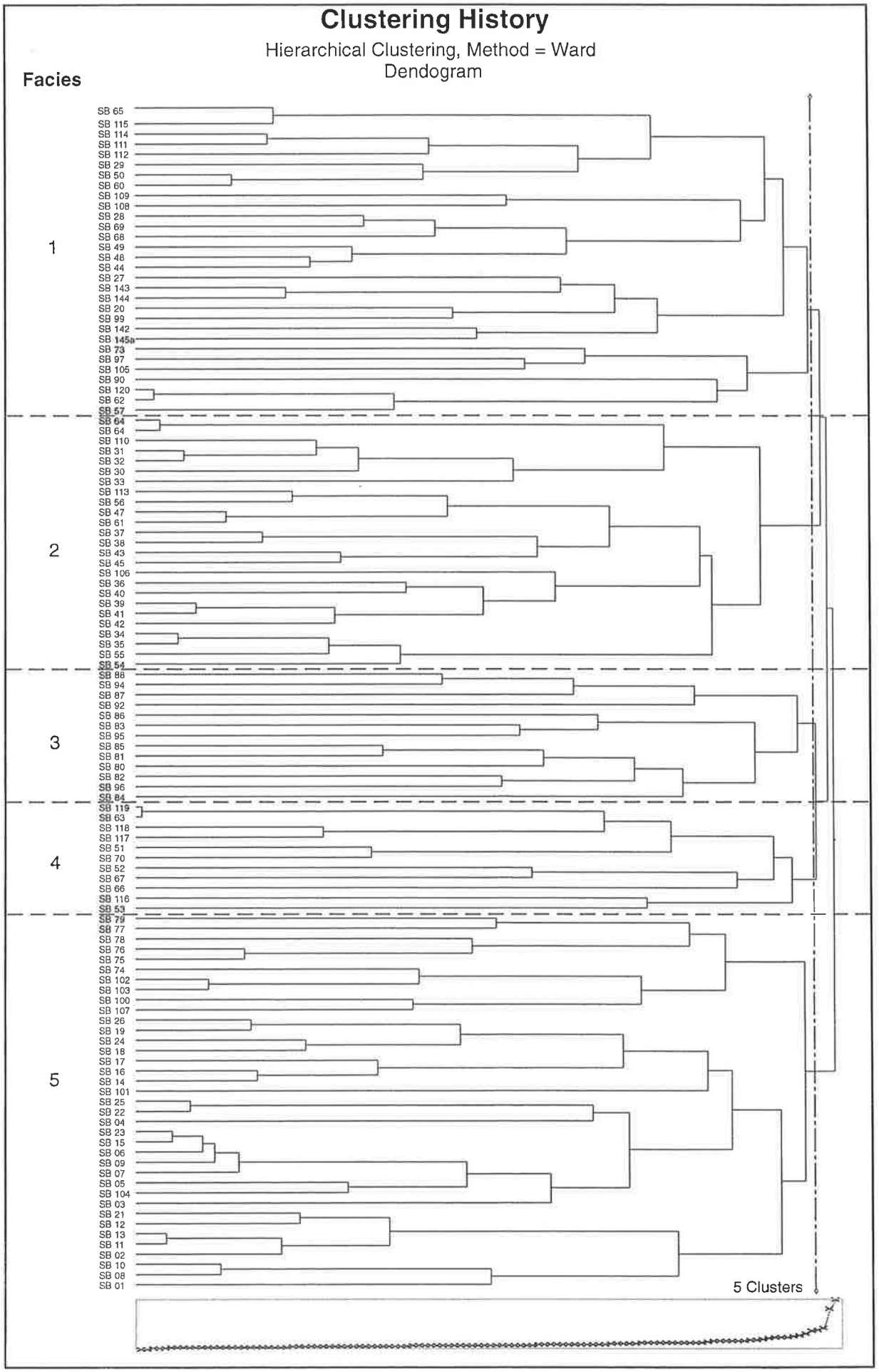
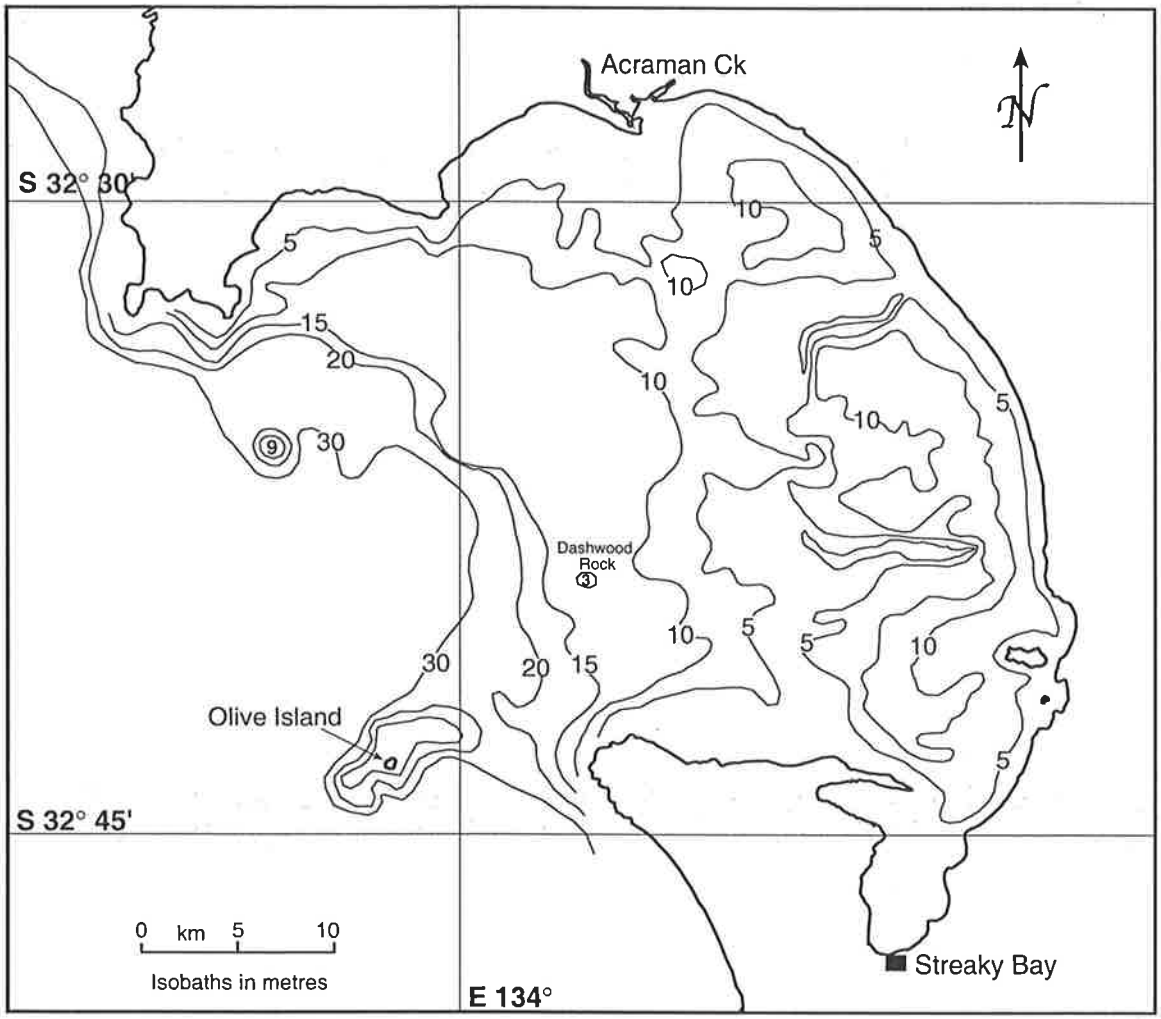



Figure 9.1 Clustering history of sampled Streaky Bay sediments, highlighting five significant clusters.




Bathymetry of Streaky Bay

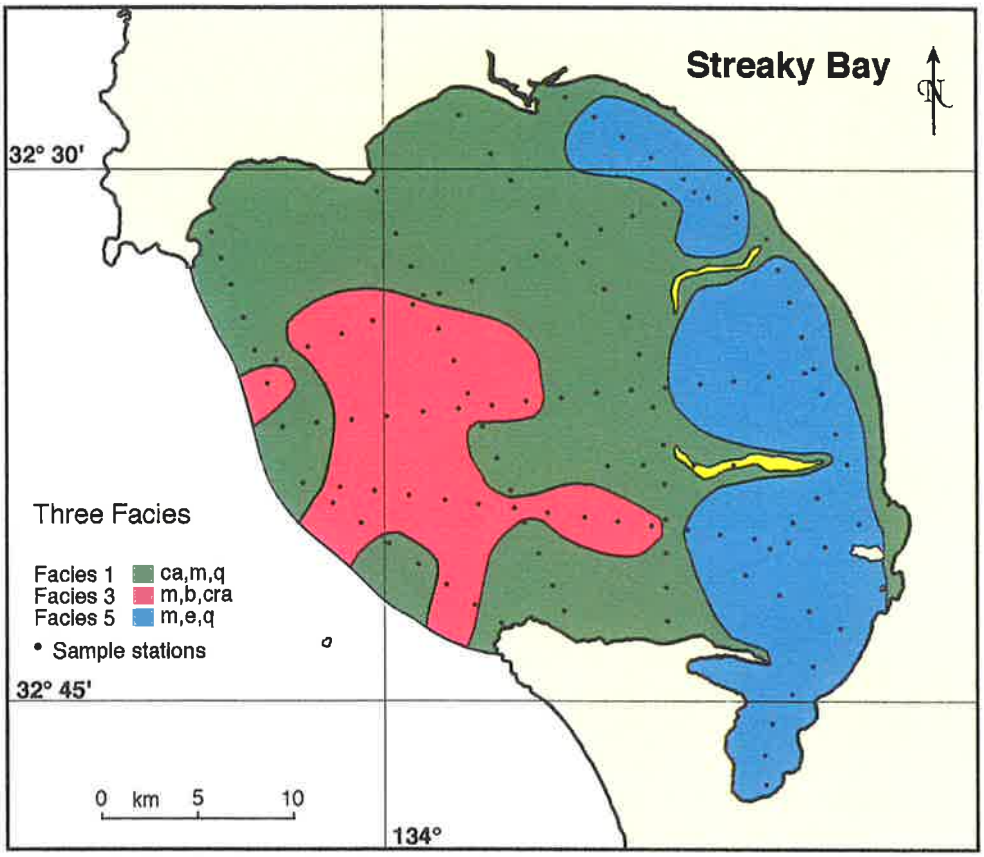



Figure 9.2 Distribution of lithofacies, clustering three dominant groups. Components of each facies is summarised in the legend, ranked in order of abundance.
Key to the summary: Molluscan-m; Foraminifer-f; Bryozoan-b; Coralline Algae-cra; Echinoderm-e; Calcareous aeolianite-ca; Quartz/lithic-q.

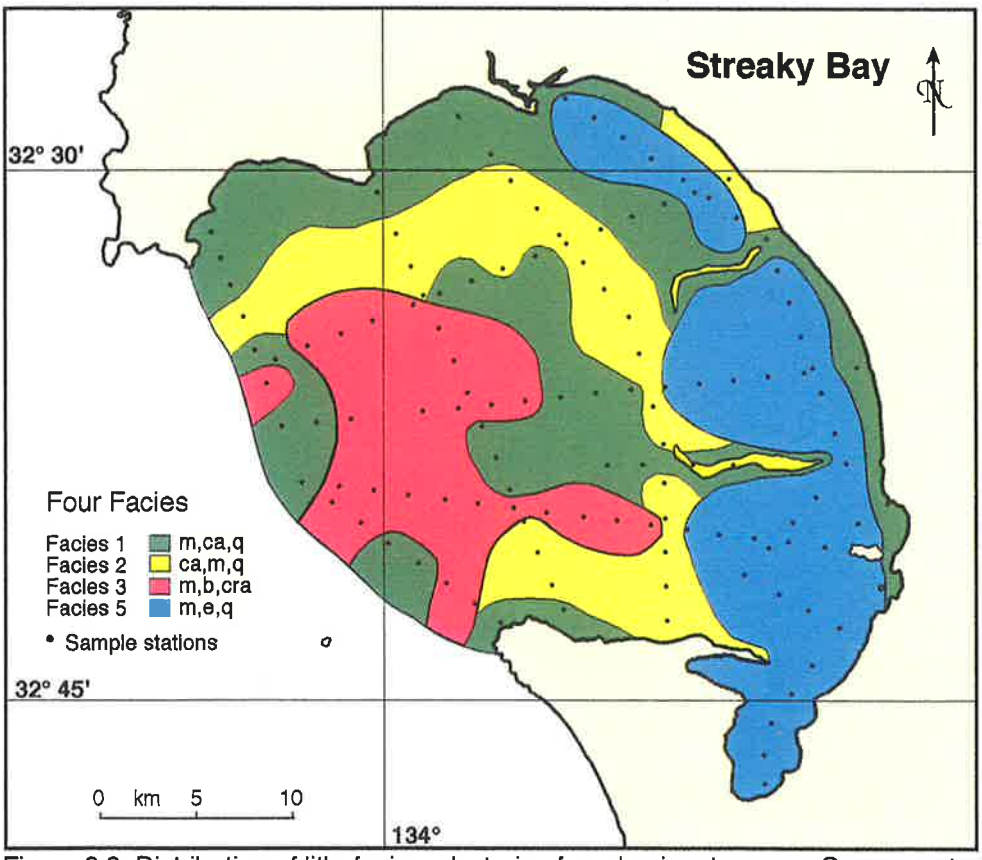



Figure 9.3 Distribution of lithofacies, clustering four dominant groups. Components of each facies is summarised in the legend, ranked in order of abundance.

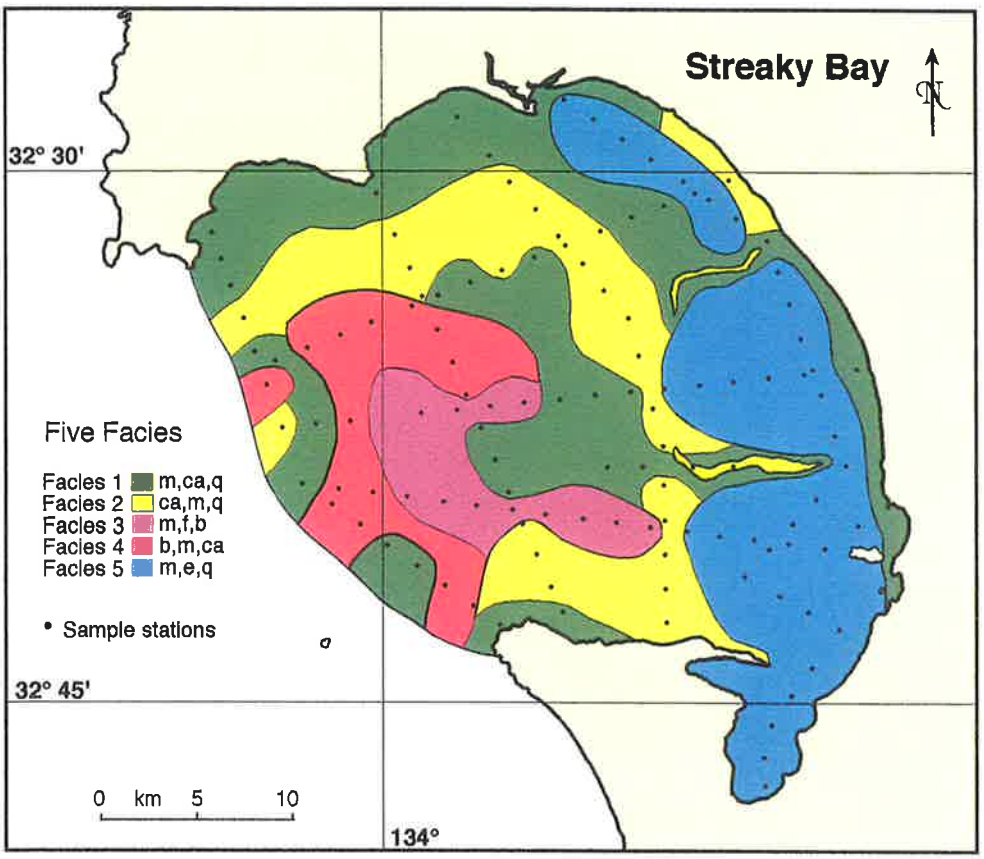



Figure 9.4 Distribution of lithofacies, clustering five dominant groups. Components of each facies is summarised in the legend, ra nked in order of abundance.
Key to the summary: Molluscan-m; Foraminifer-f; Bryozoan-b; Coralline Algae-cra; Echinoderm-e; Calcareous aeolianite-ca; Quartz/lithic-q.

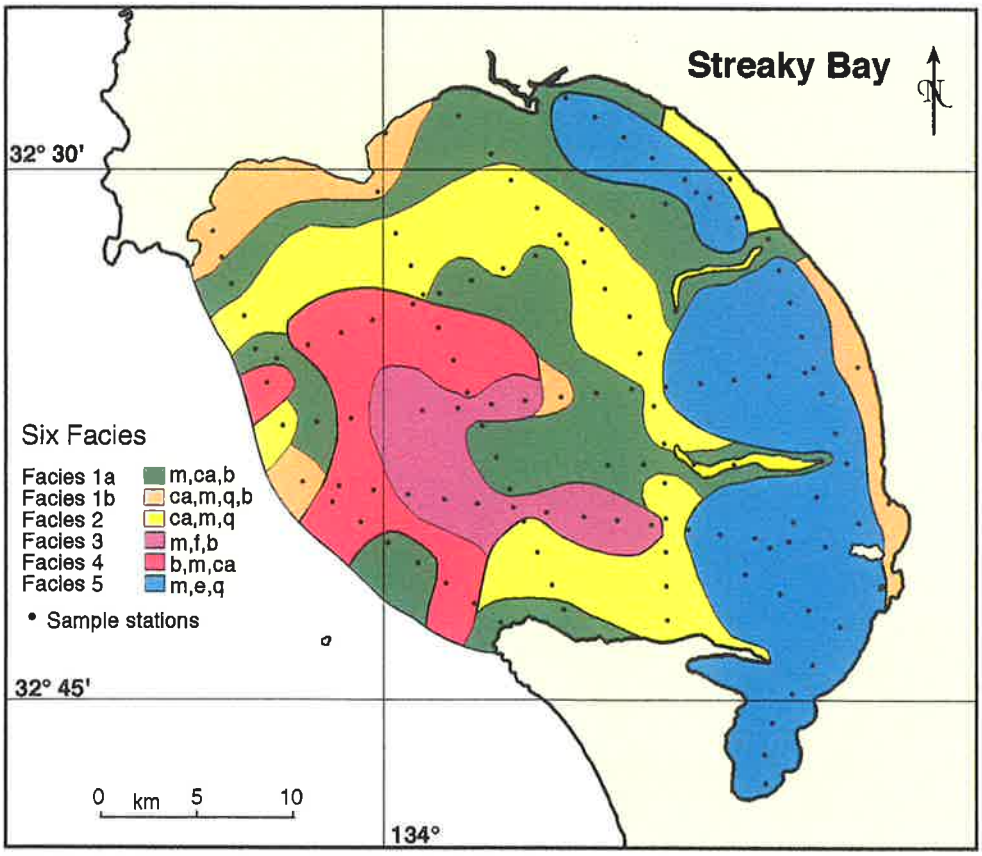



Figure 9.5 Distribution of lithofacies, clustering six dominant groups. Components of each facies is summarised in the legend, ranked in order of abundance.

Lithofacies 3; central terrace and entrance areas,
Lithofacies 5; inner marginal basins and Blanche Port (Figure 9.2).

#### 9.3.2.2 Four Lithofacies

The distribution of lithofacies is similar to the three facies model but Lithofacies 1 is subdivided. This subdivision is based on higher aeolianite and quartz content. Lithofacies 1 now consists of molluscan/ aeolianite/ quartz/ bryozoan as the dominant components and Lithofacies 2 is composed dominantly of aeolianite/ molluscan/ quartz (Figure 9.3).

Lithofacies 1 covers the area of the northern and central terrace, the central eastern coastal margin and isolated pockets in the entrance and southwest coastal margin. Lithofacies 2 is limited to the shallower areas of the sand shoals and areas on the southern coastal margin, northern and southern inner terrace with isolated occurrences on the northeast coastal margin and central entrance. Lithofacies 3 and 5 maintain the same compositions and distribution patterns as above.

#### 9.3.2.3 Five Lithofacies

Lithofacies 3 of the previous models is subdivided in this model, to a central inner Lithofacies 3, which occupies the central inner terrace area, and an outer surrounding Lithofacies 4 that occupies the entrance and part of the northern terrace. A small outlier of Lithofacies 4 occurs in the northern entrance area (Figure 9.4).

Lithofacies 3 is subdivided into 3 and 4 with respect to the variable subdominance of foraminifera and aeolianite. Lithofacies 3 is a molluscan/ foraminifera/ bryozoan lithofacies with significant coralline algae and Lithofacies 4 a bryozoan/ molluscan/ aeolianite lithofacies with significant coralline algae. Although the coralline algae component is ranked third in Lithofacies 3 of the two above clusters, the foraminifera and aeolianite components have a higher average when the facies is subdivided.

#### 9.3.2.4 Six Lithofacies

Lithofacies 1 is subdivided further in this model where isolated pockets containing high percentages of quartz and aeolianite are highlighted. This facies is subdivided into Lithofacies 1a whose dominant components are sub-equal molluscan-aeolianite/ bryozoan/ quartz and Lithofacies 1b, which is dominated by aeolianite/ molluscan/ quartz with variable amounts of bryozoans and foraminifera (Figure 9.5).

Lithofacies 1a occupies the main body of Lithofacies 1, i.e. the northern and central inner terrace, elongate sand banks and isolated areas in the entrance and southwest coastal margin. The minor Lithofacies 1b occurs in discontinuous pockets on the northwest and central eastern coastal margins with smaller areas in the northern entrance and inner central terrace.

#### 9.3.2.5 Seven and Eight Lithofacies

Clustering for seven and eight lithofacies were investigated with the programme and plotted on to a base map, but in each case the cluster divisions became unwieldy and limited in conveying an overall picture of major facies and the transitions occurring in the bay. The cluster distribution for seven lithofacies resulted in the subdivision of the inner marginal basin Lithofacies 5 that incorporated a portion of the east/ west transects based on the presence of echinoderms in the central areas of the basins. Lithofacies 3 was subdivided in the distribution of eight clusters. The middle portions of the southern and central east-west transects were divided, with coralline algae becoming significant in the clustering. These two were abandoned as being both too complicated and yielding no further understanding of the lithofacies distribution.

## 9.4 FIVE LITHOFACIES MODEL

The model of five lithofacies (Figure 9.4) is chosen as the framework for the distribution of dominant lithofacies within the bay. The possibility of using the four cluster model as a basis for the lithofacies was discounted in favour of incorporating Facies 3 which is a predominantly organism based facies in the central area of the bay. The six cluster model was discounted as a lithofacies distribution because of the relatively small subdivision (7 out of 30 stations) of Facies 1.

Arithmetic means of the facies components of the five cluster model is presented in Table 9.1 and as comparison bar graphs in Figure 9.6. These facies are briefly summarised according to the four dominant ranked components. The predominant texture of each facies is included in these descriptions:

- Lithofacies 1: Mollusc/ calcareous aeolianite/ quartz/ bryozoa, medium to fine sand lithofacies; northern and central terrace, central eastern coastal margin, isolated pockets in the entrance and southwest coastal margin (9.4.1.).

- Lithofacies 2: Calcareous aeolianite/ mollusc/ quartz, very coarse to fine sand lithofacies; sand shoals, southeast coastal margin, northern and southern inner terrace, isolated occurrences northeast coastal margin and central entrance (9.4.2.).

- Lithofacies 3: Mollusc/ foraminifera/ bryozoan/ coralline algae, gravelly fine to very coarse sand lithofacies; central inner terrace (9.4.3).

• Lithofacies 4: Bryozoa/ mollusc/ calcareous aeolianite/ coralline algae, gravelly medium to very coarse sand (medium to very coarse sandy gravel) lithofacies; entrance and portion of the northern terrace (9.4.4.).

• Lithofacies 5: Mollusc/ echinoid/ quartz/ foraminifera, fine sandy mud lithofacies; the inner marginal basins and Blanche Port. (9.4.5.)

| Component | Facies 1 Mol/ Calc Aeol/ Qtz | Facies 2 Calc Aeol/ Mol/Qtz | Facies 3 Mol/For/ Bryo | Facies 4 Bryo/Mol/ Calc Aeol | Facies 5 Mol/Ech/ Qtz |
|---|---|---|---|---|---|
| Molluscan | **23.63** | **15.84** | **26.85** | **21.23** | **48.82** |
| Foraminifera | 7.43 | 5.07 | **14.45** | 6.51 | 6.07 |
| Bryozoan | 8.58 | 6.17 | **14.02** | **21.55** | 1.97 |
| Echinoderm | 4.27 | 2.88 | 7.69 | 6.69 | **8.65** |
| Coralline Algae | 6.27 | 5.45 | 10.25 | 12.81 | 5.76 |
| Calcareous Aeolianite | **17.97** | **35.55** | 6.85 | **13.38** | 1.61 |
| Quartz/Lithic | **15.04** | **11.24** | 8.35 | 8.2 | **7.15** |

Table 9.1 Arithmetic means of components within the lithofacies of the five lithofacies models for Streaky Bay. The dominant three components are highlighted, in all cases these three components represent >55% of the total. Abraded Bioclastic component is excluded it represents the proportionate sum of recognised bioclastic constituents within each sediment sample.

### 9.4.1 Lithofacies One: Mollusc/ Calcareous aeolianite/ Quartz/ Bryozoan, Medium to fine sand

Mollusc/ calcareous aeolianite/ quartz/ bryozoan, medium to fine sand lithofacies occurs on the northern and central terrace; central eastern coastal margin; isolated pockets in the entrance and southwest coastal margin of the bay. The molluscs are represented by the bivalves: *Katelysia spp. Fulvia sp., Ostrea spp.* and *Pinna sp.* with the gastropods: *Batillaria spp., Bulla sp.,* and *Coxiella sp.* Calcareous aeolianite grains are derived from the Bridgewater Formation, which forms low cliffs (5-10m), rocky shores and islands on the northern and eastern coastal margins. The relatively high percentage of fine grained clear quartz 15% is originally derived from the felsic intrusive outcrop present on the sea-floor, and coastline flanking the outer reaches of the bay. The quartz component has been also reworked through aeolian (Bridgewater Formation) and marine (Glanville Formation) processes (Buckley et. al. 1987). This facies also includes near-shore *Posidonia sp.* seagrass with epiphytic coralline algae as well as encrusting bryozoa and minor delicate branching bryozoa. The foraminifera represented are the stenohaline types of *Elphidium sp., Discorbis sp.* and *Triloculina sp.*.

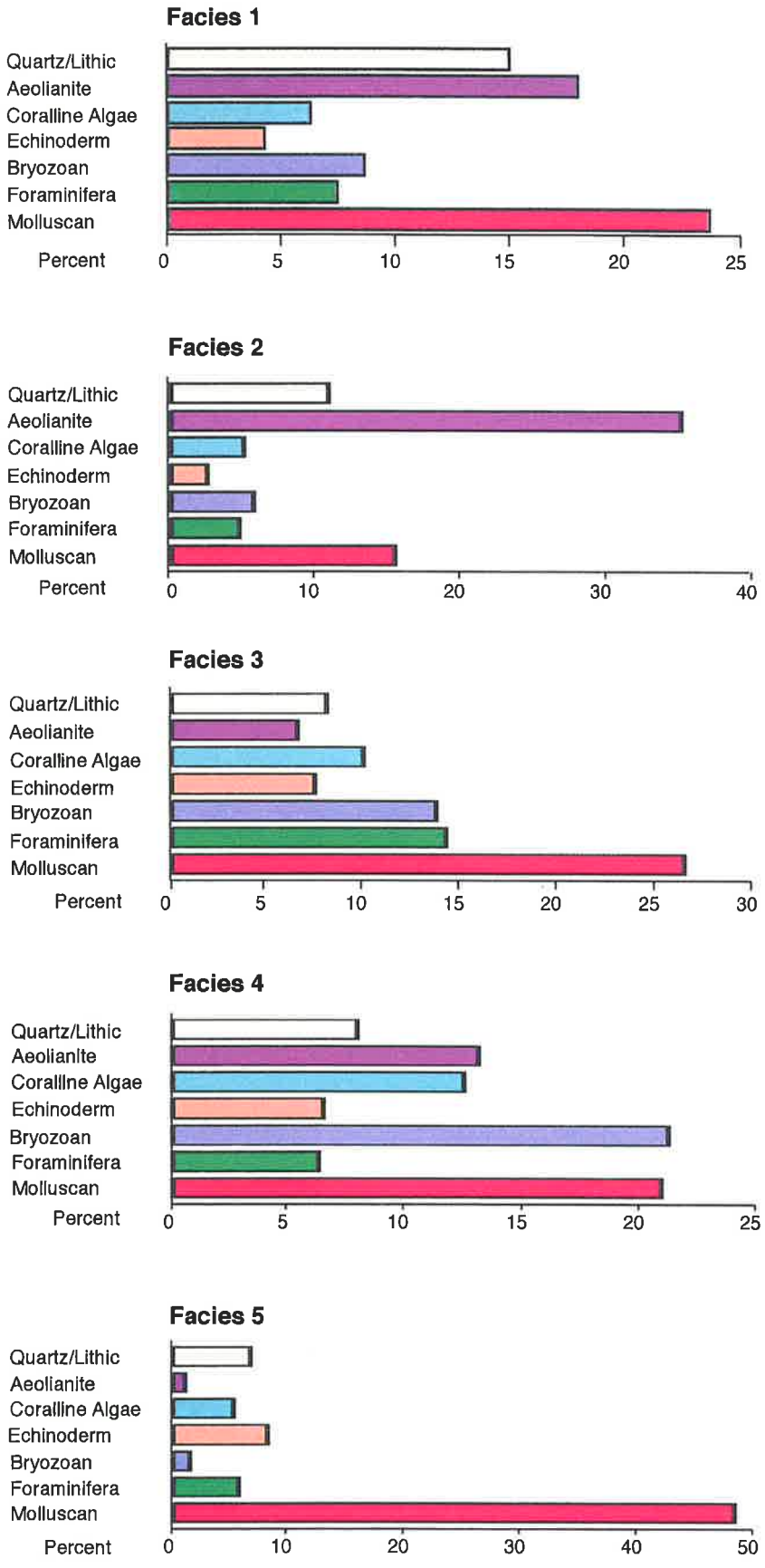



Figure 9.6 Average Composition of Lithofacies for the Five Facies Model (Abraded bioclastic fraction is assumed to be in proportion with identified skeletal organisms)

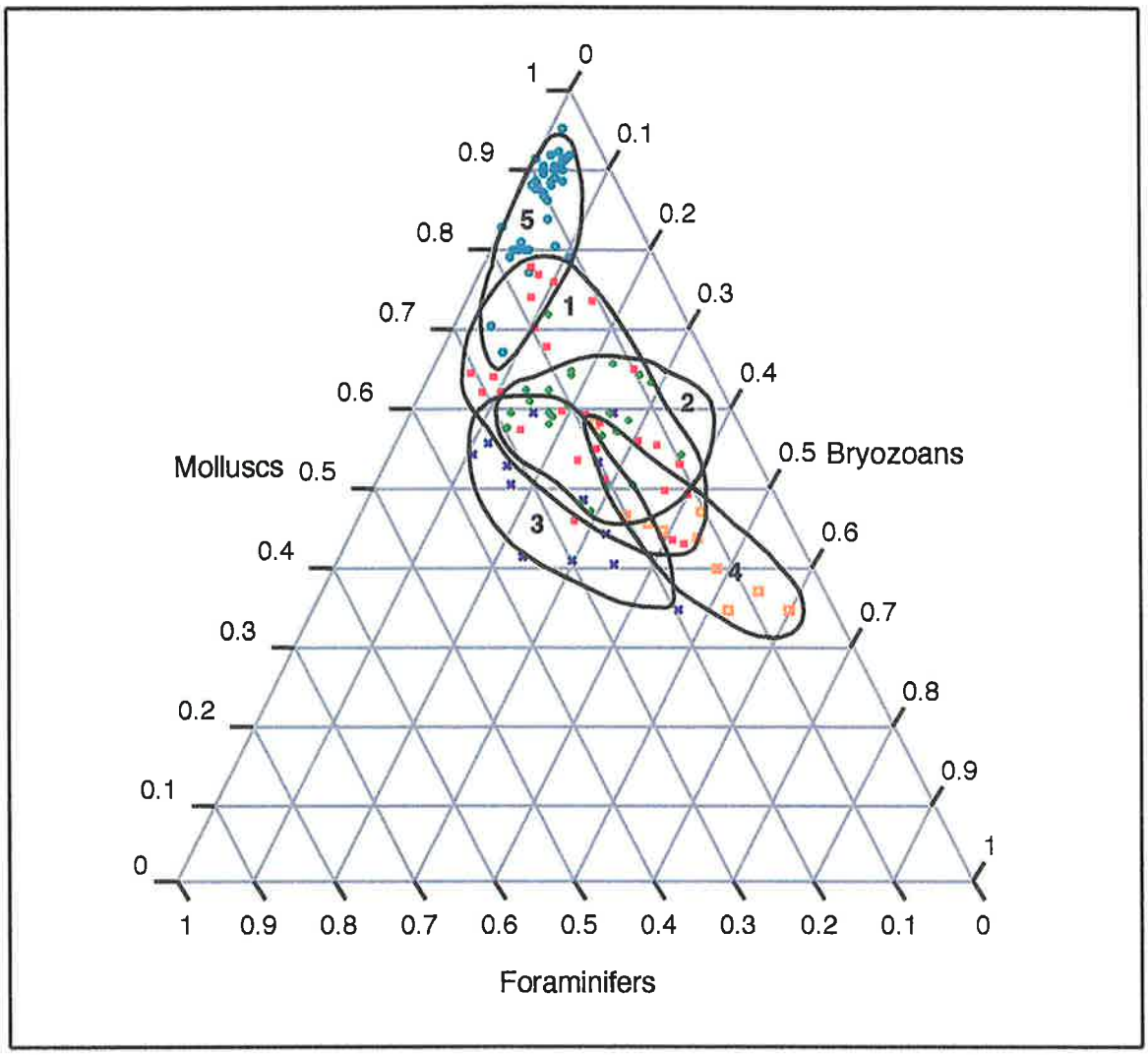



Figure 9.7 Ternary plot of molluscan, foraminifer and bryozoan components of the sand fraction. The fields are broadly similar except for the sediments of Facies 5, which contains abundant molluscan grains. The fields of facies 1, 2, 3 and 4 are differentiated by varying amounts of aeolianite and quartz/lithic grains. In general the facies are dominated by molluscan (~50%) and bryozoan (~30%) grains with ~20% foraminifers.

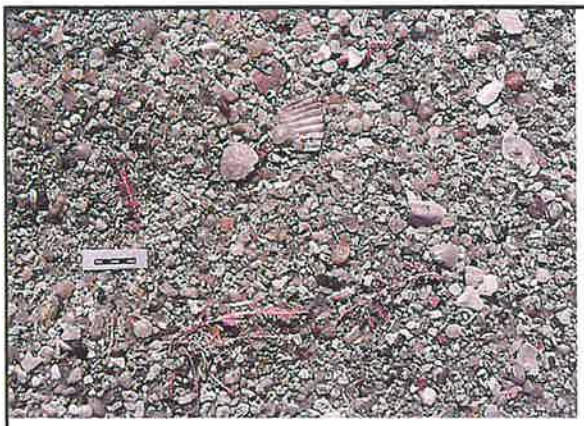




Figure 9.8 a, b. Sediments from Facies 1, highlighting molluscan, calcareous aeolianite and quartz/ lithic grains. Foraminifers, bryozoans and coralline algae are common. Seagrass meadows are extensive throughout the shallower areas of the facies. The facies occurs on the eastern and southwestern coastal margin and in pockets at the entrance. (NB. Groups of components are ranked in order of abundance). The texture of these sediments is predominantly medium to fine sand. (Scale bar 5 mm).





Figure 9.8 c, d. Sediments from Facies 2, highlighting abundant calcareous aeolianite, molluscan and quartz/ lithic grains. Bryozoans, coralline algae and foraminifers are common. The facies is prominent where calcareous aeolianite is being actively eroded, transported and deposited on the northern and southern inner terrace and southeast coastal margin. The sediments of this facies are very coarse to fine sands. (Scale bar 5 mm).





Figure 9.8 e, f. Sediments from Facies 3, showing abundant molluscan, foraminifers and bryozoan grains. Coralline algae, quartz/ lithic and echinoderm grains are common. The facies occurs in the central and southern inner terrace. The sediments are gravelly fine to very coarse sands. (Scale bar 5 mm).



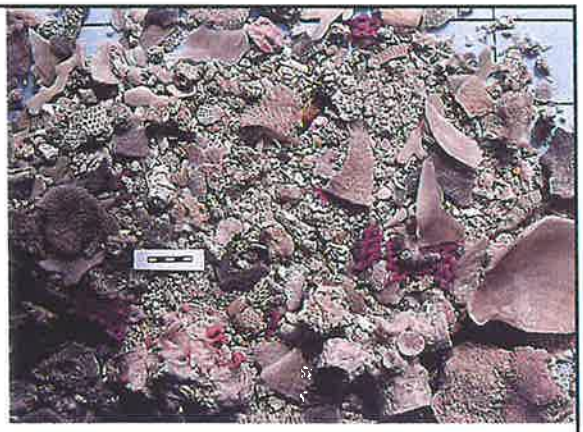


Figure 9.9 a, b Sediments representing Facies 4, highlighting bryozoan, molluscan and calcareous aeolianite grains abundant in the facies. Coralline algae, quartz/ lithic grains are common and the texture is gravelly medium to very coarse sand (medium to very coarse sandy gravel). This facies occupies the rocky substrates of the outer terrace and entrance. (Scale bar 5 mm).

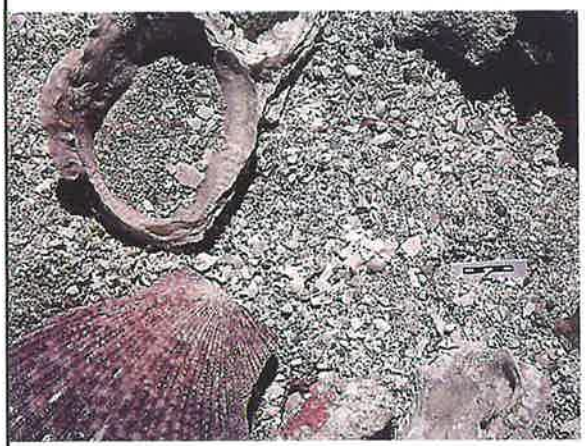




Figure 9.9 c, d Sediments representing Facies 5 highlighting abundant molluscan, echinoderm and quartz/ lithic grains. Foraminifers and coralline algae are rare to common. The texture of the sediments in this facies is a fine sandy mud and is confined to the inner marginal basins. (Scale bar 5 mm).



Figure 9.9e Common echinoid and ophiuroid fragments are found with abundant mollusc fragments in the mobile sand waves within Facies 3. (Scale bar 5 mm).

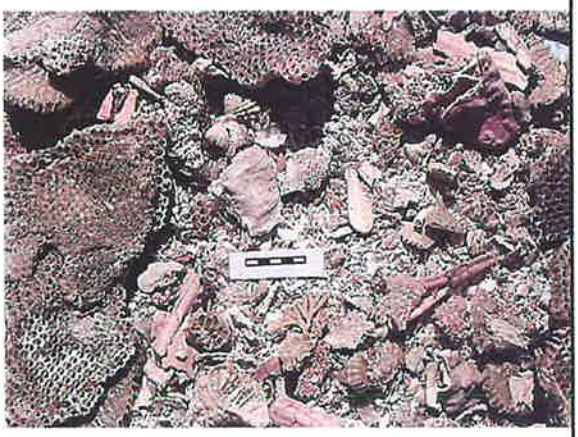


Figure 9.9 f Bryozoans and coralline algae with diverse structural architecture are abundant in patches within Facies 4. Corals and brachiopods also occur.
(Scale bar 5 mm)

### 9.4.2 Lithofacies Two:- Calcareous aeolianite/ Mollusc/ Quartz, Very coarse to fine sand

Calcareous aeolianite/ mollusc/ quartz, very coarse to fine sand lithofacies occupies the sand shoals, south-eastern coastal margin, northern and southern inner terrace, and isolated occurrences northeast coastal margin and central entrance. Calcareous aeolianite is the predominant component, which is derived from eroding Bridgewater Formation at the entrance cliffs and the sea-floor of the northern terrace. The molluscs are represented by the bivalves *Katelysia* ssp. and *Fulvia* sp., the gastropods *Batillaria* ssp., *Clanculus* sp. and *Phasianella* sp. with fragments of *Pinna* sp. Epifaunal and rare infaunal echinoids are present as lightly abraded plates and broken spines. Whole tests and larger fragments indicate common epifaunal regular echinoids whereas infaunal varieties are seen as whole tests.. Delicate branching cyclostomes are rare but fenestrate cheilostome fragments are common, along with the occasional multi layered encrusting bryozoans. Fragments of punctate brachiopod valves (Terabratullid) are present, but no whole valves have been found in this facies. The foraminifera *Peneropolis* ssp, *Cribrobulimina* sp., *Elphidium* ssp. and *Discorbis* sp. are common in the facies . The abraded bioclastic component is most abundant in this facies, being fresh, well rounded and medium to fine grained. A trace of calcareous aeolianite is recognisable throughout the facies, with the quartz fraction approximately 10%.

### 9.4.3 Lithofacies Three:- Mollusc/ Foraminifera/ Bryozoan/ Coralline algae, Gravelly fine to very coarse sand

Mollusc/ foraminifera/ bryozoan/ coralline algae, gravelly fine to very coarse sand lithofacies occupies the central inner terrace and a tongue extending towards the southern tidal delta. This facies is dominated by a mixed biogenic or heterozoan assemblage with ~15% attributable to calcareous aeolianite and quartz/lithic components. Molluscs common to the facies are the bivalves; *Modialus* sp., *Neotrigonia* sp., *Dosinia* sp. and *Glycymeris* sp. with gastropods; *Turbo* spp., *Fusinus* sp., *Cassis* sp., and *Calyptraea* sp. Bryozoans exhibiting a variety of structural architecture (encrusting unilaminate, delicate cylindrical branching, uni- and bilaminar sheet (foliaceous), fenestrate, robust and articulated branching) are present with common representatives from the genera *Membranipora, Celleporaria, Adeonellopsis, Osthimosia, Porina, Arachnopusia, Hornera, Lichenopora* and *Tubulipora.* . Abundant crustose (*Lithophyllum* sp. and *Phymatolithon* sp.), articulated branching (*Corallina* sp., *Jania* sp. and *Metagoniolithon* sp.) and minor rhodolith (*Lithothamnion* sp.) coralline algae are present with this facies. Minor echinoderms (*Heliocidaris* ssp. and *Ophionereis* sp.) and rare brachiopods (*Anakinetica* sp.) also occur. The foraminifera *Triloculina* ssp., *Quinqueloculina* ssp. *Discorbis* sp, *Peneropolis* sp., *Elphidium* sp. and *Cribrobulimina* sp. also occur in this facies.

### 9.4.4 Lithofacies Four:- Bryozoan/ mollusc/ Calcareous aeolianite/ Coralline algae, Gravelly medium to very coarse sand

Bryozoan/ mollusc/ aeolianite/ coralline algae, gravelly medium to very coarse sand (medium to very coarse sandy gravel) lithofacies; entrance and portion of the northern terrace. A diverse variety of biota exists in the facies compared with inner bay facies. A large variety of bryozoans are present, including the structural forms: encrusting unilaminate, delicate cylindrical branching, uni- and bilaminar sheet (foliaceous), fenestrate, robust and articulated branching with rare vagrants. Common bryozoan genera occurring in this facies are; *Membranipora, Celleporina, Celleporaria, Adeonellopsis, Osthimosia, Porina, Arachnopusia, Lunulites, Steginoporella, Smittina, Iodictyum, Hornera, Lichenopora, Tubulipora, Nevianopora and Diaperoecia.* Molluscs occur abundantly with gastropods the dominant and most variable group. They are represented by the gastropod genera; *Phasianella, Fulvia, Batillaria., Fusinus, Turbo, Cassis Pholas, Calytraea* and *Siliquaria* and the bivalve genera; *Glycymeris., Neotrigonia., Dosinia, Modialus* with rare *Katelysia* and *Circomphalus.*

Large lithic grains and skeletal fragments are sites for encrusting (*Lithophyllum* sp. and *Phymatolithon* sp.) and articulated branching (*Corallina* sp., *Jania* sp. and *Metagoniolithon* sp.) coralline algae with rhodoliths (*Lithothamnion* sp. and *Goniolithon* sp.) occurring in the lee of Olive Island. The foraminifer genera; *Triloculina, Discorbis, Peneropolis, Elphidium, Textularia* and *Cribrobulimina* are also recognised in this facies. Whole valves of brachiopods (*Terabratullid- Anakinetica* sp. and *Magellania* sp.) occur in and on the variable substrates. The significant calcareous aeolianite is derived from erosion and transport of Bridgewater Formation comprising the entrance cliffs and Olive Island.

### 9.4.5 Lithofacies Five:- Mollusc/ Echinoid/ Quartz/ Foraminifera, Fine sandy mud

Mollusc/ echinoid/ quartz/ foraminifera, fine sandy mud lithofacies is confined to the inner marginal basins and Blanche Port and initially recognised by the high percentage of carbonate mud and the abundance of molluscs in the sand fraction. The molluscan component comprises ~50% of the facies. Common bivalves present are *Katelysia* spp., *Dosinia* sp., *Fulvia* sp., *Anomia* sp., *Pecten* sp., *Equichlamys* sp. and isolated fragments of *Ostrea spp,* and fairly common fragments of *Pinna* sp. with the gastropods *Batillaria spp.* and *Coxiella* sp., *Bulla* sp., *Thais* sp. and *Penion* sp. Small regular echinoids (5-7 mm diameter) are common in the facies. They are present in the gravel fraction and the spines and plates range up to 8 % in the sand fraction. The range of foraminifera are reduced compared to previous facies and are significantly smaller in size. Rare bryozoans occur as small delicately branched cyclostomes (*Nevianopora* sp., *Diaperoecia* sp. and *Crisia* sp.) found cemented to fragments of *Pinna.* Other fragments of bryozoa are fenestrate (*Iodictyum* sp.), encrusting (*Membranipora, Pyripora sp., Celleporaria sp.*) and articulated branching (*Cellaria* sp.) cheilostome varieties. Quartz (< 8% average) occurs throughout the facies.

## 9.5 DISCUSSION

The spatial distribution of lithofacies indicates that the entrance/ terrace area of the bay is the principal biogenic sediment producing area. This region also contains the largest range of identifiable calcareous organisms. The variation in robustness and disintegration potential of the biota provide a range of grain-sizes to be transported to the various depositional areas i.e. the elongate banks, prograding tidal deltas and the inner basinal areas.

The ternary plot of significant biota i.e. molluscs, bryozoans and foraminifers, show that the sediments of the lithofacies in Streaky Bay fall in a broadly similar field dominated by molluscs (~50%), bryozoan (~30%) and foraminifers ~(20%) (Figure 9.7). Lithofacies 5 shows a significant departure from the common field and is dominated by molluscs over the other two groups of organisms. The fields of the lithofacies are delineated more clearly when the calcareous aeolianite component for each lithofacies is considered with the significant organism groups. As definitive grain count results are not available from the other bays on the West Coast (Eyre Peninsula) comparative ternary plots can not be shown. This skeletal composition is similar to the "foramol" associations of Simone and Carannante (1988) and derived terminology, e.g. bryomol, molechfor, rhodalgal and bryoderm (James, 1997). Unfortunately, most of these associations are from the mid to outer sediment starved continental shelves and not the shallow marine transitional area.

The larger and more robust forms i.e. gastropods, bivalves, rhodolithic and articulated red algae, fenestrate and encrusting bryozoans break down to provide the coarser sediment present in the banks and tidal channels. The more fragile forms i.e. delicate and juvenile molluscs, delicate and lightly calcified bryozoans, seagrass encrusting coralline algae and small echinoderms can provide a sediment source for the inner basins. This process acts in a continuum of sediment supply across the different depositional areas with maceration, abrasion and mastication producing smaller grain sizes.

These lithofacies present in Streaky Bay can be broadly compared with skeletal equivalents in the embayments along the west coast of the Eyre Peninsula and on the proximal open shelf (9.5.1).

### 9.5.1 Regional Distribution Of Lithofacies, Coastal Embayments, Western Eyre Peninsula

Interpretation of the lithofacies from Baird Bay, Tourville Bay, Coffin Bay and Fowlers Bay are identified with those from Streaky Bay. (i.e. SB lithofacies 1 to 5). These and other significant embayments are incorporated in a model that encompasses hydrodynamic energy, substrate and salinity. The composition of sediments is relatively uniform according to the energies and substrates of the Streaky Bay lithofacies.

#### 9.5.1.1 Baird Bay

Baird Bay (Figure 9.11) is a long, shallow inverse estuary, some 25 km long with a maximum width of 3 km and two major constrictions subdividing the bay into three domains. It is situated about 50 km south of Streaky Bay. Salinities vary from 36.5 ‰ at the entrance up to 59.7 ‰ at the northernmost point (Hill, 1994). The lithofacies present in Baird Bay are based principally on organism assemblages and sedimentary texture, which vary according to energy, salinity and substrate (Figure 9.10). Presence of calcareous aeolianite in these sediments (apart from the entrance) is minimal due to low run-off and resultant transportation, which is due to the high permeability of the Bridgewater Formation and the arid nature of the region.

• Molluscan-foraminifera sand lithofacies is restricted mainly to the entrance area of the bay and extends to the first constriction. This is an area of normal salinity and extensive *Posidonia australis* seagrass meadows. The facies contains abundant molluscs, foraminifers and quartz and is equivalent to SB Lithofacies 1. This facies also occurs along the shallow margins and sand flats to the furthest reaches of the bay where there is elevated salinity.

• Molluscan muddy sand lithofacies occurs in the low energy areas bordering the mollusc-foraminifera sands in the mid- to upper reaches of the bay and may be similar to the shallower elements of SB Lithofacies 5

• Molluscan-foraminifera-peloidal mud lithofacies is found in the north of the bay in areas of deepest water (<2 m) along the axis of the bay, marine plants are absent as a result of elevated salinities. Infaunal to semi infaunal bivalves and gastropods are the most abundant macrofauna in a lithofacies that is unique to Baird Bay.

#### 9.5.1.2 Tourville Bay

Tourville Bay (Figure 9.13) is a shallow embayment situated 15 km to the west of Ceduna, on the northern side of Denial Bay (Lablack, 1985). The lithofacies of Tourville Bay have similarities with Streaky Bay (Figure 9.10), although the description of sedimentary components are brief. Quartz and calcareous aeolianite are minimal through the lack of granitic rocks and the Bridgewater Formation respectively and the facies are correlated by texture and dominant calcareous organisms.

• Molluscan-foraminifera coarse to fine sand lithofacies occur in diverse environments such as deepwater sandy tidal channels, shallow tidal channels, tidal deltas and tidal flats with seagrass, which correlates with SB Lithofacies 1.

• Molluscan-Foraminifera fine muddy sand lithofacies are found in the subtidal to intertidal zones and shallow tidal channels which meander into the mangrove forests. This facies is similar to a mixture of

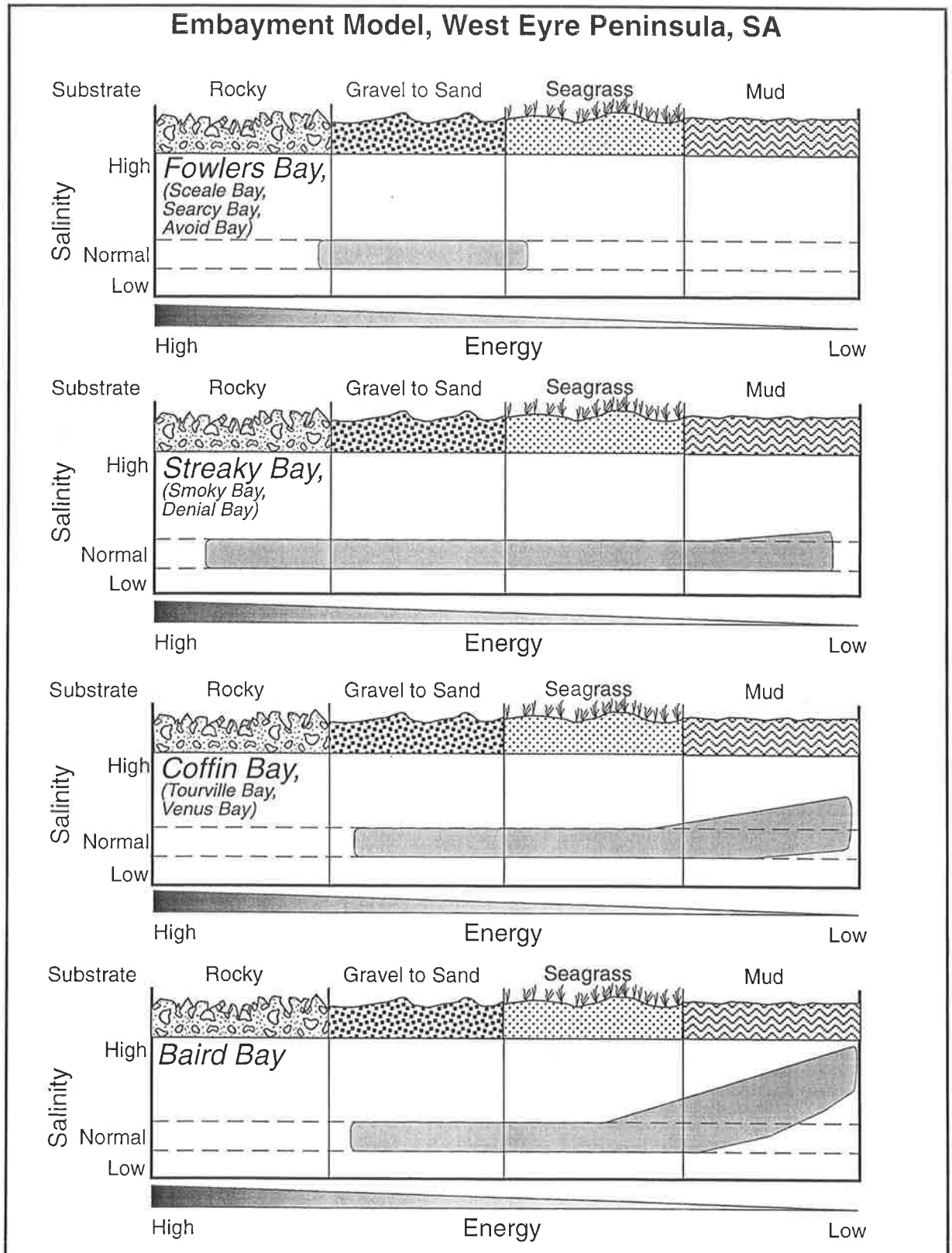



Figure 9.10 Hydrodynamic energy, substrate and salinty model for embayments on the western Eyre Peninsula, South Australia. Open sea salinities - normal range ~35-36.5‰, high salinities ~65‰. Substrate blocks represent a continuum of energy related environments from rocky to muddy. Fowlers Bay represents an open sea lithofacies , Streaky Bay semi-protected range of lithofacies, Coffin Bay protected range of lithofacies and Baird Bay protected to restricted range of lithofacies. Semi-protected to restricted embayments are generally the flooded back-dunal corridor of high coastal palaeodunes. Bays in brackets are interpreted to be of similar lithofacies range as the reference model.

SB Lithofacies 1 and SB Lithofacies 5, which by inference would occur in the mangrove mangles of northern and southern Streaky Bay.

#### 9.5.1.3 Coffin Bay

Coffin Bay is located at the south-western tip of the Eyre Peninsula (Figure 9.12) with the mouth of the bay facing to the north northwest, up the west coast of the peninsula (Freeman, 1985). The position of the mouth ensures that the high energy oceanic south-west swells are not impinging directly on Coffin Bay, but are instrumental in transporting sediment into the bay. Significant wave refraction around Point Sir Isaac is responsible for transporting reworked Bridgewater Formation (calcareous aeolianite) and modern sediments into the bay to a tidal delta complex at Point Longnose. Low energy shallow waters of the inner bays are beyond this complex (Figure 9.10) .

• Molluscan fine sandy mud lithofacies are characteristic of most of the sea floor of the inner regions of the bay in depths of over 8 m, or as 'lagoonal' mud in areas of attenuated wave energy as typified by the low energy shallow waters of the inner embayments. The sediments are generally composed of fine to very fine sandy muds containing up to 20 % molluscan shell hash in some areas. *Posidonia ssp.* grows profusely in Coffin Bay and Port Douglas. This facies generally correlates with SB Lithofacies 5 except the mud fraction is not generally as abundant as in Streaky Bay apart from the intertidal zones in the far reaches of the bay where sediments contain up to 90% mud.

• Molluscan-calcareous aeolianite sand lithofacies compose a considerable portion of Coffin Bay. The components of the sands are predominantly reworked sediment from the Bridgewater formation and modern biogenic (predominantly molluscan) material and correlates with SB Lithofacies 2 and to minor areas of SB Lithofacies 1.

• Mollusc-echinoid-calcareous aeolianite sand facies is confined to the zone between the high tide and fair-weather wave base and varies from wide, high energy beaches on the seaward side of Pt. Longnose to narrow, low energy beaches inside the spit. The sediments in this facies are generally well sorted fine sands with molluscan and echinoid spine fragments. This facies is similar in composition to SB Lithofacies 5, but texturally similar to SB Lithofacies 1. The facies probably represents the transition zone between SB Lithofacies 5 and 2.

#### 9.5.1.4 Fowlers Bay

Fowlers Bay is an open bay, situated approximately 140 km west of Ceduna, with a southerly aspect facing the high energy swells of the Southern Ocean (Figure 9.13). Recent sediments found in this area are high wave energy bioclastic beach and dune sands and low energy lagoonal and intertidal shelly and gypsiferous muds (Belperio, 1988). Limited sampling of the off-shore (45m depth) well sorted sand was carried out by James et al. (2001).

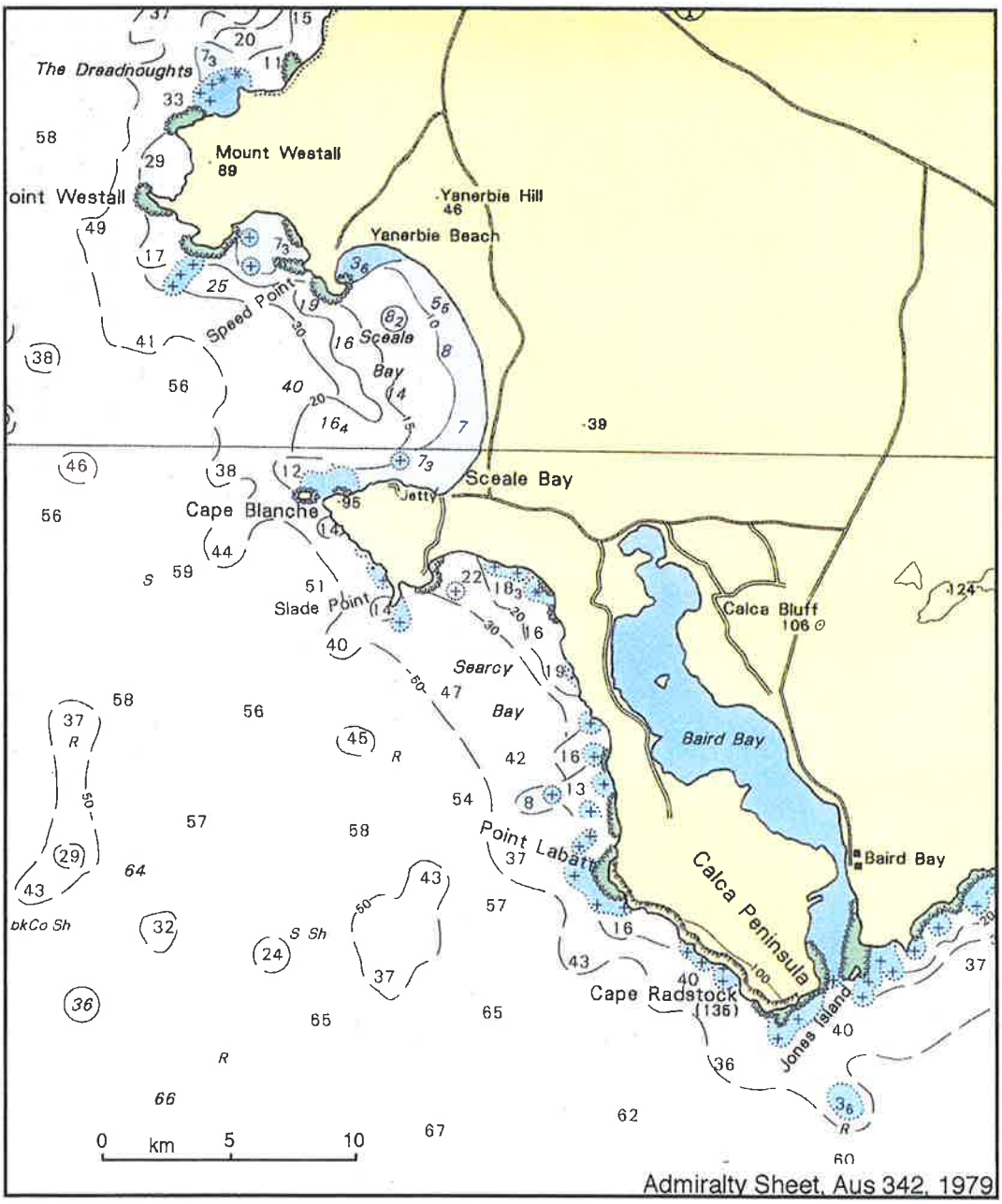



Figure 9.11 Baird Bay, West Coast, Eyre Peninsula

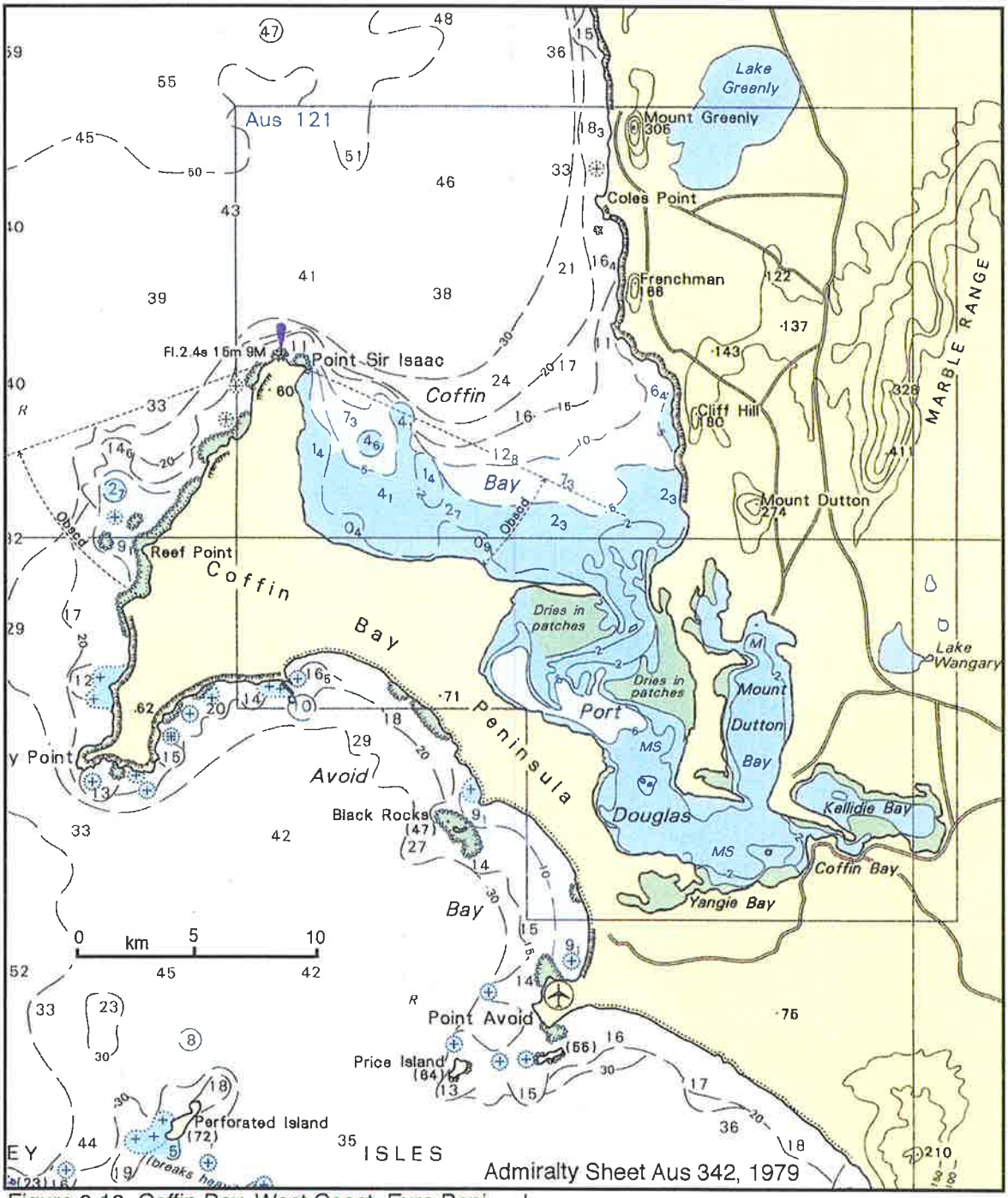



Figure 9.12 Coffin Bay, West Coast, Eyre Peninsula

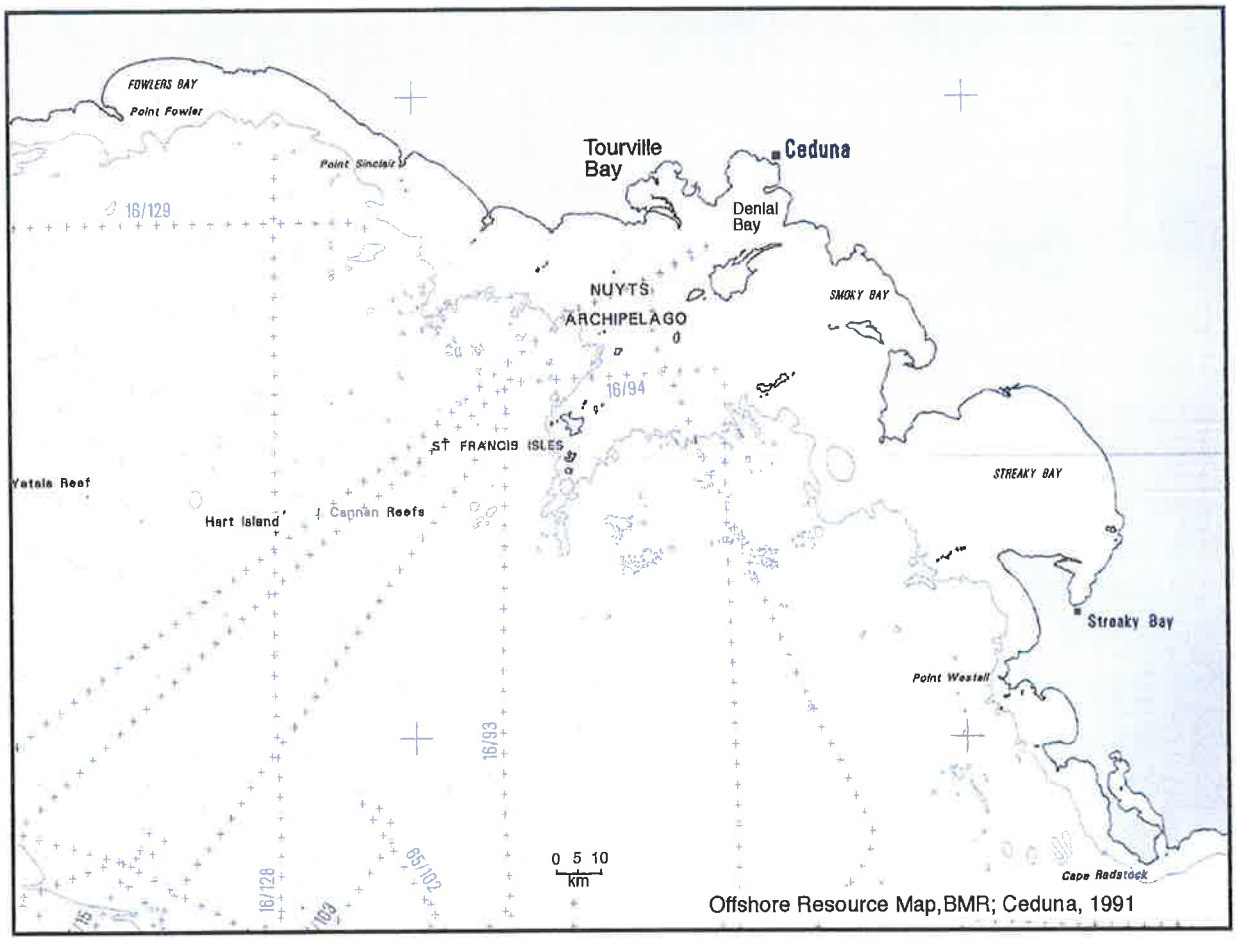



Figure 9.13 Fowlers Bay to Baird Bay, West Coast, Eyre Peninsula

• Molluscan-foraminifera medium to coarse sand lithofacies occurs in the high energy intertidal/ beach zone and is similar to SB Lithofacies 1.

• Molluscan-bryozoan-foraminifera coarse sand lithofacies contains a sediment composed of coarse bioclastic sand containing sub-equal abundant mollusc and bryozoan grains with foraminifer and coralline algae fragments. This offshore facies is similar to SB Lithofacies 3 or possibly SB Lithofacies 4 depending on the variation of calcareous aeolianite outcropping on the sea-floor (Figure 9.10)

Holocene intertidal sediments of a molluscan fine sandy mud lithofacies are capped with gypsiferous muds and occur in the Pleistocene interdunal depressions just inland from Fowlers Bay. These gypsiferous muds became common as barriers developed across the lagoonal areas when the sea-level stabilised. These deposits are similar to the sequence of sediments which occur in Acraman Creek Core No. 9 (Figure 4.9) in the now occluded early Holocene Proto Acraman embayment west of the Acraman Creek estuary.

### 9.5.2 Streaky Bay to GAB Shelf Edge: Transect from FR 03/98

Preliminary examinations of samples from the Streaky Bay Transect of the FR 03/98 RV *Franklin* cruise (Figure 2.1) revealed that the sediments on the near shelf are palimpsest, as are all inner to mid shelf sediments on the southern margin (James et al., 1992, 1997, 2001; Fuller et al., 1994). The sediments are variably composed of the following; felsic grains from the basement intrusives (inner shelf), aeolianitic (intraclasts) grains from the Bridgewater Formation and the early Holocene transgression, bioclastic grains from the latest Holocene, abraded biofragments and skeletal material from live organisms.

The distribution of major sediment components is graphed from Streaky Bay to the shelf edge (Figure 5.15) and shows that the substrate is composed of lithic bioclastic gravelly sands on the inner shelf to bioclastic gravelly muddy sands on the outer shelf. The gravel fraction on the inner shelf is composed of significant proportions of lithic grains and skeletal fragments whereas on the mid to outer shelf it is dominantly skeletal fragments. The facies on the inner shelf is mollusc/ bryozoan/ lithic coarse sand facies. Mollusc and bryozoan fraction are found in sub-equal proportions on the inner shelf facies. Of the molluscs present, bivalves are dominant on the inner shelf whereas gastropods become equal to dominant towards the outer shelf. The lithic component is comprised of calcareous aeolianite and quartz/ potassium feldspar, the sum of which ranges from ~30% on the inner shelf to zero from the mid to outer shelf. The substrate components on the outer shelf comprise; abundant bryozoan remains, common molluscan valves and fragments, pristine to abraded foraminifera with rare articulated and rigid branching fragments of coralline algae and abraded bioclastic fragments.

The lithofacies of the inner shelf GAB have been refined into four facies which broadly reflect the coastal and sea-floor lithology and near-shore shelf environment in the region off the eastern and central GAB. The predominant inner shelf lithofacies along the western side of the Eyre Peninsula is a molluscan-relict calcareous aeolianite (as intraclasts) coarse sand with minor biogenic constituents of foraminifera, bryozoa and coralline algae with up to 30% terrigenous material. Sediments taken sampled on the RV *Franklin* cruises are rarely from < 30 m and usually in higher energy swell conditions than the embayments.

This broad facies has been subdivided into (James et al, 2001):

- Mollusc Intraclast Sand (MI) facies.
- Intraclast-Mollusc Sand and Gravel (IM) facies.
- Quartzose Skeletal Sand and Gravel (Q) – bivalves ≈ bryozoans with terrigenous material between 10- 30%).
- Bryozoan Intraclast Sand (BI) – abundant bryozoans with 25-50% intraclasts.

The intraclastic or relict carbonate sand component reflects the predominance and erosion of Pleistocene calcareous aeolianite, bioclastic grainstone/packstone and calcrete horizons along the coastal margins of the western Eyre Peninsula (Wilson, 1991 and references therein) and as outcrops on the floor of the nearby shelf (James et al 1997, 2001). The terrigenous material is derived from the erosion of the numerous felsic intrusives which also outcrop along the coast and inner-shelf sea-floor. These lithofacies are also discussed and compared with the facies of Streaky Bay.

- SB Lithofacies 1 can be correlated with the near inner shelf Facies Q and MI i.e. quartz-skeletal facies and mollusc-intraclast (eroded aeolianite) facies (James et al., 2001) and their equivalents. These two facies are grouped as a result of the dominance of intraclasts and quartz with the molluscs.
- SB Facies 2 is similar to the inner shelf Facies IM (intraclast/ mollusc facies).
- SB Facies 3 is confined to Streaky Bay and is dominantly composed of fresh biogenic material with only minor quartz/ lithic and aeolianite, a true "heterozoan" facies of mollusc-bryozoan-foraminifera-coralline algae-echinoid composition.
- SB Facies 4 is similar to Facies BI (bryozoan/ intraclast) although in SB Facies 4 the bryozoan and molluscan components are subequal with significant intraclast component.
- SB Facies 5 is unique to Streaky Bay when compared with the facies of the adjacent shelf and their equivalents on the near southern margin. Although a similar facies is described from the inner lagoonal area of Coffin Bay, which contains < 10% mud and is a shallow restricted environment rather than the open exposure and comparative deep water of inner Streaky Bay.

## 9.6 LITHOFACIES OF THE SOUTHERN MARGIN, COMPARISON

Four parallel distinct zones, based on grainsize, were recognised across the shelf, down the continental slope to the abyssal plane (Conolly and von der Borch, 1967). The biogenic fragments represented in these zones include bryozoans, molluscs, foraminifera, echinoids, worm tubes, red algae sponges pteropods, corals, crustaceans asteroids, and ostracodes. The broad composition (grainsize and biota) of these zones are summarised below.

### 9.6.1 Broad-Based Southern Margin Facies

The coastal margin consists of coarse grained biogenic sands, with molluscs and foraminifera and echinoids being the dominant biota. The mid-shelf zone consists of finer grained biogenic sands derived from the breakdown of sediments from the coastal zone along with minor reworked recent and Pleistocene sediments. This zone is characterised by an infaunal molluscan/ bryozoan/ minor sponge assemblage. The deep shelf zone consists of coarse grained biogenic fragments and relic sands with minor relic Pleistocene sediments. The dominant biota are higher populations of bryozoans and sponges than the mid-shelf zone. The shelf edge zone is characterised by calcareous muds and fine sands which contain increasing amounts of planktonic organisms. Bryozoans, sponges, foraminifers and pteropods (in descending order of abundance) are the dominant biota present in this zone with molluscs being rare. Most zones, apart from the outer-most shelf, contained polished relic Pleistocene aeolianitic calcareous sands. These underlay large tracts of the shelf and also outcrop along the shelf break (Conolly and von der Borch, 1967).

The dominant constituent of the sediments dredged along the southern margin was found to be bryozoan skeletal remains, with bryozoan colonies making up a large percentage of the living fauna (Wass et al., 1970, Wass and Yoo, 1983). A broad-based biozonation using bryozoans was proposed for the south-western continental shelf:- **(a)** 30 - 55 m depth: the predominant structural forms of the bryozoa were flat robust branching and fenestrate, with minor articulated zooidal, vagrant, delicate branching and articulated branching forms (classification from Bone and James, 1993). From **(b)** 55 - 130 m depth: vagrant bryozoans were dominant in some areas almost to the exclusion of other forms. Seawards **(c)** from this zone, flat robust branching and fenestrate forms made up equal portions with the vagrant forms (Wass et al., 1970, Wass and Yoo, 1983).

### 9.6.2 Great Australian Bight

James et al. (2001) have described the inner-shelf coastal facies in the Streaky Bay area as Facies Q (Quartzose Skeletal Sand and Gravel), with Facies IM (Intraclast-Mollusc Sand and Gravel) occurring seaward to the south and south-east off the Eyre Peninsula and Facies MI (Mollusc-Intraclast Sand) occurring seaward to the south and north-west off The Eyre Peninsula. The major gravel fraction components of Facies Q in the Streaky Bay region are lithoclasts (quartzose and granitic), bryozoans, encrusting calcareous red algae, whereas the major sand components are encrusting calcareous red

algae, bryozoans and molluscs. The dominant components of Facies MR in the same region are molluscs, intraclasts (dominantly calcareous aeolianite and calcrete) and bryozoans. Facies IM is typified by intraclasts dominant over molluscs with bryozoans significant but less abundant than molluscs. It is also texturally coarser than facies MI.

The inner shelf on the western side of the Great Australian Bight consists of two major facies. West of Head of Bight (Roe Terrace) is Facies Q which consists of quartzose skeletal sands and gravel.. The skeletal content, notably molluscs and bryozoans, is slightly higher in the Western Bight region than the Eastern. The shelf is dominated by a rhodolith gravel facies (Facies R) further west on the inner Great Australian Bight from the centre of the shelf off the Roe Plain to past Israelite Bay. This comprises 70 % - 100 % granule to cobble-sized rhodoliths with molluscs and bryozoans (James et al., 2001). The mid to outer GAB facies are predominantly bryozoan assemblages with varying amounts of intraclasts and spicules. The intraclast content declines and the spicule content increases towards the outer shelf, especially in the central GAB area whereas the flanks of the outer GAB are dominated by bryozoan facies with sponges and solitary corals (James et al., 2001)

### 9.6.3 LINCOLN SHELF

The facies on the shelf, off the south western side of the Eyre Peninsula, were defined by James et al. (1997). These were based on observations of sediments recovered on the 1994 RV *Franklin* cruise (FR 06/94). The composition of the inner to mid shelf facies (**Facies 1**), in this area (from Elliston to south west of Kangaroo Island), were found to be similar to the inner shelf facies on the Lacepede/ Bonney Shelf (James et al., 1992), i.e. rich in bivalves and bryozoa with abundant rusty-coloured relict grains and/or quartz. These relict grains comprise more than 50% of the grains in the samples from the inner coastal margins of Kangaroo Island and western Eyre Peninsula (James et al. (1997). The distribution of the coarse grained branching coralline algal facies (**Facies 3D**) on the Lincoln Shelf has been discussed, above, in conjunction with the lower Spencer Gulf substrate biofacies (Facies 2 (Fuller et al., 1994) and Facies 2D (James et al., 1992).

The composition of biota in the outer shelf facies, south of Eyre Peninsula, is dominated equally by bryozoa and articulated coralline algae with minor molluscs and foraminifera. The sediments are well sorted fine to medium grained sand with minor coarse skeletal material (James et al., 1997) (this is similar to Facies 3 (Robust Bryozoa sand) on the Lacepede/ Bonney shelf). The shelf edge facies has broad similarities to the outer shelf facies except the coralline algae has been replaced by azooxanthallate coral. This facies shows an increase in gravel and mud sized grains indicating that the depositional environment is below the wave base, so the biota is not subject to sustained mechanical breakdown and the low energy of the environment allows the deposition of muds (Note that the mud deposition in Streaky Bay is the 'opposing end of the shelf spectrum' - low energy environment)

### 9.6.4 SOUTHERN SPENCER GULF, INVESTIGATOR STRAIT

The inner shelf at the entrance to the Spencer Gulf was sampled from the research vessel RV *Ngerin* in 1990 (Fuller et al., 1994). The sediments from this area, between the foot of York Peninsula and the southern coast of Eyre Peninsula, were dredged in water depths which ranged from 10 m to 50 m. These sediments from the inner shelf were found to be principally of biogenic origin with molluscs, bryozoa and calcareous algae being the dominant contributors (Fuller et al., 1994). The different facies proposed for the area included; 'molluscan sands', 'branching coralline algal gravels', 'molluscan bryozoan sands', 'mixed bioclastic sands' and 'bryozoan gravels'. The shallow water areas along the western margin of the southern gulf are the sites for the 'molluscan sand' facies which can correlated with the inner shelf facies (**Facies 1**) from the Lacepede and Bonney Shelves. The 'mixed bioclastic sand' and 'molluscan-bryozoan sand' appear to be similar to the mid-shelf facies (**Facies 2**) on the same shelves and the 'bryozoan gravel' is also similar to the same but much deeper water facies on the eastern shelves (James et al., 1992, 1997).

In the western entrance of Spencers Gulf, within 26 m of the surface, lies a branching coralline algal gravel facies (Fuller et al., 1994) which is similar to Facies 2D on the Lacepede Shelf. Both of these facies are located on the protected western lee sides of the two areas (Fuller et al., 1994). A similar facies occurs on the western side of the Gulf St. Vincent at a similar water depth (Shepherd and Sprigg, 1976). Deepwater occurrences of rigid branching corallines and rhodoliths have been observed in samples from 100m up to 240 m water depth (although not living) on the Lincoln Shelf (James et al., 1997) and as fragments on the Lacepede Shelf (James et al., 1992). Articulated corallines occur on the Lincoln Shelf (>40%) between ~120m and ~180 m and as trace fragments (<2%) on the western Lacepede Shelf (**Facies 2D**). These have been observed in thin section, but it has not been possible to readily determine whether these are relict or fresh (James et al., 1992). Deepwater rhodoliths occur in a narrow band (**Facies 3D**) on the Lincoln Shelf (>30%) in 120-250 m water depth, south of the tip of Eyre Peninsula (James et al., 1997).

### 9.6.5 LACEPEDE AND BONNEY SHELVES

The Lacepede and Bonney shelves, including the area to the south of Kangaroo Island, have been sampled by James et al. 1992, on two CSIRO R.V. *Franklin* cruises ((FR 03/89 and FR 02/91) and sedimentary biofacies have been proposed. Five main facies were described, on a broad basis which included; inner shelf bivalve rich palimpsest sands, mid shelf bivalve/ bryozoan rich sands, outer shelf bryozoan sands, upper slope bryozoan muds and continental slope pelagic muds. The outer shelf-upper slope bryozoal mud had already been partially delineated by von der Borch and Hughes Clarke (1993), on an HMAS *Cook* cruise in the southern Lacepede to the northern Bonney shelf area. This facies was proposed as an active sediment producing area for sediments found on the lower to upper continental slope.

The inner shelf sedimentary facies were subdivided by James et al. (1992) according to dominant biota, mineralogy, and grainsize (**Facies 1 and 2**). The inner facies, on the northern Lacepede Shelf, reflects the influence of the Murray River outflow with a significant component of terrestrial material. **Facies 1** was further subdivided into a 'Molluscan quartz sand' which is proximal to the river outflow, and a 'Bivalve-cobble quartz sand' being immediately adjacent the Younghusband Peninsula to a depth of 50 m. **Facies 2** still reflected the terrestrial influence of the Murray River outflow but the active biogenic contributors to the sediment had shifted from solely molluscan to sub equal parts of molluscan and bryozoan. The subdivisions in Facies 2 reflect the changing mixtures of quartz, mollusc, bryozoa, coralline algae and relict limestone gravel. Both of these inner shelf facies contain significant amounts of relict, rounded biogenic sediment which represents stranded aeolianitic material from the Pleistocene sea-level lowstands (James et al (1992),).

Assemblage facies (**Facies 3**) based on the structural architecture of bryozoans and coralline and peyssonelid algae were also outlined as being a function of the wave energy and water depth of the environment. The cheilostome bryozoan structural forms dominant on the shelf were articulated zooidal, encrusting, delicate articulated branching, fenestrate, flat robust branching adeoniform, and nodular. Nodular to multilaminar, and the more delicate structural forms were the more common varieties at greater depths (>100 m). Rigid delicate branching cyclostomes were the dominant bryozoan sediment producer at depths over 100 m (ibid.). Depth zonations based on the structural forms of calcareous algae were found to be <100 m for encrusting forms of corallines and peyssonelids, and limit for robust branching corallines was <70 m although, fragments of branching corallines were recovered from depths up to 240 m (James et al (1992)

Significant broad-based facies based on the diversity and architectural types of bryozoans are evident in Streaky Bay as indicated in the component results of the gravel fraction. However, these are controlled by substrate variation rather than water depth as are the broad shelf facies.

## 9.7 CONCLUSIONS

The lithofacies proposed for Streaky Bay and embayments on West Coast of the Eyre Peninsula are similar to heterozoan lithofacies found in temperate marine environments in the southern and northern hemispheres.

The spatial distribution lithofacies can be determined statistically by clustering the components of the dominant sediment texture. These are then modified by textural variation i.e. gravel , mud, very fine to very coarse sand. The number of lithofacies selected are optimised according to the size of clusters to the size of the sample population, the morphological variation of the area under investigation and the textural variation in the sediments. Five lithofacies were considered representative of the facies found in Streaky Bay. The selection of four lithofacies does allow for the delineation of the observed detail on the outer terrace. In contrast, the cluster population becomes too small, with six lithofacies, to transmit a concept of the hydrodynamic processes and dominant sediment compositions that are present.

Therefore the facies proposed for Streaky Bay are;

- Facies 1: Mollusc/ aeolianite/ quartz/ bryozoa, medium to fine sand lithofacies; northern and central terrace, central eastern coastal margin, isolated pockets in the entrance and southwest coastal margin.

- Facies 2: Aeolianite/ mollusc/ quartz, very coarse to fine sand lithofacies; sand shoals, southeast coastal margin, northern and southern inner terrace, isolated occurrences northeast coastal margin and central entrance.

- Facies 3: Mollusc/ foraminifera/ bryozoan/ coralline algae, gravelly fine to very coarse sand lithofacies; central inner terrace.

- Facies 4: Bryozoa/ mollusc/ aeolianite/ coralline algae, gravelly medium to very coarse sand (medium to very coarse sandy gravel) lithofacies; entrance and portion of the northern terrace.

- Facies 5: Mollusc/ echinoid/ quartz/ foraminifera, fine sandy mud lithofacies; the inner marginal basins and Blanche Port.

The spatial distribution of lithofacies indicate that the entrance/terrace area of the bay is the principal biogenic sediment producing area. This area also contains the widest range of identifiable calcareous organisms. Organism diversity varies inversely with the volume of calcareous aeolianite/quartz present in the sediment

The lithofacies present in Streaky Bay have approximate equivalents in the embayments along the west coast of the Eyre Peninsula and on the open shelf. The ranked dominant components of the Eyre Peninsula embayments are molluscs (dominant). calcareous aeolianite (highly significant), bryozoans, quartz/lithic, coralline algae and foraminifers. There are variations in these components according to

substrate type, hydrodynamic regime and the geology of each area. Variations of molluscs and calcareous aeolianite are the main contributors to the coastal lithofacies.

Lithofacies within Streaky Bay are correlated to proximal shelf lithofacies. SB Lithofacies 1 is correlated with inner-shelf Lithofacies MI (mollusc/ intraclast) and Q (quartz/ skeletal) facies. SB Lithofacies 2 is similar to the inner-shelf Facies IM and MI (intraclast/ mollusc and mollusc/ intraclast facies). SB Facies 4 is similar to Facies BI ( mid-shelf bryozoan/ intraclast), although in SB Facies 4 the bryozoan and molluscan components are subequal with significant intraclast component.

A mud-rich lithofacies situated on the outer shelf/ slope is similar to that in Streaky Bay. Although, on the outer shelf the dominant components are disarticulated and macerated bryozoan particles and sponge spicules. Therefore the shelf grainstone lithofacies can be clearly identified between the two mud-rich wackestone lithofacies of the outer shelf and proximal coastal margin.

# CHAPTER TEN

# CONCLUSIONS

The South Australian shelf is covered with cool-water carbonate sediments. The eastern shelf sector of the Great Australian Bight is the most contiguous of the southern margin shelf sectors. The coastal margin is punctuated by a variety of embayments. It was found that the sediments within the various embayments along this sector could be interpreted through comparison with one of the principal embayments, namely Streaky Bay. One of these embayments, Streaky Bay, is important as it is a relatively pristine environment, with relatively little human impact. Hence it was selected for the base-line study of sediments and lithofacies described in this study. This study has also encapsulated reports from the other embayments, and related the sediments to the general hydrodynamic regime of the western Eyre Peninsula.

The aims that were established at the beginning of this study were:

- To determine the geochronology of the late Quaternary to the present day embayment and thereby also establish the sedimentological framework.

- To ascertain and describe the sediments from Streaky Bay and thereby also provide a sedimentary facies model for the western Eyre Peninsula embayments.

• To determine and describe how biota with calcareous skeletons become carbonate sediments with the emphasis on the production of carbonate mud in the shallow cool-water carbonate setting.

The far-field tectonic stability of the Eyre Peninsula and more particularly the Streaky Bay area, has provided a unique opportunity to study marginal marine biogenic sediments. This stability is attributable to the cratonised Proterozoic basement rocks, which comprise part of the Gawler Craton and are found the beneath Streaky Bay.

The high stand sea-level of Isotope Stage 5e on the west coast of Eyre Peninsula is approximately 1.8 m above the present-day sea-level and agrees with heights reported across the globe, in areas of tectonic stability. The timing of Isotope Stage 5e in the Eyre Peninsula region is established at 124 ±9 ka BP. Glanville Formation marine sediments are spatially more extensive than present day sediments, which is attributable to this previous higher sea-level. The discovery of the present-day tropical coral *Goniopora somaliensis*, along with *Anadara trapezia* and *Marginopora vertebralis* within the Glanville Formation, establishes that the seawaters, at least on the inner GAB shelf, were significantly warmer (by 7 - 9 °C) during Isotope Stage 5e than present day conditions.

Marine conditions became re-established in the Streaky Bay region during the early Holocene prior to 7300 years BP with extensive sedimentation occurring on the coastal margins during the past 3500 years. This significant sedimentation period has led to the continued expansion of the shallow sand shoals in Streaky Bay and probably other embayments on the west coast.

The principal morphological features in Streaky Bay consist of the inner marginal basins, which are the deeper water areas of a flooded back-dunal corridor . Coastal margin spits and central shallow sand shoals prograde into these basins, the latter via large scale tidal deltas (up to 3 km wide). These calcareous sediments from the sand shoals are prograding over calcareous muds in the deep water areas. Rocky substrates with sand patches characterise the outer areas and provide a suitable substrate for epiphytic calcareous biota to flourish. The rocky areas are commonly scalloped and creviced and moderately covered with calcrete pebbles to boulders. Sandy sediments migrate across this area in mobile sand waves, driven by high energy waves from the Southern Ocean. The inner area of the bay is characterised by cyclonic and anticyclonic eddies, which have probably led to the formation of two East-West sygmoidally shaped elongate sand banks.

The sediment grainsize in Streaky Bay generally becomes finer towards the inner areas of the bay and a broad gradational coarsening of grainsize occurs from South to North due to an increasing energy regime from the swells of the Southern Ocean. A significant attenuation of wave energy in the central

shallow sand shoal region has allowed favourable conditions for the deposition of very fine sandy mud over a considerable area of the deeper inner bay.

The biogenic composition of the sediments is that of a cool-water carbonate heterozoan assemblage or more specifically variations between a foramol and a bryomol assemblages The assemblage is similar to the shallow water Great Australian Bight shelf sediments and is similar to assemblages found in the shallow cool-water shelf regions of the Northern and Southern Hemispheres.

Molluscs are the dominant living fauna in the bay with bivalves inhabiting the softer substrate and gastropods the firm or rocky substrate and seagrass meadows. Foraminifers, bryozoans and coralline algae vary in concentrations across the bay depending on the substrate present. Abraded bioclastic grains, which are composed of the above faunal groups, are concentrated in areas of active transport and deposition rather than where they actually live , ie. thanatocoenosis is common. The heterozoan assemblages in Streaky Bay are differentiated from cool-water assemblages on a global scale by the mixing of grains derived from the local underlying lithology. This modification appears within the embayments on the West Coast of the Eyre Peninsula and similar world-wide localities are equally modified by substrate and coastal geology.

Molluscs are also the dominant group in the sediments, representing a range of infaunal and epifaunal bivalves and grazing and predatory gastropods. The distribution of the mollusc fragments is controlledby the substrate variation. The subsequent disintegration characterises the sediments along the west coast of the Eyre Peninsula. The structural diversity of bryozoans increases proportionately with the areal extent of rocky substrate siutable for bryozoan colonisation. This relates to low population and diversity in low energy areas, with encrusting, delicate branching and articulated delicate branching forms common. Abundant articulated and robust crustose coralline algae and rare patches of rhodoliths occur on the high energy areas, while delicate crustose and articulated coralline algae occur in the lower energy areas.

The production, composition and morphology of marginal marine muds (<63 μm grainsize) in a temperate setting has been fully described as this size fraction has an important place as micritic matrix and is a potential source for cements. The carbonate content of the mud in Streaky Bay is approximately 93%, and the composition is aragonite < LMC = IMC < HMC. This general mud composition is similar to that of the skeletal material, which also compares closely with organisms found in other cool-water carbonate realms both in the southern and northern hemisphere.

The primary source of the significant calcium carbonate particles in the mud fraction, in order of abundance, is from molluscs, bryozoan, coralline algae, foraminifers, echinoderms, sponge spicules

and serpulids with minor contributions from brachiopods, tunicates, corals and coccoliths. These biota produce mud particles of prismatic, tabular, laminate, blocky, polygonal, bladed and composite morphologies, as highlighted in Table 10.1.

| Particle morphology | Predominant Mineralogy | Contributing Organisms |
|---|---|---|
| Prismatic | Aragonite/LMC | molluscs |
| Tabular/ Laminate | Aragonite/LMC < HMC | molluscs<br>foraminifera<br>brachiopods<br>coral<br>serpulids |
| Polygonal | Aragonite/LMC < IMC | bryozoans<br>echinoderms<br>foraminifera<br>coral |
| Blocky | LMC/Aragonite | molluscs |
| Composite | Aragonite/LMC < IMC < HMC | bryozoans<br>coralline algae<br>sponges |
| Blade / Laminate | Aragonite/LMC | brachiopods<br>bryozoans |

Table 10.1 Composition and significant origin of mud particles.

The disintegration of skeletal material, produces the muds. This is brought about by maceration coupled with medium to high energy sea movement.

The limestone equivalents of the marine sediments on the eastern Great Australian Bight embayments are predominantly fossiliferous grainstones, fossiliferous packstones and fossiliferous wackestones (or using Folk's classification - biomicrite to bio (sparite)- depending on cementation style).

This study has socio-economic significance and also relates to matters in the national interest. The realm of navigation for Harbours and Port Authorities concerns sea-floor morphology and its stability through time and space. The movement and safety of shipping can now be protected with the ability to predict stable substrates and mobile areas of active progradation. It is also imperative that the stability and type of the substrate is known before laying submarine communication cables. This study can present base-line results from environments similar to the wide variety found in most coastal settings.

Marginal cool-water marine depositional environments are important in the geological column as they can indicate the transition from marine to terrestrial sedimentary sequence in an environment where contributions from land derived sediment is minor. This lack of terrestrial sediment highlights the importance and productivity, albeit significantly lower than tropical regimes, of carbonate secreting organisms in embayments proximal to cool-water shelves.

Streaky Bay represents an interface between the present and the past, ie. it provides a model today, for embayments on the west coast of the Eyre Peninsulsa and an analogue for understanding marginal cool-water carbonate limestone shelf sequences of the past.

# References

**Aguirre, M.L.**, 1993, Palaeobiogeography of the Holocene molluscan fauna from northeastern Buenos Aires Province: its relation to coastal evolution and sea level changes: Palaeogeography, Palaeoclimatology, Palaeoecology, v. 102, p. 1-26.

**Andrews, J.E., Christidas, S., and Dennis, P.F.**, 1997, Assessing mineralogical and geochemical heterogeneity in the sub 63 micron size fraction of Holocene lime muds: Journal of Sedimentary Research, v. 67, p. 531-535.

**Arakel, A.V.**, 1980, Genesis and diagenesis of Holocene evaporitic sediments in Hutt and Leyman Lagoons, Western Australia: Journal of Sedimentary Petrology, v. 50, p. 1305-1326.

**Baker, A.N.**, 1982a, SEA-URCHINS (Class ECHINOIDEA), *in* Sherpherd, S.A., and Thomas, I.M., ed., Marine Invertebrates of Southern Australia; Part I: Adelaide, South Australia, Government Printer, p. 491.

**Baker, A.N.**, 1982b, BRITTLE-STARS (Class OPHIUROIDEA), *in* Sherpherd, S.A., and Thomas, I.M., ed., Marine Invertebrates of Southern Australia; Part I: Adelaide, South Australia, Government Printer, p. 491.

**Barnett, E.J.**, 1993, Recent sedimentary history of Lake Alexandrina and the Murray Estuary [unpublished Ph.D. thesis]: The Flinders University of South Australia, Adelaide, South Australia.

**Bathurst, R.G.C.**, 1983, Carbonate sediments and their diagenesis: Developments in Sediimentology, v. 12: Amsterdam, Elsevier Scientific, 658 p.

**Belperio, A.P., Hails, J.R. and Gostin, V.A.**, 1983, A review of Holocene sea levels in South Australia, *in* Hopley, D., ed., Australian Sea Levels in the Last 15000 years: A Review: Monograph Series: Townsville, Department of Geography, James Cook University of North Queensland, p. 37-47.

**Belperio, A.P., Hails, J.R., Gostin, V.A. and Polach, H.A.**, 1984a, The stratigraphy of coastal carbonate banks and Holocene sea levels of northern Spencer Gulf, Australia: Marine Geology, v. 61, p. 297-313.

**Belperio, A.P., Murray-Wallace, C.V., and Cann, J.H.**, 1995, The last interglacial shoreline in southern Australia: Morphostratigraphic variations in a temperate setting: Quaternary International, v. 26, p. 7-19.

**Belperio, A.P., Smith, B.W., Polach, H.A., Nittrouer, C.A., DeMaster, D.J., Prescott, J.R., Hails, J.R. and Gostin, V.A.**, 1984b, Chronological studies of the Quaternary marine sediments of northern Spencer Gulf: Marine Geology, v. 61, p. 265-296.

**Belperio, A.P., Gostin, V.A., Cann, J.H., and Murray-Wallace, C.V.**, 1988, Sediment-organism zonation and the evolution of Holocene tidal sequences in Southern Australia, *in* De Boer, P.L., van Gelder, A. and Nio, S.D., ed., Tide-Influenced sedimentary environments and facies: Dordrecht, Reidal Publishing Co., p. 475-497.

**Belperio, A.P.**, 1988, Fowlers Bay rotary drilling report and revision of the Quaternary geology around Fowlers Bay: Department of Mines and Energy, South Australia.

**Belperio, A.P., and Fotheringham, D. G.**, 1990, Geological setting of two Quaternary footprint sites, western South Australia: Australian Journal of Earth Sciences, v. 37, p. 37-42.

**Belperio, A.P.**, (compiler), 1995, Quaternary, *in* Drexel, J.F., and Priess, W.V., ed., The Geology of South Australia, The Phanerozoic: Adelaide, South Australian Geological Survey, Bull. 54. chapt. 11.

**Bird, E.C.F.**, 1984, Beaches, Spits and Barriers, Coasts: Canberra, ANU Press.

**Blom, W.M.**, 1988, Late Quaternary sediments and sealevels in the Bass Basin, southeastern Australia- a preliminary report: Search, v. 19, p. 94-96.

**Blom, W.M., and Alsop, D.B.**, 1988, Carbonate mud sedimentation on a temperate shelf: Bass Basin, southeastern Australia: Sedimentary Geology, v. 60, p. 269-280.

**Bock, P.E.**, 1982, Bryozoans (Phylum Bryozoa of Ectoprocta), *in* Sherpherd, S.A., and Thomas, I.M., ed., Marine Invertebrates of Southern Australia; Part I: Adelaide, South Australia, Government Printer, p. 491.

**Bone, Y., and James, N.P.**, 1993, Bryozoans as carbonate sediment producers on the cool-water Lacepede Shelf, southern Australia: Sedimentary Geology, v. 86, p. 247-271.

**Bone, Y., and James, N.P.**, 1997, Bryozoan stable isotope survey from the cool-water Lacepede Shelf, southern Australia, *in* James, N.P., and Clarke, J.A.D., ed., Cool-water Carbonates: Special Publications: Tulsa, USA, Society For Sedimentary Geology, p. 93-106.

**Boreen, T., James, N., Wilson, C., and Heggie, D.**, 1993, Surficial cool-water carbonate sediments on the Otway continental shelf, southeastern Australia: Marine Geology, v. 112, p. 35-66.

**Boreen, T.D., and James, N.P.**, 1993, Holocene sediment dynamics on a cool-water carbonate shelf: Otway, southeastern Australia: Journal of Sedimentary Petrology, v. 63, p. 574-588.

**Boreen, T.D., and James N.P.**, 1995, Stratigraphic sedimentology of Tertiary cool-water limestones, SE Australia: Journal for Sedimentary Research, v. B65, p. 142-159.

**Bowen, D.Q.**, 1978, Sea Level, *in* Bowen, P.Q., ed., Quaternary Geology. A Stratigraphic Framework for Multi-disciplinary Work: Oxford, Pergamon Press, p. 221.

**Bowler, J.M.**, 1976, Recent developments in reconstructing late Quaternary environments in Australia, *in* Kirk, R.L., Thorne, A. G., ed., The Origin of the Australians: Human biology series: N.J. USA, Humanities Press Inc.

**Bowman, G.M.**, 1985, Oceanic reservoir correction for marine radiocarbon datesfrom Northwestern Austalia: Australian Archeology, v. 20, p. 58-67.

**Bowman, G.M., and Harvey, N.**, 1983, Radiocarbon dating marine shells in South Australia: Australian Archeology, v. 17 113-123.

**Brandley, R.T., and Krause ,F.F.**, 1997, Upwelling, thermoclines and wave-sweeping on an equatorial carbonate ramp: lower Carboniferous strata of western Canada: *in* James, N.P., and Clarke, J.A.D., ed., Cool-Water Carbonates: Special Publication: Tulsa, U.S.A., S.E.P.M., p. 365-390.

**Brasier, M.D.**, 1980, Microfossils: London, George Allen and Unwin, 193 p.

**Brookfield, M.E.**, 1988, A mid-Ordovician temperate carbonate shelf - the Black River and Trenton Limestone Groups of southern Ontario, Canada: Sedimentary Geology, v. 60, p 137-154

**Brown, K.M., Bone, Y., James, N.P.**, 1998, Calacreous epiphytes: Their significance as carbonate producers: Geological Soceity of Australia Abstracts, v. 49, p. 55.

**Brown, K.M., Bone, Y., Cheshire, A., and James, N.P.**, 1999, Calcium carbonate from epiphytes on *Posidonia* sp. & *Amphibolis* sp., South Australian coastline: preliminary results: Fourth Australian Marine Geoscience Conference, p. 11.

**Buckley, R.C., Short, A. D., and Fotheringham, D. G.**, 1987, Late Pleistocene sea-level maxima in the Great Australin Bight: Search, v. 18, p. 86-89.

**Burne, R.V.**, 1982, Relative fall of Holocene sea level and coastal progradation, northeastern Spencer Gulf, South Australia: Journal of Australian Geology and Geophysics, v. 7, p. 35-45.

**Bureau of Meteorology**, 2001, Average mean annual SST, Australian Waters: [Online, accessed 20 July 2001]. URL: http://www.bom.gov.au/sat/sst/sst-aust

**Burne, R.V.**, 1982, Relative fall of Holocene sea level and coastal progradation, NE Spencer Gulf South Australia: Journal of Australian Geology and Geophysics, v. 7, p. 35-45.

**Bye, J.A.T.**, 1972, Oceanic circulation south of Australia, *in* Hayes, D.E., ed., Antarctic Oceanology II: The Australian-New Zealand Sector: Antarctic Research Series p. 95-99.

**Bye, J.A.T., and Ng, S.C.**, 1994, The FLOW C Model: Adelaide, Flinders Institute of Marine Science, The Flinders University of South Australia.

**Calder, C.M.**, 1989, Streaky Bay, Southwest Coast, Aus 121: Hydrographic Service, R.A.N.

**Cann, J.H.**, 1978, An exposed reference section for the Glanville Formation: Quarterly Geological Notes, v. 65, p. 2-4.

**Cann, J.H., and Gostin, V.A.**, 1985, Coastal Sedimentary facies and foraminiferal biofacies of the St. Kilda Formation at Port Gawler, South Australia: Transactions Royal Society of South Australia, v. 109, p. 121-142.

**Cann, J.H., Belperio, A. P., Gostin, V. A., and Rice, R. L.**, 1993, Contemporary benthic Foraminifera in Gulf St. Vincent, South Australia, and a refined Late Pleistocene sea-level history: Australian Journal of Earth Sciences, v. 40, p. 197-211.

**Carannante, G., Estaeban, M., Milliman, J.D. and Simone, L.**, 1988, Carbonate lithofacies as paleolatitude indicators: problems and limitations: Sedimentary Geology, v. 60, p. 333-346.

**Carannante, G., Graziano, R., Ruberti, D., and Simone, L.**, 1997, Upper Cretaceous temperate type open shelves from northern (Sardinia) and southern (Appennines-Apula) Mesozoic tethyan Margins; *in* James, N.P., and Clarke, J.A.D., ed., Cool-Water Carbonates: Special Publication: Tulsa, U.S.A., S.E.P.M., p. 309-326.

**Chappell, J., and Shackleton, N.J.**, 1986, Oxygen isotopes and sea level: Nature, v. 324, p. 137-140.

**Chappell, J.**, 1987, Late Quaternary sea-level changes in the Australian Region, *in* Tooley, M.J., and Shennan, I., ed., Sea-level Changes: Oxford, The Institute of British Geographers.

**Chappell, J.**, 1994, Quaternary sea-levels, tectonics and coral terraces at Huon Peninsula: , Reseach School of Pacific and Asian Studies, Australian National University.

**Chappell, J., Omura, A., Esat, T., McCulloch, M., Pandofi, J., Ota, Y., and Pillans, B.**, 1996, Reconciliations of late Quaternary sea-levels derived from coral terraces at Huon Peninsula with deep sea oxygen isotope records: Earth and Planetary Science Letters, v. 141, p. 227-236.

**Chave, K.E.**, 1967, Recent carbonate sediments - an unconventional view: Journal of Geological Education, v. 15, p. 200-204.

**Chelton, D.B., Hussey, K.J., and Park, M.E.**, 1981, Global satellite measurements of water vapour, wind speed and wave height: Nature, v. 294, p. 529-532.

**Christie-Blick,N., Mountain, G.S., and Miller, K.G.**, 1990, Seismic strastigraphic record of sea level change, *in* Revelle,R., (ed), Sea level change: National Research Council, Studies in Geophysics, Washinhton D.C., National Academy Presss, p. 116-140

**Clarke, J.D.A., Bone, Y. and James, N.P.**, 1996, Cool-water carbonates in an Eocene paleoestuary, Norseman Formation, Western Australia: Sedimentary Geology, v. 101, p. 213- 226.

**Clarke, P.A.**, 1994, Streaky Bay; Residual Currents: [unpublished BSc Hons thesis]: Flinders University of South Australia.

**Cloetingh, S., McQueen, H. and Lambeck, K.**, 1985, On a tectonic mechanism for regional sea-level variations: Earth and Planetary Science Letters, v. 75, p. 157-166.

**Collins, L.B.**, 1988, Sediments and history of the Rottnest Shelf, southwest Australia: a swell-dominated, non-tropical carbonate margin: Sedimentary Geology, v. 60, p. 15-49.

**Collins, L.B., France, R.E., Zhu, Z.R., and Wyroll, K-H.**, 1997, Warm-water platform shelf carbonates of the Abrolhos Shelf, southwest Australia, *in* James, N.P., and Clarke, J.A.D., ed., Cool-Water Carbonates: Special Publication: Tulsa, U.S.A., S.E.P.M., p. 23-36.

**Collins, M.B., Shimwell, S.J., Gao, S., Powell, H., Hewitson, C., and Taylor J.A.**, 1995, Water and sediment movement in the vicinity of linear sandbanks: the Norfolk Banks, southern North Sea: Marine Geology, v. 123, p. 125-142.

**Conolly, J.R., and von der Borch, C.C.**, 1967, Sedimentation and Physiography of the sea floor south of Australia: Sedimentary Geology, v. 1, p. 181-220.

**Corliss, K.E., and Honjo, S.**, 1981, Dissolution of deep-sea benthonic foraminifera: Micropaleontology, v. 27, p. 356-378.

**Cresswell, G.R.**, 1991, The Leeuwin Current - observations and recent models: Journal Royal Society of Western Australia, v. 74, p. 1-14.

**Cresswell, G.**, 1993, Ocean Depths and Currents, *in* Kailola, P.J., Williams, M.J., Stewart, P.C., Reichelt.R. E., McNee, A., and Grieve, C., ed., Australian Fisheries Resourses: Canberra, Australia, Bureau of Resourse Sciences, Department of Primary Industries and Energy, Fisheries Research and Development Corporation, p. 22-31.

**Daniel, R.F., and von der Borch, C.C.**, 1995, Carbonate sediment distribution patterns of a cool-water embayment; Streaky Bay, South Australlia: A preliminary report: Cool and Cold-water Carbonate Conference, Abstracts.

**Daniel, R.F., and von der Borch, C.C.**, 1997, Composition and grainsize distribution patterns of sediment: Streaky Bay, South Australia: Third Australian Marine Geoscience Conference, Abstracts.

**Daniel, R.F., von der Borch, C.C., James, N.P., and Bone, Y.**, 1998a, Carbonate Sediments: Streaky Bay, South Australia: 14th Australian Geological Convention, Abstracts.

**Daniel, R.F., von der Borch, C.C., Veeh, H.H., James, N.P. and Bone, Y.**, 1998b, Late Quaternary Evolution of Streaky Bay, South Australia: Relative sea-levels and timing: Eighth Biennial Conference, Australian and New Zealand Geomorphological Group, Abstracts.

**Davies, P.J.**, 1979, Marine geology of the continental shelf off southeast Austalia: Bureau of Mineral Resources, Geology and Geophysics, Canberra, Australia.

**Davies, J.L.**, 1980, Geographical Variation in Coastal Development: London, Longmans, 212p.

**Davis, R.A., Reas, C., and Robbins, L.L.**, 1995, Calcite Mud in a Back-Barrier Lagoon: Lake Reeve, Victoria, Australia: Journal of Sedimentary Research, v. A65, p. 178-184.

**De Dekker, P., Bauld, J. and Burne, R. V.**, 1982, Pillie Lake, Eyre Peninsula, South Australia: modern environment and biota, dolomite sedimentation and Holocene history: Transactions Royal Society of South Australia, v. 106, p. 169-181.

**Devoy, R.J.N.**, 1987, Introduction: first principles and the scope of sea-surface studies, *in* Devoy, R.J.N., (ed), Sea-surace studies, a global view: New York, Croom Helm, p 1-30.

**Dietz, R.S.**, 1963, Wave-base, marine profile of equilrium, and wave-built terraces: a critcal appraisal: Geological Society of America Bulletin, v. 74, p. 971-990.

**Dove, M.B.**, 1997, The geology, petrology, geochemistry and isotope geology of the eastern St. Peter Suite, western Gawler Craton, South Australia [unpublished B.Sc.(Hons) thesis]: The University of Adelaide, Adelaide, South Australia.

**Draper, J.J.**, 1988, Permian limestone in the southeastern Bowen Basin, Queensland: an example of temperate carbonate deposition: Sedimentary Geology v. 60, p. 155-162

**Dunham, R.J.**, 1962, Classification of carbonate rocks according to depositional texture, *in* Ham, W.E., ed., Classification of Carbonate Rocks: Tulsa, USA, American Association of Petroleum Geologists, p. 108-121.

**Echols, C.S.**, 1993, Diatom infestation of recent crinoid ossicles in temperate waters, Friday Harbor Laboratories, Washington: Implications for biodegradation of skeletal carbonates: Palaios, v. 8, p. 278-288.

**Exon, N.G., and Lee, C.S.**, 1987, Rig Seismic research cruise 1987: Otway Basin and west Tasmania sampling, Cruise 78: Bureau of Mineral Resourses.

**Farrand, M.G., and Belperio, A. P.**, 1987, Petrological examination of Quaternary coastal sediments from western South Australia between Head Of The Bight and Sheringa Lagoon: Dept. of Mines and Energy, South Australia.

**Farrow, G.E., Allen, N.H., and Akpan, E.B., 1984,** Bioclastic carbonate sedimentation on a high-latitude, tide dominated shelf; northeast Orkney Islands, Scotland: Journal of Sedimentary Petrology, v. 54, p. 373-393.

**Farrow, G.E., and Fyfe, J.A.**, 1988, Bioerosion and carbonate mud production on high-latitude shelves: Sedimentary Geology, v. 60, p. 281-297.

**Ferland , M.A., and Roy, P.S.**, 1997, Southeastern Australia: A sea-level dependent, cool-water carbonate margin, *in* James, N.P., and Clarke, J.A.D., ed., Cool-water Carbonates: Special Publications: Tulsa, Society for Sedimentary Geology, p. 37-52.

**Fleming, B.W.**, 1977, Depositional processes in Saldanha Bay and Langebaan Lagoon, South Africa: Marine Geology and Geophysics Division of the National Reseach Institute for Oceanography, Council for Scientific and Industrial Research, Stellenbosch, South Africa.

**Flinders, Captain M.**, 1814, Voyage to Terra Australis: Undertaken for the purpose of completing the discovery of that Vast Country, and prosecuted in the years 1801, 1802 and 1803, in His Majesty's ship the Investigator, v. 1: G. & W. Nicol, London.

**Foged, N.**, 1978, Diatoms in Eastern Australia: Bibliotheca Phycologica, v. 41, p. 1-243.

**Foged, N.**, 1979, Diatoms in New Zealand, North Island: Bibliotheca Phylocogica, v. 47, p. 1-225.

**Folk, R.L.**, 1959, Practical petrographic classification of limestones: Bulletin of American Association of Petroleum Geologists, v. 43, p. 1-38.

**Folk, R.L.**, 1962, Spectral subdivision of limestone types, *in* Ham, W.E., ed., Classification of Carbonate Rocks: Tulsa, USA, American Association of Petroleum Geologists, p. 62-84.

**Folk, R.L.**, 1968, Petrology of Sedimentary Rocks, Hemphills, Austin, Texas, USA.

**Folk, R.L.**, 1993, SEM imaging of bacteria and nannobacteria in carbonate sediments and rocks: Journal of Sedimentary Geology, v. 63, p. 990-999.

**Folk, R.L., and Lynch, F.L.**, 1997, The possible role of nannobacteria (dwarf bacteria) in clay-mineral diagenesis and the importance of careful sample preparation in high-magnification SEM study: Journal of Sedimentary Research, v. 67, p. 583-589.

**Fornos, J.J., and Ahr, W. M.**, 1997, Temperate carbonates on a modern, low-energy, isolated ramp: The Balearic Platform, Spain: Journal of Sedimentary Reseach, v. 69, p. 364-373.

**Franseen, E.K., Goldstein, R.H., and Farr, M.R.**, 1997, Substrate-slope and temperature controls on carbonate ramps: revelations from upper Miocene outcrops: *in* James, N.P., and Clarke, J.A.D., ed., Cool-Water Carbonates: Special Publication: Tulsa, U.S.A., S.E.P.M., p. 271-292.

**Freeman, A.R.**, 1985, The Quaternary geology of the Coffin Bay area, South Australia [unpublished B.Sc. Hons. thesis]: University of Adelaide, Adelaide, South Australia.

**Freiwald, A.**, 1995, Bacteria-induced carbonate degradation: A taphonomic case study of *Cibicides lobatulus* from a high-boreal carbonate setting: Palaios, v. 10, p. 337-346.

**Fuller, M.K., Bone, Y., Gostin, V.A., and Von Der Borch, C.C.**, 1994, Holocene cool-water carbonate and terrigenous sediments from southern Spencer Gulf, South Australia: Australian Journal of Earth Science, v. 41, p. 353- 363.

**Gill, E.D., and Amin, B.S.**, 1975, Interpretation of 7.5 and 4 metre last interglacial shore platforms in southeast Australia: Search, v. 6, p. 394-396.

**Gillespie, J.L., and Nelson, C.S.**, 1997, Mixed siliciclastic-skeletal carbonate facies on Wanganui Shelf, New Zealand: A contribution to the temperate carbonate model, *in* James, N.P., and Clarke, J.A.D., ed., Cool-water Carbonates: Special Publications: Tulsa, Society for Sedimentary Geology, p. 127-140.

**Gostin, V.A., Hails, J. R., and Polach, H. A**, 1981, Quaternary sea levels in upper Spencer Gulf, South Australia: Search, v. 12, p. 43-45.

**Gostin, V.A., Hails, J.R., and Belperio, A.P.**, 1984, The sedimentary framework of Northern Spencer Gulf, South Australia: Marine Geology, v. 61, p. 111-138.

**Gostin, V.A., Belperio, A.P. and Cann, J.H.**, 1988, The Holocene non-tropical coastal and shelf carbonate province of southern Australia: Sedimentary Geology, v. 60, p. 51-70.

**Grabau, A.W.**, 1913, Principles of Stratigraphy: New York, L.V. Seiler and Co., 1185 p.

**Greenstein, B.J.**, 1995, The effects of life habit and test microstructure on the preservation potential of echinoids in Graham's Harbour, San Salvador Island, Bahamas: *in* Curran H.A., and White B., eds., Terrestrial and Shallow Marine Geology of the Bahamas and Bermuda, Geological Society of America, Special Paper 300, Boulder Colorado

**Grindrod, J., and Rhodes, E.G.**, 1984, Holocene sea-level history of a tropical estuary, Missionary Bay, north Queensland, *in* Thom, B.G., ed., Coastal Geomorphology in Australia: Sydney, Academic Press, p. 151-178.

**Hageman, S.J., Bone, Y., McGowran, B., and James, N.P.**, 1995, Modern Bryozoan assemblages and distribution on the cool-water Lacepede shelf, southern Australian margin.: Australian Journal of Earth Sciences, v. 42, p. 571-580.

**Hageman, S.J., Bock, P.E., Bone, Y., and McGowran, B.**, 1998, Bryozoan growth habits: Classification and analysis: Journal of Paleontology, v. 72, p. 418-436.

**Hails, J.R., Belperio, A.P., and Gostin, V.A**, 1983, Holocene Sea Levels of Upper Spencer Gulf, South Australia, *in* Hopley, D., ed., Australian Sealevels in the Last 15,000 years: a review: Monograph series occasional paper No. 3: Townsville, James Cook University of North Queensland (Geography Dept.).

**Hails, J.R., Belperio, A.P., and Gostin, V.A.**, 1984, Quaternary Sea Levels, northern Spencer Gulf, Australia: Marine Geology, v. 61, p. 373-389.

**Ham, W.E.**, 1962, Classification of Carbonate Rocks: Tulsa, USA, American Association of Petroleum Geologists, p. 279.

**Hambin, W.K., and Christiansen, E.H.**, 1995, Earth's dynamic systems: 8th edition, Prentice -Hall, New Jersey, USA, 710 p.

**Hardy, R., and Tucker, M.**, 1988, X-ray powder diffraction of sediments, *in* Tucker, M., ed., Techniques in Sedimentology: Oxford, Blackwell Scientific Publications, p. 191-228.

**Harris, G.**, 1938, The Unknown Coast. The discovery and development of the Streaky Bay district of South Australia: Streaky Bay, West Coast Sentinal.

**Harris, P.T.**, 1994, Comparison of tropical and temperate, siliciclastic tidally dominated sedimentary deposits: Examples from the Australian continental shelf: Australian Journal of Earth Sciences, v. 41, p. 241-254.

**Harvey, N., and Belperio, A.**, 1994, Implications of climate change for the South Australian coastline: Transactions of the Royal Society of South Australia, v. 118, p. 45-52.

**Harvey, N., Barnett, E.J., Bourman, R.P., and Belperio, A.P.**, 1999, Holocene sea-level change at Port Pirie, South Australia: A contribution to global sea-level rise estimates from tide gauges: Journal of Coastal Research, v. 15, p. 607-615.

**Harwood, G.**, 1988, Microscopical techniques: Part II. Principles of sedimentary petrography, *in* Tucker, M., ed., Techniques in Sedimentology: Oxford, Blackwell Scientific Publications, p. 108-173.

**Hedges, R.E.M., and Gowlett, J.A.J.**, 1986, Radiocarbon dating by accelerator mass spectrometry: Scientific American, v. 254, p. 82-90.

**Henrich, R., and Wefer, G.**, 1986, Dissolution of biogenic carbonates: effects of skeletal structure: Marine Geology, v. 71, p. 341-362.

**Herzfeld, M.**, 1996, Sea Surface Temperatures and Circulation in the Great Australian Bight [unpublished PhD thesis]: Flinders Institute of Atmospheric and Marine Sciences, Flinders University of South Australia.

**Herzfeld, M.**, 1997, The annual cycle of sea surface temperature in the Great Australian Bight: Progress in Oceanography, v. 39, p. 1-27.

**Herzfeld, M., and Tomczak, M.**, 1997, Numerical modelling of sea surface temperature and circulation in the Great Australian Bight: Progress in Oceanography, v. 39, p. 29-78.

**Hill, R.J.**, 1994, Biofacies and the distribution of Foraminifera within Baird Bay - an inverse estuary [unpublished B.Sc. (Hons) thesis]: Flinders University of South Australia.

**Honjo, S.**, 1976, Coccoliths: production, transportation and sedimentation: Marine Micropaleontology, v. 1, p. 65-79.

**Hopley, D., and Thom, B.G.**, 1983, Australian Sea Levels in the Last 15000 years: A Review, *in* Hopley, D., ed., Australian Sea Levels in the Last 15000 years: A Review: Monograph Series: Townsville, Department of Geography, James Cook University of Northern Queensland.

**Hopley, D.**, 1983, Australian Sea Levels in the Last 15000 years: A Review, Monograph Series: Townsville, Department of Geography, James Cook University of Northern Queensland.

**Hopley, D.**, 1984, The Holocene 'high energy window' on the Central Great Barrier Reef, *in* Thom, D.G., ed., Coastal Geomorphology of Australia: Sydney, Academic Press, p. 135-150.

**Howchin, W.**, 1888, Remarks on a geological section at the new graving dock, Glanville, with special reference to a supposed old land surface now below sea-level: Transactions of the Royal Society of South Australia, v. 10, p. 31-35.

**Howchin, W.**, 1912, Notes on recurrent transgressions of the sea at Dry Creek: Transactions of the Royal Society of South Australia, v. 36, p. 34-39.

**Imbrie, J., and Purdy, E.G.**, 1962, Classification of modern Bahamian carbonate sediments, *in* Ham , W.E., ed., Classification of Carbonate Rocks: Tulsa, USA, American Association of Petroleum Geologists, p. 253-272.

**Huthnance, J.M.**, 1982, On one mechanism forming linear sand banks: Estuarine Coastal Shelf Science, v. 14, p. 79-99.

**James, N.P.**, 1997, The cool-water carbonate depositional realm, *in* James, N.P., and Clarke, J.A.D., ed., Cool-water Carbonates: Special Publications: Tulsa USA, SEPM.

**James, N.P., and Bone, Y.,** 1989, Petrogenesis of Cenozoic, temperate water calcarenites, South Australia: a model for meteoric/shallow burial diagenesis of shallow water calcite sediments: Journal of Sedimentary Petrology, v. 59, p.191-203.

**James, N.P., and Bone, Y.,** 1991, Origin of a cool-water Oligo-Miocene deep-shelf limestone, Eucla Platform, southern Australia: Sedimentology, v. 60, p. 323-341.

**James, N.P., and von der Borch, C. C.,** 1991, Carbonate shelf edge off southern Australia: A prograding open-platform margin: Geology, v. 19, p. 1005-1008.

**James, N.P., and Bone, Y.,** 1992, Synsedimentary cemented calcarenite layers in Oligo-Miocene shelf limestone, Eucla Platform, southern Australia: Journal of Sedimentary Petrology, v. 62, p.860-872.

**James, N.P., Bone, Y., von der Borch, C.C., and Gostin, V.A.,** 1992, Modern carbonate and terrigenous clastic sediments on a cool-water, high energy, mid-latitude shelf: Lacepede, southern Australia: Sedimentolgy, v. 39, p. 877-903.

**James, N.P., Bone, Y., and Kyser, T.K.,** 1993, Shallow burial dolomitizaion and dedolomitization of mid-Cenozoic, cool-water, calcitic, deep-shelf limestones, southern Australia: Journal of Sedimentary Petrology, v. 63, p. 528-538.

**James, N.P., Boreen, T.D., Bone, Y., and Feary, D.A.,** 1994, Holocene carbonate sedimentation on the west Eucla Shelf, Great Australian Bight: A shaved shelf: Sedimentary Geology, v. 90, p. 161-177.

**James, N.P., Bone, Y., Hageman, S.J., Feary, D.A., and Gostin, V.A.,** 1997, Cool-water carbonate sedimentation during the Terminal Quaternary Sealevel Cycle: Lincoln Shelf, Southern Australia., *in* James, N.P., and Clarke, J.A.D., ed., Cool-Water Carbonates: Special Publication: Tulsa, U.S.A., S.E.P.M., p. 53-76.

**James, N.P., and Clarke, J.A.D.,** 1997, Cool-water Carbonates, *in* Scholle, P.A., ed., Special Publications: Tulsa, USA, Society For Sedimentary Geology, p. 440.

**James, N.P., Bone, Y., and Kyser, K.T.,** 1997, Brachiopod ∂18O values do reflect ambient oceanography: Lacepede Shelf, southern Australia: Geology, v. 25, p. 551-554.

**James, N.P., Collins, L.B., Bone, Y., and Hallock, P.,** 1999, Sub-tropical carbonates in a temperate realm: modern sediments on the southwest Australian Shelf: Journal of Sedimentary Research, v. 69, p. 1297-1321.

**James, N.P., and Bone, Y.,** 2000, Eocene cool-water carbonate and biosiliceous sedientation dynamics, St.Vincents Basin, South Australia: Sedimentology, v. 47, p. 761-786.

**James, N.P., Bone, Y., Collins, L.B., and Kyser, T.K.,** 2001, Surficial sediments of the Great Australian Bight: facies dynamics and oceanography on a vast cool-water carbonate shelf: Journal of Sedimentary Research, v. 71, p. 549-567

**Johnson, H.J.,** 1951, An introduction to the study of organic limestones: Colorado School of Mines Quarterly, v. 46.

**Jones, H.A., and Davies, P.J.,** 1983, Superficial sediments of the Tasmanian continental shelf and part of Bass Strait: , Bureau of Mineral Resources, Geology and Geophysics, Department of Resources and Energy.

**Jones, B.**, 1990, Tunicate spicules and their syntaxial overgrowths: examples from the Pleistocene Ironshore Formation, Grand Cayman, British West Indies: Canadian Journal of Earth Sciences, v. 27, p. 525- 532.

**Jones, B. and Desrochers, A.,** 1992, Shallow platform carbonates; *in* Walker, R.G., and James, N.P., (eds): Facies models: response to sea level change: Geological Association of Canada, Dept. of Earth Sciences, Memorial University of New Foundland, Canada,: p. 277-302.

**Jutson, J.T.**, 1939, Shore platforms near Sydney, New South Wales: Journal of Geomorphology, v. 2, p. 237-250.

**Jutson, J.T.**, 1940, The shore platforms of Mt. Martha, Port Phillip Bay, Victoria, Australia: Proceedings of the Royal Society of Victoria, v. 52, p. 164-176.

**Jutson, J.T.**, 1948, The shore platforms of Flinders, Victoria: Proceedings of the Royal Society of Victoria, v. 60, p. 57-73.

**Jutson, J.T.**, 1949, The shore platforms of Lorne, Victoria: Proceedings of the Royal Society of Victoria, v. 61, p. 43-60.

**Kamp, P.J.J., Harmsen, F.J., Nelson, C.S., and Boyle, S.F.,** 1988, Barnacle dominated limestone with giant cross-beds in a non-tropical, tide swept, Pliocene forearc seaway, Hawkes Bay New zealand, Sedimetary Geology, v. 60, p. 163-172

**Keough, M.J., Jenkins, G.P.**, 1996, Seagrass meadows and their inhabitants, *in* Underwood, A.J., Chapman, M.G., ed., Coastal Marine Ecology: Sydney, Institute of Marine Ecology, University of Sydney, p. 341.

**Knight-Jones, E.W., Knight-Jones, P., and Llewellyn, L.C.**, 1971, Spirorbinae (Polychaeta: Serpulidae) from southeastern Australia: Records of the Austalian Museum, v. 29, p. 107-150.

**Kott, P.**, 1980, Algal-bearing diademnid ascidians in the Indo-West Pacific: Memoirs of the Queensland Museum, v. 20, p. 1-47.

**Kyser, K.T.**, 1995, Micro-analytical techniques in stable isotope geochemistry, *in* Hawthorne, F.C., and Martin, R.F., ed., Microbeam Techniques in the Earth Sciences: Ottawa, Canada, The Canadian Mineralogist, p. 261-278.

**Lablack, K.**, 1985, Foraminiferal biofacies analysis of Holocene sediments from Tourville Bay, South Australia [unpublished B.Sc. (Hons) thesis]: University of Adelaide, Adelaide, South Australia.

**Lambeck, K., and Nagada, M.**, 1985, Holocene fluctuations in sea-level: constraints on mantle viscosity and meltwater sources: Fifth International Coral Reef Congress, p. 79-84.

**Lambeck, K., and Nagada, M.**, 1992, Constraints on the age and duration of the last interglacial period and on sea-level variations: Nature, v. 357, p. 125-128.

**Larcombe, P., Carter, R.M., Dye, J., Gagan, M.K., and Johnson D.P.**, 1995, New Evidence for episodic post-glacial sea-level rise, central Great Barrier Reef, Australia: Marine Geology, v. 127, p. 1-44.

**Larsonneur, C.**, 1975, Tidal Deposits, Mont Saint Michel Bay, France, *in* Ginsburg, R.N., ed., Tidal Deposits: Berlin, Springer-Verlag, p. 21-30.

**Lasemi, Z., and Sandberg, P.**, 1993, Microfabric and compositional clues to dominant mud mineralogy of micrite precursors, *in* Rezak, R., and Lavoie, D.L., ed., Carbonate microfabrics: Frontiers in sedimentary geology: New York, Springer-Verlag, p. 173-185.

**Leaney, F.W., Herczeg, A.L., and Dighton, J.C.**, 1994, New developments for the direct CO2 absorbtion method for radiocarbon analysis: Quaternary Science Reviews, v. 13, p. 171-178.

**Leeder, M.R.**, 1982, Sedimentology, Process and Product: London, George Allen and Unwin, 344 p.

**Lees, A., and Buller, A.T.**, 1972, Modern temperate-water and warm-water shelf carbonate sediments contrasted: Marine Geology, v. 13, p. M67-73.

**Li, Q., James, N.P., Bone, Y., McGowran, B.**, 1996, Foraminiferal biostratigraphy and depositional environments of the mid-Cenozoic Abrakurrie Limestone, Eucla Basin, southern Australia: Australian Journal of Earth Sciences, v. 43, p. 437-450.

**Li, Q., McGowran, B., James, N.P., Bone, Y.**, 1996, Foraminiferal biofacies on the mid-latitude Lincoln Shelf, South Australia: Oceanic and sedimentological implications: Marine Geology, v. 129, p. 285-312.

**Li, Q., James, N.P., Bone, Y., and McGowran, B.**, 1999, Paleocceanographic significance of recent foraminiferal biofacies on the southern shelf of Western Australia: a preliminary study: Palaeogeography, Palaeoclimatology, Palaeoecology, v. 147, p. 101-120

**Ludbrook, N.H.**, 1984, Quaternary Molluscs of South Australia: Adelaide, South Australia, Department of Mines and Energy, 327 p.

**Ludbrook, N.H.**, 1988, Coastal Quaternary Stratigraphy: Mollusca: Department of Mines and Energy, South Australia.

**Matthews, R.K.**, 1986, Oxygen Isotope record of ice-volume history: 100 million years of glacio-eustatic sealevel fluctuation, *in* Schlee, J.S., ed., Interregional unconformities and hydrocarbon accumulation: American Association of Petroleum Geologists, p. 131-137.

**McComb, A.J., Cambridge, M.C., Kirkman, H., and Kuo, J.**, 1981, The biology of Australian seagrasses, *in* Pate, J.S., and McComb, A.J., ed., The Biology of Australian Plants: Nedlands, W.A. Australia, University of Western Australia, p. 422.

**McKee, E.D., and Ward, W.C.**, 1983, Eolian, *in* Scholle, P.A., Bebout, D.G., and Moore, C.H., ed., Carbonate Depositional Environments: Tulsa, USA, The Association of Petroleum Geologists, p. 708.

**Martindale, W., and Boreen, T.D.**, 1997, Temperature-stratified Mississippian carbonates as hydrocarbon reservoirs - examples from the foothills of the Canadian Rockies: *in* James, N.P., and Clarke, J.A.D., ed., Cool-Water Carbonates: Special Publication: Tulsa, U.S.A., S.E.P.M., p. 391-409.

**Milligan, G.W.**, 1980, An examination of the effect of six types of error perturbation on fifteen clustering algorithms: Psychmetrika, v. 45, p. 325-342.

**Millikan, M.I.**, 1994, Quaternary Geology of the Pelican Lagoon Area, Kangaroo Island, South Australia [unpublished B.Sc. Hons thesis]: University of Adelaide, Adelaide, South Australia.

**Milliman, J.D.**, 1974, Recent Sedimentary Carbonates, Part I. Marine Carbonates: Berlin, Springer, 375 p.

**Milnes, A.R., Ludbrook, N. H.**, 1986, Provenance of microfossils in calcarenites and calcretes in southern South Australia: Australian Journal of Earth Sciences, v. 33, p. 145-159.

**Morner, N.A.**, 1987a, PreQuaternary long-term changes in sea level, *in* Devoy, R.J.N., (ed), Sea-surace studies, a global view: New York, Croom Helm, p 1-30.

**Morner, N.A.**, 1987b, Quaternary sea level changes: nothern hemisphere data, *in* Devoy, R.J.N., (ed), Sea-surace studies, a global view: New York, Croom Helm, p 1-30.

**Murray-Wallace, C.V., Kimber, R.W.L., Belperio, A.P., and Gostin, V.A.**, 1988, Aminostratigraphy of the Last Interglacial in Southern Australia: Search, v. 19, p. 32-36.

**Murray-Wallace, C.V., and Belperio, A.P.**, 1991, The last interglacial shoreline in Australia- a review: Quaternary Science Reviews, v. 10, p. 441-161.

**Murray-Wallace, C.V., Belperio, A.P., Picker, K., and Kimber, R.W.L.**, 1991, Coastal Aminostratigraphy of the Last Interglaciation in South Australia: Quaternary Research, v. 35, p. 63-71.

**Murray-Wallace, C.V., Belperio, A.P., Gostin, V.A., and Cann, J.H.**, 1993, Amino acid racemisation and radiocarbon dating of interstadial marine strata (Oxygen Isotope Stage 3), Gulf St Vincent, South Australia: Marine geology, v. 110, p. 83-92.

**Murray-Wallace, C.V., Beu, A.G., Kendrick, G.W., Brown, L.J., Belperio, A.P., and Sherwood, J.E.**, 2000, Palaeoclimatic implications of the occurrence of the arcoid *Anadara trapezia* (Deshayes) in the Quaternary of Australasia: Quaternary Science Review, v. 19, p 559-590.

**Nagada, M., and Lambeck, K.**, 1988, The melting history of the late Pleistocene Antarctic ice sheet: Nature, v. 333, p. 36-40.

**Nagada, M., and Lambeck, K.**, 1989, Late Pleistocene and Holocene sea-level change in the Australian region and mantle rheology: Geophysical Journal, v. 96, p. 497-517.

**Nakiboglu, S.M., Lambeck, K. and Aharon, P.**, 1983, Post-glacial sealevels in the Pacific: Implications with respect to deglaciation regime and local tectonics: Tectonophysics, v. 91, p. 335-358.

**Nelson, C.S.**, 1978, Temperate shelf carbonate sediments in the Cenozoic of New Zealand: Sedimentology, v. 25, p. 737-771.

**Nelson, C.S.**, 1988, An introductory perspective on non-tropical shelf carbonates, Sedimentary Geology, v. 60, p, 3-14

**Nelson, C.S., and Bornhold, B.D.**, 1983, Temperate skeletal carbonate sediments on Scott Shelf, northwestern Vancouver Island, Canada: Marine Geology, v. 52, p. 241-166.

**Nelson, C.S., Harris, G.J., and Young, H.R.**, 1988a, Burial-dominated cementation in non-tropical carbonates of the Oligocene Te Kuiti Group, New Zealand: Sedimentary Geology, v. 60, p. 233-250.

**Nelson, C.S., and James, N.P.**, 2000, Marine cements in mid-Tertiary cool-water shelf limestones of New Zealand and southern Australia: Sedimentology, v. , p.609-630.

**Nelson, C.S., Keane, S.L., and Head, P.S.**, 1988b, Non-tropical carbonate deposits on the modern New Zealand shelf: Sedimentary Geology, v. 60, p. 71-94.

**Newman, W.S.**, 1986, Paleogeodesy data bank and paleogeodesy: Durham University.

**Niccolaides, S., and Wallace, M.W.**, 1997, Pressure-dissolution and cementation in an Oligo-Miocene non-tropical limestone (Clifton Formation), *in* James, N.P., and Clarke, J.A.D., ed., Cool-Water Carbonates: Tulsa, Oklahoma, Society for Sedimentary Geology, p. 440.

**Nicolaides, S.**, 1995, Cementation in Oligo-Miocene non-tropical shelf limestones, Otway Basin, Australia: Sedimentology, v. 95, p. 97-122.

**Offshore Resoursce Map,** 1991, Ceduna: Bureau of Mineral Resources and Royal Australian Navy, Canberra, Australia.

**Osleger, D.**, 1991, Subtidal carbonate cycles: Implications for allocyclic vs. autocyclic contols: Geology, v. 19, p. 917-920.

**Parker, A.J.**, 1993, Geological Framework, *in* Drexel, J.F., Priess, W.V., and Parker, A.J., ed., The Geology of South Australia. Vol. 1. The Precambrian: Adelaide, Bulletin 54, South Australian Geological Survey.

**Pattiarartchi, C., and Collins, M.B.**, 1987, Mechanisms for linear sandbank formation and maintenance in relation to dynamical oceanographic observations: Progress in Oceanography, v. 19, p. 117-176.

**Pettijohn, F.J.**, 1957, Sedimentary Rocks: New York, Harper and Bros., 718 p.

**Pirazzoli, P.A.**, 1991, World Atlas of Holocene Sea-Level Changes: Oceanographic Series No. 58: Amsterdam, Elsevier, 300 p.

**Plint, A.G., Eyles, N., Eyles, C.H., and Walker, R.G.**, 1992, Control of sea level change, *in* Walker, R.G., and James, N.P., ed., Facies Models: response to sea level change: St. John's, Geological Association of Canada, p. 15-25.

**Plumley, W.J., Risley, G.A., Graves jr, R.W., and Kaley, M.E.**, 1962, Energy index for limestone interpretation and classification, *in* Ham, W.E., ed., Classification of Carbonate Rocks: Tulsa, USA, American Association of Petroleum Geologists, p. 85-107.

**Pope, M.C., and Reid, J.F.**, 1997, High resolution stratigraphy of the Lexington Limestone (late middle Ordovician), Kentucky, USA: A cool-water carbonate clastic ramp in a tectonically active foreland basin: *in* James, N.P., and Clarke, J.A.D., ed., Cool-Water Carbonates: Special Publication: Tulsa, U.S.A., S.E.P.M., p. 411-430.

**Powers, R.W.**, 1962, Arabian Upper Jurassic carbonate reservoir rocks, *in* Ham, W.E., ed., Classification of Carbonate Rocks: Tulsa, USA, American Association of Petroleum Geologists, p. 122-192.

**Provis, D.G., and Radok, R.**, 1979, Sea-level oscillations along the Australian coast: Australian Journal of Marine and Freshwater Research, v. 30, p. 295-361.

**Provis, D.G., and Steedman, R.K.**, 1985, Wave measurements in the Great Australian Bight: Australasian Conference of Coastal Ocean Engineers, p. 51-60.

**Rankin, L.R., and Flint, R.B.**, 1991, Streaky Bay 1: 250 000 Geological Map: , South Australian Department of Mines and Energy.

**Reeckmann, S.A.**, 1988, Diagenetic alterations in temperate shelf carbonates from southeastern Australia: Sedimentary Geology, v. 60, p. 209-219.

**Reid, R.P., Macintyre, I.G., and Post, J.E.**, 1992, Micritised skeletal grains in northern Belize Lagoon: A major source of Mg-calcite mud: Journal of Sedimentary Petrology, v. 62, p. 145-156.

**Reid, R.P., and Macintyre, I.G.**, 1998, Carbonate recrystallisation in shallow marine environments: A widespread diagenetic process forming micritised grains: Journal of Sedimentary Research, v. 68, p. 928-946.

**Richardson, J.R.**, 1997, Brachiopods (Phylum Brachiopoda), *in* Shepherd, S.A., and Davies, M., ed., Marine Invertebrates of Southern Australia, Part 3: Adelaide, Government of South Australia.

**Round, F.E., Crawford, R.M., and Mann, D.G.**, 1996, The Diatoms: Cambridge, Cambridge University Press, 747 p.

**Roy, P.S.**, 1984, New South Wales estuaries: their origin and evolution, *in* Thom, B.J., ed., Coastal Geomorphology in Australia: Sydney, Academic Press Australia, p. 99-121.

**Ryan, S.**, 1998, Rhodoliths as palaeoecological indicators: Distribution, characteristics and application to the rock record of temperate coralline algae from the southern Australian continental shelf and coast [unpublished BSc (Honours) thesis]: University of Adelaide, Adelaide, South Australia.

**SAS Institute Inc.**, 1994, JMP-Statistics Made Visual: Cary, NC, USA, SAS Institute Inc.

**Schofield, J.C.**, 1971; Latest Research on the Quaternary Shorelines of Australasia. ANZAAS Quaternary Shorelines Committee: Search, v. 2, p. 58-63.

**Scholle, P.A.**, 1978, Carbonate rock constituents, textures, cements and porosities: Tulsa, USA, Memoir 27, American association of Petroleum Geologists, 241 p.

**Schwebel, D.A.**, 1984, Quaterary stratigraphy and sea level variation in the southeast of South Australia, *in* Thom, B.G., ed., Coastal Geomorphology in Australia: Sydney, Academic Press, p. 291-311.

**Scoffin, T.P.**, 1987, An introduction to carbonate sediments and rocks: Glascow, Blackie, 274 p.

**Scoffin, T.P.**, 1988, The environments of production and deposition of calcareous sediments on the shelf west of Scotland: Sedimentary Geology, v. 60, p. 107-124.

**Semenuik, V., and Searle, D. J.**, 1985, Distribution of calcrete in Holocene coastal sands in relationship to climate, southwestern Australia: Journal of Sedimentary Petrology, v. 55, p. 86-95.

**Shackleton, N.J., and Opdyke, N.D.**, 1973, Oxygen isotope and paleaomagnetic stratigraphy of equatorial Pacific core V28-238: Oxygen isotope temperatures and ice volumes on a $10^5$ year and $10^6$ year scale: Quaternary Research, v. 3, p. 39-55.

**Shackleton, J.N., and Opdyke, N.D.**, 1976, Oxygen isotope and palaeomagnetic stratigraphy of Pacific Core V28-238. Late Pliocene to latest Pleistocene: Geological Society of America, Memoir, v. 145, p. 449-464.

**Shepherd, S.A., and Sprigg, R. C.**, 1976, Substrate, sediments and subtidal ecology of Gulf St. Vincent and Investigator Strait, *in* Twidale, C.R., Tyler, M.J., and Webb, B.P., ed., Natural History of the Adelaide Region: Adeliade, Royal Society of South Australia.

**Sherbon Hills, F.**, 1972, Shore platforms and wave ramps: Geological Magazine, v. 109, p. 81-88.

**Sherherd , S.A., and Veron, J.E.N.**, 1982, Stony Corals (Order SCERACTINIA or MADREPORARIA), *in* Sherpherd, S.A., and Thomas, I.M., ed., Marine Invertebrates of Southern Australia; Part I: Adelaide, Government Printer, South Australia, p. 491.

**Short, A.D., Fotheringham, D.G., and Buckely, R.C.**, 1986, Coastal morphodynamics and Holocene evolution of the Eyre Peninsula coast, South Australia: University of Sydney.

**Short, A.D.**, 1988, The South Australia coast and Holocene sea-level transgression: Geographical Review, v. 78, p. 119-136.

**Short, A.D., Buckely, R.C., and Fotheringham, D.G.**, 1989, Preliminary investigations of beach ridge progradation on Eyre Peninsula and Kangaroo Island: Transactions Royal Society of South Australia, v. 113, p. 145-161.

**Short, A.D., Buckely, R.C., and Fotheringham, D.G.**, 1990, Reply: Preliminary investigations of beach ridge progradation on Eyre Peninsula and Kangaroo Island: Transactions Royal Society of South Australia, v. 114, p. 227.

**Simone, L., and Carannante, G.**, 1988, The fate of foramol ("temperate-type") carbonate platforms: Sedimentary Geology, v. 60, p. 347-354.

**Slowey, N.C., Henderson, G.M., and Curry, W.B.**, 1996, Direct U-Th dating of marine sediments from the two most recent interglacial periods: Nature, v. 383, p. 242-244.

**Smith, A.M.**, 1988, Prelimimary steps toward formation of a generalised budget for cold-water carbonates: Sedimentary Geology, v. 60, p. 323-331.

**Smith, A.M., Nelson, C.S., and Spencer, H.G.**, 1998, Skeletal carbonate mineralogy of New Zealand bryozoans: Marine Geology, v. 151, p. 27-46.

**Smith, A.M., and Nelson, C.S.**, 1993, Mineralogical, carbonate geochemical and diagenetic data for modern New Zealand bryozoans. Occasional Report No. 17, Department of Earth Sciences, University of Waikato, New Zealand.

**Smith, R.L., Huyer, A., Godfrey, J.S. and Church, J.A.**, 1991, The Leeuwin Current off Western Australia 1986-1987: Journal of Physical Oceanography, v. 21, p. 323-345.

**Spjeldnaes, N., and and Moissette, P.**, 1997, Celleporid (Bryozoan) thickets from the upper Pliocene of the island of Rhodes, Greece: *in* James, N.P., and Clarke, J.A.D., ed., Cool-Water Carbonates: Special Publication: Tulsa, U.S.A., S.E.P.M., p. 263-270.

**Sprigg, R.C.**, 1959, Stranded sea beaches and associated sand accumulations of the Southeast: Transactions Royal Society of South Australia, v. 82, p. 183-193.

**Sprigg, R.C.**, 1979, Stranded and submerged sea-beach systems of southeast South Australia and the aeolian desert cycle: Sedimentary Geology, v. 22, p. 53-96.

**Stanley, D.J.**, 1995, A global sea-level curve for the late Quaternary: the impossible dream?: Marine Geology, v. 125, p. 1-6.

**Stephenson, R., and Lambeck, K.**, 1985, Erosion-isostatic rebound models for uplift: An application to south-eastern Australia: Geophysical Journal of the Royal Astronomical Society, v. 82, p. 31-55.

**Stearns, C.E.**, 1984, Uranium-series dating and the history of sea level. *In* Mahaney, W.C. (ed.), Quaternary Dating Methods, pp. 53-66. Elservier, Amsterdam.

**Stirling, C.H., Esat, T.M., McCulloch, M.T., and Lambeck, K.**, 1995, High-precision U-series dating of corals from Western Australia and implications for the timing and duration of the Last Interglacial: Earth and Planetary Science Letters, v. 135, p. 115-130.

**Thom, B.G., and Chappell, J.**, 1975, Holocene Sea Levels Relative to Australia: Search, v. 6, p. 90-93.

**Thom, B.G., and Roy, P. S.**, 1985, Relative sea levels and coastal sedimentation in southeast Australia: Journal of Sedimentary Petrology, v. 55, p. 257-264.

**Thom, B.G., and Roy, P.S.**, 1985, Relative Sea Levels and Coastal Sedimentation in Southeastern Australia in the Holocene: Journal of Sedimentary Petrology, v. 55, p. 257-264.

**Tooley, M.J., and Shennan, I.**, 1987, Sea-level changes: Special Publications series, v. 20: Oxford, The Institute of British Geographers.

**Tucker, M.**, 1988, Techniques in Sedimentology: Oxford, Blackwell Scientific Publications, p. 394.

**Twenhofel, W.H.**, 1950, Principles of Stratigraphy: New York, McGraw-Hill Book Co., Inc.

**Twidale, C.R., and Bourne, J.A.**, 1990, Comment: Preliminary investigations of beach ridge progradation on Eyre Peninsula and Kangaroo Island: Transactions Royal Society of South Australia, v. 144, p. 225-226.

**van Donck, J.**, 1976, $O^{18}$ record of the Atlantic Ocean for the entire Pleistocene Epoch: Geological Society of America, Memoir, v. 145, p. 147-163.

**Veeh, H.H., and Chappell, J.**, 1970, Astronomical theory of climate change: Support from New Guinea: Science, v. 167, p. 863-865.

**Veeh, H.H., and Burnett, W.C.**, 1982, Carbonate and phosphate sediments, *in* Ivanovich, M.a.H., R.S., ed., Uranium-series disequilibrium: Applications to environmental problems: London, Oxford University Press, p. 459-480.

**Veeh, H.H., and France, R.E.**, 1988, Uranium series of corals and coexisting phospate deposits on Palseart Reef complex, Houtman-Abrolhos Islands, Western Australia: Quaternary Research, v. 30, p. 204-209.

**Veron, J.E.N.**, 1986, Corals of Australia and the Indo-Pacific: Sydney, Angus and Robertson.

**von der Borch, C.C., and Hughes Clarke, J. E.**, 1993, Slope morphology adjacent to the cool-water carbonate shelf of South Australia: GLORIA and Seabeam imaging: Australian Journal of Earth Sciences, v. 40, p. 57-64.

**Walker, R.G., and Plint, A.G.**, 1992, Wave-and storm-dominated shallow marine systems: *in* Walker, R.G. and James, N.P., (eds), Facies Models: response to sea level change: Geological Association of Canada, St. Johns, Canada, p 219-264.

**Wass, R.E., Conolly, J.R., and MacIntyre, R.J.**, 1970, Bryozoan carbonate sand continuous along southern Australia: Marine Geology, v. 9, p. 63-73.

**Wass, R.E., and Yoo, J.J.**, 1983, Cheilostome Bryozoa from the Southern Australian Continental Shelf: Australian Journal of Marine and Freshwater Research, v. 34, p. 303-354.

**Wells, P., Okada, H.**, 1996, Holocene and Pleistocene glacial palaeoceanography off southeastern Australia, based on foraminifers and nannofoosils in Vema cored hole V18-222: Australian Journal of Earth Sciences, v. 43, p. 509-523.

**Wentworth, C.K.**, 1922, A scale of grade and class terms for clastic sediments: Journal of Geology, v. 30, p. 377-392.

**Williams, M., Dunkerly, D., De Dekker, P., Kershaw, P., and Chappell, J.**, 1998, Quaternary Environments: London, Arnold/ Oxford University Press.

**Wilson, C.C.**, 1991, Geology of the Quaternary Bridgewater Formation of southwest and central South Australia [unpublished PhD thesis]: Flinders University of South Australia, Adelaide, South Australia.

**Winzar, G.**, 1998, Bryozoa of Antarctica; a first appraisal [unpublished BSc (Hons) thesis]: University of Adeliade, Adelaide, South Australia.

**Wirtz, P.D.**, 1994, The Quaternary geology of the American River area, Kangaroo Island, South Australia [unpublished B.Sc. (Hons) thesis]: Univeristy of Adelaide, Adelaide, South Australia.

**Womersley, H.B.S.**, 1996, The Marine Benthic Flora of South Australia, Part IIIb: Flora of Australia Supplementary Series No. 5: Canberra, Australian Biological Resourses Study, 392 p.

**Woodroffe, C.D.**, 1993, Late Quaternary evolution of coastal and lowland riverine plains of Southeast Asia and northern Australia: An overview: Sedimentary Geology, v. 83, p. 163-175.

**Wray, J.L.**, 1977, Calcareous Algae: Developments in Palaeontology and Statigraphy, v. 4: Amsterdam, Elservier, 185 p.

**Young, H.A., and Davies, P.J.**, 1983, Surficial sediments of the Tasmanian continental shelf and parts of Bass Strait: Bureau of Mineral Resources, Geology and Geophysics, Canberra.

**Young, H.R., and Nelson, C.S.**, 1985, Biodegradation of temperate-water skeletal carbonates by boring sponges on the Scott Shelf, British Columbia, Canada: Marine Geology, v. 65, p. 33-45.

# Appendices

# Appendix One

**Location of Seafloor Samples, Gravity Cores,**

**Slip-Hammer Cores (Streaky Bay) and**

**RV *Franklin* Sea-floor samples**

**(Shelf Transect)**

| | | |
|---|---|---|
| **Seafloor Samples** | **Location** | |
| **Sample Number** | **Latitude** | **Longitude** |
| | **Deg/ Min/ Sec** | **Deg/ Min/ Sec** |
| **Transect 4** | | |
| SB 01 | S32 47 30 | E134 12 33 |
| SB 02 | S32 46 43 | E134 12 35 |
| SB 03 | S32 45 46 | E134 12 52 |
| SB 04 | S32 44 58 | E134 13 33 |
| SB 05 | S32 44 09 | E134 14 33 |
| SB 06 | S32 43 06 | E134 15 10 |
| SB 07 | S32 42 43 | E134 14 09 |
| SB 08 | S32 42 04 | E134 13 07 |
| SB 09 | S32 41 33 | E134 12 03 |
| SB 10 | S32 40 46 | E134 12 50 |
| SB 11 | S32 40 03 | E134 13 39 |
| SB 12 | S32 39 21 | E134 14 27 |
| SB 13 | S32 38 23 | E134 15 30 |
| SB 14 | S32 37 27 | E134 15 08 |
| SB 15 | S32 36 32 | E134 14 45 |
| SB 16 | S32 35 36 | E134 14 23 |

| | | |
|---|---|---|
| SB 17 | S32 34 38 | E134 13 58 |
| SB 18 | S32 33 40 | E134 13 36 |
| SB 19 | S32 32 40 | E134 13 11 |
| SB 20 | S32 31 54 | E134 12 51 |
| SB 21 | S32 31 19 | E134 11 51 |
| SB 22 | S32 30 45 | E134 10 53 |
| SB 23 | S32 30 11 | E134 09 56 |
| SB 24 | S32 29 36 | S134 08 58 |
| SB 25 | S32 29 03 | S134 07 58 |
| SB 26 | S32 28 28 | S134 07 00 |
| SB 27 | S32 27 56 | S134 06 03 |
| **Transect 5** | | |
| SB 28 | S32 28 25 | S134 02 26 |
| SB 29 | S32 29 30 | E134 03 32 |
| SB 30 | S32 30 16 | E134 04 18 |
| SB 31 | S32 31 03 | E134 05 03 |
| SB 32 | S32 31 47 | E134 05 50 |
| SB 33 | S32 32 34 | E134 06 34 |
| SB 34 | S32 33 19 | E134 07 22 |
| SB 35 | S32 34 05 | E134 08 09 |
| SB 36 | S32 35 12 | E134 08 30 |
| SB 37 | S32 36 41 | E134 08 59 |
| SB 38 | S32 37 41 | E134 09 17 |
| SB 39 | S32 38 52 | E134 09 18 |
| SB 40 | S32 39 54 | E134 09 18 |
| SB 41 | S32 40 54 | E134 09 18 |
| SB 42 | S32 41 53 | E134 09 19 |
| SB 43 | S32 42 52 | E134 09 20 |

| | | |
|---|---|---|
| **Transect 6** | | |
| SB 44 | S32 42 45 | E134 05 52 |
| SB 45 | S32 41 51 | E134 05 26 |
| SB 46 | S32 40 56 | E134 04 58 |
| SB 47 | S32 40 00 | E134 04 31 |
| SB 48 | S32 39 05 | E134 04 03 |
| SB 49 | S32 38 10 | E134 03 36 |
| SB 50 | S32 37 15 | E134 03 07 |
| SB 51 | S32 36 20 | E134 02 40 |
| SB 52 | S32 35 26 | E134 02 12 |
| SB 53 | S32 34 30 | E134 01 43 |
| SB 54 | S32 33 35 | E134 01 16 |
| SB 55 | S32 32 40 | E134 00 49 |
| SB 56 | S32 31 44 | E134 00 20 |
| SB 57 | S32 30 30 | E133 59 42 |
| **Transect 7** | | |
| SB 58 | S32 31 34 | E134 54 10 |
| SB 59 | S32 32 13 | E133 54 27 |
| SB 60 | S32 33 07 | E133 54 51 |
| SB 61 | S32 34 05 | E133 55 11 |
| SB 62 | S32 35 03 | E133 55 37 |
| SB 63 | S32 35 59 | E133 56 00 |
| SB 64 | S32 37 12 | E133 56 30 |
| SB 65 | S32 38 49 | E133 57 10 |
| SB 66 | S32 39 24 | E133 58 07 |
| SB 67 | S32 39 59 | E133 59 03 |
| SB 68 | S32 40 34 | E133 59 58 |
| SB 69 | S32 41 10 | E134 00 58 |

| | | |
|---|---|---|
| SB 70 | S32 41 45 | E134 01 54 |
| SB 71 | S32 42 21 | E134 02 50 |
| SB 72 | S32 42 56 | E134 03 47 |
| **Transect 1** | | |
| SB 73 | S32 39 28 | E134 16 55 |
| SB 74 | S32 40 05 | E134 15 51 |
| SB 75 | S32 40 45 | E134 14 40 |
| SB 76 | S32 40 38 | E134 13 30 |
| SB 77 | S32 40 30 | E134 12 21 |
| SB 78 | S32 40 21 | E134 11 11 |
| SB 79 | S32 40 14 | E134 10 00 |
| SB 80 | S32 40 06 | E134 08 50 |
| SB 81 | S32 39 57 | E134 07 41 |
| SB 82 | S32 39 50 | E134 06 31 |
| SB 83 | S32 39 42 | E134 05 20 |
| SB 84 | S32 39 35 | E134 04 10 |
| SB 85 | S32 39 27 | E134 02 59 |
| SB 86 | S32 39 19 | E134 01 50 |
| SB 87 | S32 39 11 | E134 00 39 |
| SB 88 | S32 39 03 | E133 59 29 |
| SB 89 | S32 38 56 | E133 58 19 |
| **Transect 2** | | |
| SB 90 | S32 37 05 | E133 57 36 |
| SB 91 | S32 37 01 | E133 58 46 |
| SB 92 | S32 36 54 | E133 59 56 |
| SB 93 | S32 36 48 | E134 01 07 |
| SB 94 | S32 36 42 | E134 02 18 |
| SB 95 | S32 36 36 | E134 03 28 |

| | | |
|---|---|---|
| SB 96 | S32 36 31 | E134 38 01 |
| SB 97 | S32 36 24 | E134 05 50 |
| SB 98 | S32 36 19 | E134 06 59 |
| SB 99 | S32 36 13 | E134 08 11 |
| SB 100 | S32 36 07 | E134 09 21 |
| SB 101 | S32 36 02 | E134 10 32 |
| SB 102 | S32 35 56 | E134 11 42 |
| SB 103 | S32 35 50 | E134 12 22 |
| SB 104 | S32 35 43 | E134 14 04 |
| SB 105 | S32 35 34 | E134 16 03 |
| **Transect 3** | | |
| SB 106 | S32 30 14 | E134 11 38 |
| SB 107 | S32 30 36 | E134 10 33 |
| SB 108 | S32 30 58 | E134 09 25 |
| SB 109 | S32 31 20 | E134 08 20 |
| SB 110 | S32 31 41 | E134 07 12 |
| SB 111 | S32 32 04 | E134 06 07 |
| SB 112 | S32 32 25 | E134 05 03 |
| SB 113 | S32 32 48 | E134 03 56 |
| SB 114 | S32 33 09 | E134 02 51 |
| SB 115 | S32 33 30 | E134 01 45 |
| SB 116 | S32 33 52 | E134 00 38 |
| SB 117 | S32 34 14 | E133 59 33 |
| SB 118 | S32 34 36 | E133 58 27 |
| SB 119 | S32 34 58 | E133 57 21 |
| SB 120 | S32 35 19 | E133 56 16 |
| | | |
| | | |

| South Sand Transect | | |
|---|---|---|
| SB 142 | S32 38 22 | E134 07 22 |
| SB 143 | S32 38 20 | E134 08 34 |
| SB 144 | S32 38 19 | E134 10 15 |
| SB 145 | S32 38 18 | E134 11 27 |
| SB 145a | S32 38 16 | E134 10 43 |
| | | |
| **Gravity Cores** | **Location** | |
| Streaky Bay Gravity Core No. I | S32 34 09 | E134 12 33 |
| Streaky Bay Gravity Core No. 2 | S32 42 34 | E134 14 09 |
| Streaky Bay Gravity Core No. 3 | S32 03 11 | E134 09 56 |
| Streaky Bay Gravity Core No. 4 | S32 46 43 | E134 12 34 |
| | | |
| **Slip-Hammer Cores** | **Location** | |
| Acraman Creek Core No. 1 | S32 27 21 | E134 03 58 |
| Acraman Creek Core No. 2 | S32 27 26 | E134 04 00 |
| Acraman Creek Core No. 3 | S32 27 35 | E134 03 53 |
| Acraman Creek Core No. 4 | S32 27 45 | E134 03 59 |
| Acraman Creek Core No. 5 | S32 27 46 | E134 00 30 |

| | | |
|---|---|---|
| Acraman Creek Core No. 6 | S32 27 29 | E134 00 08 |
| Acraman Creek Core No. 7 | S32 27 49 | E134 00 05 |
| Acraman Creek Core No. 8a | S32 27 49 | E134 00 14 |
| Acraman Creek Core No. 8b | S32 27 49 | E134 00 14 |
| Acraman Creek Core No. 9 | S32 27 28 | E134 00 50 |
| Acraman Creek Core No. 10 | S32 27 28 | E134 00 50 |
| Point Gibson Core No. 1 | S32 43 33 | E134 09 09 |
| Point Gibson Core No. 2 | S32 43 37 | E134 09 49 |
| Point Gibson Core No. 3 | S32 43 29 | E134 10 02 |
| Point Gibson Bay Core No. 1 | S32 44 21 | S134 12 32 |
| Blanche Port Bay Core No. 1 | S32 47 48 | S134 11 53 |
| | | |
| **RV *Franklin* Cruise (FR 03/98)**<br>**Australian Coastal Margin (ACM)** | | |
| **Sample Number** | **Location** | |
| ACM 53 | S34 27 21 | E132 48 32 |

| | | |
|---|---|---|
| ACM 54 | S34 24 59 | E132 51 15 |
| ACM 55 | S34 23 49 | E132 51 18 |
| ACM 56 | S34 33 33 | E132 59 01 |
| ACM 57 | S33 44 05 | E133 15 00 |
| ACM 58 | S32 18 01 | E133 32 03 |
| ACM 59 | S32 53 23 | E133 48 15 |
| ACM 60 | S32 40 05 | E133 59 12 |
| ACM 61 | S32 37 00 | E133 58 33 |
| ACM 62 | S32 34 35 | E133 57 05 |
| | | |

# Appendix Two

# Sediment Descriptions

## Water Depth, Substrate,

### Streaky Bay

### Streaky Bay to the Shelf Edge

| | | | | Organism Desciptions - Gravel sized sediment- | | | | | | | | | | | | | | | | | | | | |
|---|---|---|---|---|---|---|---|---|---|---|---|---|---|---|---|---|---|---|---|---|---|---|---|---|
| Sample Number | Water Depth (M) | Sediment Description; Texture (Folk) | Seagrass, Algae, Accessory Organisms | Bivalve-structural form | | | Gastropod-structural form | | | Coralline Algae Structural form, Abundance A, C, R | | | Bryozoan-structural form, Abundance A, C, R | | | | | | | | | | Echinoid, abund A, C, R |
| Column No. | | | | Abnd A, C, R Wt.-Hvy Med Lt | Size Lge Med Sml | Ribs / Smth | Abnd A, C, R Wt. Hvy Med Lt | Spir Hi Med Lo | Orn / Smth | Artic | Encr | Rhod | Fe n | Fo l | Fl Ro | De B r | Ar B r | Zo B r | En c | No Ab | Va | Epi-Infaunal |
| 1 | 2 | 3 | 4 | 5 | 6 | 7 | 8 | 9 | 10 | 11 | 12 | 13 | 14 | 15 | 16 | 17 | 18 | 19 | 20 | 21 | 22 | 23 | | |
| SB 01 | 2 | Bioclastic v fine-fine sandy mud ; gM | Minor seagrass (Posidonia, Pos.) ($H_2S$) | A M-L | L-S | S-R | A M-L | H-M | O-S | | R | | | | | | | | C ch | | | C Epi | | |
| SB 02 | 7 | Bioclastic v fine-fine sandy mud; gM | Minor seagrass (Pos), barnacle | A M-L | M-S | | C M-L | H-L | O | | R | | | | | | | | | | | C Epi | | |
| SB 03 | 7 | Bioclastic v fine-fine sandy mud ; mS | Patchy seagrass (Pos), barnacle | C M-L | M-S | R-S | C M-L | H-M | O-S | R | R | | | | | | | | | | | R Epi | | |
| SB 04 | 2.5 | Bioclastic medium-v coarse sand; S | Minor seagrass (Pos) | A M-L | L-S | S-R | A M-L | H-M | O-S | | R | | | | | | | | C ch | | | C Epi | | |
| SB 05 | 9 | Bioclastic muddy v. fine-medium sand; mS | Minor seagrass (Pos), blood worm, oyster, pecten, barnacle. | A M-L | L-S | R-S | C H-L | H-L | O-S | | R | | | | | | | | | | | C Epi | | |
| SB 06 | 10 | Bioclastic gravelly v fine-v coarse sandy mud; gmS | Barnacle, echinoid | A H-L | L-S | R-S | A M-L | H-M | O-S | | R | | | | | | | | | | | C Epi | | |

| | | | | | | | | | | | | | | | | | | | | | | | |
|---|---|---|---|---|---|---|---|---|---|---|---|---|---|---|---|---|---|---|---|---|---|---|---|
| SB 07 | 1 1 | Bioclastic v fine sandy mud; gmS | Barnacle, echinoid | A H-L | L-S | R-S | A M-L | H-M | O-S | | R | | | | | | | | | | | | C Epi |
| SB 08 | 1 0 | Bioclastic muddy medium-v fine sand; sM | | A H-L | L-S | S-R | C L | H | O | | | | | | | | | | | | | | C Epi |
| SB 09 | 1 2 | bioclastic muddy coarse-v fine sand; sM | Barnacle, encrusting bryos common on lge bivalves | A H-L | L-S | S-R | C M-L | L-H | O-S | | R | | | | | | | | R ch | | | | C Epi |
| SB 10 | 1 2 | Bioclastic muddy coarse-v fine sand; mS | Tunicates, echinoids, bivalves | A L | S | R | C L | H | O | | | | | | | | | | | | | | R Epi |
| SB 11 | 1 0 | Bioclastic muddy coarse-v fine sand; sM | Bivalves, echinoids | A L | S-M | R | R L | H | O | | C | | | | | | | | | | | | R Epi |
| 1 | 2 | 3 | 4 | 5 | 6 | 7 | 8 | 9 | 1 0 | 1 1 | 1 2 | 1 3 | 1 4 | 1 5 | 1 6 | 1 7 | 1 8 | 1 9 | 2 0 | 2 1 | 2 2 | | 2 3 |
| SB 12 | 1 0 | Bioclastic fine sandy mud; mS | | C L | S-M | R | R L | H | O | | R-C | | | | | | | | | | | | |
| SB 13 | 1 0 | Bioclastic v fine sandy mud; sM | Barnacle on oyster shell | C H-S | L-S | S-R | C M-L | H-L | S-O | | R | | | | | | | | | | | | R Epi |
| SB 14 | 1 3 | Bioclastic muddy medium-v fine sand; mS | Barnacle | C M-L | M-S | R-S | R L | H | S | | R | | | | | | | | R ch | | | | R Epi |
| SB 15 | 1 3 | Bioclastic muddy medium-v fine sand; gmS | Barnacle | C M-L | L-S | R-S | R M | M-H | S-O | | | | | | | | | | | | | | C Epi |
| SB 16 | 1 2 | Bioclastic muddy medium-v fine sand; mS | | C M-L | M-S | R | R L | H | O | | | | | | | | | | | | | | R Epi |
| SB 17 | 1 1 | Bioclastic muddy medium-v fine sand; sM | Soft red algae, bivalves | C H-L | L-S | R-S | R L | H-M | S-O | | R | | | | | | | | C ch | | | | R Epi |
| SB 18 | 1 2 | Bioclastic fine sandy mud; mS | Barnacle, brown algae (Ecklonia), large bivalves | A H-L | L-S | R-S | R L | M-L | S-O | | R | | | | | | | | A ch | | | | C Epi |

| | | | | | | | | | | | | | | | | | | | | | | | | |
|---|---|---|---|---|---|---|---|---|---|---|---|---|---|---|---|---|---|---|---|---|---|---|---|---|
| SB 19 | 10 | Bioclastic coarse sand; mS | Barnacle, bivalves, | C M-C | S-M | S-R | C M-L | M-H | O-S | | | | | | | C cyc | | | C ch | | | C Epi |
| SB 20 | 6 | Bioclastic gravelly very coarse sand; gS | Seagrass (Pos), Ecklonia, bivalves | A H-L | L-S | R-S | A M-L | H-L | O-S | | C | | C ch | | | C cyc | C cyc | R ch | C ch | | | |
| SB 21 | 10 | Bioclastic gravelly muddy v coarse-v fine sand; gmS | Soft red algae, seagrass (Pos, Amphibolis-Amph), Pecten, | A L-M | S-M | R-S | C L-H | H-L | S-O | | C | | | | | C cyc | | | C ch | | | R Epi |
| SB 22 | 11 | Bioclastic muddy fine-v fine sand; gmS | Soft red algae, seagrass (Amph) | A H-L | L-S | R-S | C L | H-M | S-O | | C | | | | | C cyc | | | C ch | | | R Epi |
| SB 23 | 14 | Bioclastic muddy medium-v fine sand; gmS | Abundant small bivalves | A H-L | M-S | R-S | R L | H | O | | R | | | | | | | | C ch | | | C Epi |
| SB 24 | 11 | Bioclastic slightly muddy medium-v fine sand; S | Seagrass (Amph), Soft red algae | A H-M | L-S | R-S | C L | H-M | O-S | | C | | | | | | R ch | | C ch | A ch | | C Epi |
| SB 25 | 12 | Bioclastic muddy fine-v fine sand; mS | Seagrass (Pos), abundant brown algae (Ecklonia) | C M-L | M-S | R-S | R L | | S | R | C | | | | | | | | R ch cyc | | | |
| 1 | 2 | 3 | 4 | 5 | 6 | 7 | 8 | 9 | 10 | 11 | 12 | 13 | 14 | 15 | 16 | 17 | 18 | 19 | 20 | 21 | 22 | 23 |
| SB 26 | 10 | Bioclastic slightly muddy fine-v fine sand; mS | Abundant prismatic carbonate grains | A H-L | L-S | R-S | R M-L | L-H | O-S | | C | | | | | C cyc | | | C ch | | | |
| SB 27 | 5 | Bioclastic fine-v fine sand; S | Abundant seagrass (Pos) | C M | S | S | | | | R | R | | | | | | | | | | | |
| SB 28 | 4 | Bioclastic medium-v fine sand; gS | Seagrass (Pos), coralline algae | R L | S | S | | | | C | C | | | | | | | | | | | R Epi |
| SB 29 | 4 | Bioclastic v coarse-v fine sand; S | Abundant seagrass (Pos), coralline algae | R M | M | S | C M | M | S | | C | | | | | | | | C ch | | | |

| | | | | | | | | | | | | | | | | | | | | | | |
|---|---|---|---|---|---|---|---|---|---|---|---|---|---|---|---|---|---|---|---|---|---|---|
| SB 30 | 6 | Bioclastic v coarse-medium sand; S | Seagrass (Pos) | C M | M-S | R-S | R L | H | S | C | C | | | | | | | | | | | |
| SB 31 | 7 | Bioclastic coarse-fine sand; S | Tr seagrass (Pos) | C L | S | R-S | | | | | R | | | R ch | | | | | R ch | | | |
| SB 32 | 11 | Minor lithic bioclastic medium-v fine sand; S | Minor lithic | C L | S | R | | | | | R | | | | | | | | | | | |
| SB 33 | 9 | Bioclastic v fine-medium sand; S | Minor seagrass (Pos) | C M-L | S-M | S | R L-M | H-M | S | | C | R | | | | | | | R ch | | | |
| SB 34 | 6 | Bioclastic coarse-fine sand; S | Abundant seagrass (Pos) | | | | | | | C | A | | | | | | | | C ch cy c | | | |
| SB 35 | 4 | Bioclastic v coarse-v fine sand; S | Abundant seagrass (Pos) | R M | S | S | R L | M | S | | | | | | | | | | | | | |
| SB 36 | 6 | Bioclastic v fine-coarse sand; S | Abundant seagrass, coralline algae | C L | M | S-R | C M-L | M | S | C | C | | | | | | | | | | | |
| SB 37 | 8 | Bioclastic fine - coarse sand; S | Seagrass (Pos) | C L | S | S | C L | H | S | C | C | | | | | | | | R cy c | | | |
| SB 38 | 3 | Bioclastic coarse-fine sand; S | Seagrass (Pos) | C L | S | S | C L | L-H | S-O | | R | | R ch | | | | | | R ch | | | |
| SB 39 | 5 | Bioclastic gravelly v coarse-fine sand; S | Patchy seagrass | A M-L | S | R-S | A M-L | H-L | S-O | | C | R | C ch | | | | | | C ch | | | R Epi |
| SB 40 | 5- 6 | Bioclastic medium-fine sand; S | Abundant seagrass (Pos), abraded Amphistegina | R L | S | S | C L | H | O-S | | C | | R ch | | | | | C ch | R cy c | | | |

| | | | | | | | | | | | | | | | | | | | | | | | |
|---|---|---|---|---|---|---|---|---|---|---|---|---|---|---|---|---|---|---|---|---|---|---|---|
| SB 41 | 4 | Bioclastic v fine-medium sand; S | Soft red algae | C L-M | S | R | C L | H | S-O | | C | | | | | | | | C cy c | | | |
| SB 42 | 5 | Bioclastic v fine-coarse sand; S | Patchy seagrass (Pos) | C L | S | R | C L | H | S-O | R | C | | | | | | | | C ch cy c | | | |
| 1 | 2 | 3 | 4 | 5 | 6 | 7 | 8 | 9 | 10 | 11 | 12 | 13 | 14 | 15 | 16 | 17 | 18 | 19 | 20 | 21 | 22 | 23 |
| SB 43 | 2 | Bioclastic v fine-coarse sand; S | Patchy seagrass (Pos) | C L | S | S-B | R L | H | O-S | | | | | | | | | | | | | C Epi |
| SB 44 | 2 | Bioclastic fine-coarse sand; S | Abundant seagrass (Pos-Amph) | C L | S | S | | | | | C | | | | | | | R ch | C ch | | | R Epi |
| SB 45 | 8 | Bioclastic medium-coarse sand; S | Seagrass (Pos) | A L | S | R-S | R L | H | O | | | | | | | | | | | | | R Epi |
| SB 46 | 14 | Bioclastic medium sand; S, rocky bottom | Soft red algae, sponge, bryozoa | R L | S | S | | | | | | | | | | | | | R ch | | | |
| SB 47 | 12 | Bioclastic coarse to medium sand; S, rocky bottom | Barnacle | R L | S | R | R M | M | O | R | | | | | | | | | | | | R Epi |
| SB 48 | 16 | Bioclastic v coarse-coarse sand; gS rocky bottom | Barnacle, brachiopod | C L-M | S-M | S-R | R L | M-L | S | A | C | | C ch | | | | | | R ch | | | |
| SB 49 | 14 | Bioclastic v coarse sand; rocky bottom | Soft red algae, sponge, encrusting coralline algae, encrusting bryozoa | | | | | | | C | C | | | | | | | | C ch | | | |

| | | | | | | | | | | | | | | | | | | | | | | | |
|---|---|---|---|---|---|---|---|---|---|---|---|---|---|---|---|---|---|---|---|---|---|---|---|
| SB 50 | 13 | Bioclastic medium-v coarse sand; S, rocky bottom | Tr seagrass (Pos), brown algae (Ecklonia), brachiopod | | | | | | | | A | | C ch | | | | | | C ch | | | |
| SB 51 | 12 | Bioclastic medium-v. coarse sand; S rocky bottom | Sponge spicules (triaxon) | C L | M-S | S-R | R L | M | S | A | A | | | | | | | R ch | A ch | | | R Epi |
| SB 52 | 14 | Bioclstic v coarse-med sand; S rocky bottom, | Browm algae (Ecklonia), minor lithic | R M | M | R | | | | | C | | | | | | | | C ch | | | |
| SB 53 | 14 | Bioclastic gravelly v coarse-fine sand; gS, rocky bottom | Brown algae (Ecklonia) sponge, ophiuroid, brachiopod | R M | M | R | R L | M | O | C | A | | | | | | | | A ch | | | R Oph |
| SB 54 | 13 | Bioclastic gravelly v coarse-medium sand; gS, rocky bottom | Brown algae (Ecklonia), encrusting coralline algae | | | | | | | | A | | | | | | | | C ch | | | |
| SB 55 | 14 | No returns, rocky bottom | Soft red algae | | | | | | | | | | | | | | | | | | | |
| SB 56 | 13 | Bioclastic gravelly v coarse-fine sand; gS | soft red algae, agglut worm tube | C H-L | M-S | S | C M-L | H | S-O | R | C | | C ch | | | C cy c | | | C ch | | | |
| 1 | 2 | 3 | 4 | 5 | 6 | 7 | 8 | 9 | 10 | 11 | 12 | 13 | 14 | 15 | 16 | 17 | 18 | 19 | 20 | 21 | 22 | 23 |
| SB 57 | 5 | Bioclastic fine-coarse sand; gS | Tr seagrass (Pos), triaxon sponge spicules, rounded calcrete granules | R L | S | S | | | | C | C | | | | | | | | C ch | | | |
| SB 58 | | No sample taken, dangerous water | | | | | | | | | | | | | | | | | | | | |

| | | | | | | | | | | | | | | | | | | | | | | |
|---|---|---|---|---|---|---|---|---|---|---|---|---|---|---|---|---|---|---|---|---|---|---|
| SB 59 | | No sample taken, dangerous water | | | | | | | | | | | | | | | | | | | | |
| SB 60 | | Bioclastic gravelly coarse-medium sand; sG | Lithic frags | C<br>M-L | M-S | R-S | | | | | A | | | | | | C<br>ch | | C<br>ch | | | |
| SB 61 | | No returns, rocky bottom, | | | | | | | | | | | | | | | | | | | | |
| SB 62 | | Bioclastic lithic coarse-medium sand; gS | Coralline algae, radula marks on shells | R<br>L-M | S | S | | | | | A | | C<br>ch | | | | | | C<br>ch | | | |
| SB 63 | | Bioclastic lithic gravelly v coarse-coarse sand; sG | Coralline algae Gravel 85% lithic | R<br>M | M-S | R | C<br>M-L | H-L | O-S | C | C | | C<br>ch | | C<br>ch | | | | C<br>ch | R<br>ch | | C<br>Epi |
| SB 64 | | Bioclastic lithic medium-coarse sand; gS, rocky bottom | | R<br>M | M | R | | | | | | | C<br>ch | C<br>ch | R<br>ch | | | | | | | |
| SB 65 | 39 | Bioclastic lithic v coarse sandy gravel; sG, rocky bottom | Gravel 75% lithic | R<br>M | M | S-R | R<br>L | L | S | | R | | C<br>ch | | C<br>ch | C<br>ch | | | C<br>ch | | | |
| SB 66 | 38 | Bioclastic very coarse sandy gravel; sG, rocky bottom | Brachiopod, abundant bryozoans | R<br>M-L | S | S-B | R<br>L | M | O-S | | C | | A<br>ch | | R<br>ch | C<br>ch | C<br>ch | | A<br>ch | | | |
| SB 67 | 33 | Bioclastic very coarse sandy gravel; sG, rocky bottom | Brachiopod, corals (solitary + branching), abundant bryozoans | R<br>M-L | M-S | S-B | | | | | C | | A<br>ch | | C<br>ch | C<br>ch<br>cy<br>c | | | A<br>ch | C<br>ch | | |
| SB 68 | 30 | Bioclastic fine-medium sand; S | Brown algae (Ecklonia) | R<br>L | S | S | | | | | R | | | | C<br>ch | | | | | | | R<br>Epi |
| SB 69 | 24 | Bioclastic lithic medium to coarse sand; S | | R<br>L | S | S-R | | | | | | | | | | | | | | | | |

| SB 70 | 22 | Bioclastic v coarse-coarse sand; gS, rocky bottom | | R M | M-S | R-S | | | | | R | | | | | C cy c | | | C ch cy c | | | |
|---|---|---|---|---|---|---|---|---|---|---|---|---|---|---|---|---|---|---|---|---|---|---|
| 1 | 2 | 3 | 4 | 5 | 6 | 7 | 8 | 9 | 10 | 11 | 12 | 13 | 14 | 15 | 16 | 17 | 18 | 19 | 20 | 21 | 22 | 23 |
| SB 71 | | No returns, rocky bottom | | | | | | | | | | | | | | | | | | | | |
| SB 72 | | No returns, rocky bottom | | | | | | | | | | | | | | | | | | | | |
| SB 73 | 6 | Bioclastic v coarse-fine sand; S | Seagrass (Pos) | A M | S | S | A L | H | O-S | | C | | R | | | R | | | R ch | | | |
| SB 74 | 9 | Bioclastic muddy v fine-medium sand; S | Soft red algae, brown algae (brown algae) | A M | M-S | R-S | C M | L | O | | R | | | | | | | | R ch | | | |
| SB 75 | 11 | Bioclastic muddy v fine-medium sand; mS | Barnacle | A H-L | L-S | R-S | R M | H-L | S | R | C | | | | | | | | R ch | | | R Epi |
| SB 76 | 10 | Bioclastic muddy v fine to coarse sand; mS | Tunicates, agglut worm tubes, bivalves | A M-H | M | R | R L | H | O | | C | | | | | C cy c | | | R ch | | | R Epi |
| SB 77 | 11 | Bioclastic v fine-fine sandy mud; sM | agglut worm tubes | A M-H | M | R-S | R M | H | O | | R | | | | | | | | | | | R Epi |
| SB 78 | 10 | Bioclastic fine-medium sand; S | Brown algae (Ecklonia) | A H-L | L-S | R | R M | H | O | | R | | | | | | | | | | | R Epi |
| SB 79 | 5 | Bioclastic fine-coarse sand; S | Seagrass (Pos) | C M-L | M-S | R-S | C M | H | O | | R | | | | | R cy c | | | C cy c | | | R Epi |
| SB 80 | 6 | Bioclastic fine-coarse sand; S | Seagrass(Pos), brown algae (Ecklonia) | C M-L | M-S | R | C M | H | S | | C | | | | | | | | | | | R Epi |
| SB 81 | 8 | Bioclastic fine-coarse sand; s | Abundant seagrass (Pos), crab claw frag | R M | M | R-S | | | | | R | | R ch | | | | | | | | | R Epi |
| SB 82 | 8 | Bioclastic fine-coarse sand; S | Abundant seagrass (Pos) | C M | M-S | S | R M | M-L | S | | R | | C ch | | | | | | | | | |

| | | | | | | | | | | | | | | | | | | | | | | |
|---|---|---|---|---|---|---|---|---|---|---|---|---|---|---|---|---|---|---|---|---|---|---|
| SB 83 | 13 | Bioclastic medium-coarse bioclastic sand; S | Seagrass (Pos), brown algae (Ecklonia) calc worm tubes | C M-H | M | R | R L | M | S | | | | C ch | | | C ch | | | R cy c | | | |
| SB 84 | 15 | Bioclastic fine-medium sand; S, rocky bottom | | | | | | | | | | | | | | | | | | | | |
| SB 85 | 16 | Bioclastic coarse-fine sand; S, rocky bottom | Brown algae (Ecklonia) | | | | | | | | | | | | | | | | | | | |
| SB 86 | 22 | Bioclastic coarse-medium sand; S, rocky bottom | | R L | S | S | | | | C | A | | | | | C ch | | | | | | |
| 1 | 2 | 3 | 4 | 5 | 6 | 7 | 8 | 9 | 10 | 11 | 12 | 13 | 14 | 15 | 16 | 17 | 18 | 19 | 20 | 21 | 22 | 23 |
| SB 87 | 27 | Bioclastic gravelly coarse-medium sand; gS, rocky bottom | Brachiopod, coralline algae Mytilus valve | C M-H | S-L | R-S | C M | H-M | O-S | C | A | | | | | C ch | C ch | | C ch | R ch | R ch | C Epi |
| SB 88 | 32 | Bioclastic medium-coarse sand; S, rocky bottom | | R L | S | S | R M | M | O | | R | | | | | | C ch | | C ch | | | |
| SB 89 | 38 | Bioclastic coarse-v coarse sand; S | | | | | | | | | R | | | | | | | | | | | |
| SB 90 | 33 | Lithic bioclastic gravelly v coarse-coarse sand; gS | Solitary corals, large forams, 70% lithic | | | | C M | M-L | O | | C | | | | | C ch | C ch | | | R ch | R ch | |
| SB 91 | 30 | Bioclastic coarse-medium sand; S, rocky bottom | Solitary corals, abundant bryozoa lithic | R M | M-S | R | | | | C | C | | | | R ch | C cy c | R ch | C ch | C ch | | | |

| | | | | | | | | | | | | | | | | | | | | | | |
|---|---|---|---|---|---|---|---|---|---|---|---|---|---|---|---|---|---|---|---|---|---|---|
| SB 92 | 26 | Bioclastic coarse-medium sand; gS, rocky bottom | Large discoidal forams, calc worm tubes | C M | M-S | R | R L | L | S | | R | | | | | | | | C ch | | | |
| SB 93 | 18 | No returns, rocky bottom | | | | | | | | | | | | | | | | | | | | |
| SB 94 | 15 | Bioclastic gravelly v coarse-medium sand; gS, rocky bottom | Brown algae (Ecklonia) lithic | R L | S | R | R L | M-L | S | C | C | R | C ch | | | | R ch | | C ch | | | C Oph |
| SB 95 | 18 | Bioclastic coarse sandy gravel; sG rocky bottom | Brown algae (Ecklonia), bryozoa | M | M | R | | | | | C | | C ch | C ch | | C ch | | | C ch | R ch | | |
| SB 96 | 14 | Lithic bioclastic v coarse-coarse sand; S | Large discoidal and agglutinate forams | R M | S | R | R L | M | O | | R | | C ch | R ch | | | | | | | R | |
| SB 97 | 12 | Lithic bioclastic v coarse-coarse sand; S, rocky bottom | Qtz (lithic) | R L | S | S | C L | M-H | S | | C | | C ch | | | | | | C ch | | | |
| SB 98 | 10 | No returns, rocky bottom | | | | | | | | | | | | | | | | | | | | |
| SB 99 | 12 | Bioclastic gravelly v coarse-medium sand; gS | Seagrass (Pos), green algae (Ulva), large discoidal forams, barnacle calc worm tubes | A M-H | M-S | R-S | C L-M | H-M | O | | R | | R ch | | | | | | R cy c | | | |
| 1 | 2 | 3 | 4 | 5 | 6 | 7 | 8 | 9 | 10 | 11 | 12 | 13 | 14 | 15 | 16 | 17 | 18 | 19 | 20 | 21 | 22 | 23 |
| SB 100 | 12 | Bioclastic slightly muddy to gravelly v coarse-v fine sand; gS | | A L-H | L-S | R-S | C M-L | H-M | O-S | | R | | | | | | | | C ch | | | |

| | | | | | | | | | | | | | | | | | | | | | | | |
|---|---|---|---|---|---|---|---|---|---|---|---|---|---|---|---|---|---|---|---|---|---|---|---|
| SB 101 | 8 | Bioclastic v coarse-medium sand; S | Seagrass (Pos) | A H-L | L-S | R-S | C M-S | H-L | O | | A | | | | | C ch cy c | C cy c | | C ch cy c | | | |
| SB 102 | 10 | Lithic bioclastic slightly muddy v fine-fine sand; S | Seagrass (Pos), Filamentous green algae | A M-L | M-S | R-S | R L | M | O | | C | | | | | | | | | | | R Epi |
| SB 103 | 11 | Lithic bioclastic slightly muddy v fine-fine sand; S | Seagrass (Pos) | A M-L | M-S | R-S | C M-L | H | O-S | | R | | | | | | | | | | | |
| SB 104 | 12 | Lithic bioclastic v fine-fine sandy mud; sM | Agglutinate worm tubes | A M-H | M-S | R-S | R M | H | O | | R | | | | | C ch | | | | | | C Epi |
| SB 105 | 7 | Lithic bioclastic v coarse-fine sand; S | Abundant seagrass (Pos) calc worm tubes | C M-L | L-S | R | A M-L | H-M | O-S | | C | | | | | C ch cy c | | | C ch | | | |
| SB 106 | 6 | Slightly lithic bioclastic coarse-medium sand; gS | Brown algae (Ecklonia), soft red algae calc worm tubes | C L | S | R-S | A L-M | H | O-S | | C | | | | | | | | C cy c ch | | | |
| SB 107 | 12 | Bioclastic muddy medium- v fine sand; gmS | Seagrass (Amph), soft red algae | A H-L | L-S | R-S | C L-M | H | O-S | | R | | | | | | | | C ch | C ch | | C Epi |
| SB 108 | 12 | Lithic bioclastic muddy v fine-fine sand; gmS | Seagrass (Amph) | C H-L | L-S | R-S | C L | H | O-S | | R | | | | | | | | C ch | C ch | | R Epi |
| SB 109 | 12 | Lithic bioclastic slightly muddy v fine-medium sand; S | Seagrass (Pos-Amph), green algae (Ulva) agglut worm tubes | C M-L | M-S | R-S | R L | H-L | O-S | R | R | | | | | | | | C ch | | | R Epi |

| | | | | | | | | | | | | | | | | | | | | | | |
|---|---|---|---|---|---|---|---|---|---|---|---|---|---|---|---|---|---|---|---|---|---|---|
| SB 110 | 11 | Lithic bioclastic very coarse-medium sandy gravel; sG (channel lag) | Trace seagrass (Pos), Felsic and Bridgewater Formation granules <3 cm | C M-L | L | R | C H-M | H-L | O-S | | C | | C ch | | C ch | | | | | | | |
| 1 | 2 | 3 | 4 | 5 | 6 | 7 | 8 | 9 | 10 | 11 | 12 | 13 | 14 | 15 | 16 | 17 | 18 | 19 | 20 | 21 | 22 | 23 |
| SB 111 | 12 | Lithic bioclastic fine-medium sand; gS | Felsic and Bridgewater Formation granules | C M | M | R-S | C M | M-L | S | | C | | C ch | | | | | | C ch | | | |
| SB 112 | 13 | Lithic bioclastic slightly gravelly very coarse-fine sand; gS, (channel lag) | Calc worm tubes | H-M | L-S | R-S | C M-L | M-L | S | C | C | R | C ch | | | C ch | | | C ch | | | R Epi |
| SB 113 | 13 | Lithic bioclastic gravelly v coarse-fine sand; gS | Seagrass (Amph) calc worm tubes | C H-M | L-S | R | C M | M-L | S | C | C | | C ch | | R ch | C ch | | | C ch | R ch | C ch | C Epi |
| SB 114 | 12 | Lithic bioclastic fine to medium sand; S | Large agglutinate forams | C M | M-S | R | C M | M-L | S | C | C | R | C ch | R ch | | C cyc ch | | | C ch | | | C Epi |
| SB 115 | 13 | Lithic bioclastic fine-coarse sand; S | Trace seagrass (Amph) lithic frags | C M | M | R | C M | L | S | | | R | C ch | | | C ch | C ch | | C ch | R ch | | |
| SB 116 | 14 | Lithic bioclastic gravelly medium-coarse sand; gS | Barnacle, abund. large discoidal forams, lithic frags | R L | S | R-S | A M-L | L-M | S-O | C | C | R | C ch | | | | | | C ch | | | R Inf, Epi |

| | | | | | | | | | | | | | | | | | | | | | | | |
|---|---|---|---|---|---|---|---|---|---|---|---|---|---|---|---|---|---|---|---|---|---|---|---|
| SB 117 | 15 | Minimal returns, rocky bottom | Brown algae (Ecklonia), large discoidal forams, encrusting red algae, bivalve (Mytilus) | C M | S-M | R-S | | | | R | C | R | R ch | | | | C ch | | C ch | | | R Epi |
| SB 118 | 24 | No returns, rocky bottom | | | | | | | | | | | | | | | | | | | | |
| SB 119 | 27 | Bioclastic lithic coarse-v coarse sandy gravel; sG | Barnacle, discoidal + agglutinate forams, calc worm tubes (Galeolaria) lithic frags | C L-M | S-M | R-S | A L-M | H | S-O | C | C | R | C ch | C ch | C ch cy c | | C ch | | C ch | | R ch | C Epi |
| SB 120 | 29 | Lithic bioclastic gravelly medium to v coarse sand; gS, rocky bottom | Calc worm tubes (Galeolaria), brachiopod, discoidal + agglutinate forams lithic frags | C S-M | S | R | C L-M | H-M | S-O | R | C | R | C ch | R ch | | | R ch | R ch | C ch | | | R Epi |
| 1 | 2 | 3 | 4 | 5 | 6 | 7 | 8 | 9 | 10 | 11 | 12 | 13 | 14 | 15 | 16 | 17 | 18 | 19 | 20 | 21 | 22 | 23 |
| SB 142 | 5 | Lithic bioclastic fine-medium sand; S | Abundant brown algae (Ecklonia), sea grass (Pos) | C L | M | S | R L | L | O | | C | | | | | | | | C ch | | | R Epi |
| SB 143 | 4.5 | Lithic bioclastic slightly gravelly coarse-fine sand; gS | Seagrass (Pos+ Amph) calc red algae | A L-S | L-S | R-S | A M | H-L | S-O | C | A | | C ch | | R ch | | | | C ch | | | |
| SB 144 | 1 | Lithic bioclastic v fine-medium sand; S | Seagrass (Pos+Amph) | C L | S | R-S | C L | M-L | S-O | | C | | | | | | | | C ch | | | R Epi |
| SB 145a | 0.4 | Lithic bioclastic fine-coarse sand; S | Seagrass (Pos+Amph), barnacle, calc worm tubes | A M-L | M-S | R-S | A M-L | H-L | S-O | R | C | | | | | | | R ch | C ch | R ch | | |

| | | | | | | | | | | | | | | | | | | | | | | |
|---|---|---|---|---|---|---|---|---|---|---|---|---|---|---|---|---|---|---|---|---|---|---|
| FR 03/98 | | | | | | | | | | | | | | | | | | | | | | |
| ACM 53 | 500 | Bioclastic gravelly v coarse-medium sand; gS | Serpulid tubes, scaphopods, bryo>biv | C L | L | S | C L | H-L | O-S | R AB | R | C | C ch | | | A ch cy c | A ch | | C ch | R ch | C ch | R Epi |
| ACM 54 | 214-254 | Bioclastic very gravelly v coarse-medium sand; gS | Serpulid tubes, bryo>biv | C M | S | R | C M-L | H | S-O | | R | R | A ch | C ch | C ch | A ch cy c | | R ch | C ch cy c | R ch | A ch | R Epi |
| ACM 55 | 169-182 | Bryozoan bioclastic v gravelly v coarse-coarse sand; sG | Solitary coral, serpulid tubes, bryo>biv | C L | L-M | S-R | A H-L | H | S-O | | R | | A ch | C ch | | A cy c C ch | | R ch | | | A ch | C Epi |
| ACM 56 | 121 | Lithic bioclastic gravelly v coarse-fine sand; gS | bryo>biv, sponge spicules, 20% aeolianite/ calcrete | C L-M | L-M | S-R | R L | M | S | | R | R | C ch | C ch | | C cy c C ch | C ch | | C ch | | R ch | |
| ACM 57 | 94 | Lithic bioclastic gravelly v coarse-fine sand; gS | bryo>biv, solitary corals, brachiopods, sponge spicules, 10% aeolianite/ calcrete | C M-L | M-S | S-R | R L | H | S-O | C | R | C | C ch | C ch | R ch | C cy c C ch | C ch | C ch | C ch | | C ch | C Epi |
| 1 | 2 | 3 | 4 | 5 | 6 | 7 | 8 | 9 | 10 | 11 | 12 | 13 | 14 | 15 | 16 | 17 | 18 | 19 | 20 | 21 | 22 | 23 |

| | | | | | | | | | | | | | | | | | | | | | | |
|---|---|---|---|---|---|---|---|---|---|---|---|---|---|---|---|---|---|---|---|---|---|---|
| ACM 58 | 72.5 | Bioclastic lithic slightly gravelly coarse-fine sand; gS | 50% aeolianite/ calcrete/ felsic | R L | M | S | | | | | R | R | R ch | | | C cy c | | | C ch | | C ch | |
| ACM 59 | 6 2 | Bioclastic lithic slightly gravelly to slightly muddy medium-v fine sand; gS | Foram (Amphistegina) reworked? 60% aeolianite/ calcrete/ felsic | C M-C | M | S | C L | L | S | | | | R ch | R ch | | | | | | | | |
| ACM 60 | 3 1 | Bioclastic lithic slightly gravelly medium-fine sand; S | 30% aeolianite/ calcrete/ felsic | C L | S-M | S-R | R L | L | OS | | R | R | R ch | | | | | | C ch | | C ch | |
| ACM 61 | 3 1 | Lithic bioclastic v coarse-coarse sandy gravel; sG | Barnacle, soft artic zooidal bryozoan 25% felsic/ aeolianite | C M-L | R | R | R L | L-H | O | R | C | R | C ch | | | C cy c ch | | | C ch | | C ch | R Epi |
| ACM 62 | 2 6 | Lithic bioclastic v coarse-coarse sandy gravel; sG | Discoidal forams, barnacle, brachiopod, soft red algae, 20% aeolianite/ calcrete/ felsic | R L | S | R | | | | | C | C | R ch | | | R cy c | | | C ch | | R ch | |

# Appendix Three

## Grainsize Distribution % & Sand Components %

Grainsize Distribution %

| Transect 1 | SB 65 | SB 89 | SB 88 | SB 87 | SB 86 | SB 85 | SB 84 | SB 83 | SB 82 | SB 81 | SB 80 | SB 79 | SB 78 | SB 77 | SB 76 | SB 75 | SB 74 | SB 73 |
|---|---|---|---|---|---|---|---|---|---|---|---|---|---|---|---|---|---|---|
| > 2000 µm | 53 | 2 | 2 | 10 | 2 | 1 | 1 | 3 | 1 | 1 | 2 | 1 | 1 | 1 | 1 | 2 | 1 | 2 |
| 500- 2000 µm | 31 | 81 | 25 | 53 | 57 | 61 | 5 | 8 | 11 | 12 | 17 | 11 | 19 | 5 | 7 | 8 | 13 | 17 |
| 250- 500 µm | 15 | 16 | 62 | 27 | 27 | 21 | 51 | 74 | 72 | 70 | 53 | 53 | 36 | 10 | 39 | 26 | 29 | 52 |
| 250- 63 µm | 1 | 1 | 11 | 10 | 14 | 17 | 43 | 15 | 16 | 17 | 28 | 34 | 41 | 30 | 38 | 42 | 51 | 28 |
| < 63 µm | 0 | 0 | 0 | 0 | 0 | 0 | 0 | 0 | 0 | 0 | 0 | 1 | 1 | 54 | 15 | 22 | 6 | 1 |

| Transect 2 | SB 64 | SB 90 | SB 91 | SB 92 | SB 93 | SB 94 | SB 95 | SB 96 | SB 97 | SB 98 | SB 99 | SB 100 | SB 101 | SB 102 | SB 103 | SB 104 | SB 105 |
|---|---|---|---|---|---|---|---|---|---|---|---|---|---|---|---|---|---|
| > 2000 µm | 2 | 13 | 4 | 10 | 16 | 22 | 50 | 2 | 4 | 5 | 7 | 10 | 4 | 1 | 2 | 2 | 2 |
| 500- 2000 µm | 30 | 73 | 44 | 34 | 10 | 27 | 27 | 57 | 47 | 39 | 31 | 24 | 50 | 7 | 13 | 7 | 31 |
| 250- 500 µm | 57 | 13 | 35 | 54 | 44 | 33 | 16 | 32 | 40 | 43 | 46 | 35 | 31 | 10 | 16 | 10 | 44 |
| 250- 63 µm | 11 | 1 | 17 | 2 | 30 | 18 | 7 | 9 | 9 | 13 | 16 | 27 | 14 | 79 | 65 | 27 | 23 |
| < 63 µm | 0 | 0 | 0 | 0 | 0 | 0 | 0 | 0 | 0 | 0 | 0 | 4 | 1 | 3 | 4 | 54 | 0 |

| Transect 3 | SB 120 | SB 119 | SB 118 | SB 117 | SB 116 | SB 115 | SB 114 | SB 113 | SB 112 | SB 111 | SB 110 | SB 109 | SB 108 | SB 107 | SB 106 |
|---|---|---|---|---|---|---|---|---|---|---|---|---|---|---|---|
| > 2000 µm | 22 | 49 | 34 | 20 | 5 | 3 | 4 | 17 | 14 | 8 | 34 | 4 | 5 | 8 | 5 |
| 500- 2000 µm | 69 | 41 | 39 | 37 | 36 | 22 | 9 | 21 | 23 | 11 | 20 | 9 | 7 | 10 | 25 |
| 250- 500 µm | 7 | 9 | 19 | 28 | 37 | 59 | 54 | 44 | 49 | 43 | 44 | 32 | 10 | 14 | 57 |
| 250- 63 µm | 2 | 1 | 8 | 15 | 22 | 16 | 33 | 18 | 14 | 38 | 2 | 54 | 60 | 28 | 13 |
| < 63 µm | 0 | 0 | 0 | 0 | 0 | 0 | 0 | 0 | 0 | 0 | 0 | 1 | 18 | 40 | 0 |

| Transect 4 | SB 27 | SB 26 | SB 25 | SB 24 | SB 23 | SB 22 | SB 21 | SB 20 | SB 19 | SB 18 | SB 17 | SB 16 | SB 15 | SB 14 | SB 13 | SB 12 | SB 11 | SB 10 | SB 09 | SB08 | SB 07 | SB 06 | SB 05 | SB 04 | SB 03 | SB 02 | SB 01 |
|---|---|---|---|---|---|---|---|---|---|---|---|---|---|---|---|---|---|---|---|---|---|---|---|---|---|---|---|
| > 2000 µm | 1 | 3 | 1 | 4 | 5 | 14 | 8 | 20 | 2 | 3 | 2 | 3 | 5 | 0 | 3 | 1 | 2 | 2 | 3 | 4 | 7 | 12 | 2 | 0 | 3 | 5 | 7 |
| 500- 2000 µm | 3 | 2 | 6 | 13 | 10 | 14 | 18 | 25 | 12 | 11 | 7 | 8 | 11 | 8 | 6 | 7 | 7 | 11 | 7 | 11 | 15 | 26 | 11 | 40 | 14 | 10 | 14 |
| 250- 500 µm | 14 | 13 | 14 | 12 | 14 | 20 | 18 | 40 | 22 | 12 | 11 | 13 | 12 | 13 | 9 | 10 | 8 | 18 | 8 | 13 | 15 | 22 | 11 | 47 | 18 | 11 | 13 |
| 250- 63 µm | 82 | 70 | 64 | 62 | 50 | 31 | 40 | 15 | 46 | 29 | 26 | 35 | 30 | 41 | 21 | 36 | 21 | 29 | 23 | 18 | 23 | 25 | 31 | 13 | 30 | 16 | 18 |
| < 63 µm | 0 | 12 | 15 | 9 | 21 | 21 | 16 | 0 | 18 | 45 | 52 | 41 | 42 | 38 | 61 | 46 | 62 | 40 | 59 | 54 | 40 | 13 | 45 | 0 | 35 | 56 | 48 |

| Transect 5 | SB 28 | SB 29 | SB 30 | SB 31 | SB 32 | SB 33 | SB 34 | SB 35 | SB 36 | SB 37 | SB 38 | SB 39 | SB 40 | SB 41 | SB 42 | SB 43 |
|---|---|---|---|---|---|---|---|---|---|---|---|---|---|---|---|---|
| > 2000 µm | 5 | 1 | 2 | 1 | 1 | 2 | 1 | 1 | 2 | 2 | 1 | 7 | 1 | 3 | 2 | 0 |
| 500- 2000 µm | 11 | 15 | 25 | 22 | 10 | 3 | 16 | 23 | 7 | 26 | 21 | 19 | 12 | 13 | 20 | 11 |
| 250- 500 µm | 29 | 56 | 70 | 39 | 65 | 25 | 69 | 58 | 35 | 13 | 40 | 37 | 58 | 46 | 29 | 21 |
| 250- 63 µm | 55 | 28 | 3 | 36 | 24 | 70 | 14 | 18 | 56 | 59 | 38 | 37 | 29 | 37 | 48 | 67 |
| < 63 µm | 0 | 0 | 0 | 0 | 0 | 0 | 0 | 0 | 0 | 0 | 0 | 0 | 0 | 1 | 1 | 0 |

| Ttransect 6 | SB 57 | SB 56 | SB 55 | SB 54 | SB 53 | SB 52 | SB 51 | SB 50 | SB 49 | SB 48 | SB 47 | SB 46 | SB 45 | SB 44 |
|---|---|---|---|---|---|---|---|---|---|---|---|---|---|---|
| > 2000 µm | 5 | 7 | 10 | 14 | 20 | 1 | 2 | 3 | 4 | 5 | 1 | 1 | 2 | 1 |
| 500- 2000 µm | 1 | 34 | 43 | 52 | 40 | 46 | 43 | 41 | 56 | 72 | 30 | 31 | 9 | 1 |
| 250- 500 µm | 20 | 46 | 34 | 22 | 27 | 38 | 44 | 50 | 35 | 19 | 60 | 53 | 80 | 30 |
| 250- 63 µm | 74 | 13 | 13 | 12 | 13 | 15 | 11 | 6 | 5 | 4 | 9 | 15 | 9 | 68 |
| < 63 µm | 0 | 0 | 0 | 0 | 0 | 0 | 0 | 0 | 0 | 0 | 0 | 0 | 0 | 0 |

| Transect 7 | SB 60 | SB 61 | SB 62 | SB 63 | SB 64 | SB 65 | SB 66 | SB 67 | SB 68 | SB 69 | SB 70 |
|---|---|---|---|---|---|---|---|---|---|---|---|
| > 2000 µm | 35 | 20 | 5 | 30 | 2 | 53 | 65 | 75 | 1 | 1 | 12 |
| 500- 2000 µm | 27 | 22 | 17 | 58 | 30 | 31 | 19 | 14 | 1 | 76 | 64 |
| 250- 500 µm | 27 | 43 | 58 | 10 | 57 | 15 | 12 | 6 | 10 | 16 | 18 |
| 250- 63 µm | 11 | 15 | 20 | 2 | 11 | 1 | 4 | 5 | 88 | 7 | 6 |
| < 63 µm | 0 | 0 | 0 | 0 | 0 | 0 | 0 | 0 | 0 | 0 | 0 |

| Transect 8 | SB142 | SB143 | SB144 | SB145a |
|---|---|---|---|---|
| > 2000 µm | 1 | 12 | 1 | 3 |
| 500- 2000 µm | 5 | 7 | 6 | 10 |
| 250- 500 µm | 63 | 18 | 44 | 64 |
| 250- 63 µm | 31 | 63 | 49 | 23 |
| < 63 µm | 0 | 0 | 0 | 0 |

| Transect shelf | ACM53 | ACM54 | ACM55 | ACM56 | ACM57 | ACM58 | ACM59 | ACM60 | ACM61 | ACM62 |
|---|---|---|---|---|---|---|---|---|---|---|
| > 2000 µm | 28.6 | 27.8 | 44.7 | 9.4 | 25.5 | 6.4 | 6.7 | 1.3 | 35.2 | 73.5 |
| 2000- 1000 µm | 32 | 17.2 | 45.8 | 19.3 | 24.6 | 17.5 | 11.5 | 11.3 | 51.5 | 18 |
| 1000- 500 µm | 20.3 | 20.6 | 7.5 | 45.5 | 31.2 | 47.1 | 41.3 | 43.4 | 9.7 | 3.7 |
| 500- 250 µm | 9 | 21.6 | 0.6 | 25 | 15.9 | 27.8 | 27.2 | 42.3 | 2.6 | 3.7 |
| 250- 125 µm | 4.7 | 8.3 | 0.8 | 0.8 | 2.5 | 1.2 | 11.7 | 1.7 | 0.8 | 1 |
| 125- 63 µm | 3.3 | 3.5 | 0.6 | 0 | 0.3 | 0 | 1.5 | 0 | 0.1 | 0 |
| < 63 µm | 2.1 | 1 | 0 | 0 | 0 | 0 | 0 | 0 | 0 | 0 |

Components

| Transect 1 | SB 65 | SB 89 | SB 88 | SB 87 | SB 86 | SB 85 | SB 84 | SB 83 | SB 82 | SB 81 | SB 80 | SB 79 | SB 78 | SB 77 | SB 76 | SB 75 | SB 74 | SB 73 |
|---|---|---|---|---|---|---|---|---|---|---|---|---|---|---|---|---|---|---|
| Mollusc | 24.3 | 16.6 | 23.3 | 26.7 | 34.3 | 22.3 | 32.3 | 35 | 24.4 | 19.7 | 28.7 | 40.7 | 54.7 | 45 | 51 | 52 | 44.7 | 32.3 |
| Forams | 9.7 | 3.7 | 12.6 | 19 | 8.4 | 11 | 19.3 | 14.6 | 16 | 12.7 | 16.6 | 15.3 | 11.7 | 15.7 | 10 | 10 | 9 | 15.3 |
| Bryozoa | 13.3 | 2 | 17 | 19.3 | 14.7 | 12.4 | 9.4 | 9 | 4.7 | 6.7 | 6 | 4.7 | 1.7 | 3 | 2 | 3 | 0 | 2.3 |
| Echinoderm | 3 | 3 | 8.3 | 7.7 | 5 | 8.7 | 6 | 8 | 6.5 | 8.7 | 9.7 | 7 | 11.7 | 10.4 | 11 | 9.4 | 6.7 | 4.8 |
| Calcareous algae | 5.7 | 16 | 7.3 | 7.3 | 12.3 | 12.3 | 14.3 | 10.7 | 9 | 12.7 | 12 | 8 | 4.7 | 5.4 | 9 | 7.3 | 4.6 | 3.7 |
| Abraded bioclastic | 5 | 6 | 5.3 | 10.3 | 17 | 20 | 9.7 | 17 | 11.7 | 25.3 | 13.6 | 12 | 9.3 | 8.7 | 10 | 11 | 11 | 6.7 |
| Aeolianite | 26 | 2.7 | 20.3 | 6.7 | 1.3 | 0.3 | 1.3 | 0.7 | 11 | 4.7 | 0.7 | 0.3 | 0 | 2 | 0.7 | 0 | 12 | 11 |
| Quartz/ Lithic | 13 | 50 | 6.3 | 3.3 | 7 | 13 | 7.7 | 5 | 16.7 | 9.6 | 12.7 | 12 | 6.3 | 9.6 | 6.3 | 7.3 | 12 | 24.3 |

| Transect 2 | SB 64 | SB 90 | SB 91 | SB 92 | SB 94 | SB 95 | SB 96 | SB 97 | SB 99 | SB 100 | SB 101 | SB 102 | SB 103 | SB 104 | SB 105 |
|---|---|---|---|---|---|---|---|---|---|---|---|---|---|---|---|
| Mollusc | 18.9 | 25.7 | 23.3 | 26.3 | 25 | 33.4 | 17.6 | 24.3 | 33 | 56 | 75 | 44 | 47.7 | 52.7 | 21.6 |
| Forams | 7.6 | 7 | 4 | 14.7 | 15.3 | 12.7 | 15 | 11.7 | 9 | 10.7 | 4 | 10 | 9.7 | 5.8 | 9.3 |
| Bryozoa | 11 | 18.7 | 22 | 35 | 21.7 | 16.7 | 9.7 | 6 | 4.7 | 3 | 2.8 | 1.7 | 2 | 1.7 | 2.7 |
| Echinoderm | 2 | 2.7 | 42.3 | 8 | 10.3 | 5.7 | 7.4 | 5.7 | 5.7 | 6.7 | 6 | 5 | 9.4 | 10.4 | 6 |
| Calcareous algae | 2 | 6.3 | 5 | 6.4 | 7.7 | 9 | 12.3 | 8 | 8.6 | 4 | 6.7 | 4.7 | 4 | 5.4 | 3.7 |
| Abraded bioclastic | 1.4 | 2.3 | 1 | 2.3 | 3.7 | 9.7 | 5 | 6.3 | 8 | 10.6 | 4 | 20 | 17 | 15.4 | 12.4 |
| Aeolianite | 45.5 | 9.3 | 1 | 5.3 | 10 | 8.4 | 18.4 | 14.7 | 21 | 3.4 | 0.7 | 0.6 | 0.6 | 0.6 | 22 |
| Quartz/ Lithic | 11.6 | 28 | 1.7 | 2 | 6.3 | 4.4 | 14.6 | 23.3 | 12 | 5.6 | 0.8 | 11 | 9.6 | 8 | 22.3 |

| Transect 3 | SB 120 | SB 119 | SB 118 | SB 117 | SB 116 | SB 115 | SB 114 | SB 113 | SB 112 | SB 111 | SB 110 | SB 109 | SB 108 | SB 107 | SB 106 |
|---|---|---|---|---|---|---|---|---|---|---|---|---|---|---|---|
| Mollusc | 14.7 | 22.3 | 22 | 21.7 | 25.7 | 23 | 23.3 | 18.3 | 18.3 | 25.7 | 10.7 | 25 | 32.3 | 53.3 | 24.4 |
| Forams | 4.7 | 8 | 8.6 | 9.3 | 8 | 8.3 | 7 | 4.3 | 10.6 | 9 | 5 | 7 | 4.7 | 7 | 5.7 |
| Bryozoa | 5.3 | 19.7 | 17.7 | 15.7 | 10.6 | 10.3 | 9.6 | 8.7 | 10.6 | 11.8 | 2.3 | 4.6 | 6.7 | 7 | 3.7 |
| Echinoderm | 5 | 6 | 7.7 | 9.3 | 4.6 | 3.7 | 5.3 | 5.4 | 6.3 | 5.4 | 2 | 3.7 | 3 | 5.7 | 4.6 |
| Calcareous algae | 3.7 | 11.3 | 11.6 | 12 | 17.6 | 4.7 | 6.7 | 6.7 | 6.3 | 8.4 | 4 | 1.3 | 1.3 | 2.7 | 3 |
| Abraded bioclastic | 14.7 | 4 | 6.2 | 8.3 | 10.3 | 13.7 | 14.7 | 13 | 10.6 | 5.7 | 8 | 22.7 | 29.3 | 17.3 | 5 |
| Aeolianite | 29.3 | 13 | 14.2 | 15.4 | 15.9 | 24.3 | 26.7 | 32.3 | 27.3 | 28 | 53.7 | 23 | 7 | 3.7 | 44.4 |
| Quartz/ Lithic | 22.7 | 15.7 | 12 | 8.3 | 7.3 | 12 | 6.7 | 11.3 | 10 | 6 | 14.3 | 12.7 | 15.7 | 3.3 | 9 |

| Transect 4 | SB 27 | SB 26 | SB 25 | SB 24 | SB 23 | SB 22 | SB 21 | SB 20 | SB 19 | SB 18 | SB 17 | SB 16 | SB 15 | SB 14 | SB 13 | SB 12 | SB 11 | SB 10 | SB 09 | SB 08 | SB 07 | SB 06 | SB 05 | SB 04 | SB 03 | SB 02 | SB 01 |
|---|---|---|---|---|---|---|---|---|---|---|---|---|---|---|---|---|---|---|---|---|---|---|---|---|---|---|---|
| Mollusc | 33 | 50.3 | 44 | 45.6 | 45.4 | 49.4 | 49 | 31.8 | 43.7 | 47 | 54.3 | 54.7 | 49 | 51 | 52.4 | 46 | 52 | 50 | 44.7 | 48.4 | 50.4 | 45 | 39.3 | 42 | 52.3 | 49.7 | 34 |
| Forams | 8 | 4 | 2.7 | 2 | 5.4 | 3.6 | 2.8 | 5.8 | 4.7 | 5.3 | 5 | 3.7 | 5.7 | 2.7 | 4.8 | 4 | 4 | 5.7 | 4.3 | 4.4 | 4.4 | 6 | 5.7 | 3 | 1.7 | 2.7 | 7.4 |
| Bryozoa | 3.3 | 2 | 2 | 2 | 0.7 | 2.6 | 2 | 4 | 0.7 | 2 | 0 | 1 | 1 | 2 | 1 | 1.7 | 1.7 | 2 | 1.7 | 1 | 0.8 | 2.7 | 3.7 | 1.3 | 0.7 | 1.4 | 2.6 |
| Echinoderm | 7.3 | 5 | 5 | 7.7 | 8 | 4.9 | 9.7 | 5 | 6.4 | 7 | 10.7 | 7.4 | 7 | 9.3 | 10 | 10 | 9.7 | 13.7 | 8.3 | 13 | 6.7 | 7.7 | 9.3 | 6.7 | 8.7 | 11.4 | 14.3 |
| Calcareous algae | 7.4 | 8.4 | 5 | 10.4 | 5.8 | 5.2 | 5.4 | 8 | 7.7 | 11 | 8 | 7.8 | 5.7 | 8 | 3.4 | 5.7 | 3.3 | 3.7 | 6 | 4.8 | 4.7 | 4.7 | 5.7 | 4.7 | 4.3 | 3.4 | 3.8 |
| Abraded bioclastic | 26.3 | 23.7 | 32.3 | 24.3 | 28 | 26.3 | 22 | 25.4 | 26.7 | 20 | 18.3 | 20.4 | 25.3 | 20.7 | 22.4 | 30 | 23 | 19 | 26.7 | 20 | 25 | 24.7 | 25.3 | 19 | 18 | 24 | 28.6 |
| Aeolianite | 0 | 0 | 0 | 0 | 0 | 0.3 | 2.4 | 12 | 2.4 | 0 | 0 | 0 | 0 | 0 | 0.7 | 0 | 0 | 0 | 0 | 0 | 0 | 1.7 | 1.7 | 19.3 | 2.7 | 2 | 1.6 |
| Quartz/ Lithic | 14.7 | 6.6 | 9 | 8 | 6.7 | 7.8 | 6.7 | 8 | 7.7 | 7.7 | 3.7 | 5 | 6.3 | 6.3 | 5.3 | 2.7 | 6.3 | 6.3 | 8.3 | 8.4 | 8 | 7.7 | 9.3 | 4 | 11.7 | 5.4 | 7.7 |

| Transect 5 | SB 28 | SB 29 | SB 30 | SB 31 | SB 32 | SB 33 | SB 34 | SB 35 | SB 36 | SB 37 | SB 38 | SB 39 | SB 40 | SB 41 | SB 42 | SB 43 |
|---|---|---|---|---|---|---|---|---|---|---|---|---|---|---|---|---|
| Mollusc | 23 | 19 | 10.4 | 12.2 | 10.3 | 15.7 | 11.4 | 14 | 12.7 | 14.4 | 16.7 | 17.3 | 13 | 20.7 | 18.7 | 15.7 |
| Forams | 3.4 | 8 | 5.3 | 4.7 | 3.4 | 2 | 6 | 5.7 | 2.3 | 5.7 | 5.7 | 4.7 | 5.3 | 5.8 | 7.3 | 5 |
| Bryozoa | 8.8 | 8.3 | 2.3 | 3.5 | 3.3 | 7 | 6.4 | 4.4 | 4.3 | 3 | 4.3 | 4.7 | 3 | 5.7 | 5.7 | 7 |
| Echinoderm | 5 | 3.7 | 1.7 | 1.6 | 1.7 | 1.7 | 2.4 | 2 | 3.7 | 1.7 | 2.3 | 3.4 | 1.7 | 2.4 | 3.7 | 2 |
| Calcareous algae | 8 | 9 | 6.3 | 3.5 | 4 | 3 | 9 | 9.4 | 6.7 | 5.4 | 6.3 | 5.3 | 5 | 6 | 4 | 3 |
| Abraded bioclastic | 25.4 | 24 | 15.4 | 18.7 | 18.7 | 17.3 | 24.7 | 22.4 | 29.3 | 30 | 31 | 28 | 24.3 | 24 | 19.3 | 25.6 |
| Aeolianite | 12 | 17.7 | 44.3 | 43.8 | 47.3 | 43.3 | 28.7 | 31.4 | 33.3 | 25.8 | 23 | 28.3 | 39.7 | 27.4 | 32.1 | 27.7 |
| Quartz/ Lithic | 14.4 | 10.3 | 14.3 | 12.2 | 11.3 | 10 | 11.4 | 10.7 | 7.7 | 14 | 10.7 | 8.3 | 8 | 8 | 9.6 | 14.3 |

| Transect 6 | SB 57 | SB 56 | SB 55 | SB 54 | SB 53 | SB 52 | SB 51 | SB 50 | SB 49 | SB 48 | SB 47 | SB 46 | SB 45 | SB 44 |
|---|---|---|---|---|---|---|---|---|---|---|---|---|---|---|
| Mollusc | 14 | 13.7 | 13.7 | 13.7 | 14.3 | 20.3 | 18.5 | 16.7 | 16.5 | 16.3 | 21.4 | 11 | 19.3 | 18.4 |
| Forams | 5 | 2.3 | 4.6 | 7 | 5.3 | 4.4 | 5.4 | 6.3 | 5.8 | 5.4 | 5.5 | 3 | 2.7 | 3.4 |
| Bryozoa | 4.4 | 9.3 | 8.8 | 8.4 | 21.7 | 29.9 | 22.2 | 14.7 | 15.3 | 16 | 9.1 | 5.8 | 8 | 12.8 |
| Echinoderm | 4.3 | 5 | 3.6 | 2.4 | 3 | 4.7 | 4 | 3.3 | 3.7 | 4 | 4.5 | 2.4 | 4 | 4.4 |
| Calcareous algae | 5 | 6.7 | 8.5 | 10.4 | 23.3 | 9.7 | 9.5 | 9.3 | 7.6 | 6 | 5.8 | 3.8 | 4.3 | 5 |
| Abraded bioclastic | 23.7 | 12 | 15.2 | 18.3 | 13 | 16 | 14.4 | 12.7 | 12.5 | 12.3 | 15.9 | 9.3 | 15 | 18 |
| Aeolianite | 18.3 | 37.7 | 35.3 | 32.8 | 13.7 | 10.7 | 19.4 | 28 | 25.2 | 22.3 | 26.2 | 12.4 | 32 | 23 |
| Quartz/ Lithic | 25.3 | 13.3 | 10.3 | 7 | 6 | 4.3 | 6.6 | 9 | 13.6 | 17.7 | 12 | 52.3 | 14.7 | 15 |

| Transect 7 | SB 60 | SB 61 | SB 62 | SB 63 | SB 64 | SB 65 | SB 66 | SB 67 | SB 68 | SB 69 | SB 70 |
|---|---|---|---|---|---|---|---|---|---|---|---|
| Mollusc | 24.7 | 19.7 | 14.7 | 22.3 | 18.9 | 24.3 | 24 | 21 | 21.7 | 18.3 | 21.4 |
| Forams | 6 | 5.4 | 4.7 | 8 | 7.7 | 9.7 | 6.6 | 3.3 | 4.4 | 4 | 4.7 |
| Bryozoa | 13.3 | 9.3 | 5.3 | 19.7 | 11 | 13.3 | 24 | 36.5 | 12.7 | 14.7 | 19.3 |
| Echinoderm | 3.7 | 4.3 | 5 | 6 | 2 | 3 | 14.3 | 8.3 | 5.3 | 5 | 5.7 |
| Calcareous algae | 8.4 | 6 | 3.7 | 11.3 | 2 | 5.7 | 14 | 11.3 | 5 | 8.7 | 9.3 |
| Abraded bioclastic | 10.3 | 12.5 | 14.7 | 4 | 1.4 | 5 | 4.5 | 7.3 | 28.3 | 14.7 | 18.3 |
| Aeolianite | 25.3 | 27.3 | 29.3 | 13 | 45.5 | 26 | 10.6 | 10 | 6.3 | 17.3 | 11.3 |
| Quartz/ Lithic | 8.3 | 15.5 | 22.6 | 15.7 | 11.5 | 13 | 2 | 2.3 | 16.3 | 17.3 | 10 |
|  | 100 | 100 | 100 | 100 | 100 | 100 | 100 | 100 | 100 | 100 | 100 |

| Transect 8 | SB142 | SB143 | SB144 | SB145a |
|---|---|---|---|---|
| Mollusc | 26 | 33.6 | 32.2 | 24.7 |
| Forams | 11.7 | 6.8 | 6.7 | 12 |
| Bryozoa | 4 | 3.2 | 2.3 | 3 |
| Echinoderm | 2.3 | 3.2 | 2 | 2 |
| Calcareous algae | 9.7 | 6.8 | 8.1 | 6.7 |
| Abraded bioclastic | 28.6 | 31.4 | 27.7 | 28.4 |
| Aeolianite | 9 | 2 | 5.2 | 8.7 |
| Quartz/ Lithic | 8.7 | 13 | 15.8 | 14.5 |
|  | 100 | 100 | 100 | 100 |

| Transect shelf | ACM53 | ACM54 | ACM55 | ACM56 | ACM57 | ACM58 | ACM59 | ACM60 | ACM61 | ACM62 |
|---|---|---|---|---|---|---|---|---|---|---|
| Mollusc | 8 | 9 | 14 | 7 | 8 | 5 | 11 | 9 | 19 | 14 |
| Forams | 19 | 20 | 0 | 7 | 9 | 4 | 4 | 3 | 6 | 8 |
| Bryozoa | 28 | 36 | 73 | 16 | 37 | 4 | 12 | 8 | 25 | 19 |
| Echinoderm | 1 | 1 | 3 | 2 | 3 | 1 | 2 | 2 | 3 | 4 |
| Calcareous algae | 10 | 6 | 5 | 7 | 6 | 5 | 4 | 1 | 6 | 5 |
| Abraded bioclastic | 34 | 28 | 5 | 20 | 15 | 8 | 17 | 13 | 15 | 17 |
| Aeolianite | 0 | 0 | 0 | 41 | 18 | 46 | 35 | 30 | 7 | 21 |
| Quartz/ Lithic | 0 | 0 | 0 | 0 | 4 | 27 | 15 | 34 | 19 | 12 |

# Appendix Four.

## Organism Density and Structural Form: Gravel Fraction

Population density; Abundant – 3; Common – 2; Rare - 1; Absent -0

| | Qz | Mol | CA | Bry | Ech | | Bi | Ga | | CA | Encr | Rb | Rhod | | Bry | Fen | Fol | Fl | Del | Art | Zoo | Enc | No | Va | | Ech |
|---|---|---|---|---|---|---|---|---|---|---|---|---|---|---|---|---|---|---|---|---|---|---|---|---|---|---|
| SB 01 | 0 | 3 | 1 | 2 | 2 | | 3 | 3 | | 1 | 1 | 0 | 0 | | 2 | 0 | 0 | 0 | 0 | 0 | 0 | 2 | 0 | 0 | | 2 |
| SB 02 | 0 | 3 | 1 | 0 | 2 | | 3 | 2 | | 1 | 1 | 0 | 0 | | 0 | 0 | 0 | 0 | 0 | 0 | 0 | 0 | 0 | 0 | | 2 |
| SB 03 | 0 | 2 | 1 | 0 | 1 | | 2 | 2 | | 1 | 1 | 1 | 0 | | 0 | 0 | 0 | 0 | 0 | 0 | 0 | 0 | 0 | 0 | | 1 |
| SB 04 | 0 | 3 | 1 | 2 | 2 | | 3 | 3 | | 1 | 1 | 0 | 0 | | 2 | 0 | 0 | 0 | 0 | 0 | 0 | 2 | 0 | 0 | | 2 |
| SB 05 | 0 | 3 | 1 | 0 | 2 | | 3 | 2 | | 1 | 1 | 0 | 0 | | 0 | 0 | 0 | 0 | 0 | 0 | 0 | 0 | 0 | 0 | | 2 |
| SB 06 | 0 | 3 | 1 | 0 | 2 | | 3 | 3 | | 1 | 1 | 0 | 0 | | 0 | 0 | 0 | 0 | 0 | 0 | 0 | 0 | 0 | 0 | | 2 |
| SB 07 | 0 | 3 | 1 | 0 | 2 | | 3 | 3 | | 1 | 1 | 0 | 0 | | 0 | 0 | 0 | 0 | 0 | 0 | 0 | 0 | 0 | 0 | | 2 |
| SB 08 | 0 | 3 | 0 | 0 | 2 | | 3 | 2 | | 0 | 0 | 0 | 0 | | 0 | 0 | 0 | 0 | 0 | 0 | 0 | 0 | 0 | 0 | | 2 |
| SB 09 | 0 | 3 | 1 | 1 | 2 | | 3 | 2 | | 1 | 1 | 0 | 0 | | 1 | 0 | 0 | 0 | 0 | 0 | 0 | 1 | 0 | 0 | | 2 |
| SB 10 | 0 | 3 | 0 | 0 | 1 | | 3 | 2 | | 0 | 0 | 0 | 0 | | 0 | 0 | 0 | 0 | 0 | 0 | 0 | 0 | 0 | 0 | | 1 |
| SB 11 | 0 | 3 | 2 | 0 | 1 | | 3 | 1 | | 2 | 2 | 0 | 0 | | 0 | 0 | 0 | 0 | 0 | 0 | 0 | 0 | 0 | 0 | | 1 |
| SB 12 | 0 | 2 | 2 | 0 | 0 | | 2 | 1 | | 2 | 2 | 0 | 0 | | 0 | 0 | 0 | 0 | 0 | 0 | 0 | 0 | 0 | 0 | | 0 |
| SB 13 | 0 | 2 | 1 | 0 | 1 | | 2 | 2 | | 1 | 1 | 0 | 0 | | 0 | 0 | 0 | 0 | 0 | 0 | 0 | 0 | 0 | 0 | | 1 |
| SB 14 | 0 | 2 | 1 | 1 | 1 | | 2 | 1 | | 1 | 1 | 0 | 0 | | 1 | 0 | 0 | 0 | 0 | 0 | 0 | 1 | 0 | 0 | | 1 |
| SB 15 | 0 | 2 | 0 | 0 | 2 | | 2 | 1 | | 0 | 0 | 0 | 0 | | 0 | 0 | 0 | 0 | 0 | 0 | 0 | 0 | 0 | 0 | | 2 |
| SB 16 | 0 | 2 | 0 | 0 | 1 | | 2 | 1 | | 0 | 0 | 0 | 0 | | 0 | 0 | 0 | 0 | 0 | 0 | 0 | 0 | 0 | 0 | | 1 |
| SB 17 | 0 | 2 | 1 | 2 | 1 | | 2 | 1 | | 1 | 1 | 0 | 0 | | 2 | 0 | 0 | 0 | 0 | 0 | 0 | 2 | 0 | 0 | | 1 |
| SB 18 | 0 | 3 | 1 | 3 | 2 | | 3 | 1 | | 1 | 1 | 0 | 0 | | 3 | 0 | 0 | 0 | 0 | 0 | 0 | 3 | 0 | 0 | | 2 |
| SB 19 | 0 | 2 | 0 | 3 | 2 | | 2 | 2 | | 0 | 0 | 0 | 0 | | 3 | 0 | 0 | 0 | 2 | 0 | 0 | 2 | 0 | 0 | | 2 |
| SB 20 | 0 | 3 | 2 | 3 | 0 | | 3 | 3 | | 2 | 2 | 0 | 0 | | 3 | 2 | 0 | 0 | 2 | 2 | 1 | 2 | 0 | 0 | | 0 |
| SB 21 | 0 | 3 | 2 | 3 | 1 | | 3 | 2 | | 2 | 2 | 0 | 0 | | 3 | 0 | 0 | 0 | 2 | 0 | 0 | 2 | 0 | 0 | | 1 |

| | | | | | | | | | | | | | | | | | | | | | | | | |
|---|---|---|---|---|---|---|---|---|---|---|---|---|---|---|---|---|---|---|---|---|---|---|---|---|
| SB 22 | 0 | 3 | 2 | 3 | 1 | | 3 | 2 | | 2 | 2 | 0 | 0 | | 3 | 0 | 0 | 0 | 2 | 0 | 0 | 2 | 0 | 0 | | 1 |
| SB 23 | 0 | 3 | 1 | 2 | 2 | | 3 | 1 | | 1 | 1 | 0 | 0 | | 2 | 0 | 0 | 0 | 0 | 0 | 0 | 2 | 0 | 0 | | 2 |
| SB 24 | 0 | 3 | 2 | 3 | 2 | | 3 | 2 | | 2 | 2 | 0 | 0 | | 3 | 0 | 0 | 0 | 0 | 1 | 0 | 2 | 3 | 0 | | 2 |
| SB 25 | 0 | 2 | 2 | 1 | 0 | | 2 | 1 | | 2 | 2 | 1 | 0 | | 1 | 0 | 0 | 0 | 0 | 0 | 0 | 1 | 0 | 0 | | 0 |
| SB 26 | 0 | 3 | 2 | 3 | 0 | | 3 | 1 | | 2 | 2 | 0 | 0 | | 3 | 0 | 0 | 0 | 2 | 0 | 0 | 2 | 0 | 0 | | 0 |
| SB 27 | 0 | 2 | 1 | 0 | 0 | | 2 | 0 | | 1 | 1 | 1 | 0 | | 0 | 0 | 0 | 0 | 0 | 0 | 0 | 0 | 0 | 0 | | 0 |
| SB 28 | 0 | 1 | 3 | 0 | 1 | | 1 | 0 | | 3 | 2 | 2 | 0 | | 0 | 0 | 0 | 0 | 0 | 0 | 0 | 0 | 0 | 0 | | 1 |
| SB 29 | 0 | 2 | 2 | 2 | 0 | | 1 | 2 | | 2 | 2 | 0 | 0 | | 2 | 0 | 0 | 0 | 0 | 0 | 0 | 2 | 0 | 0 | | 0 |
| | Qz | Mol | CA | Bry | Ech | | Bi | Ga | | CA | Encr | Rb | Rhod | | Bry | Fen | Fol | Fl | Del | Art | Zoo | Enc | No | Va | | Ech |
| SB 30 | 0 | 2 | 3 | 0 | 0 | | 2 | 1 | | 3 | 2 | 2 | 0 | | 0 | 0 | 0 | 0 | 0 | 0 | 0 | 0 | 0 | 0 | | 0 |
| SB 31 | 0 | 2 | 1 | 1 | 0 | | 2 | 0 | | 1 | 1 | 0 | 0 | | 1 | 0 | 1 | 0 | 0 | 0 | 0 | 1 | 0 | 0 | | 0 |
| SB 32 | 1 | 2 | 1 | 0 | 0 | | 2 | 0 | | 1 | 1 | 0 | 0 | | 0 | 0 | 0 | 0 | 0 | 0 | 0 | 0 | 0 | 0 | | 0 |
| SB 33 | 0 | 2 | 2 | 1 | 0 | | 2 | 1 | | 2 | 2 | 0 | 1 | | 1 | 0 | 0 | 0 | 0 | 0 | 0 | 1 | 0 | 0 | | 0 |
| SB 34 | 0 | 0 | 3 | 2 | 0 | | 0 | 0 | | 3 | 3 | 2 | 0 | | 2 | 0 | 0 | 0 | 0 | 0 | 0 | 2 | 0 | 0 | | 0 |
| SB 35 | 0 | 1 | 0 | 0 | 0 | | 1 | 1 | | 0 | 0 | 0 | 0 | | 0 | 0 | 0 | 0 | 0 | 0 | 0 | 0 | 0 | 0 | | 0 |
| SB 36 | 1 | 2 | 3 | 0 | 0 | | 2 | 2 | | 3 | 2 | 2 | 0 | | 0 | 0 | 0 | 0 | 0 | 0 | 0 | 0 | 0 | 0 | | 0 |
| SB 37 | 0 | 2 | 3 | 1 | 0 | | 2 | 2 | | 3 | 2 | 2 | 0 | | 1 | 0 | 0 | 0 | 0 | 0 | 0 | 1 | 0 | 0 | | 0 |
| SB 38 | 0 | 2 | 1 | 1 | 0 | | 2 | 2 | | 1 | 1 | 0 | 0 | | 1 | 1 | 0 | 0 | 0 | 0 | 0 | 1 | 0 | 0 | | 0 |
| SB 39 | 1 | 3 | 2 | 3 | 1 | | 3 | 3 | | 2 | 2 | 0 | 1 | | 3 | 2 | 0 | 0 | 0 | 0 | 0 | 2 | 0 | 0 | | 1 |
| SB 40 | 0 | 2 | 2 | 2 | 0 | | 1 | 2 | | 2 | 2 | 0 | 0 | | 2 | 1 | 0 | 0 | 0 | 0 | 2 | 1 | 0 | 0 | | 0 |
| SB 41 | 0 | 2 | 2 | 2 | 0 | | 2 | 2 | | 2 | 2 | 0 | 0 | | 2 | 0 | 0 | 0 | 0 | 0 | 0 | 2 | 0 | 0 | | 0 |
| SB 42 | 0 | 2 | 2 | 2 | 0 | | 2 | 2 | | 2 | 2 | 1 | 0 | | 2 | 0 | 0 | 0 | 0 | 0 | 0 | 2 | 0 | 0 | | 0 |
| SB 43 | 0 | 2 | 0 | 0 | 2 | | 2 | 1 | | 0 | 0 | 0 | 0 | | 0 | 0 | 0 | 0 | 0 | 0 | 0 | 0 | 0 | 0 | | 2 |
| SB 44 | 0 | 2 | 2 | 2 | 1 | | 2 | 0 | | 2 | 2 | 0 | 0 | | 2 | 0 | 0 | 0 | 0 | 0 | 1 | 2 | 0 | 0 | | 1 |
| SB 45 | 0 | 3 | 0 | 0 | 1 | | 3 | 1 | | 0 | 0 | 0 | 0 | | 0 | 0 | 0 | 0 | 0 | 0 | 0 | 0 | 0 | 0 | | 1 |
| SB 46 | 0 | 1 | 0 | 1 | 0 | | 1 | 0 | | 0 | 0 | 0 | 0 | | 1 | 0 | 0 | 0 | 0 | 0 | 0 | 1 | 0 | 0 | | 0 |
| SB 47 | 0 | 1 | 1 | 0 | 1 | | 1 | 1 | | 1 | 0 | 1 | 0 | | 0 | 0 | 0 | 0 | 0 | 0 | 0 | 1 | 0 | 0 | | 1 |
| SB 48 | 0 | 2 | 3 | 2 | 0 | | 2 | 1 | | 3 | 2 | 3 | 0 | | 2 | 2 | 0 | 0 | 0 | 0 | 0 | 1 | 0 | 0 | | 0 |
| SB 49 | 0 | 0 | 3 | 2 | 0 | | 0 | 0 | | 3 | 2 | 2 | 0 | | 2 | 0 | 0 | 0 | 0 | 0 | 0 | 2 | 0 | 0 | | 0 |
| SB 50 | 0 | 0 | 3 | 2 | 0 | | 0 | 0 | | 3 | 3 | 0 | 0 | | 2 | 2 | 0 | 0 | 0 | 0 | 0 | 2 | 0 | 0 | | 0 |
| SB 51 | 0 | 2 | 3 | 3 | 1 | | 2 | 1 | | 3 | 3 | 3 | 0 | | 3 | 0 | 0 | 0 | 0 | 0 | 1 | 3 | 0 | 0 | | 1 |
| SB 52 | 1 | 1 | 2 | 2 | 0 | | 1 | 0 | | 2 | 2 | 0 | 0 | | 2 | 0 | 0 | 0 | 0 | 0 | 0 | 2 | 0 | 0 | | 0 |

| | | | | | | | | | | | | | | | | | | | | | | | | |
|---|---|---|---|---|---|---|---|---|---|---|---|---|---|---|---|---|---|---|---|---|---|---|---|---|
| SB 53 | 1 | 1 | 3 | 3 | 1 | | 1 | 1 | | 3 | 3 | 2 | 0 | | 3 | 0 | 0 | 0 | 0 | 0 | 0 | 3 | 0 | 0 | | 1 |
| SB 54 | 1 | 0 | 3 | 2 | 0 | | 0 | 0 | | 3 | 3 | 0 | 0 | | 2 | 0 | 0 | 0 | 0 | 0 | 0 | 2 | 0 | 0 | | 0 |
| SB 55 | 0 | 0 | 0 | 0 | 0 | | 0 | 0 | | 0 | 0 | 0 | 0 | | 0 | 0 | 0 | 0 | 0 | 0 | 0 | 0 | 0 | 0 | | 0 |
| SB 56 | 1 | 2 | 2 | 3 | 0 | | 2 | 2 | | 2 | 2 | 1 | 0 | | 3 | 2 | 0 | 0 | 2 | 0 | 0 | 2 | 0 | 0 | | 0 |
| SB 57 | 2 | 1 | 3 | 2 | 0 | | 1 | 0 | | 3 | 2 | 2 | 0 | | 2 | 0 | 0 | 0 | 0 | 0 | 0 | 2 | 0 | 0 | | 0 |
| SB 58 | 0 | 0 | 0 | 0 | 0 | | 0 | 0 | | 0 | 0 | 0 | 0 | | 0 | 0 | 0 | 0 | 0 | 0 | 0 | 0 | 0 | 0 | | 0 |
| SB 59 | 0 | 0 | 0 | 0 | 0 | | 0 | 0 | | 0 | 0 | 0 | 0 | | 0 | 0 | 0 | 0 | 0 | 0 | 0 | 0 | 0 | 0 | | 0 |
| SB 60 | 1 | 2 | 3 | 3 | 0 | | 2 | 0 | | 3 | 3 | 0 | 0 | | 3 | 0 | 0 | 0 | 0 | 2 | 0 | 2 | 0 | 0 | | 0 |
| SB 61 | 0 | 0 | 0 | 0 | 0 | | 0 | 0 | | 0 | 0 | 0 | 0 | | 0 | 0 | 0 | 0 | 0 | 0 | 0 | 0 | 0 | 0 | | 0 |
| SB 62 | 1 | 1 | 3 | 3 | 0 | | 1 | 0 | | 3 | 3 | 0 | 0 | | 3 | 2 | 0 | 0 | 0 | 0 | 0 | 2 | 0 | 0 | | 0 |
| SB 63 | 3 | 2 | 3 | 3 | 2 | | 1 | 2 | | 3 | 2 | 2 | 0 | | 3 | 2 | 0 | 2 | 0 | 0 | 0 | 2 | 3 | 0 | | 2 |
| SB 64 | 2 | 1 | 0 | 3 | 0 | | 1 | 0 | | 0 | 0 | 0 | 0 | | 3 | 2 | 2 | 1 | 0 | 0 | 0 | 0 | 0 | 0 | | 0 |
| SB 65 | 3 | 1 | 1 | 3 | 0 | | 1 | 1 | | 1 | 1 | 0 | 0 | | 3 | 2 | 0 | 2 | 2 | 0 | 0 | 2 | 0 | 0 | | 0 |
| SB 66 | 1 | 1 | 2 | 3 | 0 | | 1 | 1 | | 2 | 2 | 0 | 0 | | 3 | 3 | 0 | 1 | 2 | 2 | 0 | 3 | 0 | 0 | | 0 |
| SB 67 | 1 | 1 | 2 | 3 | 0 | | 1 | 0 | | 2 | 2 | 0 | 0 | | 3 | 3 | 0 | 2 | 2 | 0 | 0 | 3 | 2 | 0 | | 0 |
| SB 68 | 0 | 1 | 1 | 2 | 1 | | 1 | 0 | | 1 | 1 | 0 | 0 | | 2 | 0 | 0 | 2 | 0 | 0 | 0 | 0 | 0 | 0 | | 1 |
| SB 69 | 0 | 1 | 0 | 0 | 0 | | 1 | 0 | | 0 | 0 | 0 | 0 | | 0 | 0 | 0 | 0 | 0 | 0 | 0 | 0 | 0 | 0 | | 0 |
| SB 70 | 0 | 1 | 1 | 3 | 0 | | 1 | 0 | | 1 | 1 | 0 | 0 | | 3 | 0 | 0 | 0 | 2 | 0 | 0 | 2 | 0 | 0 | | 0 |
| | Qz | Mol | CA | Bry | Ech | | Bi | Ga | | CA | Encr | Rb | Rhod | | Bry | Fen | Fol | Fl | Del | Art | Zoo | Enc | No | Va | | Ech |
| SB 71 | 0 | 0 | 0 | 0 | 0 | | 0 | 0 | | 0 | 0 | 0 | 0 | | 0 | 0 | 0 | 0 | 0 | 0 | 0 | 0 | 0 | 0 | | 0 |
| SB 72 | 0 | 0 | 0 | 0 | 0 | | 0 | 0 | | 0 | 0 | 0 | 0 | | 0 | 0 | 0 | 0 | 0 | 0 | 0 | 0 | 0 | 0 | | 0 |
| SB 73 | 0 | 3 | 2 | 1 | 0 | | 3 | 3 | | 2 | 0 | 2 | 0 | | 1 | 0 | 0 | 0 | 0 | 0 | 0 | 1 | 0 | 0 | | 0 |
| SB 74 | 0 | 3 | 1 | 1 | 0 | | 3 | 2 | | 1 | 1 | 0 | 0 | | 1 | 0 | 0 | 0 | 0 | 0 | 0 | 1 | 0 | 0 | | 0 |
| SB 75 | 0 | 3 | 2 | 1 | 1 | | 3 | 1 | | 2 | 2 | 1 | 0 | | 1 | 0 | 0 | 0 | 0 | 0 | 0 | 1 | 0 | 0 | | 1 |
| SB 76 | 0 | 3 | 2 | 2 | 1 | | 3 | 1 | | 2 | 2 | 0 | 0 | | 2 | 0 | 0 | 0 | 2 | 0 | 0 | 1 | 0 | 0 | | 1 |
| SB 77 | 0 | 3 | 1 | 0 | 1 | | 3 | 1 | | 1 | 1 | 0 | 0 | | 0 | 0 | 0 | 0 | 0 | 0 | 0 | 0 | 0 | 0 | | 1 |
| SB 78 | 1 | 3 | 1 | 0 | 1 | | 3 | 1 | | 1 | 1 | 0 | 0 | | 0 | 0 | 0 | 0 | 0 | 0 | 0 | 0 | 0 | 0 | | 1 |
| SB 79 | 0 | 2 | 1 | 2 | 1 | | 2 | 2 | | 1 | 1 | 0 | 0 | | 2 | 0 | 0 | 0 | 1 | 0 | 0 | 2 | 0 | 0 | | 1 |
| SB 80 | 0 | 2 | 2 | 0 | 1 | | 2 | 2 | | 2 | 2 | 0 | 0 | | 0 | 0 | 0 | 0 | 0 | 0 | 0 | 0 | 0 | 0 | | 1 |
| SB 81 | 1 | 1 | 1 | 1 | 1 | | 1 | 0 | | 1 | 1 | 0 | 0 | | 1 | 1 | 0 | 0 | 0 | 0 | 0 | 0 | 0 | 0 | | 1 |
| SB 82 | 0 | 2 | 1 | 2 | 0 | | 2 | 1 | | 1 | 1 | 0 | 0 | | 2 | 2 | 0 | 0 | 0 | 0 | 0 | 0 | 0 | 0 | | 0 |
| SB 83 | 0 | 2 | 0 | 3 | 0 | | 2 | 1 | | 0 | 0 | 0 | 0 | | 3 | 2 | 0 | 0 | 2 | 0 | 0 | 1 | 0 | 0 | | 0 |

| | | | | | | | | | | | | | | | | | | | | | | | | | |
|---|---|---|---|---|---|---|---|---|---|---|---|---|---|---|---|---|---|---|---|---|---|---|---|---|---|
| SB 84 | 0 | 0 | 0 | 0 | 2 | | 0 | 0 | | 0 | 0 | 0 | 0 | | 0 | 0 | 0 | 0 | 0 | 0 | 0 | 0 | 0 | 0 | 2 |
| SB 85 | 1 | 0 | 0 | 0 | 0 | | 0 | 0 | | 0 | 0 | 0 | 0 | | 0 | 0 | 0 | 0 | 0 | 0 | 0 | 0 | 0 | 0 | 0 |
| SB 86 | 1 | 1 | 3 | 2 | 0 | | 1 | 0 | | 3 | 3 | 2 | 0 | | 2 | 0 | 0 | 0 | 2 | 0 | 0 | 0 | 0 | 0 | 0 |
| SB 87 | 1 | 2 | 3 | 3 | 1 | | 2 | 2 | | 3 | 3 | 2 | 0 | | 3 | 0 | 0 | 0 | 2 | 2 | 0 | 2 | 1 | 1 | 1 |
| SB 88 | 0 | 1 | 1 | 3 | 0 | | 1 | 1 | | 1 | 1 | 0 | 0 | | 3 | 0 | 0 | 0 | 0 | 2 | 0 | 2 | 0 | 0 | 0 |
| SB 89 | 0 | 0 | 1 | 0 | 0 | | 0 | 0 | | 1 | 1 | 0 | 0 | | 0 | 0 | 0 | 0 | 0 | 0 | 0 | 0 | 0 | 0 | 0 |
| SB 90 | 3 | 2 | 2 | 3 | 0 | | 0 | 2 | | 2 | 2 | 0 | 0 | | 3 | 0 | 0 | 0 | 2 | 2 | 0 | 0 | 1 | 1 | 0 |
| SB 91 | 2 | 1 | 3 | 3 | 0 | | 1 | 0 | | 3 | 2 | 2 | 0 | | 3 | 0 | 0 | 1 | 2 | 1 | 2 | 2 | 0 | 0 | 0 |
| SB 92 | 0 | 2 | 1 | 2 | 0 | | 2 | 1 | | 1 | 1 | 0 | 0 | | 2 | 0 | 0 | 0 | 0 | 0 | 0 | 2 | 0 | 0 | 0 |
| SB 93 | 0 | 0 | 0 | 0 | 0 | | 0 | 0 | | 0 | 0 | 0 | 0 | | 0 | 0 | 0 | 0 | 0 | 0 | 0 | 0 | 0 | 0 | 0 |
| SB 94 | 2 | 1 | 3 | 3 | 2 | | 1 | 1 | | 3 | 2 | 2 | 1 | | 3 | 2 | 0 | 0 | 0 | 1 | 0 | 2 | 0 | 0 | 2 |
| SB 95 | 0 | 1 | 2 | 3 | 0 | | 1 | 0 | | 2 | 2 | 0 | 0 | | 3 | 2 | 2 | 0 | 2 | 0 | 0 | 2 | 1 | 0 | 0 |
| SB 96 | 1 | 1 | 1 | 2 | 0 | | 1 | 1 | | 1 | 1 | 0 | 0 | | 2 | 2 | 1 | 0 | 0 | 0 | 0 | 0 | 0 | 1 | 0 |
| SB 97 | 2 | 2 | 2 | 3 | 0 | | 1 | 2 | | 2 | 2 | 0 | 0 | | 3 | 2 | 0 | 0 | 0 | 0 | 0 | 2 | 0 | 0 | 0 |
| SB 98 | 0 | 0 | 0 | 0 | 0 | | 0 | 0 | | 0 | 0 | 0 | 0 | | 0 | 0 | 0 | 0 | 0 | 0 | 0 | 0 | 0 | 0 | 0 |
| SB 99 | 0 | 3 | 1 | 1 | 0 | | 3 | 2 | | 1 | 1 | 0 | 0 | | 1 | 1 | 0 | 0 | 0 | 0 | 0 | 1 | 0 | 0 | 0 |
| SB 100 | 0 | 3 | 1 | 2 | 0 | | 3 | 2 | | 1 | 1 | 0 | 0 | | 2 | 0 | 0 | 0 | 0 | 0 | 0 | 2 | 0 | 0 | 0 |
| SB 101 | 0 | 3 | 3 | 3 | 0 | | 3 | 2 | | 3 | 3 | 0 | 0 | | 3 | 0 | 0 | 0 | 2 | 2 | 0 | 2 | 0 | 0 | 0 |
| SB 102 | 0 | 3 | 2 | 0 | 1 | | 3 | 1 | | 2 | 2 | 0 | 0 | | 0 | 0 | 0 | 0 | 0 | 0 | 0 | 0 | 0 | 0 | 1 |
| SB 103 | 0 | 3 | 1 | 0 | 0 | | 3 | 2 | | 1 | 1 | 0 | 0 | | 0 | 0 | 0 | 0 | 0 | 0 | 0 | 0 | 0 | 0 | 0 |
| SB 104 | 0 | 3 | 1 | 2 | 2 | | 3 | 1 | | 1 | 1 | 0 | 0 | | 2 | 0 | 0 | 0 | 2 | 0 | 0 | 0 | 0 | 0 | 2 |
| SB 105 | 1 | 3 | 2 | 3 | 0 | | 2 | 3 | | 2 | 2 | 0 | 0 | | 3 | 0 | 0 | 0 | 2 | 0 | 0 | 2 | 0 | 0 | 0 |
| SB 106 | 1 | 3 | 2 | 2 | 0 | | 2 | 3 | | 2 | 2 | 0 | 0 | | 2 | 0 | 0 | 0 | 0 | 0 | 0 | 2 | 0 | 0 | 0 |
| SB 107 | 0 | 3 | 1 | 3 | 2 | | 3 | 2 | | 1 | 1 | 0 | 0 | | 3 | 0 | 0 | 0 | 0 | 0 | 0 | 2 | 2 | 0 | 2 |
| SB 108 | 0 | 2 | 1 | 3 | 1 | | 2 | 2 | | 1 | 1 | 0 | 0 | | 3 | 0 | 0 | 0 | 0 | 0 | 0 | 2 | 2 | 0 | 1 |
| SB 109 | 0 | 2 | 1 | 2 | 1 | | 2 | 1 | | 1 | 1 | 1 | 0 | | 2 | 0 | 0 | 0 | 0 | 0 | 0 | 2 | 0 | 0 | 1 |
| SB 110 | 3 | 2 | 2 | 3 | 0 | | 2 | 2 | | 2 | 2 | 0 | 0 | | 3 | 2 | 0 | 2 | 0 | 0 | 0 | 0 | 0 | 0 | 0 |
| SB 111 | 2 | 2 | 2 | 3 | 0 | | 2 | 2 | | 2 | 2 | 0 | 0 | | 3 | 2 | 0 | 0 | 0 | 0 | 0 | 2 | 0 | 0 | 0 |
| | Qz | Mol | CA | Bry | Ech | | Bi | Ga | | CA | Encr | Rb | Rhod | | Bry | Fen | Fol | Fl | Del | Art | Zoo | Enc | No | Va | Ech |
| SB 112 | 2 | 2 | 3 | 3 | 1 | | 2 | 2 | | 3 | 2 | 2 | 1 | | 3 | 2 | 0 | 0 | 2 | 0 | 0 | 2 | 0 | 0 | 1 |
| SB 113 | 3 | 2 | 3 | 3 | 2 | | 2 | 2 | | 3 | 2 | 2 | 0 | | 3 | 2 | 0 | 1 | 2 | 0 | 0 | 2 | 1 | 2 | 2 |
| SB 114 | 3 | 2 | 3 | 3 | 2 | | 2 | 2 | | 3 | 2 | 2 | 0 | | 3 | 2 | 1 | 0 | 2 | 0 | 0 | 2 | 0 | 0 | 2 |

| | | | | | | | | | | | | | | | | | | | | | | | |
|---|---|---|---|---|---|---|---|---|---|---|---|---|---|---|---|---|---|---|---|---|---|---|---|
| SB 115 | 2 | 2 | 1 | 3 | 0 | | 2 | 2 | | 1 | 0 | 0 | 1 | | 3 | 2 | 0 | 0 | 2 | 2 | 0 | 2 | 1 | 0 | | 0 |
| SB 116 | 1 | 3 | 3 | 3 | 1 | | 1 | 3 | | 3 | 2 | 2 | 0 | | 3 | 2 | 0 | 0 | 0 | 0 | 0 | 2 | 0 | 0 | | 1 |
| SB 117 | 0 | 2 | 2 | 3 | 1 | | 2 | 0 | | 2 | 2 | 1 | 1 | | 3 | 1 | 0 | 0 | 0 | 2 | 0 | 2 | 0 | 0 | | 1 |
| SB 118 | 0 | 0 | 0 | 0 | 0 | | 0 | 0 | | 0 | 0 | 0 | 0 | | 0 | 0 | 0 | 0 | 0 | 0 | 0 | 0 | 0 | 0 | | 0 |
| SB 119 | 1 | 3 | 3 | 3 | 2 | | 2 | 3 | | 3 | 2 | 2 | 1 | | 3 | 2 | 2 | 2 | 0 | 2 | 0 | 2 | 0 | 1 | | 2 |
| SB 120 | 0 | 2 | 1 | 3 | 1 | | 2 | 2 | | 1 | 2 | 1 | 1 | | 3 | 2 | 1 | 0 | 0 | 1 | 1 | 2 | 0 | 0 | | 1 |
| SB 142 | 0 | 2 | 2 | 2 | 1 | | 2 | 1 | | 2 | 2 | 0 | 0 | | 2 | 0 | 0 | 0 | 0 | 0 | 0 | 2 | 0 | 0 | | 1 |
| SB 143 | 2 | 3 | 3 | 3 | 0 | | 3 | 3 | | 3 | 2 | 3 | 0 | | 3 | 2 | 0 | 1 | 0 | 0 | 0 | 2 | 0 | 0 | | 0 |
| SB 144 | 0 | 3 | 2 | 2 | 0 | | 2 | 2 | | 2 | 2 | 0 | 0 | | 2 | 0 | 0 | 0 | 0 | 0 | 0 | 2 | 0 | 0 | | 0 |
| SB 145a | 0 | 3 | 2 | 3 | 0 | | 3 | 3 | | 2 | 2 | 1 | 0 | | 3 | 0 | 0 | 0 | 0 | 0 | 1 | 2 | 1 | 0 | | 0 |
| ACM 53 | 0 | 2 | 2 | 3 | 1 | | 2 | 2 | | 2 | 1 | 2 | 1 | | 3 | 2 | 0 | 0 | 3 | 3 | 0 | 2 | 1 | 2 | | 1 |
| ACM 54 | 0 | 2 | 1 | 3 | 0 | | 2 | 2 | | 1 | 1 | 1 | 0 | | 3 | 3 | 2 | 2 | 3 | 0 | 1 | 2 | 1 | 3 | | 0 |
| ACM 55 | 0 | 3 | 1 | 3 | 2 | | 2 | 3 | | 1 | 1 | 0 | 0 | | 3 | 3 | 2 | 0 | 3 | 0 | 1 | 0 | 0 | 3 | | 2 |
| ACM 56 | 2 | 2 | 2 | 3 | 0 | | 2 | 1 | | 2 | 1 | 2 | 0 | | 3 | 2 | 2 | 0 | 2 | 2 | 0 | 2 | 0 | 1 | | 0 |
| ACM 57 | 2 | 2 | 3 | 3 | 2 | | 2 | 1 | | 3 | 2 | 2 | 0 | | 3 | 2 | 2 | 1 | 2 | 2 | 2 | 2 | 0 | 2 | | 2 |
| ACM 58 | 3 | 1 | 1 | 3 | 0 | | 1 | 0 | | 1 | 1 | 1 | 0 | | 3 | 1 | 0 | 0 | 2 | 0 | 0 | 2 | 0 | 2 | | 0 |
| ACM 59 | 3 | 2 | 0 | 1 | 0 | | 2 | 2 | | 0 | 0 | 0 | 0 | | 1 | 1 | 3 | 0 | 0 | 0 | 0 | 0 | 0 | 0 | | 0 |
| ACM 60 | 3 | 2 | 1 | 3 | 0 | | 2 | 1 | | 1 | 1 | 0 | 0 | | 3 | 1 | 0 | 0 | 0 | 0 | 0 | 2 | 0 | 2 | | 0 |
| ACM 61 | 2 | 2 | 2 | 3 | 1 | | 2 | 1 | | 2 | 2 | 1 | 1 | | 3 | 2 | 0 | 0 | 2 | 0 | 0 | 2 | 0 | 2 | | 1 |
| ACM 62 | 2 | 1 | 2 | 3 | 0 | | 1 | 0 | | 2 | 2 | 0 | 2 | | 3 | 1 | 0 | 0 | 1 | 0 | 0 | 2 | 0 | 1 | | 0 |

# Appendix Five

## Definitions of Carbonate Mud

The definition and size range of carbonate mud as variously described in the literature (see references below), uncovers a disparity in fraction size which does not appear to have been resolved. Carbonate mud was defined by various authors at a joint symposium organised by the American Association of Petroleum Geologists (AAPG) and the Society of Economic Paleontologists and Mineralogists (SEPM) on the classification of carbonate rocks and sediments in 1961. The results of this symposium, which was published by the AAPG (Ham, 1962), showed a wide variation in classification concepts based on texture, fabric and mineral composition.

Earlier classifications were acknowledged at the symposium, especially those of Folk (1959), Pettijohn (1957), Johnson (1951), Twenhofel (1950), and Grabau (1913). A textural classification for detrital or clastic limestones with the major subdivisions of calcirudite (>2mm), calcarenite (2 mm – 0.0625 mm) and calcilutite (< 0.0625 mm) was in use at the time of the symposium (principally those of Pettijohn and Folk), although a category had been created for the matrix grain-size which was < 20 μm (Pettijohn, 1957). The term "micrite" was introduced at this time. This referred to microcrystalline calcium carbonate with grain-size < 4 μm, which was formed by rapid chemical or biochemical precipitation in sea-water (Folk, 1959). Micrite sized dust produced by the abrasion of skeletal debris was acknowledged, though it was not chemically precipitated. However it was considered to be of minor importance. The term "lime mud" (and latterly micrite) was used to designate carbonates of grain size less than 0.0625 μm before this time (Folk, 1959).

The proposed size range and definition of carbonate mud as presented at the symposium was significantly varied ie:

- **Lime mud**, which was either unconsolidated or lithified, was equivalent to a micrite or matrix (old term) and refers to an ooze of either chemical or mechanical origins. It was given an upper limit of ~31 μm (Leighton and Pendexter, 1962). Further descriptive subdivisions within the lime mud classification was established to correlate with the Udden-Wentworth scale (Wentworth, 1922) where grains of < 4 μm were "cryptograined"; 4 μm to 31 μm were "finely micrograined" and 31 μm to 62.5 μm were "coarsely micrograined" (Leighton and Pendexter, 1962).

- **Micrite** was confirmed as a microcrystalline calcite with grain-sizes ranging from 1-4 μm (Folk 1962), but within this reiteration Folk stated that micrite had also been used as a term in place of "lime mudstone", "calcilutite" and "aphanitic limestone", the grain-sizes of which range from silt-sized to

clay-sized. The above terms should refer to 'mud-sized' carbonates, which incorporates a variable amount of micrite within the sediment. This carbonate grain-size definition is clear and logical but when Folk introduced his Classification of Carbonate Rocks (Folk 1962, Table 1, Figure 3 and 4) the silt-sized textures had been left out or incorporated into the micrite category further on in the text. This omission leaves the calcisiltite and mud fraction of detrital carbonates without a place in his classification table and subsequently creates a point of confusion when dealing with the spectrum of mud-sized carbonates. The nexus within Folk's paper on the classification of carbonate sediments of < 62.5μm appears to be the underlying notion that "lime mud" represents the unconsolidated state and "micrite" represents the lithified state.

• **Micrograined or microclastic carbonate** is the term used by Plumley et al (1962) for grain-sizes between 60 μm and 3.9 μm, in which the grains can be interpreted as being of clastic origin. Microcrystalline carbonate refers to inorganic or biochemical precipitation and post-depositional recrystallisation of grains < 60 μm. These grain-sizes, as well as the full spectrum of grain-size, are related to an Energy Index Classification where textural and compositional information is used to determine the genetic grouping of the limestones. This classification was used for determining the environments of deposition of carbonates in subsurface profiles so that models of sedimentary history can be constructed. It was primarily created for use in petroleum exploration (Plumley et al 1962).

• The significance of **mud** is fundamental in the distinction of whether a carbonate is deposited in calm or agitated water (Dunham, 1962). The effect of water currents and their potential to remove carbonate (and other) sediment from a depo-site is a method of characterising carbonate deposition in terms of the hydraulic environment. Calm water, therefore, has the character of allowing mud-sized grains to settle and remain on the seafloor. The grain-size of carbonate "mud" within the context of Dunham's classification is < 20 μm, with the term "grains" reserved for components > 20 μm. A sediment which contained > 1 % of mud was deemed to be significant in terms of the hydraulic setting, under this classification. This is clearly important in the context of Streaky Bay where a significant percentage of the 'muddy' sediment (< 62.5 μm) in the inner marginal basins occurs with grain-sizes < 20 μm (Figure 6.xx, SEMs of general views showing broad range of grainsize).

• The category of **mud or aphanitic limestone** in the context of Powers' classification (Powers, 1962) is similar to the Udden-Wentworth scale although the boundary between sand and mud is rounded off to 60 μm with a clay/silt boundary at 4 μm. The study also found the depositional pathways of carbonate grains were similar to comparably sized siliceous grains. Therefore the techniques which are used in siliceous sediment grainsize analysis can be cautiously utilised in the grainsize study of carbonate sediments. This classification was created as a result of a thorough study of carbonate sequences from the Arabian Upper Jurassic.

• Modern **lime mud** from the Bahama Banks was defined as a "sufficient quantity" of grains < 125 μm (Imbrie and Purdy, 1962) with two subfacies or subgroups being skeletal mud and pellétal mud. Both of these subgroups contained carbonate grains of clay-size which was significantly finer than the skeletal or pellet grains, although this was inferred and not actually stated.

Since the time of these seminal papers, common use points to **lime mud** as having a grain size of < 62.5 μm (Young and Davies, 1983; Nelson and Bornhold, 1983; Young and Nelson, 1985; Blom and Alsop, 1988; Farrow and Fyfe, 1988; Reid et al 1992; Davis et al 1995; Andrews et al, 1997; Reid and Macintyre, 1998, amongst others).

Use of the term **micrite** has continued to refer to calcite or aragonite microcrystallites with a grain-size < 4 μm (op. cit.), although there is also support for including the category "microspar" under an expanded "micrite" category to encompass grainsizes < 7 μm (Leighton and Pendexter, 1962; Lasemi and Sandberg, 1993).

The choice of grain-size for the terms **'carbonate or lime mud'** with a grainsize < 62.5 μm, or more generally < 63 μm, has been selected in this study for purposes of clarity and within the context of the above discussion. **Micrite** is used for microcrystalline sediment with a grainsize < 4 μm. However the differentiation between crystallites of inorganic and organic origin in micrite becomes unclear as does the difference between crystallites of tropical (Lasemi and Sandberg 1993) and temperate organic origins (this study)